Pinch Technique: Theory and Applications

Daniele Binosi [a], Joannis Papavassiliou [b]

[a]*ECT*, Villa Tambosi, Str. delle Tabarelle 286, I-38100 Villazzano (Trento), Italy*

[b]*Departamento de Física Teórica and IFIC, Centro Mixto, Universidad de Valencia-CSIC, E-46100, Burjassot, Valencia, Spain*

Abstract

We review the theoretical foundations and the most important physical applications of the Pinch Technique (PT). This general method allows the construction of off-shell Green's functions in non-Abelian gauge theories that are independent of the gauge-fixing parameter and satisfy ghost-free Ward identities. We first present the diagrammatic formulation of the technique in QCD, deriving at one loop the gauge independent gluon self-energy, quark-gluon vertex, and three-gluon vertex, together with their Abelian Ward identities. The generalization of the PT to theories with spontaneous symmetry breaking is carried out in detail, and the profound connection with the optical theorem and the dispersion relations are explained within the electroweak sector of the Standard Model. The equivalence between the PT and the Feynman gauge of the Background Field Method (BFM) is elaborated, and the crucial differences between the two methods are critically scrutinized. A variety of field theoretic techniques needed for the generalization of the PT to all orders are introduced, with particular emphasis on the Batalin-Vilkovisky quantization method and the general formalism of algebraic renormalization. The main conceptual and technical issues related to the extension of the technique beyond one loop are described, using the two-loop construction as a concrete example. Then the all-order generalization is thoroughly examined, making extensive use of the field theoretic machinery previously introduced; of central importance in this analysis is the demonstration that the PT-BFM correspondence persists to all orders in perturbation theory. The extension of the PT to the non-perturbative domain of the QCD Schwinger-Dyson equations is presented systematically, and the main advantages of the resulting self-consistent truncation scheme are discussed. A plethora of physical applications relying on the PT are finally reviewed, with special emphasis on the definition of gauge-independent off-shell form-factors, the construction of non-Abelian effective charges, the gauge-invariant treatment of resonant transition amplitudes and unstable particles, and finally the dynamical generation of an effective gluon mass.

prepared for Physics Reports

Contents

1 Introduction

When quantizing gauge theories in the continuum one usually resorts to an appropriate gauge-fixing procedure in order to remove redundant (non-dynamical) degrees of freedom originating from the gauge invariance of the theory [1]. Thus, one adds to the gauge invariant (classical) Lagrangian, $\mathcal{L}_{\mathrm{I}}$, a gauge-fixing term, $\mathcal{L}_{\mathrm{GF}}$, which allows for the consistent derivation of Feynman rules. At this point a new type of redundancy makes its appearance, this time at the level of the building blocks defining the perturbative expansion. In particular, individual off-shell Green's functions (n-point functions) carry a great deal of unphysical information, which disappears when physical observables are formed. S-matrix elements, for example, are independent of the gauge-fixing scheme and parameters chosen to quantize the theory are unitary and well-behaved at high energies. Green's functions, on the other hand, depend explicitly (and, in general, non-trivially) on the gauge-fixing parameter (gfp) entering in the definition of $\mathcal{L}_{\mathrm{GF}}$, contain unphysical thresholds, and grow much faster than physical amplitudes at high energies (*e.g.*, they grossly violate the Froissart-Martin bound [2]). Evidently, in going from unphysical Green's functions to physical amplitudes, subtle field-theoretic mechanisms are at work, enforcing vast cancellations among the various Green's functions. While it is clear that the realization of these cancellations mixes non-trivially contributions stemming from Feynman diagrams of different kinematic nature (propagators, vertices, boxes), the prevailing attitude is to condense all this down to the standard statement that the Becchi-Rouet-Stora-Tyutin (BRST) symmetry [3,4] guarantees eventually the gauge-independence of physical observables, and nothing more.

It turns out, however, that all aforementioned cancellations inside physical amplitudes (such as S-matrix elements, Wilson loops, etc) take place in a very particular way: not only is the entire physical amplitude gauge-independent, but it may be decomposed into kinematically distinct subamplitudes that are themselves *individually* gauge-independent. In addition to being gauge-independent, these subamplitudes are endowed with further properties, such as analyticity and a profound connection with the optical theorem. The precise field-theoretic method that exposes this particular stronger version of gauge independence and enforces all ensuing physical properties is the Pinch Technique (PT) [5–9]. The basic observation is that all relevant cancellations are realized when a very particular subset of longitudinal momenta, circulating inside vertex and box diagrams, extracts out of them, through the "pinching" of internal lines, structures that are in all respects propagator-like, and should therefore be reassigned to the conventional self-energy Feynman graphs. This particular reshuffling of terms has far-reaching consequences, giving rise to effective Green's functions, which, in contradistinction to the conventional unphysical Green's functions, have properties generally associated with physical observables. In particular, the PT Green's functions are independent of the gauge-fixing scheme and parameters chosen to quantize the theory (ξ in covariant gauges, n_μ in axial gauges, etc.) are gauge-invariant, *i.e.*, they satisfy the all-order simple tree-level Ward Identities (WIs), associated with the gauge symmetry of the classical Lagrangian $\mathcal{L}_{\mathrm{I}}$, instead of the ghost-infested Slavnov-Taylor identities (STIs), they display only physical thresholds, and they are well-behaved at high energies.

But why should one worry at all about the gauge-dependence or other unphysical properties that individual Green's functions may have? After all, when one uses them to construct observables, they do conspire to furnish the right answer, which is all that really matters. Things are

not so simple, however; in fact, as we will explain in detail in this report, there are considerable theoretical and phenomenological advantages in reformulating the perturbative expansion in terms of off-shell Green's functions with improved properties.

Even within a fixed order perturbative calculation, the sharp difference between observables and Green's functions suggests a great deal of redundancy in the conventional diagrammatic formulation of gauge theories, in the sense that extensive underlying cancellations beg to be made manifest and be explicitly exploited as early within a calculation as possible. Implementing these cancellations at an early stage renders the book-keeping aspects more tractable [10]. Moreover, there is an unpleasant mismatch between our intuition based on Quantum Electrodynamics (QED) and the way non-Abelian theories seem to work; however, very often this mismatch is not due to inherent properties of the non-Abelian physics, but is rather an artifact of the quantization procedure, and of the way this affects individual Green's functions. For example, the text-book concept of the effective charge, so familiar in QED, becomes completely obscured in a non-Abelian setting, because of the gauge-dependence of the vector meson's self-energy, a complication that is automatically resolved in the PT context.

The main reason that clearly favors employing the PT Green's functions, however, is the fact that a variety of important physical problems cannot be addressed within the framework of fixed-order perturbation theory, *i.e.*, by simply computing all Feynman diagrams contributing to a given process at a given order. This is often the case within Quantum Chromodynamics (QCD), where, due to the large disparities of the physical scales involved, a complicated interplay between perturbative and non-perturbative effects takes place. Similar limitations appear when physical kinematic singularities, such as resonances, render the perturbative expansion divergent at any finite order, or when perturbatively exact symmetries prohibit the appearance of certain phenomena, such as chiral symmetry breaking or gluon mass generation. In such cases one often resorts to various reorganizations of the perturbative expansion, or to completely non-perturbative techniques such as the Schwinger-Dyson equations (SDEs). One of the main difficulties encountered when dealing with the problems mentioned above is the fact that several physical properties, which are automatically preserved in fixed-order perturbative calculations by virtue of powerful field-theoretic principles, may be easily compromised when rearrangements of the perturbative series, such as resummations, are carried out. These complications may, in turn, be traced down to the fundamental fact that we have emphasized from the outset: in non-Abelian gauge theories individual off-shell Green's functions are unphysical.

We now take a closer look at some of the aforementioned issues, in order to fully appreciate the usefulness of the PT formalism.

∗ *Non-Abelian effective charges*. The unambiguous extension of the concept of the gauge-independent, renormalization group invariant, and process-independent effective charge from QED to QCD [7,11] is of special interest for several reasons [12]. The PT construction of this quantity accomplishes the explicit identification of the conformally-variant and conformally-invariant subsets of QCD graphs [13], usually assumed in the field of renormalon calculus [14]. Moreover, the PT effective charge can serve as the natural scheme for defining the coupling in the proposed "event amplitude generators" based on the the light-cone formulation of QCD [15]. In addition, the electroweak effective charges constructed with the PT are used to define the physical renormalization schemes [16], which provide a superior framework for the study of gauge coupling unification.

∗ *Off-shell form-factors.* In non-Abelian theories their proper definition poses in general problems related to the gauge invariance [17]. Specifically, if one attempts to define the form-factors from the conventional vertices, for off-shell momentum transfers, one is invariably faced with residual gauge-dependences, together with the various pathologies that these imply. Some representative cases are the magnetic dipole and electric quadrupole moments of the W [18], the top-quark magnetic moment [19], and the neutrino charge radius [20]. The PT allows for an unambiguous definition of such quantities, without any additional assumptions whatsoever: one must simply extract the corresponding physical off-shell form-factors from the corresponding gauge-independent PT vertex. A celebrated example of such a successful construction has been the neutrino charge radius; the gauge-independent, renormalization-group-invariant, and target-independent neutrino charge radius obtained from the corresponding PT vertex constitutes a genuine *physical* observable, since it can be extracted (at least in principle) from an appropriate combination of scattering experiments [21].

∗ *Resonant transition amplitudes.* The Breit-Wigner procedure used for regulating the physical singularity appearing in the vicinity of resonances ($\sqrt{s} \sim M$) is equivalent to a *reorganization* of the perturbative series [22]. In particular, the Dyson summation of the self-energy, which is the standard way for treating resonant amplitudes, effectively amounts to removing a particular term from each order of the perturbative expansion, since from all the Feynman graphs contributing to a given order one only keeps the part that contains self-energy bubbles. Given that non-trivial cancellations involving the various Green's function generally take place at any given order of this expansion, the act of removing one of them from each order may distort those cancellations; this is indeed what happens when constructing non-Abelian *running widths*. The way the PT solves this problem is by ensuring that all unphysical contributions contained inside the conventional self-energies have been identified and properly discarded, *before* any resummations are carried out [23].

∗ *Schwinger-Dyson equations.* The most widely used framework for studying in the continuum various dynamical questions that lie beyond perturbation theory are the Schwinger-Dyson equations (SDE) [24,25]. This infinite system of coupled non-linear integral equations for all Green's functions of the theory is inherently non-perturbative, and captures the full content of the quantum equations of motion. Even though these equations are derived by an expansion about the free-field vacuum, they finally make no reference to it, or to perturbation theory, and can be used to address problems related to chiral symmetry breaking, dynamical mass generation, formation of bound states, and other non-perturbative effects [26,27]. Since this system involves an infinite hierarchy of equations, in practice one is severely limited in their use, and the need for a self-consistent truncation scheme is evident. Devising such a scheme, however, is far from trivial; the crux of the matter is that the SDEs, in their conventional formulation, are built out of unphysical Green's functions. Thus, the extraction of reliable physical information depends crucially on delicate all-order cancellations, which may be inadvertently distorted in the process of the truncation. The PT addresses this problem at its root, by introducing a drastic modification already at the level of the building blocks of the SD series, namely the off-shell Green's functions themselves.

Let us emphasize from the beginning that, to date, there is no formal definition of the PT procedure at the level of the functional integral defining the theory. In particular, let us assume that the path integral has been defined using an arbitrary gauge-fixing procedure (*e.g.*, linear covariant gauges); then, there is no known a priori procedure (such as, *e.g.*, functional differentiation with respect to some combination of appropriately defined sources) that would furnish directly the gauge-independent PT Green's functions. The definition of the PT procedure is operational, and is intimately linked to the diagrammatic expansion of the theory (*i.e.*, one must know the Feynman rules). In fact, the starting point of the PT construction can be any gauge-fixing scheme that furnishes a set of well-defined Feynman rules and gauge-independent physical observables. Specifically, one operates at a certain well-defined subset of diagrams, and the subsequent rearrangements give rise to the same gfp-independent PT answer, regardless of the gauge-fixing scheme chosen for deriving the Feynman rules. However, as we will see in the last sections of this report, the PT in its ultimate formulation is not diagrammatic, in the sense that one does not need to operate on individual graphs but rather on a handful of classes of diagrams (each one containing an infinite number of individual graphs).

Today's distilled wisdom on the structure of the PT can be essentially captured by the profound connection between the PT and the the well-known quantization scheme known as the Background Field Method (BFM) [28–38]. The BFM is a special gauge-fixing procedure, implemented at the level of the generating functional. In particular, it preserves the symmetry of the action under ordinary gauge transformations with respect to the background (classical) gauge field $\widehat{A}_\mu$, while the quantum gauge fields A_μ appearing in the loops transform homogeneously under the gauge group, *i.e.*, as ordinary matter fields which happened to be assigned to the adjoint representation [39]. As a result of the background gauge symmetry, the BFM n-point functions $\langle 0|T\left[\widehat{A}_{\mu_1}(x_1)\widehat{A}_{\mu_2}(x_2)\cdots\widehat{A}_{\mu_n}(x_n)\right]|0\rangle$ satisfy naive QED-like Ward-identities, but they do depend explicitly on the quantum gauge-fixing parameter ξ_Q used to define the tree-level propagators of the quantum gluons. It turns out that, to all orders in perturbation theory, the gauge-fixing parameter-independent effective n-point functions constructed by means of the PT (starting from any gauge-fixing scheme) *coincide* with the corresponding background n-point functions when the latter are computed at the special value $\xi_Q = 1$ (BFM Feynman gauge, BFG in short) [40–42] . Some important conceptual issues related to this correspondence will be discussed extensively in the corresponding sections.

We now turn to a somewhat more technical issue, and discuss briefly the formal machinery necessary for the implementation of the PT. Evidently, there is a gradual increase in the sophistication of the field-theoretic tools employed when going from the one-loop construction, presented in the early articles, all the way to the recently derived new SD series.

The original one-loop [7] and two-loop [43] PT calculations consist in carrying out algebraic manipulations inside individual box- and vertex-diagrams, following well-defined rules. In particular, one tracks down the rearrangements induced when the action of (virtual) longitudinal momenta (k) on the bare vertices of diagrams trigger elementary WIs. The longitudinal momenta responsible for these rearrangements stem either from the bare gluon propagators or from a very characteristic decomposition of the tree-level (bare) three-gluon vertex. Eventually, a WI of the form $k_\mu \gamma^\mu = S^{-1}(\not{k}+\not{p}) - S^{-1}(\not{p})$ gives rise to propagator-like parts, by removing (pinching out) the internal bare fermion propagator $S(\not{k}+\not{p})$. Depending on the order and topology of the diagram under consideration, the final WI may be activated immediately, as happens

10

at one loop, or as the final outcome of a sequential triggering of intermediate WIs, as happens at two loops. The propagator-like contributions so obtained are next reassigned to the usual gluon self-energies, giving rise to the PT gluon self-energy.

The direct diagram-by-diagram treatment followed up until the two-loops cannot be possibly used to generalize the PT to all orders. Indeed, the resulting logistic complexity clearly advocates for the use of a non-diagrammatic approach, *i.e.*, a method that treats at once entire subsets of diagrams. The non-diagrammatic formulation of the PT introduced in [44] accomplishes this, by recognizing that the aforementioned one- and two-loop rearrangements are but lower-order manifestations of a more fundamental cancellation. This cancellation takes place when computing the divergence (STI) of a special Green's function, which serves as a common kernel to all higher order self-energy and vertex diagrams. In addition, and most importantly, the parts of the Feynman diagrams that are shuffled around during the pinching process are expressed in terms of well-defined field-theoretic objects, namely the ghost Green's functions appearing as a standard ingredient in the STI satisfied by the three-gluon vertex [45]. These ghost Green's functions involve composite operators, such as $\langle 0|T[s\Phi(x)\cdots]|0\rangle$, where s is the BRST operator and Φ is a generic QCD field. It turns out that the most efficient framework for dealing with these type of objects is the Batalin-Vilkovisky formalism [46]. In this framework, one adds to the original gauge-invariant Lagrangian $\mathcal{L}_\mathrm{I}$ the term $\mathcal{L}_\mathrm{BRST} = \sum_\Phi \Phi^* s\Phi$, thus coupling the composite operators $s\Phi$ to the BRST invariant external sources (usually called anti-fields) Φ^*, to obtain the new Lagrangian $\mathcal{L}_\mathrm{BV} = \mathcal{L}_\mathrm{I} + \mathcal{L}_\mathrm{BRST}$. One advantage of this formulation is that it allows one to express the STIs of the theory in terms of auxiliary functions, which can be constructed using a well-defined set of Feynman rules (derived from $\mathcal{L}_\mathrm{BRST}$). The Batalin-Vilkovisky formalism, and in particular a multitude of useful identities derived from it, is used extensively in the derivation of the new series of gauge-invariant SDEs.

We conclude by presenting a roadmap of the topics discussed in this report.

Section 2. This section contains a detailed introduction to the one-loop PT in the context of a theory like QCD, *i.e.*, without tree-level symmetry breaking. The method is implemented at the level of every single one-loop Feynman diagram contributing to a quark-quark scattering amplitude. The PT two-point functions at one-loop are derived, with particular emphasis on the PT gluon self-energy and the quark-gluon vertex. The QED-like WI satisfied by the latter is derived in detail. A similar construction is carried out for the one-loop three-gluon vertex, the corresponding Abelian WI is presented, and the supersymmetric structure of its form-factors is discussed. We dedicate a large part of the first section in establishing the precise connection between the imaginary parts of the one-loop PT Green's functions and the optical theorem, together with the corresponding dispersion relations.

Section 3. Here we review the formal aspects of the BFM, and derive the corresponding set of Feynman rules, emphasizing the dependence of the *bare* three- and four-gluon vertices on the gfp, and the characteristic ghost sector containing a symmetric $\widehat{A}\bar{c}c$ vertex, and a new $\widehat{A}\widehat{A}\bar{c}c$ four-field vertex. We next establish the correspondence between the PT and the BFG at the one-loop level, and clarify various conceptual issues regarding this correspondence and its correct interpretation. The final item in this section is the introduction to the "generalized" PT, which is a diagrammatic procedure that permits one to start out with any arbitrary conventional gauge and be dynamically projected to the corresponding BFM gauge.

Section 4. In this section, the one-loop PT construction for the electroweak sector of the Standard Model (SM) is presented. This exercise is significantly more involved than in the case of QCD, mainly due to the book-keeping complications introduced by the proliferation of particles. We pay particular attention to the modifications introduced to the PT procedure due to the spontaneous breaking of the symmetry through the Higgs mechanism. We first present the technically simpler situation of massless external test fermions, an assumption that considerably simplifies the algebra. The absorptive construction of the first section is repeated, and the same underlying principles and patterns are recovered. The generalization of the method to the case of massive external fermions is then discussed, and the central role of the would-be Goldstone bosons for maintaining gauge-invariance is elucidated. We demonstrate how in this latter case the requirement of the complete gauge-independence of the PT-rearranged scattering amplitude furnishes non-trivial WIs relating the various PT Green's functions.

Section 5. We present some of the most characteristic applications of the PT, that can be worked out based on the material presented in the previous three sections. We focus on four particular subjects. First, we study in detail the construction of non-Abelian effective charges that satisfy the same properties as the prototype QED effective charge. The analysis includes the QCD effective charge, as well as the those appearing in the electroweak sector, most notably the effective electroweak mixing angle. We demonstrate how the unitarity and analyticity properties built into these charges allow (at least in principle) their reconstruction from experiments. As a particularly interesting phenomenological application of the PT effective charges, we focus on the so-called "physical renormalization schemes", relevant for the correct quantitative study of the unification of the gauge couplings. Second, we explain how to define gauge-independent off-shell form-factors with the PT. Particular emphasis is placed on the more recent case of the neutrino charge radius, which is shown to be endowed with a plethora of physical properties, and to constitute a genuine physical observable. The third application is related to the gauge-independent definition of some important electroweak parameters, such as the S, T, and U, and the universal part of the ρ parameter. The fourth main application is the gauge-invariant framework for treating self-consistently resonant transition amplitudes. The intricate nature of this problem requires an elaborate synthesis of practically all the material that has been presented in the first three sections. In the corresponding subsections the reader may fully appreciate how tightly intertwined the various physical principles really are, and eventually recognize the superiority of the PT-based resonant transition formalism over any other similar attempt that has appeared in the literature to date.

Section 6. The application of the PT beyond one loop is presented. We start with the explicit two-loop construction, which still proceeds by applying the PT algorithm on individual graphs. The upshot of the analysis is that all the PT properties known from the one-loop construction are replicated at two loops, without any additional assumptions; most notably, it is established that the PT-BFG correspondence persists at two loops. Next, we shift gears and turn into the non-diagrammatic formulation of the PT: the all-order construction is carried out by recognizing that all crucial PT cancellations are encoded into the STI satisfied by a special Green's function, and the PT-BFG correspondence is proven to be valid to all orders.

Section 7. We introduce the powerful quantization formalism of Batalin and Vilkovisky, which will allow us to streamline elegantly the entire PT procedure, in a way especially suited for accomplishing the important task of the next section. After introducing the basic formalism, we revisit the one- and two-loop cases, and show how the various terms participating in the construction are expressed in terms of the auxiliary Green's functions characteristic of the Batalin-Vilkovisky formalism. In addition, we derive a set of identities relating the conventional and BFM Green's functions, which will turn out to be of paramount importance for the SD analysis that follows.

Section 8. This section contains the holy grail of the PT. We first explain that the naive truncation of the conventional SD series is bound to introduce artifacts, such as the violation of the transversality of the gluon self-energy. We then show that the application of the PT to the conventional SDE for the gluon propagator and three-gluon vertex gives rise to new SDEs endowed with special properties. The fully dressed vertices appearing in this new SD series satisfy Abelian all-order WIs instead of the STIs satisfied by their conventional counterparts. As a result, and contrary to the standard case, the new series can be truncated *gauge-invariantly* at any order in the dressed loop expansion, and *separately* for gluonic and ghost contributions.

Section 9. Here we present a highly non-trivial application of the new SD formalism derived in the previous section. In particular, after truncating the SD series gauge-invariantly, we solve the resulting system of coupled integral equations, and determine the infrared behavior of the gluon and ghost propagator (in the Landau gauge). We explain that, under very special assumptions for the three-gluon vertex entering into the SDE, one can obtain an infrared finite gluon propagator. The physics behind this behavior is associated with the phenomenon of dynamical gluon mass generation, which is the $4 - d$ analogue of the $2 - d$ Schwinger mechanism. In addition, the numerical treatment of the SD system reveals that the dressing function of the ghost propagator is also finite in the infrared. These results are then compared with several recent large-volume lattice simulations, and are found to be in good qualitative agreement.

The review ends with some concluding remarks in Section 10, and three appendices collecting material used in the main text.

2 The one-loop pinch technique in QCD

In this section, we present in detail the PT construction at one-loop for a non-Abelian gauge theory like QCD, where there is no tree-level symmetry breaking (no Higgs mechanism). The analysis we present here applies to any gauge group [$SU(N)$, exceptional groups, etc], but for concreteness we will adopt the QCD terminology (thus talking about quarks, gluons, etc). The calculations presented in this section are purposefully very detailed, and aim to provide a completely self-contained guide to the one-loop PT.

2.1 The QCD Lagrangian, gauge-fixing, and BRST symmetry

Throughout this report we will adopt the conventions of the book by Peskin & Schröder [47]. The QCD Lagrangian density is given by

$$\mathcal{L} = \mathcal{L}_{\mathrm{I}} + \mathcal{L}_{\mathrm{GF}} + \mathcal{L}_{\mathrm{FPG}}. \tag{2.1}$$

$\mathcal{L}_{\mathrm{I}}$ represents the gauge invariant $SU(3)$ Lagrangian, namely

$$\mathcal{L}_{\mathrm{I}} = -\frac{1}{4} F_a^{\mu\nu} F_{\mu\nu}^a + \bar{\psi}_{\mathrm{f}}^i \left(i\gamma^\mu \mathcal{D}_\mu - m \right)_{ij} \psi_{\mathrm{f}}^j, \tag{2.2}$$

where $a = 1, \ldots, 8$ (respectively $i, j = 1, 2, 3$) is the color index for the adjoint (respectively fundamental) representation, while "f" is the flavor index. The field strength is

$$F_{\mu\nu}^a = \partial_\mu A_\nu^a - \partial_\nu A_\mu^a + g f^{abc} A_\mu^b A_\nu^c, \tag{2.3}$$

and the covariant derivative is defined as

$$(\mathcal{D}_\mu)_{ij} = \partial_\mu (\mathbb{I})_{ij} - ig A_\mu^a (t^a)_{ij}, \tag{2.4}$$

with g the (strong) coupling constant. Finally, the $SU(N)$ generators t^a satisfy the commutation relations

$$[t^a, t^b] = i f^{abc} t^c, \tag{2.5}$$

with f^{abc} the totally antisymmetric $SU(N)$ structure constants. Useful formulas involving the $SU(N)$ structure constants are reported in Appendix A.

$\mathcal{L}_{\mathrm{I}}$ is invariant under the (infinitesimal) local gauge transformations

$$\delta A_\mu^a = -\frac{1}{g} \partial_\mu \theta^a + f^{abc} \theta^b A_\mu^c \qquad \delta_\theta \psi_{\mathrm{f}}^i = -i\theta^a (t^a)_{ij} \psi_{\mathrm{f}}^j \qquad \delta_\theta \bar{\psi}_{\mathrm{f}}^i = i\theta^a \bar{\psi}_{\mathrm{f}}^j (t^a)_{ji}, \tag{2.6}$$

where $\theta^a(x)$ are the local infinitesimal parameters corresponding to the $SU(N)$ generators t^a.

In order to quantize the theory, the gauge invariance needs to be broken; this is achieved through a (covariant) gauge fixing function $\mathcal{F}^a$, giving rise to the (covariant) gauge fixing Lagrangian $\mathcal{L}_{\mathrm{GF}}$ and its associated Faddeev-Popov ghost term $\mathcal{L}_{\mathrm{FPG}}$. The most general way of writing these terms is through the BRST operator s [48,3] and the Nakanishi-Lautrup multiplier

B^a [49,50] which represents an auxiliary, non-dynamical field, that can be eliminated through its (trivial) equation of motion. Then

$$
\begin{aligned}
\mathcal{L}_{\text{GF}} &= -\frac{\xi}{2}(B^a)^2 + B^a \mathcal{F}^a, \\
\mathcal{L}_{\text{FPG}} &= -\bar{c}^a s \mathcal{F}^a,
\end{aligned}
\tag{2.7}
$$

where

$$
\delta_{\text{BRST}} \Phi = \epsilon s \Phi,
\tag{2.8}
$$

with ϵ a Grassmann constant parameter, and s the BRST operator acting on the QCD fields as

$$
\begin{aligned}
s A_\mu^a &= \partial_\mu c^a + g f^{abc} A_\mu^b c^c & s c^a &= -\frac{1}{2} g f^{abc} c^b c^c, \\
s \psi_{\text{f}}^i &= i g c^a (t^a)_{ij} \psi_{\text{f}}^j & s \bar{c}^a &= B^a, \\
s \bar{\psi}_{\text{f}}^i &= -i g c^a \bar{\psi}_{\text{f}}^j (t^a)_{ji} & s B^a &= 0.
\end{aligned}
\tag{2.9}
$$

We thus see that the sum of the gauge fixing and Faddev-Popov terms can be written as a total BRST variation

$$
\mathcal{L}_{\text{GF}} + \mathcal{L}_{\text{FPG}} = s \left(\bar{c}^a \mathcal{F}^a - \frac{\xi}{2} \bar{c}^a B^a \right).
\tag{2.10}
$$

This is of course expected, since it is well known that total BRST variations cannot appear in the physical spectrum of the theory, implying, in turn, the gfp independence of the S-matrix elements and physical observables.

As far as the gauge fixing function is concerned, there are several possible choices. The usual linear R_ξ gauges, correspond to the covariant choice

$$
\mathcal{F}_{R_\xi}^a = \partial^\mu A_\mu^a.
\tag{2.11}
$$

In this case one has

$$
\begin{aligned}
\mathcal{L}_{\text{GF}} &= \frac{1}{2\xi}(\partial^\mu A_\mu^a)^2, \\
\mathcal{L}_{\text{FPG}} &= \partial^\mu \bar{c}^a \partial_\mu c^a + g f^{abc} (\partial^\mu \bar{c}^a) A_\mu^b c^c;
\end{aligned}
\tag{2.12}
$$

the Feynman rules corresponding to such gauge are reported in Appendix B. One can also consider non-covariant gauge fixing functions, such as [51–58]

$$
\mathcal{F}_\eta^a = \frac{\eta^\mu \eta^\nu}{\eta^2} \partial_\mu A_\nu^a,
\tag{2.13}
$$

where η^μ is an arbitrary but constant four-vector. In general, we can classify these gauges from the different value of η^2, i.e., $\eta^2 < 0$ (axial gauges), $\eta^2 = 0$ (light-cone gauge) and, finally, $\eta^2 > 0$ (Hamilton or time-like gauge). In this case

$$\mathcal{L}_{\mathrm{GF}} = \frac{1}{2\xi(\eta^2)^2}(\eta^\mu \eta^\nu \partial_\mu A_\nu^a)^2,$$

$$\mathcal{L}_{\mathrm{FPG}} = \frac{\eta^\mu \eta^\nu}{\eta^2}\left[\partial_\mu \bar{c}^a \partial_\nu c^a + gf^{abc}(\partial^\mu \bar{c}^a)A_\nu^b c^c\right]. \tag{2.14}$$

Notice that these non-covariant gauges are ghost-free, since it can be shown that, in dimensional regularization, the ghosts decouple completely from the S-matrix [57,58]. Another non-covariant gauge fixing function is the one determining the Coulomb gauge, which arises from choosing

$$\mathcal{F}^a = \left(g_{\mu\nu} - \frac{\eta^\mu \eta^\nu}{\eta^2}\right)\partial_\mu A_\nu^a. \tag{2.15}$$

Finally, due to their central importance for the PT, the particular class of gauges known as background field gauges [59,34] will be described in detail in Section 3.

Throughout this report we will use dimensional regularization to regulate loop integrals. We will employ the short-hand notation

$$\int_k \equiv \mu^{2\varepsilon}(2\pi)^{-d}\int d^d k, \tag{2.16}$$

where $d = 4 - \epsilon$ is the dimension of space-time and μ the 't Hooft mass-scale, introduced to guarantee that the coupling constant remains dimensionless in d dimensions. In addition, the standard result

$$\int_k \frac{1}{k^2} = 0, \tag{2.17}$$

will be often used to set to zero various terms appearing in the PT procedure.

2.2 Gauge cancellations in the S-matrix and the origin of the pinch technique

Consider the S-matrix element T for the elastic scattering of two fermions of masses m_1 and m_2. To any order in perturbation theory T is independent of the gfp ξ. On the other hand, the conventionally defined proper box, vertex, and self-energy, collectively depicted in Fig. 1 (a), (b), and (c), respectively, depend on *explicitly* on the gfp ξ already at one-loop level. Specifically, since $s + t + u = 2(m_1^2 + m_2^2)$, we have that

$$T(s, t, m_i) = T_1(t, \xi) + T_2(t, m_i, \xi) + T_3(t, s, m_i, \xi). \tag{2.18}$$

where the gfp-dependent subamplitudes T_1, T_2, and T_3 are composed of self-energy, vertex, and box diagrams, respectively; for example, $T_1(t, \xi)$ corresponds to the standard propagator, depending kinematically only on $t = (r_1 - r_2)^2 = (p_1 - p_2)^2$, but not on $s = (r_1 + p_1)^2 = (r_2 + p_2)^2$, nor on the external masses.

The central observation of the PT is that the ξ-dependence of the proper self-energy will cancel against contributions from the vertex- and box-graphs, which, at first glance, do not seem to contain propagator-like parts. In turn, this cancellation can be employed to define *gfp-independent* subamplitudes with distinct kinematic properties. Indeed, given that the total sum

16
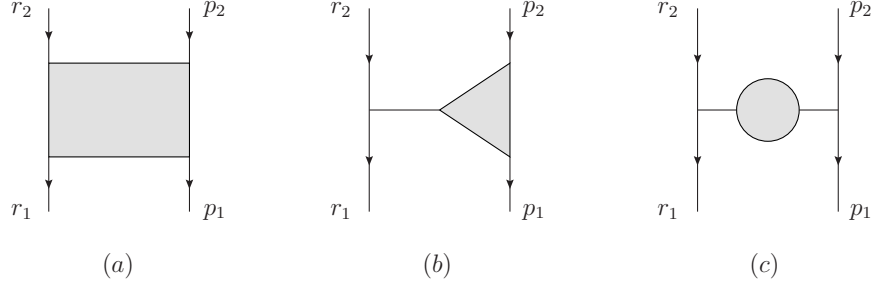
Fig. 1. The diagrams contributing to the S-matrix, grouped according to their topologies and their dependence on the Mandelstam variables s, t, and u, with $s = (r_1 + p_1)^2 = (r_2 + p_2)^2$, $t = (r_1 - r_2)^2 = (p_1 - p_2)^2$, and $u = (r_1 - p_2)^2 = (p_1 - r_2)^2$, with $s + t + u = \Sigma_i m_i^2$. Evidently, box-diagrams (a) depend on s, t, m_i^2, vertex-diagrams (b) depend on t, m_i^2, and self-energy diagrams (c) depend only on t.

$T(s, t, m_i)$ is gfp-independent, it is relatively easy to show that Eq. (2.18) can be recast in the form

$$T(s, t, m_i) = \widehat{T}_1(t) + \widehat{T}_2(t, m_i) + \widehat{T}_3(t, s, m_i), \tag{2.19}$$

where the $\widehat{T}_i$ ($i = 1, 2, 3$) are *individually* ξ-independent. An immediate way to see this is by differentiating both sides of (2.18) with respect to ξ and s; the rhs vanishes because $dT(s, t, m_i)/d\xi = 0$; on the lhs we have that $dT_1(t, \xi)/ds = dT_2(t, m_i, \xi)/ds = 0$. Thus,

$$\frac{d^2 T_3(t, s, m_i, \xi)}{ds\, d\xi} = 0, \tag{2.20}$$

from which it follows that T_3 can be written as a sum of two functions, one independent of ξ and one independent of s, *i.e.*,

$$T_3(t, s, m_i, \xi) = \widehat{T}_3(t, s, m_i) + h(t, m_i, \xi). \tag{2.21}$$

So, we have

$$T(s, t, m_i) = T_1(t, \xi) + \tilde{T}_2(t, m_i, \xi) + \widehat{T}_3(t, s, m_i), \tag{2.22}$$

where $\tilde{T}_2(t, m_i, \xi) \equiv T_2(t, m_i, \xi) + h(t, m_i, \xi)$. The argument may be continued by differentiating both sides of Eq. (2.22) with respect to ξ and m_i, now obtaining

$$\frac{d^2 \tilde{T}_2(t, m_i, \xi)}{dm_i\, d\xi} = 0, \tag{2.23}$$

and thus

$$\tilde{T}_2(t, m_i, \xi) = \widehat{T}_2(t, m_i) + f(t, \xi). \tag{2.24}$$

The last step is to write $\widehat{T}_1(t, \xi) \equiv T_1(t, \xi) + f(t, \xi)$; clearly, since $dT(s, t, m_i)/d\xi = 0$, we must have that $d\widehat{T}_1(t, \xi)/d\xi = 0$, and therefore $\widehat{T}_1(t, \xi) = \widehat{T}_1(t)$, thus arriving at Eq. (2.19).

The above proof is meant to demonstrate the possibility of decomposing $T(s, t, m_i)$ in terms of individually gfp-independent subamplitudes, as in (2.19), but does not specify how this decomposition is realized operationally, nor whether it is physically unique. To be sure, at the level presented above, the decomposition is not mathematically unique, since one can always add an arbitrary function $g(t)$ to $\widehat{T}_1(t)$ and subtract it from $\widehat{T}_2(t, m_i)$; this changes the definition

of what the individual subamplitudes are, without changing the value of the full $T(s, t, m_i)$. However, when the $\widehat{T}_i$ are endowed with physical properties, such as unitarity and analyticity, Dyson resummability, and invariance under the renormalization group (RG), to name a few, the above arbitrariness disappears. As we will see in the rest of this review, the PT Green's functions, which, by construction, have all the aforementioned physical properties built in, provide the field-theoretically and physically unique way of realizing the decomposition of Eq. (2.19).

2.3 The pinch technique mechanism of gauge fixing parameter cancellations at one loop

Let us start by considering the S-matrix element for the quark-quark elastic scattering process $q(p_1)q(r_1) \to q(p_2)q(r_2)$ in QCD. We have that $p_1 + r_1 = p_2 + r_2$, and set $q = r_2 - r_1 = p_1 - p_2$, with $t = q^2$ the square of the momentum transfer. The longitudinal momenta responsible for triggering the kinematical rearrangements characteristic of the PT stem either from the bare gluon propagator, $\Delta_{\alpha\beta}^{(0)}(k)$, or from the *external* bare (tree-level) three-gluon vertices, *i.e.*, the vertices where the physical momentum transfer q is entering.

To study the origin of the longitudinal momenta in detail, consider first the gluon propagator $\Delta_{\alpha\beta}(k)$; after factoring out the trivial color factor δ^{ab}, in the R_ξ gauges it has the form [1]

$$i\Delta_{\alpha\beta}(q, \xi) = -i\left[P_{\alpha\beta}(q)\Delta(q^2, \xi) + \xi\frac{q_\alpha q_\beta}{q^4}\right], \tag{2.25}$$

with $P_{\alpha\beta}(q)$ the dimensionless transverse projector defined as

$$P_{\alpha\beta}(q) = g_{\alpha\beta} - \frac{q_\alpha q_\beta}{q^2}. \tag{2.26}$$

The scalar function $\Delta(q^2, \xi)$ is related to the all-order gluon self-energy

$$\Pi_{\alpha\beta}(q, \xi) = P_{\alpha\beta}(q)\Pi(q^2, \xi), \tag{2.27}$$

through

$$\Delta(q^2, \xi) = \frac{1}{q^2 + i\Pi(q^2, \xi)}. \tag{2.28}$$

Since $\Pi_{\alpha\beta}$ has been defined in (2.28) with the imaginary factor i factored out in front, it is simply given by the corresponding Feynman diagrams in Minkowski space. The inverse of $\Delta_{\alpha\beta}$ can be found by requiring that

$$i\Delta_{\alpha\mu}^{am}(q, \xi)(\Delta^{-1})_{mb}^{\mu\beta}(q, \xi) = \delta^{ab}g_\alpha^\beta, \tag{2.29}$$

---

[1] In the definition of the gluon propagator $\Delta_{\alpha\beta}$ we explicitly pull out an i factor on the lhs, which accounts for the slightly unusual (but totally equivalent) form of writing Eq. (2.29). This is done in order to be consistent with the definition of the Green's functions in terms of functional differentiation of the generating functional introduced later on (Section 7).

and it is given by

$$\Delta_{\alpha\beta}^{-1}(q,\xi) = iP_{\alpha\beta}(q)\Delta^{-1}(q^2,\xi) + \frac{i}{\xi}q_\alpha q_\beta. \tag{2.30}$$

At tree-level we have that

$$i\Delta_{\alpha\beta}^{(0)}(q,\xi) = -id(q^2)\left[g_{\alpha\beta} - (1-\xi)\frac{q_\alpha q_\beta}{q^2} \right],$$

$$d(q^2) = \frac{1}{q^2}. \tag{2.31}$$

Evidently, the longitudinal (pinching) momenta are proportional to $(1-\xi)$, and vanish for the particular choice $\xi = 1$, to be referred to as the "Feynman gauge"; in that gauge the propagator is simply proportional to $g_{\alpha\beta}d(q^2)$. The case $\xi = 0$, known as the "Landau gauge", gives rise to a transverse $\Delta_{\alpha\beta}^{(0)}(k)$, but does not eliminate the pinching momenta.

In order to gradually build up the concepts, and at the same time introduce some useful notation, let us see what happens to the pinching momenta at tree-level. Defining

$$\mathcal{V}^{a\alpha}(p_1,p_2) = \bar{u}(p_1)gt^a\gamma^\alpha u(p_2), \tag{2.32}$$

the tree-level amplitude reads

$$\mathcal{T}^{(0)} = i\mathcal{V}^{a\alpha}(r_1,r_2)i\Delta_{\alpha\beta}^{(0)}(q)i\mathcal{V}^{a\beta}(p_1,p_2). \tag{2.33}$$

Then, since the on-shell spinors satisfy the equations of motion

$$\bar{u}(p)(\not{p} - m) = 0 = (\not{p} - m)u(p), \tag{2.34}$$

the longitudinal part coming from $\Delta_{\alpha\beta}^{(0)}$ vanishes, and we obtain

$$\mathcal{T}^{(0)} = i\mathcal{V}^{a\alpha}(r_1,r_2)d(q^2)\mathcal{V}_\alpha^a(p_1,p_2). \tag{2.35}$$

Let us next consider the conventional three-gluon vertex, to be denoted by $\Gamma_{\alpha\mu\nu}^{amn}(q,k_1,k_2)$; of course, in the case of the specific process we consider this vertex appears for the first time at one loop. It is given by the following manifestly Bose-symmetric expression (all momenta are incoming, *i.e.*, $q + k_1 + k_2 = 0$)

$$i\Gamma_{\alpha\mu\nu}^{amn}(q,k_1,k_2) = gf^{amn}\Gamma_{\alpha\mu\nu}(q,k_1,k_2),$$

$$\Gamma_{\alpha\mu\nu}(q,k_1,k_2) = g_{\mu\nu}(k_1 - k_2)_\alpha + g_{\alpha\nu}(k_2 - q)_\mu + g_{\alpha\mu}(q - k_1)_\nu. \tag{2.36}$$

It is elementary to verify that the vertex satisfies the following WIs:

$$q^\alpha\Gamma_{\alpha\mu\nu}(q,k_1,k_2) = k_2^2 P_{\mu\nu}(k_2) - k_1^2 P_{\mu\nu}(k_1),$$

$$k_1^\mu\Gamma_{\alpha\mu\nu}(q,k_1,k_2) = q^2 P_{\alpha\nu}(q) - k_2^2 P_{\alpha\nu}(k_2),$$

$$k_2^\nu\Gamma_{\alpha\mu\nu}(q,k_1,k_2) = k_1^2 P_{\alpha\mu}(k_1) - q^2 P_{\alpha\mu}(q). \tag{2.37}$$

19

To show how the relevant pinching momenta are identified in the conventional three-gluon vertex, we split $\Gamma_{\alpha\mu\nu}(q, k_1, k_2)$ into two parts,

$$\Gamma_{\alpha\mu\nu}(q, k_1, k_2) = \Gamma^{\mathrm{F}}_{\alpha\mu\nu}(q, k_1, k_2) + \Gamma^{\mathrm{P}}_{\alpha\mu\nu}(q, k_1, k_2), \tag{2.38}$$

with

$$\Gamma^{\mathrm{F}}_{\alpha\mu\nu}(q, k_1, k_2) = (k_1 - k_2)_\alpha g_{\mu\nu} + 2q_\nu g_{\alpha\mu} - 2q_\mu g_{\alpha\nu},$$
$$\Gamma^{\mathrm{P}}_{\alpha\mu\nu}(q, k_1, k_2) = k_{2\nu} g_{\alpha\mu} - k_{1\mu} g_{\alpha\nu}. \tag{2.39}$$

The vertex $\Gamma^{\mathrm{F}}_{\alpha\mu\nu}(q, k_1, k_2)$ is Bose-symmetric only with respect to the μ and ν legs. Evidently the above decomposition assigns a special role to the q-leg, and allows $\Gamma^{\mathrm{F}}_{\alpha\mu\nu}(q, k_1, k_2)$ to satisfy the WI

$$q^\alpha \Gamma^{\mathrm{F}}_{\alpha\mu\nu}(q, k_1, k_2) = (k_2^2 - k_1^2)g_{\mu\nu}. \tag{2.40}$$

where the rhs is the difference of two inverse tree-level propagators in the Feynman gauge. The term $\Gamma^{\mathrm{P}}_{\alpha\mu\nu}(q, k_1, k_2)$, which in configuration space corresponds to a pure divergence, contains the longitudinal momenta that will pinch.

When considering a vertex or a box diagram, the effect of the pinching momenta, regardless of their origin (gluon propagator or three-gluon vertex), is to trigger the elementary WI

$$k_\nu \gamma^\nu = (\not{k} + \not{p} - m) - (\not{p} - m)$$
$$= -i[S^{-1}_{(0)}(k + p) - S^{-1}_{(0)}(p)], \tag{2.41}$$

where the rhs is the difference of two inverse tree-level quark propagators. The first of these terms removes (pinches out) the internal tree-level fermion propagator $S^{(0)}(k + p)$, whereas the second term on the rhs vanishes when hitting the on-shell external leg, i.e. using the appropriate Dirac equation of 2.34. Diagrammatically, what appears in the place where the $S^{(0)}(k + p)$ was is an unphysical effective vertex, *i.e.*, a vertex that does not appear in the original Lagrangian; as we will see, all such vertices cancel in the full, gauge-invariant amplitude.

We next consider all one-loop graphs contributing to the S-matrix element shown in Fig. 2, and isolate their gfp-dependent parts using the PT procedure; what we will find is that all gfp-dependent parts, irrespective of whether they come from box- or vertex-diagrams, are effectively propagator-like (we emphasize that no integration over virtual momenta is necessary for carrying out the pinching procedure).

2.3.1   The box

We start our one-loop analysis from the two box diagrams, direct and crossed, shown in graphs (a) of Fig. 2 (for the kinematics used see Fig. 3). For the sum of the two graphs we have
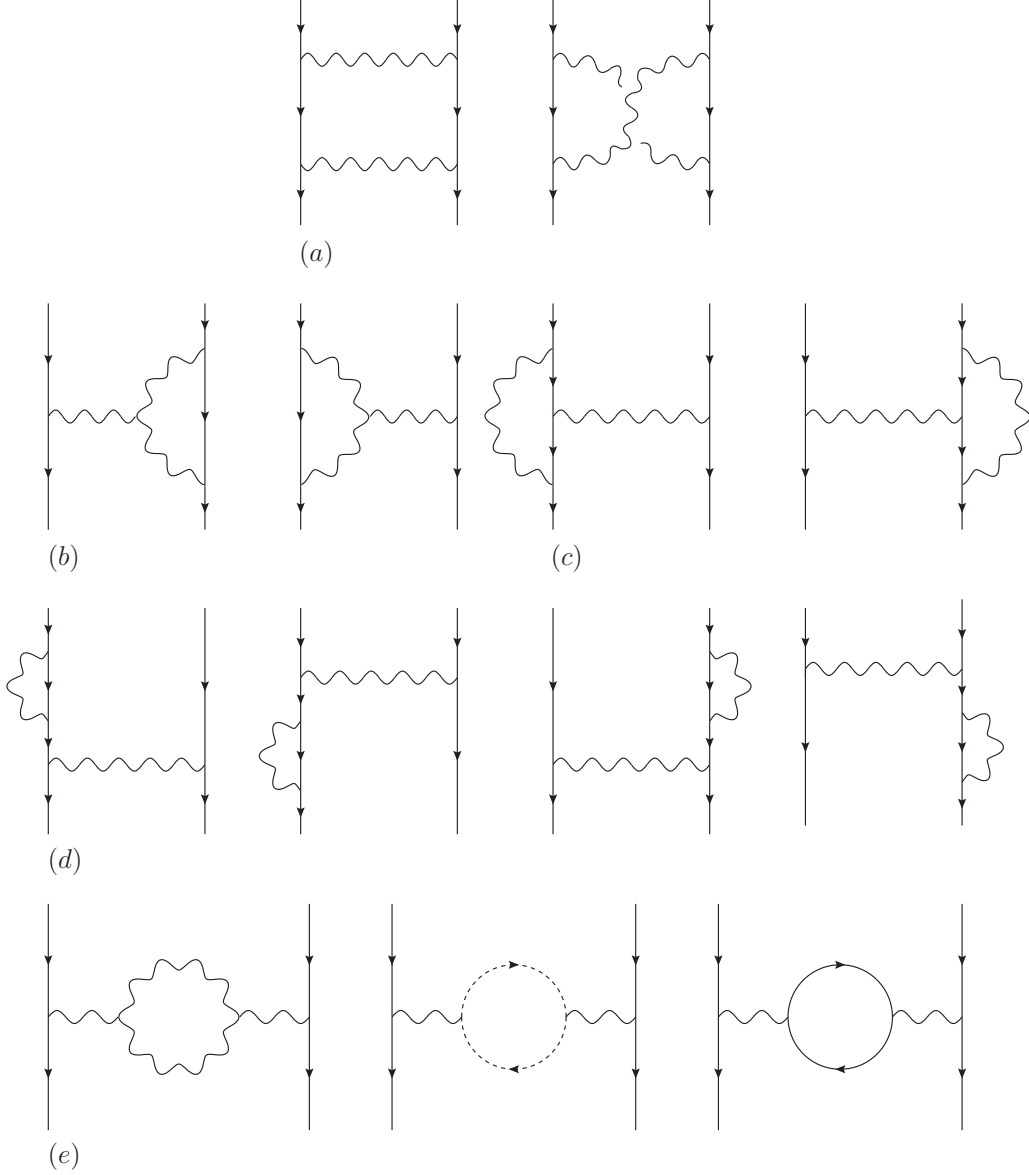
Fig. 2. The diagrams contributing to the one-loop quark elastic scattering S-matrix element. (a) box contributions, (b) non-Abelian and (c) Abelian vertex contributions, (d) quark self-energy corrections, and (e) gluon self-energy contributions.

$$(a) = g^2 \int_k \bar{u}(r_1)\gamma^\alpha t^a S^{(0)}(r_2 - k)\gamma^\rho t^r u(r_2)\Delta^{(0)}_{\alpha\beta}(k - q)\Delta^{(0)}_{\rho\sigma}(k) \times$$

$$\times g^2\bar{u}(p_1)\left\{\gamma^\beta t^a S^{(0)}(p_2 + k)\gamma^\sigma t^r + \gamma^\sigma t^r S^{(0)}(p_1 - k)\gamma^\beta t^a\right\} u(p_2). \tag{2.42}$$

To see how the PT works, we must now study the action of the longitudinal momenta appearing in the product $\Delta^{(0)}_{\alpha\beta}(k - q)\Delta^{(0)}_{\rho\sigma}(k)$. Therefore, let us, for concreteness, see what happens to the term $k_\rho k_\sigma$ coming from $\Delta^{(0)}_{\rho\sigma}(k)$. Using Eqs (2.41) and (2.34), we find that the contraction of k_σ with the term contained in the brackets in the second line on the rhs of Eq. (2.42) gives rise to the expression
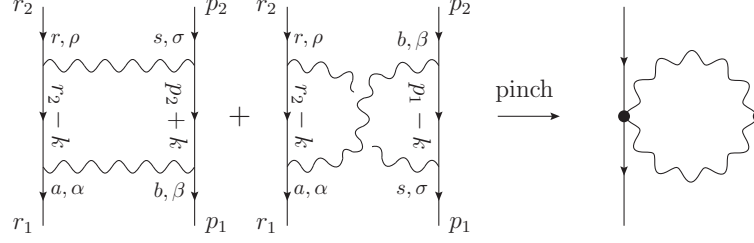
Fig. 3. Schematic representation of the propagator-like parts extracted from the boxes for a general ξ. Black dots indicate effective vertices that do not exist in the original theory.

$$
\begin{aligned}
g^2 \bar{u}(p_1) k_\sigma \{\cdots\}^{\beta\sigma} u(p_2) &= g^2 \bar{u}(p_1) \gamma^\beta \{t^a t^r - t^r t^a\} u(p_2) \\
&= i g^2 f^{arn} \bar{u}(p_1) \gamma^\beta t^n u(p_2) \\
&= g f^{arn} P_\nu^\beta(q) \bar{u}(p_1) i g \gamma^\nu t^n u(p_2) \\
&= \left[g f^{arn} P_\nu^\beta(q) \right] i \mathcal{V}^{n\nu}(p_1, p_2).
\end{aligned}
\tag{2.43}
$$

Notice that in the second step we have used the commutation relation of Eq. (2.5), while in the third step we have used the fact that, for the on-shell process we consider, longitudinal pieces proportional to $q_\beta q_\nu$ may be added for free (since they vanish anyway due to current conservation), thus converting g_ν^β to $P_\nu^\beta(q)$. The term in the last line of Eq. (2.43) couples to the external on-shell quarks as a propagator; evidently all reference to the internal (off-shell) quarks inside the brackets has disappeared. To continue the calculation, (*i*) multiply the result by k_ρ, (*ii*) let k_ρ get contracted with the γ^ρ in the first line of Eq. (2.42), (*iii*) employ again the WI of Eq. (2.41), and (*iv*) use that $i f^{abc} t^a t^b = -\frac{1}{2} C_A t^c$, where C_A is the Casimir eigenvalues of the adjoint representation, defined in Appendix A. The final result is a purely propagator-like term, *i.e.*, a term that only depends on q (even though it originates from a box diagram), and couples to the external on-shell quarks as a propagator (see Fig. 3). Armed with these observations, it is relatively easy to track down the action of all terms proportional to $(1-\xi)$; setting $\lambda \equiv (1-\xi)$, we can write the two boxes as follows,

$$
(a) = (a)_{\xi=1} + \mathcal{V}_\alpha^a(r_1, r_2) d(q^2) \Pi_{\text{box}}^{\alpha\beta}(q, \lambda) d(q^2) \mathcal{V}_\beta^a(p_1, p_2),
\tag{2.44}
$$

where the gfp-dependent propagator-like term $\Pi_{\text{box}}^{\alpha\beta}$ is given by

$$
\Pi_{\text{box}}^{\alpha\beta}(q, \lambda) = \lambda g^2 C_A q^4 \left[\frac{\lambda}{2} P^{\alpha\mu}(q) P^{\beta\nu}(q) \int_k \frac{k_\mu k_\nu}{k^4 (k+q)^4} - P^{\alpha\beta}(q) \int_k \frac{1}{k^4 (k+q)^2} \right].
\tag{2.45}
$$

2.3.2 *The quark-gluon vertex*

We next turn to the two vertex graphs, the non-Abelian graphs (b) and the Abelian graphs (c), shown in Fig. 2. We will analyze only one graph per subgroup, since the mirror graphs are to be treated in exactly the same way. As in the case of the boxes, we want to isolate the gfp-dependent pieces coming from the internal gluon propagators. The action of the corresponding longitudinal momenta is determined following the PT procedure; again, they give rise to effectively propagator-like terms, as shown schematically in Fig. 4, where the kinematics

22
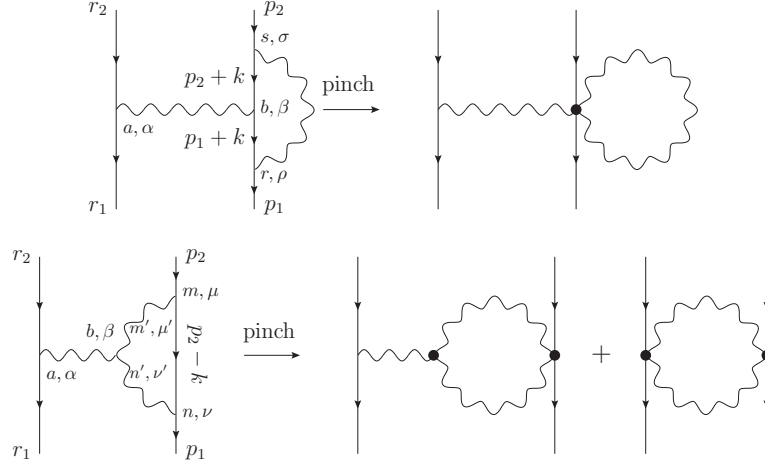
Fig. 4. Schematic representation of the propagator-like parts extracted from the one-loop vertex graphs for general ξ.

used are explicitly shown. Note that we do *not* yet split the three gluon vertex as described in Eq. (2.38); for the moment we simply collect the terms proportional to different powers of λ. After a straightforward calculation, we find for the corresponding results

$$
\begin{aligned}
(b) &= (b)_{\xi=1} + \mathcal{V}_\alpha^a(r_1, r_2) d(q^2) \Pi_{\text{nav}}^{\alpha\beta}(q, \lambda) d(q^2) \mathcal{V}_\beta^a(p_1, p_2), \\
(c) &= (c)_{\xi=1} + \mathcal{V}_\alpha^a(r_1, r_2) d(q^2) \Pi_{\text{av}}^{\alpha\beta}(q, \lambda) d(q^2) \mathcal{V}_\beta^a(p_1, p_2),
\end{aligned}
\tag{2.46}
$$

with the propagator-like pieces given by

$$
\begin{aligned}
\Pi_{\text{nav}}^{\alpha\beta}(q, \lambda) &= -\frac{\lambda^2}{2} g^2 C_A q^4 P^{\alpha\mu}(q) P^{\beta\nu}(q) \int_k \frac{k_\mu k_\nu}{k^4 (k+q)^4} \\
&\quad + \lambda g^2 C_A q^2 \left[q^2 P^{\alpha\beta}(q) \int_k \frac{1}{k^2 (k+q)^4} + P^{\beta\mu}(q) \int_k \frac{k^\alpha k_\mu}{k^4 (k+q)^2} - P^{\alpha\beta}(q) \int_k \frac{1}{k^4} \right], \\
\Pi_{\text{av}}^{\alpha\beta}(q, \lambda) &= \lambda g^2 \left(\frac{C_A}{2} - C_f \right) q^2 P^{\alpha\beta}(q) \int_k \frac{1}{k^4},
\end{aligned}
\tag{2.47}
$$

where C_f is the Casimir eigenvalues in the fundamental representation, see again Appendix A.

2.3.3 The quark self-energy

Let us now turn to the one-loop corrections to the self-energy of the on-shell test quarks shown in the group (d) of Fig. 2; notice that these four graphs are multiplied by a factor of $\frac{1}{2}$. Let us then concentrate on one of these graphs, shown in Fig. 5. It reads

$$
(d) = \frac{1}{2} \mathcal{V}^{a\alpha}(r_1, r_2) \Delta_{\alpha\beta}^{(0)}(q) \bar{u}(p_1) g \gamma^\beta t^a S^{(0)}(p_2) \Sigma_\xi(p_2) u(p_2),
\tag{2.48}
$$

23
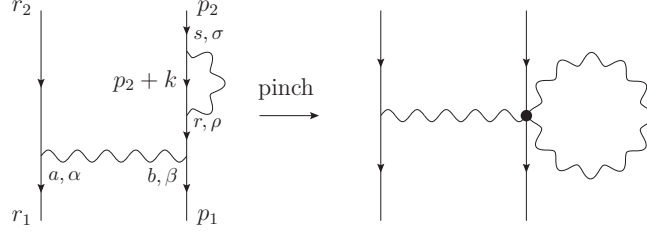
Fig. 5. Schematic representation of the propagator-like parts extracted from (one of) the quark self-energy corrections graphs for general ξ.

where

$$\Sigma_\xi(p_2) = g^2 C_f \int_k \gamma^\rho \Delta_{\rho\sigma}^{(0)}(k) S^{(0)}(p_2 + k) \gamma^\sigma. \tag{2.49}$$

Using the same methodology employed so far, it is easy to show that

$$
\begin{aligned}
\Sigma_\xi(p_2) &= \Sigma_{\xi=1}(p_2) - \lambda g^2 C_f (\not{p}_2 - m) \int_k \frac{1}{k^4} S^{(0)}(p_2 + k) \not{k} \\
&= \Sigma_{\xi=1}(p_2) - \lambda g^2 C_f \left\{ (\not{p}_2 - m) \int_k \frac{1}{k^4} - (\not{p}_2 - m) \int_k \frac{1}{k^4} S^{(0)}(p_2 + k)(\not{p}_2 - m) \right\}.
\end{aligned}
\tag{2.50}
$$

We next insert the rhs of (2.50) back into Eq. (2.48). Clearly, the second term in the brackets vanish on-shell as the second fermion inverse propagator will trigger the Dirac equation; also the term $\Sigma_{\xi=1}(p_2)$ gives simply $(d)_{\xi=1}$. Thus the only term furnishing a propagator part will be the first one in the brackets and we will have

$$(d) = (d)_{\xi=1} + \mathcal{V}_\alpha^a(r_1, r_2) d(q^2) \Pi_{\mathrm{qse}}^{\alpha\beta}(q, \lambda) d(q^2) \mathcal{V}_\beta^a(p_1, p_2), \tag{2.51}$$

where

$$\Pi_{\mathrm{qse}}^{\alpha\beta}(q, \lambda) = \frac{1}{2} \lambda g^2 C_f q^2 P^{\alpha\beta}(q) \int_k \frac{1}{k^4}. \tag{2.52}$$

Notice that $\Pi_{\mathrm{qse}}^{\alpha\beta}$ is proportional to C_f instead of C_A, and is in that sense of Abelian nature. Indeed, after multiplying it by a factor of 2 (accounting for both quark fields), Π_{qse} cancels exactly against the part of Π_{av} proportional to C_f in Eq. (2.47). For $C_f = 1$ this is simply the standard QED gfp-cancellation between the elector-photon vertex and the electron wave-function.

Note that in obtaining the rhs of (2.50) we have not assumed that $\Sigma(p_2)$ is actually sandwiched between on-shell spinors, as indicated in Eq. (2.48). Thus, the gfp-independent quark self-energy should be identified with the first term on the rhs of (2.50), *i.e.*,

$$\widehat{\Sigma}(p) = \Sigma_{\xi=1}(p). \tag{2.53}$$

A more thorough analysis [60,61], where an off-shell $\Sigma(p)$ is embedded into a quark-gluon scattering process $[g(k_1)q(k_2) \rightarrow g(k_3)q(k_4)$, with $p = k_1 + k_2 = k_3 + k_4]$ and the pinching procedure is repeated, shows that Eq. (2.53) is absolutely general: the gfp-independent off-shell quark self-energy *coincides* with the conventional quark self-energy calculated in the Feynman gauge.

24
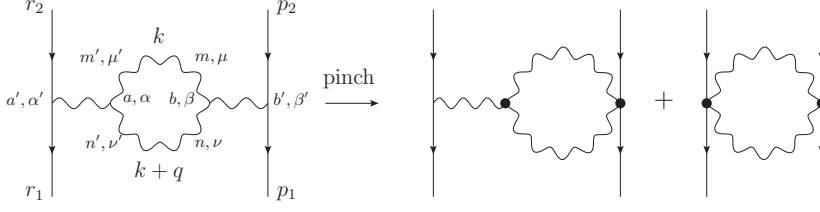
Fig. 6. Schematic representation of the propagator-like parts extracted from the gluon self-energy corrections graph for general ξ.

2.3.4 Final cancellation of all gauge fixing parameter dependence

We will now show that the propagator-like parts extracted from all the previous diagrams cancel exactly against analogous terms contained in the conventional self-energy graphs (e) of Fig. 2. Of course this cancellation is guaranteed to take place, regardless of how one may choose to organize the calculation, given that it amounts to the gfp-independence of the one-loop amplitude. It is conceptually important, however, to establish a systematic way for extracting the relevant terms from the conventional one-loop self-energy using nothing but tree-level WIs.

To that end, we concentrate only on the graph containing the three-gluon vertices (see Fig. 6); the ghost and fermion graphs have no pinching momenta and thus will be inert. We have

$$(e) = \mathcal{V}_\alpha^a(r_1, r_2) d(q^2) \Pi^{\alpha\beta}(q, \lambda) d(q^2) \mathcal{V}_\beta^a(p_1, p_2). \tag{2.54}$$

Then, we let the longitudinal momenta coming from the tree-level propagators act on the two bare three-gluon vertices, triggering the two WIs of Eqs (2.37). It turns out that only the terms proportional to the transverse projector $P_{\alpha\beta}(q)$ survive, furnishing

$$\Pi^{\alpha\beta}(q, \lambda) = \Pi_{\xi=1}^{\alpha\beta}(q) + \Pi_{\text{gse}}^{\alpha\beta}(q, \lambda), \tag{2.55}$$

with

$$\Pi_{\text{gse}}^{\alpha\beta}(q, \lambda) = \frac{\lambda^2}{2} g^2 C_A q^4 P^{\alpha\mu}(q) P^{\beta\nu}(q) \int_k \frac{k_\mu k_\nu}{k^4 (k+q)^4}$$
$$- \lambda g^2 C_A q^2 \left[q^2 P^{\alpha\beta}(q) \int_k \frac{1}{k^2 (k+q)^4} + 2 P^{\beta\mu}(q) \int_k \frac{k^\alpha k_\mu}{k^4 (k+q)^2} - P^{\alpha\beta}(q) \int_k \frac{1}{k^4} \right]. \tag{2.56}$$

We are now in the position of showing the cancellation of the gfp-dependent pieces; in fact, adding all the terms we have been isolating, we find

$$\Pi_{\text{gse}}^{\alpha\beta}(q, \lambda) + \Pi_{\text{box}}^{\alpha\beta}(q, \lambda) + 2 \left[\Pi_{\text{av}}^{\alpha\beta}(q, \lambda) + \Pi_{\text{nav}}^{\alpha\beta}(q, \lambda) \right] + 4 \Pi_{\text{qse}}^{\alpha\beta}(q, \lambda) = 0. \tag{2.57}$$

In the above formula the multiplicative factor of 2 comes from the mirror vertex graphs and the 4 from the four external quarks. The contributions of each term to the different gfp-dependent structures appearing in the PT process is shown in Table 1.

	$\lambda^2 \int_k \frac{k_\mu k_\nu}{k^4(k+q)^4}$	$\lambda \int_k \frac{k_\mu k_\nu}{k^4(k+q)^2}$	$\lambda \int_k \frac{1}{k^2(k+q)^4}$	$\lambda \int_k \frac{1}{k^4}$
Π_{box}	$\frac{1}{2}C_A$	0	$-C_A$	0
$2\Pi_{\text{av}}$	0	0	0	$C_A - 2C_f$
$2\Pi_{\text{nav}}$	$-C_A$	$2C_A$	$2C_A$	$-2C_A$
$4\Pi_{\text{qse}}$	0	0	0	$2C_f$
Π_{gse}	$\frac{1}{2}C_A$	$-2C_A$	$-C_A$	C_A
Total	0	0	0	0

Table 1

Contributions of the box, vertex and self-energy diagrams to the different ξ-dependent structures appearing in the PT process. The sum of each column is zero, showing the well-known property of the gfp-independence of the S-matrix elements.

In summary, all gfp-dependent terms have been eliminated in a very particular way. Specifically, due to the PT procedure employed, all gfp-dependent pieces turned out to be propagator-like. As a result, all gfp-dependence has canceled giving rise to subamplitudes that maintain their original kinematic identity (boxes, vertices, and self-energies), and are, in addition, individually gfp-independent. It is important to appreciate the fact that the explicit cancellation carried out amounts effectively to choosing the Feynman gauge, $\xi = 1$, from the beginning. Of course, there is no doubt that this can be done for the entire physical amplitude considered; the point is that, thanks to the PT, one may move from general ξ to the specific $\xi = 1$ without compromising the notion of individual topologies. Such a notion would have been lost if, for instance, the demonstration of the gfp-independence involved the integration over virtual momenta; had one opted for this latter approach, one would have eventually succeeded to demonstrate the ξ-independence of the entire S-matrix element, but would have missed out on the ability to identify gfp-independent subamplitudes, as we did. In addition, this result indicates that there is no loss of generality in choosing $\xi = 1$ from the beginning, thus eliminating a major source of longitudinal pieces, that are bound to cancel anyway, through the special pinching procedure outlined above.

It would be tempting at this point to identify the gfp-independent subamplitudes obtained here with the $\widehat{T}_i$ $(i = 1, 2, 3)$ introduced in Eq. (2.19). While this identification would be justified, as far as the gfp-independence is concerned, it will be postponed until the end of the next two subsections, in order to endow the $\widehat{T}_i$ with one additional powerful ingredient: QED-like WIs.

2.4 The one-loop pinch technique Green's functions

2.4.1 The one-loop pinch technique quark-gluon vertex and its Ward identity

Let us now turn to the longitudinal terms contained in the pinching part $\Gamma^{\text{P}}_{\alpha\mu\nu}$ of the three-gluon vertex [see Eq. (2.39)] appearing in the non-Abelian vertex graph (b) (first line of Fig. 4), and the two such vertices inside the gluon self-energy graph (Fig. 6). One may ask at this point

$$iH^a(p,q) = -gt^a \quad + \quad$$

Fig. 7. The auxiliary function H appearing in the quark-gluon vertex STI. The gray blob represents the (connected) ghost-fermion kernel appearing in the usual QCD skeleton expansion.

what is the purpose of carrying the PT decomposition of the vertex given that one has already achieved ξ-independent structures. The answer is that the effect of the pinching momenta of $\Gamma^{\mathrm{P}}_{\alpha\mu\nu}$ is to make the effective ξ-independent Green's functions satisfy, in addition, QED-like WIs instead of the usual STIs.

This is best seen in the case of one-loop quark-gluon vertex $\Gamma^a_\alpha(p_1, p_2)$, composed by graphs (b) and (c) of Fig. 2 now written (after the ξ-cancellations described above) in the Feynman gauge. It is well known that the QED counterpart of $\Gamma^a_\alpha(p_1, p_2)$, namely the photon-electron vertex $\Gamma_\alpha(p_1, p_2)$, satisfies to all orders (and for every gfp) the WI

$$q^\alpha \Gamma_\alpha(p_1, p_2) = ie \left\{ S_e^{-1}(p_1) - S_e^{-1}(p_2) \right\}, \tag{2.58}$$

where S_e is the (all-order) electron propagator; Eq. (2.58) is the naive, all-order generalization of the tree-level WI of (2.41).

The quark-gluon vertex $\Gamma^a_\alpha(p_1, p_2)$ also obeys the WI of (2.41) at tree-level (multiplied by t^a):

$$q^\alpha \Gamma^a_\alpha(p_1, p_2) = igt^a \left\{ S_e^{-1}(p_1) - S_e^{-1}(p_2) \right\}. \tag{2.59}$$

However, at higher orders it obeys an STI that is not the naive generalization of this tree-level WI. Instead, $\Gamma^\alpha_a(p_1, p_2)$ satisfies the STI [62]

$$q^\alpha \Gamma^a_\alpha(p_1, p_2) = \left[q^2 D^{aa'}(q) \right] \left\{ S^{-1}(p_2) H^{a'}(q, p_1) + \bar{H}^{a'}(p_1, q) S^{-1}(p_2) \right\}, \tag{2.60}$$

where $D^{aa'}(q)$ and $S(p)$ represents the full ghost and quark propagator respectively, and H^a is a composite operator defined as (see also Fig. 7)

$$iS(p) iD^{aa'}(q) iH^a(p,q) = -gt^d \int d^4x \int d^4y \; \mathrm{e}^{ip\cdot x} \; \mathrm{e}^{iq\cdot y} \left\langle 0 \left| T \left\{ \bar{q}(x)\bar{c}^{a'}(y) \left[c^d(0)q(0) \right] \right\} \right| 0 \right\rangle, \tag{2.61}$$

where T denotes the time-ordered product of fields, and $\bar{H}$ is the hermitian conjugate of H. At tree-level, H^a_{ij} reduces to $H^{(0)a}_{ij} = t^a_{ij}$.

After these general considerations, let us carry out the decomposition of Eq. (2.38) to the non-Abelian vertex of graph (b) in Fig. 2. Then, let us write, suppressing again the color indices,

$$(b)_{\xi=1} = i\mathcal{V}^\alpha_a id(q^2)\bar{u}(p_1) i\widetilde{\Gamma}^a_\alpha(p_1, p_2) u(p_2), \tag{2.62}$$

and concentrate on the (one-loop) non-Abelian contribution to the quark-gluon vertex $\widetilde{\Gamma}^a_\alpha$. We have
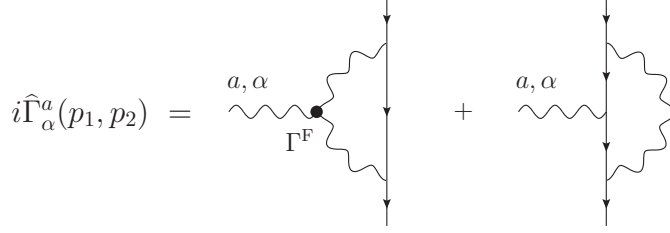
Fig. 8. Diagrammatic representation of the PT quark-gluon vertex at one-loop.

$$i\widetilde{\Gamma}_\alpha^a(p_1, p_2) = \frac{1}{2}g^3 C_A t^a \int_k \frac{\Gamma_{\alpha\mu\nu}\gamma^\nu S^{(0)}(p_2 - k)\gamma^\mu}{k^2(k+q)^2}$$
$$= \frac{1}{2}g^3 C_A t^a \left\{ \int_k \frac{\Gamma_{\alpha\mu\nu}^{\mathrm{F}}\gamma^\nu S^{(0)}(p_2 - k)\gamma^\mu}{k^2(k+q)^2} + \int_k \frac{\Gamma_{\alpha\mu\nu}^{\mathrm{P}}\gamma^\nu S^{(0)}(p_2 - k)\gamma^\mu}{k^2(k+q)^2} \right\}, \quad (2.63)$$

where in this case

$$\Gamma_{\alpha\mu\nu}^{\mathrm{F}} = g_{\mu\nu}(2k + q)_\alpha + 2q_\nu g_{\alpha\mu} - 2q_\mu g_{\alpha\nu},$$
$$\Gamma_{\alpha\mu\nu}^{\mathrm{P}} = -(k + q)_\nu g_{\alpha\mu} - k_\mu g_{\alpha\nu}. \tag{2.64}$$

Despite appearances, if we use that $\bar{u}(p_2)(\not{p}_2 - m) = 0$ and $(\not{p}_1 - m)u(p_1) = 0$, the part of the vertex graph containing Γ^{P} is in fact purely propagator-like:

$$\int_k \frac{\Gamma_{\alpha\mu\nu}^{\mathrm{P}}\gamma^\nu S^{(0)}(p_2 - k)\gamma^\mu}{k^2(k+q)^2} \xrightarrow{\overset{\mathrm{PT}}{\mathrm{Dirac\,Eq.}}} 2\gamma_\alpha \int_k \frac{1}{k^2(k+q)^2}. \tag{2.65}$$

Thus, using the by now familiar methodology employed before, one obtains from the one-loop quark-gluon vertex a propagator-like contribution, to be denoted by $\Pi_{\mu\nu}^{\mathrm{P}}(q)$, given by

$$\Pi_{\mu\nu}^{\mathrm{P}}(q) = g^2 C_A q^2 P_{\mu\nu}(q) \int_k \frac{1}{k^2(k+q)^2}. \tag{2.66}$$

This term, together with an identical one coming from the mirror vertex, will be reassigned to the PT self-energy, soon to be constructed; for the moment let us concentrate on the remaining terms in the vertex. In fact, the part of the vertex graph containing Γ^{F} remains unchanged, since it has no longitudinal momenta. Adding it to the usual Abelian-like graph, we obtain the one-loop PT quark-gluon vertex, to be denoted by $\widehat{\Gamma}_\alpha^a$, given by (see Fig. 8)

$$i\widehat{\Gamma}_\alpha^a(p_1, p_2) = g^3 t^a \left\{ \frac{1}{2}C_A \int_k \frac{\Gamma_{\alpha\mu\nu}^{\mathrm{F}}\gamma^\nu S^{(0)}(p_2 - k)\gamma^\mu}{k^2(k+q)^2} \right.$$
$$\left. + \left(C_f - \frac{C_A}{2} \right) \int_k \frac{\gamma^\mu S^{(0)}(p_1 + k)\gamma_\alpha S^{(0)}(p_2 + k)\gamma_\mu}{k^2} \right\}. \tag{2.67}$$

Now it is easy to derive the WI that the $\widehat{\Gamma}_\alpha^a(p_1, p_2)$ satisfies, simply by contracting the rhs of (2.67); this will trigger inside the integrands the corresponding tree-level WIs. Thus, using Eqs (2.41) and (2.40), together with the definitions (2.49) and (2.53), we have that

$$\widehat{\Pi}^{ab}_{\alpha\beta}(q) = \quad \frac{1}{2} \; {}^{a,\,\alpha}\,\langle\langle\langle\!\langle\rangle\rangle\rangle\rangle\,{}^{b,\,\beta} \quad + \quad {}^{a,\,\alpha}\,\langle\!\langle\,\bigcirc\,\rangle\!\rangle\,{}^{b,\,\beta} \quad + \quad {}^{a,\,\alpha}\,\bigcirc\,{}^{b,\,\beta} \quad + \quad 2\,\langle\!\langle\!\langle\rangle\!\rangle\!\rangle\bullet\, \delta^{ab} P_{\alpha\beta}(q)$$

$$\qquad\qquad (a) \qquad\qquad\qquad (b) \qquad\qquad\qquad (c) \qquad\qquad\qquad (d)$$

Fig. 9. Diagrammatic representation of the one-loop PT gluon self-energy $\widehat{\Pi}_{\alpha\beta}$ as the sum of the conventional gluon self-energy terms and the pinch contributions coming from the vertex.

$$q^\alpha \widehat{\Gamma}^a_\alpha(p_1, p_2) = -igt^a \left\{ g^2 C_f \int_k \frac{\gamma^\mu S^{(0)}(p_2 + k)\gamma_\mu}{k^2} - g^2 C_f \int_k \frac{\gamma^\mu S^{(0)}(p_1 + k)\gamma_\mu}{k^2} \right\}$$
$$= igt^a \left\{ \widehat{\Sigma}(p_1) - \widehat{\Sigma}(p_2) \right\}. \tag{2.68}$$

Clearly, Eq. (2.68) is the naive generalization of (2.59) at one-loop, *i.e.*, the WI satisfied by Γ^a_α at tree-level; this makes the analogy with Eq. (2.58) fully explicit. An immediate consequence of Eq. (2.68) is that the renormalization constants of $\widehat{\Gamma}^a_\alpha$ and $\widehat{\Sigma}$, to be denoted by $\widehat{Z}_1$ and $\widehat{Z}_2$, respectively, are related by the relation $\widehat{Z}_1 = \widehat{Z}_2$, which is none other than the textbook relation $Z_1 = Z_2$ of QED, but now realized in a non-Abelian context.

A direct comparison of the STI of Eq. (2.60), obeyed by the conventional vertex Γ^a_α, with the WI of Eq. (2.68), satisfied by the PT vertex $\widehat{\Gamma}^a_\alpha$, suggests a connection between the terms removed from Γ^a_α during the process of pinching and the ghost-related quantities D^{ab} and H^a_{ij}. As we will see in detail in the next chapter, such a connection indeed exists, and is, in fact, of central importance for the generalization of the PT to all orders.

2.4.2 The pinch technique gluon self-energy at one loop

Next, we construct the PT gluon self-energy, to be denoted by $\widehat{\Pi}_{\alpha\beta}(q)$. It is given by the sum of the conventional self-energy graphs and the self-energy-like parts extracted from the two vertices, as shown schematically in Fig. 9, *i.e.*,

$$\widehat{\Pi}_{\alpha\beta}(q) = \Pi_{\alpha\beta}(q) + 2\Pi^P_{\alpha\beta}(q). \tag{2.69}$$

Specifically, in a closed form [8],

$$\widehat{\Pi}_{\alpha\beta}(q) = \frac{1}{2}g^2 C_A \left\{ \int_k \frac{\Gamma_{\alpha\mu\nu}\Gamma^{\mu\nu}_\beta}{k^2(k+q)^2} - \int_k \frac{k_\alpha(k+q)_\beta + k_\beta(k+q)_\alpha}{k^2(k+q)^2} \right\} + 2g^2 C_A \int_k \frac{q^2 P_{\alpha\beta}(q)}{k^2(k+q)^2}, \tag{2.70}$$

where we have symmetrized the ghost contribution [graph (b) in Fig. 8] for later convenience, and neglected the fermion contribution [graph (c) of the same figure].

It would be elementary to compute $\widehat{\Pi}_{\alpha\beta}$ directly from the rhs of (2.70). It is very instructive, however, to identify exactly the parts of the conventional $\Pi_{\alpha\beta}$ that combine with (and eventually cancel against) the term $\Pi^P_{\alpha\beta}$. To make this cancellation manifest, one carries out the following rearrangement of the two elementary three-gluon vertices appearing in graph (a) of Fig. 8

$$\Gamma_{\alpha\mu\nu}\Gamma_\beta^{\mu\nu} = \left[\Gamma_{\alpha\mu\nu}^{\mathrm{F}} + \Gamma_{\alpha\mu\nu}^{\mathrm{P}}\right]\left[\Gamma_\beta^{\mathrm{F}\,\mu\nu} + \Gamma_\beta^{\mathrm{P}\,\mu\nu}\right]$$
$$= \Gamma_{\alpha\mu\nu}^{\mathrm{F}}\Gamma_\beta^{\mathrm{F}\,\mu\nu} + \Gamma_{\alpha\mu\nu}^{\mathrm{P}}\Gamma_\beta^{\mu\nu} + \Gamma_{\alpha\mu\nu}\Gamma_\beta^{\mathrm{P}\,\mu\nu} - \Gamma_{\alpha\mu\nu}^{\mathrm{P}}\Gamma_\beta^{\mathrm{P}\,\mu\nu}. \tag{2.71}$$

Then, using the elementary WIs of Eqs (2.37) we have

$$\Gamma_{\alpha\mu\nu}^{\mathrm{P}}\Gamma_\beta^{\mu\nu} + \Gamma_{\alpha\mu\nu}\Gamma_\beta^{\mathrm{P}\,\mu\nu} = -4q^2 P_{\alpha\beta}(q) - 2k_\alpha k_\beta - 2(k+q)_\alpha(k+q)_\beta,$$
$$\Gamma_{\alpha\mu\nu}^{\mathrm{P}}\Gamma_\beta^{\mathrm{P}\,\mu\nu} = 2k_\alpha k_\beta + (k_\alpha q_\beta + q_\alpha k_\beta), \tag{2.72}$$

where several terms have been set to zero by virtue of Eq. (2.17). Thus we obtain [8]

$$\widehat{\Pi}_{\alpha\beta}(q) = \frac{1}{2}g^2 C_A \left\{ \int_k \frac{\Gamma_{\alpha\mu\nu}^{\mathrm{F}}\Gamma_\beta^{\mathrm{F}\,\mu\nu}}{k^2(k+q)^2} - \int_k \frac{2(2k+q)_\alpha(2k+q)_\beta}{k^2(k+q)^2} \right\}, \tag{2.73}$$

which may be further evaluated, using

$$\Gamma_{\alpha\mu\nu}^{\mathrm{F}}\Gamma_\beta^{\mathrm{F}\,\mu\nu} = d(2k+q)_\alpha(2k+q)_\beta + 8q^2 P_{\alpha\beta}(q), \tag{2.74}$$

and

$$\int_k \frac{(2k+q)_\alpha(2k+q)_\beta}{k^2(k+q)^2} = -\left(\frac{1}{d-1}\right) q^2 P_{\alpha\beta}(q) \int_k \frac{1}{k^2(k+q)^2}, \tag{2.75}$$

to finally cast $\widehat{\Pi}_{\alpha\beta}(q)$ in the simple form

$$\widehat{\Pi}_{\alpha\beta}(q) = \left(\frac{7d-6}{d-1}\right) g^2 \frac{C_A}{2} q^2 P_{\alpha\beta}(q) \int_k \frac{1}{k^2(k+q)^2}. \tag{2.76}$$

Writing

$$\widehat{\Pi}_{\alpha\beta}(q) = P_{\alpha\beta}(q)\widehat{\Pi}(q^2), \tag{2.77}$$

and following the standard integration rules for the Feynman integral, we obtain for the unrenormalized $\widehat{\Pi}$

$$\widehat{\Pi}(q^2) = ibg^2 q^2 \left[\frac{2}{\epsilon} + \ln 4\pi - \gamma_E - \ln \frac{q^2}{\mu^2} + \frac{67}{33}\right], \tag{2.78}$$

where γ_E is the Euler-Mascheroni constant ($\gamma_E \approx 0.57721$) and

$$b = \frac{11 C_A}{48\pi^2}, \tag{2.79}$$

is the one-loop coefficient of the β function of QCD ($\beta = -bg^3$) in the absence of quark loops.

The appearance of b in front of the logarithm is not accidental, and is exactly what happens with the vacuum polarization of QED. In the latter case the corresponding coefficient is $-\alpha/3\pi$; of course, the difference in the sign is related to the fact that QCD is asymptotically free, whereas QED is not. The fact that the PT gluon propagator captures the leading RG logarithms is a direct consequence of the WI of Eq. (2.68) and the corresponding relation $\widehat{Z}_1 = \widehat{Z}_2$. Indeed, if $\widehat{Z}_1 = \widehat{Z}_2$, then the charge renormalization constant, Z_g, and the wave-function renormalization of the PT gluon self-energy, $\widehat{Z}_A$, are related by $Z_g = \widehat{Z}_A^{-1/2}$, exactly as in QED.
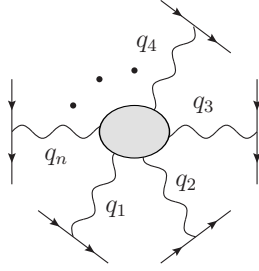
Fig. 10. S-matrix embedding necessary for constructing a gfp-independent, fully off-shell gluonic n-point function.

2.4.3   Process-independence of the pinch technique

It is important to stress, at this point, that the only completely off-shell Green's function involved in the previous construction was the gluon self-energy; instead, the quark-gluon vertex has the incoming gluon off-shell and the two quarks on shell, while the box has all four incoming quarks on shell. These latter quantities were also made gfp-independent in the process of constructing the fully off-shell gfp-independent gluonic two-point function. Similarly, as already mentioned after Eq. (2.53), the construction of a fully off-shell PT quark self-energy requires its embedding in a process such as quark-gluon elastic scattering. The generalization of the methodology is now clear; for example, for constructing a gfp-independent, fully off-shell gluonic n-point function (*i.e.*, with n off-shell gluons) one must consider the entire gfp-independent process consisting of n-pairs of quarks, $q(p_1)q(k_1)$, $q(p_2)q(k_2)$, $\cdots$, $q(p_n)q(k_n)$ and hook each gluon A_i to one pair of test quarks; the off-shell momentum transfer q_i of the ith gluonic leg will be $q_i = p_i - k_i$ (see Fig. 10). Note, however, that one may equally well use gluons as external test particles, or even (not observed) fundamental scalars carrying color. Provided that the embedding process is gfp-independent, the answer that the PT furnishes for a given fully off-shell n-point function is unique, *i.e.*, it is independent of the embedding process. This property is usually referred to as the process-independence of the PT, and the PT Green's functions are said to be process-independent or universal. The universality of the one-loop gluon self-energy has been demonstrated through explicit computations, using a variety of external test particles [63]. For example, when gluons are used as external test particles, the pinching isolates propagator-like pieces that are attached to the external gluons through a tree-level three-gluon vertex (see Fig. 11). In this case the analogue of the quark-gluon vertex $\widehat{\Gamma}^a_\alpha$ is a gfp one-loop vertex with one off-shell and two on-shell gluons, which, as we will see in a later section, is the one-loop generalization of Γ^{F}. This latter vertex should not be confused with the PT three-gluon vertex with all three gluons off-shell, that can be constructed by embedding it into a six quark process (one pair for each leg), to be discussed in the next subsection. The distinction between these two three-gluon vertices is crucial, and will be made more explicit later on; in addition, a more precise field-theoretic notation will be adopted, that will allow us to distinguish them unambiguously.

We emphasize that the PT construction is not restricted to the use of on-shell S-matrix amplitudes, and works equally well inside, for example, a gauge-invariant current correlation function or a Wilson loop. This fact is particularly relevant for the correct interpretation of the correspondence between PT and BFM, which will be discussed in the Section 3. Actually, in the first PT
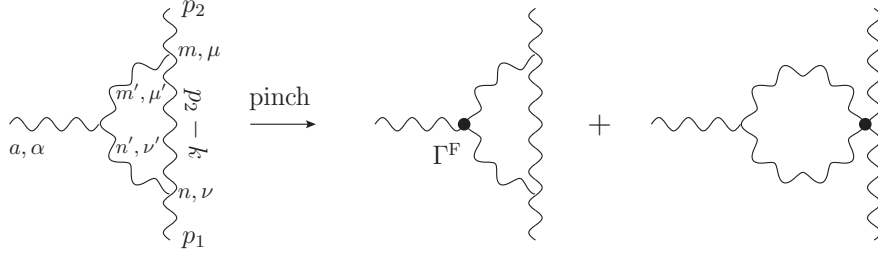
Fig. 11. The pinching procedure when the embedding particles are "on-shell" gluons. Despite appearances, the vertex to which the pinching contribution is connected to the external gluons is a three-gluon vertex.

calculation ever [7], Cornwall studied the set of one-loop Feynman diagrams contributing to the *gauge-invariant* Green's function $G(x, y) = \left\langle 0 \left| T \left\{ \mathrm{Tr} \left[\Phi(x) \Phi^\dagger(x) \right] \mathrm{Tr} \left[\Phi(y) \Phi^\dagger(y) \right] \right\} \right| 0 \right\rangle$, where $\Phi(x)$ is a matrix describing a set of scalar test particles in an appropriate representation of the gauge group. In this case, the special momentum, with respect to which the vertex decomposition of Eq. (2.38) should be carried out (*i.e.*, the equivalent of q in that same equation), is the momentum transfer between the two sides of the scalar loop (*i.e.*, one should count loops as if the Φ loop had been opened at x and y). The advantage of using an S-matrix amplitude is purely operational: the PT construction becomes more expeditious, because several terms can be set to zero directly due to the equation of motion of the on-shell test particles. Instead, in the case of a Wilson loop, one would have to carry out the additional step of demonstrating explicitly their cancellation against other similar terms.

2.4.4 *Intrinsic pinch technique and the gauge-independent three-gluon vertex at one loop*

The central achievement of the previous subsections has been the construction of the gfp-independent off-shell gluon self-energy, $\widehat{\Pi}_{\mu\nu}$, through its embedding into a physical S-matrix element, corresponding to quark-quark elastic scattering. This was accomplished by identifying propagator-like pieces from the vertices and the boxes contributing to the embedding process, and reassigning them to the conventional gluon self-energy, $\Pi_{\mu\nu}$. This procedure has been carried out for a general value of the gfp, leading to a unique answer, which is most economically reached by choosing the Feynman gauge from the beginning. Thus, $\widehat{\Pi}_{\mu\nu}$ is obtained by adding to $\Pi_{\mu\nu}$ the propagator-like pieces $2\Pi_{\mu\nu}^{\mathrm{P}}$ extracted from the vertices, as shown in Eq. (2.70). In the analysis following Eq. (2.70) it became clear that these latter terms cancel very precise terms of the conventional self-energy $\Pi_{\mu\nu}$, furnishing finally $\widehat{\Pi}_{\mu\nu}$. Specifically, after the vertex decomposition of Eq. (2.71), the terms Γ^{P} acted on the corresponding Γ, triggering the WIs of Eqs (2.37): the term $2\Pi_{\mu\nu}^{\mathrm{P}}$ cancels against the terms of the WIs that are proportional to $q^2 P_{\mu\nu}$. This observation motivates the following more expeditious course of action: instead of identifying the propagator-like pieces from the various graphs, focus on $\Pi_{\mu\nu}$, carry out the decomposition of Eq. (2.71), and discard the terms coming from the WIs that are proportional to $q^2 P_{\mu\nu}$; what is left is then the PT answer.

This alternative, and completely equivalent, approach to pinching was first introduced in [8] and is known as "intrinsic" PT. Its main virtue is that it avoids as much as possible the embed-

32
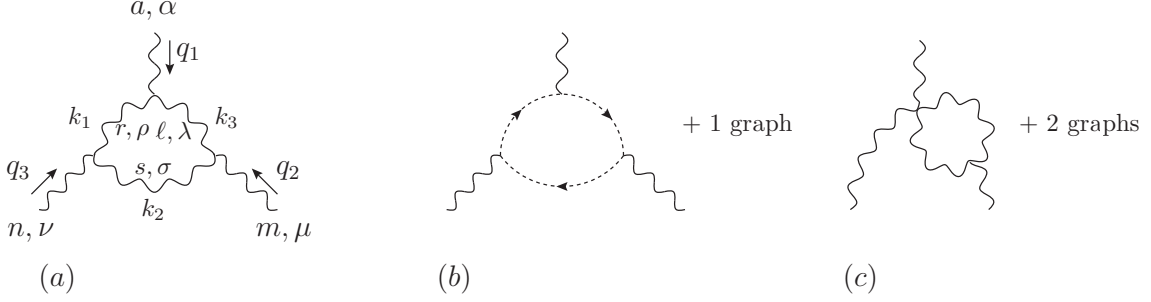
Fig. 12. R_ξ diagrams contributing to the one-loop three-gluon vertex. Diagrams (c) carry a $\frac{1}{2}$ symmetry factor. Fermion diagrams are not shown.

ding of the Green's function under construction into a physical amplitude. As we will see later on, the intrinsic approach is particularly suited for extending the PT construction at the level of the SDE of the theory.

As an application of the intrinsic PT algorithm, we will construct the one-loop PT three gluon vertex [8]. The conventional R_ξ diagrams are shown in Fig. 12 and read

$$\Gamma^{amn}_{\alpha\mu\nu}(q_1, q_2, q_3) = -\frac{1}{2}g^3 C_A f^{amn} \left\{ \int_{k_1} \frac{1}{k_1^2 k_2^2 k_3^2} N_{\alpha\mu\nu} + B_{\alpha\mu\nu} \right\}, \tag{2.80}$$

with

$$N_{\alpha\mu\nu} = \Gamma_{\alpha\lambda\rho}(q_1, k_3, -k_1)\Gamma_{\mu\sigma\lambda}(q_2, k_2, -k_3)\Gamma_{\nu\rho\sigma}(q_3, k_1, -k_2) - k_{1\alpha}k_{2\nu}k_{3\mu} - k_{1\alpha}k_{2\nu}k_{3\mu},$$

$$B_{\alpha\mu\nu} = \frac{9}{2}\left(g_{\alpha\mu}q_{1\nu} - g_{\alpha\nu}q_{1\mu}\right)\int_k \frac{1}{k^2(k+q_1)^2} + \frac{9}{2}\left(g_{\alpha\mu}q_{2\nu} - g_{\mu\nu}q_{2\alpha}\right)\int_k \frac{1}{k^2(k+q_2)^2}$$

$$+ \frac{9}{2}\left(g_{\mu\nu}q_{3\alpha} - g_{\alpha\nu}q_{3\mu}\right)\int_k \frac{1}{k^2(k+q_3)^2}. \tag{2.81}$$

Let us then introduce the short-hand notation $\Gamma_1\Gamma_2\Gamma_3$ for the product of (bare) three gluon vertices appearing in Eq. (2.81). In this notation all the Lorentz indices are suppressed and the number appearing in each vertex is the one corresponding to its external momentum q_i. Then, decomposing each of the Γ_i into $\Gamma_i^{\rm F} + \Gamma_i^{\rm P}$, we obtain the analogue of (2.71), namely

$$\Gamma_1\Gamma_2\Gamma_3 = \Gamma_1^{\rm F}\Gamma_2^{\rm F}\Gamma_3^{\rm F} + \Gamma_1^{\rm P}\Gamma_2\Gamma_3 + \Gamma_1\Gamma_2^{\rm P}\Gamma_3 + \Gamma_1\Gamma_2\Gamma_3^{\rm P} - \Gamma_1^{\rm P}\Gamma_2^{\rm P}\Gamma_3 - \Gamma_1^{\rm P}\Gamma_2\Gamma_3^{\rm P} - \Gamma_1\Gamma_2^{\rm P}\Gamma_3^{\rm P}$$
$$+ \Gamma_1^{\rm P}\Gamma_2^{\rm P}\Gamma_3^{\rm P}. \tag{2.82}$$

Now, the first term contains no pinching momenta, and therefore will be kept in the PT answer, giving rise to the term

$$(\widehat{a}) = -\frac{i}{2}g^3 C_A f^{amn} \int_{k_1} \frac{1}{k_1^2 k_2^2 k_3^2} \Gamma^{\rm F}_{\alpha\lambda\rho}(q_1, k_3, -k_1)\Gamma^{\rm F}_{\mu\sigma\lambda}(q_2, k_2, -k_3)\Gamma^{\rm F}_{\nu\rho\sigma}(q_3, k_1, -k_2). \tag{2.83}$$

Each of the next six terms gives rise to pinching contributions, generated when $\Gamma_i^{\rm P}$ acts on the full Γ's, thus triggering the WIs of (2.37). Some of the terms so generated will be proportional to

$d^{-1}(q_i^2)$, i.e. inverse *external* gluon propagators; according to the rules of the intrinsic pinch, we simply discard them. However, all other terms generated from the WIs of (2.37) must be kept; as we will see, they are crucial for furnishing the correct final answer. For example, collectively denoting the terms discarded with ellipses, one has

$$\Gamma_1^{\mathrm{P}}\Gamma_2\Gamma_3 = d^{-1}(k_3^2)\left[\Gamma_{\nu\alpha\mu}(k_1, -k_2) + \Gamma_{\mu\nu\alpha}(k_2, -k_3)\right] + k_{2\mu}\left[d^{-1}(k_1^2)g_{\alpha\nu} - k_{1\alpha}k_{1\nu}\right]$$
$$+ k_{2\nu}\left[d^{-1}(k_3^2)g_{\alpha\mu} - k_{3\alpha}k_{3\mu}\right] + \cdots,$$
$$\Gamma_1^{\mathrm{P}}\Gamma_2^{\mathrm{P}}\Gamma_3 = d^{-1}(k_3^2)\Gamma_{\nu\alpha\mu}(k_1, -k_2) - k_{3\alpha}\left[d^{-1}(k_2^2)g_{\mu\nu} - k_{2\mu}k_{2\nu}\right]$$
$$- k_{3\mu}\left[d^{-1}(k_1^2)g_{\nu\alpha} - k_{1\nu}k_{1\alpha}\right] + \cdots, \tag{2.84}$$

with similar expressions for the other such terms on on the rhs of Eq. (2.82). The last term on the rhs of Eq. (2.82) does not have terms proportional to $d^{-1}(q_i^2)$, so there is nothing to discard; it must be kept in its entirety. Specifically,

$$\Gamma_1^{\mathrm{P}}\Gamma_2^{\mathrm{P}}\Gamma_3^{\mathrm{P}} = -d^{-1}(k_1^2)\left(g_{\mu\nu}k_{3\alpha} + g_{\alpha\mu}k_{1\alpha}\right) - d^{-1}(k_2^2)\left(g_{\alpha\mu}k_{1\nu} + g_{\alpha\nu}k_{3\mu}\right)$$
$$- d^{-1}(k_3^2)\left(g_{\alpha\nu}k_{2\mu} + g_{\mu\nu}k_{1\alpha}\right) - k_{1\alpha}k_{2\mu}k_{3\nu} - k_{1\nu}k_{2\mu}k_{3\alpha}. \tag{2.85}$$

Isolating all terms that are not proportional to a $d^{-1}(k_i^2)$, and adding them to the conventional ghost graph (b) of Fig. 12, we get the result

$$(\widehat{b}) = \frac{i}{2}g^3 C_A f^{amn} \int_{k_1} \frac{1}{k_1^2 k_2^2 k_3^2} 2(k_1 + k_3)_\alpha (k_2 + k_3)_\mu (k_1 + k_2)_\nu. \tag{2.86}$$

Evidently, all terms proportional to $d^{-1}(k_i^2)$ will cancel against one internal gluon propagator, giving rise to integrands with only two such propagators, i.e.

$$(\widetilde{c}) = -\frac{i}{2}g^3 C_A f^{amn} \int_{k_2} \frac{1}{k_2^2 k_3^2}\left[g_{\alpha\mu}(k_1 - q_3)_\nu + 2g_{\alpha\nu}(q_3 - q_1)_\mu + g_{\mu\nu}(k_1 + q_1)_\alpha\right]$$
$$- \frac{i}{2}g^3 C_A f^{amn} \int_{k_1} \frac{1}{k_1^2 k_3^2}\left[g_{\alpha\mu}(k_2 + q_3)_\nu + g_{\alpha\nu}(k_2 - q_2)_\mu + 2g_{\mu\nu}(q_2 - q_3)_\alpha\right]$$
$$- \frac{i}{2}g^3 C_A f^{amn} \int_{k_1} \frac{1}{k_1^2 k_2^2}\left[2g_{\alpha\mu}(q_1 - q_2)_\nu + g_{\alpha\nu}(k_3 + q_2)_\mu + g_{\mu\nu}(k_3 - q_1)_\alpha\right]. \tag{2.87}$$

This is, however, not the end of the story. As we have seen, in the presence of longitudinal momenta the topology of a Feynman diagram is not a well-defined property, since longitudinal momenta will pinch out internal propagators, turning t-channel diagrams into s-channel ones. This same caveat applies also to the notion of one particle reducibility. Remember that a diagram is called one-particle irreducible (1PI) if it cannot be split into two disjoined pieces by cutting a single internal line; otherwise it is called one-particle reducible (1PR). Now, it turns out that by pinching out internal propagators, one can effectively convert 1PR diagrams into 1PI ones (see Fig. 13); of course the opposite cannot happen. Evidently the notion of a 1PR diagram is gauge-dependent! Thus, when constructing the purely (1PI) gauge-invariant three-gluon vertex at one-loop, one has to take into account possible 1PI pinching contribution coming from seemingly

(d_1) $(d_1)^{\mathrm{P}}$ $(d_1')^{\mathrm{P}}$
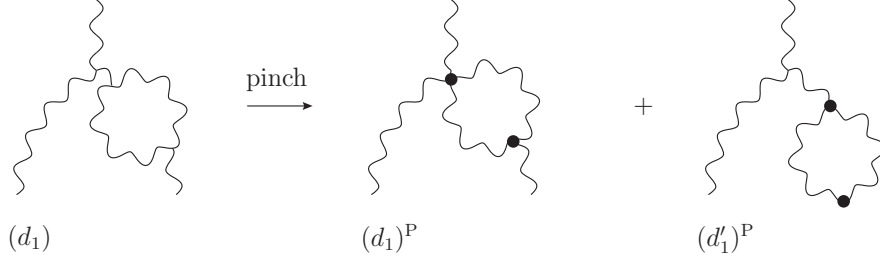
Fig. 13. 1PR diagram giving to effectively 1PI pinching contributions [diagram $(d_1)^{\mathrm{P}}$]. Two more diagrams (corresponding to having the gluon self-energy correction on the remaining legs) that give rise to similar terms are not shown.

1PR diagrams, such as those shown in Fig. 13. How do we actually obtain these terms ? Simply by carrying out the intrinsic PT construction inside the self-energy graph (d_1): in doing so, the terms that will remove the "internal" gluon propagator will furnish the (effectively 1PI) diagram $(d_1)^{\mathrm{P}}$, while those proportional to an inverse "external" gluon propagator [diagram $(d_1')^{\mathrm{P}}$] ought to be discarded, in full accordance with the rules of the intrinsic PT. Indeed, as the reader should be able to verify, in the S-matrix PT implementation these latter terms will cancel anyway against analogous contribution coming from non-Abelian vertices attached to the external test-quark.

Let us see in detail what happens in the case shown in Fig. 13. One has

$$(d_1) = -\frac{\mathrm{i}}{2} g^2 C_A \Gamma_{\alpha\mu'\nu}(q_1, q_2, q_3) d(q_2^2) g^{\mu'\nu'} \times$$
$$\times \int_k \frac{1}{k^2(k+q_2)^2} \Gamma_{\nu'\rho\sigma}(-q_2, k+q_2, -k) \Gamma^{\rho\sigma}_\mu(-q_2, k+q_2, -k). \tag{2.88}$$

As explained above, of all the possible pinching contributions appearing after the splitting of the two three gluon vertices inside this gluon self-energy according to (2.71) and (2.72), one needs to retain only half of the first term appearing in the rhs of Eq. (2.72), the other half removing instead the external propagator, thus generating diagram $(d_1')^{\mathrm{P}}$ of Fig. 13. Therefore one has

$$(d_1)^{\mathrm{P}} = ig^3 C_A f^{amn} \Gamma_{\alpha\mu\nu}(q_1, q_2, q_3) \int_k \frac{1}{k^2(k+q_2)^2}, \tag{2.89}$$

where we kept only the $g^{\mu\sigma}$ part of the $P^{\mu\sigma}$ appearing in the pinching term, since the $q_2^\mu q_2^\sigma$ term will remove the external propagator and thus ought to be discarded. Adding this to the first term on the rhs of Eq. (2.87), to be denoted by $(\tilde{c}_1)$, we find

$$(\tilde{c}_1) + (d_1)^{\mathrm{P}} = -i\frac{7}{4} g^3 C_A f^{amn}(g_{\alpha\mu}q_{2\nu} - g_{\mu\nu}q_{2\alpha}) \int_k \frac{1}{k^2(k+q_2)^2}. \tag{2.90}$$

The same procedure can be repeated for the diagrams (d_2) and (d_3); after adding them to the corresponding contributions, $(\tilde{c}_2)$ and $(\tilde{c}_3)$, we obtain

$$(\tilde{c}_2) + (d_2)^{\mathrm{P}} = -i\frac{7}{4}g^3 C_A f^{amn} (g_{\mu\nu}q_{3\alpha} - g_{\alpha\nu}q_{3\mu}) \int_k \frac{1}{k^2(k+q_3)^2},$$

$$(\tilde{c}_3) + (d_3)^{\mathrm{P}} = -i\frac{7}{4}g^3 C_A f^{amn} (g_{\alpha\mu}q_{1\nu} - g_{\alpha\nu}q_{1\mu}) \int_k \frac{1}{k^2(k+q_1)^2}. \tag{2.91}$$

Notice that these terms have exactly the same structure as the conventional (c) diagrams, to which they can be added.

Thus, the PT one-loop three-gluon vertex is finally given by

$$i\widehat{\Gamma}^{amn}_{\alpha\mu\nu}(q_1, q_2, q_3) = -\frac{i}{2}g^3 C_A f^{amn} \left\{ \int_{k_1} \frac{1}{k_1^2 k_2^2 k_3^2} \widehat{N}_{\alpha\mu\nu} + \widehat{B}_{\alpha\mu\nu} \right\}, \tag{2.92}$$

where

$$\widehat{N}_{\alpha\mu\nu} = \Gamma^{\mathrm{F}}_{\alpha\lambda\rho}(q_1, k_3, -k_1)\Gamma^{\mathrm{F}}_{\mu\sigma\lambda}(q_2, k_2, -k_3)\Gamma^{\mathrm{F}}_{\nu\rho\sigma}(q_3, k_1, -k_2)$$
$$- 2(k_1 + k_3)_\alpha (k_2 + k_3)_\mu (k_1 + k_2)_\nu,$$

$$\widehat{B}_{\alpha\mu\nu} = 8\,(g_{\alpha\mu}q_{1\nu} - g_{\alpha\nu}q_{1\mu}) \int_k \frac{1}{k^2(k+q_1)^2} + 8\,(g_{\alpha\mu}q_{2\nu} - g_{\mu\nu}q_{2\alpha}) \int_k \frac{1}{k^2(k+q_2)^2}$$
$$+ 8\,(g_{\mu\nu}q_{3\alpha} - g_{\alpha\nu}q_{3\mu}) \int_k \frac{1}{k^2(k+q_3)^2}. \tag{2.93}$$

Note that $\widehat{\Gamma}^{amn}_{\alpha\mu\nu}(q_1, q_2, q_3)$ is manifestly Bose-symmetric with respect to all three of its legs.

It is now of central importance to recognize that, unlike the conventional three gluon vertex that satisfies an STI, the $\widehat{\Gamma}^{amn}_{\alpha\mu\nu}(q_1, q_2, q_3)$ constructed above satisfies a simple Abelian-like WI. Specifically, the conventional three-gluon vertex (in the R_ξ gauges) satisfies at all orders the STI [45]

$$q_1^\alpha \Gamma^{amn}_{\alpha\mu\nu}(q_1, q_2, q_3) = \left[q_1^2 D^{aa'}(q_1) \right] \left\{ \Delta^{-1}(q_2^2) P_\mu^\gamma(q_2) H^{a'nm}_{\nu\gamma}(q_3, q_2) \right.$$
$$\left. + \Delta^{-1}(q_3^2) P_\nu^\gamma(q_3) H^{a'mn}_{\mu\gamma}(q_2, q_3) \right\}, \tag{2.94}$$

where the auxiliary function $H_{\alpha\beta}$ is the 1PI part of the composite operator

$$i\Delta^{nn'}_{\nu\nu'}(k) i D^{aa'} i H^{adn}_{\nu\gamma}(k, q) = -ig f^{eds} \int d^4x \int d^4y \, e^{iq\cdot x} \, e^{ik\cdot y} \times$$
$$\times \left\langle 0 \left| T \left\{ \bar{c}^{a'}(x) A^{n'}_{\nu'}(y) [c^e(0) A^s_\gamma(0)] \right\} \right| 0 \right\rangle^{\mathrm{1PI}}. \tag{2.95}$$

and it is defined in Fig. 14. Notice that the kernel appearing in this auxiliary function is the conventional connected ghost-ghost-gluon-gluon kernel appearing in the usual QCD skeleton expansion [27,64]. Also, $H_{\alpha\beta}(k, q)$ is related to the conventional gluon-ghost vertex $\Gamma_\beta(k, q)$ (with k the gluon and q the anti-ghost momentum) by [62,45,27,64].

$$q^\alpha H_{\alpha\beta}(k, q) = \Gamma_\beta(k, q). \tag{2.96}$$

$$H_{\nu\gamma}^{adn}(k,q) = gf^{adn}g_{\nu\gamma} +$$

Fig. 14. The auxiliary function H appearing in the three-gluon vertex STI. The gray blob represents the (connected) ghost-gluon kernel $\mathcal{K}$ appearing in the usual QCD skeleton expansion.

Of course, the STI of (2.94) reduces at tree-level to that of (2.37).

On the other hand, contracting Eq. (2.92) with q_1^α, one obtains easily the result [8]

$$q_1^\alpha \widehat{\Gamma}_{\alpha\mu\nu}^{amn}(q_1, q_2, q_3) = gf^{amn} \left\{ \widehat{\Delta}^{-1}(q_2)P_{\mu\nu}(q_2) - \widehat{\Delta}^{-1}(q_3)P_{\mu\nu}(q_3) \right\}, \tag{2.97}$$

with $\widehat{\Delta}^{-1}(q) = q^2 + i\widehat{\Pi}(q^2)$; of course, contracting with respect q_2^μ and q_3^ν furnishes the expected Bose-symmetric analogues of (2.97). Thus, rather remarkably, we find the naive one-loop generalization of the tree-level identity of Eq. (2.40). Note, in particular, that any reference to auxiliary ghost Green's functions has disappeared: Eq. (2.97) is completely gauge-invariant.

Let us now focus on a very interesting property of the one-loop PT three-gluon vertex, discovered recently by Binger and Brodsky [65]. These authors have first added quark and scalar loops to $\widehat{\Gamma}_{\alpha\mu\nu}^{amn}(q_1, q_2, q_3)$; this is straightforward, from the point of view of gauge-independence and gauge-invariance, since these loops are automatically gfp-independent and satisfy (2.97). Then, all resulting one-loop integrals, including those of (2.93) and (2.93), were evaluated for the first time, thus determining the precise tensorial decomposition of $\widehat{\Gamma}_{\alpha\mu\nu}^{amn}(q_1, q_2, q_3)$. Then, after choosing a convenient tensor basis, $\widehat{\Gamma}_{\alpha\mu\nu}^{amn}(q_1, q_2, q_3)$ was expressed as a linear combination of fourteen independent tensors, each one multiplied by its own scalar form-factor. Every form-factor receives, in general, contributions from gluons(G), quarks(Q), and scalars(S). It turns out that these three types of contributions satisfy very characteristic relations, that are closely linked to supersymmetry and conformal symmetry, and in particular the $\mathcal{N} = 4$ non-renormalization theorems. Specifically, for all form-factors F (in d-dimensions) it was shown that

$$F_G + 4F_Q + (10 - d)F_S = 0, \tag{2.98}$$

which encodes the vanishing contribution of the $\mathcal{N} = 4$ supermultiplet in four dimensions. Similar relations have been found in the context of supersymmetric scattering amplitudes [66,67].

It should be emphasized that relations such as Eq.(2.98) do *not* exist for the gauge-dependent three-gluon vertex [68], since the gluon contributions depend on the gfp, while the quarks and scalars do not. Indeed, it is uniquely the PT (or equivalently BFM in the BFG $\xi_Q = 1$, see next section) Green's function that satisfies this homogeneous sum rule. Most importantly, calculating in the BFM with $\xi_Q \neq 1$ leads to a nonzero rhs of Eq. (2.98).

2.4.5 The pinch technique four-gluon vertex at one loop

The construction of the gauge-invariant four-gluon vertex has been outlined in detail in [69], in the context of the S-matrix PT. The actual derivation is technically rather cumbersome because of (*i*) the large number of graphs and (*ii*) certain subtle exchange of pinching contributions between 1PI and 1PR diagrams (some of which have been seen in the construction carried out in the previous subsection). The exact closed form of this vertex (see, *e.g.*, [41]) is too lengthy to be reported here. Far more interesting is the WI that this vertex satisfies: it is simply the naive one-loop generalization of the tree-level result, as can be easily confirmed using the explicit expressions for the bare three- and four-gluon vertices. Specifically, we have [69]

$$
\begin{aligned}
q^{\alpha}\Gamma^{amnr}_{\alpha\mu\nu\rho}(q,k_1,k_2,k_3) = {} & gf^{adm}\widehat{\Gamma}^{dnr}_{\mu\nu\rho}(q+k_1,k_2,k_3) + gf^{adr}\widehat{\Gamma}^{drm}_{\nu\rho\mu}(q+k_2,k_3,k_1) \\
& + gf^{adn}\widehat{\Gamma}^{dmr}_{\nu\mu\rho}(q+k_3,k_1,k_2),
\end{aligned}
\tag{2.99}
$$

where the three-gluon vertices appearing are the PT ones constructed in the previous subsection. Again we find a fully gauge invariant, Abelian-like WI, that makes no reference to ghost Green's functions.

2.5 The absorptive pinch technique construction

In the previous subsection, we worked at the level of one-loop perturbation theory, and constructed non-Abelian Green's functions that are gfp-independent and satisfy QED-like WIs. The analogy between the PT Green's functions and those of QED is best exemplified by comparing the PT gluon self-energy with that of the photon (vacuum polarization): they are both gfp-independent and capture the leading RG logarithms. It is therefore natural to want to explore until what point this analogy with QED may persist. Specifically, in QED knowledge of the vacuum polarization spectral function determined from the tree level $e^+e^- \to \mu^+\mu^-$ cross sections, together with a single low energy measurement of the fine structure constant α, enables the construction of the one-loop vacuum polarization, and the corresponding effective charge, $\alpha_{\mathrm{eff}}(q^2)$, for all q^2. What makes this possible in the case of QED is the unitarity of the S-matrix, expressed in the form of the optical theorem, and the requirement of the analyticity of Green's functions, as captured by the so-called dispersion relations (see, *e.g.*, [70]). In this subsection we will study in detail how the above crucial properties are encoded into the Green's functions constructed by the PT. Specifically, we will see that, in a non-Abelian context, the PT construction enforces *at the level of individual Green's functions* properties of unitarity and analyticity that are completely analogous to those of QED.

2.5.1 Optical theorem and analyticity

The T-matrix element of a reaction $i \to f$ is defined via the relation

$$
\langle f|S|i\rangle \;=\; \delta_{fi} \;+\; i(2\pi)^4\delta^{(4)}(P_f - P_i)\langle f|T|i\rangle,
\tag{2.100}
$$

where P_i (P_f) is the sum of all initial (final) momenta of the $|i\rangle$ ($|f\rangle$) state. Furthermore, imposing the unitarity relation $S^\dagger S = 1$ leads to the generalized optical theorem:

$$\langle f|T|i\rangle - \langle i|T|f\rangle^* = i\sum_j (2\pi)^4 \delta^{(4)}(P_j - P_i)\langle j|T|f\rangle^* \langle j|T|i\rangle. \qquad (2.101)$$

In Eq. (2.101), the sum $\sum_j$ should be understood to be over the entire phase space and spins of all possible on-shell intermediate particles j.

An important corollary of this theorem is obtained if $f = i$, corresponding to the case of the so-called "forward scattering". For this particular kinematic choice, setting on the lhs $T^{ii} \equiv \langle i|T|i\rangle$ and on the rhs $\mathcal{T}^{ij} \equiv \langle j|T|i\rangle$ and $\mathcal{M}^{ij} \equiv |\langle j|T|i\rangle|^2 = |\mathcal{T}^{ij}|^2$ we have

$$\Im m\{T^{ii}\} = \frac{1}{2}\sum_j (2\pi)^4 \delta^{(4)}(P_j - P_i)\mathcal{M}^{ij}. \qquad (2.102)$$

For the rest of this review we will be referring to the relation given in Eq. (2.102) as the optical theorem (OT).

The rhs of the OT consists of the sum of the (squared) amplitudes, $\mathcal{M}^{ij}$, of all kinematically allowed elementary processes connecting the initial and final states. Note, in particular, that only *physical particles* may appear as intermediate $|j\rangle$ states. If the particles involved are fermions and/or gauge bosons, when calculating $\mathcal{M}^{ij}$ one averages over the initial state polarizations and sums over the final state polarizations. In addition, the integration over all available phase-space, implicit in the sum $\sum_j$, must be carried out. The lhs of the OT is given by the imaginary part of the *entire* amplitude, *i.e.*, including all Feynman diagrams contributing to it. For example, in the case of non-Abelian gauge theories to obtain the lhs of the OT one must calculate the imaginary part of all diagrams, regardless of whether they contain physical (gluons, quarks) or unphysical (ghosts or would-be Goldstone bosons) fields inside their loops. The way how these imaginary parts will be actually computed is a mathematics rather than a physics question. For instance, in the simple case of one-loop graphs one may carry out the integration over virtual momenta, and then determine where the resulting expressions develop imaginary parts. Equivalently, one can use a set of rules known as "Cutkosky rules" or "cutting rules". One has to first cut through all diagrams on the lhs of the OT in all possible ways such that the cut propagators can be put simultaneously on-shell. Note that one cuts through physical and unphysical particles (given that we are operating on the lhs of the OT), and that higher order diagrams have, in general, multiple (two-particle, three-particle, etc.) cuts. Then, for each cut propagator one must substitute

$$(k^2 - m^2 + i\epsilon)^{-1} \rightarrow -2i\pi\delta_+(k^2 - m^2), \qquad (2.103)$$

where

$$\delta_+(k^2 - m^2) \equiv \theta(k^0)\delta(k^2 - m^2), \qquad (2.104)$$

and carry out the resulting integral. Finally, one must sum up the contributions of all cuts. This approach has the advantage of casting the lhs of the OT into a form that, for certain simple theories such as scalar field theories or QED, makes the equality with the rhs manifest.

An issue of central importance for what follows is the way that the OT is realized at the level of the conventional diagrammatic expansion, or equivalently, at the level of the propagator-, vertex-, and box-like amplitudes, T_1, T_2, and T_3, respectively, introduced in subsection 2.2.
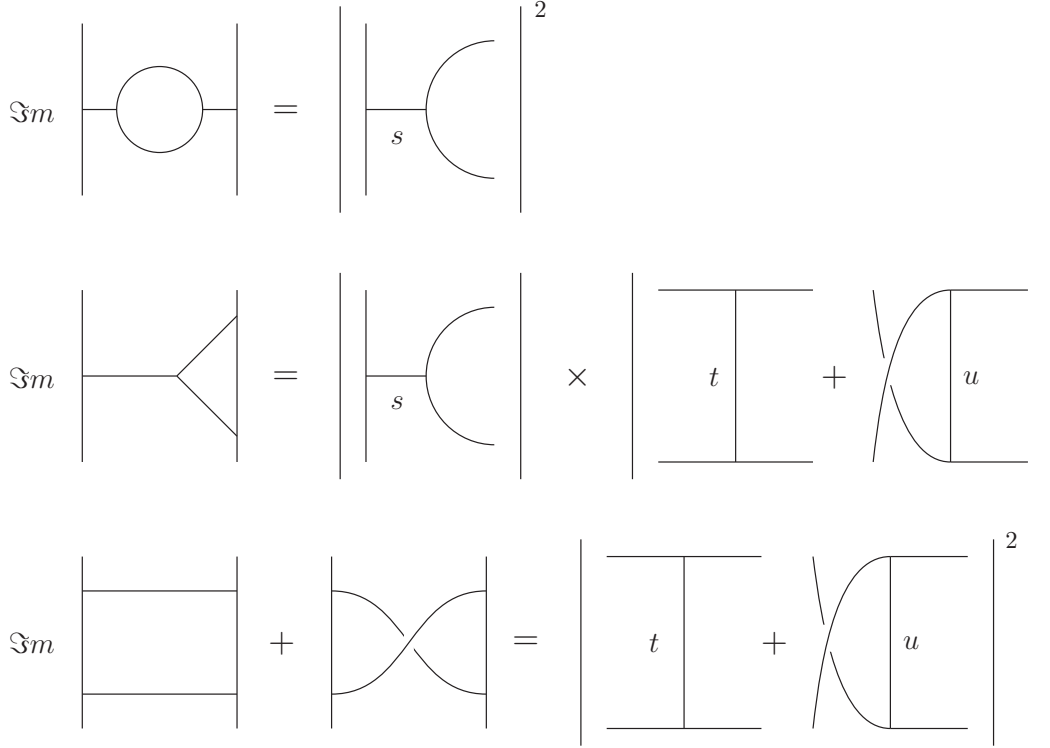
Fig. 15. The stronger version of the OT in the case of a scalar theory.

Specifically, in its general formulation of Eq. (2.102), the OT is a statement at the level of *entire* amplitudes and not of individual Feynman graphs, nor of the corresponding subamplitudes. Thus, the imaginary part of a given diagram appearing on the rhs does *not* necessarily correspond to an easily identifiable diagrammatic (or kinematic) piece on the rhs. For example, in QCD the *conventional* propagator-like pieces of the two sides, *i.e.*, those defined from the *standard* (as opposed to the "pinched") diagrammatic expansion, do not have to coincide in general. Of course, there are theories where the OT holds also at the level of individual graphs and kinematic subamplitudes. This stronger version of the OT is realized in scalar theories, but fails in non-Abelian gauge theories, such as QCD and the electroweak model. A crucial advantage of the PT is that it permits the realization of the OT at the level of kinematically distinct, well-defined subamplitudes, even in the context of non-Abelian gauge-theories; these privileged subamplitudes are, of course, none other than the $\widehat{T}_1$, $\widehat{T}_2$, and $\widehat{T}_3$.

In order to see a concrete example where the OT holds at the level of individual subamplitudes, let us turn to a scalar, $\lambda\phi^3$ theory, where pinching is impossible (no WIs), and therefore the topological structures given by the Feynman graphs cannot be modified. We will consider the process $\phi(p_1)\phi(p_2) \to \phi(p_1)\phi(p_2)$; thus, $|i\rangle = |\phi(p_1)\phi(p_2)\rangle$, and, at lowest order, the only intermediate state possible is $|j\rangle = |\phi(k_1)\phi(k_2)\rangle$ (see Fig. 15). In such a case, the OT assumes its stronger version

$$\Im m\{T_\ell^{ii}\} = \frac{1}{2}\sum_j (2\pi)^4 \delta^{(4)}(P_j - P_i)\mathcal{M}_\ell^{ij}, \qquad (2.105)$$

where $\ell = 1, 2, 3$ denotes, respectively, the propagator-, the vertex-, and box-like parts of either side (to recover the full OT, one simply sums both sides over ℓ).

The way the $\mathcal{M}_\ell^{ij}$ are determined is simply through the dependence on the Mandelstam variables s, t, and u; the latter are defined in this case as $s = (p_1 + p_2)^2 = (k_1 + k_2)^2$, $t = (p_1 - k_1)^2 = (p_2 - k_2)^2$, and $u = (p_1 - k_2)^2 = (p_2 - k_1)^2$. Specifically (suppressing the superscript ij),

$$\mathcal{T} = \lambda^2 \left[\frac{1}{s - m^2} + \frac{1}{t - m^2} + \frac{1}{u - m^2} \right], \qquad (2.106)$$

and so

$$
\begin{aligned}
\mathcal{M}_1 &= \lambda^4 \left(\frac{1}{s - m^2} \right)^2, \\
\mathcal{M}_2 &= 2\lambda^4 \left[\frac{1}{t - m^2} + \frac{1}{u - m^2} \right] \frac{1}{s - m^2}, \\
\mathcal{M}_3 &= \lambda^4 \left[\frac{1}{t - m^2} + \frac{1}{u - m^2} \right]^2.
\end{aligned}
\qquad (2.107)
$$

As we will see later on, this simple identification fails in the case of non-Abelian theories.

Let us now verify Eq. (2.105) for the propagator-like parts of the amplitude ($\ell = 1$) and at the lowest non-trivial order in λ. We have that

$$
\begin{aligned}
T_1^{ii} &= -\lambda^2 i \Delta(q^2, m^2) \\
&= -\lambda^2 \frac{i}{q^2 - m^2 - i\Pi(q^2, m^2)} \\
&= -\lambda^2 i D^{(0)}(q^2, m^2) + \lambda^2 D^{(0)}(q^2, m^2) \Pi(q^2, m^2) D^{(0)}(q^2, m^2), \\
\mathcal{M}_1^{ij} &= \lambda^4 [D^{(0)}(q^2, m^2)]^2
\end{aligned}
\qquad (2.108)
$$

with $D^{(0)}(q^2, m^2) = (q^2 - m^2)^{-1}$ the tree-level scalar propagator and $\Pi(q^2, m^2)$ its one-loop self-energy, given by

$$i\Pi(q^2, m^2) = \frac{\lambda^2}{2} \int_k \frac{1}{(k^2 - m^2)[(k + q)^2 - m^2]}. \qquad (2.109)$$

Then, denoting the two sides of the OT by $(\text{lhs})_1$ and $(\text{rhs})_1$, we have

$$
\begin{aligned}
(\text{lhs})_1 &= \lambda^2 \Im m \{T_1^{ii}\}, \\
(\text{rhs})_1 &= \frac{1}{2} \times \frac{1}{2} \lambda^4 [D^{(0)}(q^2)]^2 \int_{\text{PS}},
\end{aligned}
\qquad (2.110)
$$

where the additional combinatorial $\frac{1}{2}$ factor accounts for having two identical particles in the final state. The integral $\int_{\text{PS}}$ is the two-body phase-space integral, given by

$$\int_{\text{PS}} = \frac{1}{(2\pi)^2} \int d^4k_1 \int d^4k_2 \, \delta_+(k_1^2 - m_1^2) \delta_+(k_2^2 - m_2^2) \delta^{(4)}(q - k_1 - k_2), \qquad (2.111)$$

41
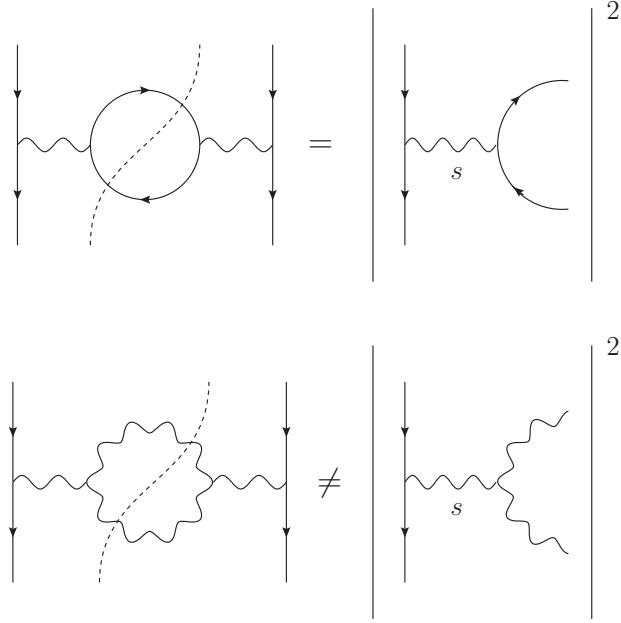
Fig. 16. The stronger version of the OT in QCD: it holds for the quark loop but fails for the gluon loop.

where m_1 and m_2 are the masses of the intermediate particles produced (in the case at hand $m_1 = m_2 = m$). To demonstrate the equality $(\mathrm{lhs})_1 = (\mathrm{rhs})_1$, use for $(\mathrm{rhs})_1$ the standard result

$$\int_{\mathrm{PS}} = \theta(q^0)\theta[q^2 - (m_1 + m_2)^2]\frac{1}{8\pi q^2}\lambda^{1/2}(q^2, m_1^2, m_2^2), \qquad (2.112)$$

where $\lambda(x, y, z) = (x - y - z)^2 - 4yz$, and for $(\mathrm{lhs})_1$ that

$$
\begin{aligned}
\Im m\{\Pi(q^2)\} &= -\frac{\lambda^2}{32\pi^2}\Im m\left\{\int_0^1 dx \ln[m^2 - q^2 x(1 - x)]\right\}\\
&= \frac{\lambda^2}{32\pi}\frac{\theta(q^2 - 4m^2)}{q^2}\lambda^{1/2}(q^2, m^2, m^2)\\
&= \frac{\lambda^2}{4}\int_{\mathrm{PS}},
\end{aligned}
\qquad (2.113)
$$

obtained from Eq. (2.109) after the Feynman parametrization and standard integration over k. It is relatively straightforward to show, to lowest order, the validity of (2.105) for $\ell = 2, 3$, especially if the Cutkosky rules are employed to determine the rhs. Notice that, in QCD, the stronger version of the OT holds for the quark loop but fails when the virtual particles circulating in the loop are gluons (see Fig. 16).

An additional important ingredient that accompanies the OT is that of analyticity; together they provide a powerful framework that restricts severely the allowed structure of Green's functions. Specifically, Green's functions are considered to be analytic functions of their kinematic variables; this property, in turn, relates their real and imaginary parts by the so-called dispersion relations.

In particular, let us recall that if a complex function $f(z)$ is analytic in the interior of and
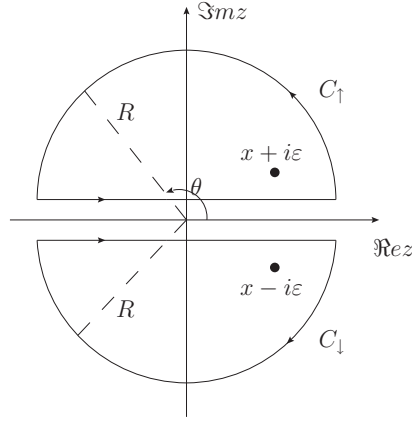
Fig. 17. Contours of complex integration for the dispersion relations

upon a closed curve, say $C_\uparrow$ in Fig. 17, and $x + i\varepsilon$ (with $x, \varepsilon \in \mathbb{R}$ and $\varepsilon > 0$) is a point within the closed curve $C_\uparrow$, we then have the Cauchy's integral form,

$$f(x + i\varepsilon) = \frac{1}{2\pi i} \oint_{C_\uparrow} dz \, \frac{f(z)}{z - x - i\varepsilon} , \tag{2.114}$$

where $\oint$ denotes that the path $C_\uparrow$ is singly wound. Using Schwartz's reflection principle, one also obtains

$$f(x - i\varepsilon) = -\frac{1}{2\pi i} \oint_{C_\downarrow} dz \, \frac{f(z)}{z - x + i\varepsilon} . \tag{2.115}$$

Note that $C_\uparrow^* = C_\downarrow$. Sometimes, an analytic function is called holomorphic; both terms are equivalent for complex functions.

Then, let us assume that the analytic function $f(z)$ has the asymptotic behavior, $|f(z)| \leq C/R^k$, for large radii R with C a real non-negative constant and $k > 0$. Taking the limit $\varepsilon \to 0$, it is easy to evaluate $\Re e f(x)$ through

$$2\Re e f(x) = \text{`}\lim_{\varepsilon \to 0}\text{'} \left[ f(x + i\varepsilon) + f^*(x - i\varepsilon) \right] = \text{`}\lim_{\varepsilon \to 0}\text{'} \frac{1}{\pi} \int_{-\infty}^{+\infty} dx' \, \Im m \left(\frac{f(x')}{x' - x - i\varepsilon} \right) + \Gamma_\infty. \tag{2.116}$$

Here, '$\lim_{\varepsilon \to 0}$' means that the limit should be taken *after* the integration has been performed, and

$$\Gamma_\infty = \frac{1}{\pi} \lim_{R \to \infty} \Re e \int_0^\pi d\theta \, f(Re^{i\theta}) . \tag{2.117}$$

Because of the assumed asymptotic behavior of $f(z)$ at infinity, the integral over the upper infinite semicircle in Fig. 17 can be easily shown to vanish: $\Gamma_\infty = 0$. Then, employing the well-known identity for distributions,

$$\text{`}\lim_{\varepsilon \to 0}\text{'} \frac{1}{x' - x - i\varepsilon} = \mathrm{P}\frac{1}{x' - x} + i\pi\delta(x' - x), \tag{2.118}$$

43

we arrive at the unsubtracted dispersion relation,

$$\Re ef(x) = \frac{1}{\pi} \mathrm{P} \int\limits_{-\infty}^{+\infty} dx' \frac{\Im mf(x')}{x'-x}. \tag{2.119}$$

where the "P" denotes the principle value of the integral. Following similar arguments, one can express the imaginary part of $f(x)$ as an integral over $\Re ef(x)$.

In the previous derivation, the assumption that $|f(z)|$ approaches zero sufficiently fast at infinity has been crucial, since it guarantees that $\Gamma_\infty \to 0$. However, if this assumption does not hold, additional subtractions need be included in order to arrive at a finite expression. For instance, for $|f(z)| \le CR^k$ with $k < 1$, it is sufficient to carry out a single subtraction at a point $x = a$. In this way, one has

$$\Re ef(x) = \Re ef(a) + \frac{(x-a)}{\pi} \mathrm{P} \int\limits_{-\infty}^{+\infty} dx' \frac{\Im mf(x')}{(x'-a)(x'-x)}. \tag{2.120}$$

From Eq. (2.120), it is obvious that $\Re ef(x)$ can be obtained from $\Im mf(x)$, up to an unknown, real constant $\Re ef(a)$. Usually, the point a is chosen in a way such that $\Re ef(a)$ takes a specific value on account of some physical requirement or normalization condition.

To see how analyticity works in a simple case, let us return to the scalar self-energy $\Pi(s)$ of Eq. (2.109). Setting $q^2 = s$, and defining the "velocity"

$$\beta(s, m^2) \equiv (1 - 4m^2/s)^{1/2} = s^{-1}\lambda^{1/2}(s, m^2, m^2), \tag{2.121}$$

a standard integration yields

$$\Pi(s, m^2) = \frac{\lambda^2}{32\pi^2} \left[\frac{2}{\epsilon} - \gamma_E + \ln \frac{4\pi\mu^2}{m^2} + 2 - \beta(s) \ln \frac{\beta(s, m^2) + 1}{\beta(s, m^2) - 1} \right], \tag{2.122}$$

where s should be analytically continued to $s + i\varepsilon$. In fact, for $s > 4m^2$, the logarithmic function in Eq. (2.122) assumes the form

$$\ln \frac{1 + \beta(s, m^2)}{1 - \beta(s, m^2)} - i\pi\theta(s - 4m^2). \tag{2.123}$$

Evidently, the absorptive part of $\Pi(s)$ obtained from Eq. (2.122) is equal to the $\Im m\Pi(s)$ appearing in Eq. (2.113). Furthermore, one can verify the validity of the dispersion relation of Eq. (2.120), singly subtracted at $s = 0$. Since

$$\Pi(0, m^2) = \frac{\lambda^2}{32\pi^2} \left[\frac{2}{\epsilon} - \gamma_E + \ln \frac{4\pi\mu^2}{m^2} \right], \tag{2.124}$$

the renormalized $\Pi(s)$ is obtained simply as $\Pi_\mathrm{R}(s, m^2) = \Pi(s, m^2) - \Pi(0, m^2)$. Noting that $\Im m\Pi(s, m^2) = \Im m\Pi_\mathrm{R}(s, m^2)$ (the divergent parts have to be real in order for the hermiticity of the Lagrangian to be preserved), it is elementary to demonstrate that indeed (principle value

implied),

$$\Re e \Pi_{\mathrm{R}}(s, m^2) = \frac{s}{\pi} \int\limits_{4m^2}^{\infty} ds' \frac{\Im m \Pi(s', m^2)}{s'(s' - s)}. \tag{2.125}$$

The synergy between unitarity (OT) and analyticity (dispersion relations) constitutes the basis of the dynamical framework known from the sixties as "S-matrix theory" (see, *e.g.*, [71]). In the context relevant to our purposes, one may resort to this framework in order to (re)construct dynamically (at least in principle) a given Green's function. A possible procedure one may adopt to accomplish this is the following. The lhs of the OT is an experimentally measurable quantity: up to simple kinematic ingredients (flux-factors, etc) it can be identified with a physical cross-section. In fact, in the case of scalar theories or QED, the contributions of the *individual* sub-amplitudes $\mathcal{M}_\ell^{ij}$ to this cross-section may be projected out; for example, in the center-of-mass frame the $\mathcal{M}_\ell^{ij}$ display a different dependence on the scattering angle θ, which, in turn, allows their extraction from the entire cross-section. Then, through the lhs of the OT, the measured $\mathcal{M}_\ell^{ij}$ is identified with the imaginary part of the Green's function under construction, namely (up to trivial factors) the T_ℓ^{ii} (for example, the propagator, for $\ell = 1$). Having determined the $\Im m T_\ell^{ii}$ from the OT, the dispersion relation can finally furnish (up to subtractions) the real part of T_ℓ^{ii}.

2.5.2 *The fundamental s-t cancellation*

As already alluded to in the previous subsection, the strong version of the OT, expressed in Eq. (2.105), does not hold in general in the case of non-Abelian theories. This is so because, with the exception of certain gauges, the naive (diagrammatic) propagator-, vertex-, and box-like subamplitudes of each side are totally different. For example, in the case of the forward QCD process $q(p_1)\bar{q}(p_2) \to q(p_1)\bar{q}(p_2)$ the propagator-like part of the lhs, computed in the renormalizable gauges, is determined by cutting through one-loop graphs containing ξ-dependent gluon propagators and unphysical ghosts (omit quark-loops), while the propagator-like part of the rhs contains the polarization tensors corresponding to physical massless particles of spin 1 (two physical polarizations). This profound difference complicates the diagrammatic verification of the OT, and invalidates, at the same time, its stronger version.

As we will demonstrate in this subsection, the application of the PT on the rhs (the physical side) of the OT is tantamount to the explicit use of an underlying fundamental cancellation between s-channel and t-channel graphs [72,73]. This cancellation is exposed after the judicious combination of two fundamental WIs, one operating on the s-channel and one on the t-channel amplitude. This cancellation results in a non-trivial reshuffling of terms, which, in turn, allows for the definition of kinematically distinct contributions, to be denoted by $\widehat{\mathcal{M}}_\ell^{ij}$; interestingly enough, they correspond to the imaginary parts of the one-loop PT subamplitudes constructed in the previous section. Specifically, the PT subamplitudes satisfy the strongest version of the OT, *i.e.*,

$$\Im m \widehat{T}_\ell^{ii} = \frac{1}{2} \sum_j (2\pi)^4 \delta^{(4)}(P_j - P_i) \widehat{\mathcal{M}}_\ell^{ij}, \tag{2.126}$$

In other words, the strong version of the OT holds iff the identification of the subamplitudes on each side occurs *after* the application of the PT.
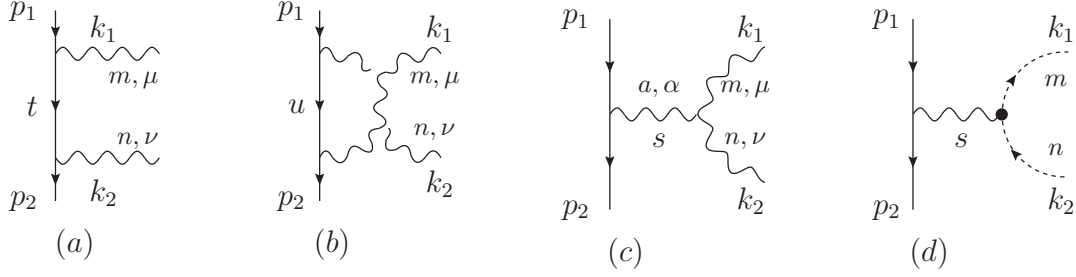
Fig. 18. Diagrams defining the amplitudes $\mathcal{T}_t$ [graphs (a) and (b)] and $\mathcal{T}_s$ [graph (c)]. Diagram (d) will contribute to the amplitude $\mathcal{S}$ defined in Eq. (2.138).

To see all this in detail, we consider the forward scattering process $q(p_1)\bar{q}(p_2) \to q(p_1)\bar{q}(p_2)$, and concentrate on the OT to lowest order. Obviously, the intermediate states appearing on the rhs may involve quarks or gluons. The quarks can be treated essentially as in QED, and are, in that sense, completely straightforward. We will therefore focus on the part of the OT where the intermediate states are two gluons; we have that

$$\Im m\langle q\bar{q}|T|q\bar{q}\rangle = \frac{1}{2} \times \frac{1}{2} \int_{\mathrm{PS}_{gg}} \langle q\bar{q}|T|gg\rangle\langle gg|T|q\bar{q}\rangle^*. \tag{2.127}$$

The extra $\frac{1}{2}$ factor is statistical and arises from the fact that the final on-shell gluons should be considered as identical particles in the total rate.

In Eq. (2.127) we set for the lhs $T \equiv \langle q\bar{q}|T|q\bar{q}\rangle$ and for the rhs $\mathcal{T} \equiv \langle q\bar{q}|T|gg\rangle$ and $\mathcal{M} \equiv \mathcal{T}\mathcal{T}^*$. Let us now focus on the rhs of Eq. (2.127). Diagrammatically, the tree-level amplitude $\mathcal{T}$ consists of two distinct parts: t and u-channel graphs that contain an internal quark propagator, $\mathcal{T}_{t\mu\nu}^{mn}$, as shown in diagrams (a) and (b) of Fig. 18, and an s-channel amplitude, $\mathcal{T}_{s\mu\nu}^{mn}$, given in diagram (c) of that same figure. The subscript s and t refers as usual to the corresponding Mandelstam variables, $i.e.$, $s = q^2 = (p_1 + p_2)^2 = (k_1 + k_2)^2$, and $t = (p_1 - k_1)^2 = (p_2 - k_2)^2$.

Defining the analogue of Eq. (2.32) for these kinematics, namely

$$i\mathcal{V}_\rho^a(p_2, p_1) = \bar{v}(p_2)igt^a\gamma_\rho u(p_1), \tag{2.128}$$

we have that

$$\mathcal{T}_{\mu\nu}^{mn} = \mathcal{T}_{s\mu\nu}^{mn} + \mathcal{T}_{t\mu\nu}^{mn}, \tag{2.129}$$

with

$$\mathcal{T}_{s\mu\nu}^{mn} = -gf^{amn}\mathcal{V}^{a\rho}\Delta_{\rho\alpha}^{(0)}(q,\xi)\Gamma_{\mu\nu}^\alpha(q,-k_1,-k_2),$$
$$\mathcal{T}_{t\mu\nu}^{mn} = -ig^2\bar{v}(p_2)\left[t^n\gamma_\nu S^{(0)}(p_1-k_1)t^m\gamma_\mu + t^m\gamma_\mu S^{(0)}(p_1-k_2)\gamma_\nu t^n\right]u(p_1). \tag{2.130}$$

We then have

$$\mathcal{M} = \mathcal{T}_{\mu\nu}^{mn}L^{\mu\mu'}(k_1)L^{\nu\nu'}(k_2)\mathcal{T}_{\mu'\nu'}^{mn*}$$
$$= [\mathcal{T}_s + \mathcal{T}_t]_{\mu\nu}^{mn}L^{\mu\mu'}(k_1)L^{\nu\nu'}(k_2)[\mathcal{T}_s^* + \mathcal{T}_t^*]_{\mu'\nu'}^{mn}, \tag{2.131}$$

46

where the polarization tensor $L^{\mu\nu}(k)$ corresponding to a massless spin one particle is given by

$$L_{\mu\nu}(k) \;=\; -g_{\mu\nu} + \frac{n_\mu k_\nu + n_\nu k_\mu}{n \cdot k} + \eta^2 \frac{k_\mu k_\nu}{(n \cdot k)^2} \,. \tag{2.132}$$

Notice that in accordance with Eq. (2.127), the rhs of Eq. (2.131) is inside the phase space integral $\frac{1}{4} \int_{\mathrm{PS}_{gg}}$, which we will suppress for simplicity. Also, the auxiliary four-vectors n_μ are unphysical, and any dependence on them must cancel in a physical process. The same holds for the parameter η^2, which acts as a gauge-fixing term.

It is clear now that if we were to apply at this point the same criterion for determining the $\mathcal{M}_\ell$ as in the scalar case [see Eqs (2.107)] we would get (we suppress Lorentz and color indices)

$$
\begin{aligned}
\mathcal{M}_1 &= \mathcal{T}_s L(k_1) L(k_2) \mathcal{T}_s^* , \\
\mathcal{M}_2 &= \mathcal{T}_s L(k_1) L(k_2) \mathcal{T}_t^* + \mathcal{T}_t L(k_1) L(k_2) \mathcal{T}_s^* , \\
\mathcal{M}_3 &= \mathcal{T}_t L(k_1) L(k_2) \, \mathcal{T}_t^* .
\end{aligned}
\tag{2.133}
$$

However, the $\mathcal{M}_\ell$ appearing in the equations above cannot play the role of the subamplitudes appearing on the rhs of the strong version of OT, for at least one obvious reason: they depend explicitly on the unphysical n_μ and η^2. This is the crux of the matter: the cancellation of n_μ and η^2 at the level of the entire $\mathcal{M}$ becomes possible only by combining contributions between the s- and the t-channel graphs. It is only *after* this cancellation has taken place that the criterion of Eqs (2.107) may be used to define the $\widehat{\mathcal{M}}_\ell^{ij}$ that will appear on the rhs of Eq. (2.126).

We now study the above points concretely. Before turning to the n_μ and η^2 cancellations, let us demonstrate the cancellation of gfp inside the off-shell tree-level gluon propagator, $\Delta_{\mu\nu}^{(0)}(q, \xi)$, appearing in the s-channel graph. To that end note that the external quark current is conserved, namely $q^\rho \mathcal{V}_\rho^a = 0$. In addition, we have that for "on-shell" gluons, *i.e.*, for $k^2 = 0$, $k^\mu L_{\mu\nu}(k) = 0$. By virtue of this last property, we see immediately that if we carry out the PT decomposition of Eq. (2.38) to the three-gluon vertex Γ, the term Γ^{P} vanishes after being contracted with the polarization vectors, and only the Γ^{F} piece of the vertex survives. Then, it is immediate to verify that the longitudinal (gfp-dependent) parts of $\Delta^{(0)}$ either vanish because of current conservation, or because they trigger the WI

$$q^\alpha \Gamma_{\alpha\mu\nu}^{\mathrm{F}}(q, -k_1, -k_2) = g_{\mu\nu}(k_1^2 - k_2^2), \tag{2.134}$$

which vanishes on-shell. This last WI is crucial because, in general, current conservation alone is not sufficient to guarantee the gfp-independence of the final answer. Clearly, in the covariant gauges the gauge fixing term is proportional to $q^\mu q^\nu$ and therefore current conservation ensures that such a term vanishes. However, had we chosen an axial gauge instead, the gluon propagator would be of the form

$$\Delta_{\mu\nu}^{(0)}(q, \tilde{\eta}) = \frac{L_{\mu\nu}(q, \tilde{n}, \tilde{\eta})}{q^2}, \tag{2.135}$$

where $\tilde{n} \neq n$ in general; then only the term $\tilde{\eta}_\nu q_\mu$ vanishes because of current conservation, whereas the term $\tilde{n}_\nu q_\mu$ can only disappear if Eq. (2.134) holds. Thus, either way, Eq. (2.131) finally becomes

$$\mathcal{M} = \frac{1}{4}(\mathcal{T}_s^{\mathrm{F}} + \mathcal{T}_t)_{\mu\nu}^{mn} L^{\mu\mu'}(k_1) \, L^{\nu\nu'}(k_2)(\mathcal{T}_s^{\mathrm{F}} + \mathcal{T}_t)_{\mu'\nu'}^{mn*}, \tag{2.136}$$

where the gfp-independent quantity $\mathcal{T}_s^{\mathrm{F}}$ is given by

$$\mathcal{T}_{s\,\mu\nu}^{\mathrm{F},mn} = gf^{amn}g^{\rho\alpha}d(q^2)\Gamma_{\alpha\mu\nu}^{\mathrm{F}}(q,-k_1,-k_2)\mathcal{V}_\rho^a. \tag{2.137}$$

We now want to show that the dependence on the unphysical quantities n_μ and η^2, coming from the polarization vectors, disappears. The exact way this happens is very instructive, and can be traced to a very particular cancellation operating between the s- and t- channel components. This cancellation, in turn, is crucial for the PT construction (and its all-order generalization, see Section 6), because it captures precisely the mechanism that enforces the corresponding cancellations inside Feynman diagrams (where the gluons are off-shell).

To see this s-t cancellation in detail, let us first define the quantities $\mathcal{S}^{mn}$ and $\mathcal{R}_\mu^{mn}$ as follows:

$$\mathcal{S}^{mn} = \frac{1}{2}gf^{amn}d(q^2)(k_1 - k_2)^\mu\mathcal{V}_\mu^a,$$
$$\mathcal{R}_\mu^{mn} = gf^{amn}\mathcal{V}_\mu^a, \tag{2.138}$$

which are related by

$$k_1^\mu\mathcal{R}_\mu^{mn} = -k_2^\mu\mathcal{R}_\mu^{mn} = q^2\mathcal{S}^{mn}. \tag{2.139}$$

Second, using the conditions $k_1^2 = k_2^2 = 0$, together with current conservation, $q^\rho\mathcal{V}_\rho^a = 0$, we obtain the elementary WIs

$$k_1^\mu\Gamma_{\alpha\mu\nu}^{\mathrm{F}}(q,-k_1,-k_2) = -q^2g_{\alpha\nu} + (k_1 - k_2)_\alpha k_{2\nu},$$
$$k_2^\nu\Gamma_{\alpha\mu\nu}^{\mathrm{F}}(q,-k_1,-k_2) = q^2g_{\alpha\mu} + (k_1 - k_2)_\alpha k_{1\mu}. \tag{2.140}$$

Now the crucial point is that the q^2 term on the rhs of the above WIs will cancel against the $d(q^2)$ inside $\mathcal{T}_s^{\mathrm{F}}$, allowing the communication of this part with the (contracted) t-channel graph. Specifically, we will have

$$k_1^\mu\mathcal{T}_{s\,\mu\nu}^{\mathrm{F},mn} = 2k_{2\nu}\mathcal{S}^{mn} - \mathcal{R}_\nu^{mn},$$
$$k_2^\nu\mathcal{T}_{s\,\mu\nu}^{\mathrm{F},mn} = 2k_{1\mu}\mathcal{S}^{mn} + \mathcal{R}_\mu^{mn},$$
$$k_1^\mu\mathcal{T}_{t\,\mu\nu}^{mn} = \mathcal{R}_\nu^{mn},$$
$$k_2^\nu\mathcal{T}_{t\,\mu\nu}^{mn} = -\mathcal{R}_\mu^{mn}, \tag{2.141}$$

so that, evidently,

$$k_1^\mu[\mathcal{T}_s^{\mathrm{F}} + \mathcal{T}_t]_{\mu\nu}^{mn} = 2k_{2\nu}\mathcal{S}^{mn},$$
$$k_2^\nu[\mathcal{T}_s^{\mathrm{F}} + \mathcal{T}_t]_{\mu\nu}^{mn} = 2k_{1\mu}\mathcal{S}^{mn}. \tag{2.142}$$

This is the s-t cancellation [72,73]: the term $\mathcal{R}$ comes with opposite sign, and drops out in the sum. In addition, notice also that

$$k_1^\mu k_2^\nu \mathcal{T}_{s\,\mu\nu}^{\mathrm{F},mn} = q^2 \mathcal{S}^{mn},$$
$$k_1^\mu k_2^\nu \mathcal{T}_{t\,\mu\nu}^{mn} = -q^2 \mathcal{S}^{mn}. \tag{2.143}$$

Using the above results, it is now easy to check that indeed, all dependence on both n_μ and η^2 cancels in Eq. (2.136), as it should, and we are finally left with (omitting the fully contracted color and Lorentz indices)

$$\mathcal{M} = \left(\mathcal{T}_s^{\mathrm{F}} \mathcal{T}_s^{\mathrm{F}*} - 8\mathcal{S}\mathcal{S}^* \right) + \left(\mathcal{T}_s^{\mathrm{F}} \mathcal{T}_t^* + \mathcal{T}_s^{\mathrm{F}*} \mathcal{T}_t \right) + \mathcal{T}_t \mathcal{T}_t^* \tag{2.144}$$

At this point we can naturally define the genuine propagator-like, vertex-like, and box-like sub-amplitudes, as in the scalar case, *i.e.*,

$$\widehat{\mathcal{M}}_1 = \mathcal{T}_s^{\mathrm{F}} \mathcal{T}_s^{\mathrm{F}*} - 8\mathcal{S}\mathcal{S}^*,$$
$$\widehat{\mathcal{M}}_2 = \mathcal{T}_s^{\mathrm{F}} \mathcal{T}_t^* + \mathcal{T}_s^{\mathrm{F}*} \mathcal{T}_t,$$
$$\widehat{\mathcal{M}}_3 = \mathcal{T}_t \mathcal{T}_t^*. \tag{2.145}$$

Let us now focus on $\widehat{\mathcal{M}}_1$; employing the relation

$$\Gamma_{\rho\mu\nu}^{\mathrm{F}} \Gamma_\alpha^{\mathrm{F},\mu\nu} = 8q^2 P_{\alpha\rho}(q) + 4(k_1 - k_2)_\alpha (k_1 - k_2)_\rho, \tag{2.146}$$

and

$$\mathcal{S}\mathcal{S}^* = \frac{1}{4} g^2 C_A \mathcal{V}_\alpha^a d(q^2) \left[(k_1 - k_2)^\alpha (k_1 - k_2)^\rho \right] d(q^2) \mathcal{V}_\rho^a, \tag{2.147}$$

we obtain for $\widehat{\mathcal{M}}_1$

$$\widehat{\mathcal{M}}_1 = g^2 C_A \mathcal{V}_\mu^a d(q^2) \left[8q^2 P^{\mu\nu}(q) + 2(k_1 - k_2)^\mu (k_1 - k_2)^\nu \right] d(q^2) \mathcal{V}_\nu^a, \tag{2.148}$$

and the propagator-like part of the rhs of the OT reads

$$(\mathrm{rhs})_1 = \frac{1}{2} \times \frac{1}{2} \int_{\mathrm{PS}_{gg}} \widehat{\mathcal{M}}_1. \tag{2.149}$$

Using the result of Eq. (2.112), together with the additional general formula

$$\int_{\mathrm{PS}} (k_1 - k_2)_\mu (k_1 - k_2)_\nu = -\frac{\lambda(q^2, m_1^2, m_2^2)}{3q^2} P_{\mu\nu}(q) \int_{\mathrm{PS}}$$
$$+ \left[\frac{\lambda(q^2, m_1^2, m_2^2)}{q^2} - q^2 + 2(m_1^2 + m_2^2) \right] \frac{q_\mu q_\nu}{q^2} \int_{\mathrm{PS}}, \tag{2.150}$$

we obtain for the case of two massless gluons in the final state

$$\int_{\mathrm{PS}_{gg}} = \frac{1}{8\pi},$$
$$\int_{\mathrm{PS}_{gg}} (k_1 - k_2)_\mu (k_1 - k_2)_\nu = -\frac{1}{8\pi} \frac{1}{3} q^2 P_{\mu\nu}(q), \tag{2.151}$$

49

and thus (2.149) becomes

$$(\text{rhs})_1 = \mathcal{V}_a^\mu d(q^2)\pi bg^2 q^2 P_{\mu\nu}(q) d(q^2)\mathcal{V}_a^\nu. \tag{2.152}$$

On the other hand, for the propagator-like part of the lhs of the OT we have

$$(\text{lhs})_1 = \Im m \widehat{T}_1 = \mathcal{V}_\mu^a d(q^2)\Im m \widehat{\Pi}^{\mu\nu}(q) d(q^2)\mathcal{V}_\nu^a, \tag{2.153}$$

Equating (2.152) and (2.153) we finally obtain

$$\Im m \widehat{\Pi}_{\mu\nu}(q) = \pi bg^2 q^2 P_{\mu\nu}(q). \tag{2.154}$$

Let us now write the (dimensionful) $\widehat{\Pi}(q^2)$ introduced in Eq. (2.77) as $\widehat{\Pi}(q^2) = q^2\widehat{\mathbf{\Pi}}(q^2)$. From (2.154) we have that $\Im m \widehat{\mathbf{\Pi}}(q^2) = \pi bg^2$, with the renormalized $\widehat{\mathbf{\Pi}}_R(q^2)$ given by

$$\widehat{\mathbf{\Pi}}_R(q^2) = \widehat{\mathbf{\Pi}}(q^2) - \widehat{\mathbf{\Pi}}(\mu^2), \tag{2.155}$$

and from the corresponding single subtraction dispersion relation

$$\Re e\widehat{\mathbf{\Pi}}_R(q^2) = \int_0^\infty ds \left[\frac{1}{s-q^2} - \frac{1}{s-\mu^2}\right] \frac{\Im m\widehat{\mathbf{\Pi}}(s)}{\pi}$$

$$= -bg^2 \ln \frac{q^2}{\mu^2}. \tag{2.156}$$

We emphasize that the above procedure furnishes an alternative way for constructing the gfp-independent PT Green's functions at one-loop, for *every* gauge-fixing scheme. Indeed, in our derivation we have solely relied on the rhs of the OT, which we have rearranged in a well-defined way, *after* having explicitly demonstrated its gfp-independence. The proof of the gfp-independence of the rhs presented here is, of course, expected on physical grounds, and it only relies on the use of WIs, triggered by the longitudinal parts of the tree-level gluon propagators. Since the gfp-dependence at the level of the Feynman rules is carried entirely by the longitudinal parts of the gluon tree-level propagator, its cancellation at the level of $\mathcal{M}$ proceeds exactly as described before Eq. (2.137). Obviously, the final step of reconstructing the real part from the imaginary by means of a (once subtracted) dispersion relation does not introduce any new gauge-dependences.

In addition, in the context of theories with tree-level (spontaneous) symmetry breaking (such as the electroweak theory) the lhs of the OT contains, in general, would-be Goldstone bosons or ghost fields, with gfp-dependent masses. Such contributions manifest themselves as unphysical cuts, *e.g.*, at $q^2 = \xi M_W^2$ for a W propagator in the renormalizable R_ξ gauges, and, eventually, as unphysical thresholds, at *e.g.*, $s = 4\xi M_W^2$. However, unitarity requires that these unphysical contributions should vanish, as can be read off from the rhs of Eq. (2.102). As we will see in detail in Section 5, this observation is of central importance when devising a gauge-invariant resummation formalism for resonant transition amplitudes [23,74–76].

3 The background field method and its correspondence with the PT

As we have seen in the previous section, in the conventional formulation of gauge theories the Lagrangian $\mathcal{L}$– consisting of the classical term plus the gauge-fixing and Faddeev-Popov ghost terms– is no longer gauge invariant, but rather BRST invariant. As a consequence, off-shell Green's functions satisfy complicated STIs reflecting BRST invariance. In this context we have seen how the PT implements a rearrangement of the perturbative series, that allows the construction of *effective* one-loop Green's functions which, among several other important properties, satisfy naive, QED-like WIs.

It turns out that there exists a formal framework, known as the background field method (BFM), which gives rise to Green's functions that satisfy automatically this last property (but not all others).

The BFM was initially introduced at the one-loop level [28,29,31,32,77–83], and was generalized soon afterwards to higher orders [33,34,84–86]. In the BFM one arranges things such that the explicit gauge invariance present at the level of the classical Lagrangian is retained even after the gauge-fixing and ghost terms have been added. Thus, the (formally defined) off-shell Green's functions of the BFM obey the naive WIs dictated by gauge invariance, exactly as the (diagrammatically defined) PT Green's functions. Notice however two important points: The BFM Green's functions (*i*) depend explicitly on the (quantum) gfp, denoted by ξ_Q, and (*ii*) obey the aforementioned WIs for every value of ξ_Q. Thus one encounters a situation very similar to that of QED: the photon-electron vertex and the electron self-energy depend explicitly on the gfp, and for every value of the gfp they satisfy the text-book WI of Eq. (2.58). The reason why the BFM has become so relevant in the study of the PT was the observation [40,41,60] that for a very simple choice of ξ_Q the BFM Green's functions become identical to those of the PT. This particular value is the BFG, $\xi_Q = 1$.

The purpose of this section is twofold. First, we introduce the BFM quantization, discussing its advantages over the conventional quantization formalism. Second, we will establish (at the one-loop level) the important correspondence between the PT and BFM Green's functions mentioned above. Since this correspondence will accompany us for the rest of this report, we will pay particular attention in explaining the conceptual differences that distinguish the PT from the BFM (for a related general discussion see also Section 1, as well as subsection 5.4 for further physical arguments sharpening this distinction).

3.1 The background field method

Let us start by considering a theory describing a (scalar) field ϕ with an associated classical action

$$S[\phi] = \int d^4x \mathcal{L}[\phi]. \tag{3.1}$$

The S-matrix of this theory can be derived from the knowledge of its corresponding Green's functions through the LSZ reduction formula (see below). The Green's functions of the theory can, in turn, be obtained by taking functional derivatives with respect to a suitable source J of

the generating functional

$$Z[J] = \int [d\phi]\, \mathrm{e}^{i\{S[\phi]+J\cdot\phi\}}, \qquad J\cdot\phi = \int d^4x\, J(x)\phi(x). \tag{3.2}$$

The functional integral appearing in the equation above is performed over all the possible configurations of the field ϕ. The disconnected Green's functions of the theory are then defined through the relation

$$\langle 0|T(\phi\cdots\phi)|0\rangle = \int [d\phi](\phi\cdots\phi)\, \mathrm{e}^{iS[\phi]} = \left(\frac{1}{i}\frac{\delta}{\delta J}\right)^n Z[j]\bigg|_{J=0}. \tag{3.3}$$

Since the disjoined pieces appearing in the Green's function do not contribute to the S-matrix, it is more convenient to work with the connected Green's functions which are generated by taking functional derivatives with respect to the source J of the generating functional $W[J]$ defined as

$$\mathrm{e}^{iW[J]} = Z[J]. \tag{3.4}$$

Finally, yet another simplification can be achieved by expressing connected Green's functions in terms of 1PI pieces, which are generated by the effective action defined through the Legendre transform

$$\Gamma[\overline{\phi}] = W[J] - J\cdot\overline{\phi}, \tag{3.5}$$

where

$$\overline{\phi} = \frac{\delta W}{\delta J}. \tag{3.6}$$

Notice the difference between ϕ and $\overline{\phi}$; since

$$\overline{\phi} = -i\frac{1}{Z[J]}\frac{\delta}{\delta J}Z[J] = \frac{\langle 0|\phi|0\rangle_J}{\langle 0|0\rangle_J}, \tag{3.7}$$

we see that $\overline{\phi}$ corresponds to the vacuum expectation value of the field ϕ in the presence of a source J. In particular notice that the equation

$$\frac{\delta\Gamma}{\delta\overline{\phi}} = -J, \tag{3.8}$$

corresponds to the quantum mechanical field equation for $\overline{\phi}$, which replaces the classical field equation

$$\frac{\delta S}{\delta\phi} = -J, \tag{3.9}$$

in the quantized theory.

Thus, the key quantity to calculate in field theories is the effective action (3.5), because, once it is known, the S-matrix can be constructed through the LSZ reduction formula, *i.e.*, by stringing together trees of 1PI Green's functions (thus generating the connected ones), amputating external propagators, putting external momenta on-shell, and adding appropriate external wavefunctions renormalization factors.

At this stage the BFM can be seen as a convenient way of computing the effective action. Let

us begin by defining a new generating functional $\widetilde{Z}$ by shifting the argument of the classical action $S[\phi]$ appearing in Eq. (3.1) by an arbitrary background field φ independent of J:

$$\widetilde{Z}[J, \varphi] = \int [d\phi]\, e^{i\{S[\phi+\varphi]+J\cdot\phi\}}. \tag{3.10}$$

By analogy we can now go on and define $\widetilde{W}$ as

$$e^{i\widetilde{W}[J,\varphi]} = \widetilde{Z}[J, \varphi], \tag{3.11}$$

and, finally, the corresponding effective action

$$\widetilde{\Gamma}[J, \varphi] = \widetilde{W}[J, \varphi] - J \cdot \widetilde{\phi}, \tag{3.12}$$

with

$$\widetilde{\phi} = \frac{\delta \widetilde{W}}{\delta J}. \tag{3.13}$$

Therefore the background effective action constructed in Eq. (3.12) is a conventional effective action computed in the presence of a background field φ, and, as such, will give rise to 1PI Green's functions in the presence of this background field φ.

Let us now look for a connection between the generating functionals $\widetilde{Z}$ and Z. Shifting the variable of the functional integration in Eq. (3.10) through $\phi \to \phi - \varphi$, we arrive immediately at the relation

$$\widetilde{Z}[J, \varphi] = Z[J]\, e^{-iJ\cdot\varphi}, \tag{3.14}$$

and thus we are led to

$$\widetilde{W}[J, \varphi] = W[J] - J \cdot \varphi. \tag{3.15}$$

Differentiating this last equation with respect to J and taking into account the definitions of Eqs (3.6) and (3.13) we find

$$\widetilde{\phi} = \overline{\phi} - \varphi. \tag{3.16}$$

Finally, making use of Eqs (3.5) and (3.12) we find

$$\widetilde{\Gamma}[\widetilde{\phi}, \varphi] = W[J] - J \cdot (\widetilde{\phi} + \varphi) = \Gamma[\overline{\phi}] = \Gamma[\widetilde{\phi} + \varphi]. \tag{3.17}$$

As a special case of the above equation we can choose $\widetilde{\phi} = 0$ to get

$$\widetilde{\Gamma}[0, \varphi] = \Gamma[\varphi]. \tag{3.18}$$

Notice that the background effective action $\widetilde{\Gamma}[0, \varphi]$ has no dependence on $\widetilde{\phi}$, so that it can only generate 1PI vacuum graphs in the presence of the background field φ; on the other hand Eq. (3.18) tells us that the effective action of the theory can be obtained precisely by summing up all these vacuum diagrams. However, unless φ is a very simple background field (*e.g.*, a constant), the calculation of $\widetilde{\Gamma}[0, \varphi]$, treating φ exactly, is not possible. Thus, one needs to resort to a perturbative treatment of the background field φ, in which case the background field appearing in external lines is arbitrary, and does not need to be specified at all.

To pursue this latter approach, one starts generating Feynman rules from $\mathcal{L}[\phi + \varphi]$. From this process there will be two type of interaction vertex emerging: (*i*) those involving only ϕ

fields, which must be used inside diagrams only, and (*ii*) those involving ϕ and φ fields, which ought to be used in order to generate external lines. This, in turn, means that in the BFM one will calculate the same diagrams needed in the conventional formulation, with the only proviso that vertices appearing inside loops might have different Feynman rules compared to those connecting external legs.

3.2 Background field gauges

All the results discussed above for the simplified setting of a scalar field theory have analogs in non-Abelian gauge theories, with the obvious complications coming from the fact that, in the latter cases, one must choose a gauge fixing term; this, in turn, implies the appearance of the corresponding Faddeev-Popov ghost determinant. The generating functional for pure gluodynamics (since fermions play no role in the BFM construction they will be neglected in what follows) can be written as

$$Z[J] = \int [dA] \text{Det} \left[\frac{\delta \mathcal{F}^a}{\delta \theta^b} \right] e^{i\{S_\text{I}[A] + S_\text{GF}[A;\xi] + J \cdot A\}}, \qquad J \cdot A = \int d^4x\, J^a_\mu A^\mu_a. \tag{3.19}$$

The gauge invariant and gauge-fixing Lagrangian have been introduced in Section 2 and read

$$S_\text{I}[A] = \int d^4x\, \mathcal{L}^A_\text{I} = -\frac{1}{4} \int d^4x\, F^a_{\mu\nu} F^{\mu\nu}_a, \qquad S_\text{GF}[A;\xi] = \frac{1}{2\xi} \int d^4x\, \mathcal{F}^a \mathcal{F}^a, \tag{3.20}$$

with $\mathcal{F}^a$ the gauge fixing function; finally, $\delta \mathcal{F}^a / \delta \theta^b$ represents the derivative of the gauge fixing function with respect to the infinitesimal gauge transformation of the gluon field, see Eq. (2.6), with the determinant of this term expressing the result of the integral over the ghost and anti-ghost field variables of the Faddeev-Popov Lagrangian term, introduced in Eq. (2.7).

The background field generating functional can be defined in an way completely analogous to the scalar case [see Eq. (3.10)], namely [2]

$$\widetilde{Z}[J, \widehat{A}] = \int [dA] \text{Det} \left[\frac{\delta \widehat{\mathcal{F}}^a}{\delta \theta^b} \right] e^{i\left\{ S_\text{I}[A + \widehat{A}] + S_\text{GF}[A;\xi_Q] + J \cdot A \right\}}, \tag{3.21}$$

where now $\widehat{\mathcal{F}} = \widehat{\mathcal{F}}(A, \widehat{A})$, with $\delta \widehat{\mathcal{F}}^a / \delta \theta^b$ represents the derivative of the gauge fixing function with respect to an infinitesimal gauge transformation

$$\delta A^a_\mu = -\frac{1}{g} \partial_\mu \theta^a + f^{abc} \theta^b \left(\widehat{A}^c_\mu + A^c_\mu \right). \tag{3.22}$$

At this point, all quantities defined in the scalar case can be also defined here. Moreover, since the relation between normal and background quantities can be found, as before, by shifting

---

[2] From now on we will indicate background fields with a caret. Notice however that we will indicate Green's functions containing background fields with a tilde, to distinguish them from the PT ones.

the integration variable in the path integral through $A \to A - \widehat{A}$, one finds in analogy with Eq. (3.18),

$$\widetilde{\Gamma}[0, \widehat{A}] = \Gamma[\overline{A}]\big|_{\overline{A}=\widehat{A}}. \tag{3.23}$$

Notice that for arriving at this equation one has to write $\widetilde{Z}[J, \widehat{A}]$ in terms of $Z[J]$; this, as already said, can be easily done by shifting the integration variable. Thus, for Eq.(3.23) to be valid, if on the lhs the effective action is calculated using the gauge fixing function $\widehat{\mathcal{F}}(A, \widehat{A})$, then on the rhs we must use the gauge fixing function $\mathcal{F} = \widehat{\mathcal{F}}(A - \widehat{A}, \widehat{A})$ (and the gauge fixing parameter $\xi = \xi_Q$). Then, while it is clear that the BFM will give rise to different Green's functions with respect to those appearing in the conventional formalism, the gauge independence of the physical observables, together with Eq. (3.23), guarantee that one will finally obtain the same S-matrix.

The crucial feature that makes the BFM such an advantageous way of quantizing gauge theories is the following. There exist special choices of the gauge fixing function $\widehat{\mathcal{F}}$ for which the form of the BFM effective action $\widetilde{\Gamma}[0, \widehat{A}]$ is severely restricted, being a gauge invariant functional of $\widehat{A}$, $i.e.$, invariant under the gauge transformations

$$\delta \widehat{A}_\mu^a = -\frac{1}{g} \partial_\mu \widehat{\theta}^a + f^{abc} \widehat{\theta}^b \widehat{A}_\mu^c,$$
$$\delta J_\mu^a = -f^{abc} \widehat{\theta}^b J_\mu^c. \tag{3.24}$$

Notice that the (infinitesimal) parameter of the gauge transformations above has been denoted by $\widehat{\theta}$, because it is different from the one appearing in the gauge transformations of the quantum field A, shown $e.g.$, in Eq. (3.22). The (covariant) gauge fixing function that enforces the background gauge invariance is

$$\widehat{\mathcal{F}}^a = (\widehat{\mathcal{D}}^\mu A_\mu)^a$$
$$= \partial^\mu A_\mu^a + g f^{abc} \widehat{A}_\mu^b A_c^\mu, \tag{3.25}$$

where $\widehat{\mathcal{D}}^\mu$ is the covariant background field derivative.

In order to prove the invariance of the effective action under the transformations (3.24) and (3.24), we carry out the following change of variables in the functional integral appearing in Eq. (3.21)

$$A_\mu^a \to A_\mu'^a = A_\mu^a - f^{abc} \widehat{\theta}^b A_\mu^c = O^{ab}(\widehat{\theta}) A_\mu^b, \tag{3.26}$$

where

$$O^{ab}(\widehat{\theta}) = \delta^{ab} - f^{abc} \widehat{\theta}^c \tag{3.27}$$

is an orthogonal matrix representing a rotation by an infinitesimal amount $\widehat{\theta}$ in the vector space spanned by the generators of the $SU(N)$ gauge group. Thus it is clear that this change of variables leaves the integral measure invariant. Also, on the one hand, since both Eqs (3.24) and (3.26) represent adjoint group rotations, the term $J \cdot A$ is clearly invariant. On the other hand, one has that

$$\int [dA] \, \mathrm{e}^{iS[A+\widehat{A}]} \to \int [dA'] \, \mathrm{e}^{iS[A'+\widehat{A}+\delta(A+\widehat{A})]}, \tag{3.28}$$

with

$$\delta(A_\mu^a + \widehat{A}_\mu^a) = -\frac{1}{g}\partial_\mu\widehat{\theta}^a + f^{abc}\widehat{\theta}^b\left(\widehat{A}_\mu^c + A_\mu^c\right). \tag{3.29}$$

The latter represents a gauge transformation (with parameter $\widehat{\theta}$) of the $A + \widehat{A}$ field, so that also this part of the generating functional is invariant.

As far as the gauge fixing term is concerned, one has that it transforms as follows

$$\begin{aligned}\widehat{\mathcal{F}}(\widehat{A} + \delta\widehat{A}, A) &= \widehat{\mathcal{F}}^a(\widehat{A}, A) - f^{abc}\partial^\mu\left(\widehat{\theta}^b A_\mu^c\right) + gf^{abc}\widehat{\theta}^b\partial^\mu A_\mu^c + gf^{abc}f^{bde}\widehat{\theta}^d\widehat{A}_\mu^e A_c^\mu \\ &= \widehat{\mathcal{F}}^a(\widehat{A}, A') + f^{abc}\widehat{\theta}^b\widehat{\mathcal{F}}^c(\widehat{A}, A'),\end{aligned} \tag{3.30}$$

where in the last step the Jacobi identity has been used, and $\widehat{\theta}^2$ terms have been discarded. Thus we can write

$$\widehat{\mathcal{F}}^a(\widehat{A} + \delta\widehat{A}, A) = O_{ac}^{\mathrm{T}}\widehat{\mathcal{F}}^c(\widehat{A}, A'), \tag{3.31}$$

and therefore since $(\mathcal{F}^a)^2$ is manifestly invariant under orthogonal rotations, the background gauge invariance of the gauge fixing term is evident. Finally for the derivative term $\delta\widehat{\mathcal{F}}^a/\delta\theta^b$ one has the relation [42]

$$\frac{\delta}{\delta\theta^b}\mathcal{F}^a(\widehat{A} + \delta\widehat{A}, A^\theta(\widehat{A} + \delta\widehat{A})) = O^{T,ac}(\widehat{\theta})\frac{\delta}{\delta\widetilde{\theta}^b}\mathcal{F}^c(\widehat{A}, A'^{\widetilde{\theta}}(\widehat{A}))O^{db}(\widehat{\theta}), \tag{3.32}$$

where $\widetilde{\theta}^a = O^{ab}(\widehat{\theta})\theta^b$, and we have explicitly indicated the dependence of the variation of the quantum field A on the background field $\widehat{A}$ and the infinitesimal parameter θ. From the above identity follows that the determinant is also invariant, since the determinant of an orthogonal matrix is equal to 1. Thus, this concludes our proof of the gauge invariance of the background effective action.

Summarizing, the general idea behind the BFM is to first make a linear decomposition of the gauge field appearing in the classical action in terms of a background field, $\widehat{A}$, and the quantum field, A, which is the variable of integration in the path integral. Then, using the Faddeev-Popov quantization method, one eliminates the unphysical degrees of freedom of the gauge field by breaking the gauge invariance of the classical Lagrangian through a gauge fixing condition, which is usually taken to be of covariant form, even if such a choice may not be unique (see the next subsection). Most importantly, it is possible to choose a gauge fixing condition that is invariant under the gauge transformations of the background field $\widehat{A}$, so that the whole Lagrangian retains (background) gauge invariance with respect to the latter field, which only appears in external lines. The gauge symmetry is, however, explicitly broken by the quantum field A, which enters only in loops.

3.2.1 Generalized background gauges

An interesting question to ask is whether the gauge fixing function of Eq. (3.25) is unique. To address this issue, we start by noticing that, in order to get from the conventional R_ξ gauge fixing function $\partial^\mu A_\mu^a$ to the covariant background equivalent given in Eq. (3.25), it has been

sufficient to make the replacement

$$\delta^{ab}\partial_\mu \to \widehat{D}_\mu^{ab}, \tag{3.33}$$

where $\widehat{D}_\mu^{ab} = \widehat{D}_\mu^{ab}(\widehat{A}) = \delta^{ab}\partial_\mu + gf^{amb}\widehat{A}_\mu^m$. On the other hand, Eq. (3.30) tells us that the background covariant derivative transforms under the background gauge transformation (3.24) as

$$\widehat{D}_\mu^{ab}(\widehat{A} + \delta\widehat{A})A_\nu^b = O_{ab}^{\mathrm{T}}\widehat{D}_\mu^{bc}(\widehat{A})A_\nu'^b, \tag{3.34}$$

which, in turn, ensures that the corresponding Faddeev-Popov determinant transforms as in Eq. (3.32). In fact, we see that Eq. (3.34), together with the fact that the gauge fixing Lagrangian is given by the group space scalar product of the corresponding function, ensures that $\widehat{\mathcal{F}}^a$ leaves $Z[J, \widehat{A}]$ invariant under background field gauge transformations. Thus, using Eq. (3.33), all the non-covariant gauge fixing functions introduced in subsection 2.1 can be converted into background gauge fixing functions that preserve the background gauge invariance of the effective action.

3.3 Advantages over the conventional formalism

3.3.1 Preliminaries: Green's function and S-matrix calculation in the BFM

The background gauge invariance of the effective action $\widetilde{\Gamma}[0, \widehat{A}]$, imposes a drastic restriction on the form of the 1PI Green's functions generated by taking functional derivative of the background effective action with respect to the background fields $\widehat{A}$. In fact, exactly as happens in the Abelian (QED) case, these functions are forced to satisfy naive WIs rather than the usual STIs associated with the non-Abelian character of the theory.

BFM Green's functions are calculated starting from the shifted Lagrangian $\mathcal{L}_I[A, \widehat{A}]$, the gauge fixing term $\mathcal{L}_{\mathrm{GF}}^{\mathrm{BFM}} = \frac{1}{2\xi_Q}\widehat{\mathcal{F}}^a\widehat{\mathcal{F}}^a$, and the Faddeev-Popov determinant, which can be written in terms of an anti-commuting scalar field c, giving rise to the Faddeev-Popov ghost Lagrangian

$$\begin{aligned}
\mathcal{L}_{\mathrm{FPG}}^{\mathrm{BFM}} = {} & \partial^\mu\bar{c}^a\partial_\mu c^a + gf^{abc}(\partial^\mu\bar{c}^a)A_\mu^b c^c + gf^{abc}(\partial^\mu\bar{c}^a)\widehat{A}_\mu^b c^c - gf^{abc}\bar{c}^a\widehat{A}_\mu^b(\partial^\mu c^c) \\
& - g^2 f^{abe}f^{cde}\bar{c}^a\widehat{A}_\mu^b(A_c^\mu + \widehat{A}_\mu^c)c^d. \tag{3.35}
\end{aligned}$$

Notice the appearance of a modified ghost sector: the interactions between ghosts and background gluons are very characteristic, consisting of a symmetric $\widehat{A}c\bar{c}$ ghost vertex and a completely new, four particle vertex, $\widehat{A}\widehat{A}c\bar{c}$.

As discussed in the scalar case, vertices appearing inside loops contain only quantum fields A, while vertices involving the background field $\widehat{A}$ connect external lines. Notice that all the propagators ought to be those of the quantum fields, since gauge invariance is unbroken in the background sector, and therefore the $\widehat{A}$ propagator is not defined. The complete set of Feynman rules for QCD in the BFM gauge are reported in Appendix B. As a rule of thumb to remember what vertices we expect to have different Feynman rules, notice that the BFM covariant gauge fixing term is linear in the quantum fields A; therefore, apart from vertices involving ghost fields, only vertices containing exactly two quantum fields can differ from the conventional ones. Thus, for example, the vertex $\widehat{A}AAA$ will have to lowest order the same Feynman
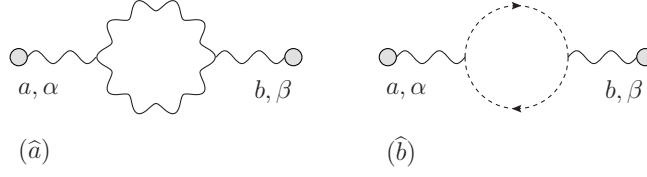
Fig. 19. Feynman diagrams contributing to the one-loop background gluon self-energy. Gray circles on external lines represent background fields. Seagull contribution are not shown since, perturbatively, they do not contribute to the self-energy.

rule as the conventional vertex $AAAA$. Despite the distinction between background and quantum fields, calculations in the BFM are, in general, simpler. This is particularly so in the BFG, where many vertices simplify considerably (see again Appendix B).

When calculating S-matrix elements from the BFM Feynman rules remember that fields inside loops (*i.e.*, fields irrigated by virtual momenta) are always quantum, while those irrigated by physical momentum transfers are background. As a result, box diagrams are exactly the same as in the conventional case, *i.e.*, all fields are quantum. On the other hand, self-energy and vertex diagrams are attached to the on-shell particles by background gluons, having quantum gluons and quarks inside their loops. Note also that, eventually, one must choose a gauge for the background fields $\widehat{A}$ as well, which is completely unrelated to the gauge used for the quantum fields. For example, the propagators inside the loops may be in the BFG, while the background propagators in the axial gauge. After the background gauge is fixed, the background field propagator is well-defined, and one can use it to build up strings of 1PI functions, thus generating the connected Green's functions. Finally, the S-matrix will be determined from the LSZ reduction formula.

3.3.2 Special transversality properties of the BFM

To show what are the simplifications that the explicit preservation of gauge invariance implies at the practical level, let us consider the calculation of the gluon two-point function. The diagrams contributing to the one-loop background gluon self-energy are shown in Fig. 19 (seagull terms do not contribute due to the dimensional regularization result $\int_k k^{-2} = 0$). Choosing the background Feynman gauge (the β function being, of course, a ξ-independent quantity) and using the BFM Feynman rules reported in Appendix B one has

$$(\widehat{a})_{\alpha\beta} = g^2 \frac{C_A}{2} \int_k \frac{1}{k^2(k+q)^2} \widehat{\Gamma}_{\alpha\mu\nu}(q, -k-q, k)\widehat{\Gamma}_\beta^{\mu\nu}(q, -k-q, k),$$

$$(\widehat{b})_{\alpha\beta} = -g^2 C_A \int_k \frac{1}{k^2(k+q)^2}(2k+q)_\alpha(2k+q)_\beta, \qquad (3.36)$$

Introducing, then, the function

$$f(q^2, \epsilon) = i\frac{C_A}{3}\frac{g^2}{(4\pi)^2}\Gamma\left(\frac{\epsilon}{2}\right)\left(\frac{q^2}{\mu^2}\right)^{-\frac{\epsilon}{2}}, \qquad (3.37)$$

58

(Γ being the Euler gamma function) we get [3]

$$\begin{cases} (\widehat{a})_{\alpha\beta} = 10 f(q^2, \epsilon) q^2 P_{\alpha\beta}(q), \\ (\widehat{b})_{\alpha\beta} = f(q^2, \epsilon) q^2 P_{\alpha\beta}(q), \end{cases} \quad \Rightarrow \quad \widetilde{\Pi}^{(1)}_{\alpha\beta}(q) = 11 f(q^2, \epsilon) q^2 P_{\alpha\beta}(q). \qquad (3.38)$$

Notice that each of the contributions above is individually transverse, as a result of background gauge invariance. This is to be contrasted with $e.g.$, the R_ξ result, where

$$(a)_{\alpha\beta} = g^2 \frac{C_A}{2} \int_k \frac{1}{k^2(k+q)^2} \Gamma_{\alpha\mu\nu}(q, -k-q, k) \Gamma^{\mu\nu}_\beta(q, -k-q, k),$$

$$(b)_{\alpha\beta} = -g^2 C_A \int_k \frac{1}{k^2(k+q)^2} k_\alpha (k+q)_\beta, \qquad (3.39)$$

and (a) and (b) are the diagrams corresponding to those shown in Fig. 19, when the external gluons are quantum gluons. Carrying out the integrals, we obtain

$$\begin{cases} (a)_{\alpha\beta} = \frac{1}{4} f(q^2, \epsilon) \left(19 q^2 g_{\alpha\beta} - 22 q_\alpha q_\beta\right) \\ (b)_{\alpha\beta} = \frac{1}{4} f(q^2, \epsilon) \left(q^2 g_{\alpha\beta} + 2 q_\alpha q_\beta\right) \end{cases} \quad \Rightarrow \quad \Pi^{(1)}_{\alpha\beta}(q) = 5 f(q^2, \epsilon) q^2 P_{\alpha\beta}(q).$$

Thus, while the sum of the two diagrams results in a transverse one-loop gluon self-energy (as it should), the individual diagrams are not transverse.

At two loops the diagrams to be calculated are shown in Fig. 20. Let us start by noticing that out of these diagrams one can form combinations that corresponds to the one-loop dressed gluonic and ghost contributions, and two-loop (dressed) gluonic and ghost contributions. Using the notation of Fig. 77, one has respectively

$$[(d_1) + (d_2)]^{(2)} = (a) + \frac{1}{2}[(b) + (c)] + (d) + (g) + (h) + \frac{1}{2}[(q) + (r)],$$

$$[(d_3) + (d_4)]^{(2)} = (e) + (f) + (i) + (j) + (k) + \frac{1}{2}[(m) + (n) + (o) + (p)],$$

$$[(d_5) + (d_6)]^{(2)} = \frac{1}{2}[(b) + (c)] + (\ell),$$

$$[(d_7) + (d_8) + (d_9) + (d_{10})]^{(2)} = \frac{1}{2}[(q) + (r)] + (s) + \frac{1}{2}[(m) + (n) + (o) + (p)], \quad (3.40)$$

and focussing on the divergent parts of the diagrams, we obtain [34]

---

[3] Notice that from this result, and the fact that in the BFM $Z_g = Z_{\widehat{A}}^{-\frac{1}{2}}$ one immediately obtains that $\beta^{(1)} = -\frac{11}{3} C_A \frac{g_R^3}{(4\pi)^2}$. This has to be contrasted with the conventional formalism ($e.g.$, R_ξ gauges), where in order to get Z_g one must calculate the divergent parts of the gauge and ghost self-energies, as well as the ghost-gauge vertex [87–89].

$$a,\alpha \qquad b,\beta$$

$$(a) \qquad\qquad (b) \qquad\qquad (c) \qquad\qquad (d)$$

$$(e) \qquad\qquad (f) \qquad\qquad (g) \qquad\qquad (h)$$

$$(i) \qquad\qquad (j) \qquad\qquad (k) \qquad\qquad (\ell)$$

$$(m) \qquad\qquad (n) \qquad\qquad (o) \qquad\qquad (p)$$

$$(q) \qquad\qquad (r) \qquad\qquad (s)$$
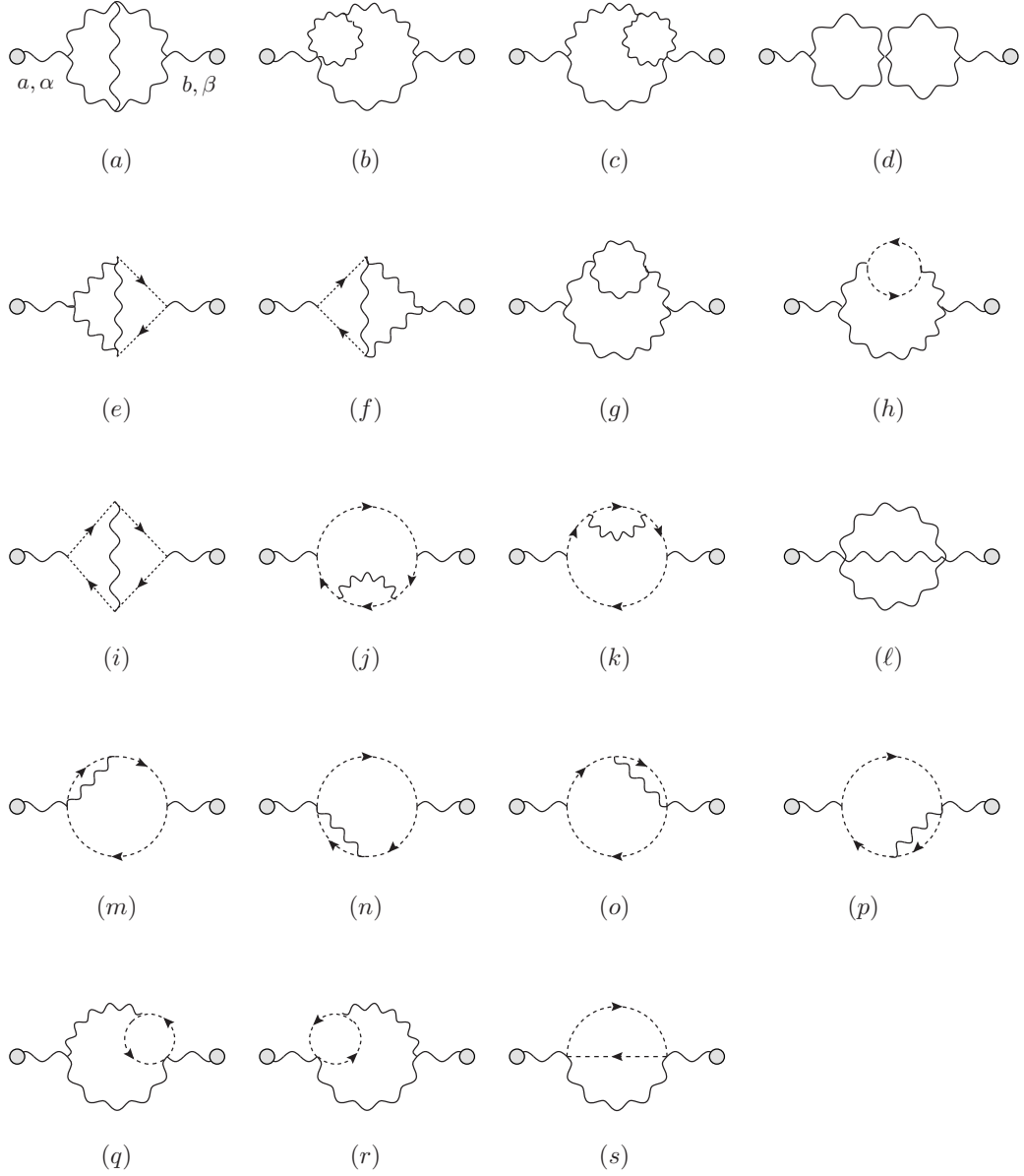
Fig. 20. The Feynman diagrams contributing to the BFM two-loop gluon self-energy $\widetilde{\Pi}^{(2)}_{\alpha\beta}$.

$$[(d_1) + (d_2)]^{(2)}_{\alpha\beta} = i\frac{g^4 C_A^2}{(4\pi)^4}\frac{7}{2\epsilon^2}\left(1 + \frac{43}{12}\epsilon - \rho\epsilon\right)q^2 P_{\alpha\beta}(q),$$

$$[(d_3) + (d_4)]^{(2)}_{\alpha\beta} = -i\frac{g^4 C_A^2}{(4\pi)^4}\frac{1}{2\epsilon^2}\left(1 + \frac{3}{4}\epsilon - \rho\epsilon\right)q^2 P_{\alpha\beta}(q),$$

$$[(d_5) + (d_6)]^{(2)}_{\alpha\beta} = -i\frac{g^4 C_A^2}{(4\pi)^4}\frac{9}{4\epsilon^2}\left(1 + \frac{31}{12}\epsilon - \rho\epsilon\right)q^2 P_{\alpha\beta}(q),$$

$$[(d_7) + (d_8) + (d_9) + (d_{10})]^{(2)}_{\alpha\beta} = -i\frac{g^4 C_A^2}{(4\pi)^4}\frac{3}{4\epsilon^2}\left(1 + \frac{9}{4}\epsilon - \rho\epsilon\right)q^2 P_{\alpha\beta}(q), \qquad (3.41)$$

with $\rho = \gamma_{\rm E} - \ln 4\pi + \ln(q^2/\mu^2)$. Then, adding up all the contributions, we get

$$\widetilde{\Pi}^{(2)}_{\alpha\beta}(q) = \sum_{i=1}^{10}(d_i)^{(2)}_{\alpha\beta} = i\frac{g^4 C_A^2}{(4\pi)^4}\frac{14}{3\epsilon}q^2 P_{\alpha\beta}(q). \qquad (3.42)$$

60

Notice that, as happened in the one-loop case, the contribution of each of the four subgroups is *individually* transverse. This property is certainly not accidental; in fact, as we will see in Section 8, it is valid to all orders. Its validity has been established for the first time in [90], and is a direct consequence of the linear WIs satisfied by the (fully-dressed) vertices entering in the SD expansion of the background gluon self-energy. As we will explain there in detail, this grouping of diagrams into individually transverse subsets has profound implications, constituting the cornerstone of the gauge-invariant truncation scheme implemented by the PT.

3.4 The pinch technique/background Feynman gauge correspondence

The key observation [40,41] that immediately suggests a connection between the PT and BFM Green's functions is related to the form of the ξ_Q-dependent tree-level BFM vertex $\widehat{A}_\alpha(q)A_\mu(k_1)A_\nu(k_2)$, denoted by $\tilde{\Gamma}^{\xi_Q}_{\alpha\mu\nu}(q, k_1, k_2)$ (see the BFM Feynman rules of Appendix B). Specifically, using the PT decomposition of Eq. (2.38) for the standard tree-level three-gluon vertex $\Gamma_{\alpha\mu\nu}(q, k_1, k_2)$, we find that

$$
\begin{aligned}
\tilde{\Gamma}^{(\xi_Q)}_{\alpha\mu\nu}(q, k_1, k_2) &= \Gamma^{\mathrm{F}}_{\alpha\mu\nu}(q, k_1, k_2) + \left(\frac{\xi_Q - 1}{\xi_Q}\right)\Gamma^{\mathrm{P}}_{\alpha\mu\nu}(q, k_1, k_2), \\
&= \Gamma_{\alpha\mu\nu}(q, k_1, k_2) - \frac{1}{\xi_Q}\Gamma^{\mathrm{P}}_{\alpha\mu\nu}(q, k_1, k_2).
\end{aligned}
\tag{3.43}
$$

Evidently, at $\xi_Q = 1$ we have that

$$
\tilde{\Gamma}^{(\xi_Q=1)}_{\alpha\mu\nu}(q, k_1, k_2) \equiv \Gamma^{\mathrm{F}}_{\alpha\mu\nu}(q, k_1, k_2).
\tag{3.44}
$$

Given that, in addition, at $\xi_Q = 1$ the longitudinal parts of the gluon propagator vanish also, one realizes that at this point there is nothing there that could pinch. Thus, ultimately, the BFG is singled out because of the total absence, in this particular gauge, of any pinching momenta.

In what follows we will only prove the PT/BFG correspondence by means of explicit calculations at the one-loop level, following the aforementioned original articles. An all-order, more profound proof of this correspondence will be postponed until Section 6; there we will show that, as a result of the BRST symmetry, the PT/BFG correspondence persists to all orders in perturbation theory. Finally, in Section 8, the proof will be generalized to the non-perturbative case of the SDEs.

The case of the gluon self-energy is almost immediate: simply compare the two terms on the rhs of Eq. (2.73) with the two terms given in Eqs (3.36). Evidently the PT and BFG gluon self-energies are identical at one loop.

Then, let us consider the case of the three-gluon vertex [41]. The one-loop diagrams contributing to the BFM three-gluon vertex (i.e., with three incoming background gluons) are shown in Fig. 21; there we also fix the conventions for momenta, Lorentz, and color indices, used in what
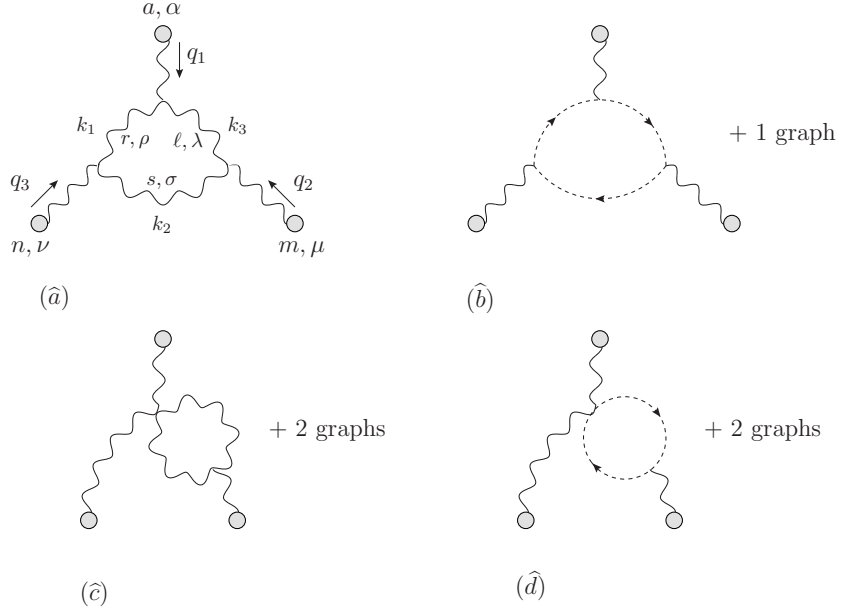
Fig. 21. One-loop diagrams contributing to the three-gluon vertex in the BFM. Diagrams $(\widehat{c})$ carry a $\frac{1}{2}$ symmetry factor.

follows. From diagram $(\widehat{a})$ one has

$$(\widehat{a}) = -\frac{i}{2}g^3 C_A f^{amn} \int_{k_1} \frac{1}{k_1^2 k_2^2 k_3^2} \tilde{\Gamma}^{(\xi_Q=1)}_{\alpha\lambda\rho}(q_1, k_3, -k_1)\tilde{\Gamma}^{(\xi_Q=1)}_{\mu\sigma\lambda}(q_2, k_2, -k_3)\tilde{\Gamma}^{(\xi_Q=1)}_{\nu\rho\sigma}(q_3, k_1, -k_2).$$
(3.45)

For diagram $(\widehat{b})$, and the one with the ghost charge running in the opposite direction, we have instead

$$(\widehat{b}) = ig^3 C_A f^{amn} \int \frac{1}{k_1^2 k_2^2 k_3^2}(k_1 + k_3)_\alpha(k_2 + k_3)_\mu(k_1 + k_2)_\nu.$$
(3.46)

For diagrams $(\widehat{c})$, and the two other possible diagrams of the same type, we get (using the BFG for the four-gluon vertex with two background legs)

$$(\widehat{c}) = 4g^3 C_A f^{amn} \left(g_{\alpha\nu}q_{1\mu} - g_{\alpha\mu}q_{1\nu}\right) \int_k \frac{1}{k^2(k + q_1)^2}$$
$$+ 4g^3 C_A f^{amn} \left(g_{\mu\nu}q_{2\alpha} - g_{\alpha\mu}q_{2\nu}\right) \int_k \frac{1}{k^2(k + q_2)^2}$$
$$+ 4g^3 C_A f^{amn} \left(g_{\alpha\nu}q_{3\mu} - g_{\mu\nu}q_{3\alpha}\right) \int_k \frac{1}{k^2(k + q_3)^2}.$$
(3.47)

Finally, diagram $(\widehat{d})$ (and the other two similar diagrams) turns out to be zero at this order, due to group-theoretical identities for the structure constants such as

$$f^{ead}(f^{dbx} f^{xce} + f^{dcx} f^{xbe}) = 0.$$
(3.48)

Adding the contributions found, notice that the sum $(\widehat{a}) + (\widehat{b})$ coincides with the term $\widehat{N}_{\alpha\mu\nu}$ of Eq. (2.93), while $(\widehat{c})$ coincides exactly with $\widehat{B}_{\alpha\mu\nu}$ of Eq. (2.93). Thus the BFM result matches

the expression of Eq.(2.92), obtained by the (intrinsic) PT.

The calculation of the one-loop four-gluon vertex in the BFM Feynman gauge has been carried out in [41]; again it was found to coincide with the one constructed through the PT algorithm.

3.5 The pinch technique/background Feynman gauge correspondence: conceptual issues

While it is a remarkable and extremely useful fact that the one-loop PT Green's functions can be calculated in the BFG, particular care is needed for the correct interpretation of this correspondence.

First of all, the PT is a way of enforcing gauge independence (and several other physical properties, such as unitarity and analyticity) on off-shell Green's functions, whereas the BFM, in a general gauge, is not. This is reflected in the fact that the BFM n-point functions are gauge-invariant, in the sense that they satisfy (by construction) QED-like WIs, but are *not* gauge-independent, *i.e.*, they depend explicitly on ξ_Q. For example, the BFM gluon self-energy at one loop is given by

$$\tilde{\Pi}_{\alpha\beta}^{(\xi_Q)}(q) = \tilde{\Pi}_{\alpha\beta}^{(\xi_Q=1)}(q) + \frac{i}{4(4\pi)^2}g^2 C_A(1-\xi_Q)(7+\xi_Q)q^2 P^{\alpha\beta}(q). \tag{3.49}$$

Had the BFM n-point functions been ξ_Q-independent, in addition to being gauge-invariant, there would be no need for introducing, independently, the PT.

We emphasize that the objective of the PT construction is not to derive diagrammatically the BFG, but rather to exploit the underlying BRST symmetry in order to expose a large number of cancellations, and eventually define gauge-independent Green's functions satisfying Abelian WIs. Thus, that the PT Green's functions can also be calculated in the BFG always needs a very extensive demonstration. Therefore, the correspondence must be verified at the end of the PT construction and should not be assumed beforehand.

Moreover, the ξ_Q-dependent BFM Green's functions are *not* physically equivalent. This is best seen in theories with spontaneous symmetry breaking: the dependence of the BFM Green's functions on ξ_Q gives rise to *unphysical* thresholds inside these Green's functions for $\xi_Q \neq 1$, a fact which limits their usefulness for resummation purposes (this point will be studied in detail in subsection 5.4). Only the case of the BFG is free from unphysical poles; that is because then (and only then) the BFM results collapse to the physical PT Green's functions.

It is also important to realize that the PT construction goes through unaltered under circumstances where the BFM Feynman rules cannot even be applied. Specifically, if instead of an S-matrix element one were to consider a different observable, such as a current correlation function or a Wilson loop (as was in fact done by Cornwall in the original formulation [7], and more recently in [61]), one could not start out using the background Feynman rules, because *all* fields appearing inside the first non-trivial loop are quantum ones. Instead, by following the PT rearrangement inside these physical amplitudes the unique PT answer emerges again.

Perhaps the most compelling fact that demonstrates that the PT and the BFM are intrinsically two completely disparate methods is that one can apply the PT within the BFM. Operationally, this is easy to understand: away from $\xi_Q = 1$ even in the BFM there are longitudinal (pinch-
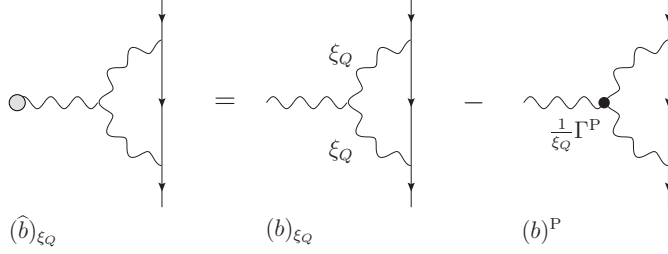
Fig. 22. Relation between the one loop non-Abelian BFM vertex, and the standard non-Abelian graph in the R_ξ gauge (with the substitution $\xi \to \xi_Q$), for a general value of the gfp parameter ξ_Q. The difference is a pinching contribution.

ing momenta) that will initiate the pinching procedure. Thus, one starts out with the S-matrix written with the BFM Feynman rules using a general ξ_Q, and applies the PT algorithm as in any other gauge-fixing scheme; one will recover again the unique PT answer for all Green's functions involved (*i.e.*, will get projected dynamically to $\xi_Q = 1$).

3.5.1 Pinching within the background field method

Let us study in some detail how pinching works within the BFM. It is expeditious to organize this calculation using as reference point the corresponding one-loop construction presented in the the previous section, in the context of the R_ξ gauges. The reason is that a great deal of the results needed here can be recovered directly from the analysis of the one-loop pinching in subsection 2.3, simply by setting $\xi \to \xi_Q$.

To begin with, the box diagrams in the BFM are identical to those of the R_ξ, shown in Fig. 3, with the trivial replacement $\xi \to \xi_Q$. Therefore, their pinching proceeds exactly as described in 2.3, and the results are precisely those found in subsection 2.3.1, Eqs (2.44) and (2.45), with $\xi \to \xi_Q$.

We then turn to the vertex graphs. The topologies are the same as in the R_ξ gauges. The Abelian graph, together with the external leg corrections are again identical, with the replacement $\xi \to \xi_Q$. The non-Abelian graph of Fig. 4, however, needs particular treatment, because the ξ_Q dependent BFM three-gluon vertex does not coincide with the conventional three-gluon vertex (of the R_ξ gauge). In fact, as we can see from Eq. (3.43), the two vertices differ by an amount proportional to Γ^P. So, we will use Eq. (3.43) inside the non-Abelian graph: the first term converts the graph into its conventional counterpart (with $\xi \to \xi_Q$ for the gluon propagators in the loop); the second term is purely pinching in nature, and we will track down its effect [Note that one could equally well employ (3.43) directly, as was done in [60], but then one could not use the results of the R_ξ so straightforwardly].

The term $\Gamma^P_{\alpha\mu\nu}(q, k_1, k_2)$, when multiplied by the two gluons inside the non-Abelian graph, leads to the expression

$$\frac{1}{\xi_Q}\Gamma^{P\,\mu\nu}_\alpha(q, k_1, k_2)\Delta^{(\xi_Q)}_{\mu\rho}(k_1)\Delta^{(\xi_Q)}_{\nu\sigma}(k_2) = \frac{k_{1\rho}}{k_1^2}\Delta^{(\xi_Q)}_{\alpha\sigma}(k_2) - \frac{k_{2\sigma}}{k_2^2}\Delta^{(\xi_Q)}_{\alpha\rho}(k_1), \tag{3.50}$$

which, after pinching, generates propagator-like terms. In particular, the original non-Abelian vertex graph, $(\widehat{b})_{\xi_Q}$, can be written as (Fig. 22)

64

$$(\widehat{b})_{\xi_Q} = (b)_{\xi_Q} + (b)^{\mathrm{P}}$$

$$= (b)_{\xi_Q} + g^2 C_A \delta^{ab} \int_k \left[-\frac{g_{\alpha\beta}}{k^2(k+q)^2} + \lambda_Q \frac{k_\alpha k_\beta}{k^4(k+q)^2} \right] [g\gamma^\beta t^b], \qquad (3.51)$$

where $(b)_{\xi_Q}$ denotes the standard non-Abelian graph in the R_ξ gauge when $\xi \to \xi_Q$. Then, we can convert $(b)_{\xi_Q}$ directly to $(\widehat{b})_{\xi_Q=1}$, *i.e.*, the PT answer, following exactly the procedure described in subsections 2.3.2 and 2.4.1; in this way the total pinching contribution coming from the BFM non-Abelian vertex is

$$(\widehat{b})_{\xi_Q} \to \Pi_{\mathrm{nav}}^{\alpha\beta}(q, \lambda_Q) + \lambda_Q g^2 C_A q^2 P^{\beta\mu}(q) \int_k \frac{k^\alpha k_\mu}{k^4(k+q)^2}. \qquad (3.52)$$

After these observations, it is easy to determine the total propagator-like pinching contribution, $\tilde{\Pi}_{\mathrm{P}}^{\alpha\beta}(q, \lambda_Q)$, that should be added to the BFM self-energy $\tilde{\Pi}_{\alpha\beta}^{\xi_Q}(q)$ (following the universal PT rules): one has

$$\tilde{\Pi}_{\mathrm{P}}^{\alpha\beta}(q, \lambda_Q) = \Pi_{\mathrm{box}}^{\alpha\beta}(q, \lambda_Q) + 2\left[\Pi_{\mathrm{nav}}^{\alpha\beta}(q, \lambda_Q) + \Pi_{\mathrm{nav}}^{\alpha\beta}(q, \lambda_Q) \right] + 4\Pi_{\mathrm{qse}}^{\alpha\beta}(q, \lambda_Q)$$

$$+ 2\lambda_Q g^2 C_A q^2 P^{\beta\mu}(q) \int_k \frac{k^\alpha k_\mu}{k^4(k+q)^2}$$

$$= -\Pi_{\mathrm{gse}}^{\alpha\beta}(q, \lambda_Q) + 2\lambda_Q g^2 C_A q^2 P^{\beta\mu}(q) \int_k \frac{k^\alpha k_\mu}{k^4(k+q)^2}, \qquad (3.53)$$

where the last step is by virtue of Eq. (2.57). Thus,

$$\tilde{\Pi}_{\mathrm{P}}^{\alpha\beta}(q, \lambda_Q) = \lambda_Q g^2 C_A q^2 \left\{ -\frac{\lambda_Q}{2} q^2 P^{\alpha\mu}(q) P^{\beta\nu}(q) \int_k \frac{k_\mu k_\nu}{k^4(k+q)^4} \right.$$

$$\left. + \left[q^2 P^{\alpha\beta}(q) \int_k \frac{1}{k^2(k+q)^4} + 4P^{\beta\mu}(q) \int_k \frac{k^\alpha k_\mu}{k^4(k+q)^2} - P^{\alpha\beta}(q) \int_k \frac{1}{k^4} \right] \right\}. \qquad (3.54)$$

Using the exact relation

$$P^{\beta\mu}(q) \int_k \frac{4k^\alpha k_\mu}{k^4(k+q)^2} = P^{\alpha\beta}(q) \int_k \frac{1}{k^2(k+q)^2}, \qquad (3.55)$$

we finally find that

$$\tilde{\Pi}_{\mathrm{P}}^{\alpha\beta}(q, \lambda_Q) = -\lambda_Q g^2 C_A q^2 \left[\frac{\lambda_Q}{2} q^2 P^{\alpha\mu}(q) P^{\beta\nu}(q) \int_k \frac{k_\mu k_\nu}{k^4(k+q)^4} + P^{\alpha\beta}(q) \int_k \frac{2q \cdot k}{k^4(k+q)^2} \right]. \qquad (3.56)$$

Note that the result is ultraviolet (UV) finite, as expected. After carrying out the integration, we obtain

$$\tilde{\Pi}_{\mathrm{P}}^{\alpha\beta}(q, \lambda_Q) = -\frac{i}{4(4\pi)^2} g^2 C_A (1 - \xi_Q)(7 + \xi_Q) q^2 P^{\alpha\beta}(q), \qquad (3.57)$$

which, when added to $\tilde{\Pi}_{\alpha\beta}^{(\xi_Q)}(q)$ given in Eq. (3.49) will give $\tilde{\Pi}_{\alpha\beta}^{(\xi_Q=1)}(q)$, as announced.

3.6 Generalized pinch technique

As we have seen in detail, the PT is an algorithm that gives rise to the same unique Green's functions, regardless of the gauge-fixing scheme one starts out from. Thus, irrespective of the starting point, the PT projects one dynamically to the BFG. A question one may naturally ask at this point is the following: could we devise a PT-like procedure that would project us to some other value of the background gfp ξ_Q? Or, going one step further, could one rearrange the Feynman graphs is such a way as to be projected to the generalized background gauges introduced in subsection 3.2.1? As was shown by Pilaftsis [42], such a construction is indeed possible; the systematic algorithm that accomplishes this is known as the *generalized* pinch technique (GPT). The GPT essentially modifies the starting point of the PT algorithm, namely Eq. (2.38), distributing differently the longitudinal momenta between (the now modified) $\Gamma^F_{\alpha\mu\nu}$ and $\Gamma^P_{\alpha\mu\nu}$ type of terms.

As explained by the author of [42], the GPT represents a fundamental departure from the primary aim of the PT, which is to construct gfp-independent off-shell Green's functions. The GPT, instead, deals exclusively with gfp-dependent Green's functions, with all the pathologies that this dependence entails. Nonetheless, it is certainly useful to have a method that allows us to move systematically from one gauge-fixing scheme to another, at the level of individual Green's functions. In addition to the possible applications mentioned in [42], we would like to emphasize the usefulness of the GPT in truncating gauge-invariantly (*i.e.*, maintaining transversality) sets of SDEs written in gauges other than the Feynman gauge (see Section 8). This possibility becomes particularly relevant, for example, when one attempts to compare SDE predictions with lattice simulations, carried out usually in the Landau gauge.

So, let us suppose, for starters, that we want to devise an algorithm that will take us from the R_ξ gluon self-energy, calculated at $\xi = \xi_0$, to the corresponding BFM self-energy, calculated at the same $\xi_Q = \xi_0$ (for example, say we want to go from the normal Yennie gauge, $\xi = 3$, to the BFM Yennie gauge, now at $\xi_Q = 3$).

It is clear that in this case the box diagrams in both schemes are automatically identical. So, what one should focus on is the one-loop vertex. What we want to do is get from the conventional vertex graph (with a normal (ξ-independent!) three-gluon vertex, and gluon propagators written at $\xi = \xi_0$) to the corresponding BFM graph (with the ξ_Q-dependent three-gluon vertex, and gluon propagators written at $\xi_Q = \xi_0$), and hope that the remainder is a purely propagator-like piece. Then, the solution is almost obvious: one must simply use Eq. (3.43), with the term proportional to Γ^P moved to the lhs, *i.e.*,

$$\Gamma_{\alpha\mu\nu}(q, k_1, k_2) = \tilde{\Gamma}^{(\xi_0)}_{\alpha\mu\nu}(q, k_1, k_2) + \frac{1}{\xi_0}\Gamma^P_{\alpha\mu\nu}(q, k_1, k_2). \tag{3.58}$$

In fact, this particular decomposition predates the GPT by two decades; it appears for the first time in Eq.(4.4) of [11], and has also been employed by Haeri in [91]. It was essentially motivated by the observation that the first term, corresponding to Γ^F in the usual PT procedure, satisfies precisely the correct generalization of the WI given in (2.40), namely

$$q^\alpha \Gamma^{(\xi_0)}_{\alpha\mu\nu}(q, k_1, k_2) = i\left\{\Delta^{(0)-1}_{(\xi_0)}(k_1) - \Delta^{(0)-1}_{(\xi_0)}(k_2)\right\}_{\mu\nu}, \tag{3.59}$$

66

with the inverse propagator given in Eq. (2.30). This property, in turn, guarantees that the resulting one-loop vertex satisfies the correct Abelian WI (see below). Evidently, Eq. (3.58) reduces to the usual PT decomposition of Eq. (2.38) when $\xi_0 = 1$.

Now, the first term on the rhs, when inserted into the original non-Abelian graph, gives exactly the corresponding graph in the BFM (at $\xi_Q = \xi_0$); of course, the Abelian graphs and the external leg corrections are identical. Thus, one eventually obtains the BFM one-loop gluon-quark vertex, $\tilde{\Gamma}_\alpha^{(\xi_Q)}(p_1, p_2)$, at $\xi_Q = \xi_0$. As is known from the general discussion on the formal properties of the BFM Green's function, or as can be demonstrated explicitly (at one-loop) using Eq. (3.59), $\tilde{\Gamma}_\alpha^{(\xi_0)}(p_1, p_2)$ satisfies a naive QED-like WI, namely

$$q^\alpha \tilde{\Gamma}_\alpha^{(\xi_0)}(p_1, p_2) = g \left\{ \widehat{\Sigma}^{(\xi_0)}(p_1) - \widehat{\Sigma}^{(\xi_0)}(p_2) \right\}, \tag{3.60}$$

where $\widehat{\Sigma}^{(\xi_0)}$ is the GPT quark self-energy coinciding with the usual quark self-energy when evaluated in the gauge $\xi_Q = \xi_0$.

The final step is to determine the (exclusively propagator-like) contributions of the remaining term Γ^P, coming from Eq. (3.58). In fact, Γ^P will trigger first Eq. (3.50), and then pinch, as usual. Once the propagator-like contributions have been alloted to $\Pi_{\alpha\beta}^{(\xi_0)}$, the conventional R_ξ one-loop self-energy at $\xi = \xi_0$, we will obtain $\tilde{\Pi}_{\alpha\beta}^{(\xi_0)}$, namely the BFM one-loop self-energy at $\xi_Q = \xi_0$, thus concluding the construction.

The method can be systematically generalized to more complicated situations [42]. For instance, one may be projected from the R_ξ gauges to one of the generalized BFM gauges, such as the BFM axial gauge; this would lead to a proliferation of pinching momenta. The resulting construction is therefore more cumbersome, but remains conceptually rather straightforward.

4 The Pinch Technique one-loop construction in the electroweak sector of the Standard Model

In this section we give a general overview of how the PT construction is modified in a case of a theory with spontaneous (tree-level) symmetry breaking (Higgs mechanism) [9,92,93], using the electroweak sector of the SM as the reference theory.

4.1 The electroweak lagrangian

In order to define the relevant quantities and set up the notation used throughout this section, we begin by writing the classical (gauge invariant) SM Lagrangian as

$$\mathcal{L}_{\mathrm{SM}}^{\mathrm{cl}} = \mathcal{L}_{\mathrm{YM}} + \mathcal{L}_{\mathrm{H}} + \mathcal{L}_{\mathrm{F}}. \tag{4.1}$$

The gauge invariant $SU(2)_W \otimes U(1)_Y$ Yang-Mills part $\mathcal{L}_{\mathrm{YM}}$ consists of an isotriplet W_μ^a (with $a = 1, 2, 3$) associated with the weak isospin generators T_w^a, and an isosinglet W_μ^4 with weak hypercharge Y_w associated to the group factor $U(1)_Y$; it reads

$$\begin{aligned}
\mathcal{L}_{\mathrm{YM}} &= -\frac{1}{4} F_{\mu\nu}^a F^{a\,\mu\nu} \\
&= -\frac{1}{4} \left(\partial_\mu W_\mu^a - \partial_\nu W_\mu^a + g_w f^{abc} W_\mu^b W_\nu^c \right)^2 - \frac{1}{4} \left(\partial_\mu W_\nu^4 - \partial_\nu W_\mu^4 \right)^2 .
\end{aligned} \tag{4.2}$$

The Higgs-boson part $\mathcal{L}_{\mathrm{H}}$ involves a complex $SU(2)_W$ scalar doublet field Φ and its complex (charge) conjugate $\widetilde{\Phi}$, given by

$$\Phi = \begin{pmatrix} \phi^+ \\ \frac{1}{\sqrt{2}} (H + i\chi) \end{pmatrix}, \qquad \widetilde{\Phi} \equiv i\sigma^2 \Phi^* = \begin{pmatrix} \frac{1}{\sqrt{2}} (H - i\chi) \\ -\phi^- \end{pmatrix}. \tag{4.3}$$

Here σ denotes the Pauli matrices, H denotes the physical Higgs field, while $\phi^\pm$ and χ represents, respectively, the charged and neutral unphysical degrees of freedom (would-be Goldstone bosons) . Then $\mathcal{L}_{\mathrm{H}}$ takes the form

$$\mathcal{L}_{\mathrm{H}} = (\mathcal{D}_\mu \Phi)^\dagger (\mathcal{D}^\mu \Phi) - V(\Phi), \tag{4.4}$$

with the covariant derivative $\mathcal{D}_\mu$ defined as

$$\mathcal{D}_\mu = \partial_\mu - ig_w T_w^a W_\mu^a + ig_1 \frac{Y_w}{2} W_\mu^4, \tag{4.5}$$

and the Higgs potential as

$$V(\Phi) = \frac{\lambda}{4} \left(\Phi^\dagger \Phi \right)^2 - \mu^2 \left(\Phi^\dagger \Phi \right). \tag{4.6}$$

The SM leptons (we neglect the quark sector in what follows) are grouped into left-handed doublets

$$\Psi_i^L = P_L \Psi_i = \begin{pmatrix} \nu_i^L \\ \ell_i^L \end{pmatrix}, \tag{4.7}$$

which transform under the fundamental representation of $SU(2)_W \otimes U(1)_Y$, and right-handed singlets (which comprise only the charged leptons)

$$\psi_i^R = P_R \psi_i = \ell_i^R \tag{4.8}$$

transforming with respect to the Abelian subgroup $U(1)_Y$ only. In the previous formulas, i is the generation index, and the chirality projection operators are defined according to $P_{L,R} = (1 \mp \gamma_5)/2$. In this way the leptonic part of $\mathcal{L}_F$ reads

$$\mathcal{L}_F = \sum_i \left(i\overline{\Psi}_i^L \gamma^\mu \mathcal{D}_\mu \Psi_i^L + i\overline{\psi}_i^R \gamma^\mu \mathcal{D}_\mu \psi_i^R - \overline{\Psi}_i^L G_i^\ell \psi_i^R \Phi + \text{h.c.} \right), \tag{4.9}$$

with G_i^ℓ the Yukawa coupling.

The Higgs field H will give mass to all the SM fields, by acquiring a vacuum expectation value (vev) v; in particular, the masses of the gauge fields are generated after absorbing the massless would-be Goldstone bosons $\phi^\pm$ and χ. The physical massive gauge-bosons $W^\pm$, Z and the (massless) photon A are then obtained by diagonalizing the mass matrix; they are given by

$$W_\mu^\pm = \frac{1}{\sqrt{2}} \left(W_\mu^1 \mp iW_\mu^2 \right), \qquad \begin{pmatrix} Z_\mu \\ A_\mu \end{pmatrix} = \begin{pmatrix} c_w & s_w \\ -s_w & c_w \end{pmatrix} \begin{pmatrix} W_\mu^3 \\ W_\mu^4 \end{pmatrix}, \tag{4.10}$$

where

$$c_w = \cos\theta_w = \frac{g_w}{\sqrt{g_1^2 + g_w^2}}, \qquad s_w = \sin\theta_w = \sqrt{1 - c_w^2}, \tag{4.11}$$

with θ_w the weak mixing angle. The resulting gauge-boson masses are

$$M_W = \frac{1}{2} g_w v, \qquad M_Z = \frac{1}{2}\sqrt{g_1^2 + g_w^2}\, v, \qquad M_A = 0, \tag{4.12}$$

which for the weak mixing angle give the relation

$$c_w = \frac{M_W}{M_Z}. \tag{4.13}$$

Finally, identifying the photon-electron coupling constant with the usual electrical charge e, we find

$$e = \frac{g_1 g_w}{\sqrt{g_1^2 + g_w^2}}, \qquad g_1 = \frac{e}{c_w}, \qquad g_w = \frac{e}{s_w}. \tag{4.14}$$

For quantizing the theory, a gauge fixing term must be added to the classical Lagrangian $\mathcal{L}_{\text{SM}}^{\text{cl}}$. To avoid tree-level mixing between gauge and scalar fields, a renormalizable R_ξ gauge of the 't Hooft type is most commonly chosen [17]. This latter gauge is specified by introducing a

different gauge parameter for each gauge-boson, and is defined through the linear gauge fixing (no sum over the color index a) functions

$$\mathcal{F}^a = \partial^\mu W_\mu^a - \frac{i}{2} g_w \xi_a \left[v_i^\dagger \sigma_{ij}^a \phi_j - \phi_i^\dagger \sigma_{ij}^a v_j \right],$$

$$\mathcal{F}^4 = \partial^\mu W_\mu^4 + \frac{i}{2} g_1 \xi_4 \left[v_i^\dagger \phi_i - \phi_i^\dagger v_i \right], \tag{4.15}$$

with $v_1 = 0$, $v_2 = v$, and the gfp parameters given by $\xi_1 = \xi_2 = \xi_W$, $\xi_3 = \xi_4 = \xi_Z$. In terms of the mass eigenstates these translate into the gauge fixing functions

$$\mathcal{F}^\pm = \partial^\mu W_\mu^\pm \mp i\xi_W M_W \phi^\pm,$$

$$\mathcal{F}^Z = \partial^\mu Z_\mu - \xi_Z M_Z \chi,$$

$$\mathcal{F}^A = \partial^\mu A_\mu, \tag{4.16}$$

finally yielding to the R_ξ gauge fixing Lagrangian

$$\mathcal{L}_{\mathrm{GF}} = -\frac{1}{\xi_W} \mathcal{F}^+ \mathcal{F}^- - \frac{1}{2\xi_Z} \left(\mathcal{F}^Z \right)^2 - \frac{1}{2\xi_A} \left(\mathcal{F}^A \right)^2. \tag{4.17}$$

The Faddeev-Popov ghost sector corresponding to the above gauge fixing Lagrangian reads

$$\mathcal{L}_{\mathrm{FPG}} = -\bar{u}^+ s\mathcal{F}^+ - \bar{u}^- s\mathcal{F}^- - \bar{u}^Z s\mathcal{F}^Z - \bar{u}^A s\mathcal{F}^A, \tag{4.18}$$

with s the BRST operator for the SM fields (for the full set of the BRST transformation see *e.g.*, [94]). Notice that the ghost Lagrangian contains kinetic terms for the Faddeev-Popov fields, allowing one to introduce them as dynamical fields of the theory.

In the case of the BFM gauge-fixing one replaces the Higgs vev by the background scalar field

$$\widehat{\Phi} = \begin{pmatrix} \widehat{\phi}^+ \\ \frac{1}{\sqrt{2}} \left(v + \widehat{H} + i\widehat{\chi} \right) \end{pmatrix}, \tag{4.19}$$

and adds to the derivative term the background $SU(2)_W$ triplet field $\widehat{W}_\mu^a$. Thus we get

$$\mathcal{F}^a = \left(\delta^{ac} \partial^\mu + g_w f^{abc} \widehat{W}_\mu^b \right) W^{c\mu} - \frac{i}{2} g_w \xi_Q^W \left[\widehat{\phi}_i^\dagger \sigma_{ij}^a \phi_j - \phi_i^\dagger \sigma_{ij}^a \widehat{\phi}_j \right],$$

$$\mathcal{F}^4 = \partial^\mu W_\mu^4 + \frac{i}{2} g_1 \xi_Q^4 \left[\widehat{\phi}_i^\dagger \phi_i - \phi_i^\dagger \widehat{\phi}_j \right]. \tag{4.20}$$

Notice that: (*i*) the background scalar doublet $\widehat{\Phi}$ field has the usual non-vanishing vev v, while that of the quantum field Φ is zero, and (*ii*) the background field gauge invariance restricts the number of quantum gauge parameters to two, one for $SU(2)_W$ and one for $U(1)_Y$. Setting $\xi_Q^W = \xi_Q^4 = \xi_Q$, to avoid tree-level mixing between the photon and the Z boson, we get

$$\mathcal{F}^{\pm} = \partial^{\mu} W^{\pm}_{\mu} \pm ig_w \left(s_w \widehat{A}^{\mu} - c_w \widehat{Z}^{\mu} \right) W^{\pm}_{\mu} \mp ig_w \left(s_w A^{\mu} - c_w Z^{\mu} \right) \widehat{W}^{\pm}_{\mu}$$

$$\mp \frac{i}{2} g_w \xi_Q \left[\left(v + \widehat{H} \mp i\widehat{\chi} \right) \phi^{\pm} - (H \mp i\chi) \widehat{\phi}^{\pm} \right],$$

$$\mathcal{F}^{Z} = \partial^{\mu} Z_{\mu} - ig_w c_w \left(\widehat{W}^{+}_{\mu} W^{-\mu} - W^{+}_{\mu} \widehat{W}^{-\mu} \right) - \frac{i}{2} g_w \frac{c_w^2 - s_w^2}{2c_w} \xi_Q \left(\widehat{\phi}^{-} \phi^{+} - \widehat{\phi}^{+} \phi^{-} \right)$$

$$+ \frac{1}{2c_w} g_w \xi_Q \left(\widehat{\chi} H - \widehat{H} \chi - v\chi \right),$$

$$\mathcal{F}^{A} = \partial^{\mu} A_{\mu} + ig_w s_w \left(\widehat{W}^{+}_{\mu} W^{-\mu} - W^{+}_{\mu} \widehat{W}^{-\mu} \right) + ig_w s_w \xi_Q \left(\widehat{\phi}^{-} \phi^{+} - \widehat{\phi}^{+} \phi^{-} \right). \tag{4.21}$$

After setting the gauge parameters all equal to ξ_Q, the corresponding gauge-fixing and Faddeev-Popov terms are still given by Eqs (4.17) and (4.18).

Summarizing, the complete electroweak sector of the SM Lagrangian in the R_ξ/BFM gauges is given by

$$\mathcal{L}_{\text{SM}} = \mathcal{L}_{\text{SM}}^{\text{cl}} + \mathcal{L}_{\text{F}} + \mathcal{L}_{\text{GF}} + \mathcal{L}_{\text{FPG}}. \tag{4.22}$$

The full set of Feynman rules derived from this Lagrangian can be found in [95], and will be used throughout this section.

4.2 Pinch technique with Higgs mechanism: general considerations

Before proceeding with the general discussion, we report some useful ingredients. In particular, in the R_ξ gauges the tree-level gauge boson propagators– three massive gauge bosons ($W^{\pm}$ and Z), and a massless photon (A)– are given by [notice the i factor difference with respect to our definitions of Eq. (2.31) and (2.31) in the previous section]

$$\Delta^{\mu\nu}_i(q) = \left[g^{\mu\nu} - \frac{(1 - \xi_i) q^{\mu} q^{\nu}}{q^2 - \xi_i M_i^2} \right] d_i(q^2)$$

$$d_i(q^2) = \frac{-i}{q^2 - M_i^2} \tag{4.23}$$

where $i = W, Z, A$, and $M_A^2 = 0$. In general, the gfps ξ_W, ξ_Z, and ξ_A will be considered to be different from one another. The inverse of the gauge boson propagators (4.23), to be denoted by $\Delta^{-1}_{i,\mu\nu}$, is given by

$$\Delta^{-1}_{i,\mu\nu}(q) = i \left[(q^2 - M_i^2) g_{\mu\nu} - q_{\mu} q_{\nu} + \frac{1}{\xi_i} q_{\mu} q_{\nu} \right]. \tag{4.24}$$

There are three unphysical (would-be) Goldstone bosons associated with the three massive gauge boson, to be denoted by $\phi^{\pm}$ and χ. Their tree-level propagators are ξ-dependent, and are given by

$$D_i(q) = \frac{i}{q^2 - \xi_i M_i^2}, \tag{4.25}$$

71

with $i = W, Z$ (of course, there should be no Goldstone boson associated with the photon). In addition, the ghost propagators are also given by $D_i(q)$, with $i = W, Z, A$ (there is, however, a massless ghost associated with the photon). Finally, the bare propagator of the Higgs-boson is given by

$$\Delta_H(q) = \frac{i}{q^2 - M_H^2}, \tag{4.26}$$

For the massive gauge bosons ($i = W, Z$) the following identities, valid for any value of ξ_i, will be used frequently:

$$\Delta_i^{\mu\nu}(q) = U_i^{\mu\nu}(q) - \frac{q^\mu q^\nu}{M_i^2} D_i(q), \tag{4.27}$$

where

$$U_i^{\mu\nu}(q) = \left(g^{\mu\nu} - \frac{q^\mu q^\nu}{M_i^2} \right) d_i(q^2), \tag{4.28}$$

is the corresponding propagator in the so-called *unitary gauge* ($\xi_i \to \infty$). In addition, in order to rearrange various expressions appearing in the computations, we will often employ the algebraic identity

$$\frac{1}{k^2 - \xi_i M_i^2} = \frac{1}{k^2 - M_i^2} - \frac{(1 - \xi_i) M_i^2}{(k^2 - M_i^2)(k^2 - \xi_i M_i^2)}. \tag{4.29}$$

Finally, when dealing with the case where the fermions are considered to be massive, we will use extensively the identities [93]

$$
\begin{aligned}
ig_\alpha^\nu &= i\Delta_i^{\nu\mu}(q)\Delta_{i\,\mu\alpha}^{-1}(q) \\
&= q^\nu q_\alpha D_i(q) - \Delta_i^{\nu\mu}(q)\left[(q^2 - M_i^2)g_{\mu\alpha} - q_\mu q_\alpha\right], \\
iq^\mu &= q^2 D_i(q)q^\mu + M_i^2 q_\nu \Delta_i^{\mu\nu}(q).
\end{aligned}
\tag{4.30}
$$

Now, the application of the PT in the electroweak sector is significantly more involved than in the QCD case; in addition to the general proliferation of graphs intrinsic to the electroweak sector, there are three PT-specific reasons that complicate the construction [9,93].

i. In addition to the longitudinal momenta coming from the propagators of the gauge bosons (proportional to $\lambda_i = 1 - \xi_i$) and the PT decomposition of the vertices involving three gauge bosons, a new source of pinching momenta appears, originating from graphs having an external (*i.e.*, carrying the physical momentum q) would-be Goldstone boson. Specifically, interaction vertices such as $\Gamma_{A_\alpha \phi^\pm \phi^\mp}$, $\Gamma_{Z_\alpha \phi^\pm \phi^\mp}$, $\Gamma_{W_\alpha^\pm \phi^\mp \chi}$, and $\Gamma_{W_\alpha^\pm \phi^\mp H}$ also furnish pinching momenta, when the gauge boson is inside the loop carrying (virtual) momentum k. Such a vertex will then be decomposed as (see Fig. 23)

$$\Gamma_\alpha^{(0)}(q, k, -q-k) = \Gamma_\alpha^{\text{F}}(q, k, -q-k) + \Gamma_\alpha^{\text{P}}(q, k, -q-k), \tag{4.31}$$

with

$$
\begin{aligned}
\Gamma_\alpha^{(0)}(q, k, -q-k) &= (2q+k)_\alpha, \\
\Gamma_\alpha^{\text{F}}(q, k, -q-k) &= 2q_\alpha, \\
\Gamma_\alpha^{\text{P}}(q, k, -q-k) &= k_\alpha,
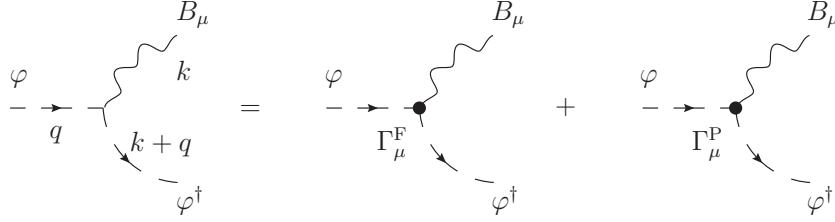\end{aligned}
\tag{4.32}
$$

72

Fig. 23. The PT decomposition of the generic elementary gauge-boson-scalar vertex $\Gamma_{B_\mu \varphi \varphi^\dagger}$.

which is the scalar case analogue of (2.38), (2.39) and (2.39).

ii. When the fermions involved (external or inside loops) are massive, the WI of Eq. (2.41) receives additional contributions, which correspond precisely to the tree-level coupling of the would-be Goldstone bosons to the fermions. To see this concretely, let us consider the analogue of the fundamental pinching WI of Eq. (2.41) *e.g.*, in the case where the incoming boson is a W. Contracting with k^μ the $\Gamma_{W_\mu^+ \bar{u} d}$ vertex (the fermions u and d are isodoublet partners), we have (we omit a factor $g_w/\sqrt{2}$)

$$ \slashed{k} P_L = P_R S_d^{-1}(k+p) - S_u^{-1}(p) P_L + [m_d P_R - m_u P_L]. \tag{4.33} $$

The first two terms will pinch and vanish on-shell, respectively, as they did in the case of Eq. (2.41); the leftover term in the square bracket corresponds precisely to the coupling $\phi^+ \bar{u} d$ (the case involving the $\Gamma_{W_\mu^- \bar{d} u}$ is identical). A completely analogous WI is obtained when the incoming boson is a Z. Again, contraction with the vertex $\Gamma_{Z \bar{f} f}$ furnishes a WI completely analogous to (4.33), with the additional term proportional to $m_f \gamma_5$, which corresponds to the coupling $\Gamma_{\chi \bar{f} f}$.

iii. After the various pinch contributions have been identified, particular care is needed when allotting them among the PT quantities that one is constructing. So, unlike the QCD case where all propagator-like pinch contributions were added to the only available self-energy, $\Pi_{\alpha\beta}$ (in order to construct $\widehat{\Pi}_{\alpha\beta}$), in the electroweak case such pinch contributions must, in general, be split among various propagators. Thus, in the case of the charged channel, they will be shared, in general, between the self-energies $\Pi_{W_\alpha W_\beta}$, $\Pi_{W_\alpha \phi}$, $\Pi_{\phi W_\beta}$, and $\Pi_{\phi\phi}$. This is equivalent to saying that, when forming the inverse of the W self-energy, in general the longitudinal parts may no longer be discarded from the four-fermion amplitude, since the external current is not conserved, up to terms proportional to the fermion masses. As we will see in detail, the correct way of treating the longitudinal pieces is provided by the identities (4.30). The neutral channel is even more involved; one has to split the propagator-like pinch contributions among the self-energies $\Pi_{Z_\alpha Z_\beta}$, $\Pi_{A_\alpha A_\beta}$, $\Pi_{Z_\alpha A_\beta}$, $\Pi_{A_\alpha Z_\beta}$, $\Pi_{Z_\alpha \chi}$, $\Pi_{\chi Z_\beta}$, $\Pi_{\chi\chi}$, and Π_{HH}.

We emphasize that points (*i*), (*ii*), and (*iii*) above are tightly intertwined. The extra terms appearing in the WI are precisely needed to cancel the gauge-dependence of the corresponding graph where the gauge boson is replaced by its associated Goldstone boson. In addition, as we will see later, when the external currents are not conserved, the appearance of the scalar–scalar or scalar–gauge-boson self-energies is crucial for enforcing the gfp-independence of the physical

amplitude.

We close this general discussion by briefly presenting an alternative approach to the PT, known as the "current algebra formulation of the PT", introduced in [92]. In this approach the interaction of gauge bosons with external fermions is expressed in terms of current correlation functions, *i.e.*, matrix elements of Fourier transforms of time-ordered products of current operators. This is particularly economical because these amplitudes automatically include several closely related Feynman diagrams. When one of the current operators is contracted with the appropriate four-momentum, a WI is triggered. The pinch part is then identified with the contributions involving the equal-time commutators in the WIs, and therefore involve amplitudes where the number of current operators has been reduced by one or more. A basic ingredient in this formulation are the following equal-time commutators

$$
\begin{aligned}
\delta(x_0 - y_0)[J_W^0(x), J_Z^\mu(y)] &= c_w^2 J_W^\mu(x)\delta^4(x - y), \\
\delta(x_0 - y_0)[J_W^0(x), J_W^{\mu\dagger}(y)] &= -J_3^\mu(x)\delta^4(x - y), \\
\delta(x_0 - y_0)[J_W^0(x), J_A^\mu(y)] &= J_W^\mu(x)\delta^4(x - y), \\
\delta(x_0 - y_0)[J_V^0(x), J_{V'}^\mu(y)] &= 0.
\end{aligned}
\tag{4.34}
$$

where $J_3^\mu \equiv 2(J_Z^\mu + s_w^2 J_A^\mu)$ and $V, V' \in \{A, Z\}$. To demonstrate the method with an example, consider the one-loop vertex Γ_μ, where the gauge particles in the loop are Ws, and the incoming ($|\psi_i\rangle$) and outgoing ($|\psi_f\rangle$) fermions are massless. It can be written as follows (with $\xi = 1$):

$$
\Gamma_\mu = \int_k \Gamma_{\mu\alpha\beta}(q, k, -k - q) \int d^4x\; \mathrm{e}^{ik\cdot x} \left\langle \psi_f \left| T[J_W^{\alpha\dagger}(x) J_W^\beta(0)] \right| \psi_i \right\rangle.
\tag{4.35}
$$

When an appropriate momentum, say k_α, from the vertex is pushed into the integral over dx, it gets transformed into a covariant derivative d/dx_α acting on the time ordered product $\left\langle \psi_f \left| T[J_W^{\alpha\dagger}(x) J_W^\beta(0)] \right| \psi_i \right\rangle$. Then, after using current conservation and differentiating the θ-function terms, implicit in the definition of the T^* product, we end up with the lhs of Eq. (4.34). So, the contribution of each such term is proportional to the matrix element of a single current operator, namely $\langle \psi_f | J_3^\mu | \psi_i \rangle$; this is precisely the pinch part.

4.3   The case of massless fermions

We will now study the application of the PT in the case where all fermions involved are massless. This simplification facilitates the PT procedure considerably, because no scalar particles can be attached to the massless fermions. As a result (*i*) the scalars can appear only *inside* the self-energy graphs, where they obviously cannot pinch; (*ii*) Eq.(4.33) is practically reduced to its QCD equivalent; (*iii*) there are no self-energies with incoming scalars (*i.e.*, no $\Pi_{W_\alpha\phi}$, $\Pi_{Z_\alpha\chi}$, $\Pi_{\phi\phi}$, etc).

Let us now focus, for simplicity, on the the process $f_1(p_1)\bar{f}_1(p_2) \rightarrow f_2(r_1)\bar{f}_2(r_2)$, mediated at tree-level by a Z-boson and a photon. At one-loop order, the box and vertex graphs furnish propagator-like contributions, every time the WI of Eq.(4.33) is triggered by a pinching momentum. Specifically, the term in Eq. (4.33) proportional to the inverse of the internal fermion
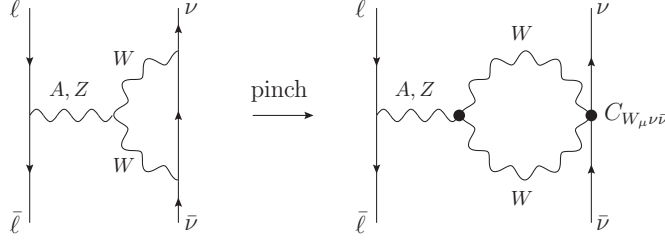
Fig. 24. The basic pinching and one of the unphysical vertex produced in the process $\ell\bar{\ell} \to \nu\nu$ with ℓ a lepton.

propagator gives rise to a propagator-like term, whose coupling to the external fermions f and $\bar{f}$ (with $f = f_1, f_2$) is proportional to an effective vertex $C_{W_\alpha f\bar{f}}$ given by (see also Fig. 24)

$$C_{W_\alpha f\bar{f}} = -i\left(\frac{g_w}{2}\right)\gamma_\alpha P_L. \tag{4.36}$$

Note that this effective vertex is unphysical, in the sense that it does not correspond to any of the elementary vertices appearing in the electroweak Lagrangian. However, it can be written as a linear combination of the two *physical* tree-level vertices $\Gamma_{A_\alpha f\bar{f}}$ and $\Gamma_{Z_\alpha f\bar{f}}$ given by

$$\Gamma_{A_\alpha f\bar{f}} = -ig_w s_w Q_f \gamma_\alpha,$$
$$\Gamma_{Z_\alpha f\bar{f}} = -i\left(\frac{g_w}{c_w}\right)\gamma_\alpha[(s_w^2 Q_f - T_z^f)P_L + s_w^2 Q_f P_R], \tag{4.37}$$

as follows:

$$C_{W_\alpha f\bar{f}} = \left(\frac{s_w}{2T_z^f}\right)\Gamma_{A_\alpha f\bar{f}} - \left(\frac{c_w}{2T_z^f}\right)\Gamma_{Z_\alpha f\bar{f}}. \tag{4.38}$$

In the above formulas, Q_f is the electric charge of the fermion f, and T_z^f its z-component of the weak isospin. The identity established in Eq. (4.38) above, allows one to combine the propagator-like parts with the conventional self-energy graphs by writing $1 = d_i(q^2)d_i^{-1}(q^2)$.

4.3.1 Gauge fixing parameter cancellations

Next, we will describe how the cancellation of the gfp proceeds at one-loop level for the simple case where f_1 is a lepton, to be denoted by ℓ, and f_2 is a neutrino, denoted by ν. Of course, based on general field-theoretic principles, one knows in advance that the entire amplitude will be gfp-independent. What is important to recognize, however, is that this cancellation goes through without having to carry out any of the integrations over virtual loop momenta, exactly as happened in the case of QCD. From the practical point of view, the extensive gauge cancellations that are implemented through the PT finally amount to the statement that one may start out in the Feynman gauge, *i.e.*, set directly $\xi_W = 1$ and $\xi_Z = 1$, with no loss of generality.

Demonstrating the cancellation of ξ_Z is rather easy. First of all, it is straightforward to verify that the box diagrams containing two Z-bosons (direct and crossed, see Fig. 25) form a ξ_Z-independent subset. The way this works is completely analogous to the QED case, where
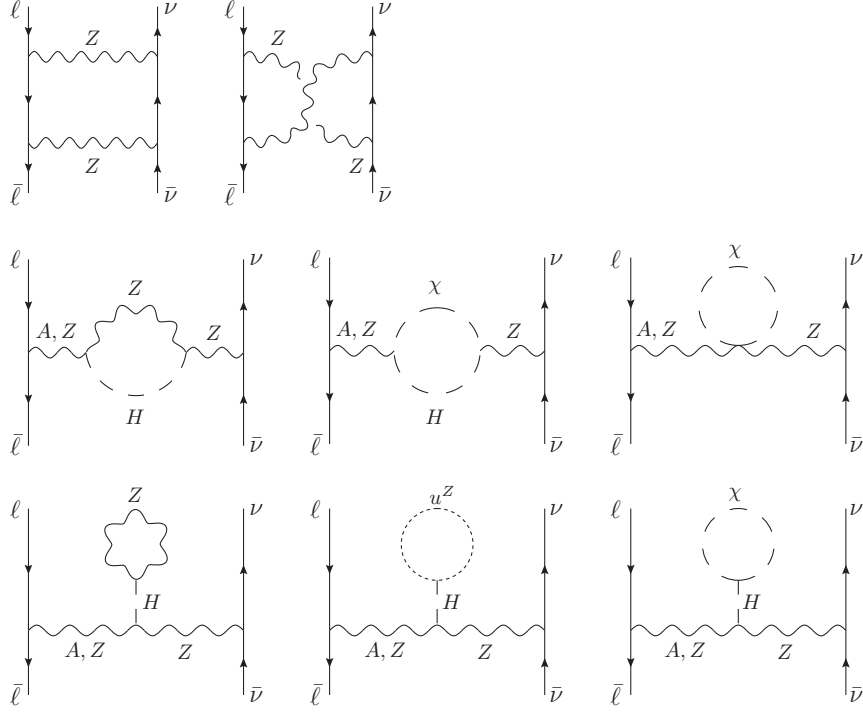
Fig. 25. The subset of diagrams of the process that depends on the gfp ξ_Z.

the two boxes contain photons: the ξ_Z-dependence of the direct box cancels exactly against the gfp-dependence of the crossed.

The only other graphs with a ξ_Z dependence are the self-energy graphs shown in Fig. 25; it is easy to show by employing Eq. (4.29) that their sum is independent of ξ_Z, separately for ZZ and AZ. In fact, from the PT point of view it is clear why this must be so: at one-loop there are no vertex graphs containing Z, χ, or H, that could possibly furnish pinch contributions which might mix with (and cancel against) the self-energy graphs. Therefore, the ξ_Z dependent contributions are isolated in the self-energy, and must cancel completely, since the S-matrix is gfp independent.

Proving the cancellation of ξ_W is significantly more involved. In what follows we set $\lambda_W \equiv 1 - \xi_W$, and suppress a factor $g_w^2 \int_k$. We also define

$$I_3 \equiv \left[(k^2 - \xi_W M_W^2)(k^2 - M_W^2)[(k+q)^2 - M_W^2]\right]^{-1},$$

$$I_4 \equiv \left[(k^2 - \xi_W M_W^2)[(k+q)^2 - \xi_W M_W^2](k^2 - M_W^2)[(k+q)^2 - M_W^2]\right]^{-1}, \tag{4.39}$$

Note that terms proportional to q_μ or q_ν may be dropped directly, because the external currents are conserved (massless fermions).

To get a feel of how the PT organizes the various gauge-dependent terms, consider the box graphs shown in Fig. 26. We have:

$$(a) = (a)_{\xi_W=1} + \mathcal{V}_{W^\alpha \ell \bar{\ell}} \left(\lambda_W^2 I_4 k_\alpha k_\beta - 2\lambda_W I_3 g_{\alpha\beta}\right) \mathcal{V}_{W^\beta \nu \bar{\nu}}, \tag{4.40}$$
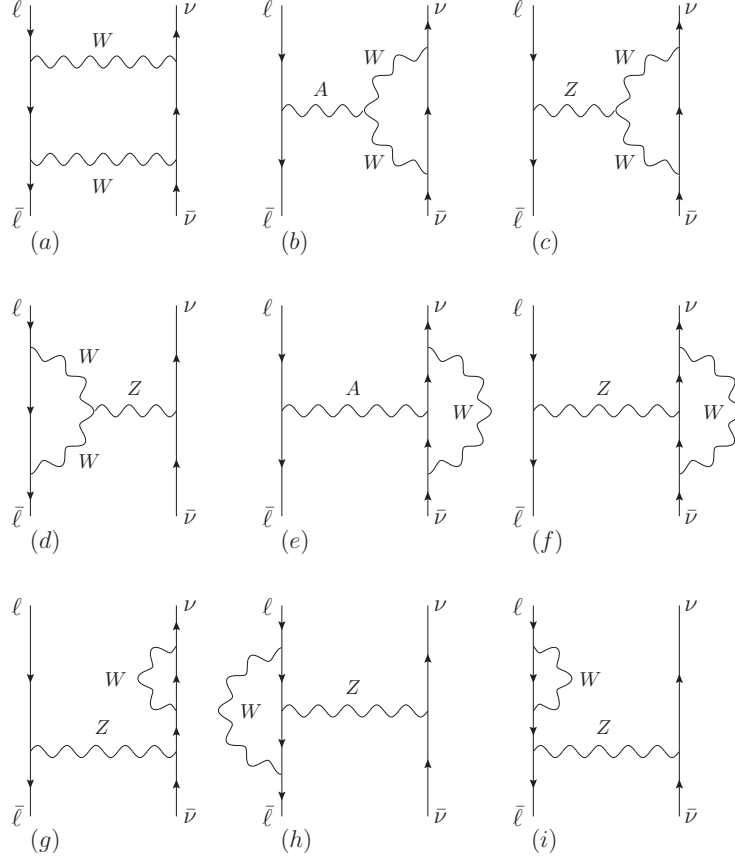
where the vertices $\mathcal{V}$ are defined according to

Fig. 26. The box and vertex diagrams that depends on the gfp ξ_W.

$$\mathcal{V}_{W_\alpha f\bar{f}} = \bar{v}_f C_{W_\alpha f\bar{f}} u_f,$$
$$\mathcal{V}_{V_\alpha f\bar{f}} = \bar{v}_f \Gamma_{V_\alpha f\bar{f}} u_f, \qquad V = A,\ Z. \tag{4.41}$$

The first term on the rhs of (4.40) is the "pure" box, *i.e.*, the part that does not contain any propagator-like structures, whereas the second term is the propagator-like contribution that must be combined with the conventional propagator graphs of Fig. 27. To accomplish this, we employ Eq. (4.38), in order to write the unphysical vertices $\mathcal{V}_{W\ell\bar{\ell}}$ and $\mathcal{V}_{W\nu\bar{\nu}}$ in terms of the physical ones, $\mathcal{V}_{A\ell\bar{\ell}}$, $\mathcal{V}_{Z\ell\bar{\ell}}$, and $\mathcal{V}_{Z\nu\bar{\nu}}$. Specifically, using that in our case $T_z^\ell = -\frac{1}{2}$ and $T_z^\nu = \frac{1}{2}$, we have

$$C_{\ell\bar{\ell}}^\alpha = -s_w \Gamma_{A^\alpha\ell\bar{\ell}} + c_w \Gamma_{Z^\alpha\ell\bar{\ell}},$$
$$C_{\nu\bar{\nu}}^\alpha = -c_w \Gamma_{Z^\alpha\nu\bar{\nu}}. \tag{4.42}$$

The equations above determine, unambiguously, the parts that must be appended to $\Pi_{Z_\alpha Z_\beta}$ and $\Pi_{A_\alpha Z_\beta}$ self-energies. To make this separation manifest, one must take the extra step of writing $d_Z(q^2)d_Z^{-1}(q^2) = d_A(q^2)d_A^{-1}(q^2) = 1$, in order to force the external tree-level propagators to appear explicitly [see Fig. 28]. Thus, from the propagator-like part of the box we finally obtain
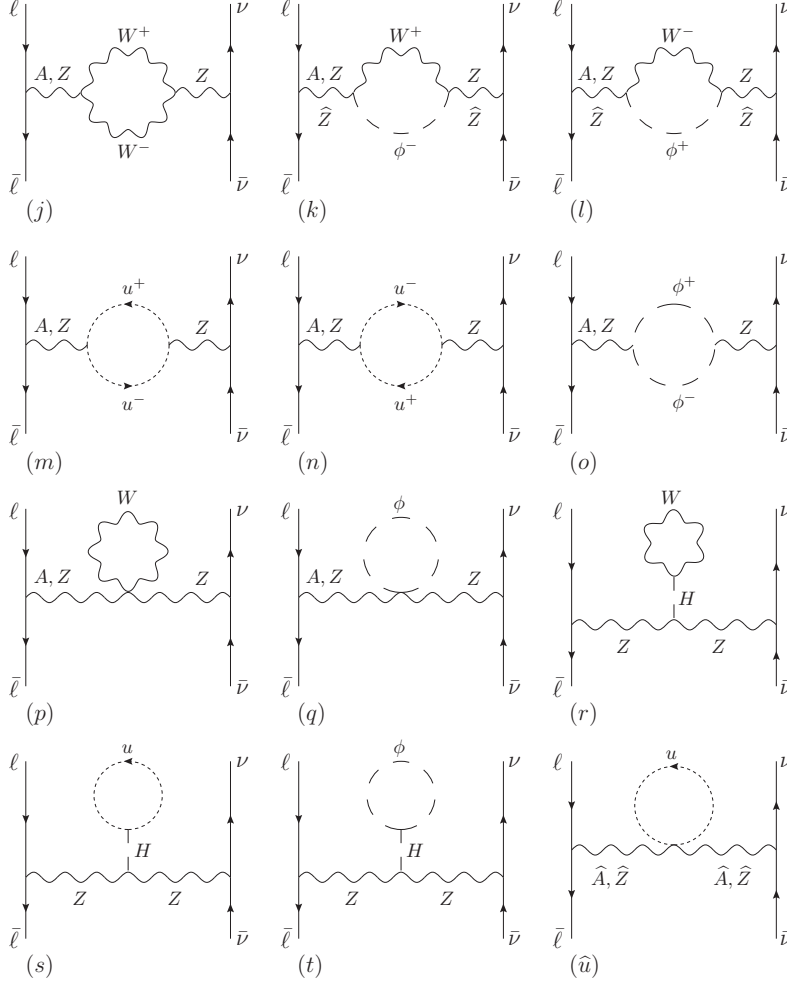
Fig. 27. The self-energy diagrams that depends on the gfp ξ_W.

$$(a)_{A_\alpha Z_\beta} = s_w c_w q^2 (q^2 - M_Z^2) \left(\lambda_W^2 I_4 k_\alpha k_\beta - 2\lambda_W I_3 g_{\alpha\beta} \right),$$

$$(a)_{Z_\alpha Z_\beta} = -c_w^2 (q^2 - M_Z^2)^2 \left(\lambda_W^2 I_4 k_\alpha k_\beta - 2\lambda_W I_3 g_{\alpha\beta} \right). \tag{4.43}$$

A similar procedure must be followed for the vertex graphs shown in Fig. 26. In doing so, recall that there is a relative minus sign between the ZW^+W^- and AW^+W^- vertices, namely $\Gamma_{A_\alpha W_\mu W_\nu}(q, k_1, k_2) = i g_w s_w \Gamma_{\alpha\mu\nu}(q, k_1, k_2)$, while $\Gamma_{Z_\alpha W_\mu W_\nu}(q, k_1, k_2) = -i g_w c_w \Gamma_{\alpha\mu\nu}(q, k_1, k_2)$. Then, all propagator-like terms identified from the boxes and the vertex-graphs must be added to the conventional self-energy diagrams, given in Fig. 27. At this point, it would be a matter of straightforward algebra to verify that all ξ_W-dependent terms cancel. Of course, this cancellation proceeds completely independently for the ZZ and AZ contributions. To make the cancellation explicit (*i.e.*, identify exactly the parts of the conventional self-energy diagrams that will cancel against those coming from the boxes and the vertex-graphs) we can repeat what we did in the case of QCD. Thus, employing the WIs of Eqs (2.37) triggered by the action of the longitudinal parts of the internal W propagators on the three-boson vertices we can rearrange diagram (j), exposing a large part of the underlying gfp-cancellation. For the rest of the diagrams in Fig. 27 one must instead use the identity of Eq. (4.29). Note that the inclusion of the tadpole graphs,
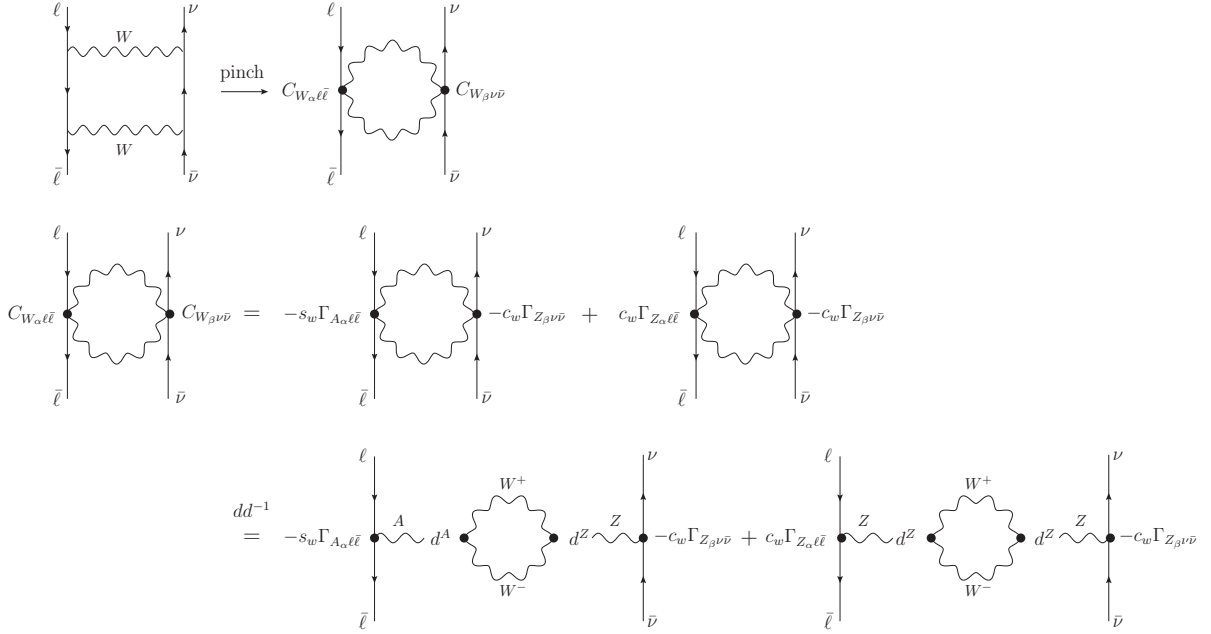
78

Fig. 28. The procedure needed for splitting the propagator-like pieces coming from the WW box among the different AZ and ZZ self-energies.

namely (r), (s), and (t), is crucial for the final cancellation of the gfp-dependent contributions that do not depend on q^2.

4.3.2 Final rearrangement and connection with the background Feynman gauge

Exactly as happened in the QCD case, the gfp-cancellations described in the previous subsection amount effectively to choosing the Feynman gauge, $\xi_W = 1$ (the self-energy diagrams of Fig. 25 are also in $\xi_Z = 1$ and we will suppress them in what follows). The next step is to consider the action of the remaining pinching momenta stemming from the three-gauge-boson vertices inside the non-Abelian diagrams (o), (p), and (q), exposed after employing the PT decomposition of Eqs (2.38) and (2.39). The propagator-like contributions that will emerge from the action of Γ^{P} must be then reassigned to the conventional self-energy graphs, thus giving rise to the one-loop PT self-energies, in this case $\widehat{\Pi}_{Z_\alpha Z_\beta}$ and $\widehat{\Pi}_{A_\alpha Z_\beta}$. The part of the vertex graph containing the Γ^{F}, together with the Abelian graph which in the Feynman gauge remains unchanged, constitute the one-loop PT vertices $A\nu\bar{\nu}$, $Z\nu\bar{\nu}$, and $Z\ell\bar{\ell}$, to be denoted by $\widehat{\Gamma}_{A\nu\bar{\nu}}$, $\widehat{\Gamma}_{Z\nu\bar{\nu}}$, and $\widehat{\Gamma}_{Z\ell\bar{\ell}}$, respectively.

Let us see this in detail. Setting

$$I_{WW}(q) = \int_k \frac{1}{(k^2 - M_W^2)[(k+q)^2 - M_W^2]}, \tag{4.44}$$

we obtain from the non-Abelian vertex graphs (now in the Feynman gauge):

79

$$(b)_{\xi_W=1} = (b)^{\mathrm{F}} - 2\mathcal{V}_{A^\alpha \ell \bar{\ell}}\, d_A(q^2) \left[s_w c_w (q^2 - M_Z^2) I_{WW}(q) g_{\alpha\beta} \right] d_Z(q^2)\, \mathcal{V}_{Z^\beta \nu \bar{\nu}},$$

$$(c)_{\xi_W=1} = (c)^{\mathrm{F}} + 2\mathcal{V}_{Z^\alpha \ell \bar{\ell}}\, d_Z(q^2) \left[c_w^2 (q^2 - M_Z^2) I_{WW}(q) g_{\alpha\beta} \right] d_Z(q^2) \mathcal{V}_{Z^\beta \nu \bar{\nu}},$$

$$(d)_{\xi_W=1} = (d)^{\mathrm{F}} - 2\mathcal{V}_{A^\alpha \ell \bar{\ell}}\, d_A(q^2) \left[s_w c_w q^2 I_{WW} g_{\alpha\beta} \right] d_Z(q^2) \mathcal{V}_{Z^\beta \nu \bar{\nu}},$$

$$+ 2\mathcal{V}_{Z^\alpha \ell \bar{\ell}}\, d_Z(q^2) \left[c_w^2 (q^2 - M_Z^2) I_{WW}(q) g_{\alpha\beta} \right] d_Z(q^2) \mathcal{V}_{Z^\beta \nu \bar{\nu}}. \tag{4.45}$$

The one-loop PT vertices $\widehat{\Gamma}_{A\nu\bar{\nu}}$, $\widehat{\Gamma}_{Z\nu\bar{\nu}}$, and $\widehat{\Gamma}_{Z\ell\bar{\ell}}$, are given by

$$(e) + (b)^{\mathrm{F}} = \mathcal{V}_{A^\alpha \ell \bar{\ell}}\, d_A(q^2)\, \widehat{\Gamma}_{A^\alpha \nu \bar{\nu}},$$

$$(f) + (c)^{\mathrm{F}} = \mathcal{V}_{Z^\alpha \ell \bar{\ell}}\, d_Z(q^2)\, \widehat{\Gamma}_{Z^\alpha \nu \bar{\nu}},$$

$$(h) + (d)^{\mathrm{F}} = \widehat{\Gamma}_{Z^\alpha \ell \bar{\ell}}\, d_Z(q^2)\, \mathcal{V}_{Z^\alpha \nu \bar{\nu}}, \tag{4.46}$$

whereas the PT self-energies $\widehat{\Pi}_{Z_\alpha Z_\beta}$ and $\widehat{\Pi}_{Z_\alpha Z_\beta}$ are simply the sum of all propagator-like contributions, namely

$$\widehat{\Pi}_{Z_\alpha Z_\beta}(q) = \Pi^{(\xi_W=1)}_{Z_\alpha Z_\beta}(q) + 4 g_w^2 c_w^2 (q^2 - M_Z^2) g_{\alpha\beta} I_{WW}(q),$$

$$\widehat{\Pi}_{A_\alpha Z_\beta}(q) = \Pi^{(\xi_W=1)}_{A_\alpha Z_\beta}(q) - 2 g_w^2 s_w c_w (2q^2 - M_Z^2) g_{\alpha\beta} I_{WW}(q). \tag{4.47}$$

It is now relatively straightforward to prove that the ξ_W-independent PT self-energies constructed in Eqs (4.47) coincide with their BFM counterparts computed at $\xi_W^Q = 1$, *i.e.*,

$$\widehat{\Pi}_{Z_\alpha Z_\beta}(q) = \tilde{\Pi}^{(\xi_W^Q=1)}_{Z_\alpha Z_\beta}(q),$$

$$\widehat{\Pi}_{A_\alpha Z_\beta}(q) = \tilde{\Pi}^{(\xi_W^Q=1)}_{A_\alpha Z_\beta}(q). \tag{4.48}$$

To see this explicitly, we will start from the rhs of (4.47) and reorganize, appropriately, the individual Feynman diagrams contributing to the ZZ and AZ self-energies. Specifically, we will cast all diagrams in Fig. 27, computed at $\xi_W = 1$, into the form of the corresponding diagrams in the BFM at $\xi_W^Q = 1$, plus the leftover contributions.

Let us then start with diagrams $(j)_{Z_\alpha Z_\beta}$ and $(j)_{A_\alpha Z_\beta}$, and employ Eq. (2.71), together with Eqs (2.72), to write them in the form

$$(j)_{Z_\alpha Z_\beta} = (\widehat{j})_{Z_\alpha Z_\beta} - 2 g_w^2 c_w^2 \left[2q^2 I_{WW}(q) g_{\alpha\beta} + \int_k \frac{3 k_\alpha k_\beta - k^2 g_{\alpha\beta}}{(k^2 - M_W^2)[(k+q)^2 - M_W^2]} \right],$$

$$(j)_{A_\alpha Z_\beta} = (\widehat{j})_{A_\alpha Z_\beta} + 2 g_w^2 s_w c_w \left[2q^2 I_{WW}(q) g_{\alpha\beta} + \int_k \frac{3 k_\alpha k_\beta - k^2 g_{\alpha\beta}}{(k^2 - M_W^2)[(k+q)^2 - M_W^2]} \right]. \tag{4.49}$$

Notice that the terms $(\widehat{j})_{Z_\alpha Z_\beta}$ and $(\widehat{j})_{A_\alpha Z_\beta}$ on the rhs come from the $\Gamma^{\mathrm{F}}\Gamma^{\mathrm{F}}$ part, while the remainders come from the expressions given in Eqs (2.72), when the terms proportional to

q_α and q_β are set equal to zero (due to current conservation).

For the remaining diagrams, simple algebra yields:

$$(k)_{Z_\alpha Z_\beta} + (l)_{Z_\alpha Z_\beta} = (\widehat{k})_{Z_\alpha Z_\beta} + (\widehat{l})_{Z_\alpha Z_\beta} + 2g_w^2 c_w^2 (2M_Z^2 - M_W^2) I_{WW}(q) g_{\alpha\beta},$$

$$(m)_{Z_\alpha Z_\beta} + (n)_{Z_\alpha Z_\beta} = (\widehat{m}_{Z_\alpha Z_\beta} + (\widehat{n})_{Z_\alpha Z_\beta} + 6g_w^2 c_w^2 \int_k \frac{k_\alpha k_\beta}{(k^2 - M_W^2)[(k+q)^2 - M_W^2]},$$

$$(p)_{Z_\alpha Z_\beta} = (\widehat{p})_{Z_\alpha Z_\beta} + (\widehat{u})_{Z_\alpha Z_\beta} - 2g_w^2 c_w^2 \int_k \frac{g_{\alpha\beta}}{k^2 - M_W^2}, \tag{4.50}$$

and

$$(k)_{A_\alpha Z_\beta} + (l)_{A_\alpha Z_\beta} = -2g_w^2 s_w c_w (M_Z^2 - M_W^2) I_{WW}(q) g_{\alpha\beta},$$

$$(m)_{A_\alpha Z_\beta} + (n)_{A_\alpha Z_\beta} = (\widehat{d})_{A_\alpha Z_\beta} + (\widehat{e})_{A_\alpha Z_\beta} - 6g_w^2 s_w c_w \int_k \frac{k_\alpha k_\beta}{(k^2 - M_W^2)[(k+q)^2 - M_W^2]},$$

$$(p)_{A_\alpha Z_\beta} = (\widehat{p})_{A_\alpha Z_\beta} + (\widehat{u})_{A_\alpha Z_\beta} + 2g_w^2 s_w c_w \int_k \frac{g_{\alpha\beta}}{k^2 - M_W^2}. \tag{4.51}$$

Then, adding by parts all the terms above, we obtain

$$\Pi_{Z_\alpha Z_\beta}^{(\xi_W = 1)} = \tilde{\Pi}_{Z_\alpha Z_\beta}^{(\xi_W^Q = 1)} - 4g_w^2 c_w^2 (q^2 - M_Z^2) g_{\alpha\beta} \, I_{WW}(q),$$

$$\Pi_{A_\alpha Z_\beta}^{(\xi_W = 1)} = \tilde{\Pi}_{A_\alpha Z_\beta}^{(\xi_W^Q = 1)} + 2g_w^2 s_w c_w (2q^2 - M_Z^2) g_{\alpha\beta} \, I_{WW}(q). \tag{4.52}$$

Substituting Eqs (4.52) into the rhs of Eqs (4.47) we obtain immediately Eqs (4.48), as announced. In particular, notice that: (*i*) in the BFM there is no $\widehat{A} W^\pm \phi^\mp$ interaction, and therefore graphs (k) and (l) are absent in $\tilde{\Pi}_{A_\alpha Z_\beta}$, and (*ii*) diagram $(\widehat{u})$, corresponding to the characteristic BFM four-field coupling $\widehat{V}\widehat{V}uu$, has been generated dynamically from the simple rearrangement of terms.

With a small extra effort we can now obtain the closed expressions for the $\widehat{\Pi}_{Z_\alpha Z_\beta}$ and $\widehat{\Pi}_{A_\alpha Z_\beta}$ in terms of the Passarino-Veltman functions [96]. We will only focus on the parts of the self-energies originating from Feynman graphs containing W propagators, together with the associated Goldstone boson and ghosts. The contributions coming form the rest of the diagrams (*e.g.*, containing loops with fermions, or Z- and H-bosons) are common to the conventional and PT self-energies, *i.e.*, $\Pi_{AZ}^{(\bar{f}f)} = \widehat{\Pi}_{AZ}^{(\bar{f}f)}$ and $\Pi_{ZZ}^{(\bar{f}f)} = \widehat{\Pi}_{ZZ}^{(\bar{f}f)}$, and we do not report them here. Therefore the only Passarino-Veltman function that will appear is $B_0(q^2, M_W^2, M_W^2)$.

To that end, one may use the closed expressions for $\Pi_{Z_\alpha Z_\beta}^{(\xi_W = 1)}$ and $\Pi_{A_\alpha Z_\beta}^{(\xi_W = 1)}$ given in [97], and add to them the pinch terms given in Eqs (4.47). Equivalently, one may employ the correspondence established in Eqs (4.48), and calculate directly the graphs contributing to $\tilde{\Pi}_{A_\alpha Z_\beta}^{(\xi_W^Q = 1)}$ and $\tilde{\Pi}_{A_\alpha Z_\beta}^{(\xi_W^Q = 1)}$ using the Feynman rules of [95]. Opting for the former procedure, and concentrating on the part proportional to $g_{\alpha\beta}$ (which we factor out), from [97] we have that

$$
\Pi_{AZ}^{(WW)}(q^2)\Big|_{\xi_W=1} = \frac{\alpha}{4\pi}\frac{1}{3s_w c_w}\left\{\left[\left(9c_w^2 + \frac{1}{2}\right)q^2 + (12c_w^2 + 4)M_W^2\right]B_0(q^2, M_W^2, M_W^2)\right.
$$
$$
\left. - (12c_w^2 - 2)M_W^2 B_0(0, M_W^2, M_W^2) + \frac{1}{3}q^2\right\},
$$
$$
\Pi_{ZZ}^{(WW)}(q^2)\Big|_{\xi_W=1} = -\frac{\alpha}{4\pi}\frac{1}{6s_w^2 c_w^2}\left\{\left[\left(18c_w^4 + 2c_w^2 - \frac{1}{2}\right)q^2 + (24c_w^4 + 16c_w^2 - 10)M_W^2\right]\times\right.
$$
$$
\times B_0(q^2, M_W^2, M_W^2) - (24c_w^4 - 8c_w^2 + 2)M_W^2 B_0(0, M_W^2, M_W^2)
$$
$$
\left. + \frac{1}{3}(4c_w^2 - 1)q^2\right\}. \tag{4.53}
$$

Adding to the above expressions the pinch terms given in Eqs (4.47), and using the identity $iB_0(q^2, M_W^2, M_W^2) = 16\pi^2\, I_{WW}(q)$, we finally obtain

$$
\widehat{\Pi}_{AZ}^{(WW)}(q^2) = \frac{\alpha}{4\pi}\frac{1}{3s_w c_w}\left\{\left[\left(21c_w^2 + \frac{1}{2}\right)q^2 + (12c_w^2 - 2)M_W^2\right]B_0(q^2, M_W^2, M_W^2)\right.
$$
$$
\left. - (12c_w^2 - 2)M_W^2 B_0(0, M_W^2, M_W^2) + \frac{1}{3}\,q^2\right\},
$$
$$
\widehat{\Pi}_{ZZ}^{(WW)}(q^2) = -\frac{\alpha}{4\pi}\frac{1}{6s_w^2 c_w^2}\left\{\left[\left(42c_w^4 + 2c_w^2 - \frac{1}{2}\right)q^2 + (24c_w^4 - 8c_w^2 - 10)M_W^2\right]\times\right.
$$
$$
\times B_0(q^2, M_W^2, M_W^2) - (24c_w^4 - 8c_w^2 + 2)M_W^2 B_0(0, M_W^2, M_W^2)
$$
$$
\left. + \frac{1}{3}(4c_w^2 - 1)\,q^2\right\}. \tag{4.54}
$$

It is easy to establish from the closed expressions reported in [97] that $\Pi_{AZ}^{(f\bar{f})}(0) = 0$ and $\widehat{\Pi}_{AZ}^{(f\bar{f})}(0) = 0$. On the other hand, from Eqs (4.53) we see that $\Pi_{AZ}^{(WW)}(0) \neq 0$, while $\widehat{\Pi}_{AZ}^{(WW)}(0) = 0$. Evidently, as a result of the PT rearrangement, bosonic and fermionic radiative corrections are treated on the same footing. As we will see in the next section, this last property is of great importance for phenomenological applications, such as the self-consistent generalization of the universal part of the ρ-parameter, the unambiguous definition of the physical charge radius of the neutrinos, and the gauge-invariant formalism for treating resonant transition amplitudes.

4.3.3   A very special case: the unitary gauge

In the previous subsections we have applied the PT in the framework of the linear renormalizable R_ξ gauges, and we have obtained ξ-independent one-loop self-energies for the gauge bosons. What would happen, however, if one were to work *directly* in the unitary gauge? The unitary gauge is reached after gauging away the would-be Goldstone bosons, through an appropriate field redefinition (which, at the same time, corresponds to a gauge transformation) $\phi(x) \to \phi'(x) = \phi(x)\exp\left(-i\zeta(x)/v\right)$, where $\zeta(x)$ denotes, generically, the Goldstone fields. Note that the unitary gauge is defined completely independently of the R_ξ gauges; of course, operationally, it is identical to the $\xi_W, \xi_Z \to \infty$ limit of the latter. In particular, in the unitary gauge the W and Z propagators are given by (4.28), where $i = W, Z$.

Given that the contributions of unphysical scalars and ghosts cancel in this gauge, the unitar-

ity of the theory becomes *manifest* [and hence its name]. In the language employed in subsection 2.5, "manifest unitarity" means that, in the unitary gauge, the OT (a direct consequence of unitarity) holds in its strong version. The most immediate way to realize this is by noticing that the unitary gauge propagators, (4.28), and the expression for the sum over the polarization vectors of a massive spin one vector boson [see (4.60) in the following subsection] are practically identical.

Since the early days of spontaneously broken non-Abelian gauge theories, the unitary gauge has been known to give rise to non-renormalizable Green's functions, in the sense that their divergent parts cannot be removed by the usual mass and field-renormalization counter-terms. It is easy to deduce from the tree-level expressions of the gauge-boson propagators why this happens: the longitudinal contribution in (4.28) is divided by a squared mass instead of a squared momentum, i.e. $q^\mu q^\nu / M_i^2$ instead of $q^\mu q^\nu / q^2$, and therefore, $U_{\mu\nu}^i(q) \sim 1$ as $q \to \infty$. As a consequence, when $U_{\mu\nu}^i(q)$ is inserted inside quantum loops (and q is the virtual momentum that is being integrated over), it gives rise to highly divergent integrals. If dimensional regularization is applied, this hard short-distance behavior manifests itself in the occurrence of divergences proportional to high powers of q^2. Thus, at one loop, the divergent part of the W or Z self-energies proportional to $g_{\mu\nu}$ has the general form

$$\Pi_{WW}^{\rm div}(q^2) = \frac{1}{\epsilon}(c_1 q^6 + c_2 q^4 + c_3 q^2 + c_4), \tag{4.55}$$

where the coefficients c_i, of appropriate dimensionality, depend on the gauge coupling and combinations of M_W^2 and M_Z^2. The important point is that, whereas the last two terms on the rhs of (4.55) can be absorbed into mass and wave-function renormalization as usual, the first two *cannot* be absorbed into a redefinition of the parameters in the original Lagrangian, because they are proportional to q^6 and q^4.

As was shown in a series of papers [98–100], when one puts together the individual Green's functions to form S-matrix elements, an extensive cancellation of all non-renormalizable divergent terms takes place, and the resulting S-matrix element can be rendered finite through the usual mass and gauge coupling renormalization. Actually, in retrospect, this cancellation is nothing but another manifestation of the PT (of course, the papers mentioned above predate the PT). Even though this situation may be considered acceptable from the practical point of view, in the sense that S-matrix elements may be still computed consistently, the inability to define renormalizable Green's functions has always been a theoretical shortcoming of the unitary gauge.

The actual demonstration of how to construct renormalizable Green's functions at one-loop starting from the unitary gauge was given in [101]. The methodology is identical to that used in the context of the R_ξ gauges: the propagator-like parts of vertices and boxes are identified and subsequently redistributed among the various gauge-boson self-energies. Evidently, the pinch contributions contain, themselves, divergent terms proportional to q^6 and q^4, which, when added to the analogous contributions contained in the conventional propagators, cancel exactly. After this cancellation, the remaining terms reorganize themselves in such a way as give rise *exactly* to the unique PT gauge boson self-energies, *viz.* Eqs (4.53).

4.3.4 Pinch technique absorptive construction in the electroweak sector

We will now study exactly how the PT subamplitudes of the electroweak theory satisfy the OT [72,73]. The upshot of this section is that the conclusions drawn from the corresponding QCD analysis, in particular the s-t cancellations and the validity of the strong OT version for the PT Green's functions, persist in the case of tree-level symmetry breaking. The richness of the electroweak spectrum and the complexity of the corresponding Feynman rules make the actual demonstrations slightly more cumbersome, but the underlying philosophy of the construction is very similar to that of QCD.

We consider the forward process $f(p_1)\bar{f}(p_2) \to f(p_1)\bar{f}(p_2)$ and study both sides of the OT to lowest order. The PT rearrangement of the one-loop amplitude of this process proceeds as described in the previous section, giving rise to one-loop PT Green's functions, such as the PT self-energies $\widehat{\Pi}_{Z_\alpha Z_\beta}(q)$, $\widehat{\Pi}_{A_\alpha Z_\beta}(q)$, $\widehat{\Pi}_{A_\alpha A_\beta}(q)$, the PT vertices $\widehat{\Gamma}_{A_\alpha \nu\bar{\nu}}$, $\widehat{\Gamma}_{Z_\alpha f\bar{f}}$, $\widehat{\Gamma}_{Z_\alpha \nu\bar{\nu}}$, and the PT boxes. From them the corresponding subamplitudes may be straightforwardly constructed; their imaginary parts will determine the propagator-, vertex-, and box-like parts of the rhs of the OT, to be denoted by $(\mathrm{rhs})_i$, $i = 1, 2, 3$ as usual.

Let us now focus on the lhs of the OT. Evidently, there are several intermediate states $|j\rangle$ that may appear; specifically, depending on the available center-of-mass energy, all fermionic pairs (quarks and leptons) $|f_i \bar{f}_i\rangle$ (with i the flavor index), together with the bosonic channels $|W^+W^-\rangle$ and $|ZH\rangle$, may enter in principle. Notice, however, that the energy thresholds for the appearance of all these intermediate states are different, being given by $s_{\mathrm{th}} = (m_1 + m_2)^2$; for instance, the intermediate state $|W^+W^-\rangle$ will appear on the rhs of the OT when $s \geq 4M_W^2$, while the $|ZH\rangle$ channel opens up when $s \geq (M_Z + M_H)^2$. This clear kinematic separation of the various possible channels indicates that the pertinent PT cancellations (*i.e.*, the s-t cancellation) take place *independently* within each intermediate state; indeed, there is no way that the $|W^+W^-\rangle$ and $|ZH\rangle$ can talk to each other (unless $M_H = 2M_W - M_Z$, which is experimentally excluded). Therefore, on the rhs of the OT we will keep only the contribution of the S-matrix element $\langle f\bar{f}|T|W^+W^-\rangle$, *i.e.*,

$$\Im m\langle f\bar{f}|T|f\bar{f}\rangle_{WW} = \frac{1}{2}\int_{\mathrm{PS}_{WW}} \langle f\bar{f}|T|W^+W^-\rangle\langle W^+W^-|T|f\bar{f}\rangle^*. \qquad (4.56)$$

Notice that, unlike Eq. (2.127), now there is no additional statistical factor, since the two (positively and negatively charged) W's are distinguishable particles. The two-body phase space integral is given by Eq. (2.111) with $m_1 = m_2 = M_W$. As in the QCD case, in what follows we set $T = \langle f\bar{f}|T|f\bar{f}\rangle_{WW}$, $\mathcal{T} = \langle f\bar{f}|T|W^+W^-\rangle$, and $\mathcal{M} = |\mathcal{T}|^2$.

Let us now focus on the rhs of (4.56), considering the process $f(p_1)\bar{f}(p_2) \to W^+(k_1)W^-(k_2)$, with $q = p_1 + p_2 = k_1 + k_2$, and $s = q^2 = (p_1 + p_2)^2 = (k_1 + k_2)^2 > 4M_W^2$. In this case, we have that $\mathcal{T}^{\mu\nu}$ is given by two s-channel graphs, one mediated by a photon and the other by a Z-boson, to be denoted by $\mathcal{T}_A^{\mu\nu}$ and $\mathcal{T}_Z^{\mu\nu}$, respectively, and one t-channel graph, to be denoted by $\mathcal{T}_t^{\mu\nu}$, *i.e.*, (see also Fig. 29)

$$\mathcal{T}^{\mu\nu} = \mathcal{T}_{s,A}^{\mu\nu} + \mathcal{T}_{s,Z}^{\mu\nu} + \mathcal{T}_t^{\mu\nu}, \qquad (4.57)$$
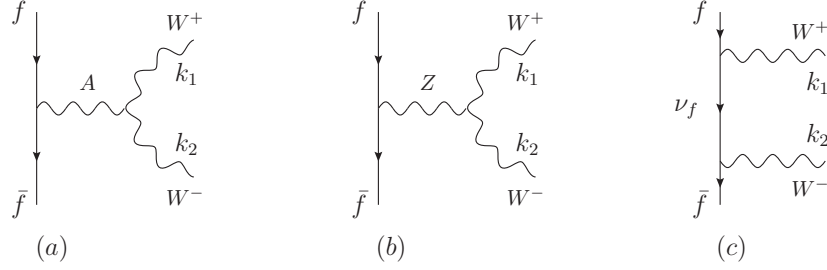
where

Fig. 29. The two s-channel and one t-channel graphs contributing to the tree-level process $f(p_1)\bar{f}(p_2) \to W^+(k_1)W^-(k_2)$.

$$\mathcal{T}_{s,A}^{\mu\nu} = -\mathcal{V}_{A^\alpha f \bar{f}} d_A(q^2) g_w s_w \Gamma_\alpha^{\mu\nu}(q, k_1, k_2),$$
$$\mathcal{T}_{s,Z}^{\mu\nu} = \mathcal{V}_{Z^\alpha f \bar{f}} d_Z(q^2) g_w c_w \Gamma_\alpha^{\mu\nu}(q, k_1, k_2),$$
$$\mathcal{T}_t^{\mu\nu} = -\frac{g_w^2}{2} \bar{v}_f(p_2) \gamma^\mu P_L\, S_{f'}^{(0)}(p_1 - k_1) \gamma^\nu P_L u_f(p_1). \tag{4.58}$$

Note that we have already used current conservation to eliminate the (gfp-dependent) longitudinal parts of the tree-level photon and Z-boson propagators. Then,

$$\mathcal{M} = [\mathcal{T}_{s,A} + \mathcal{T}_{s,Z} + \mathcal{T}_t]^{\mu\nu}\, L_{\mu\mu'}(k_1) L_{\nu\nu'}(k_2) \left[\mathcal{T}_{s,A}^* + \mathcal{T}_{s,Z}^* + \mathcal{T}_t^*\right]^{\mu'\nu'}, \tag{4.59}$$

where now the polarization tensor $L^{\mu\nu}(k)$ corresponds to a massive gauge boson (and thus with *three* polarization states), *i.e.*,

$$L_{\mu\nu}(k) = \sum_{\lambda=1}^{3} \varepsilon_\mu^\lambda(k) \varepsilon_\nu^\lambda(k) = -g_{\mu\nu} + \frac{k_\mu k_\nu}{M_W^2}. \tag{4.60}$$

On shell ($k^2 = M_W^2$) we have that $k^\mu L_{\mu\nu}(k) = 0$. Therefore, as in the QCD case, when the two non-Abelian vertices are decomposed as in Eq. (2.38), the Γ^P parts vanish, and only the Γ^F parts contribute in the s-channel graphs; we denote them by $\mathcal{T}_{s,A}^{F,\mu\nu}$ and $\mathcal{T}_{s,Z}^{F,\mu\nu}$, respectively.

Let us then study what happens when $\mathcal{T}_{\mu\nu}$ is contracted by a longitudinal momentum, k_1^μ or k_2^ν, coming from the polarization tensors. The WIs of Eqs (2.37) will operate at the two s-channel graphs, whereas that of Eq. (4.33) at the t-channel graph (Fig. 30), yielding

$$k_{1\mu}\mathcal{T}_{s,A}^{F,\mu\nu} = -s_w \mathcal{V}_{A^\nu f\bar{f}} + \mathcal{S}_A^\nu,$$
$$k_{1\mu}\mathcal{T}_{s,Z}^{F,\mu\nu} = c_w \mathcal{V}_{Z^\nu f\bar{f}} + \mathcal{S}_Z^\nu,$$
$$k_{1\mu}\mathcal{T}_t^{\mu\nu} = \mathcal{V}_{W^\nu f\bar{f}}, \tag{4.61}$$

with

$$\mathcal{S}_A^\nu = -\mathcal{V}_{A^\alpha f\bar{f}} d_A(q^2) g_w s_w (k_1 - k_2)_\alpha k_2^\nu,$$
$$\mathcal{S}_Z^\nu = \mathcal{V}_{Z^\alpha f\bar{f}} d_Z(q^2) g_w c_w \left[(k_1 - k_2)_\alpha k_2^\nu - M_Z^2 g_{\alpha\nu}\right]. \tag{4.62}$$
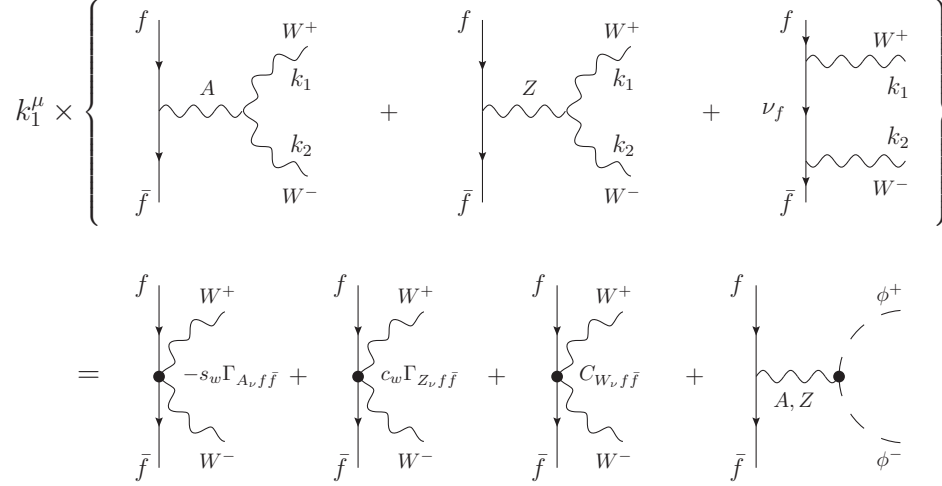
85

Fig. 30. The fundamental s-t cancellation in the SM case.

Adding by parts both sides of Eqs (4.61) we see that a major cancellation takes place: the pieces containing the vertices $\mathcal{V}_{A^\nu f\bar{f}}$ and $\mathcal{V}_{Z^\nu f\bar{f}}$ cancel against $\mathcal{V}_{W^\nu f\bar{f}}$ by virtue of Eq. (4.42), and one is left on the rhs with purely s-channel contribution, namely

$$k_{1\mu}\mathcal{T}^{\mu\nu} = \mathcal{S}_A^\nu + \mathcal{S}_Z^\nu. \tag{4.63}$$

An exactly analogous cancellation takes place when one contracts with k_2^ν. Of course, Eq. (4.63) is nothing more than the manifestation of the s-t cancellation already encountered in QCD, in a slightly more involved context.

It is important to recognize [20] that the cancellation described above goes through, even when the initial fermions are right-handedly polarized, regardless of the fact that, in that particular case, there is no t-channel graph, since the fermions do not couple to the W (Fig. 31). What happens, then, is that the elementary vertices given in Eqs (4.37), together with the corresponding $\mathcal{V}_{A_\alpha f\bar{f}}$ and $\mathcal{V}_{Z_\alpha f\bar{f}}$ are appropriately modified. Specifically,

$$\Gamma_{A_\alpha f_R \bar{f}_R} = -ig_w s_w Q_f \gamma_\alpha,$$
$$\Gamma_{Z_\alpha f_R \bar{f}_R} = -i\frac{g_w}{c_w} s_w^2 Q_f \gamma_\alpha, \tag{4.64}$$

and

$$\mathcal{V}_{Z_\alpha f_R \bar{f}_R} = \frac{s_w}{c_w}\mathcal{V}_{A_\alpha f_R \bar{f}_R}. \tag{4.65}$$

Clearly, in that case, from Eqs (4.42) it follows immediately that

$$\mathcal{V}_{W_\alpha f_R \bar{f}_R} = 0, \tag{4.66}$$

so that Eq. (4.63) is still satisfied. Let us now simplify the algebra, by choosing the initial fermions to be neutrinos, i.e., let us consider the process $\nu\bar{\nu} \to W^+W^-$. This choice eliminates all terms mediated by a photon, and one has

$$\mathcal{M} = \left[\mathcal{T}_{s,Z}^F + \mathcal{T}_t\right]^{\mu\nu} L_{\mu\mu'}(k_1) L_{\nu\nu'}(k_2) \left[\mathcal{T}_{s,Z}^{F*} + \mathcal{T}_t^*\right]^{\mu'\nu'}, \tag{4.67}$$

86
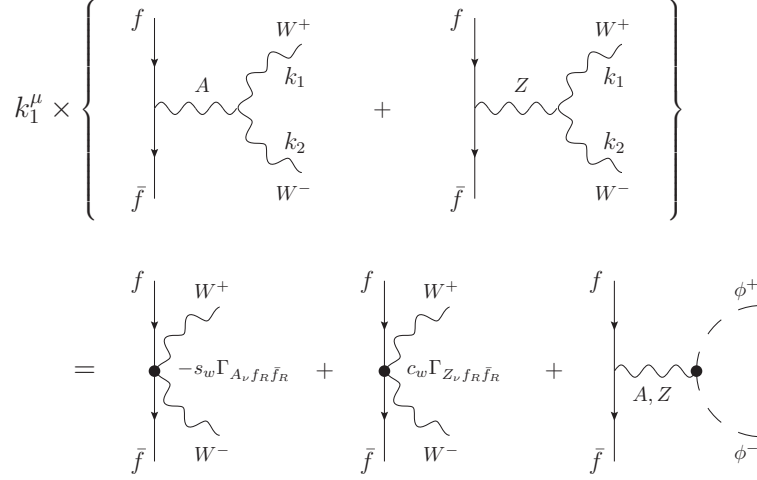
Fig. 31. The fundamental cancellation in the case of right-handed fermions; due to the absence of the t-channel graph, it is implemented through the two remaining s-channel graphs.

Then, Eqs (4.61) simplify to

$$
\begin{aligned}
k_{1\mu}[\mathcal{T}^F_{s,Z} + \mathcal{T}_t]^{\mu\nu} &= \mathcal{S}^\nu_Z, \\
k_{2\nu}[\mathcal{T}^F_{s,Z} + \mathcal{T}_t]^{\mu\nu} &= \bar{\mathcal{S}}^\mu_Z.
\end{aligned}
\tag{4.68}
$$

with

$$
\begin{aligned}
\mathcal{S}^\nu_Z &= \mathcal{V}_{Z^\alpha\nu\bar\nu} d_Z(q^2)\, g_w c_w \left[(k_1 - k_2)_\alpha k_2^\nu - M_Z^2 g_\alpha^\nu \right], \\
\bar{\mathcal{S}}^\mu_Z &= \mathcal{V}_{Z^\alpha\nu\bar\nu} d_Z(q^2)\, g_w c_w \left[(k_1 - k_2)_\alpha k_1^\mu + M_Z^2 g_\alpha^\mu \right],
\end{aligned}
\tag{4.69}
$$

In addition,

$$
\begin{aligned}
k_{2\nu}\mathcal{S}^\nu_Z &= k_{1\mu}\bar{\mathcal{S}}^\mu_Z \\
&= \mathcal{V}_{Z^\alpha\nu\bar\nu} d_Z(q^2) g_w c_w \left[M_W^2 + \frac{1}{2}M_Z^2 \right] (k_1 - k_2)_\alpha.
\end{aligned}
\tag{4.70}
$$

Now we will isolate from (4.67) the part that is purely s-channel (or, equivalently, purely propagator-like), to be denoted by $\widehat{\mathcal{M}}_1$. It is composed by the sum of the following terms

$$
\widehat{\mathcal{M}}_1 = \mathcal{T}^F_Z \cdot \mathcal{T}^{F*}_Z - \frac{\mathcal{S}_Z \cdot \mathcal{S}^*_Z}{M_W^2} - \frac{\bar{\mathcal{S}}_Z \cdot \bar{\mathcal{S}}^*_Z}{M_W^2} + \frac{(k_2 \cdot \mathcal{S}_Z) \cdot (k_2 \cdot \mathcal{S}^*_Z)}{M_W^4}.
\tag{4.71}
$$

Using (2.146), (4.69), (4.69) and (4.70), we find

$$
\widehat{\mathcal{M}}_1 = \mathcal{V}_{Z^\alpha\nu\bar\nu} d_Z(q^2) K_{\alpha\beta} d_Z(q^2) \mathcal{V}_{Z^\beta\nu\bar\nu}
\tag{4.72}
$$

87

with

$$K_{\alpha\beta} = -\frac{g_w^2}{c_w^2}\left[\left(8q^2c_w^4 - 2M_W^2\right)g_{\alpha\beta} + \left(3c_w^4 - c_w^2 + \frac{1}{4}\right)(k_1 - k_2)_\alpha(k_1 - k_2)_\beta\right]. \tag{4.73}$$

Thus, the propagator-like part of the rhs of the OT becomes

$$(\text{rhs})_1 = \frac{1}{2}\int_{\text{PS}_{WW}}\widehat{\mathcal{M}}_1. \tag{4.74}$$

Now, from Eq. (2.150), we have that $\lambda(q^2, M_W^2, M_W^2) = q^2(q^2 - 4M_W^2)$, and therefore

$$\int_{\text{PS}_{WW}}(k_1 - k_2)_\alpha(k_1 - k_2)_\beta = -\frac{1}{3}(q^2 - 4M_W^2)g_{\alpha\beta}\int_{\text{PS}_{WW}} + \cdots, \tag{4.75}$$

where the ellipses stand for terms proportional to $q_\alpha q_\beta$. Then, using the elementary result

$$8\pi^2\int_{\text{PS}_{WW}} = \Im m B_0(q^2, M_W^2, M_W^2), \tag{4.76}$$

Eq. (4.74) becomes

$$(\text{rhs})_1 = \mathcal{V}_{Z^\alpha\nu\bar{\nu}}d_Z(q^2)Kd_Z(q^2)\mathcal{V}_{Z_\alpha\nu\bar{\nu}}, \tag{4.77}$$

with

$$K = -\frac{\alpha}{4\pi}\frac{1}{6s_w^2c_w^2}\left[\left(42c_w^4 + 2c_w^2 - \frac{1}{2}\right)q^2 + (24c_w^4 - 8c_w^2 - 10)M_W^2\right]\Im m B_0(q^2, M_W^2, M_W^2). \tag{4.78}$$

Let us now compare Eq. (4.74) with the propagator-like part of the lhs of the OT, given by

$$(\text{lhs})_1 = \mathcal{V}_{Z^\alpha\nu\bar{\nu}}d_Z(q^2)\left[\Im m\widehat{\Pi}_{ZZ}^{(WW)}(q)\right]d_Z(q^2)\mathcal{V}_{Z_\alpha\nu\bar{\nu}}. \tag{4.79}$$

The equality between Eq. (4.79) and (4.77) requires that

$$\Im m\widehat{\Pi}_{ZZ}^{(WW)}(q) = -\frac{\alpha}{4\pi}\frac{1}{6s_w^2c_w^2}\left[\left(42c_w^4 + 2c_w^2 - \frac{1}{2}\right)q^2 + (24c_w^4 - 8c_w^2 - 10)M_W^2\right]\times$$
$$\times\Im m B_0(q^2, M_W^2, M_W^2). \tag{4.80}$$

Taking the imaginary part of $\widehat{\Pi}_{ZZ}^{(WW)}$ given in Eq. (4.54) we see that Eq. (4.80) is indeed fulfilled.

At this point one could go one step further, and employ a twice subtracted dispersion relation, in order to reconstruct from (4.80) the real part of the $\widehat{\Pi}_{ZZ}^{(WW)}(q)$. The end result of this procedure will coincide with the corresponding expression obtained from Eq. (4.54) after renormalization. (for a detailed derivation, see [73]).

Finally, let us return to the non-renormalizability of the unitary gauges, now seen from the absorptive point of view. As mentioned in the previous subsection, in the unitary gauge the strong version of the OT is satisfied; to make contact with this section, what this means is that the OT is satisfied diagram-by-diagram, *without* having to resort explicitly to the s-t cancellation.

For example, the imaginary part of the conventional self-energy $\Pi_{ZZ}^{(WW)}(s)$ in the unitary gauge is

$$\Im m\Pi_{ZZ}^{(WW)}(s) \sim (s - M_Z)^2 \int_{\mathrm{PS}_{WW}} \mathcal{T}_Z^{\mu\nu} L_{\mu\mu'}(k_1) L_{\nu\nu'}(k_2) \mathcal{T}_Z^{*\mu'\nu'} \,. \tag{4.81}$$

What is the price one pays for *not* implementing the $s - t$ cancellation? Simply, the conventional subamplitudes, such as the one given above, contain terms that grow as s^2 or as s^3 [see, e.g., [102,73]]; indeed, the s-t cancellation eliminates precisely terms of this type. Consequently, if one were to substitute the $\Im m\Pi_{ZZ}^{(WW)}(s)$ obtained from the rhs of (4.81) into a twice subtracted dispersion relation –the maximum number of subtractions allowed by renormalizability– one would encounter UV divergent real parts proportional to q^4 or as q^6. Of course, these are precisely the non-renormalizable terms encountered in (4.55), now obtained not from a direct one-loop calculation but rather from the combined use of unitarity and analyticity (and with a hard UV cutoff instead of $1/\epsilon$).

4.3.5 Background field method away from $\xi_Q = 1$: physical versus unphysical thresholds

As we have seen in the previous section, from the fact that the BFM Green's functions satisfy the same QED-like WIs for every value of the quantum gfp ξ_Q one should *not* conclude that the PT Green's functions, reproduced from the BFM at $\xi_Q = 1$, are simply one among an infinity of physically equivalent choices, parametrized by ξ_Q. This interpretation is not correct: the BFM Green's functions obtained away from $\xi_Q = 1$ are *not* physically equivalent to the privileged case of $\xi_Q = 1$.

In addition to the reasons outlined in Section 3, when dealing with the SM the following crucial observation clarifies the above point beyond any doubt: for $\xi_Q \neq 1$ the imaginary parts of the BFM electroweak self-energies include terms with *unphysical thresholds* [73,72]. For example, for the one-loop contributions of the W and its associated would-be Goldstone boson and ghost to $\tilde{\Pi}_{ZZ}^{(WW)}(\xi_Q, s)$ one obtains

$$\Im m\tilde{\Pi}_{ZZ}^{(WW)}(s, \xi_Q) = \Im m\hat{\Pi}_{ZZ}^{(WW)}(s) + \frac{\alpha}{24 s_w^2 c_w^2} \left(\frac{s - M_Z^2}{s M_Z^4} \right) [W_1(s) + W_2(s, \xi_Q) + W_3(s, \xi_Q)],$$

$$\tag{4.82}$$

with

$$\begin{aligned}
W_1(s) &= f_1(s)\theta(s - 4M_W^2), \\
W_2(s, \xi_Q) &= f_2(s, \xi_Q)\lambda^{1/2}(s, \xi_Q M_W^2, \xi_Q M_W^2)\theta(s - 4\xi_Q M_W^2), \\
W_3(s, \xi_Q) &= f_3(s, \xi_Q)\lambda^{1/2}(s, M_W^2, \xi_Q M_W^2)\theta(s - M_W^2(1 + \sqrt{\xi_Q})^2),
\end{aligned} \tag{4.83}$$

and

$$\begin{aligned}
f_1(s) &= \left(8M_W^2 + s\right)\left(M_Z^2 + s\right) + 4M_W^2\left(4M_W^2 + 3M_Z^2 + 2s\right), \\
f_2(s, \xi_Q) &= f_1(s) - 4\left(\xi_Q - 1\right)M_W^2\left(4M_W^2 + M_Z^2 + s\right), \\
f_3(s, \xi_Q) &= -2\left[8M_W^2 + s - 2\left(\xi_Q - 1\right)M_W^2 + \left(\xi_Q - 1\right)^2 M_W^4 s^{-1}\right]\left(M_Z^2 + s\right).
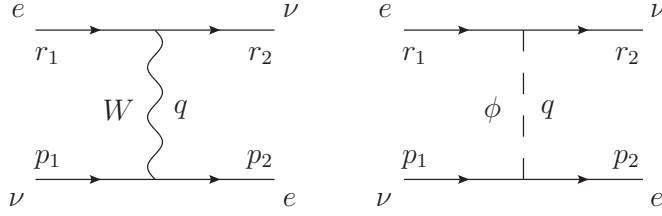\end{aligned} \tag{4.84}$$

Fig. 32. The process $e\nu_e \to e\nu_e$ at tree level in the SM.

These gauge-dependent unphysical thresholds (see the arguments of the θ functions) are artifacts of the BFM gauge fixing procedure, and exactly cancel in the calculation of any physical process against unphysical contributions from the imaginary parts of the one-loop vertices and boxes. After these cancellations have been implemented one is left just with the contribution proportional to the tree level cross section for the on-shell physical process $\nu\bar{\nu} \to W^+W^-$, given in Eq. (4.80), with thresholds only at $q^2 = 4M_W^2$. In fact, by obtaining in the previous subsection the full W-related contribution to the PT self-energy, namely $\widehat{\Pi}_{WW}^{ZZ}(s)$, directly from the on-shell physical process $\nu\bar{\nu} \to W^+W^-$, we have shown explicitly that, in the BFM at $\xi_Q = 1$, the thresholds that occur at $q^2 = 4M_W^2$ are due *solely* to the *physical* W^+W^- pair.

We therefore conclude that the particular value $\xi_Q = 1$ in the BFM *is* distinguished on physical grounds from all other values of ξ_Q. In the next section we will further elaborate on this point, by exposing various pathologies resulting in from the Dyson summation of self-energies with unphysical thresholds.

4.4   PT with massive fermions: an explicit example

In this section, we discuss the technical subtleties encountered in the application of the PT when the fermions are massive. Consider the elastic process $e^-(r_1)\nu_e(p_1) \to e^-(p_2)\nu_e(r_2)$, and concentrate on the charged channel which, at tree-level, is shown in Fig. 32. The momentum transfer q is defined as $q = p_1 - p_2 = r_2 - r_1$. We will consider the electrons to be massive, with a mass m_e, while the neutrinos will be treated for simplicity as if they were massless. The tree-level propagators of the W and the corresponding Goldstone boson are those given in Eq. (4.23) and Eq. (4.25) (for $i = W$); the index "W" will be suppressed in what follows. The elementary vertices describing the coupling of the charged bosons with the external fermions are $\Gamma_\alpha \equiv \Gamma_{W_\alpha^+ \bar{\nu}_e e} = \Gamma_{W_\alpha^- \bar{e}\nu_e}$, $\Gamma_+ \equiv \Gamma_{\phi^+ \bar{\nu}_e e}$, and $\Gamma_- \equiv \Gamma_{\phi^- \bar{e}\nu_e}$, and are given by

$$\Gamma_\alpha = \frac{ig_w}{\sqrt{2}}\gamma_\alpha P_L, \qquad \Gamma_{+(-)} = -\frac{ig_w}{\sqrt{2}}\frac{m_e}{M_W}P_{R(L)}. \tag{4.85}$$

We also define the corresponding vertices sandwiched between the external spinors, *i.e.*,

$$\begin{aligned}
\Gamma_1^\alpha &= \bar{u}_{\nu_e}(r_2)\,\Gamma^\alpha u_e(r_1), & \Gamma_2^\alpha &= \bar{u}_e(p_2)\,\Gamma^\alpha u_{\nu_e}(p_1),\\
\Gamma_1 &= \bar{u}_{\nu_e}(r_2)\,\Gamma_+ u_e(r_1), & \Gamma_2 &= \bar{u}_e(p_2)\,\Gamma_- u_{\nu_e}(p_1).
\end{aligned} \tag{4.86}$$

90

Note that both Γ_1^α and Γ_2^α contain a P_L, whereas Γ_1 and Γ_2 a P_R and a P_L, respectively. The subscripts $(1,2)$ are related to the electric charge carried by the $W^\pm$ entering into the corresponding tree-level vertices by setting $+ \to 1, - \to 2$. The following elementary identities

$$
\begin{aligned}
q_\alpha \Gamma_{1,2}^\alpha &= M_W \Gamma_{1,2}, \\
i\Gamma_{1,2} &= M_W q^\beta \Delta_{\beta\alpha}(q)\Gamma_{1,2}^\alpha + q^2 D(q)\Gamma_{1,2},
\end{aligned}
\tag{4.87}
$$

valid for every ξ_W (which will be indicated simply as ξ in what follows), will be frequently used [in deriving (4.87) we have used Eq. (4.30)].

We will start by considering the S-matrix at tree-level (Fig. 32), to be denoted by T_0, given by

$$
T_0 = \Gamma_1^\alpha \, \Delta_{\alpha\beta}(q) \, \Gamma_2^\beta + \Gamma_1 \, D(q) \, \Gamma_2 \, .
\tag{4.88}
$$

Of course, T_0 must be ξ-independent, and it is easy to demonstrate that this is indeed so. There are three, algebraically equivalent but physically rather distinct, ways of writing the ξ-independent expression for T_0.

i. Using Eqs (4.29) and (4.87) we can see immediately that all dependence on ξ cancels, and one can cast T_0 in terms of $\Delta_{\beta\alpha}^{\xi=1}(q)$ and $D^{\xi=1}(q)$ as follows

$$
T_0 = \Gamma_1^\alpha \Delta_{\alpha\beta}^{\xi=1}(q)\Gamma_2^\beta + \Gamma_1 D^{\xi=1}(q)\Gamma_2.
\tag{4.89}
$$

The physical amplitude is the sum a massive gauge boson and a massive (would-be) Goldstone boson. The fact that the Goldstone boson is massive is, of course, a consequence of the gauge-fixing used, namely the R_ξ-gauges.

ii. Using Eqs (4.27) and (4.87), it is elementary to verify that T_0 can also be written as

$$
T_0 = \Gamma_1^\alpha U_{\alpha\beta}(q)\Gamma_2^\beta.
\tag{4.90}
$$

Thus, even though one works in the R_ξ gauge, making no assumption on the value of ξ (in particular, not taking the limit $\xi \to \infty$) one is led *effectively* to the unitary gauge, with no (unphysical) would-be Golstone bosons present.

iii. The third way of writing T_0 is slightly more subtle, as far as its physical interpretation is concerned. It is well-known (but often underemphasized) that the so-called "spontaneous symmetry breaking" is not actually "breaking" the local gauge symmetry, but simply realizing it in a different way. Specifically, the WIs or STIs of the theory, which encompass the gauge symmetry at the level of Green's functions, maintain their form, at the expense of introducing massless longitudinal poles. The role of these massless poles is obscured by the fact that, through the process of gauge fixing, they can be changed to poles of arbitrary mass (as explained above). These massless poles do not appear in the S-matrix, to the extent that they are absorbed by gauge bosons. However, simple algebra can recast the tree-level amplitude into a form where the presence of the massless poles becomes manifest. Using the algebraic
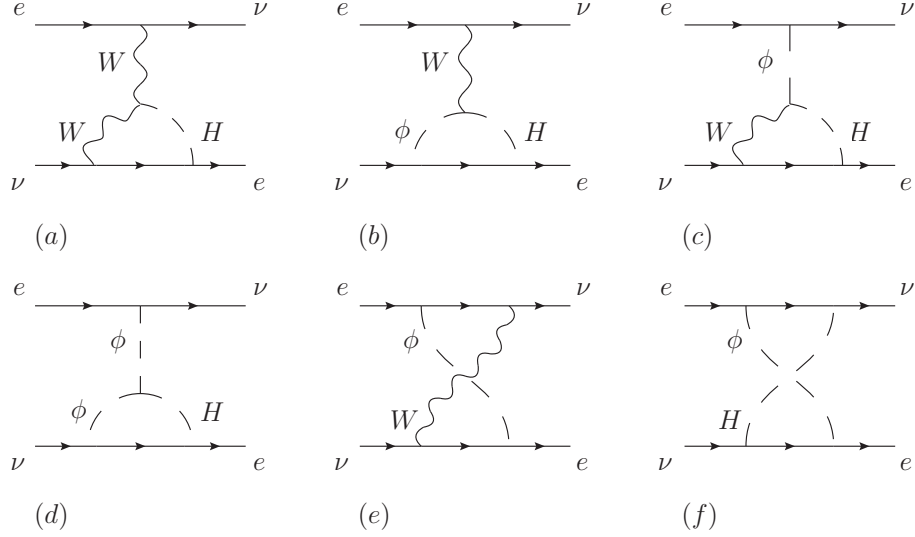
Fig. 33. The subset of box and vertex diagrams containing a W gauge boson and a Higgs field H.

identity

$$\frac{1}{M^2} = \frac{1}{q^2} + \frac{q^2 - M^2}{q^2 M^2},\tag{4.91}$$

we can write $U_{\alpha\beta}(q)$ as

$$U_{\alpha\beta}(q) = P_{\alpha\beta}(q)d_W(q^2) + \frac{q_\alpha q_\beta}{M_W^2}\frac{i}{q^2},\tag{4.92}$$

where we have used the transverse projector $P_{\alpha\beta}(q)$ defined in Eq. (2.26). Then Eq. (4.90) can be rewritten as

$$T_0 = \Gamma_1^\alpha P_{\alpha\beta}(q)d_W(q^2)\Gamma_2^\beta + \Gamma_1\frac{i}{q^2}\Gamma_2.\tag{4.93}$$

As we will see later on, thanks to the PT, the ways of writing the S-matrix given in Eqs (4.90) and (4.93) go through at one-loop, and eventually at all orders.

4.4.1 *Gauge fixing parameter cancellations*

Let us now turn to the one-loop PT construction. The main motivation is to construct via the PT the gfp-independent self-energies $\Pi_{W_\alpha W_\beta}$, $\Pi_{W_\alpha \phi}$, $\Pi_{\phi W_\beta}$, and $\Pi_{\phi\phi}$, to be denoted by $\widehat{\Pi}_{\alpha\beta}$, $\widehat{\Theta}_\alpha$, $\widehat{\Theta}_\beta$, and $\widehat{\Omega}$, respectively, as well as gfp-independent $W f_1 \bar{f}_2$ and $\phi f_1 \bar{f}_2$ vertices, which we denote by $\widehat{\Gamma}_\alpha$ and $\widehat{\Gamma}_\pm$, respectively.

We will show the PT construction for a characteristic subset of diagrams contributing to the amplitude $e^-(r_1)\nu_e(p_1) \to e^-(p_2)\nu_e(r_2)$. Specifically, we will consider the subset of all Feynman graphs that contain, inside the loop, a W- and a H-propagator. The relevant vertex and box diagrams are shown in Fig. 33 and the self-energy diagrams in Fig. 34 . It is relatively easy to understand why this subset must be gfp-independent by itself: The dependence on the Higgs mass forces the gfp-cancellation to take place within this subset (as we will see, up to seagull-

92
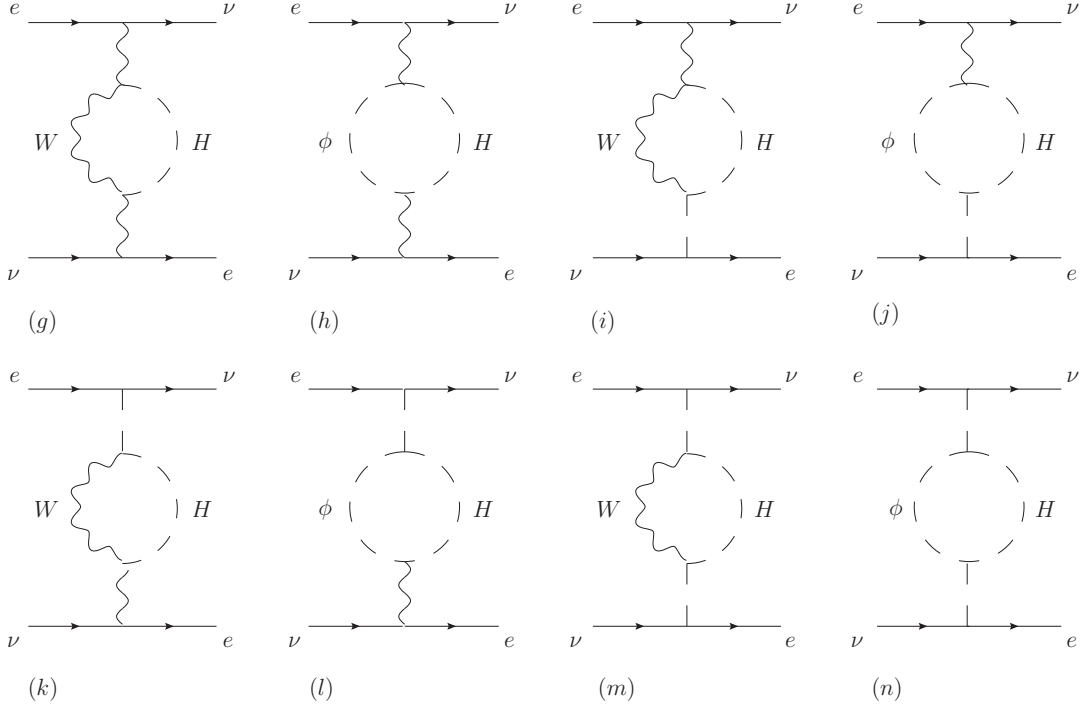
Fig. 34. The self-energy diagrams containing a WH or ϕH loop. The various SM self-energies are given by the diagrams' combinations $(g)+(h) = \Pi^{(WH)}_{\alpha\beta}$, $(i)+(j) = \Theta^{(WH)}_{\alpha}$, $(k)+(l) = \Theta^{(WH)}_{\beta}$ and, finally, $(m)+(n) = \Omega^{(WH)}$.

like terms). From the absorptive point of view, the graphs we consider display a threshold (*i.e.*, they develop imaginary parts if cut) at $q^2 \geq (M_W + M_H)^2$; therefore they should form a gfp-independent subset, since they cannot communicate with the rest (this absorptive argument does not apply to seagulls and tadpoles, since they do not have imaginary parts, but the PT construction takes care of them as well). In what follows, we will use the sub- or super-script "WH" for the aforementioned subset; for example, $\widehat{\Pi}^{(WH)}_{\alpha\beta}$ denotes the subset of graphs contributing to the WW self-energy that contain, in their loop, a W or ϕ propagator and a Higgs-boson propagator (see Fig. 34).

We will introduce the following ingredients appearing in the intermediate steps of our demonstration:

i. The coupling of the Higgs boson to the electrons $\Gamma_H \equiv \Gamma_{H\bar{e}e}$ is given by

$$\Gamma_H = -i\frac{g_w}{2}\frac{m_e}{M_W}, \tag{4.94}$$

and we have that

$$\Gamma_H P_{R(L)} = \frac{1}{\sqrt{2}}\Gamma_{+(-)}. \tag{4.95}$$

ii. We set

$$A^{\xi}_{WH}(q,k) = \left[(k^2 - M_W^2)(k^2 - \xi M_W^2)\left((k+q)^2 - M_H^2\right)\right]^{-1}, \tag{4.96}$$

93

and define the propagator-like structures

$$F_{WH}(q) = (1 - \xi) g_w^2 \int_k A_{WH}^{\xi}(q, k),$$

$$J_{WH}^{\alpha}(q) = (1 - \xi) g_w^2 \int_k k^{\alpha} A_{WH}^{\xi}(q, k),$$

$$K_{WH}^{\alpha\beta}(q) = (1 - \xi) g_w^2 \int_k k^{\alpha} k^{\beta} A_{WH}^{\xi}(q, k), \tag{4.97}$$

the vertex-like structures

$$L_{WH}(q, p_1) = (1 - \xi) g_w \int_k \left[\Gamma_H S_e^{(0)}(p_1 + k) \Gamma_- \right] A_{WH}^{\xi}(q, k),$$

$$\bar{L}_{WH}(q, r_2) = (1 - \xi) g_w \int_k \left[\Gamma_+ S_e^{(0)}(r_2 + k) \Gamma_H \right] A_{WH}^{\xi}(q, k),$$

$$N_{WH}^{\alpha}(q, p_1) = (1 - \xi) g_w \int_k \left[\Gamma_H S_e^{(0)}(p_1 + k) \Gamma_- \right] k^{\alpha} A_{WH}^{\xi}(q, k), \tag{4.98}$$

and, finally, the box-like structure

$$R_{WH}(q, p_1, r_2) = (1 - \xi) g_w \int_k \left[\Gamma_H S_e^{(0)}(p_1 + k) \Gamma_- \right] \left[\Gamma_+ S_e^{(0)}(r_2 + k) \Gamma_H \right] A_{WH}^{(\xi)}(q, k). \tag{4.99}$$

Then, we start with the vertex diagrams (a) and (c) in Fig. 33 and we let the ξ-dependent longitudinal parts appearing in the tree-level W trigger the WI of Eq. (4.33). Now that the electrons are considered to be massive, the term on the rhs in the square brackets of Eq. (4.33) is turned on; as a result, and for the first time until now, the outcome of the pinching action is *not* only propagator-like contributions: in addition, we obtain a vertex-like contribution, precisely due to the additional term in Eq. (4.33) proportional to the electron mass. As we will see, this vertex-like term will mix with the graphs (b) and (d), and will combine to form a ξ-independent vertex-like structure.

Specifically, we have (suppressing a common factor $\Gamma_1^{\beta} \Delta_{\beta\alpha}(q)$ in front)

$$(a)^{\alpha} = (a)_{\xi=1}^{\alpha} + \left\{ \frac{1}{2} M_W J_{WH}^{\alpha}(q) \right\} (i\Gamma_2) - i M_W^2 N_{WH}^{\alpha}(q, p_1),$$

$$(b)^{\alpha} = (b)_{\xi=1}^{\alpha} + \frac{i}{2} q^{\alpha} M_W^2 L_{WH}(q, p_1) + i M_W^2 N_{WH}^{\alpha}(q, p_1), \tag{4.100}$$

We next turn to graphs (c) and (d). As far as diagram (c) is concerned, one of the longitudinal momenta coming from the W-propagator will pinch as before; however, in addition, we will use the identity $(2q + k) \cdot k = [(k + q)^2 - M_H^2] + M_H^2 - q^2$, triggered when the second longitudinal momentum is contracted with the $\Gamma_{\phi WH}$ vertex. The first term in this identity will cancel the M_H-dependent part appearing in $A_{WH}^{\xi}(q, k)$, thus generating a term that is independent of M_H. These terms cancel against other similar terms, coming from the M_H-independent Feynman graphs that are not considered, and will be discarded. Therefore, keeping only M_H-dependent terms, we have [suppressing a common factor $\Gamma_1 D(q)$ in front]

$$(c) = (c)_{\xi=1} + \left\{ -\frac{1}{4}(q^2 - M_H^2)F_{WH}(q) \right\}(i\Gamma_2) + \frac{i}{2}(q^2 - M_H^2)M_W L_{WH}(q, p_1),$$

$$(d) = (d)_{\xi=1} + \frac{i}{2}M_H^2 M_W L_{WH}(q, p_1). \tag{4.101}$$

Finally, following a similar methodology for the boxes (e) and (f), we have

$$(e) = (e)_{\xi=1} + (i\Gamma_1)\left\{ \frac{1}{4}F_{WH}(q) \right\}(i\Gamma_2) - R_{WH}(q, p_1, r_2)$$

$$+ \frac{1}{2}\left[\Gamma_1 M_W L_{WH}(q, p_1) + \Gamma_2 M_W \bar{L}_{WH}(q, r_2) \right],$$

$$(f) = (f)_{\xi=1} + R_{WH}(q, p_1, r_2). \tag{4.102}$$

It is now straightforward to verify that:

i. the vertex-like N_{WH}^α in $(a)^\alpha$ and $(b)^\alpha$, and the box-like R_{WH} in (e) and (f) cancel directly;

ii. the vertex-like terms proportional to L_{WH} in $(b)^\alpha$, (c), (d) and (e) cancel (after restoring the suppressed factors in front) by evoking the identity of Eq (4.87);

iii. the term proportional to $\bar{L}_{WH}$ will cancel, in exactly the same way described above, against the contributions coming from the mirror vertex graphs, not shown.

Thus one is left only with ξ-dependent propagator-like pieces, contained in the curly brackets in Eqs (4.100), (4.101) and (4.102), together with the contributions coming from the mirror vertex graphs; the latter are identical to those already identified, up to trivial adjustments. All aforementioned terms will cancel exactly against the ξ-dependent parts of the conventional self-energy graphs, shown in Fig. 34.

Let us now turn to this remaining cancellation. Separating out the contributions at $\xi = 1$ from the rest, we have for the self-energy graphs of Fig. 34

$$(g)^{\alpha\beta} + (h)^{\alpha\beta} = (g)_{\xi=1}^{\alpha\beta} + (h)_{\xi=1}^{\alpha\beta}$$

$$- \frac{1}{4}q^\alpha q^\beta M_W^2 F_{WH}(q) - \frac{1}{2}M_W^2 \left[q^\alpha J_{WH}^\beta(q) + q^\beta J_{WH}^\alpha(q) \right],$$

$$(i)^\alpha + (j)^\alpha = (i)_{\xi=1}^\alpha + (j)_{\xi=1}^\alpha - \frac{1}{2}q^2 M_W J_{WH}^\alpha(q) - \frac{1}{4}q^\alpha M_W M_H^2 F_{WH}(q),$$

$$(k)^\beta + (l)^\beta = (k)_{\xi=1}^\beta + (l)_{\xi=1}^\beta - \frac{1}{2}q^2 M_W J_{WH}^\beta(q) - \frac{1}{4}q^\beta M_W M_H^2 F_{WH}(q),$$

$$(m) + (n) = (m)_{\xi=1} + (n)_{\xi=1} + \frac{1}{4}q^2(q^2 - 2M_H^2)F_{WH}(q). \tag{4.103}$$

Using again the identity of Eq. (4.87) one may separate, unambiguously, the ξ-dependent propagator like pieces from Eqs (4.100), (4.101) and (4.102) into WW, $W\phi$, ϕW, and $\phi\phi$ structures, and add them to the corresponding contributions in the equation above. It is then straightforward to verify that a complete cancellation of all ξ-dependent terms takes place; in fact, the terms pro-

portional to F_{WH} and J^α_{WH} cancel separately. Even though we have restricted ourselves to the subset of Feynman diagrams that depend explicitly on M_H, the methodology presented goes through, unchanged, also for the remaining graphs. We emphasize again that, as in all previous examples, the conceptual and technical advantage of this demonstration lies precisely in the fact that all cancellations take place systematically, by identifying the appropriate kinematic structures, with no need to carry out any integrations.

Notice, finally, the following important point: all aforementioned cancellations take place *inside* the loops, *without* touching the ξ-dependence of the (external) bare propagators attached to the external fermions; indeed, all we have used, in addition to pinching, is the algebraic identity of Eq (4.87), which is valid for every ξ. As we will see shortly, after the completion of the PT procedure at one-loop, the requirement that this residual ξ-dependence also cancels imposes Abelian-like WIs on the PT Green's functions.

4.4.2 Final rearrangement and comparison with the background Feynman gauge

Let us now turn again to the subset of graphs considered above. As we have demonstrated, inside the loops all propagators have been dynamically reduced to the Feynman gauge, $\xi = 1$. At this point the genuine box contributions have been isolated; thus, the WH-part of the one-loop PT box is given simply by $(e)_{\xi=1} + (f)_{\xi=1}$.

To get the corresponding part of the one-loop PT vertices and self-energies, an additional step is required: we must extract from the vertex graphs in the Feynman gauge possible propagator-like pieces generated by the momentum-dependent vertices. For the case at hand, the only graph that can furnish such a contribution is (c); the propagator-like piece is generated when the longitudinal momentum k_μ, coming from the elementary vertex $\Gamma_{\phi WH} \propto (2q + k)_\mu$ in (c) is allowed to pinch, according to our earlier general discussion [subsection 4.2 point (i)] (Of course, had we considered the entire set of vertex diagrams then the three-boson vertices Γ_{ZWW} and Γ_{AWW} should also undergo the standard PT splitting).

Then, separate $(c)_{\xi=1}$ into the purely vertex-like part, denoted by $(c)^{\mathrm{v}}_{\xi=1}$, and the propagator-like part, $(c)^{\mathrm{se}}_{\xi=1}$,

$$(c)_{\xi=1} = (c)^{\mathrm{v}}_{\xi=1} + (c)^{\mathrm{se}}_{\xi=1} \tag{4.104}$$

with

$$(c)^{\mathrm{v}}_{\xi=1} = \frac{g_w}{2} \int_k \left[\Gamma_H S^{(0)}_e(p_1 + k)\Gamma_\mu(2q^\mu) \right] d_W(k^2)\Delta_H(k + q)$$
$$+ \frac{g_w}{2} M_W \int_k \left[\Gamma_H S^{(0)}_e(p_1 + k)\Gamma_- \right] d_W(k^2)\Delta_H(k + q)$$
$$(c)^{\mathrm{se}}_{\xi=1} = \frac{g_w^2}{4} I_{WH}(q)\,(i\Gamma_2). \tag{4.105}$$

and

$$I_{WH}(q) = \int_k d_W(k^2)\Delta_H(k + q) = \int_k \frac{1}{(k^2 - M_W^2)[(k + q)^2 - M_H^2]}. \tag{4.106}$$

Then, the WH-parts of the one-loop $\Gamma_{W^-_\mu \bar{e}\nu_e}$ and $\Gamma_{\phi^- \bar{e}\nu_e}$ PT vertices, to be denoted by $\widehat{\Gamma}^{(WH)}_\alpha$ and $\widehat{\Gamma}^{(WH)}_-$, respectively, are given schematically by

$$\widehat{\Gamma}_\alpha^{(WH)} = (a)_\alpha^{\xi=1} + (b)_\alpha^{\xi=1},$$
$$\widehat{\Gamma}_-^{(WH)} = (c)_{\xi=1}^{\text{v}} + (d)_{\xi=1}. \tag{4.107}$$

Finally, to obtain the corresponding parts of the one-loop PT self-energies, to be denoted by $\widehat{\Pi}_{\alpha\beta}^{(WH)}$, $\widehat{\Theta}_\alpha^{(WH)}$, $\widehat{\Theta}_\beta^{(WH)}$, and $\widehat{\Omega}^{(WH)}$, we must use Eq. (4.87) in order to distribute among the different self-energies the contributions coming from $(c)_{\xi=1}^{\text{se}}$ and its mirror graph. Evidently, these terms will not contribute anything to $\widehat{\Pi}_{\alpha\beta}^{(WH)}$, and therefore $\widehat{\Pi}_{\alpha\beta}^{(WH)}$ will be identical to the conventional one-loop $\Pi_{\alpha\beta}^{(WH)}$ (of course, the non WH-parts will differ). Then, we will have

$$\widehat{\Pi}_{\alpha\beta}^{(WH)}(q) = (g)_{\alpha\beta}^{\xi=1} + (h)_{\alpha\beta}^{\xi=1},$$
$$\widehat{\Theta}_\alpha^{(WH)}(q) = (i)_\alpha^{\xi=1} + (j)_\alpha^{\xi=1} + \frac{g_w^2}{4}M_W I_{WH}(q)q_\alpha,$$
$$\widehat{\Theta}_\beta^{(WH)}(q) = (k)_\beta^{\xi=1} + (l)_\beta^{\xi=1} + \frac{g_w^2}{4}M_W I_{WH}(q)q_\beta,$$
$$\widehat{\Omega}^{(WH)}(q) = (m)^{\xi=1} + (n)^{\xi=1} + \frac{g_w^2}{2}q^2 I_{WH}(q). \tag{4.108}$$

It is a relatively straightforward exercise to verify that the parts of the PT Green's functions constructed above *coincide* with the corresponding quantities calculated in the BFG; of course, this coincidence holds for the entire Green's functions, and it is not restricted to the WH-parts analyzed here.

In the case of $\widehat{\Gamma}_\alpha^{(WH)}$ given in (4.107), the coincidence with the BFG is obvious; the external W's may be converted into $\widehat{W}$'s for free, since the corresponding (lowest-order) vertices are identical in the R_ξ and the BFM gauges. The case of $\widehat{\Gamma}_-^{(WH)}$ is more interesting; the coincidence with the BFG takes place because of the extraction of the propagator-like piece $(c)_{\xi=1}^{\text{se}}$ from $(c)_{\xi=1}$, as described in Eq. (4.104) and (4.105). Specifically, the purely vertex-like piece $(c)_{\xi=1}^{\text{v}}$ in Eq. (4.105) consists of two parts, the first one corresponds to graph (c) computed in the BFG [indeed, the factor $(2q^\mu)$ is proportional to the bare BFM vertex $\Gamma_{\widehat{\phi}WH}$], while the second part, when added to $(d)_{\xi=1}$, furnishes the graph (d) computed in the BFG, given that the BFM vertex $\Gamma_{\widehat{\phi}\phi H}$ and the R_ξ vertex $\Gamma_{\phi\phi H}$ are related by $\Gamma_{\widehat{\phi}\phi H} = \Gamma_{\phi\phi H} + ig_w\xi_Q M_W/2$.

Turning to the self-energies of Eq. (4.108), $\widehat{\Pi}_{\alpha\beta}^{(WH)}$ coincides with the corresponding BFM quantity, for the same reason as in the case of the $\widehat{\Gamma}_\alpha^{(WH)}$ vertex: the elementary vertices appearing in (g) and (h) coincide in both gauge-fixing schemes, R_ξ and BFM. As for $\widehat{\Theta}_\alpha^{(WH)}$, the term $(g_w^2/4)M_W I_{WH}(q)q_\beta$ accounts precisely for the difference between $\Gamma_{\widehat{\phi}\phi H}$ and $\Gamma_{\phi\phi H}$. Finally, the case of $\widehat{\Omega}^{(WH)}$ is slightly more involved: to demonstrate the equality one must write the $(2q+k)^2$ appearing in (m) in the form

$$(2q + k)^2 = 2q^2 + 2[(k + q)^2 - M_H^2] - (k^2 - M_W^2) + (2M_H^2 - M_W^2). \tag{4.109}$$

Then for the terms on the rhs we have that the first is added to $(g_w^2/2)q^2 I_{WH}$ and furnishes graph (m) in the BFG; the second combines with other M_H-independent parts (note that in the BFM we have also the coupling $\Gamma_{\widehat{\phi}^+\widehat{\phi}^- u^\pm \bar{u}^\mp} \propto -\xi_Q/2$; the third cancels with the $(g_w^2/2)q^2 I_{WH}$; the
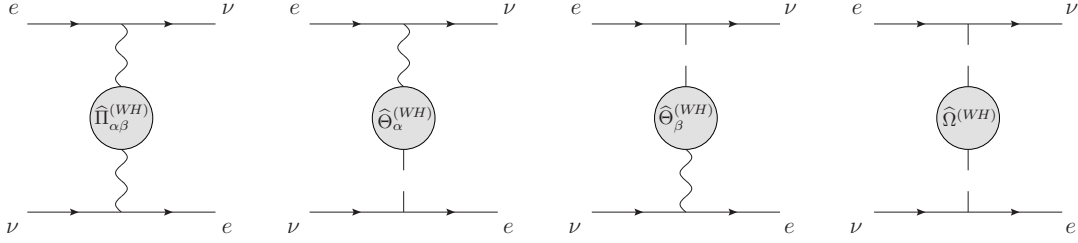
Fig. 35. The (one-loop) ξ-independent PT self-energies (gray blobs); the tree-level propagators are still ξ-dependent. By requiring that any gfp-dependence coming from these tree-level propagators must cancel, imposes a set of non-trivial WIs on the one-loop PT self-energies (and vertices).

third converts the seagull graph containing a Higgs-boson propagator (not shown) to the same graph in the BFM, given that $\Gamma_{\widehat{\phi}^+\widehat{\phi}^- HH} = \Gamma_{\phi^+\phi^- HH} - ig_w^2 \xi_Q/2$; finally, the last term converts (n) into its BFM counterpart.

4.4.3   Deriving Ward identities from the gfp-independence of the S-matrix.

In the previous subsections we showed explicitly how the application of the PT gives rise to gfp-independent self energies, vertices, and boxes. As already emphasized there, the gfp-cancellation proceeded without reference to the tree-level propagators connecting the one-loop graphs to the external fermions. Any gfp-dependence coming from these tree-level propagators [see Eqs (4.23) and (4.25)] must also cancel, in order to obtain fully gfp-independent subamplitudes $\widehat{T}_1$ and $\widehat{T}_2$ ($\widehat{T}_3$ being box-like does not have external propagators and is already fully gfp-independent). It turns out that, quite remarkably, the requirement of this final gfp-cancellation imposes a set of non-trivial WIs on the one-loop PT self-energies and vertices [9,93]. These WIs are identical to those obtained some years later within the BFM [95], but are derived through a procedure that has no apparent connection with the BFM; all that one evokes really is the full gfp-independence of the S-matrix. Actually, this S-matrix derivation could be considered as an all-order proof of the above WIs, assuming that the various Green's functions [the gray blobs in Fig. 35)] can be made gfp-independent to all orders.

Let us see how the WIs for the self-energies are derived from the gfp-independence of $\widehat{T}_1$. Neglecting tadpole contributions from the external fermions, we have that $\widehat{T}_1$ is given by

$$\widehat{T}_1 = \Gamma_1^\mu \Delta_{\mu\alpha}(q)\widehat{\Pi}^{\alpha\beta}(q)\Delta_{\beta\nu}(q)\Gamma_2^\nu + \Gamma_1 D(q)\,\widehat{\Omega}(q)\,D(q)\Gamma_2$$
$$+ \Gamma_1^\mu \Delta_{\mu\alpha}(q)\widehat{\Theta}^\alpha(q)D(q)\Gamma_2 + \Gamma_1 D(q)\widehat{\Theta}^\beta(q)\Delta_{\beta\nu}(q)\Gamma_2^\nu, \tag{4.110}$$

or, after using Eq. (4.27),

$$\widehat{T}_1 = \Gamma_1^\mu \left[U_{\mu\alpha}(q) - \frac{q_\mu q_\alpha}{M_W^2} D(q) \right] \widehat{\Pi}^{\alpha\beta}(q) \left[U_{\beta\nu}(q) - \frac{q_\beta q_\nu}{M_W^2} D(q) \right] \Gamma_2^\nu$$

$$+ \Gamma_1^\mu \left[U_{\mu\alpha}(q) - \frac{q_\mu q_\alpha}{M_W^2} D(q) \right] \widehat{\Theta}^\alpha(q) D(q) \Gamma_2$$

$$+ \Gamma_1 D(q) \widehat{\Theta}^\beta(q) \left[U_{\beta\nu}(q) - \frac{q_\beta q_\nu}{M_W^2} D(q) \right] \Gamma_2^\nu + \Gamma_1 D(q) \widehat{\Omega}(q) D(q) \Gamma_2. \tag{4.111}$$

This way of writing $\widehat{T}_1$ has the advantage of isolating all residual ξ-dependence inside the propagators $D(q)$. Demanding that $\widehat{T}_1$ should be ξ-independent, we obtain as a condition for the cancellation of the terms quadratic in $D(q)$

$$q^\beta q^\alpha \widehat{\Pi}_{\alpha\beta}(q) - 2 M_W q^\alpha \widehat{\Theta}_\alpha(q) + M_W^2 \widehat{\Omega}(q) = 0, \tag{4.112}$$

while for the cancellation of the linear terms we must have

$$q^\alpha \widehat{\Pi}_{\alpha\beta}(q) - M_W \widehat{\Theta}_\beta(q) = 0. \tag{4.113}$$

From Eqs (4.112) and (4.113) it follows that

$$q^\beta q^\alpha \widehat{\Pi}_{\alpha\beta}(q) = M_W^2 \widehat{\Omega}(q), \tag{4.114}$$

and

$$q^\alpha \widehat{\Theta}_\alpha(q) = M_W \widehat{\Omega}(q). \tag{4.115}$$

Eqs (4.112) and (4.115) are the announced WIs. Applying an identical procedure for $\widehat{T}_2$ one obtains the corresponding WI relating the one-loop PT vertices $\widehat{\Gamma}_\alpha$ and $\widehat{\Gamma}_\pm$.

Finally, the gfp-independent $\widehat{T}_1$ is given by

$$\widehat{T}_1 = \Gamma_1^\mu U_{\mu\alpha}(q) \widehat{\Pi}^{\alpha\beta}(q) U_{\beta\nu}(q) \Gamma_2^\nu. \tag{4.116}$$

Notice that Eq. (4.116) is the one-loop generalization of Eq. (4.90).

We can now use the WIs derived above in order to reformulate the S-matrix in a very particular way; specifically, we will show that the higher-order physical amplitude given above may be cast in the tree-level form of Eq. (4.93). Such a reformulation gives rise to a new transverse gfp-independent W self-energy $\widehat{\Pi}_{\alpha\beta}^t$ with a gfp-independent longitudinal part, exactly as in Eq. (4.93). To be sure, the cost of such a reformulation is the appearance of *massless* Goldstone poles in our expressions. However, since both the old and the new quantities originate from the same *unique* S-matrix, all poles introduced by this reformulation will cancel against each other, because the S-matrix contains no massless poles to begin with.

To see how this works out, write $\widehat{\Theta}_\alpha$ in the form

$$\widehat{\Theta}_\alpha(q) = q_\alpha \widehat{\Theta}(q) ; \tag{4.117}$$

from (4.115) follows that

$$\widehat{\Theta}(q) = \frac{M_W}{q^2} \widehat{\Omega}(q) \tag{4.118}$$

Then, we can define $\widehat{\Pi}^{t}_{\alpha\beta}(q)$ in terms of $\widehat{\Pi}^{\alpha\beta}(q)$ and $\widehat{\Theta}(q)$ as follows:

$$\widehat{\Pi}^{t}_{\alpha\beta}(q) = \widehat{\Pi}_{\alpha\beta}(q) - \frac{q_{\alpha}q_{\beta}}{q^2}M_W\widehat{\Theta}(q) \tag{4.119}$$

Evidently $\widehat{\Pi}^{t}_{\alpha\beta}(q)$ is transverse, *e.g.*, $q^{\alpha}\widehat{\Pi}^{t}_{\alpha\beta}(q) = q^{\beta}\widehat{\Pi}^{t}_{\alpha\beta}(q) = 0$. Moreover, using Eqs (4.113) and (4.118),

$$\widehat{\Pi}^{t}_{\alpha\beta}(q) = P_{\alpha\mu}(q)\widehat{\Pi}^{\mu\nu}(q)P_{\beta\nu}(q). \tag{4.120}$$

We may now re-express $\widehat{T}_1$ of (4.116) in terms of $\widehat{\Pi}^{t}_{\alpha\beta}$ and $\widehat{\Omega}$; using (4.92) and (4.87) we have

$$\widehat{T}_1 = \Gamma^{\alpha}_1 d_W(q^2)\widehat{\Pi}^{t}_{\alpha\beta}(q)d_W(q^2)\Gamma^{\beta}_2 + \Gamma_1\frac{i}{q^2}\widehat{\Omega}(q)\frac{i}{q^2}\Gamma_2. \tag{4.121}$$

Eq. (4.121) is the generalization of Eq. (4.93): $\widehat{T}_1$ is the sum of two self-energies, one corresponding to a *transverse massive vector field* and one to a *massless Goldstone boson*. It is interesting to notice that the above rearrangements have removed the mixing terms $\widehat{\Theta}_{\alpha}$ and $\widehat{\Theta}_{\beta}$ between W and ϕ, thus leading to the generalization of the well known tree-level property of the R_{ξ} gauges to higher orders. It is important to emphasize again that the massless poles in the above expressions would not have appeared had we not insisted on the transversality of the W self-energy (or the vertex); notice in particular that they are *not* related to any particular gauge choice, such as the Landau gauge ($\xi = 0$). A completely analogous procedure may be followed for the one-loop (and beyond) vertex [9], yielding the corresponding Abelian-like WI; as in the case of te self-energy studied above, the WI of the vertex is realized by means of massless Goldstone bosons.

The rearrangement of the S-matrix carried out above, in additional to the conceptual transparency that it provides, brings about considerable calculational simplifications, since it organizes the transverse and longitudinal pieces in individually gauge-invariant blocks. As was first recognized in [103], this is particularly economical if one is only interested in gauge-invariant longitudinal contributions, *e.g.*, in the context of resonantly enhanced CP violation.

5 Applications - I

In this section we will present a variety of phenomenological applications of the PT. Specifically, we will focus on the following representative topics:

i. The field-theoretic construction and the observable nature of the PT effective charges, as well as the conceptual and practical advantages of the physical renormalization schemes, which use these effective charges, over the unphysical schemes, such as the popular $\overline{MS}$.

ii. The definition and measurement of gauge-invariant off-shell form-factors, with particular emphasis on the neutrino charge radius.

iii. The gauge-invariant definition of basic electroweak parameters, such as the S,T, and U, and the universal part of the ρ parameter.

iv. The gauge-invariant resummation formalism for resonant transition amplitudes.

5.1 Non-Abelian effective charges

The possibility of extending the concept of an effective charge [104] from QED to non-Abelian gauge theories is of fundamental interest for at least three reasons. First, in QCD, the existence of an effective charge analogous to that of QED is explicitly assumed in renormalon studies [105–107]. However, in the absence of a concrete guiding principle (such as the PT), the diagrammatic identification of the subset of (conformally-variant) corrections that should be resummed is rather obscure. Second, in theories involving unstable particles (*e.g.*, in the electroweak SM) the Dyson summation of (appropriately defined) self-energies is needed, in order to regulate the kinematic singularities of the corresponding tree-level propagators in the vicinity of resonances [108–111]. Third, in theories involving disparate energy scales (*e.g.*, grand unified theories) the extraction of accurate low-energy predictions requires an exact treatment of threshold effects due to heavy particles [112–114]. The construction of effective charges, valid for all momenta q^2 and not just the asymptotic regime governed by the β-functions, constitutes the natural way to account for such threshold effects. In all cases, the fundamental problem is the gfp-dependence of the conventionally defined gauge boson self-energies. The PT cures this problem and leads to the definition of physical effective charges, both in QCD and the electroweak sector of the SM.

5.1.1 QED effective charge: the prototype

The quantity that serves as the field-theoretic prototype for guiding our analysis is the effective charge of QED. In the rest of this section, a '0' super or subscript will indicate (bare) unrenormalized quantities.

In QED consider the unrenormalized photon self-energy $\Pi_0^{\mu\nu}(q) = P^{\mu\nu}(q)\Pi_0(q^2)$, where

$\Pi_0(q^2)$ has dimensions of mass squared, and is gfp-independent to all orders in perturbation theory. One usually sets $\Pi(q^2) = q^2\boldsymbol{\Pi}(q^2)$, where the dimensionless quantity $\boldsymbol{\Pi}(q^2)$ is referred to as the "vacuum polarization". Carrying out the standard Dyson summation, we obtain the dressed photon propagator between conserved external currents,

$$\Delta_0^{\mu\nu}(q^2) = \frac{g^{\mu\nu}}{q^2[1 + \boldsymbol{\Pi}_0(q^2)]}. \tag{5.1}$$

$\Delta_0^{\mu\nu}(q^2)$ is renormalized multiplicatively according to $\Delta_0^{\mu\nu}(q^2) = Z_A\Delta^{\mu\nu}(q^2)$, where Z_A is the wave-function renormalization of the photon ($A_0 = Z_A^{1/2}A$). Imposing the on-shell renormalization condition for the photon we obtain

$$1 + \boldsymbol{\Pi}(q^2) = Z_A[1 + \boldsymbol{\Pi}_0(q^2)], \tag{5.2}$$

where $Z_A = 1 - \boldsymbol{\Pi}_0(0)$, and $\boldsymbol{\Pi}(q^2) = \boldsymbol{\Pi}_0(q^2) - \boldsymbol{\Pi}_0(0)$; clearly $\boldsymbol{\Pi}(0) = 0$.

The renormalization procedure introduces, in addition, the standard relations between renormalized and unrenormalized electric charge,

$$e = Z_e^{-1}e^0 = Z_f Z_A^{1/2} Z_1^{-1}e^0, \tag{5.3}$$

where Z_e is the charge renormalization constant, Z_f the wave-function renormalization constant of the fermion, and Z_1 the vertex renormalization.

The Abelian symmetry of the theory gives rise to the well-known WI [given also in (2.58)]

$$q^\mu\Gamma_\mu^0(p, p + q) = S_0^{-1}(p + q) - S_0^{-1}(p), \tag{5.4}$$

where Γ_μ^0 and $S_0(k)$ are the unrenormalized one-loop photon-electron vertex and electron propagator, respectively. The requirement that the renormalized vertex $\Gamma_\mu = Z_1\Gamma_\mu^0$ and the renormalized self-energy $S = Z_f^{-1}S_0$ should satisfy the same WI imposes the equality

$$Z_1 = Z_f, \tag{5.5}$$

from which it immediately follows that

$$Z_e = Z_A^{-1/2}. \tag{5.6}$$

Given these relations between the renormalization constants, we can now form the following renormalization group (RG) invariant combination:

$$R_0^{\mu\nu}(q^2) = \frac{(e^0)^2}{4\pi}\Delta_0^{\mu\nu}(q^2) = \frac{e^2}{4\pi}\Delta^{\mu\nu}(q^2) = R^{\mu\nu}(q^2). \tag{5.7}$$

From $R_{\mu\nu}(q^2)$, after pulling out a the trivial kinematic factor $(1/q^2)$, one may define the QED *effective charge* $\alpha_{\text{eff}}(q^2)$, namely

$$\alpha_{\text{eff}}(q^2) = \frac{\alpha}{[1 + \boldsymbol{\Pi}(q^2)]}, \tag{5.8}$$

where α is the fine-structure constant.

The QED effective charge of (5.8) has the following crucial properties:

i. It is gfp-independent, to all orders in perturbation theory.

ii. It is RG-invariant by virtue of the WI of 5.4 and the resulting relation (5.6).

iii. Given that $\mathbf{\Pi}(0) = 0$, at low energies the effective charge matches the fine structure constant: $\alpha_{\text{eff}}(0) = \alpha = 1/137.036\cdots$.

iv. For asymptotically large values of q^2, *i.e.*, for $q^2 \gg m_f^2$, where m_f denotes the masses of the fermions contributing to the vacuum polarization loop ($f = e, \mu, \tau,...$), $\alpha(q^2)$ matches the *running coupling* $\bar{\alpha}(q^2)$ defined from the RG: at the one-loop level,

$$\alpha_{\text{eff}}(q^2) \xrightarrow{q^2 \gg m_f^2} \bar{\alpha}(q^2) = \frac{\alpha}{1 - (\alpha\beta_1/2\pi)\log(q^2/m_f^2)}, \tag{5.9}$$

where $\beta_1 = \frac{2}{3}n_f$ is the coefficient of the QED β function for n_f fermion species.

v. The effective charge has a non-trivial dependence on the masses m_f, which allows its re-construction from physical amplitudes by resorting to the OT and analyticity, *i.e.*, dispersion relations. Specifically, given a particular contribution to the spectral function $\Im m\mathbf{\Pi}(s)$, the corresponding contribution to $\mathbf{\Pi}(q^2)$ can be reconstructed via a *once-subtracted dispersion relation* (see, e.g. [115]). For example, for the one-loop contribution of the fermion f, choosing the on-shell renormalization scheme,

$$\mathbf{\Pi}_{f\bar{f}}(q^2) = \frac{1}{\pi}q^2 \int_{4m_f^2}^{\infty} ds \frac{\Im m\mathbf{\Pi}_{f\bar{f}}(s)}{s(s - q^2)}. \tag{5.10}$$

For $f \neq e$, $\Im m\mathbf{\Pi}_{f\bar{f}}(s)$ is *measured directly* in the tree-level cross-section for $e^+e^- \to f^+f^-$, see Fig. 36. For $f = e$, it is necessary to isolate the self-energy-like component of the tree-level Bhabha cross-section, see Fig. 37. This is indeed possible because the self-energy-, vertex- and box-like components of the Bhabha *differential* cross-section are *linearly independent functions* of $\cos\theta$; they may therefore be projected out by convoluting the *differential* cross-section with appropriately chosen polynomials in $\cos\theta$.

Thus, in QED, knowledge of the spectral function $\Im m\mathbf{\Pi}_{f\bar{f}}(s)$, determined from the tree-level $e^+e^- \to f^+f^-$ cross sections, together with a single low energy measurement of the fine structure constant α (obtained *e.g.*, from the Josephson effect and the quantized Hall effect, or from the anomalous magnetic moment of the electron [116]), enables the construction of the one-loop effective charge $\alpha_{\text{eff}}(q^2)$ for all q^2.
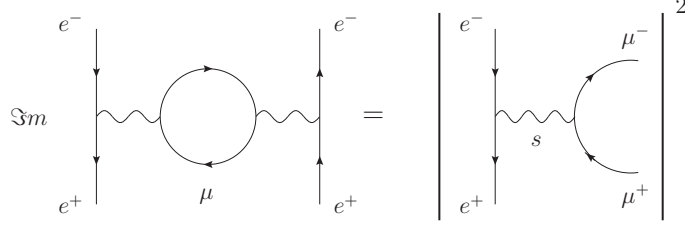
Fig. 36. The OT relation between the imaginary part of the muon contribution to $\mathbf{\Pi}(s)$ and the tree-level cross section $\sigma(e^+e^- \to \mu^+\mu^-)$ in QED.

5.1.2 QCD effective charge

In non-Abelian gauge theories the crucial equality $Z_1 = Z_f$ does not hold in general. Furthermore, in contrast to the photon case, the gluon vacuum polarization depends on the gfp, already at one-loop order. These facts make the non-Abelian generalization of the QED concept of the effective charge non-trivial. The possibility of defining an effective charge for QCD in the framework of the PT was established first by Cornwall [7], and was further investigated in a series of papers [12,23,74,72,117,118].

As we have shown in detail in Section 2 the PT rearrangement of physical amplitudes gives rise to a gfp-independent effective gluon self-energy, restoring, at the same time, the equalities

$$\widehat{Z}_1 = \widehat{Z}_f, \qquad \widehat{Z}_{g_s} = \widehat{Z}_A^{-1/2}, \tag{5.11}$$

where g_s is the QCD coupling. Then, using the additional fact that the PT self-energy is process-independent [63] and can be Dyson-resummed to all orders [23,74,72,12], the construction of the universal RG-invariant combination and the corresponding QCD effective charge is immediate. We have

$$\widehat{R}_0^{\mu\nu}(q^2) = \frac{(g_s^0)^2}{4\pi}\widehat{\Delta}_{\mu\nu}^0(q) = \frac{g_s^2}{4\pi}\widehat{\Delta}_{\mu\nu}(q) = \widehat{R}^{\mu\nu}(q^2). \tag{5.12}$$

and after pulling out a $1/q^2$ factor we arrive at the QCD effective charge,

$$\alpha_{s,\text{eff}}(q^2) = \frac{\alpha_s}{1 + \widehat{\mathbf{\Pi}}(q^2)}, \tag{5.13}$$

where $\alpha_s = g_s^2/4\pi$.

Let us now turn to properties (*iii*)–(*v*) of the QED effective charge, and see how they are modified due to the fact that the low-energy sector of QCD is strongly coupled and must be treated non-perturbatively.

Evidently point (*iii*) must be replaced by a measurement where perturbation theory holds, such as the $\alpha(M_Z)$. Point (*iv*) remains true; actually, due to asymptotic freedom, the high energy limit is where the QCD charge is completely unambiguous. Finally, point (*v*) is trickier: clearly, the absorptive analysis of Section 2 demonstrates that, perturbatively, the imaginary part of $\widehat{\mathbf{\Pi}}(\mathbf{s})$ may be identified with a well-defined part of the $q\bar{q} \to gg$ tree-level cross-section. These parts may be, in principle, extracted out of the full differential cross-section through the convolution with an appropriately constructed function of the scattering angle [see subsection 5.1.4 on the electroweak effective charges], and then be fed into the dispersion relation
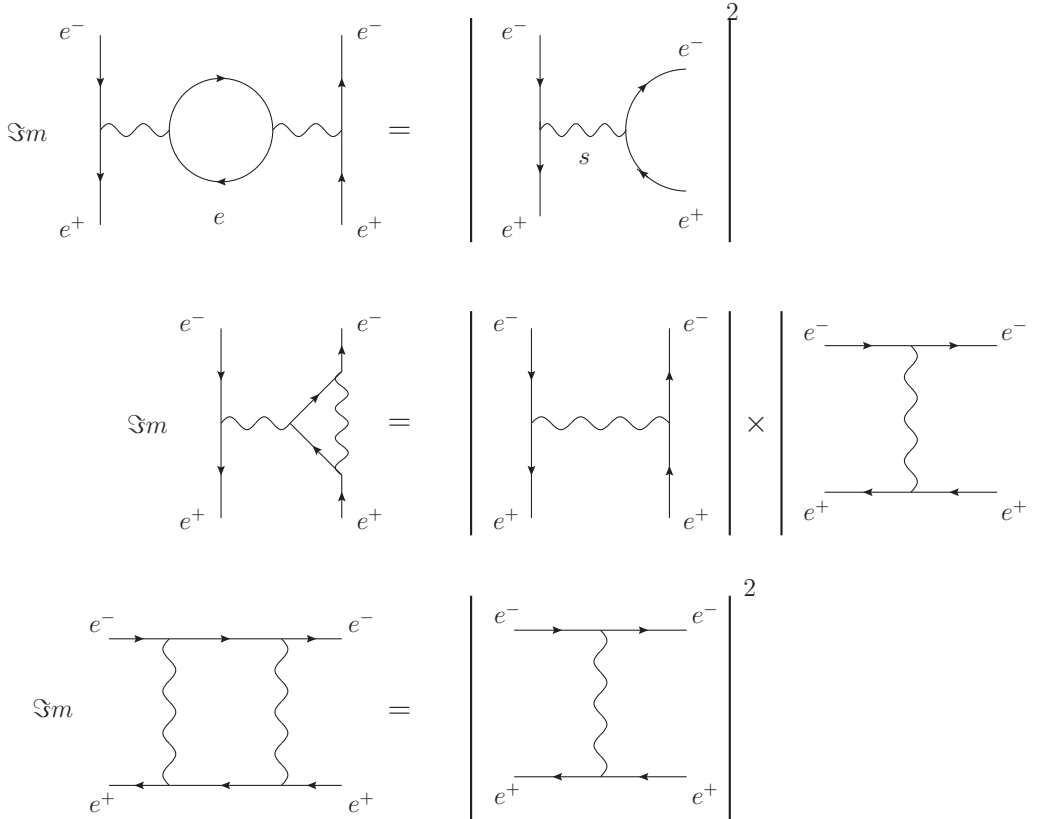
Fig. 37. The OT relation between the imaginary parts of the electron contribution to the one-loop vacuum polarization, vertex and box diagrams and the components of the tree-level cross section $\sigma(e^+e^- \to e^+e^-)$ in QED

(2.120) to furnish $\widehat{\Pi}(q^2)$. The problem is that, in QCD, such a procedure is not feasible, even at the level of a thought-experiment, because in the limit of low s QCD is strongly coupled, and non-perturbative effects become significant.

An additional important point related to the non-perturbative nature of QCD is the following. As has been argued long ago by Cornwall [7], and has been corroborated by a large number of lattice simulations and SDE studies, the gluons generate dynamically an effective mass, which cures the Landau singularity and makes the gluon propagator finite in the infrared [we will revisit this issue in much more detail in Section 9]. In such a case, it would of course be wrong to define the effective charge as in Eq. (5.13), *i.e.*, by forcing out a factor of $1/q^2$ from Eq. (5.12). Such a procedure would furnish a completely unphysical strong QCD coupling, namely one that would vanish in the deep infrared(!) where QCD is supposed to be strongly coupled. The correct treatment (see again Section 9) yields, instead, an effective coupling that in the deep infrared "freezes" at a *finite value*, in complete agreement with a plethora of phenomenological and theoretical works.

5.1.3 Effective mixing (Weinberg) angle

We now turn to the electroweak sector of the SM, and consider the subset of neutral gauge boson self-energies, $\widehat{\Pi}_{\mu\nu}^{AA}(q)$, and $\widehat{\Pi}_{\mu\nu}^{ZZ}(q)$, together with the mixed self-energies $\widehat{\Pi}_{\mu\nu}^{AZ}(q)$ and $\widehat{\Pi}_{\mu\nu}^{ZA}(q)$. Let us now see how the above self-energies organize themselves into RG-invariant combinations. We will assume that we are working between massless fermions (conserved currents) and we will therefore retain only the parts of the self-energies proportional to $g_{\mu\nu}$. The general framework presented in this subsection has been established in [95] and [75]; here we will adopt the notation and philosophy of the latter article.

We begin by listing the relations between the bare and renormalized parameters for the neutral part of the electroweak sector. For the masses we have

$$(M_W^0)^2 = M_W^2 + \delta M_W^2, \qquad (M_Z^0)^2 = M_Z^2 + \delta M_Z^2. \tag{5.14}$$

The wave-function renormalizations for the neutral sector are defined as

$$\begin{pmatrix} Z_0 \\ A_0 \end{pmatrix} = \begin{pmatrix} \widehat{Z}_{ZZ}^{1/2} & \widehat{Z}_{ZA}^{1/2} \\ \widehat{Z}_{AZ}^{1/2} & \widehat{Z}_{AA}^{1/2} \end{pmatrix} \begin{pmatrix} Z \\ A \end{pmatrix} = \begin{pmatrix} 1 + \frac{1}{2}\delta\widehat{Z}_{ZZ} & \frac{1}{2}\delta\widehat{Z}_{ZA} \\ \frac{1}{2}\delta\widehat{Z}_{AZ} & 1 + \frac{1}{2}\delta\widehat{Z}_{AA} \end{pmatrix} \begin{pmatrix} Z \\ A \end{pmatrix}. \tag{5.15}$$

In addition, the coupling renormalization constants are defined by

$$e_0 = \widehat{Z}_e e = (1 + \delta\widehat{Z}_e)e, \qquad g_w^0 = \widehat{Z}_{g_w} g_w = (1 + \delta\widehat{Z}_{g_w})g_w, \qquad c_w^0 = \widehat{Z}_{c_w} c_w, \tag{5.16}$$

with

$$\widehat{Z}_{c_w} = \left(1 + \frac{\delta M_W^2}{M_W^2}\right)^{1/2} \left(1 + \frac{\delta M_Z^2}{M_Z^2}\right)^{-1/2}. \tag{5.17}$$

If we expand $\widehat{Z}_{c_w}$ perturbatively, we have that $\widehat{Z}_{c_w} = 1 + \frac{1}{2}(\delta c_w^2/c_w^2) + \cdots$, with

$$\frac{\delta c_w^2}{c_w^2} = \frac{\delta M_W^2}{M_W^2} - \frac{\delta M_Z^2}{M_Z^2}, \tag{5.18}$$

which is the usual one-loop result.

Imposing the requirement that the PT Green's functions should respect the same WI's before and after renormalization we arrive at the following relations:

$$\widehat{Z}_{AA} = \widehat{Z}_e^{-2}, \qquad \widehat{Z}_{ZZ} = \widehat{Z}_{g_w}^{-2} \widehat{Z}_{c_w}^2, \tag{5.19}$$

or, equivalently, at the level of the counter-terms

$$\delta\widehat{Z}_{AA} = -2\delta\widehat{Z}_e,$$

$$\delta\widehat{Z}_{ZZ} = -2\delta\widehat{Z}_e - \frac{c_w^2 - s_w^2}{s_w^2}\left(\frac{\delta c_w^2}{c_w^2}\right),$$

$$\delta\widehat{Z}_{AZ} = 2\frac{c_w}{s_w}\left(\frac{\delta c_w^2}{c_w^2}\right),$$

$$\delta\widehat{Z}_{ZA} = 0. \tag{5.20}$$

The corresponding propagators relevant for the neutral sector may be obtained by inverting the matrix $\widehat{L}$, whose entries are the PT self-energies, *i.e.*,

$$\widehat{L} = \begin{pmatrix} q^2 + \widehat{\Pi}_{AA}(q^2) & \widehat{\Pi}_{AZ}(q^2) \\ \widehat{\Pi}_{AZ}(q^2) & q^2 - M_Z^2 + \widehat{\Pi}_{ZZ}(q^2) \end{pmatrix}. \tag{5.21}$$

Casting the inverse in the form

$$\widehat{L}^{-1} = \begin{pmatrix} \widehat{\Delta}_{AA}(q^2) \; \widehat{\Delta}_{AZ}(q^2) \\ \widehat{\Delta}_{AZ}(q^2) \; \widehat{\Delta}_{ZZ}(q^2) \end{pmatrix} \tag{5.22}$$

one finds that

$$\widehat{\Delta}_{AA}(q^2) = \frac{-[q^2 - M_Z^2 + \widehat{\Pi}_{ZZ}(q^2)]}{\widehat{\Pi}_{AZ}^2(q^2) - [q^2 - M_Z^2 + \widehat{\Pi}_{ZZ}(q^2)][q^2 + \widehat{\Pi}_{AA}(q^2)]},$$

$$\widehat{\Delta}_{ZZ}(q^2) = \frac{-[q^2 + \widehat{\Pi}_{AA}(q^2)]}{\widehat{\Pi}_{AZ}^2(q^2) - [q^2 - M_Z^2 + \widehat{\Pi}_{ZZ}(q^2)][q^2 + \widehat{\Pi}_{AA}(q^2)]},$$

$$\widehat{\Delta}_{AZ}(q^2) = \frac{-\widehat{\Pi}_{AZ}(q^2)}{\widehat{\Pi}_{AZ}^2(q^2) - [q^2 - M_Z^2 + \widehat{\Pi}_{ZZ}(q^2)][q^2 + \widehat{\Pi}_{AA}(q^2)]}. \tag{5.23}$$

The above expressions at one-loop reduce to

$$\widehat{\Delta}_{AA}(q^2) = \frac{1}{q^2 + \widehat{\Pi}_{AA}(q^2)},$$

$$\widehat{\Delta}_{ZZ}(q^2) = \frac{1}{q^2 - M_Z^2 + \widehat{\Pi}_{ZZ}(q^2)},$$

$$\widehat{\Delta}_{AZ}(q^2) = \frac{\widehat{\Pi}_{AZ}(q^2)}{q^2(q^2 - M_Z^2)}. \tag{5.24}$$

The standard re-diagonalization procedure of the neutral sector [119–121] may then be followed, for the PT self-energies; it will finally amount to introducing the effective (running) weak mixing angle. In particular, after the PT rearrangement, the propagator-like part $\widehat{\mathcal{D}}_{ff'}$ of the neutral current amplitude for the interaction between fermions with charges Q, Q' and isospins T_z^f, $T_z^{f'}$, is given in terms of the inverse of the matrix $\widehat{L}$ by the expression

$$\widehat{\mathcal{D}}_{ff'} = \left(eQ_f, \; \frac{g_w}{c_w} \left[s_w^2 Q_f - T_z^f P_L \right] \right) \widehat{L}^{-1} \begin{pmatrix} eQ_{f'} \\ \frac{g_w}{c_w}(s_w^2 Q_{f'} - T_z^{f'} P_L) \end{pmatrix}$$

$$= \left(eQ_f, \; \frac{g_w}{c_w} \left[\bar{s}_w^2(q^2) Q_f - T_z^f P_L \right] \right) \widehat{L}_D^{-1} \begin{pmatrix} eQ_{f'} \\ \frac{g_w}{c_w} \left[\bar{s}_w^2(q^2) Q_{f'} - T_z^{f'} P_L \right] \end{pmatrix}, \tag{5.25}$$

where

$$\widehat{L}_D^{-1} = \begin{pmatrix} \widehat{\Delta}_{AA}(q^2) & 0 \\ 0 & \widehat{\Delta}_{ZZ}(q^2) \end{pmatrix}. \tag{5.26}$$

The rhs of this equation, where the neutral current interaction between the fermions has been written in diagonal (*i.e.*, Born-like) form, defines the diagonal propagator functions $\widehat{\Delta}_{AA}$ and $\widehat{\Delta}_{ZZ}$ and the effective weak mixing angle $\bar{s}_w^2(q^2)$

$$\bar{s}_w^2(q^2) = (s_w^0)^2 \left[1 - \left(\frac{c_w^0}{s_w^0} \right) \frac{\widehat{\Pi}_{AZ}^0(q^2)}{q^2 + \widehat{\Pi}_{AA}^0(q^2)} \right] = s_w^2 \left[1 - \left(\frac{c_w}{s_w} \right) \frac{\widehat{\Pi}_{AZ}(q^2)}{q^2 + \widehat{\Pi}_{AA}(q^2)} \right]. \tag{5.27}$$

It is easy to show that, by virtue of the special relations of Eq. (5.19), $\bar{s}_w^2(q^2)$ is an RG-invariant quantity.

Using the fact that $\widehat{\Pi}_{AZ}(0) = 0$, we may write $\widehat{\Pi}_{AZ}(q^2) = q^2 \widehat{\mathbf{\Pi}}_{AZ}(q^2)$; then, Eq. (5.19) yields

$$\begin{aligned} \bar{s}_w^2(q^2) &= s_w^2 \left[1 - \left(\frac{c_w}{s_w} \right) \frac{\widehat{\mathbf{\Pi}}_{AZ}(q^2)}{1 + \widehat{\mathbf{\Pi}}_{AA}(q^2)} \right] \\ &= s_w^2 \left[1 - \left(\frac{c_w}{\alpha\, s_w} \right) \alpha_{\text{eff}}(q^2) \widehat{\mathbf{\Pi}}_{AZ}(q^2) \right], \end{aligned} \tag{5.28}$$

where in the last step we used Eq. (5.8). At one-loop level, $\bar{s}_w^2(q^2)$ reduces to

$$\bar{s}_w^2(q^2) = s_w^2 \left[1 - \left(\frac{c_w}{s_w} \right) \widehat{\mathbf{\Pi}}_{AZ}(q^2) \right]. \tag{5.29}$$

Notice that in the case where the fermion f' is a neutrino ($f' = \nu$, with $Q_\nu = 0$ and $T_z^\nu = 1/2$), Eq. (5.25) assumes the form

$$\widehat{\mathcal{D}}_{f\nu} = \left(eQ_f,\ \frac{g_w}{c_w} \left[\bar{s}_w^2(q^2)Q_f - T_z^f P_L \right] \right) \widehat{L}_D^{-1} \begin{pmatrix} 0 \\ -\frac{g_w}{2c_w} P_L \end{pmatrix} \tag{5.30}$$

Evidently, $\bar{s}_w^2(q^2)$ constitutes a universal modification to the effective vertex of the charged fermion.

5.1.4   Electroweak effective charges

The analogue of Eq. (5.8) may be defined for the Z- and W-boson propagators. In particular, the bare and renormalized PT resummed Z-boson propagators, $\widehat{\Delta}_{ZZ,0}^{\mu\nu}(q)$ and $\widehat{\Delta}_{ZZ}^{\mu\nu}(q)$ respectively, satisfy the following relation

$$\widehat{\Delta}_{ZZ}^{0,\mu\nu}(q) = \widehat{Z}_{ZZ} \widehat{\Delta}_{ZZ}^{\mu\nu}(q). \tag{5.31}$$

In what follows we only consider the cofactors of $g^{\mu\nu}$, *i.e.*, $\widehat{\Delta}_{ZZ}^{0,\mu\nu}(q) = \widehat{\Delta}_{ZZ}^0(q)g^{\mu\nu}$ and $\widehat{\Delta}_{ZZ}^{\mu\nu}(q) = \widehat{\Delta}_{ZZ}(q)g^{\mu\nu}$, since the longitudinal parts vanish when contracted with the conserved external currents of massless fermions. The standard renormalization procedure is to define the

wave function renormalization, $\widehat{Z}_{ZZ}$, by means of the transverse part of the resummed Z-boson propagator:

$$\widehat{Z}_{ZZ}[q^2 - (M_Z^0)^2 + \widehat{\Pi}_{ZZ}^0(q^2)] = q^2 - M_Z^2 + \widehat{\Pi}_{ZZ}(q^2). \tag{5.32}$$

It is then straightforward to verify that the universal RG-invariant quantity for the Z boson, which constitutes a common part of all neutral current processes, is given by (we omit a factor $g^{\mu\nu}$):

$$\bar{R}_Z^0(q^2) = \frac{1}{4\pi}\left(\frac{g_w^0}{c_w^0}\right)^2 \widehat{\Delta}_{ZZ}^0(q^2) = \frac{1}{4\pi}\left(\frac{g_w}{c_w}\right)^2 \widehat{\Delta}_{ZZ}(q^2) = \bar{R}_Z(q^2). \tag{5.33}$$

A completely analogous analysis holds also for the $\widehat{\Delta}_{WW}(q^2)$ propagator; in this case the corresponding RG-invariant combination is

$$\bar{R}_W(q^2) = \left(\frac{g_w^2}{4\pi}\right)\widehat{\Delta}_{WW}(q^2). \tag{5.34}$$

If one retains only the real parts in the above equation, one may define from $\bar{R}_i(q^2)$ ($i = W, Z$) a dimensionless quantity, corresponding to an effective charge by casting $\Re e\widehat{\Pi}(q^2)_{ii}$ in the form $\Re e\widehat{\Pi}_{ii}(q^2) = \Re e\widehat{\Pi}_{ii}(M_i^2) + (q^2 - M_i^2)\Re e\widehat{\Pi}_{ii}(M_i^2)$ and then pulling out a common factor $(q^2 - M_i^2)$. In that case,

$$\bar{R}_i(q^2) = \frac{\alpha_{i,\text{eff}}(q^2)}{q^2 - M_i^2}, \qquad i = W, Z \tag{5.35}$$

with

$$\alpha_{w,\text{eff}}(q^2) = \frac{\alpha_w}{1 + \Re e\widehat{\mathbf{\Pi}}_{WW}(q^2)},$$
$$\alpha_{z,\text{eff}}(q^2) = \frac{\alpha_z}{1 + \Re e\widehat{\mathbf{\Pi}}_{ZZ}(q^2)}, \tag{5.36}$$

where

$$\widehat{\mathbf{\Pi}}_{ii}(q^2) = \frac{\widehat{\Pi}_{ii}(q^2) - \widehat{\Pi}_{ii}(M_i^2)}{q^2 - M_i^2}, \qquad i = W, Z. \tag{5.37}$$

and $\alpha_w = g_w^2/4\pi$ and $\alpha_z = \alpha_w/c_w^2$. Notice, however, that, whereas Eqs (5.33) and (5.34) remain valid in the presence of imaginary parts (*i.e.*, when $\widehat{\Pi}_{ii}(q^2)$ develops physical thresholds) the above separation into a dimensionful and a dimensionless part is ambiguous and should be avoided [76] .

5.1.5 Electroweak effective charges and their relation to physical cross-sections

Let us now turn to the relation of the RG-invariant and universal quantity $\bar{R}_Z(q^2)$ to physical cross-sections, and the procedure that would allow, at least in principle, its extraction from experiment [73]. In general, the renormalization of $\widehat{\Pi}_{ZZ}$ requires two subtractions, for mass and field renormalization. If we denote the subtraction point by s_0, then the twice-subtracted
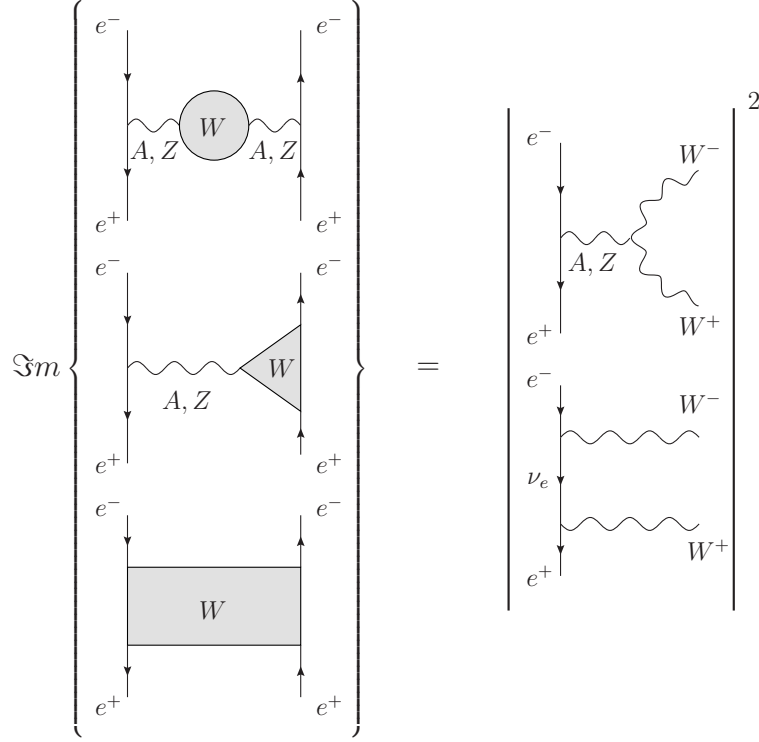
Fig. 38. The OT relation between the imaginary parts of the subset of the W-related one-loop corrections to $e^+e^- \to e^+e^-$ and the tree-level process $e^+e^- \to W^+W^-$.

dispersion relation corresponding to the W^+W^- contributions reads

$$\widehat{\Pi}_{ZZ}^{(WW)}(q^2) = \frac{1}{\pi}(q^2 - s_0)^2 \int_{4M_W^2}^{\infty} ds \frac{\Im m \widehat{\Pi}_{ZZ}^{(WW)}(s)}{(s - q^2)(s - s_0)^2}. \tag{5.38}$$

The property that is instrumental for the observability of $\bar{R}_Z^{(WW)}(q^2)$ is that, in contrast to the conventional gauge-dependent self-energies, the absorptive parts of the PT self-energies appearing on the rhs of Eq. (5.38) are directly related to components of the physical cross-section $e^+e^- \to W^+W^-$ which are *experimentally observable* (see Fig. 38). Indeed, as we have already seen in Section 4, the characteristic s-t cancellation, triggered by the longitudinal momenta of the on-shell polarization tensors, rearranges the tree-level cross-section $e^+e^- \to W^+W^-$ into subamplitudes, which, through the use of the OT, can be connected unambiguously with the absorptive parts of the one-loop PT Green's functions.

To simplify the algebra without compromising the principle, let us consider the limit of $e^+e^- \to W^+W^-$ when the electroweak mixing angle vanishes, $s_w^2 = 0$. In this limit all photon related contributions are switched off , and the two massive gauge bosons become degenerate ($M_Z = M_W \equiv M$). Let us denote by θ the center-of-mass scattering angle, and set $x = \cos\theta$, $\beta = \sqrt{1 - 4M^2/s}$, and $z = (1 + \beta^2)/2\beta$. Then, it is relatively straightforward to show that the differential tree-level cross-section for $e^+e^- \to W^+W^-$ can be cast in the form [73]

$$(z - x)^2 \left(\frac{d\sigma}{dx}\right)_{s_w=0} = \frac{g^4}{64\pi} \frac{s\beta}{(s - M^2)^2} \theta(s - 4M^2) \sum_{i=1}^{5} A_i(s) F_i(s, x) \tag{5.39}$$

110

where

$$F_1(s,x) = (z-x)^2 \qquad\qquad A_1(s) = \frac{5}{32}\left(\beta^2 - 12\right),$$

$$F_2(s,x) = (z-x)^2 x^2 \qquad\qquad A_2(s) = -\frac{9}{32}\beta^2,$$

$$F_3(s,x) = (z-x)(1-x^2) \qquad\qquad A_3(s) = -\frac{\beta}{2}\left(\frac{s-M^2}{s}\right),$$

$$F_4(s,x) = (z-x)(1-\beta x) \qquad\qquad A_4(s) = \frac{2}{\beta}\left(\frac{s-M^2}{s}\right),$$

$$F_5(s,x) = 1 - x^2 \qquad\qquad A_5(s) = \frac{1}{2}\left(\frac{s-M^2}{s}\right)^2. \qquad (5.40)$$

Let us emphasize an important point: for $s \to \infty$, the $A_i(s)$ reported above go asymptotically to constant values. This good high-energy behavior is to be contrasted with that of the conventional subamplitudes, corresponding to the $A_i(s)$, obtained in [102] (no s-t cancellation explicitly carried out): they grow rapidly as functions of s, violating individually unitarity (see also comments at the end of subsection 4.3.4). Notice also that the five polynomials $F_i(s,x)$, $i = 1, 2 \ldots 5$ are *linearly independent*, and also that the coefficients $A_1(s)$ and $A_2(s)$ contribute only to the self-energy-like component of the cross-section, being related to $\Im m\, \widehat{\Pi}_{ZZ}^{(WW)}(s)$ by

$$\Im m\, \widehat{\Pi}_{ZZ}^{(WW)}(s)\Big|_{s_w=0} = \frac{g^2}{4\pi}\beta s\left(A_1(s) + \frac{1}{3}A_2(s)\right). \qquad (5.41)$$

To project out the functions $A_i(s)$, we construct a further set of five polynomials $\tilde{F}_i(s,x)$ satisfying the orthogonality conditions

$$\int_{-1}^{1} dx\, F_i(s,x)\tilde{F}_j(s,x) = \delta_{ij}. \qquad (5.42)$$

The explicit expressions for the $\tilde{F}_i(s,x)$ can be found in [73]. The coefficient functions $A_i(s)$ may then be projected out from the observable formed by taking the product of the differential cross section with the kinematic factor $(z-x)^2$:

$$\int_{-1}^{1} dx\, \tilde{F}_i(s,x)\,(z-x)^2 \left(\frac{d\sigma}{dx}\right)_{s_w=0} = \frac{g^4}{64\pi}\frac{s\beta}{(s-M^2)^2}A_i(s). \qquad (5.43)$$

Thus, it is is possible to extract $\Im m\, \widehat{\Pi}_{ZZ}^{(WW)}(s)|_{s_w=0}$ directly from $d\sigma(e^+e^- \to W^+W^-)/dx|_{s_w=0}$. The general case with $s_w^2 \neq 0$ requires, in addition, the observation of spin density matrices [122]; though technically more involved, the procedure is, in principle, the same.

Finally notice the following:

i. In order to use the dispersion relation of (5.38) to compute $\widehat{\Pi}_{ZZ}^{(WW)}(q^2)$, one needs to integrate the spectral density $\Im m\, \widehat{\Pi}_{ZZ}^{(WW)}(s)$ over a large number of values of s. This, in turn,

means that one needs experimental data for the process $e^+e^- \to W^+W^-$ for a variety of center-of-mass energies s, and for each value of s one must repeat the procedure described above. Regardless of whatever practical difficulties this might entail, it does not constitute a problem of principle.

ii. The experimental extraction of the contributions $\widehat{\Pi}_{ZZ}^{(ZH)}(q^2)$ is conceptually far more straight-forward, given that it involves the *entire* cross-section of the process $e^+e^- \to ZH$ (known as "Bjorken process" or "Higgsstrahlung"); specifically, we have that

$$e^2 \frac{(a^2 + b^2)}{s_w^2 c_w^2} \frac{\Im m \widehat{\Pi}_{ZZ}^{(ZH)}(s)}{(s - M_Z^2)^2} = \sigma(e^+e^- \to ZH). \tag{5.44}$$

5.1.6   *The effective charge of the Higgs boson*

As has been shown in [75], there is a universal RG-invariant quantity related to the Higgs boson that leads to the *novel concept* of the "Higgs boson effective charge". Specifically, after applying the PT algorithm, the linearity of the WI satisfied by the PT Green's functions provides us with the following relations

$$\widehat{Z}_W \;=\; \widehat{Z}_{g_w}^{-2}, \qquad \widehat{Z}_H = \widehat{Z}_\chi = \widehat{Z}_\phi = \widehat{Z}_W(1 + \delta M_W^2/M_W^2), \tag{5.45}$$

where $\widehat{Z}_W$ and $\widehat{Z}_H$ are the wave-function renormalizations of the W and H fields, respectively, $\widehat{Z}_{g_w}$ is the coupling renormalization. The renormalization of the bare resummed Higgs-boson propagator $\widehat{\Delta}_H^0(s)$ proceeds, then, as follows:

$$\widehat{\Delta}_H^0(s) = [\, s - (M_H^0)^2 + \widehat{\Pi}_{HH}^0(s)]^{-1} = \widehat{Z}_H[\, s - M_H^2 + \widehat{\Pi}_{HH}(s)]^{-1} = \widehat{Z}_H \widehat{\Delta}^H(s), \tag{5.46}$$

with $(M_H^0)^2 = M_H^2 + \delta M_H^2$. The renormalized Higgs-boson mass M_H^2 may be defined as the real part of the complex pole position of $\widehat{\Delta}^H(s)$. Employing the relations of Eq. (5.45), together with the relation between $(M_W^0)^2$ and M_W^2 given in (5.14), we observe that the universal (process-independent) quantity

$$\bar{R}_H^0(s) = \frac{(g_w^0)^2}{(M_W^0)^2} \widehat{\Delta}_H^0(s) = \frac{g_w^2}{M_W^2} \widehat{\Delta}_H(s) = \bar{R}_H(s) \tag{5.47}$$

constitutes, in fact, a RG-invariant. Interestingly enough, $\bar{R}^H(s)$ provides a natural extension of the notion of the QED effective charge for the SM Higgs boson: H couples universally to matter with an effective "charge" inversely proportional to its vev.

5.1.7   *Physical renormalization schemes vs $\overline{MS}$*

It is well-known, but often overlooked, that the widely used (unphysical) renormalization schemes, such as $\overline{\text{MS}}$ and $\overline{\text{DR}}$, are plagued with persistent threshold and matching errors. The origin of these errors can be understood by noting that the aforementioned unphysical schemes implicitly integrate out all masses heavier than the physical energy scale until they are crossed,

and then they turn them back on abruptly, by means of a step function. Integrating out heavy fields, however, is only valid for energies well below their masses. This procedure is conceptually problematic, since it does not correctly incorporate the finite probability that the uncertainty principle gives for a particle to be pair produced below threshold [16]. In addition, complicated matching conditions must be applied when crossing thresholds to maintain consistency for such desert scenarios. In principle, these schemes are only valid for theories where all particles have zero or infinite mass, or if one knows the full field content of the underlying physical theory.

Instead, in the physical renormalization scheme defined with the PT, gauge couplings are defined directly in terms of *physical observables*, namely the effective charges. The latter run smoothly over space-like momenta and have non-analytic behavior only at the expected physical thresholds for time-like momenta; as a result, the thresholds associated with heavy particles are treated with their correct analytic dependence. In particular, particles will contribute to physical predictions even at energies below their threshold [16].

Historically, the gauge-invariant parametrization of physics offered by the PT has been first systematized by Hagiwara, Haidt, Kim, and Matsumoto [123], and has led to an alternative framework for confronting the precision electroweak data with the theoretical predictions. This approach resorts to the PT in order to separate the one-loop corrections into gfp-independent universal (process-independent) and process-specific pieces; the former are parametrized using the PT effective charges, $\alpha_{\text{eff}}(q^2)$, $\bar{s}_w^2(q^2)$, $\alpha_{w,\text{eff}}(q^2)$, and $\alpha_{z,\text{eff}}(q^2)$, defined earlier. There is a total of nine electroweak parameters that must be determined in this approach: the eight universal parameters M_W, M_Z, $\alpha_{\text{eff}}(0)$, $\bar{s}_w^2(0)$, $\alpha_{w,\text{eff}}(0)$, $\alpha_{z,\text{eff}}(0)$, $\bar{s}_w^2(M_Z^2)$, $\alpha_{z,\text{eff}}(M_Z^2)$, and one process-dependent parameter $\delta_b(M_Z^2)$, related to the form-factor of the $Z\bar{b}_L b_L$ vertex.

The authors of [123] explain in detail the advantage of their approach over the $\overline{MS}$ scheme. In particular they emphasize that the non-decoupling nature of the $\overline{MS}$ forces one to adopt an effective field theory approach, where the heavy particles are integrated out of the action. The couplings of the effective theories are then related to each other by matching conditions ensuring that all effective theories give identical results at zero momentum transfer, since the effects of heavy particles in the effective light field theory must be proportional to q^2/M^2, where M is the heavy mass scale. This procedure, however, is not only impractical in the presence of many quark and lepton mass scales, but it introduces errors due to the mistreatment of the threshold effects. In addition, the direct use of the $\overline{MS}$ couplings leads to expressions where the masses used for the light quarks are affected by sizable non-perturbative QCD effects.

The relevance of the effective charges in the quantitative study of threshold corrections due to heavy particles in Grand Unified Theories (GUTs) was already recognized in [123], but it was not until a decade later when this was actually accomplished by Binger and Brodsky [16]. As was shown by these authors, the effective charges defined with the PT furnish a conceptually superior and calculationally more accurate framework for studying the important issue of gauge coupling unification. The main advantage of the effective charge formalism is that it provides a template for calculating all mass threshold effects for any given grand unified theory; such threshold corrections may be instrumental in making the measured values of the gauge couplings consistent with unification.

The analysis presented in [16] in the context of a toy model makes a most compelling case in favor of the *physical renormalization schemes*; here we reproduce it practically unchanged (up to minor notational modifications).

Consider QED with three fermions e, μ, and τ, and focus on the process $e^-\mu^-\rightarrow e^-\mu^-$. The

corresponding amplitude can be written as a dressed skeleton expansion, *i.e.*, the dressed tree-level graph plus the dressed box diagram plus the dressed double box, etc. It is easy to see (*e.g.*, , by carrying out the standard Dyson summation) that the tree-level diagram, dressed to all orders in perturbation theory, is equal to the tree-level diagram with one modification: the QED coupling (fine structure constant) α is replaced by the effective charge $\alpha_{\text{eff}}(q^2)$ given in Eq. (5.8).

Let us now consider two rather disparate scales, denoted by q_h (for "high") and q_ℓ (for "low"). From measurements of the cross-section, one can actually extract the the value of the effective charge at these two scales, $\alpha_{\text{eff}}(q_h^2)$ and $\alpha_{\text{eff}}(q_\ell^2)$. Let us suppose for a moment that the electron charge is not known, and we are trying to test the predictions of QED. The way to proceed is to use one measurement, say at the low scale q_ℓ, as an input to determine e. Once e is known the prediction at the high scale q_h is well defined, and represents a test of the theory. More directly, we could just write $\alpha_{\text{eff}}(q_h^2)$ in terms of $\alpha_{\text{eff}}(q_\ell^2)$, which would lead us to the same prediction.

Since the cross-section $\sigma_{e^-\mu^-\to e^-\mu^-}(q^2)$ is proportional to $\alpha_{\text{eff}}^2(q^2)$, we are clearly relating one observable to another. Such a scheme is referred to as an *effective charge scheme*, since a given observable, here just $\sigma_{e^-\mu^-\to e^-\mu^-}(q_h^2)$ (or $\alpha_{\text{eff}}(q_h^2)$), is expressed in terms of an effective charge, $\alpha_{\text{eff}}(q_\ell^2)$, defined from a measurement of the cross-section at the scale q_ℓ. One could equally well express any observable in terms of this effective charge. Note that this approach to renormalization works for arbitrary scales, even if the low scale lies below some threshold, say $q_\ell < m_\tau$, while $q_h > m_\tau$. Thus, the decoupling and the smooth (not through a θ function!) "turning on" of the τ is manifest, due to the intrinsic analyticity and unitarity properties of the vacuum polarization (see subsection 2.5.1).

Let us now consider the results obtained by using the conventional implementation of $\overline{MS}$. In this case one begins by calculating the cross-section at q_ℓ using the rules of $\overline{MS}$, which stipulate that *only* the electrons and muons are allowed to propagate in loops, since $q_\ell < m_\tau$. Comparing the observed cross section to this result will fix the value of the $\overline{MS}$ coupling for two flavors, $\hat{\alpha}_2(q_\ell)$. To predict the result of the same experiment at scale $q_h > m_\tau$, we need to evolve $\hat{\alpha}_2$ to the τ threshold using the *two-flavor* β function, match with a three-flavor coupling, $\hat{\alpha}_3$, through the relation $\hat{\alpha}_2(m_\tau) = \hat{\alpha}_3(m_\tau)$, and then evolve $\hat{\alpha}_3(m_\tau)$ to q_h using the *three-flavor* β function. We will now have a prediction for $\sigma_{e^-\mu^-\to e^-\mu^-}(q_h^2) \propto \alpha^2(q_h^2)$.

Now, one might expect, from the general principle of RG-invariance of physical predictions, that this result should be the same as the prediction derived using the physical effective charge scheme above. However, there is a discrepancy arising from the incorrect treatment of the threshold effects in the $\overline{MS}$. One finds that the ratio of the cross section derived using $\overline{MS}$ with the cross section derived using effective charges, to first order in perturbation theory, is given by [16]

$$\frac{\hat{\sigma}(q_h^2)}{\sigma(q_h^2)} = 1 + \frac{2\alpha_{\text{eff}}(q_\ell^2)}{3\pi}\left[L\left(\frac{q_\ell}{m_\tau}\right) - 5/3\right], \tag{5.48}$$

with

$$L_\tau\left(\frac{q}{m}\right) = \int_0^1 dx\, 6x(1-x)\log\left(1 + \frac{q^2}{m^2}x(1-x)\right) + \frac{5}{3}$$
$$= [\beta\tanh^{-1}(\beta^{-1}) - 1](3-\beta^2) + 2, \tag{5.49}$$

114

where $\beta = \sqrt{1 + 4m^2/q^2}$. Since $L_\tau(0) = 5/3$, there is no discrepancy when the low reference scale q_ℓ is much lower than the τ mass threshold. This reflects the important fact that unphysical schemes, such as $\overline{MS}$, are formally consistent only in *desert regions* where particle masses can be neglected. Notice that in this example there is an error only for $q_l < m_\tau$. However, in the more general case of multiple flavor thresholds, as well as in the analysis of grand unification, there are errors from both high and low scales.

An important difference between the physical effective charges and the unphysical $\overline{MS}$, intimately related to the analyticity properties built into the former, is the distinction between time-like and space-like momenta. As emphasized in [16], in conventional approaches the thresholds are treated using a step function approximation [θ functions], and hence, the running is always logarithmic. The analytic continuation from space-like to time-like momenta is trivial, yielding $i\pi$ imaginary terms on the time-like side; thus, the real parts of such couplings are the same [modulo three loop $(i\pi)^2$ corrections]. In contrast, the PT charges on time-like and space-like sides have considerable differences at one-loop. Specifically, the relevant quantities to consider are functions such as the $L_\tau(q/m)$ defined above. The analytic continuation to time-like momenta below threshold, $0 < q^2 = -Q^2 < 4m^2$, is obtained by replacing

$$\beta \to i\bar{\beta}, \quad \text{where} \quad \bar{\beta} = \sqrt{\frac{4m^2}{q^2} - 1}, \quad \text{and} \quad \tanh^{-1}(\beta^{-1}) \to -i\tan^{-1}(\bar{\beta}^{-1}). \tag{5.50}$$

Above threshold, $q^2 > 4m^2$, one should replace

$$\tanh^{-1}(\beta^{-1}) \to \tanh^{-1}(\beta) + i\frac{\pi}{2}, \quad \text{where} \quad \beta = \sqrt{1 - \frac{4m^2}{q^2}}. \tag{5.51}$$

From these results, it is clear that significant differences will arise between the space-like and time-like couplings evaluated at scale M_Z^2, mainly due to the $W^\pm$ boson threshold asymmetry.

In [16] the effective charges $\alpha_{\text{eff}}(q^2)$, $\alpha_{s,\text{eff}}(q^2)$, and the effective mixing angle $\bar{s}_w^2(q^2)$ [defined in (5.8), (5.13), and (5.29), respectively], were used to define new effective charges, $\tilde{\alpha}_1(q^2)$, $\tilde{\alpha}_2(q^2)$, and $\tilde{\alpha}_3(q^2)$, which correspond to the standard combinations of gauge couplings used to study gauge-coupling unification. Specifically,

$$\tilde{\alpha}_1(q^2) = \left(\frac{5}{3}\right) \frac{\alpha_{\text{eff}}(q^2)}{1 - \bar{s}_w^2(q^2)} \qquad \tilde{\alpha}_2(q^2) = \frac{\alpha_{\text{eff}}(q^2)}{\bar{s}_w^2(q^2)} \qquad \tilde{\alpha}_3(q^2) = \alpha_{s,\text{eff}}(q^2). \tag{5.52}$$

The above couplings were used to obtain novel heavy and light threshold corrections, and the resulting impact on the unification predictions for a general GUT model were studied. Notice that even in the absence of new physics (*i.e.*, using only the known SM spectrum) there are appreciable numerical discrepancies between the values of of the conventional and PT couplings at M_Z (see Table I in [16]). Given that these values are used as initial conditions for the evolution of the couplings to the GUT scale, these differences alone may affect the unification properties of the couplings (*i.e.*, even if no additional threshold effects due to new particles are considered).

It is well-known that renormalizability and gauge-invariance severely restricts the type of inter-action vertices that can appear at the level of the fundamental Lagrangian. Thus, the tensorial possibilities allowed by Lorentz invariance are drastically reduced down to relatively simple tree-level vertices. Beyond tree-level, the tensorial structures that have been so excluded appear due to quantum corrections, *i.e.*, they are generated from loops. This fact is not in contradiction with renormalizability and gauge-invariance, provided that the tensorial structures generated, not present at the level of the original Lagrangian, are *UV finite*, *i.e.*, no counterterms need be introduced to the fundamental Lagrangian proportional to the forbidden structures.

In order to fix the ideas, let us consider a concrete, text-book example. In standard QED the tree-level photon-electron vertex is simply proportional to γ_μ, while kinematically one may have, in addition, (for massive on-shell electrons, using the Gordon decomposition) a term proportional to $\sigma_{\mu\nu}q^\nu$, that would correspond to a non-renormalizable interaction. Of course, the one-loop photon-electron vertex generates such a term; specifically, one has

$$\Gamma_\mu(q) = \gamma_\mu F_1(q^2) + \frac{i\sigma_{\mu\nu}q^\nu}{2m_e}F_2(q^2)\,, \tag{5.53}$$

where the scalar cofactors multiplying the two tensorial structures are the corresponding form-factors; they are, in general, non-trivial functions of the photon momentum transfer (the photon "off-shellness"). $F_1(q^2)$ is the electric form-factor, whereas $F_2(q^2)$ is the magnetic form-factor. $F_1(q^2)$ is UV divergent, and becomes finite after carrying out the standard vertex renormalization. On the other hand, $F_2(q^2)$ comes out UV finite, as it should, given that there is no term proportional to $\sigma_{\mu\nu}q^\nu$ (in configuration space) in the original Lagrangian, where a potential UV divergence could be absorbed. Of course, in the limit of $q^2 \to 0$ the magnetic form-factor $F_2(q^2)$ reduces to the famous Schwinger anomaly [124] (see, e.g., [47]).

At the level of an Abelian theory, such as QED, the above discussion exhausts more or less the theoretical complications associated with the calculation of off-shell form-factors. However, in non-Abelian theories, such as the electroweak sector of the SM, there is an additional important complication: The off-shell form-factors obtained from the conventional one-loop vertex (and beyond) depend explicitly on the gfp. This dependence disappears when going to the on-shell limit of the incoming gauge boson ($q^2 \to 0$ for a photon, $q^2 \to M_Z^2$ for a Z boson, etc) but is present for any other value of q^2. This fact becomes phenomenologically relevant, because one often wants to study the various form-factors of particles that are produced in high-energy collisions, where the gauge boson mediating the interaction is far off-shell. In the case of e^+e^- annihilation into heavy fermions, the value of q^2 must be above the heavy fermion threshold. For example, top quarks may be pair-produced through the reaction $e^+e^- \to t\bar{t}$, with center-of-mass energy $s = q^2 \geq 4m_t^2$. Due to their large masses, the produced top quarks are expected to decay weakly ($t\bar{t} \to bW^+\bar{b}W^-$, with subsequent leptonic decays of the W), before hadroniza-tion takes place; therefore electroweak properties of the top can be studied in detail, and QCD corrections can be reliably evaluated in the context of perturbation theory, when the energy of the collider is well above the threshold for $t\bar{t}$ production. The problem is that, in such a case, the intermediate photon and Z are far off-shell, and therefore, the form-factors F_i^V, appearing
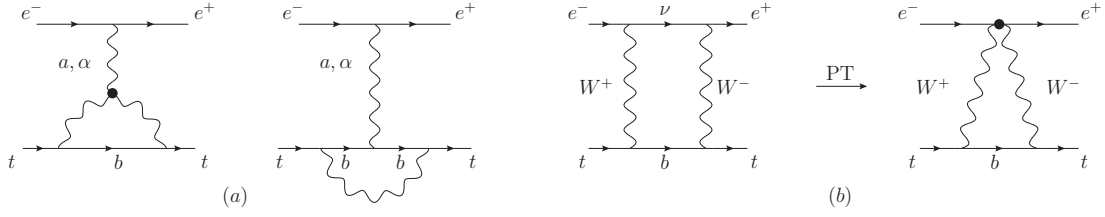
Fig. 39. The conventional one-loop vertex (a) and the vertex-like piece extracted from the box for $\xi \neq 1$

in the standard decompositions

$$\Gamma_\mu^V(q^2) = \gamma_\mu F_1^V(q^2, \xi) + \frac{i\sigma_{\mu\nu}q^\nu}{2m_t} F_2^V(q^2, \xi) + \gamma_\mu\gamma_5 F_3^V(q^2, \xi) + \frac{i\sigma_{\mu\nu}q^\nu}{2m_t}\gamma_5 F_4^V(q^2, \xi), \quad (5.54)$$

depend explicitly on ξ, which stands collectively for ξ_W, ξ_Z, ξ_A, and $V = A, Z$.

The situation described above is rather general and affects most form-factors; very often the residual gauge-dependences have serious physical consequences. For example, the form-factors display unphysical thresholds, bad high-energy behavior, and sometimes they are UV and infrared (IR) divergent. The way out is to use the PT construction, and extract the physical, gauge-independent form-factors from the corresponding off-shell one-loop PT vertex (and beyond). Applying the PT to the case of the form-factors amounts to saying that one has to identify vertex-like contributions (with the appropriate tensorial structure corresponding to the form-factor considered) contained in box diagrams, as shown in Fig. 39. The latter, when added to the usual vertex graphs, render all form-factors ξ-independent and well-behaved in all respects.

In what follows, we will present certain characteristic examples, in order for the reader to appreciate the nature of the pathologies encountered in the conventional formulation, and see how the PT resolves all of them at once.

5.2.1 Anomalous gauge boson couplings

A significant amount of research activity has been devoted to the study of the three-boson vertices AW^+W^- and ZW^+W^-, with the neutral gauge bosons *off-shell* and the W pair on-shell, or off-shell and subsequently decaying to on-shell particles. Historically, the main motivation for exploring their properties was the fact that they were going to be tested at LEP2 by direct W-pair production, proceeding through the process $e^+e^- \to W^+W^-$; their experimental scrutiny could provide invaluable information on non-Abelian nature of the electroweak sector of the SM. Particularly appealing in this quest has been the possibility of measuring anomalous gauge boson couplings, *i.e.*, the appearance of contributions to AW^+W^- and ZW^+W^- not encoded in the fundamental Lagrangian of the SM. Such contributions may originate from two sources: (*i*) from radiative corrections within the SM, and/or (*ii*) from physics beyond the SM. Therefore the first theoretical task one is faced with is to carry out the necessary calculations for completing part (*i*).

The most general parametrization of the trilinear gauge boson vertex for on-shell Ws and off-shell $V = A, Z$ is given by (see Fig. 40)
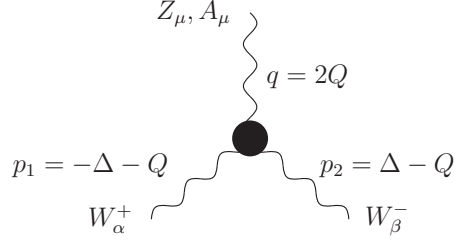
117

Fig. 40. The kinematics of the trilinear gauge boson vertex VW^+W^- (all momenta incoming)

$$\Gamma^V_{\mu\alpha\beta} = -ig_V \Big\{ f \left[2g_{\alpha\beta}\Delta_\mu + 4(g_{\alpha\mu}Q_\beta - g_{\beta\mu}Q_\alpha) \right] + 2\Delta\kappa_V \left(g_{\alpha\mu}Q_\beta - g_{\beta\mu}Q_\alpha \right)$$

$$+ 4\frac{\Delta Q_V}{M_W^2} \left(\Delta_\mu Q_\alpha Q_\beta - \frac{1}{2}Q^2 g_{\alpha\beta}\Delta_\mu \right) \Big\} + \cdots , \tag{5.55}$$

with $g_A = g_w s_w$, $g_Z = g_w c_w$, and the ellipses denote omission of C, P, or T violating terms. The four-momenta Q and Δ are related to the incoming momenta q, p_1 and p_2 of the gauge bosons V, W^- and W^+ respectively, by $q = 2Q$, $p_1 = \Delta - Q$ and $p_2 = -\Delta - Q$ [125]. The *off-shell* form-factors $\Delta\kappa_V$ and ΔQ_V, also defined as $\Delta\kappa_V = \kappa_V + \lambda_V - 1$, and $\Delta Q_V = -2\lambda_V$, are compatible with C, P, and T invariance, and are related to the magnetic dipole moment μ_W and the electric quadrupole moment Q_W, by the following expressions:

$$\mu_W = \frac{e}{2M_W}(2 + \Delta\kappa_A), \qquad Q_W = -\frac{e}{M_W^2}(1 + \Delta\kappa_A + \Delta Q_A). \tag{5.56}$$

In the context of the SM their canonical, tree-level values are $f = 1$ and $\Delta\kappa_V = \Delta Q_V = 0$. To determine the radiative corrections to these quantities one must cast the resulting one-loop expressions in the form

$$\Gamma^V_{\mu\alpha\beta} = -ig_V[a_1^V g_{\alpha\beta}\Delta_\mu + a_2^V(g_{\alpha\mu}Q_\beta - g_{\beta\mu}Q_\alpha) + a_3^V \Delta_\mu Q_\alpha Q_\beta], \tag{5.57}$$

where a_1^V, a_2^V, and a_3^V are complicated functions of the momentum transfer Q^2, and the masses of the particles appearing in the loops. It then follows that $\Delta\kappa_V$ and ΔQ_V are given by

$$\Delta\kappa_V = \frac{1}{2}(a_2^V - 2a_1^V - Q^2 a_3^V), \qquad \Delta Q_V = \frac{M_W^2}{4}a_3^V . \tag{5.58}$$

Calculating the one-loop expressions for $\Delta\kappa_V$ and ΔQ_V is a non-trivial task, both from the technical and the conceptual point of view. Let us focus, for concreteness, on the case $V = A$. If one calculates just the Feynman diagrams contributing to the AW^+W^- vertex and then extracts from them the contributions to $\Delta\kappa_A$ and ΔQ_A, one arrives at expressions that are plagued with several pathologies, gfp-dependence being one of them. Indeed, even if the two Ws are considered to be on-shell ($p_1^2 = p_2^2 = M_W^2$) since the incoming photon is not, there is no *a priori* reason why a gfp-independent answer should emerge. Indeed, in the context of the renormalizable R_ξ gauges the final answer depends on the choice of the gfp ξ, which enters into the one-loop calculations through the gauge-boson propagators (W, Z,A, and unphysical "would-be" Goldstone bosons). In addition, as shown by an explicit calculation performed in the Feynman gauge
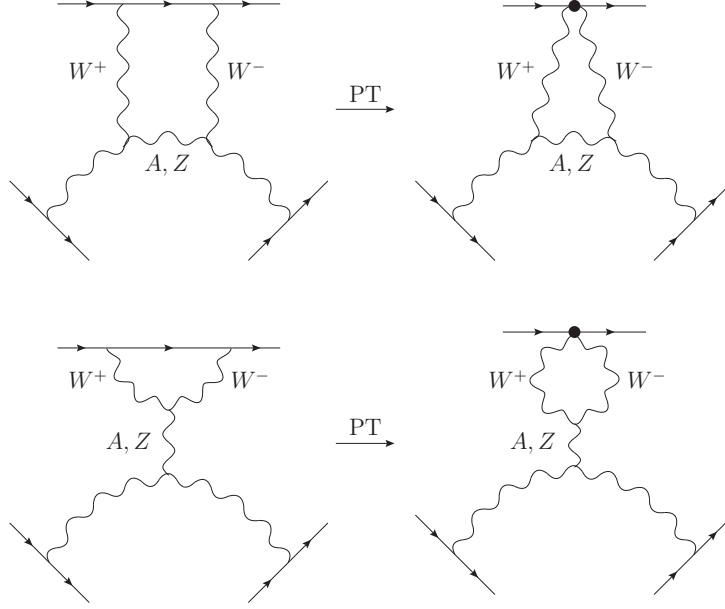
118

Fig. 41. Two of the graphs contributing pinching parts to the gauge independent VW^+W^- vertex.

($\xi = 1$), the answer for $\Delta\kappa_A$ is *infrared divergent* and violates perturbative unitarity, *e.g.*, it grows monotonically for $Q^2 \to \infty$ [126].

All the above pathologies may be circumvented if one uses the PT definition of the relevant (off-shell) gauge boson vertices [18]. The application of the PT identifies vertex-like contributions from the box graphs, as shown in Fig. 41, which are subsequently distributed, in a unique way, among the various form-factors. The final outcome is that one arrives at new expressions, to be denoted by $\widehat{\Delta}\kappa_A$ and $\widehat{\Delta}Q_A$, which are gauge fixing parameter (ξ) independent, ultraviolet *and* infrared finite, and monotonically decreasing for large momentum transfers Q^2.

Using "hats" to denote the gfp-independent one-loop contributions, we have

$$
\begin{aligned}
\widehat{\Delta}\kappa_A &= \Delta\kappa_A^{(\xi=1)} + \Delta\kappa_A^P, \\
\widehat{\Delta}Q_A &= \Delta Q_A^{(\xi=1)} + \Delta Q_A^P,
\end{aligned}
\tag{5.59}
$$

where $\Delta Q_A^{(\xi=1)}$ and $\Delta Q_A^{(\xi=1)}$ are the contributions of the usual vertex diagrams in the Feynman gauge [126], whereas ΔQ_A^P and ΔQ_A^P are the analogous contributions from the pinch parts. A straightforward calculation yields

$$
\Delta\kappa_A^P = -\frac{Q^2}{M_W^2} \sum_V \frac{\alpha_V}{\pi} \int_0^1 da \int_0^1 dt \, \frac{t(at-1)}{L_V^2},
\tag{5.60}
$$

where

$$
L_V^2 = t^2 - t^2 a(1-a)\left(\frac{4Q^2}{M_W^2}\right) + (1-t)\frac{M_V^2}{M_W^2},
\tag{5.61}
$$

and

$$
\Delta Q_A^P = 0.
\tag{5.62}
$$

119

Notice an important point: $\Delta\kappa_A^P$ contains an infrared divergent term, stemming from the double integral shown above, when $V = A$. This term cancels *exactly* against a similar infrared divergent piece contained in $\Delta\kappa_A^{(\xi=1)}$, thus rendering $\widehat{\Delta}\kappa_A$ infrared finite. After the infrared pieces have been canceled, one notices that the remaining contribution of $\Delta\kappa_A^P$ decreases monotonically as $Q^2 \to \pm\infty$; due to the difference in relative signs, this contribution cancels asymptotically against the monotonically increasing contribution from $\Delta\kappa_A^{(\xi=1)}$. Thus, by including the pinch parts the unitarity of $\widehat{\Delta}\kappa_A$ is restored and $\widehat{\Delta}\kappa_A \to 0$ for large values of Q^2.

5.2.2 *Neutrino charge radius*

The neutrino electromagnetic form-factor and the neutrino charge radius (NCR) have constituted an important theoretical puzzle for over three decades. Since the dawn of the SM it was pointed out that radiative corrections will induce an effective one-loop $A^*(q^2)\nu\nu$ vertex, to be denoted by $\Gamma_{A\nu\bar{\nu}}^{\mu}$, with $A^*(q^2)$ an off-shell photon. Such a vertex would, in turn, give rise to a small but non-vanishing NCR. Traditionally (and, of course, non-relativistically and rather heuristically) the NCR has been interpreted as a measure of the "size" of the neutrino ν_i when probed electromagnetically, owing to its classical definition (in the static limit) as the second moment of the spatial neutrino charge density $\rho_\nu(\mathbf{r})$, *i.e.*,

$$\langle r_\nu^2 \rangle \sim \int d\mathbf{r}\, r^2 \rho_\nu(\mathbf{r}). \tag{5.63}$$

From the quantum field theory point of view, the NCR is defined as follows. If we write $\Gamma_{A\nu\bar{\nu}}^{\mu}$ in the form

$$\Gamma_{A\nu\bar{\nu}}^{\mu}(q^2) = \gamma_\mu(1 - \gamma_5)F_D(q^2), \tag{5.64}$$

where $F_D(q^2)$ is the (dimensionless) Dirac electromagnetic form-factor, then the NCR is given by

$$\langle r_\nu^2 \rangle = 6 \left. \frac{\partial F_D(q^2)}{\partial q^2} \right|_{q^2=0}. \tag{5.65}$$

Gauge invariance (if not compromised) requires that, in the limit $q^2 \to 0$, $F_D(q^2)$ must be proportional to q^2, *i.e.*, that it can be cast in the form $F_D(q^2) = q^2 F(q^2)$, with the dimensionful form-factor $F(q^2)$ being regular as $q^2 \to 0$. As a result, the q^2 contained in $F_D(q^2)$ cancels against the $(1/q^2)$ coming from the propagator of the off-shell photon, and one effectively obtains a contact interaction between the neutrino and the sources of the (background) photon, as one would expect from classical considerations.

Even though in the SM the one-loop computation of the *entire* S-matrix element describing the electron-neutrino scattering, shown in Fig. 42, is conceptually straightforward, the identification of a *subamplitude*, which would serve as the effective $\Gamma_{A\nu\bar{\nu}}^{\mu}$ has been faced with serious complications, associated with the simultaneous reconciliation of crucial requirements such as gauge-invariance, finiteness, and target-independence. Specifically, various attempts to define the value of the NCR within the SM from the one-loop $\Gamma_{A\nu\bar{\nu}}^{\mu}$ vertex calculated in the renormalizable (R_ξ) gauges reveal that the corresponding electromagnetic form-factor depends explicitly on the gauge-fixing parameter ξ in a prohibiting way. In particular, even though in the static limit of zero momentum transfer, $q^2 \to 0$, the Dirac form-factor becomes independent of ξ, its first
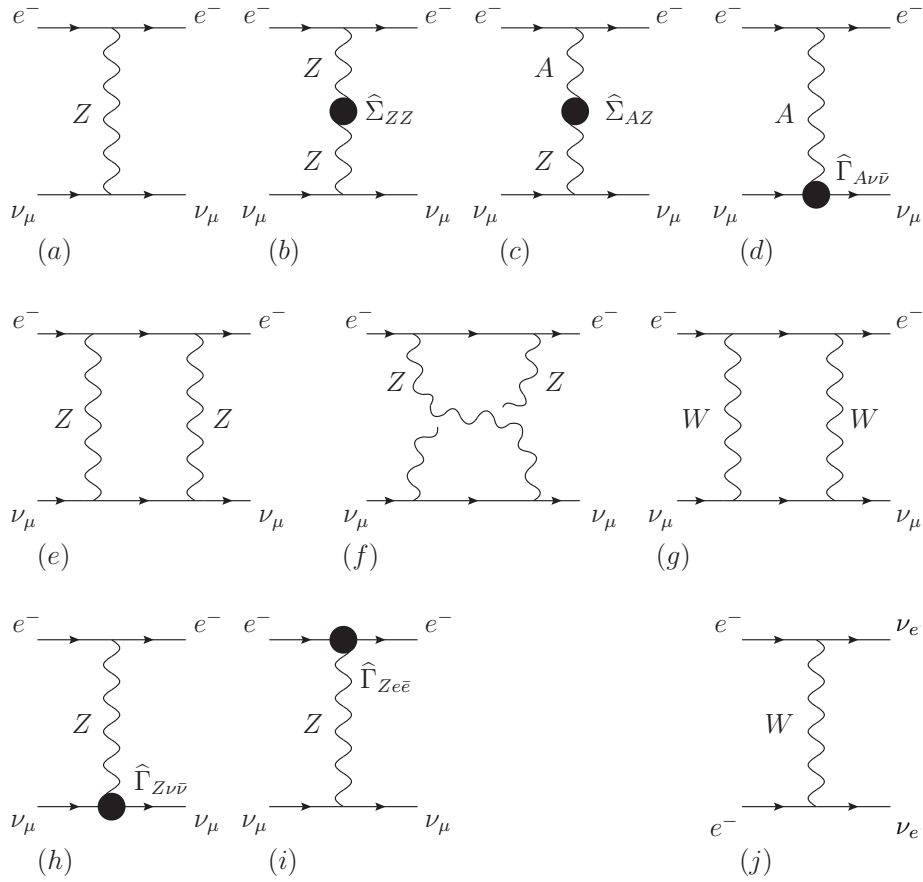
Fig. 42. The electroweak diagrams contributing to the entire electron-neutrino scattering process at one-loop. The last diagram (and all of its dressing) is absent when the neutrino species is muonic.

derivative with respect to q^2, which corresponds to the definition of the NCR, continues to depend on it. Similar (and sometimes worse) problems occur in the context of other gauges (*e.g.*, unitary gauge). These complications have obscured the entire concept of an NCR, and have casted serious doubts on whether it can be regarded as a genuine physical observable.

5.2.3   The physical NCR

Of course, if a quantity is gauge-dependent it is not physical. But the fact that the off-shell vertex is gauge-dependent only means that it just does not serve as a physical definition of the NCR. It does not mean that an *effective* NCR cannot be encountered which satisfies *all* necessary physical properties, gauge-independence being one of them. Indeed, several authors have attempted to find a *modified* vertex-like amplitude, that would lead to a consistent definition of the electromagnetic NCR (see [20,21,127] for an extended list of references). The common underlying idea in all these works is to rearrange, somehow, the Feynman graphs contributing to the scattering amplitude of neutrinos with charged particles, in an attempt to find a vertex-like combination that would satisfy all desirable properties. What makes this exercise so difficult is that, in addition to gauge-independence, a multitude of other crucial physical requirements

need to be satisfied as well. For example, one should not enforce gauge-independence at the expense of introducing target-dependence. Therefore, a definite guiding-principle is needed, allowing for the construction of physical subamplitudes with definite kinematic structure (*i.e.*, self-energies, vertices, boxes).

The guiding-principle in question has been provided by the PT. As was shown for the first time in [9], the rearrangement of the physical amplitude $f^\pm \nu \to f^\pm \nu$, where $f^\pm$ are the target fermions, into PT self-energies, vertices, and boxes conclusively settles the issue: the *proper* PT vertex with an off-shell photon and two on-shell neutrinos (see Fig. 43), denoted by $\widehat{\Gamma}^\mu_{A\nu_i\bar{\nu}_i}$, *furnishes unambiguously and uniquely the physical NCR*. As we know from the general discussion of the previous section, $\widehat{\Gamma}^\mu_{A\nu_i\bar{\nu}_i}$ *coincides* with the BFM vertex involving an off-shell background photon and two on-shell neutrinos, calculated by putting the quantum W-bosons inside the loops in the Feynman gauge (the BFG).

Several years after its original resolution within the PT [9], the NCR issue was revisited in [20]. There, in addition to an exhaustive demonstration of the various gauge cancellations, two important conceptual points have been conclusively settled:

i. As already explained in [9], the box diagrams furnish gauge-dependent (propagator-like) contributions that are crucial for the gauge-cancellations, but once these contributions have been identified and extracted, the remaining "pure" box cannot form part of the NCR, because it would introduce process-dependence (due to its non-trivial dependence on the target-fermion masses, for one thing). The most convincing way to understand why the pure box could not possibly enter into the NCR definition is to consider the case of right-handedly polarized target fermions, which do not couple to the Ws: in that case, the box diagram is not even there! (the gauge-cancellations proceed now differently, since the coupling of the Z boson to the target fermions is also modified) [20].

ii. The mixing self-energy $\widehat{\Pi}_{AZ}(q^2)$ should *not* be included in the definition of the NCR either. The reason is more subtle (and had not been recognized in [9]): $\widehat{\Pi}_{AZ}(q^2)$ is *not* an RG-invariant quantity; adding it to the finite contribution coming from the proper vertex would convert the resulting NCR to a μ-dependent, and therefore unphysical quantity. Instead, $\widehat{\Pi}^{AZ}(q^2)$ must be combined with the appropriate Z-mediated *tree-level* contributions (which evidently do not enter into the definition of the NCR) in order to form, with them, the RG-invariant combination $\bar{s}^2_w(q^2)$ of Eq.(5.29), whereas the ultraviolet-finite NCR will be determined from the *proper* vertex only.

Writing $\widehat{\Gamma}^\mu_{A\nu_i\bar{\nu}_i} = q^2\widehat{F}_i(q^2)\gamma_\mu(1-\gamma_5)$, the physical NCR is then defined as $\left\langle r^2_{\nu_i}\right\rangle = 6\widehat{F}_i(0)$, and the explicit calculation yields

$$\left\langle r^2_{\nu_i}\right\rangle = \frac{G_F}{4\sqrt{2}\pi^2}\left[3 - 2\log\left(\frac{m^2_i}{M^2_W}\right)\right], \tag{5.66}$$

where $i = e, \mu, \tau$, m_i denotes the mass of the charged isodoublet partner of the neutrino under consideration, and G_F is the Fermi constant. Note that the logarithmic term on the rhs of Eq. (5.66) originates from the Abelian graph, and is not affected by the PT procedure, *i.e.*, it is, from the beginning, gauge-independent. This term may be obtained directly if one considers
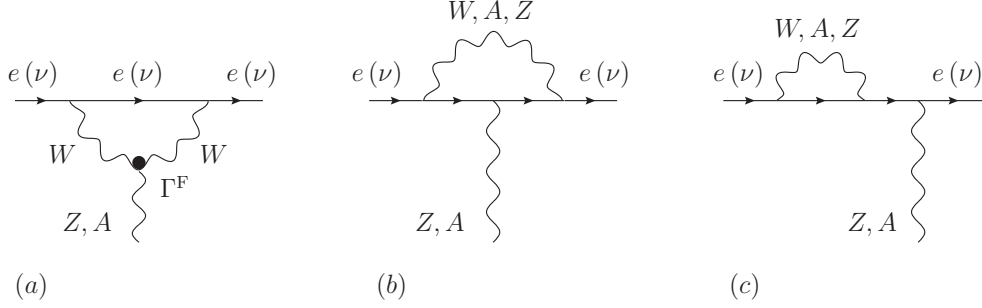
Fig. 43. The PT vertex with an off-shell gauge-boson (A,Z) and two on-shell fermions (ν, e)

the problem from an effective field theory point of view, in the limit of a very heavy W-boson.

The observable nature of the NCR was established in [21], by demonstrating that, at least in principle, the probe-independent NCR may be extracted from a judicious combination of scattering experiments involving neutrinos and anti-neutrinos.

Consider, in fact, the elastic processes $f(k_1)\nu(p_1) \to f(k_2)\nu(p_2)$ and $f(k_1)\bar{\nu}(p_1) \to f(k_2)\bar{\nu}(p_2)$, where f denotes an electrically charged fermion belonging to a different isodoublet than the neutrino ν, in order to eliminate the diagrams mediated by a charged W-boson. The Mandelstam variables are defined as $s = (k_1 + p_1)^2 = (k_2 + p_2)^2$, $t = q^2 = (p_1 - p_2)^2 = (k_1 - k_2)^2$, $u = (k_1 - p_2)^2 = (k_2 - p_1)^2$, and $s + t + u = 0$. In what follows, we will restrict ourselves to the limit $t = q^2 \to 0$ of the above amplitudes, assuming that all external (on-shell) fermions are massless. As a result of this special kinematic situation we have the following relations: $p_1^2 = p_2^2 = k_1^2 = k_2^2 = p_1 \cdot p_2 = k_1 \cdot k_2 = 0$ and $p_1 \cdot k_1 = p_1 \cdot k_2 = p_2 \cdot k_1 = p_2 \cdot k_2 = s/2$. In the center-of-mass system, we have that $t = -2E_\nu E'_\nu (1-x) \leq 0$, where E_ν and E'_ν are the energies of the neutrino before and after the scattering, respectively, and $x \equiv \cos\theta_{cm}$, where θ_{cm} is the scattering angle. Clearly, the condition $t = 0$ corresponds to the exactly forward amplitude, with $\theta_{cm} = 0$, $x = 1$.

At tree-level the amplitude $f\nu \to f\nu$ is mediated by an off-shell Z-boson. At one-loop, the relevant contributions are determined through the PT rearrangement of the amplitude, giving rise to gauge-independent subamplitudes. In particular, $\widehat{\Pi}_{AZ}^{\mu\nu}(q^2)$ obtained is transverse, for *both* the fermionic and the bosonic contributions, *i.e.*, $\widehat{\Sigma}_{AZ}^{\mu\nu}(q^2) = (q^2 g^{\mu\nu} - q^\mu q^\nu)\widehat{\mathbf{\Pi}}_{AZ}(q^2)$, and we only keep the $g^{\mu\nu}$ part of $\widehat{\Pi}_{ZZ}^{\mu\nu}(q^2)$. The one-loop vertex $\widehat{\Gamma}_{ZF\bar{F}}^{\mu}(q, p_1, p_2)$, with $F = f$ or $F = \nu$, satisfies a QED-like WI, relating it to the one-loop inverse fermion propagators $\widehat{\Sigma}_F$, *i.e.*, $q_\mu \widehat{\Gamma}_{Zf\bar{F}}^{\mu}(q, p_1, p_2) = \widehat{\Sigma}_F(p_1) - \widehat{\Sigma}_F(p_2)$. In the limit of $q^2 \to 0$, $\widehat{\Gamma}_{ZF\bar{F}}^{\mu} \sim q^2 \gamma^\mu (c_1 + c_2 \gamma_5)$; since it is multiplied by a massive Z boson propagator $(q^2 - M_Z)^{-1}$, its contribution to the amplitude vanishes when $q^2 \to 0$. This is to be contrasted with the $\widehat{\Gamma}_{A\nu_i\bar{\nu}_i}^{\mu}$, which is accompanied by a $(1/q^2)$ photon-propagator, thus giving rise to a contact interaction between the target-fermion and the neutrino, described by the NCR.

In order to experimentally isolate from the amplitude the contribution due to the NCR, we first eliminate the box-contributions. The basic observation is that the tree-level amplitudes $\mathcal{M}_{\nu f}^{(0)}$, as well as the part of the one-loop amplitude $\mathcal{M}_{\nu f}^{(B)}$ consisting of the propagator and vertex corrections (namely the "Born-improved" amplitude), are proportional to

$$[\bar{u}_f(k_2)\gamma_\mu(v_f + a_f\gamma_5)u_f(k_1)][\bar{v}(p_1)\gamma_\mu P_L v(p_2)], \qquad (5.67)$$

123

and therefore transform differently than the boxes under the replacement $\nu \to \bar{\nu}$, since [128]

$$\bar{u}(p_2)\gamma_\mu P_L u(p_1) \to -\bar{v}(p_1)\gamma_\mu P_L v(p_2) = -\bar{u}(p_2)\gamma_\mu P_R u(p_1). \tag{5.68}$$

Thus, under the above transformation, $\mathcal{M}_{\nu f}^{(0)} + \mathcal{M}_{\nu f}^{(B)}$ reverse sign once, whereas the box contributions reverse sign twice. These distinct transformation properties allow for the isolation of the box contributions when the forward differential cross-sections $(d\sigma_{\nu f}/dx)_{x=1}$ and $(d\sigma_{\bar{\nu} f}/dx)_{x=1}$ are appropriately combined. In particular, the combination

$$\sigma_{\nu f}^{\pm} \equiv \left.\frac{d\sigma_{\nu f}}{dx}\right|_{x=1} \pm \left.\frac{d\sigma_{\bar{\nu} f}}{dx}\right|_{x=1} \tag{5.69}$$

either does not contain boxes (when choosing the plus sign), or precisely isolates the contribution of the boxes (when choosing the minus sign).

Finally, a detailed analysis shows that in the kinematic limit considered, the Bremsstrahlung contribution vanishes, due to a completely destructive interference between the two relevant diagrams corresponding to the processes $fA\nu(\bar{\nu}) \to f\nu(\bar{\nu})$ and $f\nu(\bar{\nu}) \to fA\nu(\bar{\nu})$. The absence of such corrections is consistent with the fact that there are no infrared divergent contributions from the (vanishing) vertex $\widehat{\Gamma}_{ZF\bar{F}}^\mu$, to be canceled against.

$\sigma_{\nu f}^+$ receives contributions from the tree-level exchange of a Z-boson, the one-loop contributions from the ultraviolet divergent quantities $\widehat{\Sigma}_{ZZ}(0)$ and $\widehat{\Pi}^{AZ}(0)$, and the (finite) NCR, coming from the proper vertex $\widehat{\Gamma}_{A\nu_i\bar{\nu}_i}^\mu$. The first three contributions are universal (*i.e.*, common to all neutrino species) whereas that of the proper vertex $\widehat{\Gamma}_{A\nu_i\bar{\nu}_i}^\mu$ is flavor-dependent. After organizing the one-loop corrections of $\sigma_{\nu f}^{(+)}$ in terms of the RG-invariant quantities $\bar{R}_Z$ and $\bar{s}_w^2(q^2)$, one may fix $\nu = \nu_\mu$, and then consider three different choices for f: (*i*) right-handed electrons, e_R; (*ii*) left-handed electrons, e_L, and (*iii*) neutrinos, ν_i other than ν_μ, *i.e.*, $i = e, \tau$. Thus, we arrive at the system

$$\sigma_{\nu_\mu\nu_i}^+ = s\pi\bar{R}^2(0),$$
$$\sigma_{\nu_\mu e_R}^+ = s\pi\bar{R}^2(0)\bar{s}_w^4(0) - 2\lambda s_w^2 \left\langle r_{\nu_\mu}^2 \right\rangle,$$
$$\sigma_{\nu_\mu e_L}^+ = s\pi\bar{R}^2(0)\left(\frac{1}{2} - \bar{s}_w^2(0)\right)^2 + \lambda(1 - 2s_w^2)\left\langle r_{\nu_\mu}^2 \right\rangle, \tag{5.70}$$

where $\lambda \equiv (2\sqrt{2}/3)s\alpha\, G_F$. Now $\bar{R}^2(0)$, $\bar{s}_w^2(0)$, and $\left\langle r_{\nu_\mu}^2 \right\rangle$ are treated as three unknown quantities, to be determined from the above algebraic equations. Substituting $s\pi\bar{R}^2(0) \to \sigma_{\nu_\mu\nu_i}^+$ into the equations above, we arrive at a system which is linear in the unknown quantity $\left\langle r_{\nu_\mu}^2 \right\rangle$, and quadratic in $\bar{s}_w^2(0)$. The corresponding solutions are given by

$$\bar{s}_w^2(0) = s_w^2 \pm \Omega^{1/2}$$
$$\left\langle r_{\nu_\mu}^2 \right\rangle = \lambda^{-1}\left[\left(s_w^2 - \frac{1}{4} \pm \Omega^{1/2}\right)\sigma_{\nu_\mu\nu_i}^+ + \sigma_{\nu_\mu e_L}^+ - \sigma_{\nu_\mu e_R}^+\right], \tag{5.71}$$

where the discriminant Ω is given by

$$\Omega = (1 - 2s_w^2)\left(\frac{\sigma_{\nu_\mu e_R}^+}{\sigma_{\nu_\mu \nu_i}^+} - \frac{1}{2}s_w^2\right) + 2s_w^2\frac{\sigma_{\nu_\mu e_L}^+}{\sigma_{\nu_\mu \nu_i}^+} \tag{5.72}$$

and must satisfy $\Omega > 0$. The actual sign in front of Ω may be chosen by requiring that it correctly accounts for the sign of the shift of $\bar{s}_w^2(0)$ with respect to s_w^2 predicted by the theory [123].

To extract the experimental values of the quantities $\bar{R}^2(0)$, $\bar{s}_w^2(0)$, and $\left\langle r_{\nu_\mu}^2 \right\rangle$, one must substitute in the above equations the experimentally measured values for the differential cross-sections $\sigma_{\nu_\mu e_R}^+$, $\sigma_{\nu_\mu e_L}^+$, and $\sigma_{\nu_\mu \nu_i}^+$. Thus, one would have to carry out three different pairs of experiments.

5.2.4 Neutrino-Nuclear coherent scattering and the NCR

The above analysis establishes the observable nature of the NCR in terms of Gedanken-type of experiments. In practice, however, one needs to resort to a more feasible procedure, even at the expense of using as an input the theoretical SM values for certain parts of the process (*e.g.*, boxes).

One such proposal aims to extract the value of the NCR from the *coherent scattering* of a neutrino against a heavy nucleus [129]. The notion of coherent nuclear scattering is well-known from electron scattering. In the neutrino case it was developed in connection with the discovery of weak neutral currents, with a component proportional to the number operator [130].

When a projectile (*e.g.*, a neutrino) scatters elastically from a composite system (*e.g.*, a nucleus), the amplitude $F(\mathbf{p}', \mathbf{p})$ for scattering from an incoming momentum $\mathbf{p}$ to an outgoing momentum $\mathbf{p}'$ is given as the sum of the contributions from each constituent,

$$F(\mathbf{p}', \mathbf{p}) = \sum_{j=1}^{A} f_j(\mathbf{p}', \mathbf{p})e^{i\mathbf{q}\cdot\mathbf{x}_j}, \tag{5.73}$$

where $\mathbf{q} = \mathbf{p}' - \mathbf{p}$ is the momentum transfer and the individual amplitudes $f_j(\mathbf{p}', \mathbf{p})$ are added with a relative phase-factor, determined by the corresponding wave function. The differential cross-section is then

$$\frac{d\sigma}{d\Omega} = |F(\mathbf{p}', \mathbf{p})|^2 = \sum_{j=1}^{A} |f_j(\mathbf{p}', \mathbf{p})|^2 + \sum_{j,i}^{i\neq j} f_i(\mathbf{p}', \mathbf{p})f_j^\dagger(\mathbf{p}', \mathbf{p})e^{i\mathbf{q}\cdot(\mathbf{x}_j - \mathbf{x}_i)}. \tag{5.74}$$

In principle, due to the presence of the phase factors, major cancellations may take place among the $A(A - 1)$ terms in the second (non-diagonal) sum. This happens for $qR \gg 1$, where R is the size of the composite system, and the scattering would be incoherent. On the contrary, under the condition that $qR \ll 1$, then all phase factors may be approximated by unity, and the terms in (5.74) add coherently. If there were only one type of constituent, *i.e.*, $f_j(\mathbf{p}', \mathbf{p}) = f(\mathbf{p}', \mathbf{p})$ for all j, then (5.74) would reduce to

$$\frac{d\sigma}{d\Omega} = A^2 |f(\mathbf{p}', \mathbf{p})|^2 \tag{5.75}$$

Evidently, in that case, the *coherent* scattering cross-section would be enhanced by a factor of A^2 compared to that of a single constituent. In the realistic case of a nucleus with Z protons and N neutrons, and assuming zero nuclear spin, the corresponding differential cross-section reads [130]

$$\frac{d\sigma}{d\Omega} = \frac{G_F^2}{4(2\pi)^2}E^2(1+\cos\theta)\left[(1-4s_w^2)Z - N\right]^2,\tag{5.76}$$

where s_w is the sine of the weak mixing angle, $d\Omega = d\phi\, d(\cos\theta)$, and θ is the scattering angle.

In such an experiment the relevant quantity to measure is the kinetic energy distribution of the recoiling nucleus, which, in turn, may be directly related to the shift in the value of s_w^2 produced by the NCR. Specifically, the UV-finite contribution from the NCR may be absorbed into an additional (flavor-dependent!) shift of $\bar{s}_w^2(q^2)$. In fact, a detailed analysis based on the methodology developed in [123], reveals that, in the kinematic range of interest, the numerical impact of $\bar{R}_Z(q^2)$ and $\bar{s}_w^2(q^2)$ is negligible, *i.e.*, these quantities do not run appreciably. Instead, the contribution from the NCR amounts to a correction of few percent to s_w^2, given by an expression of the form $s_w^2 \longrightarrow s_w^2\left(1 - \frac{2}{3}M_W^2\left\langle r_{\nu_i}^2\right\rangle\right)$ [129]. The contributions of the boxes are of the order g_W^4/M_W^2, and they may have to be subtracted out "by hand". This type of experiment has been proposed in order to observe the coherent elastic neutrino-nuclear scattering for the first time, and it could also furnish the first *terrestrial* measurement of the NCR.

Finally, it is interesting to mention that if one were to consider the differences in the cross-sections between two *different* neutrino species scattering coherently off the same nucleus, as proposed by Sehgal long ago [131], one would eliminate all unwanted contributions, such as boxes, thus measuring the *difference* between the two corresponding charge radii. Such a difference would contribute to a difference for the neutrino index of refraction in nuclear matter [132].

5.3 Gauge-independent definition of electroweak parameters

The PT offers the possibility to define a set of electroweak parameters that are completely gauge-independent. This is useful because one usually tends to place bounds on new physics by comparing with the most sensitive electroweak parameters. Clearly, gauge artifacts may give misleading information on the viability and relevance of possible extensions of the SM.

5.3.1 The S, T, and U parameters

One of the most frequently used parametrizations of the leading contributions of electroweak radiative corrections is in terms of the S, T, and U parameters [47]. The expressions for these parameters are suitable combinations of self-energies (usually referred to also as "oblique corrections"); in terms of the conventional SM self-energies they are given by

$$\hat{\alpha}S = \frac{4\hat{c}^2\hat{s}^2}{M_Z^2}\Re e\Big\{\Pi_{ZZ}(M_Z^2) - \Pi_{ZZ}(0)$$

$$- \frac{\hat{c}^2 - \hat{s}^2}{\hat{c}\hat{s}}\Big[\Pi_{AZ}(M_Z^2) - \Pi_{AZ}(0)\Big] - \Pi_{AA}(M_Z^2)\Big\},$$

$$\hat{\alpha}T = \frac{\Pi_{WW}(0)}{M_W^2} - \frac{\hat{c}^2}{M_W^2}\Big[\Pi_{ZZ}(0) + \frac{2\hat{s}}{\hat{c}}\Pi_{AZ}(0)\Big],$$

$$\hat{\alpha}U = 4\hat{s}^2\Re e\Big\{\frac{\Pi_{WW}(M_W^2) - \Pi_{WW}(0)}{M_W^2} - \hat{c}^2\frac{\Pi_{ZZ}(M_Z^2) - \Pi_{ZZ}(0)}{M_Z^2}$$

$$-2\hat{c}\hat{s}\frac{\Pi_{AZ}(M_Z^2) - \Pi_{AZ}(0)}{M_Z^2} - \hat{s}^2\frac{\Pi_{AA}(M_Z^2)}{M_Z^2}\Big\}, \tag{5.77}$$

where Π_{WW}, Π_{ZZ}, Π_{AZ}, and Π_{AA} are the cofactors of $g^{\mu\nu}$ in the WW, ZZ, AZ, and AA self-energies, respectively. The $\overline{\text{MS}}$ values $\hat{e}^2 \equiv \hat{e}^2(M_Z)$, $\hat{s}^2 \equiv \sin^2\hat{\theta}_w(M_Z)$ are usually employed, since they are considered well suited to describe physics at the M_Z scale.

The main practical function of these parameters is to furnish constraints for models of new physics; this is done by computing the contributions of the new physics to these parameters, and then comparing them against the SM values. However, a serious problem arises already at the level of the SM, *i.e.*, before any new physics has been put in: the above expressions for the S, T, and U are *not* gfp-independent. Specifically, as was shown by Degrassi, Kniehl, and Sirlin [133], they become infested with gauge-dependencies as soon as the one-loop SM bosonic contributions are taken into account. In addition, these quantities are, in general, ultraviolet divergent, unless one happens to work within a very special class of gauges, namely those satisfying the relation

$$\xi_W = \hat{c}^2\xi_Z + \hat{s}^2\xi_A. \tag{5.78}$$

The above shortcomings may be circumvented automatically if one defines the S, T, and U parameters through the corresponding gfp-independent PT self-energies, *i.e.*, simply by replacing, in Eqs (5.77), all Πs by the corresponding $\widehat{\Pi}$s. If one restricts oneself only to the contributions within the SM (no new physics) one obtains the following relation between the conventional and gfp-independent (hatted) quantities (note that the SM tadpoles cancel exactly)

$$\hat{\alpha}\widehat{S}_{\text{SM}} = \hat{\alpha}S_{\text{SM}} + 8\hat{e}^2\hat{c}^2[I_{WW}(M_Z^2) - I_{WW}(0)],$$

$$\hat{\alpha}\widehat{T}_{\text{SM}} = \hat{\alpha}T_{\text{SM}} + 4\hat{g}^2[\hat{c}^2 I_{ZW}(0) + \hat{s}^2 I_{AW}(0) - I_{WW}(0)],$$

$$\hat{\alpha}\widehat{U}_{\text{SM}} = \hat{\alpha}U_{\text{SM}} + 16\hat{e}^2\Big\{\hat{c}^2\left[I_{WW}(0) - I_{ZW}(0)\right] + \hat{s}^2[I_{WW}(M_Z^2) - I_{AW}(0)]\Big\}, \tag{5.79}$$

where

$$I_{ij}(q^2) = i\int_k \frac{1}{(k^2 - M_i^2)[(k+q)^2 - M_j^2]}. \tag{5.80}$$

Note that, since $\widehat{\Pi}_{AZ}(0) = 0$, we have that

$$\hat{\alpha}\widehat{T}_{\text{SM}} = \frac{\widehat{\Pi}^{WW}(0)}{M_W^2} - \frac{\widehat{\Pi}^{ZZ}(0)}{M_Z^2}; \tag{5.81}$$

thus, $\hat{\alpha}\widehat{T}_{\mathrm{SM}}$ serves as the gfp-independent definition of the universal part of the ρ parameter at one loop (see next topic).

It goes without saying that the additional contributions to the $\widehat{S}$, $\widehat{T}$, and $\widehat{U}$ parameters from new physics must also be cast in a PT form (unless they involve only fermion loops). Thus, contributions to the self-energies from new gauge bosons (such as, *e.g.*, the Kaluza-Klein modes in models with universal extra dimensions [134–136]) must undergo the PT rearrangement, and be written in the form $\widehat{\Pi}_{\mathrm{NP}}$; for some recent applications of this methodology in various SM extensions, see, *e.g.*, [137–142].

5.3.2 *The universal part of the ρ parameter beyond one loop*

The ρ parameter [143] is defined as the ratio of the relative strength between neutral and charged current interactions, at low momentum transfer, namely

$$\rho = \frac{G_{NC}(0)}{G_{CC}(0)} = \frac{1}{1 - \Delta\rho} \tag{5.82}$$

where G_{NC} and G_{CC} are the corresponding full amplitudes, with all Feynman diagrams included. The ρ parameter displays a strong dependence on m_t and affects most electroweak parameters such as Δr, M_W, and $\sin^2\theta_{\mathrm{eff}}(M_Z)$. The ρ parameter defined above as the ratio of two amplitudes is a gauge independent and finite quantity. In addition, it is manifestly process dependent, since its value depends on the quantum numbers of the external particles chosen. To fully determine the value of ρ for a given neutral and charged process, one must compute the complete set of Feynman diagrams (self-energy, vertex, and box graphs) to a given order in perturbation theory. However, traditionally one focuses instead on the quantity Δ_{un}, defined in terms of the subset of Feynman diagrams containing only the gauge-boson self-energies, *i.e.*,

$$\Delta_{\mathrm{un}} = \frac{\Pi_{WW}(0)}{M_W^2} - \frac{\Pi_{ZZ}(0) + (2s_w/c_w)\Pi_{AZ}(0)}{M_Z^2}. \tag{5.83}$$

The quantity Δ_{un} is meant to capture the "universal" (*i.e.*, process-independent) part of ρ, since, by definition, it does not depend on the details of the process. According to the standard lore [144–147], Δ_{un} contains the dominant contributions to ρ.

From Eq. (5.77) we see that, at one-loop, $\Delta_{\mathrm{un}} = \hat{\alpha}T_{\mathrm{SM}}$. Given the discussion of the previous subsection, the problematic nature of this identification, as well as its one-loop remedy, should be clear by now. Specifically, the leading one-loop m_t contributions (of order $G_\mu m_t^2$) to Δ_{un} are trivially gauge-independent (since the gfp does not appear in the fermion loop), and UV finite. On the other hand, the one-loop bosonic contributions (subleading in m_t^2, of order $g^2 m_t^0$) to Δ_{un} are gauge-dependent and, except when formulated within a restricted class of gauges given in Eq. (5.78), UV divergent. The remedy is, of course, to use, instead, the definition appearing on the rhs of Eq. (5.81).

As one may imagine, things do not get any better at two-loops. Thus, if one attempts to use Eq. (5.83) at two loops (a dubious proposition, given that it does not even work at one loop) one encounters more problems (compounded by the book-keeping complications typical of the two loops) [148,149]. In particular, the leading two-loop contributions (of order $G_\mu^2 m_t^4$) to Δ_{un}

are also gauge-independent and UV finite, exactly as their one-loop counterparts. On the other hand, subleading two-loop m_t contributions (of order $G_\mu^2 m_t^2 M_Z^2$) are ξ-dependent in the context of the R_ξ gauges. In addition, even when computed in the Feynman gauge ($\xi_W = \xi_Z = 1$), which satisfies the (one-loop) relation of (5.78), the answer turns out to be UV divergent.

In order to understand the origin of the problems associated with the subleading contributions, one should first establish the mechanism that enforces the good behavior of the leading contributions– in particular their UV finiteness [150]. If we denote the leading (fermionic) contributions (both at one and two loops) to the WW and ZZ self-energies by $\Pi_{WW}^{(\ell)\mu\nu}(q)$ and $\Pi_{ZZ}^{(\ell)\mu\nu}(q)$, respectively (the label ℓ stands for "leading"), and use the important fact that

$$\Pi_{AZ}^{(\ell)}(0) = 0, \tag{5.84}$$

(valid for fermionic contributions only!) we can write for $\Delta_{\text{un}}^{(\ell)}$

$$\Delta_{\text{un}}^{(\ell)} = \frac{\Pi_{WW}^{(\ell)}(0)}{M_W^2} - \frac{\Pi_{ZZ}^{(\ell)}(0)}{M_Z^2}. \tag{5.85}$$

The finiteness of $\Delta_{\text{un}}^{(\ell)}$ may be established as follows. The WW and ZZ self-energies appearing in this problem, denoted by $\Pi_{ii}^{\mu\nu}(q)$ ($i = W, Z$) may be written in the form

$$\Pi_{ii}^{\mu\nu}(q) = \Pi_{ii}(q^2)g_{\mu\nu} + \Pi_{ii}^L(q^2)q^\mu q^\nu, \tag{5.86}$$

and the dimensionality of $\Pi_{ii}(q^2)$ will be saturated either by q^2 or by the masses appearing in the theory, the latter being all proportional to the value v of the vev. Thus, we have

$$\Pi_{ii}(q^2) = v^2 \Pi_{1\,ii}(q^2) + q^2 \Pi_{2\,ii}(q^2), \tag{5.87}$$

and therefore

$$\Pi_{ii}(0) = v^2 \Pi_{1\,ii}(0). \tag{5.88}$$

Then it is elementary to establish that

$$\Pi_{ii}(0) = \frac{d}{dq^2} \left\{ q_\mu q_\nu \Pi_{ii}^{\mu\nu}(q^2) \right\} \bigg|_{q^2=0}. \tag{5.89}$$

Next, combine this last result with the WIs (valid only for the fermionic loops, and, in particular, the leading contributions containing top-quark loops)

$$q_\mu q_\nu \Pi_{(\ell)\mu\nu}^{WW}(q) = M_W^2 \Pi_{\phi\phi}^{(\ell)}(q^2), \tag{5.90}$$
$$q_\mu q_\nu \Pi_{ZZ}^{(\ell)\mu\nu}(q) = M_Z^2 \Pi_{\chi\chi}^{(\ell)}(q^2),$$

where $\Pi_{\phi\phi}^{(\ell)}$ and $\Pi_{\chi\chi}^{(\ell)}$ are the leading contributions of the $\phi\phi$ and $\chi\chi$ self-energies, respectively. We may then write $\Delta_{\text{un}}^{(\ell)}$ of Eq. (5.85) as

$$\Delta_{\text{un}}^{(\ell)} = \frac{d}{dq^2} \left\{ \Pi_{\phi\phi}^{(\ell)}(q^2) - \Pi_{\chi\chi}^{(\ell)}(q^2) \right\} \bigg|_{q^2=0}. \tag{5.91}$$

129

The final ingredient that enforces the finiteness of $\Delta_{\rm un}^{(\ell)}$ is the equality of the divergent parts of $\Pi_{\phi\phi}^{(\ell)}(q^2)$ and $\Pi_{\chi\chi}^{(\ell)}(q^2)$, reflected in the corresponding equality

$$Z_{\phi\phi}^{(\ell)} = Z_{\chi\chi}^{(\ell)}, \tag{5.92}$$

between the wave-function renormalization constants.

Notice, however, that the crucial relations (5.84), (5.91), and (5.92) are not longer valid when one includes the bosonic (subleading) parts of $\Pi_{WW}^{\mu\nu}(q)$ and $\Pi_{ZZ}^{\mu\nu}(q)$ in the framework of the R_ξ gauges. Consequently, since the mechanism enforcing the finiteness does not operate any more, the resulting expressions do not have to be UV finite, and indeed, as an explicit calculation showed, they are not.

The easy way out of these complications would be to abandon the notion of a "universal" part of ρ, and adopt the conservative point of view that the entire process must be considered in order to restore the finiteness and gauge-independence of the final answer. In that case, one would introduce vertex and box corrections, which would render the result gauge-independent and finite, at the expense of making it process-dependent, and therefore non-universal.

Of course, as the reader must have realized by now, this unpleasant trade-off between gauge-independence and process-independence is completely artificial, and can be easily avoided by defining $\widehat{\Delta}_{\rm un}$ beyond one loop in terms of the physical PT self-energies, namely [150]

$$\widehat{\Delta}_{\rm un} = \frac{\widehat{\Pi}_{WW}(0)}{M_W^2} - \frac{\widehat{\Pi}_{ZZ}(0)}{M_Z^2}, \tag{5.93}$$

i.e., use exactly the same definition [*viz.* (5.81)] as at one loop! Indeed, all PT self-energies are gauge-independent, and due to the Abelian WIs they satisfy, for *both fermionic and bosonic contributions*, all aforementioned conditions enforcing the finiteness of $\Delta_{\rm un}^{(\ell)}$, and in particular (5.84), (5.91), and (5.92) are valid *both for leading and subleading* contributions. Evidently, the PT restores the mechanism for the cancellation of the UV divergences, and guarantees at the same time the gauge- and process-independence of the final answer.

Thus the $\widehat{\Delta}_{\rm un}$ defined in (5.93) in terms of the PT self-energies constitutes the natural extension of the universal part of the ρ-parameter, that can accommodate consistently both leading and subleading contributions, at one and two loops. $\widehat{\Delta}_{\rm un}$ is endowed with three crucial properties; it is (*i*) independent of the gfp, (*ii*) UV finite, and (*iii*) process-independent (universal). In addition to the above important conceptual advantages, the calculation of $\widehat{\Delta}_{\rm un}$ is facilitated enormously from the fact that no vertex or box diagrams need to be calculated, since the terms that restore the good properties are all propagator-like. Therefore, the answer can be expressed in a closed analytic form up to two loops. The actual calculation of the two-loop subleading corrections of order $G_\mu^2 m_t^2 M_Z^2$ was carried out in the typical limit of $s_w^2 = 0$, where $M_Z = M_W$ (custodial symmetry restored). It turned out that their relative size is about 25% with respect to the leading ones [150]; this result is in complete agreement with naive expectations, given that the expansion parameter employed is $M_W^2/m_t^2 \approx 1/4$.

130

The physics of unstable particles and the computation of resonant transition amplitudes has attracted significant attention in recent years, because it is both phenomenologically relevant and theoretically challenging. The practical interest in the problem is related to the resonant production of various particles in all sorts of accelerators, most notably LEPI and LEP2 in the past, the TEVATRON at present, and, of course, the LHC in the very near future. From the theoretical point of view, the issue comes up every time fundamental resonances, *i.e.*, unstable particles that appear as basic degrees of freedom in the original Lagrangian of the theory (as opposed to composite bound-states), can be produced resonantly. The presence of such fundamental resonances makes it impossible to compute physical amplitudes for arbitrary values of the kinematic parameters, unless a resummation has taken place first. Simply stated, perturbation theory breaks down in the vicinity of resonances, and information about the dynamics to "all orders" needs be encoded already at the level of Born amplitudes. The difficulty arises from the fact that in the context of non-Abelian gauge theories the standard Breit-Wigner resummation used for regulating physical amplitudes near resonances is at odds with gauge invariance, unitarity, and the equivalence theorem [151–153]. Consequently, the resulting Born-improved amplitudes, in general, fail to capture faithfully the underlying dynamics.

Whereas the need for a resummed propagator is evident when dealing with unstable particles within the framework of the S-matrix perturbation theory, its incorporation to the amplitude of a resonant process is non-trivial. When this incorporation is done naively (*e.g.*, by simply replacing the bare propagators of a tree-level amplitude by resummed propagators) one is often unable to satisfy basic field theoretical requirements, such as the gfp-independence of the resulting S-matrix element, the $U(1)_{em}$ symmetry, high-energy unitarity, and the OT. This fact is perhaps not so surprising, since the naive resummation of the self-energy graphs takes into account higher order corrections, for *only* certain parts of the tree-level amplitude. Indeed, resumming the conventional two-point function of a gauge boson in order to construct a Breit-Wigner type of propagator does not include properly crucial contributions originating from box and vertex diagrams. Even though the amplitude possesses all the desired properties, this unequal treatment of its parts distorts subtle cancellations, resulting in numerous pathologies, that are artifacts of the resummations method used. It is therefore important to devise a self-consistent calculational scheme, which *manifestly* preserves the aforementioned field theoretical properties, *intrinsic* to every S-matrix element. In what follows we will briefly review how this is accomplished using the PT; the presentation is almost exclusively based on a series of articles written on the subject by A. Pilaftsis and one of the authors [23,72,74–76].

5.4.1   *The Breit-Wigner Ansatz and the Dyson summation*

The mathematical expressions for computing transition amplitudes are ill-defined in the vicinity of resonances, because the tree-level propagator of the particle mediating the interaction (*i.e.*, $\Delta = (s - M^2)^{-1}$), becomes singular as the center-of-mass energy approaches the mass of the resonance, *i.e.*, as $\sqrt{s} \sim M$. The standard way for regulating this physical kinematic singularity is to use a Breit-Wigner type of propagator; thus, near the resonance, one carries out the

substitution

$$\frac{1}{s - M^2} \longrightarrow \frac{1}{s - M^2 + iM\Gamma}, \tag{5.94}$$

where Γ is the width of the unstable (resonating) particle. The presence of the $iM\Gamma$ in the denominator prevents the amplitude from being divergent, even at the physical resonance, *i.e.*, when $s = M^2$.

This physically motivated Breit-Wigner Ansatz may seem unjustified at first, considering the fact that the width of the particle is a parameter that does not appear in the fundamental Lagrangian density defining the theory; indeed, such a term would violate immediately the hermiticity of $\mathcal{L}$, thus producing all sorts of complications. The actual field-theoretic mechanism that justifies a replacement similar to that of (5.94) is the Dyson resummation of the self-energy $\Pi(s)$ of the unstable particle. This bubble resummation amounts to the rigorous substitution

$$\frac{1}{s - M^2} \longrightarrow \frac{1}{s - M^2 + \Pi(s)}. \tag{5.95}$$

The running width of the particle is then defined as $M\Gamma(s) = \Im m\Pi(s)$, whereas the usual (on-shell) width is simply its value at $s = M^2$; thus, (5.94) is a special case of (5.95).

It is relatively easy to realize now that the Breit-Wigner procedure, as described above, is tantamount to a reorganization of the perturbative series. Indeed, resumming the self-energy $\Pi(s)$ amounts to removing a particular piece from each order of the perturbative expansion, since, from all the Feynman graphs contributing to a given order n we only pick the part that contains the corresponding string of self-energy bubbles $\Pi(s)$, and then take $n \to \infty$. Notice, however, that the off-shell Green's functions contributing to a physical quantity, at any finite order of the conventional perturbative expansion, participate in a subtle cancellation, which eliminates all unphysical terms. Therefore, the act of resummation, which treats unequally the various Green's functions, is in general liable to distort these cancellations. To put it differently, if $\Pi(s)$ contains unphysical contributions (which would eventually cancel against other terms within a given order), resumming it naively would mean that these unphysical contributions have also undergone infinite summation (they now appear in the denominator of the propagator $\Delta(s)$). In order to remove them, one would have to add the remaining perturbative pieces to an infinite order, clearly an impossible task, since the latter (boxes and vertices) do not constitute a resumable set. Thus, if the resumed $\Pi(s)$ happened to contain such unphysical terms, one would finally arrive at predictions for the physical amplitude close to the resonance which would be plagued with unphysical artifacts. It turns out that, while in scalar field theories $\Pi(s)$ does not contain such unphysical contributions, this ceases to be true in the case of non-Abelian gauge theories. The crucial novelty introduced by the PT is that the resummation of the (physical) self-energy graphs must take place only *after* the amplitude of interest has been cast via the PT algorithm into manifestly physical subamplitudes, with distinct kinematic properties, order by order in perturbation theory. Put in the language employed earlier, the PT ensures that all unphysical contributions contained inside $\Pi(s)$ have been identified and properly discarded, *before* $\Pi(s)$ undergoes resummation.
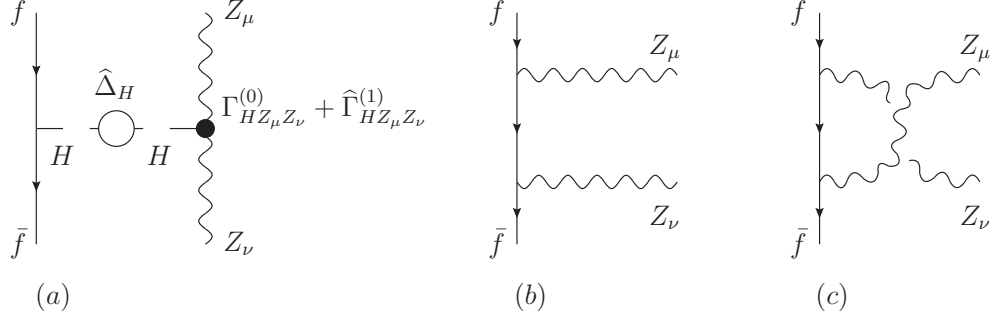
Fig. 44. The amplitude for the process $f\bar{f} \to ZZ$. The s-channel graph (a) may become resonant, and must be regulated by appropriate resummation of the Higgs propagator and dressing of the HZZ vertex

5.4.2 The non-Abelian setting

We now turn to the case of a non-Abelian gauge theory, such as the electroweak sector of the SM. As has been discussed extensively in the relevant literature, the physical requirements that must be encoded into a properly regulated resonant amplitude are the following [23,72,74–76]:

i. The resonant amplitude must be gfp-independent.

ii. Unitarity (OT) and analyticity (dispersion relations) must hold.

iii. The position of the pole must be unchanged.

iv. The external gauge-invariance must remain intact.

v. The equivalence theorem must be satisfied.

vi. The resonant amplitude must be invariant under the renormalization group.

vii. The amplitude must display good asymptotic (high-energy) behavior.

Note that if all incoming and outgoing particles are fermions then points (*iv*) and (*v*) do not enter into the discussion.

In order to fully appreciate the subtle interplay between all these issues, let us consider a concrete example that has sufficient structure for all the above points to make their appearance. Specifically, we study the process $f(p_1)\bar{f}(p_2) \to Z(k_1)Z(k_2)$, shown in Fig. 44, and $s = (p_1 + p_2)^2 = (k_1 + k_2)^2$ is the c.m. energy squared. The tree-level amplitude of this process is the sum of an s- and a t- channel contribution, denoted by $\mathcal{T}_s$ and $\mathcal{T}_t$, respectively, given by

$$
\begin{aligned}
\mathcal{T}_s^{\mu\nu} &= \Gamma_{HZZ}^{\mu\nu}\Delta_H(s)\,\bar{v}(p_2)\Gamma_{Hf\bar{f}}u(p_1), \\
\mathcal{T}_t^{\mu\nu} &= \bar{v}(p_2)\left[\Gamma_{Zf\bar{f}}^{\nu}S^{(0)}(\not{p}_1 + \not{k}_1)\Gamma_{Zf\bar{f}}^{\mu} + \Gamma_{Zf\bar{f}}^{\mu}S^{(0)}(\not{p}_1 + \not{k}_2)\Gamma_{Zf\bar{f}}^{\nu}\right]u(p_1),
\end{aligned}
\tag{5.96}
$$

133

where

$$\Gamma_{HZZ}^{\mu\nu} = ig_w \frac{M_Z^2}{M_W} g^{\mu\nu}, \qquad \Gamma_{Hf\bar{f}} = -ig_w \frac{m_f}{2M_W}, \qquad \Gamma_{Zf\bar{f}}^{\mu} = -i\frac{g_w}{c_w}\gamma_\mu\,(T_z^f P_L - Q_f s_w^2), \quad (5.97)$$

are the tree-level HZZ, $Hf\bar{f}$ and $Zf\bar{f}$ couplings, respectively.

Obviously the s-channel contribution is mediated by the Higgs boson of mass M_H and becomes resonant if the kinematics are such that $\sqrt{s}$ lies in the vicinity of M_H; in that case the resonant amplitude must be properly regulated, as explained earlier. As we will see in detail in what follows, the minimal way for accomplishing this is by: (i) Dyson-resumming the one-loop PT self-energy of the (resonating) Higgs boson, and (ii) by appropriately "dressing" the tree-level vertex $\Gamma_{HZZ}^{\mu\nu}$, $i.e.$, by replacing in the amplitude the vertex $\Gamma_{HZZ}^{\mu\nu}$ by the one-loop PT vertex $\widehat{\Gamma}_{HZZ}^{\mu\nu}$.

i. gfp-independence

Let us first see what happens if one attempts to regulate the resonant amplitude by means of the conventional one-loop Higgs self-energy in the R_ξ gauges. A straightforward calculation yields (tadpole and seagull terms omitted) [75,76]:

$$\Pi_{HH}^{(WW)}(s,\xi_W) = \frac{\alpha_w}{4\pi}\left[\left(\frac{s^2}{4M_W^2} - s + 3M_W^2\right)B_0(s, M_W^2, M_W^2)\right.$$
$$\left. + \frac{M_H^4 - s^2}{4M_W^2}B_0(s, \xi_W M_W^2, \xi_W M_W^2)\right]. \tag{5.98}$$

We see that for $\xi_W \neq 1$ the term growing as s^2 survives and is proportional to the difference $B_0(s, M_W^2, M_W^2) - B_0(s, \xi_W M_W^2, \xi_W M_W^2)$. For any finite value of ξ_W this term vanishes for sufficiently large s, $i.e.$, $s \gg M_W^2$ and $s \gg \xi_W M_W^2$. Therefore, the quantity in Eq. (5.98) displays good high energy behavior in compliance with high energy unitarity. Notice, however, that the onset of this good behavior depends crucially on the choice of ξ_W. Since ξ_W is a free parameter, and may be chosen to be arbitrarily large, but finite, the restoration of unitarity may be arbitrarily delayed as well. This fact poses no problem as long as one is restricted to the computation of physical amplitudes at a finite order in perturbation theory. However, if the above self-energy were to be resummed in order to regulate resonant transition amplitudes, it would lead to an artificial delay of unitarity restoration, which becomes numerically significant for large values of ξ_W. In addition, a serious pathology occurs for any value of $\xi_W \neq 1$, namely the appearance of unphysical thresholds [23,74,72]. Such thresholds may be particularly misleading if ξ_W is chosen in the vicinity of unity, giving rise to distortions in the lineshape of the unstable particle.

How does the situation change if instead we compute the corresponding part of the Higgs-boson self-energy in the BFM, for an *arbitrary* value of ξ_Q? Denoting it by $\widetilde{\Pi}_{(WW)}^{HH}(s,\xi_Q)$, and using the appropriate set of Feynman rules [95], we obtain

$$\widetilde{\Pi}_{HH}^{(WW)}(s,\xi_Q) = \frac{\alpha_w}{4\pi}\left[\left(\frac{s^2}{4M_W^2} - s + 3M_W^2\right)B_0(s,M_W^2,M_W^2)\right.$$
$$\left. + \frac{M_H^4 - s^2}{4M_W^2}B_0(s,\xi_Q M_W^2,\xi_Q M_W^2)\right]$$
$$- \frac{\alpha_w}{4\pi}\xi_Q(s - M_H^2)B_0(s,\xi_Q M_W^2,\xi_Q M_W^2), \tag{5.99}$$

or simply

$$\widetilde{\Pi}_{HH}^{(WW)}(s,\xi_Q) = \Pi_{HH}(s,\xi_W \to \xi_Q) - \frac{\alpha_w}{4\pi}\xi_Q(s - M_H^2)B_0(s,\xi_Q M_W^2,\xi_Q M_W^2) \tag{5.100}$$

Evidently, away from $\xi_Q = 1$, $\widetilde{\Pi}_{HH}^{(WW)}(s,\xi_Q)$ displays the same unphysical characteristics mentioned above for $\Pi_{HH}^{(WW)}(s,\xi_W)$! Therefore, when it comes to the study of resonant amplitudes, calculating in the BFM for general ξ_Q is as pathological as calculating in the conventional R_ξ gauges.

To solve these problems one has to simply follow the PT procedure, within either gauge-fixing scheme, R_ξ or BFM, identify the corresponding Higgs-boson related pinch parts from the vertex and box diagrams, and add them to (5.98) or (5.99). Then a unique answer emerges, the PT one-loop Higgs boson self-energy, given by $\widehat{\Pi}_{HH}(q^2)$,

$$\widehat{\Pi}_{HH}^{(WW)}(s) = \frac{\alpha_w}{16\pi}\frac{M_H^4}{M_W^2}\left[1 + 4\frac{M_W^2}{M_H^2} - 4\frac{M_W^2}{M_H^4}(2s - 3M_W^2)\right]B_0(s,M_W^2,M_W^2). \tag{5.101}$$

Setting $\xi_Q = 1$ in the expression of Eq. (5.99), we recover the full PT answer of Eq. (5.101), as expected. Clearly, $\widehat{\Pi}_{(WW)}^{HH}(s)$ has none of the pathologies observed above.

At this point one may wonder why not use simply the R_ξ expression for $\Pi_{HH}(s,\xi_W)$ at $\xi_W = 1$, given that it too becomes free of the aforementioned problems. The answer is that if the external particles are gauge bosons then the vertices connecting them with the resonating Higgs boson will not satisfy an Abelian WI, but rather an STI, and this, in turn, will make it impossible to satisfy the external gauge invariance [see also subsection (*iv*)].

Exactly the same arguments presented above hold for the part of the Higgs self-energy containing the Z-bosons, together with the associated would-be Golstone bosons and ghosts. The corresponding one-loop PT result reads

$$\widehat{\Pi}_{HH}^{(ZZ)}(s) = \frac{\alpha_w}{32\pi}\frac{M_H^4}{M_W^2}\left[1 + 4\frac{M_Z^2}{M_H^2} - 4\frac{M_Z^2}{M_H^4}(2s - 3M_Z^2)\right]B_0(s,M_Z^2,M_Z^2). \tag{5.102}$$

ii. Running width and the optical theorem.

When the kinematic singularity of the resonant amplitude is regulated through the resummation of the self-energy of the resonating particle, then, in the Breit-Wigner language, one obtains automatically a running (s-dependent) width. The main reason why a s-dependent instead of a constant width must be used comes from the OT. To appreciate this in a simpler context, we consider a toy model [22], with interaction Lagrangian $\mathcal{L}_{int} = \frac{\lambda}{2}\phi^2\Phi$, and assume

that $M_\Phi > 2M_\phi$, so that the decay of Φ into a pair of ϕs is kinematically allowed. For concreteness, let us consider the reaction $\phi\phi \to \Phi^*(s) \to \phi\phi$ at c.m.s. energies $s \simeq M_\Phi^2$. There are three relevant graphs, one resonant s-channel graph, and two non-resonant t and u graphs. We next focus on the resonant channel, $T_{\text{res}}(s)$, and carry out the Dyson summation of the (irreducible) $\Phi\Phi$ self-energy, to be denoted by $\Pi(s)$, obtaining for the transition amplitude

$$T_{\text{res}}(s) = -\frac{\lambda^2}{s - M_\Phi^2 + \Re e\Pi(s) + i\Im m\Pi(s)}. \tag{5.103}$$

For the case at hand the OT states that

$$\Im m\, T_{\text{res}}(s) = \frac{1}{2} \int (dPS)_{\phi\phi} |T_s(s)|^2\,; \tag{5.104}$$

on the other hand, the lhs of Eq. (5.104) is given simply by the imaginary part of Eq. (5.103), namely

$$\Im m\, T_{\text{res}}(s) = \frac{\lambda^2\Im m\Pi(s)}{\left[s - M_\Phi^2 + \Re e\Pi(s)\right]^2 + \left[\Im m\Pi(s)\right]^2}. \tag{5.105}$$

Eq. (5.104) is consistent with Eq. (5.105) in a perturbative sense; if one is sufficiently away from the resonance, such that the perturbative expansion makes sense, then Eq. (5.105) expanded to first order reproduces Eq. (5.104). Notice, however, that this becomes possible *only* when the resummation involves an s-dependent two-point function and width for the unstable scalar Φ. If a constant width for Φ had been considered instead, unitarity would have been violated, *i.e.*, Eq. (5.105) would not go over to Eq. (5.104), when $s \neq M_\Phi^2$.

It is therefore evident that the regulator of a resummed propagator in a scalar theory should be s-dependent. Needless to say, a similar situation occurs if one attempts to use a constant pole expansion in the context of a gauge field theory; indeed, it would be unrealistic to expect that one could consistently describe gauge theories using a resummation procedure that is defective even for scalar theories. The reorganization of the perturbative expansion implemented by the PT and, in particular the resummation of the PT self-energies, strictly enforces the required unitarity relations. The reason for this is that the PT self-energies satisfy the OT *individually*, as explained in Sections 2 and 4.

To verify that $\widehat{\Pi}_{HH}^{(ZZ)}(s)$ has indeed this property, in complete analogy to the methodology developed in sections I and III, we must turn to the tree-level version of the process shown in Fig. 44, [no dressing for graph (a)], and study the quantity

$$\mathcal{M} = [\mathcal{T}_s^{\mu\nu} + \mathcal{T}_t^{\mu\nu}]\, L_{\mu\rho}(k_1)L_{\nu\sigma}(k_2)[\mathcal{T}_s^{\rho\sigma} + \mathcal{T}_t^{\rho\sigma}]^*, \tag{5.106}$$

where the s-channel contribution comes from graph (a) and the t-channel from graphs (b) and (c). $L_{\mu\nu}(k)$ is the usual polarization tensor introduced in Eq. (4.60). Then we must use the longitudinal momenta coming from $L_{\mu\rho}(k_1)$ and $L_{\nu\sigma}(k_2)$ to extract from $\mathcal{T}_t^{\mu\nu}$ the effectively s-dependent, Higgs-boson mediated, part, to be denoted by $\mathcal{T}_s^P$ (see Fig. 45) Specifically,

$$\frac{k_{1\mu}k_{2\nu}}{M_Z^2}\,\mathcal{T}_t^{\mu\nu} = \mathcal{T}_s^P + \cdots = -\frac{ig_w}{2M_W}\bar{v}(p_2)\Gamma_{Hf\bar{f}}u(p_1) + \cdots, \tag{5.107}$$

where the ellipses denote genuine t-channel (not Higgs-boson related) contributions. Then, one must append the piece $\mathcal{T}_s^P\mathcal{T}_s^{P*}$ to the "naive" Higgs-dependent part $\mathcal{T}_s^{\mu\nu}L_{\mu\rho}(k_1)L_{\nu\sigma}(k_2)\mathcal{T}_s^{\rho\sigma}$.
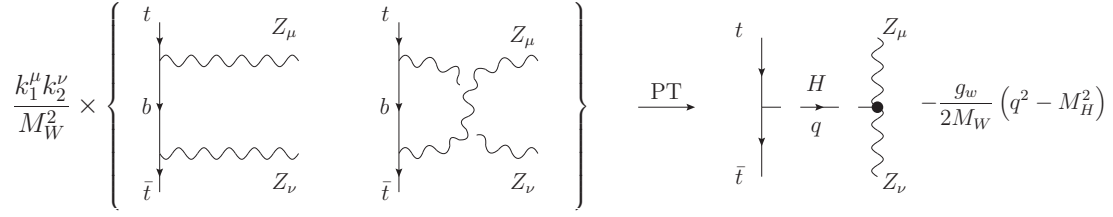
Fig. 45. The Higgs-boson related contribution extracted from the boxes through pinching; to get it we must contract with both momenta.

Integrating the expression obtained in Eq. (5.107) over the two-body phase space of two Z bosons we finally arrive at the imaginary part of Eq. (5.102), which is the announced result. A completely analogous procedure must be applied to the process $f(p_1)\bar{f}(p_2) \to W^+(k_1)W^-(k_2)$, in order to verify that the $\widehat{\Pi}_{HH}^{(WW)}(s)$ of Eq. (5.101) has the same property.

iii. Position of the pole

Since the position of the pole is the only gauge-invariant quantity that one can extract from conventional self-energies, any acceptable resummation procedure should give rise to effective self-energies that do not shift the position of the pole. This requirement is rather stringent and constrains significantly any alternative resummation procedure. It is a non-trivial exercise to demonstrate that, indeed, the PT self-energies do not shift the position of the pole. The easiest way to see that at one-loop is by noticing that the pinch terms are always proportional to $(q^2 - M^2)$, and therefore vanish at the pole. The all-order demonstration becomes far more involved, and relies on a careful construction, where the contributions coming from the 1PR diagrams must be properly taken into account.

Let us mention in passing that an early attempt towards a self-consistent resummation scheme has been based on the observation that the position of the complex pole is a gauge independent quantity [154–157,109,110]. Exploiting this fundamental property of the S-matrix, a perturbative approach in terms of three gauge invariant quantities has been proposed: the constant complex pole position of the resonant amplitude, the residue of the pole, and a s-dependent non-resonant background term. Even though this approach, which finally boils down to a Laurent series expansion of the resonant transition element [155–157], furnishes a gauge invariant result, it clashes with point (ii) above: the use of a constant instead of a running width leads to the violation of the OT. The perturbative treatment of these three gfp-independent quantities [158] introduces unavoidably residual space-like threshold terms, which become more apparent in CP-violating scenarios of new-physics [108]. In fact, the precise q^2-dependent shape of a resonance [109,110] is reproduced, to a given loop order, by considering quantum corrections to the three gfp-independent quantities mentioned above [155–158], while the space-like threshold contributions, even though shifted to higher orders, do not disappear completely.

iv. External gauge-invariance

As is well-known already from the studies of QED, gauge-invariance imposes WIs on physical amplitudes. Let us consider a physical (on-shell) amplitude with n incoming photons $A^{\mu_i}(k_i)$, $i = 1, \ldots, n$ [n must be even, otherwise the amplitude vanishes by Furry's theorem].
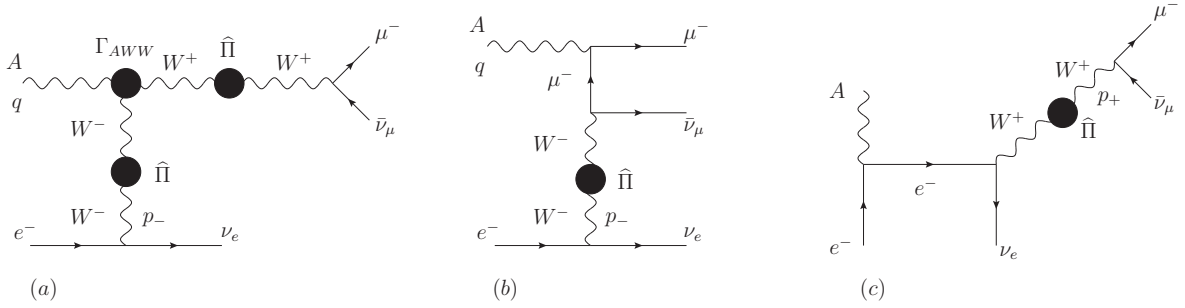
Fig. 46. The process $\gamma e^- \to \mu^- \bar{\nu}_\mu \nu_e$ appropriately dressed.

Denoting the amplitude by $T_{\mu_1 \mu_2 \ldots \mu_i \ldots \mu_n}(k_1, k_2, \ldots, k_i, \ldots, k_n, p)$, where p stands collectively for the momenta of the incoming fermions, gauge invariance imposes the relation

$$k_i^{\mu_i} T_{\mu_1 \mu_2 \cdots \mu_i \cdots \mu_n}(k_1, k_2, \ldots, k_i, \ldots, k_n, p) = 0, \qquad (5.108)$$

for every i. This result is valid to all orders in perturbation theory as well as non-perturbatively. In non-Abelian theories without tree-level symmetry breaking, such as QCD, the result mentioned above holds unchanged for the corresponding gauge bosons mediating the interaction (gluons). In the case of QCD such an example is given in Eqs (2.142); note that the rhs of these equations vanish when contracted with the corresponding (on-shell) polarization tensors. In the case of non-Abelian theories with spontaneous symmetry breaking (electroweak sector), the above result gets, in general, modified by symmetry breaking effects. When the amplitude is contracted by the momentum carried by a massive gauge boson (W or Z), the result does not vanish up to terms related to the would-be Goldstone bosons and the corresponding gauge boson masses. However, for the particular case of the photons, *i.e.*, the gauge boson corresponding to the unbroken $U(1)_{em}$, the vanishing of the contracted amplitude persists (no mass nor would-be Goldstone boson associated with the photon).

The way the fundamental property of Eq. (5.108) is realized diagrammatically at tree-level is through a number of delicate cancellations triggered by the elementary Abelian WIs satisfied by the bare photonic vertices. Beyond tree-level, to any finite order in perturbation theory, Eq. (5.108) is still valid. However, its diagrammatic demonstration is more involved, due to the proliferation of graphs and the fact that, in a non-Abelian context, the quantum corrections (concretely, the bosonic loops) to the conventional photonic vertex introduce new terms that convert the simple tree-level WI into a more complicated STI. Nonetheless, at the conceptual level, the situation is straightforward; all one has to do is contract with the relevant momentum all Feynman diagrams contributing to the amplitude in that order, and sum up the terms: the various contributions conspire in such a way as to enforce Eq. (5.108). The PT rearrangement of the amplitude facilitates the demonstration, for one thing because it restores the simple tree-level WIs to higher orders, but, strictly speaking, is not necessary.

The PT becomes indispensable, however, when one attempts to maintain Eq. (5.108) near the resonance. Let us imagine that the kinematic configuration is such that a part of the amplitude becomes resonant and must be regulated through appropriate resummation of some of its parts. Since the Dyson resummation is not a fixed order calculation, it leads, in general, to the distortion of the cancellations enforcing the validity of Eq. (5.108) at any finite order. Moreover,

near resonance a great number of graphs become numerically subleading (box diagrams are not resonant, etc), and the tendency is to omit them, even though, away from the resonance, when fixed order perturbation theory works, their inclusion is necessary for Eq. (5.108) to be valid. Evidently, the fixed-order wisdom does not carry over easily to the resonant case. The question that arises naturally, therefore, is under what conditions the resummed amplitude will be still gauge-invariant, *i.e.*, it will satisfy the crucial Eq. (5.108). To put it differently, what is the *minimum number of graphs* that must be kept, and what is the *minimum amount of "dressing"* they must undergo, in order to maintain Eq. (5.108) in the vicinity of a resonance?

Let us focus on the concrete example of the process $\gamma e^- \to \mu^- \bar{\nu}_\mu \nu_e$, shown in Fig. 46 (recall that Furry's theorem does not apply in non-Abelian theories). We assume, for simplicity, that the external fermions are all massless, and therefore we keep only the $g^{\mu\nu}$ parts of the propagators involved. At tree-level, and away from the resonance, it is elementary to demonstrate that the amplitude $T_\alpha^{(0)}$ satisfies

$$q^\alpha T_\alpha^{(0)} = 0. \tag{5.109}$$

To that end, one must employ the the WI satisfied by Ae^+e^- and $A\mu^+\mu^-$, *i.e.*, Eq. (2.41), together with the elementary WI of the tree-level AW^+W^- vertex, namely ($q + p_- + p_+ = 0$)

$$q_\alpha \Gamma_{AWW}^{\alpha\mu\nu} = (p_-^2 - M_W^2)g^{\mu\nu} - (p_+^2 - M_W^2)g^{\mu\nu}, \tag{5.110}$$

where we have omitted longitudinal momenta, since they vanish when contracted with the conserved currents.

It is clear that the negatively charged W (carrying momentum p_-) in graphs (a) may become resonant, in which case the tree-level expression for its propagator must be regulated. It is important to notice, however, that if one were to simply replace, by hand, the tree-level propagator by a Dyson-resummed one, with no further modifications, one would violate (5.110) and, as a consequence, also (5.109). In order to maintain (5.110) one must:

i. Replace in *all three graphs* the tree-level W propagators by the (one-loop) Dyson-resummed PT propagators $\widehat{\Delta}_W^{\mu\nu}(p_\pm)$,

$$\widehat{\Delta}_W^{\mu\nu}(p_\pm) = \frac{-ig^{\mu\nu}}{p_\pm^2 - M_W^2 + \widehat{\Pi}_{WW}(p_\pm^2)}; \tag{5.111}$$

ii. Add to the tree-level vertex $\Gamma_{AWW}^{\alpha\mu\nu}$ of graph (a) the one-loop PT vertex $\widehat{\Gamma}_{AWW}^{\alpha\mu\nu}$, satisfying the WI

$$q_\alpha \widehat{\Gamma}_{AWW}^{\alpha\mu\nu} = \widehat{\Pi}_{WW}^{\mu\nu}(p_-) - \widehat{\Pi}_{WW}^{\mu\nu}(p_+). \tag{5.112}$$

Thus, one arrives at the following resonant transition amplitude,

$$
\begin{aligned}
\widehat{T}_{\text{res}}^\alpha = {} & \Gamma_{We\nu_e} \widehat{\Delta}_W(p_+) \left[\Gamma_{AWW}^\alpha + \widehat{\Gamma}_{AWW}^\alpha \right] \widehat{\Delta}_W(p_-) \Gamma_{W\mu\nu_\mu} \\
& + \Gamma^{We\nu_e} S_e^{(0)} \Gamma_{Aee}^\alpha \widehat{\Delta}_W(p_-) \Gamma_{W\mu\nu_\mu} + \Gamma_{We\nu_e} \widehat{\Delta}_W(p_+) \Gamma_{A\mu\mu}^\alpha S_\mu^{(0)} \Gamma_{W\mu\nu_\mu},
\end{aligned}
\tag{5.113}
$$

where contraction over all Lorentz indices except of the photonic one is implied.

Then, since by virtue of (5.112) we have that

$$q_\alpha \left[\Gamma^{\alpha\mu\nu}_{AWW} + \widehat{\Gamma}^{\alpha\mu\nu}_{AWW} \right] = \widehat{\Delta}^{-1}_W(p_-)g^{\mu\nu} - \widehat{\Delta}^{-1}_W(p_+)g_{\mu\nu}, \tag{5.114}$$

namely the generalization of Eq. (5.110), it is straightforward to verify that the $U(1)_{em}$ gauge invariance of this resonant process is maintained, *i.e.*, that

$$q_\alpha \widehat{T}^\alpha_{\text{res}} = 0. \tag{5.115}$$

v. Equivalence theorem

The equivalence theorem states that at very high energies ($s \gg M_Z^2$) the amplitude for emission or absorption of a longitudinally polarized gauge boson becomes equal to the amplitude in which the gauge boson is replaced by the corresponding would-be Goldstone boson [151–153,159]. The above statement is a consequence of the underlying local gauge invariance of the SM, and has been known to hold to all orders in perturbation theory for multiple absorptions and emissions of massive vector bosons. Compliance with this theorem is a necessary requirement for any resummation algorithm, since any Born-improved amplitude which fails to satisfy it is bound to be missing important physical information. The reason why most resummation methods are at odds with the equivalence theorem is that, in the usual diagrammatic analysis, the underlying symmetry of the amplitudes is not manifest. Just as happens in the case of the OT, the conventional subamplitudes, defined in terms of Feynman diagrams, do *not* satisfy the equivalence theorem individually. The resummation of such a subamplitude will, in turn, distort several subtle cancellations, thus giving rise to artifacts and unphysical effects. Instead, the PT subamplitudes satisfy the equivalence theorem *individually*; as usual, the only non-trivial step for establishing this is the proper exploitation of elementary WIs.

To see an explicit example, let us return to the process $f(p_1)\bar{f}(p_2) \rightarrow Z(k_1)Z(k_2)$. The equivalence theorem states that the full amplitude $\mathcal{T} = \mathcal{T}_s + \mathcal{T}_t$ satisfies

$$\mathcal{T}(Z_L Z_L) = -\mathcal{T}(\chi\chi) - i\mathcal{T}(\chi z) - i\mathcal{T}(z\chi) + \mathcal{T}(\chi\chi), \tag{5.116}$$

where Z_L is the longitudinal component of the Z boson, χ is its associated would-be Goldstone boson, and $z_\mu(k) = \varepsilon_\mu^L(k) - k_\mu/M_Z$ is the energetically suppressed part of the longitudinal polarization vector ε_μ^L. It is crucial to observe, however, that already at the tree-level, the conventional s- and t- channel subamplitudes $\mathcal{T}_s$ and $\mathcal{T}_t$ fail to satisfy the equivalence theorem individually [75,76].

To verify that, one has to calculate $\mathcal{T}_s(Z_L Z_L)$, using explicit expressions for the longitudinal polarization vectors, and check if the answer obtained is equal to the Higgs-boson mediated s-channel part of the lhs of Eq. (5.116). In particular, in the center of mass (c.m.) system, we have

$$z_\mu(k_1) = \varepsilon_\mu^L(k_1) - \frac{k_{1\mu}}{M_Z} = -2M_Z\frac{k_{2\mu}}{s} + \mathcal{O}\left(\frac{M_Z^4}{s^2}\right), \tag{5.117}$$

140

and an exactly analogous expressions for $z_\mu(k_2)$. The residual vector $z^\mu(k)$ has the properties $k^\mu z_\mu = -M_Z$ and $z^2 = 0$. After a straightforward calculation, we obtain

$$\mathcal{T}_s(Z_L Z_L) = -\mathcal{T}_s(\chi\chi) - i\mathcal{T}_s(z\chi) - i\mathcal{T}_s(\chi z) + \mathcal{T}_s(zz) - \mathcal{T}_s^P, \qquad (5.118)$$

where

$$\mathcal{T}_s(\chi\chi) = \Gamma_{H\chi\chi} \Delta_H(s) \bar{v}(p_2) \Gamma^{(0)}_{Hf\bar{f}} u(p_1),$$
$$\mathcal{T}_s(z\chi) + \mathcal{T}_s(\chi z) = [z_\mu(k_1)\Gamma^\mu_{HZ\chi} + z_\nu(k_2)\Gamma^\nu_{H\chi Z}]\Delta_H(s)\bar{v}(p_2)\Gamma_{Hf\bar{f}}u(p_1),$$
$$\mathcal{T}_s(zz) = z_\mu(k_1)z_\nu(k_2)\mathcal{T}_s^{\mu\nu}(ZZ), \qquad (5.119)$$

with $\Gamma_{H\chi\chi} = -ig_w M_H^2/(2M_W)$ and $\Gamma^\mu_{HZ\chi} = -g_w(k_1+2k_2)_\mu/(2c_w)$. Evidently, the presence of the term $\mathcal{T}_s^P$ prevents $\mathcal{T}_s^H(Z_L Z_L)$ from satisfying the equivalence theorem. This is, of course, not surprising, given that an important Higgs-boson mediated s-channel part has been omitted. Specifically, the momenta k_1^μ and k_2^ν, stemming from the leading parts of the longitudinal polarization vectors $\varepsilon_L^\mu(k_1)$ and $\varepsilon_L^\nu(k_2)$, extract such a term from $\mathcal{T}_t(Z_L Z_L)$ (see Fig. 45). Just as happens in Eq. (5.107), this term is precisely $\mathcal{T}_s^P$, and must be added to $\mathcal{T}_s(Z_L Z_L)$, in order to form a well-behaved amplitude at high energies. In other words, the amplitude

$$\widehat{\mathcal{T}}_s(Z_L Z_L) = \mathcal{T}_s(Z_L Z_L) + \mathcal{T}_s^P \qquad (5.120)$$

satisfies the equivalence theorem by itself [see Eq. (5.116)].

In fact, this crucial property persists *after resummation*, provided that one follows the same methodology for maintaining the external gauge-invariance, presented in the previous subsection. Indeed, as shown in Fig. 44(a), the resummed amplitude, to be denoted by $\overline{\mathcal{T}}_s(Z_L Z_L)$, may be constructed from $\mathcal{T}_s(Z_L Z_L)$ in Eq. (5.96), if $\Delta_H(s)$ is replaced by the resummed Higgs-boson propagator $\widehat{\Delta}_H(s)$, and $\Gamma^{\mu\nu}_{HZZ}$ by the expression $\Gamma^{\mu\nu}_{HZZ} + \widehat{\Gamma}^{\mu\nu}_{HZZ}$, where $\widehat{\Gamma}^{\mu\nu}_{HZZ}$ is the one-loop HZZ vertex calculated within the PT. It is then straightforward to show that the Higgs-mediated amplitude $\widetilde{\mathcal{T}}_s(Z_L Z_L) = \overline{\mathcal{T}}_s(Z_L Z_L) + \mathcal{T}_s^P$ respects the equivalence theorem *individually*; to that end we only need to employ the following tree-level-type PT WIs

$$k_{2\nu}\widehat{\Gamma}^{\mu\nu}_{HZZ}(q, k_1, k_2) + iM_Z\widehat{\Gamma}^\mu_{HZ\chi}(q, k_1, k_2) = -\frac{g_w}{2c_w}\widehat{\Pi}^\mu_{Z\chi}(k_1),$$

$$k_{1\mu}\widehat{\Gamma}^\mu_{HZ\chi}(q, k_1, k_2) + iM_Z\widehat{\Gamma}_{H\chi\chi}(q, k_1, k_2) = -\frac{g_w}{2c_w}\left[\widehat{\Pi}_{HH}(q^2) + \widehat{\Pi}_{\chi\chi}(k_2^2)\right],$$

$$k_{1\mu}k_{2\nu}\widehat{\Gamma}^{\mu\nu}_{HZZ}(q, k_1, k_2) + M_Z^2\widehat{\Gamma}_{H\chi\chi}(q, k_1, k_2) = \frac{ig_w M_Z^2}{2c_w}\left[\widehat{\Pi}_{HH}(q^2) + \widehat{\Pi}_{\chi\chi}(k_1^2) + \widehat{\Pi}_{\chi\chi}(k_2^2)\right],$$

$$(5.121)$$

where $\widehat{\Gamma}^{HZ\chi}_\mu$ and $\widehat{\Gamma}^{H\chi\chi}$ are the one-loop PT $HZ\chi$ and $H\chi\chi$ vertices, respectively. In addition, one should also make use of the PT WI involving the $Z\chi$- and $\chi\chi$- self-energies, namely

$$k_\mu\widehat{\Pi}^\mu_{Z\chi}(k) = -iM_Z\widehat{\Pi}_{\chi\chi}(k^2), \qquad (5.122)$$

which is the exact analogue of Eq. (4.115).

vi. Renormalization group invariance

Physical quantities, such as scattering amplitudes, must be invariant under the RG, *i.e.*, they should not depend on the renormalization point μ chosen to carry out the subtractions, nor the renormalization scheme ($\overline{\text{MS}}$, on-shell scheme, momentum subtraction, etc).

Let us consider, for concreteness, a two-to-two amplitude, mediated (at tree-level) by a gauge boson (photon, gluon, W or Z). In QED the RG-invariance of such an amplitude is realized in a very particular way. Due to the characteristic relations (5.5) and (5.6), the amplitude may be decomposed in a unique way into three parts that are individually RG-invariant: (*i*) a universal (process-independent) part, corresponding to the effective charge defined in (5.8), [expanded to the given order], which is RG-invariant due to (5.6); (*ii*) a process-dependent part composed by the vertex corrections and the wave-function renormalization of the external particles, which is RG-invariant due to (5.5); (*iii*) a process-dependent part, coming from UV finite boxes; this is trivially RG-invariant, since it is UV finite and does not get renormalized.

In non-Abelian theories the RG-invariance of scattering amplitudes is enforced order-by-order in perturbation theory, regardless of the PT rearrangement, by virtue of equations such as (5.3), which hold also in a non-Abelian context [but not (5.5) and (5.6)]. There is an important difference, however, with respect to the QED case: while the entire amplitude is RG-invariant, the identification of a universal part corresponding to an effective charge is no longer possible. Since the PT rearrangement restores relations of the type (5.5) and (5.6), the three individually RG-invariant quantities introduced above for QED can also be identified in a non-Abelian context; in particular, non-Abelian effective charges constitute the universal part of the amplitude.

It should be clear from the above discussion, together with the analysis of the previous subsections, that when resonant amplitudes are regulated following the PT procedure they are automatically RG-invariant. In fact, in the cases where the resonating particles are W, Z, or Higgs bosons, one can isolate a universal part, which, in turn, may be identified with the *lineshape* of the corresponding particle.

vii. Good high energy behavior.

On physical grounds one expects that far from the resonance the Born-improved amplitude must behave exactly as its tree-level counterpart; in fact, a self-consistent resummation formalism should have this property built in, *i.e.*, far from resonance one should recover the correct high energy behavior *without* having to re-expand the Born-improved amplitude perturbatively. Recovering the correct asymptotic behavior is particularly tricky, however, when the final particles are gauge bosons. In order to accomplish this, in addition to the correct one-loop (running) width, the appropriate one-loop vertex corrections must be supplemented; these vertex corrections and the width must be related by a crucial tree-level Ward identity. In practice this WI ensures that the massive cancellations, which take place at tree-level, will still go through after the Born-amplitude has been "dressed". The exact mechanism that enforces the correct high energy behavior of the Born-improved amplitude, when the PT width and vertex are used, has been studied in detail in [160], for the specific reference process $f(p_1)\bar{f}(p_2) \rightarrow Z(k_1)Z(k_2)$ used above.

6 Beyond one loop: from two loops to all orders

In this section we generalize the PT to two loops and beyond; this is a rather more difficult problem than pinching at one loop, both conceptually and operationally. In the first part of this section we will establish the rules of the game beyond one-loop; the final upshot of these considerations is simple but cumbersome to implement: one must repeat exactly what one did at one loop, only now with many more diagrams. There are essentially two important lessons that can be learned from the two-loop construction: (*i*) the PT works perfectly well beyond one loop, and (*ii*) the PT must evolve into a non-diagrammatic procedure. The second lesson is taken seriously in the second part of this section, where the all-order PT construction is presented. There we show that the entire pinching action is actually encoded into the STI satisfied by a very special all-order kernel shared by propagator and vertex diagrams. This fundamental observation allows us to rise beyond the diagram-by-diagram treatment, and eventually generalize the PT to all orders.

6.1 The pinch technique at two loops

In this subsection we present the PT construction at two loops [43,161]. Specifically, we will show that the PT can be generalized at two loops by resorting *exactly* to the same physical and field-theoretical principles as at one-loop. In addition, it will become clear that the correspondence between the PT and BFG, established at one-loop, persists also at the two-loop level.

Historically, the basic conceptual difficulty associated with the generalization of the PT beyond one loop has been to determine the origin of the pinching momenta. Let us assume that, without loss of generality, one chooses from the beginning the conventional Feynman gauge. Then, the only sources of possible pinching momenta are the three-gluon vertices. The question is whether all such vertices must be somehow forced to pinch, or, in other words, whether the standard PT decomposition of Eq. (2.38) should be carried out to all available three-gluon vertices. The problem with such an operation, however, is the following: for the case of a three-gluon vertex nested inside a Feynman diagram, how does one choose what is the "special" momentum? Or, in other words, which way is one supposed to break the Bose-symmetry of the vertex? It turns out that the solution to these questions is very simple: one should only apply Eq. (2.38) to the vertices that have the physical momentum incoming (or outgoing) in one of their legs (not mixed with virtual momenta); the special leg is precisely the one carrying q. We will call such a vertex "external". All other vertices are not to be touched, i.e. they should not be decomposed in any way; such vertices have virtual momenta in every one of their three legs, and are called "internal" (see Fig. 47). A simple way to understand why the decomposition of internal vertices would lead to inconsistencies is to consider the special unitarity properties that the PT subamplitude must satisfy (see corresponding subsection).

We emphasize that throughout the entire two-loop analysis we will maintain a diagrammatic interpretation of the various contributions. In particular, no sub-integrations should to be carried out. This additional feature renders the method all the more powerful, because unitarity is manifest, and can be easily verified by means of the Cutkosky cuts.
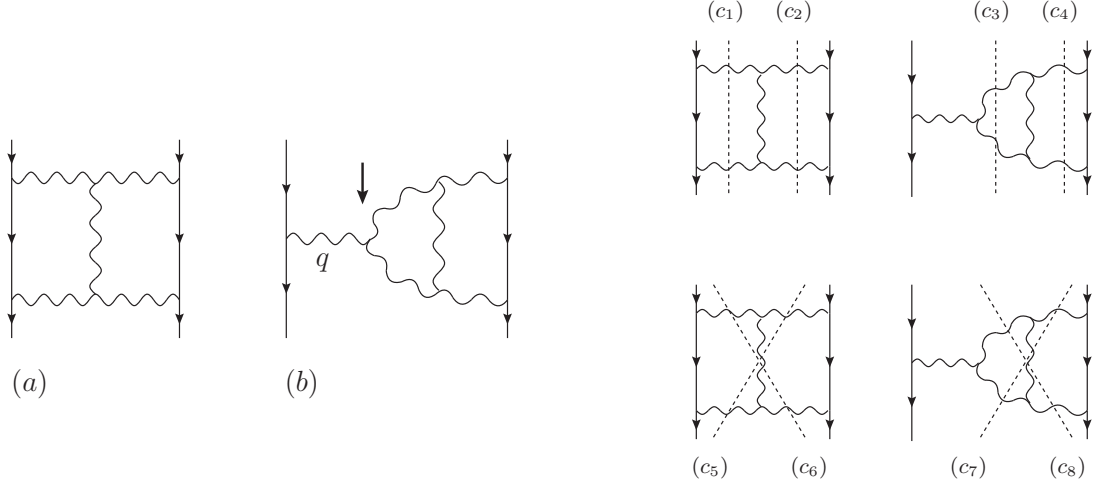
143

Fig. 47. Left panel:Some examples of external and internal vertices which appears in the two-loop graphs. Diagram (a) has only internal three-gluon vertices, while diagram (b) has two internal vertices and an external one (indicated by the arrow). Right panel: The two- and three-particle Cutkosky cuts (cutting through gluons only).

In addition to the result of Eq. (2.17), throughout this section we will employ the following formulas, valid in dimensional regularization:

$$
\int_k \frac{k_\alpha k_\beta}{k^4} = \left(\frac{1}{4-\epsilon}\right) \int_k \frac{1}{k^2} = 0,
$$
$$
\int_k \frac{(2k+q)_\alpha}{k^2(k+q)^2} = 0,
$$
$$
\int_k \frac{\ln^n(k^2)}{k^2} = 0 \qquad n = 0, 1, 2, \ldots \tag{6.1}
$$

Finally, in order to make contact with the notation of [43,161], we introduce the dimensionful projection operator

$$
t_{\mu\nu}(q) \equiv q^2 P_{\mu\nu}(q). \tag{6.2}
$$

6.1.1 The one-particle reducible graphs

We begin the two-loop construction by treating the 1PR graphs, collectively shown in Fig. 48. All such graphs are the product of two one-loop subgraphs, which may be individually converted into their PT counterparts, following precisely the standard PT procedures established in section II. Note, in fact, that, as has been explained in detail in [23,74,72], the resummability of the one-loop PT self-energy requires precisely this: the conversion of one-particle reducible (1PR) strings of conventional self-energies $\Pi^{(1)}$ into strings containing PT self-energies $\widehat{\Pi}^{(1)}$.

There is an important point, however, that one must realize. The conversion of the 1PR graphs into the corresponding PT does not take place for free; instead, the process of the conversion

gives rise to certain residual pieces, all of which have the crucial characteristic of being effectively 1PI. The way these pieces are produced is (*i*) because there is a mismatch between the propagator-like terms obtained from the available quark-gluon vertices $\Gamma^{(1)}$, and those needed to convert the string of two $\Pi^{(1)}$s into a string of two $\widehat{\Pi}^{(1)}$s [this happens with graphs (a), (b), (c) and (d) in Fig. 49], or (*i*) terms that in the one-loop construction were vanishing, due to the on-shell conditions, now they do not vanish, because they do not communicate with the external quarks (i.e., the Dirac equation cannot be triggered) [see graph (b) in Fig. 49] .

To see this in detail, let us return for a moment to the one-loop construction, and consider the conventional quark-gluon vertex at one-loop, to be denoted by $\Gamma^{(1)}_\alpha(p_1, p_2)$. We will repeat the calculation of subsection 2.4.1, but now we will not assume that the external quarks are on-shell; this is because, at two-loops, we can have the situation depicted in Fig. 49. In particular,

$$\Gamma^{(1)}_\alpha = \widehat{\Gamma}^{(1)}_\alpha + \frac{1}{2} V^{(1)}_{P\alpha\sigma}(q)\gamma^\sigma + X^{(1)}_{1\alpha}(p_1, p_2)(\slashed{p}_2 - m) + (\slashed{p}_1 - m)X^{(1)}_{2\alpha}(p_1, p_2)\,, \qquad (6.3)$$

where

$$X^{(1)}_{1\alpha}(p_1, p_2) = g^2 C_A \int_k \frac{1}{k^2(k+q)^2}\gamma_\alpha S^{(0)}(p_2 + k),$$

$$X^{(1)}_{2\alpha}(p_1, p_2) = g^2 C_A \int_k \frac{1}{k^2(k+q)^2} S^{(0)}(p_2 + k)\gamma_\alpha. \qquad (6.4)$$

By $\frac{1}{2} V^{(1)}_{P\alpha\beta}(q)$ we denote the dimensionless propagator-like contribution to be alloted to $\Pi^{(1)}(q)$, i.e.

$$V^{(1)}_{P\alpha\beta}(q) = 2g^2 C_A P_{\alpha\beta}(q) \int_k \frac{1}{k^2(k+q)^2} \qquad (6.5)$$

Thus, Eq. (2.66) reads (completely equivalently)

$$\Pi^{(1)}_{P\alpha\beta}(q) = q^2 V^{(1)}_{P\alpha\beta}(q) \qquad (6.6)$$

or

$$\Pi^{(1)}_{P\alpha\beta}(q) = V^{(1)}_{P\alpha\sigma}(q)t^\sigma_\beta(q)\,. \qquad (6.7)$$

Of course, on-shell ($\slashed{p}_1 = \slashed{p}_2 = m$) the $\Gamma^{(1)}_\alpha$ of (6.3) collapses to that of (2.67).

It is relatively straightforward to establish that

$$(2a) = (2\widehat{a}) - d(q) R^{(2)}_{P\alpha\beta}(q) d(q)\,,$$

$$(2b) + (2c) + (2d) + (2e) = (2\widehat{b}) + (2\widehat{c}) + (2\widehat{d}) + (2\widehat{e}) - F^{(2)}_{P\alpha}(p_1, p_2)\,, \qquad (6.8)$$

with

$$iR^{(2)}_{P\alpha\beta}(q) = \Pi^{(1)}_{\alpha\rho}(q)V^{(1)\rho}_{P\beta}(q) + \frac{3}{4} q^2 V^{(1)}_{P\alpha\rho}(q)V^{(1)\rho}_{P\beta}(q)\,,$$

$$F^{(2)}_{P\alpha}(p_1, p_2) = \Pi^{(1)\beta}_{P\alpha}(q) d(q) \widehat{\Gamma}^{(1)}_\beta(p_1, p_2) + d(q) Y^{(2)}_{P\alpha}(p_1, p_2), \qquad (6.9)$$
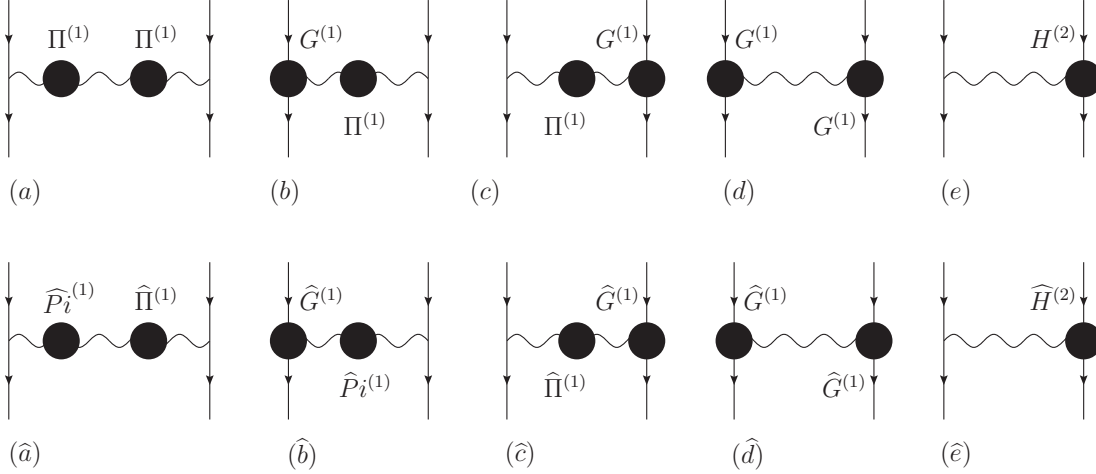
145

Fig. 48. The one-particle reducible graphs (a), (b), (c), (d), and (e) before the PT rearrangement. $G^{(1)}$ denotes the sum of the conventional one-loop quark-gluon vertex and one-loop wave-function corrections to the external quarks. $H^{(2)}$ is the product of the one-loop quark-gluon vertex times the one-loop wave-function corrections to the external quarks (see also Fig. 49). Note that (a), (b), (c), and (d) become disconnected by cutting a gluon line, whereas (e) by cutting an external quark line. All these graphs are converted into their PT equivalent graphs, i.e. $(\widehat{a})$, $(\widehat{b})$, $(\widehat{c})$, $(\widehat{d})$, and $(\widehat{e})$ are produced, together with some residual terms that, due to the pinching action, are effectively 1PI.

with

$$Y_{\mathrm{P}\alpha}^{(2)}(p_1, p_2) \equiv X_{1\alpha}^{(1)}(p_1, p_2)\Sigma^{(1)}(p_1) + X_{2\alpha}^{(1)}(p_1, p_2)\Sigma^{(1)}(p_2). \tag{6.10}$$

Notice that

$$R_{\mathrm{P}\alpha\beta}^{(2)}(q) = I_2 \left[L_{\alpha\beta}(q, k) + 3t_{\alpha\beta}(q) \right], \tag{6.11}$$

where

$$L_{\alpha\beta}(q, k) \equiv \Gamma_\alpha^{\sigma\rho}(q, k, -k-q)\Gamma_{\beta\sigma\rho}(q, k, -k-q) - 2k_\alpha(k+q)_\beta \tag{6.12}$$

is simply the numerator of the conventional $\Pi_{\alpha\beta}^{(1)}(q)$ [*i.e.*, the terms in square brackets on the rhs of Eq. (2.70)].

6.1.2   *Quark-gluon vertex and gluon self-energy at two loops*

In this subsection we will first demonstrate the construction of the two-loop PT quark-gluon vertex $\widehat{\Gamma}_\alpha^{(2)}(p_1, p_2)$, which turns out to have the exact same properties as its one-loop counterpart $\widehat{\Gamma}_\alpha^{(1)}(p_1, p_2)$. At the same time we will determine the two-loop propagator-like contributions $V_{\mathrm{P}\alpha\sigma}^{(2)}\gamma_\sigma$, which will be subsequently converted into $\Pi_{\mathrm{P}\alpha\sigma}^{(2)}$, i.e. the two-loop version of $\Pi_{\mathrm{P}\alpha\sigma}^{(1)}$ of Eq. (6.7). In addition, out of this procedure the terms $Y_{\mathrm{P}\alpha}^{(2)}(p_1, p_2)$ of Eq. (6.10) will emerge again, but with opposite sign. Then, we will turn to the two-loop gluon self-energy, and we will outline the basic steps that must be followed in its construction.

The construction of the two-loop quark-gluon vertex proceeds as follows: the Feynman graphs contributing to $\Gamma_\alpha^{(2)}(p_1, p_2)$ can be classified into two sets: (*i*) those containing an "external" three-gluon vertex i.e. a three-gluon vertex where the momentum q is incoming, as shown in Fig.s 50 and 51, and (*ii*) those which do not have an "external" three-gluon vertex. This latter set contains either graphs with no three gluon vertices (Abelian-like), or graphs with internal
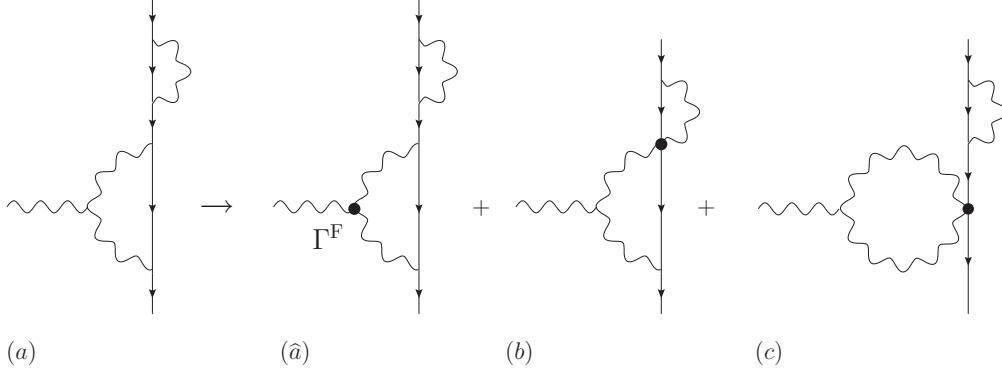
Fig. 49. The PT rearrangement of the non-Abelian part of $\mathbf{H}^{(2)}$ [graph (a)], giving rise to its PT counterpart [graph $\widehat{a}$], and to additional contributions [graphs (b) and (c)]. Diagram (b) is effectively 1PI, and is alloted to $Y_{\mathrm{P}}^{(2)}$, whereas (c) contributes to the first term of $F_{\mathrm{P}}^{(2)}$.

three-gluon vertices (all three legs are irrigated by virtual momenta, i.e. q never enters alone into any of the legs). Of course, all three-gluon vertices appearing in the computation of the one-loop S-matrix are external, and so are those appearing in the 1PR part of the two-loop S-matrix (see previous subsection). Then one carries out the decomposition of Eq. (2.38) to the external three-gluon vertex of all graphs belonging to set (i), leaving *all* their other vertices unchanged, and identifies the propagator-like pieces generated at the end of this procedure.

Let us define the following quantities (the two loop integration symbol $\int_k \int_\ell$ will be suppressed throughout)

$$
\begin{aligned}
iI_1 &= g^4 C_A^2 [\ell^2 (\ell - q)^2 k^2 (k + \ell)^2 (k + \ell - q)^2]^{-1}, \\
iI_2 &= g^4 C_A^2 [\ell^2 (\ell - q)^2 k^2 (k + q)^2]^{-1}, \\
iI_3 &= g^4 C_A^2 [\ell^2 (\ell - q)^2 k^2 (k + \ell)^2]^{-1}, \\
iI_4 &= g^4 C_A^2 [\ell^2 \ell^2 (\ell - q)^2 k^2 (k + \ell)^2]^{-1}, \\
iI_5 &= g^4 C_A^2 [\ell^2 k^2 (k + q)^2]^{-1},
\end{aligned}
\tag{6.13}
$$

which will be used extensively in what follows. The calculation is straightforward, but lengthy [see also again Fig.s 50 and 51]; we find

$$
\Gamma_\alpha^{(2)}(p_1, p_2) = \frac{1}{2} F_{\mathrm{P}\,\alpha}^{(2)}(p_1, p_2) + \frac{1}{2} V_{\mathrm{P}\alpha\sigma}^{(2)} \gamma^\sigma + \widehat{\Gamma}_\alpha^{(2)}(p_1, p_2),
\tag{6.14}
$$

with

$$
V_{\mathrm{P}\alpha\sigma}^{(2)}(q) = I_4 L_{\alpha\sigma}(\ell, k) + (2I_2 + I_3) g_{\alpha\sigma} - I_1 \left[k_\sigma g_{\alpha\rho} + \Gamma_{\rho\sigma\alpha}^{(0)}(-k, -\ell, k + \ell) \right] (\ell - q)^\rho.
\tag{6.15}
$$

The interpretation of the three terms appearing on the rhs of Eq. (6.14) is as follows:

i. The term $\frac{1}{2} F_{\mathrm{P}\,\alpha}^{(2)}(p_1, p_2)$ is half of the vertex-like part necessary to cancel the corresponding term appearing in Eq. (6.8), during the conversion of conventional 1PR graphs into their PT counterparts. The other half will come from the mirror vertex (not shown).
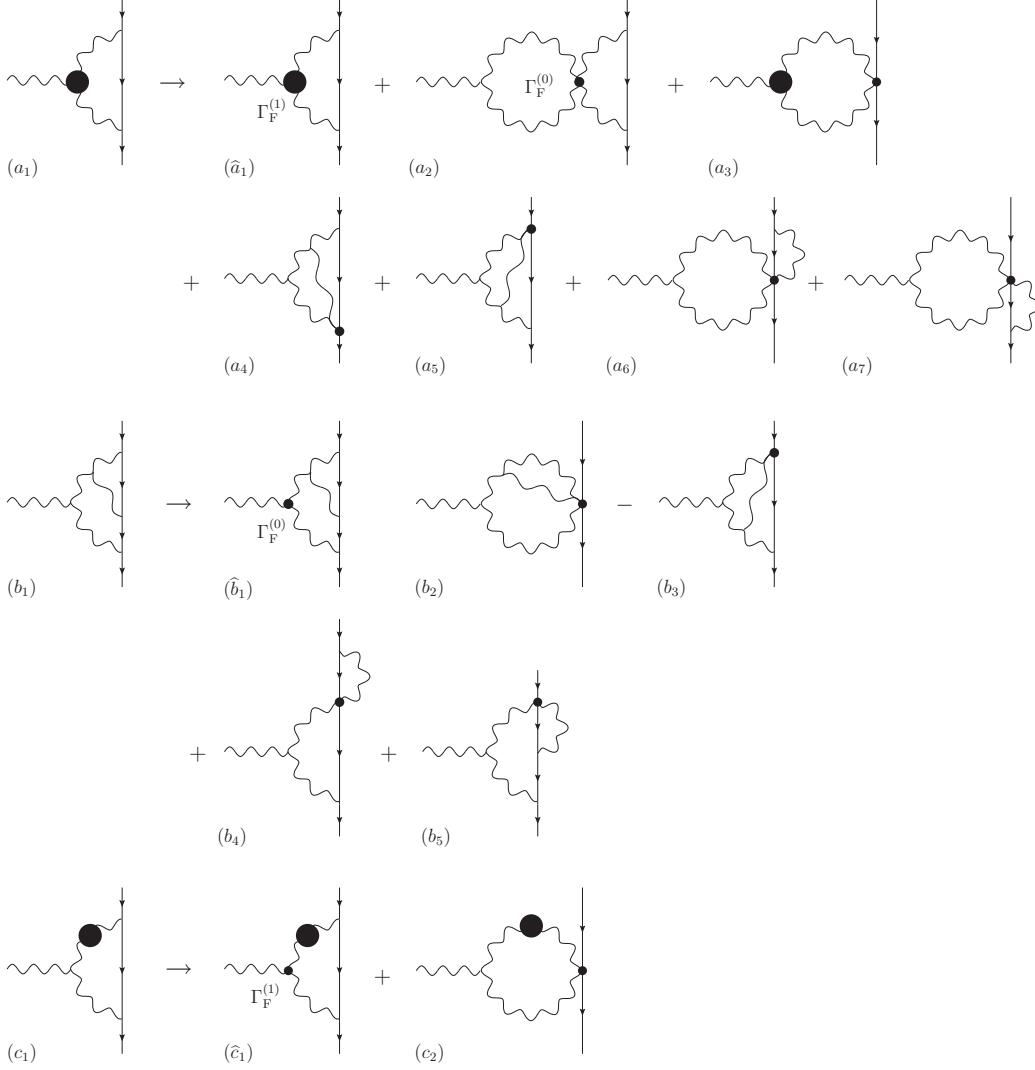
Fig. 50. The result of enforcing the PT decomposition on the external vertices of some of the two-loop Feynman diagrams contributing the conventional two-loop quark-gluon vertex $\Gamma_\alpha^{(2)}$

ii. $\frac{1}{2}V_{\mathrm{P}\alpha\sigma}^{(2)}\gamma^\sigma$ is the total propagator-like term originating from the two-loop quark-gluon vertex; together with the equal contribution from the mirror set of two-loop vertex graphs (not shown) will give rise to the self-energy term

$$\Pi_{\mathrm{P}\alpha\beta}^{(2)}(q) = V_{\mathrm{P}\alpha\sigma}^{(2)}(q)t_\beta^\sigma(q), \tag{6.16}$$

which will be part of the effective two-loop PT gluon self-energy, to be constructed below.

iii. $\widehat{\Gamma}_\alpha^{(2)}(p_1, p_2)$ is the PT two-loop quark-gluon vertex; it *coincides* with the corresponding two-loop quark-gluon vertex computed in the BFG, *i.e.*,

$$\widehat{\Gamma}_\alpha^{(2)}(p_1, p_2) = \widetilde{\Gamma}_\alpha^{(2)}(p_1, p_2, \xi_Q = 1) \tag{6.17}$$

as happens in the one-loop case. Either by virtue of the above equality and the formal prop-
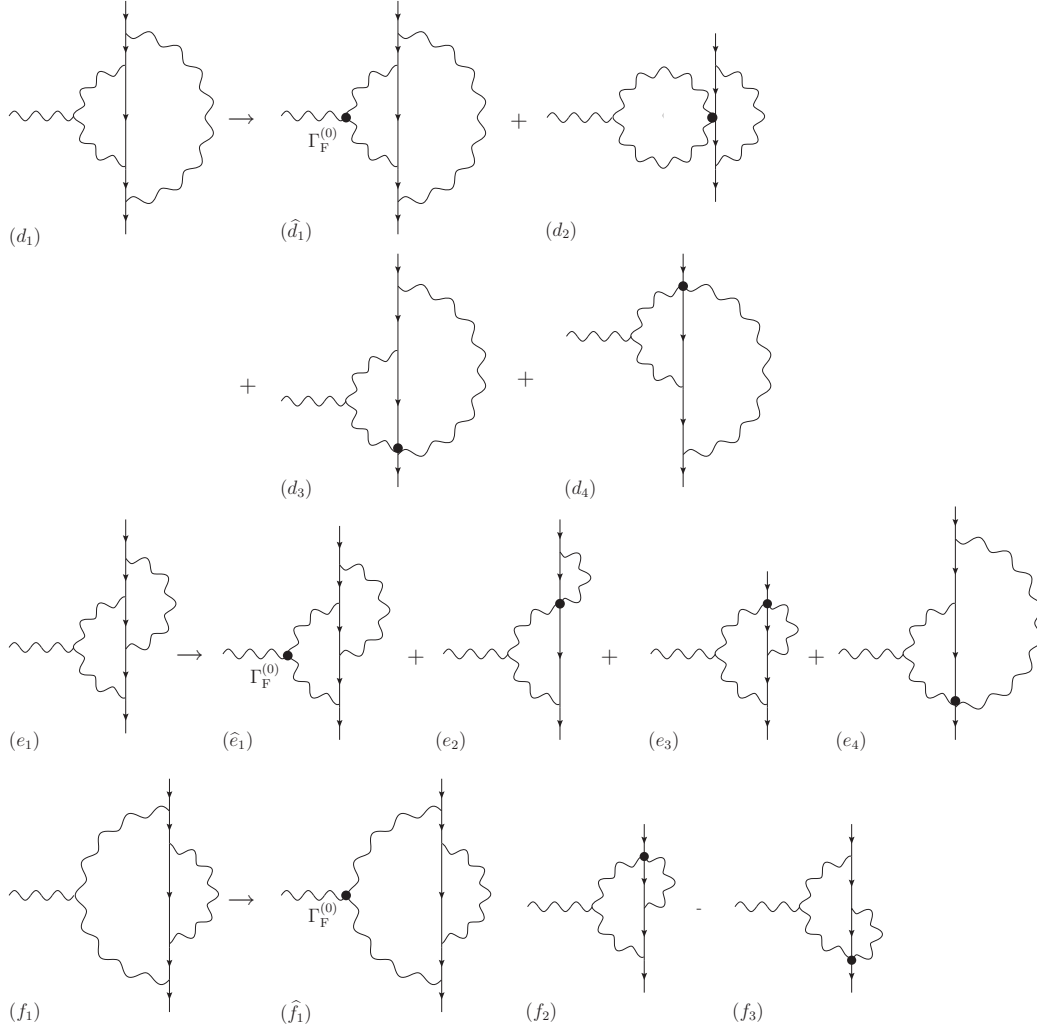
148

Fig. 51. The result of enforcing the PT decomposition on the external vertices of some of the remaining two-loop vertex graphs.

erties of the BFM, or by means of an explicit diagrammatic calculation, where one acts with q^α on individual diagrams, one can establish that $\widehat{\Gamma}_\alpha^{(2)}(p_1, p_2)$ satisfies the WI

$$q^\alpha \widehat{\Gamma}_\alpha^{(2)}(p_1, p_2) = \widehat{\Sigma}^{(2)}(p_1) - \widehat{\Sigma}^{(2)}(p_2), \tag{6.18}$$

which is the exact two-loop analogue of Eq. (2.68). $\widehat{\Sigma}^{(2)}(p)$ is the two-loop PT fermion self-energy; it is given by

$$\widehat{\Sigma}^{(2)}(p) = \widetilde{\Sigma}^{(2)}(p, \xi_Q = 1) = \Sigma^{(2)}(p, \xi = 1). \tag{6.19}$$

Again, this is the precise generalization of the one-loop result of Eq. (2.53). At this point this result comes as no surprise, since all three gluon vertices appearing in the Feynman graphs contributing to $\Sigma^{(2)}(p, \xi)$ are internal; therefore, at $\xi = 1$ there will be no pinching.

Notice that, as happened in the one-loop case, in deriving the above results no integrations (or sub-integrations) over virtual momenta have been carried out.
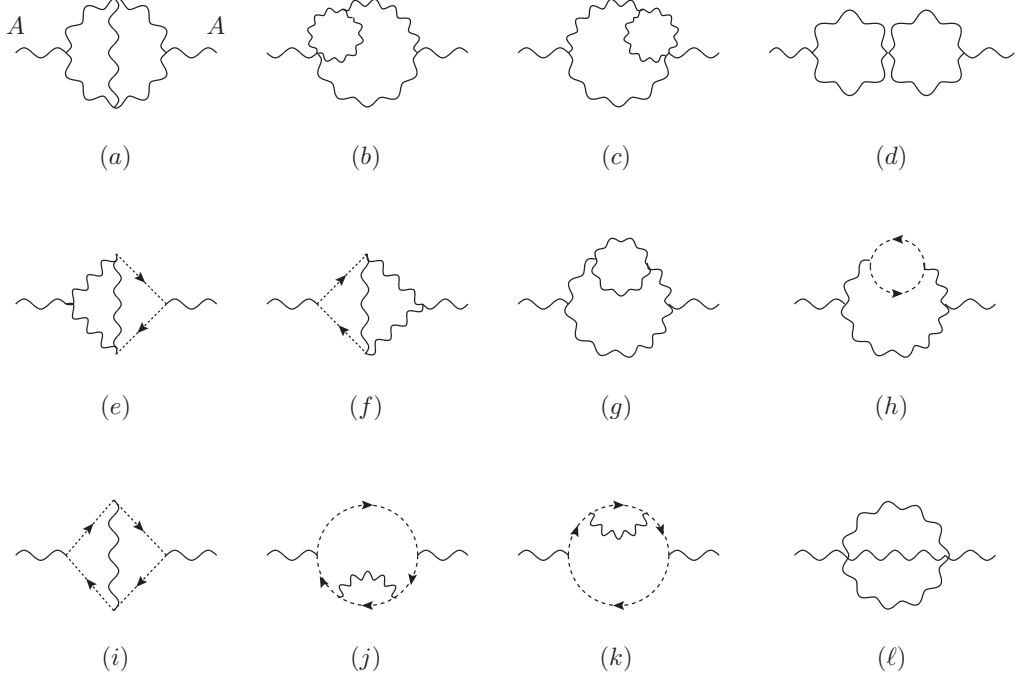
149

Fig. 52. The Feynman diagrams contributing to the conventional two-loop gluon self-energy $\Pi^{(2)}_{\alpha\beta}$, in the R_ξ gauges.

The construction of $\widehat{\Pi}^{(2)}_{\alpha\beta}(q)$ proceeds as follows: To the conventional two-loop gluon self-energy $\Pi^{(2)}_{\alpha\beta}(q)$ (shown in Fig. 52) we add two additional terms; (*i*) the propagator-like term $\Pi^{(2)}_{\mathrm{P}\alpha\beta}(q)$ derived in the previous subsection, Eq. (6.16), and (*ii*) the propagator-like part $-R^{(2)}_{\mathrm{P}\alpha\beta}(q)$ given in Eq. (6.9), stemming from the conversion of the conventional string into a PT string; this term must be removed from the 1PR reducible set and be alloted to $\widehat{\Pi}^{(2)}_{\alpha\beta}(q)$, as described in [23,74,72]. Thus, $\widehat{\Pi}^{(2)}_{\alpha\beta}(q)$ reads

$$\widehat{\Pi}^{(2)}_{\alpha\beta}(q) = \Pi^{(2)}_{\alpha\beta}(q) + \Pi^{(2)}_{\mathrm{P}\alpha\beta}(q) - R^{(2)}_{\mathrm{P}\alpha\beta}(q). \tag{6.20}$$

It is a rather lengthy exercise to establish that the two-loop PT gluon self-energy coincides with that of the BFG, *i.e.*,

$$\widehat{\Pi}^{(2)}_{\alpha\beta}(q) = \widetilde{\Pi}^{(2)}_{\alpha\beta}(q, \xi_Q = 1). \tag{6.21}$$

To verify this important result explicitly, we simply start out with the diagrams contributing to $\Pi^{(2)}_{\alpha\beta}(q)$, and convert them into the corresponding diagrams contributing to $\widetilde{\Pi}^{(2)}_{\alpha\beta}(q, \xi_Q = 1)$, shown in Fig. 20, keeping track of the terms that are left over. In doing so we only need to carry out algebraic manipulations in the numerators of individual Feynman diagrams, and use judiciously the identity of Eq. (2.71). Again, no integrations over virtual momenta need be carried out, except for identifying vanishing contributions by means of the formulas listed in Eqs (6.1), (6.1) and (6.1). It turns out that all terms left over after this diagram-by-diagram conversion cancel exactly against the terms $[\Pi^{(2)}_{\mathrm{P}\alpha\beta}(q) - R^{(2)}_{\mathrm{P}\alpha\beta}(q)]$, finally furnishing the crucial equality of Eq. (6.21).

Since we have used dimensional regularization throughout, and no integrations have been
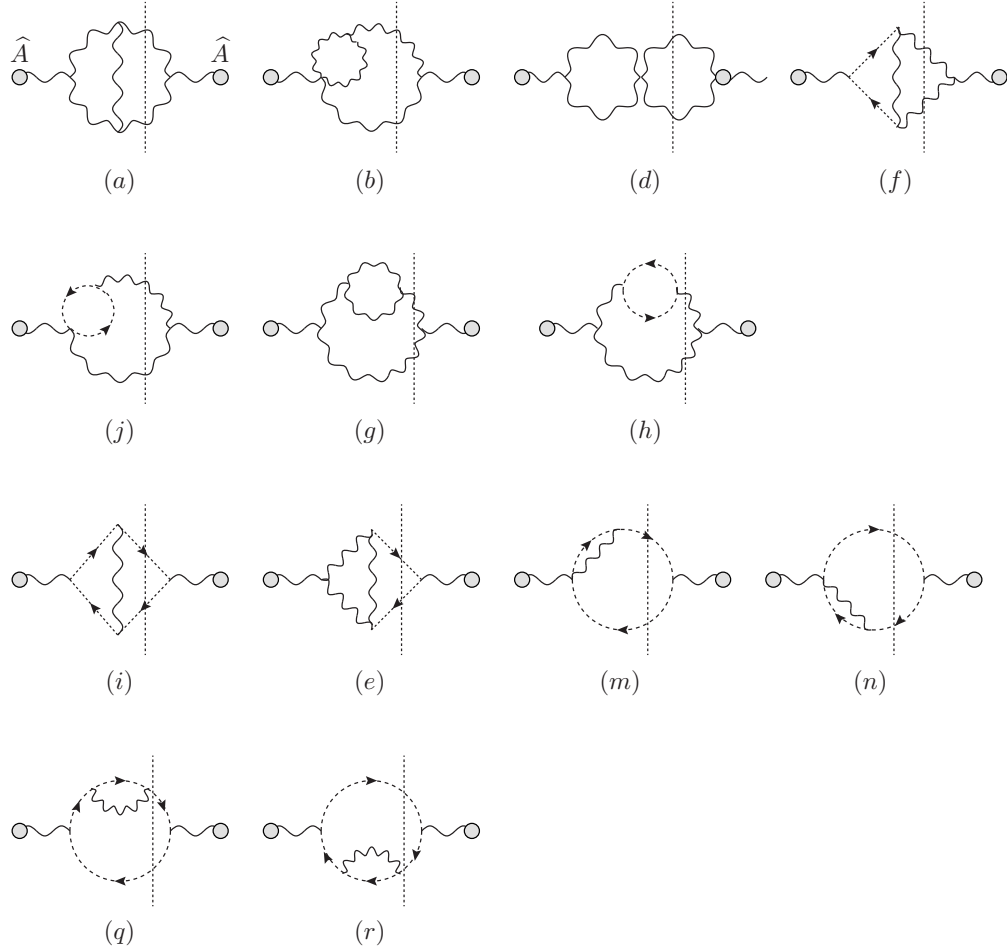
150

Fig. 53. The two-particle Cutkosky cuts of the PT (and BFG) two-loop gluon self-energy. We have used the same labeling of individual diagrams as in Fig. 20. The two upper (lower) rows show graphs where two gluon (ghost) lines have been cut.

performed, the results of this section do not depend on the value d of the space-time; in particular they are valid for $d = 3$, which is of additional field-theoretical interest [162–164]. Clearly, when $d \to 4$ the renormalization program should also be carried out (for details see [161]).

6.1.3 The two-loop absorptive construction

We now turn to the absorptive two-loop construction. Operationally the situation is significantly more involved compared to the one-loop case; the full details have been presented in [161]. Here we will give a brief qualitative description of how this construction proceeds.

The central result is that the strong version of the OT, given in (2.126), holds also for the two-loop case. Specifically, the imaginary parts of the two-loop PT Green's functions (under construction) are related by the OT to precisely identifiable and very special parts of two different squared amplitudes, namely the one-loop squared amplitude for the process $q\bar{q} \to gg$ and the tree-level squared amplitude for the process $q\bar{q} \to ggg$. For example, the two-particle Cutkosky cuts of the two-loop PT self-energy, Fig. 53, are related to the propagator-like part of the PT-rearranged one-loop squared amplitude for $q\bar{q} \to gg$, Fig. 54, while, at the same time,

151

the three-particle Cutkosky cuts of the same quantity, Fig. 55, are related to the s-channel part of the PT-rearranged tree-level squared amplitude for $q\bar{q} \to ggg$ (Fig. 56). The same holds for vertex- and box-like contributions. The aforementioned PT-rearranged squared amplitudes are to be constructed in a way exactly analogous to the PT-rearranged tree-level $q\bar{q} \to gg$ squared amplitude.

In order to get a firmer understanding of the above statements, let us consider the OT for the forward scattering process $q(p_1)\bar{q}(p_2) \to q(p_1)\bar{q}(p_2)$ at two loops. We have that

$$\Im m \langle q\bar{q}|T^{[6]}|q\bar{q}\rangle = \frac{1}{2}\left(\frac{1}{3!}\right)\int_{\mathrm{PS}_{3g}} \langle ggg|T^{[2]}|q\bar{q}\rangle^* \langle ggg|T^{[2]}|q\bar{q}\rangle$$
$$+ \frac{1}{2}\left(\frac{1}{2!}\right)\int_{\mathrm{PS}_{2g}} 2\,\Re e\left(\langle gg|T^{[4]}|q\bar{q}\rangle^* \langle gg|T^{[2]}|q\bar{q}\rangle\right), \tag{6.22}$$

where $\int_{\mathrm{PS}_{2g}}$ and $\int_{\mathrm{PS}_{3g}}$ stand for the two- and three-body phase-space for massless gluons, respectively. The superscripts $[n]$ denotes the order of the corresponding amplitude in the coupling constant g; when counting powers of g remember the couplings from hooking up the external particles. The lhs of (6.22) can be obtained by carrying out all possible Cutkosky cuts on the two-loop diagrams contributing to the process $q(p_1)\bar{q}(p_2) \to q(p_1)\bar{q}(p_2)$. Specifically, one must sum the contributions of both two-particle and three-particle cuts; the cuts involve gluons and ghosts. Equivalently, on the rhs one has intermediate physical process involving two and three gluons [$q\bar{q} \to gg$ and $q\bar{q} \to ggg$]; as usual one averages over the initial state polarizations and sums over the final state polarizations.

Let us now assume that the amplitude $q(p_1)\bar{q}(p_2) \to q(p_1)\bar{q}(p_2)$ has been cast in its PT form, as described in the previous subsection. That means that the subamplitudes $\widehat{T}_\ell^{[6]}$ have been constructed, where $\ell = 1, 2, 3$ denotes (as in the one-loop case) the propagator-like subamplitudes ($\ell = 1$), the vertex-like subamplitudes ($\ell = 2$), and the box-like ones ($\ell = 3$). Thus $\widehat{T}_1^{[6]}$ is composed of the two-loop PT gluon self-energy $\widehat{\Pi}_{\alpha\beta}^{(2)}(q)$, $\widehat{T}_2^{[6]}$ of the two-loop PT vertex $\widehat{\Gamma}_\alpha^{(2)}(p_1, p_2)$ (and its mirror), and $\widehat{T}_3^{[6]}$ of the two-loop PT box (which coincides with the regular two-loop box in the Feynman gauge).

Then, one can show that

$$\Im m \langle q\bar{q}|\widehat{T}_\ell^{[6]}|q\bar{q}\rangle = \frac{1}{2}\left(\frac{1}{3!}\right)\int_{\mathrm{PS}_{3g}} [\langle ggg|\widehat{T}^{[2]}|q\bar{q}\rangle^* \langle ggg|\widehat{T}^{[2]}|q\bar{q}\rangle]_\ell$$
$$+ \frac{1}{2}\left(\frac{1}{2!}\right)\int_{\mathrm{PS}_{2g}} 2\,\Re e\left(\langle gg|\widehat{T}^{[4]}|q\bar{q}\rangle^* \langle gg|\widehat{T}^{[2]}|q\bar{q}\rangle\right)_\ell. \tag{6.23}$$

Lets us now see how one constructs the "PT-rearranged" squared amplitudes appearing on the rhs of (6.23); the construction is identical to what we did in the one-loop case, but is sufficiently more complicated at the technical level to merit some additional clarifying remarks.

A PT-rearranged squared amplitude means the following. Consider a normal squared amplitude, i.e. the product of two regular amplitudes [remember that "product" means that they are also connected (multiplied) by the corresponding polarization tensors]. Then each amplitude must be first cast into its PT form; this is done following simply the PT rules for converting
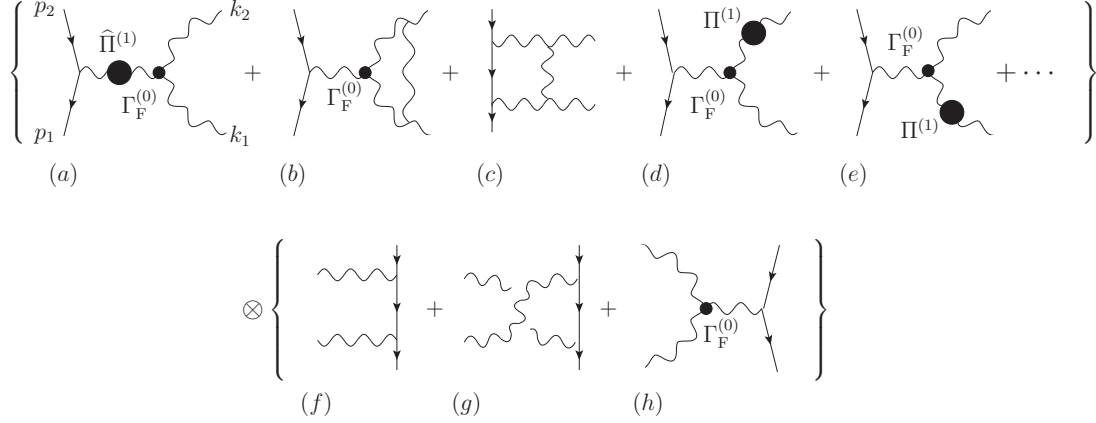
Fig. 54. The product of the PT-rearranged amplitudes of the process $q\bar{q} \rightarrow q\bar{q}$ at one-loop (up) and tree-level (down). The longitudinal momenta from the polarization tensors will produce additional cancellations between s-channel and t-channel graphs furnishing finally the first term on the rhs of Eq. (6.22).

a on-shell amplitude into its PT form. However, this is not the end of the story as far as the PT-rearrangement of the square is concerned. One must go through the additional exercise of letting the longitudinal momenta coming from the polarization vectors trigger the s-t cancellation at that order. That will identify the genuine propagator-like piece of the entire product.

The reader should recognize that this is exactly the procedure followed in the one-loop absorptive construction of Section 2 for arriving at the $\widehat{\mathcal{M}}_\ell$. First, the tree-level amplitude $\mathcal{T}_s$ was converted into $\mathcal{T}_s^F$; this is the conversion of $\mathcal{T}_s$ into its PT form. This was done simply by carrying out the PT decomposition of (2.38) to the only available three-gluon vertex; note that this vertex has a preferred momentum (q) (employing the terminology introduce in this chapter, it is "external"), because the momenta of the other two legs are integrated over all available phase-space. Then, the longitudinal momenta from the polarization tensors were used to trigger the s-t cancellation, which, in turn, furnished the three $\widehat{\mathcal{M}}_\ell$.

For the two-loop case at hand this procedure must be applied for both squared amplitudes appearing on the rhs of (6.23). For $\langle ggg|\widehat{T}^{[2]}|q\bar{q}\rangle^* \langle ggg|\widehat{T}^{[2]}|q\bar{q}\rangle$ we cast the tree-level process $q(p_1)\bar{q}(p_2) \rightarrow g(k_1)g(k_2)g(k_3)$ into its PT form. This means to carry out (2.38) only to the three-gluon vertices shown in Fig. 56; all other vertices are internal, because they are irrigated by momenta (the k_i) that are being integrated over in $\int_{\mathrm{PS}_{3g}}$. It turns out that the Γ^P parts cancel completely, as expected; this takes some algebra to demonstrate. Then, the longitudinal momenta (k_1^μ, $k_1^{\mu'}$, k_2^ν, $k_2^{\nu'}$, k_3^ρ, $k_3^{\rho'}$) contained in the three polarization tensors will act, giving rise to the s-t cancellations corresponding to this particular process; its realization is operationally more complicated, but otherwise completely analogous to the one showed in Section 2. For $\langle gg|\widehat{T}^{[4]}|q\bar{q}\rangle^* \langle gg|\widehat{T}^{[2]}|q\bar{q}\rangle$ things are more involved. Now the amplitude $q(p_1)\bar{q}(p_2) \rightarrow g(k_1)g(k_2)$ must be cast into its PT form both at tree-level [for $\langle gg|\widehat{T}^{[2]}|q\bar{q}\rangle$], and at one-loop [for $\langle gg|\widehat{T}^{[4]}|q\bar{q}\rangle^*$]. The tree-level PT amplitude is, of course, known from the absorptive construction of subsection 2.5. The construction of the one-loop PT amplitude $q(p_1)\bar{q}(p_2) \rightarrow g(k_1)g(k_2)$ has been described in great detail in the literature [63,165]. In fact, as mentioned in subsection 2.4.3, this process was the first explicit example [63] where the universality (process-independence) of the PT gluon self-energy was explicitly demonstrated; the end result is shown
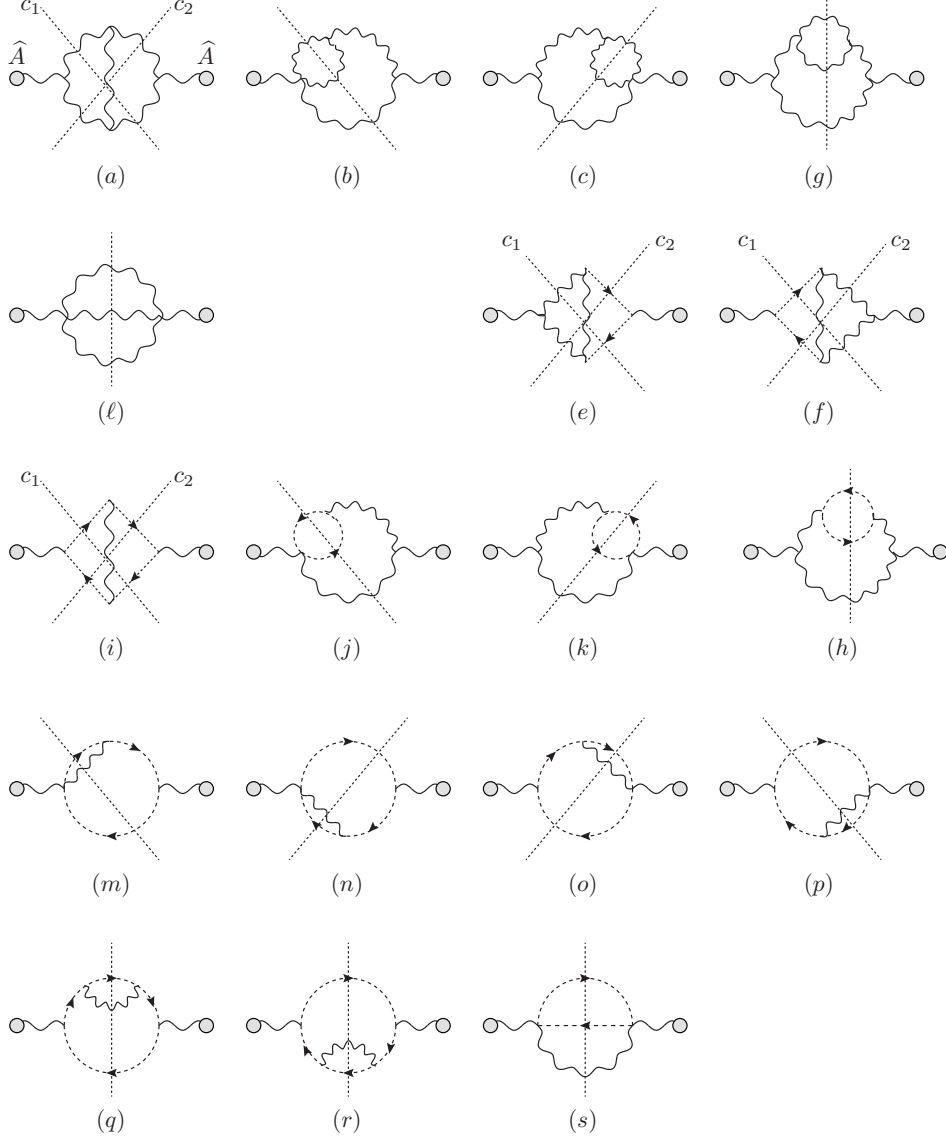
Fig. 55. The three-particle Cutkosky cuts of the PT two-loop gluon self-energy. The first five graphs have three-gluon cuts, the next two have two-gluon–one-ghost cuts, while the remaining ones have one-gluon-on-two-ghost cuts.

in Fig. 54. As we see there, the procedure of the PT rearrangement leads to the appearance of $\widehat{\Pi}(q)$ and the conversion of the conventional one-loop three-gluon vertex $\Gamma^{(1)}_{\alpha\mu\nu}(q, k_1, k_2)$ into $\Gamma^{(1)}_{F\,\alpha\mu\nu}(q, k_1, k_2)$, which is the BFG three-gluon vertex at one-loop, with one background gluon (q) and two quantum ones (k_1, k_2). It is straightforward to show that $\Gamma^{(1)}_{F\,\alpha\mu\nu}(q, k_1, k_2)$ satisfies the following WI

$$q^{\alpha}\Gamma^{(1)}_{F\,\alpha\mu\nu}(q, k_1, k_2) = \Pi^{(1)}_{\mu\nu}(k_1) - \Pi^{(1)}_{\mu\nu}(k_2), \tag{6.24}$$

which is the exact one-loop analogue of the tree-level WI of Eq. (2.40); indeed the rhs is the difference of two one-loop self-energies computed in the conventional Feynman gauge. Then, one must let the longitudinal momenta in the polarization tensors trigger the corresponding s-t cancellation. When they hit on $\langle gg|\widehat{T}^{[2]}|q\bar{q}\rangle$ they will simply trigger the prototype tree-level
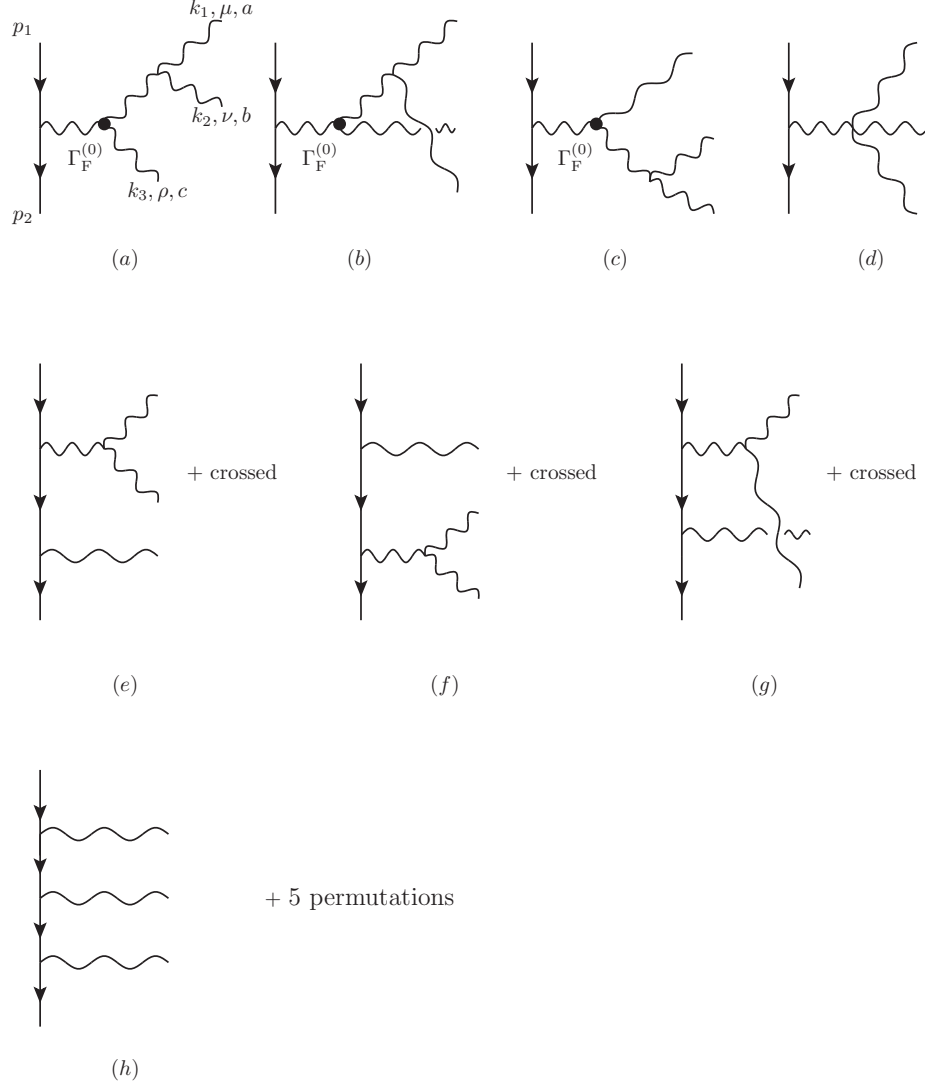
154

Fig. 56. The tree-level graphs contributing to the process $q(p_1)\bar{q}(p_2) \to g(k_1)g(k_2)g(k_3)$, after the PT rearrangement. The momenta k_i are to be integrated over in the three-body phase-space integral.

s-t cancellation of Section 2; but when they hit on $\langle gg|\widehat{T}^{[4]}|q\bar{q}\rangle^*$ they will trigger the *one-loop* version of the same s-t cancellation [43,161]. To demonstrate this latter cancellation one needs to know the result of the action of the longitudinal momenta k_1^μ and k_2^ν on $\Gamma^{(1)}_{F\,\alpha\mu\nu}(q,k_1,k_2)$, exactly as happened in the tree-level construction, see Eq.(2.140). Given that these momenta correspond to quantum fields (as opposed to the q^α, which corresponds to a background field) the result of their contraction with $\Gamma^{(1)}_{F\,\alpha\mu\nu}(q,k_1,k_2)$ is not a WI, as in (6.24), but rather an STI, which is given in Eq.(C.30).

The reader should appreciate at this point that any rearrangement of the (internal) vertices of two-loop box-diagrams cannot be reconciled with the arguments of the simultaneous two- and three-particle Cutkosky cuts presented here. To see this with an example, let us return to the two representative two-loop diagrams of Fig. 47. After their PT rearrangement, the two-particle Cutkosky cut on (a), denoted by (c_2) in Fig. 47, must reproduce $(c) \otimes [(f) + (g)]$ in Fig. 54, and cut (c_4) on (b) must reproduce $(b) \otimes [(f) + (g)]$. Obviously, if we were to modify the
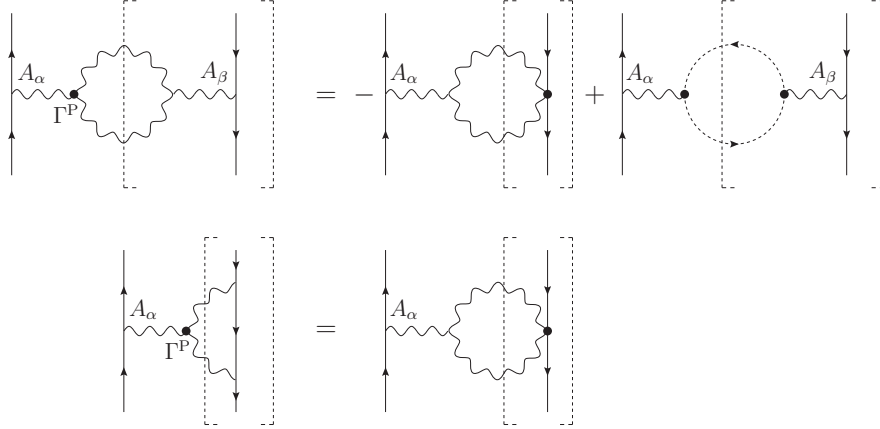
155

Fig. 57. The one-loop PT algorithm seen in terms of the fundamental s-t cancellation. The self-energy like contribution coming from the vertex is exactly canceled by the one coming from the propagator. Notice that none of the vertices appearing in the rhs of the above diagrammatic identities is an elementary vertex of the theory, they are all *unphysical* vertices.

internal three-gluon vertices of (a) or (b) in Fig. 47 in any way, this identification would not work: one must modify *only* the vertex injected with q (turning it to Γ^{F}). This argument may be generalized to include all remaining two-particle and three-particle cuts, making the above conclusion completely airtight.

We emphasize that the arguments presented here do not postulate at any point the existence of any relation between the PT and the BFM. On the other hand, in hindsight, all conclusions drawn are in complete agreement with the known PT/BFM correspondence. Specifically, switching now to the BFM language, the fact that internal vertices should not be touched is precisely what the BFM Feynman rules dictate: since one cannot have background fields propagating inside loops, all internal vertices have three *quantum* gluons merging.

Let us finally comment on an additional point. The philosophy of this subsection has been to establish that the two-loop PT Green's functions, constructed explicitly in the previous subsection, satisfy the strong version of the OT. Evidently, one could adopt an alternative approach, and consider the absorptive formulation as the defining construction for the PT Green's functions. Thus, one can start from the rhs of the OT, carry out the same analysis that we did here, and postulate that the sum of the propagator-like parts of the rhs furnish the imaginary part of the (now unknown) two-loop gluon self-energy on the lhs, and similarly for vertices and boxes. Then, the real parts would have to be reconstructed from the corresponding dispersion relation, in the spirit of subsection 2.5. The advantage of this strategy is that all the PT-rearranged (squared) amplitudes appearing on the rhs are at least one loop lower than the amplitude on the lhs. Therefore, one can actually reconstruct the lhs, by working directly on the rhs, because one knows already how to pinch at lower orders. Of course, the downside is that, in order to obtain the final answer, one would have to carry out complicated phase-space and dispersion integrations.
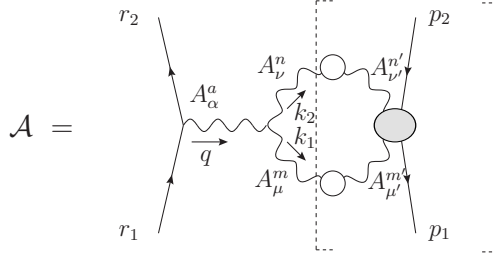
Fig. 58. The fundamental amplitude receiving the action of the longitudinal momenta stemming from Γ^{P}. The gray blob represent the (connected) kernel corresponding to the process $AA \to q\bar{q}$.

6.2 The PT to all orders in perturbation theory

The two-loop construction of the PT quark-gluon vertex and gluon propagator outlined in the previous subsections follows to the letter the one-loop recipe: we have tracked down the rearrangements induced to individual Feynman diagrams when the longitudinal pinching momenta acting on their bare vertices trigger elementary WIs. Clearly such a method does not lend itself to an all-order generalization; realistically speaking, the two-loop construction is as far as one can push this diagrammatic procedure.

In order to generalize the PT to higher orders one must find an expeditious way of enforcing the crucial cancellations without manipulating individual diagrams, but, instead, through the collective treatment of entire sets of diagrams. It turns out that such a breakthrough is indeed possible [44,166]: the PT algorithm can be successfully generalized to *all orders* in perturbation theory through the judicious use of the STI satisfied by a special Green's function, which serves as a common kernel to all higher order self-energy and vertex diagrams.

In fact, as was first realized in [44,166], the one- and two-loop PT rearrangements are but lower-order manifestations of a fundamental cancellation, taking place between graphs of distinct kinematic nature when computing the divergence of the four-point function $AAq\bar{q}$ (with the gluons off-shell, and the quarks on-shell). At tree-level, this is nothing else than the "s-t cancellation" that we already encountered in the absorptive PT construction of Section 2 and 4. As for the one-loop PT rearrangement, it is actually encoded in the two graphs of Fig. 57: both graphs have the Γ^{P} terms in common, while their terms shown in dotted brackets are the tree-level t- and s-channel contributions, respectively, to the four-particle amplitude $AA \to q\bar{q}$. Dressing the above amplitude with higher order corrections, and exploiting its STI, will eventually provide a compact way of generalizing the PT to all orders.

6.2.1 The four-point kernel $AAq\bar{q}$ and its Slavnov-Taylor identity

With this intention in mind, of all the diagrams contributing to the QCD amplitude under consideration we will focus on the subset that will receive the action of the longitudinal momenta stemming from Γ^{P}, to be denoted by $\mathcal{A}$. It is given by (see Fig. 58)
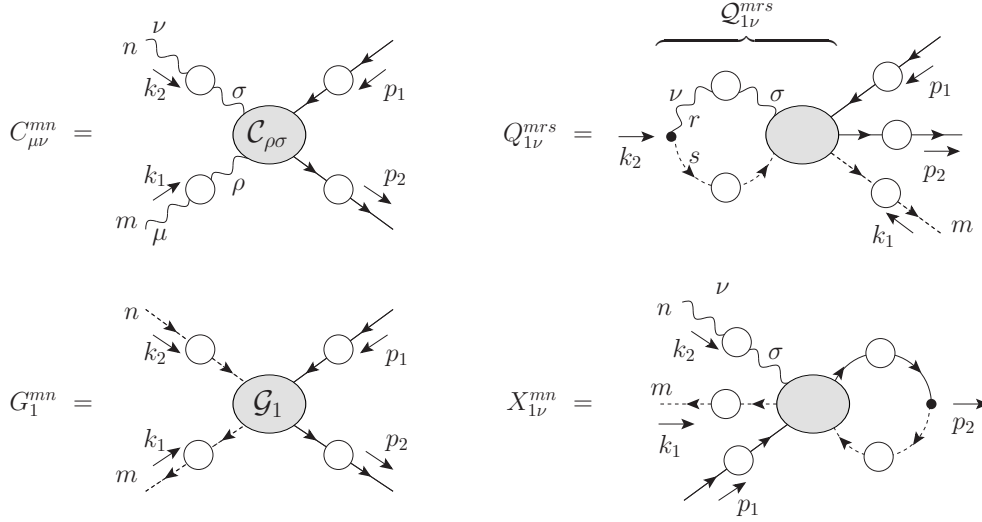
Fig. 59. Diagrammatic representation of the Greens functions appearing in the Slavnov-Taylor identity (6.27). The function $\bar{X}_{1\nu}^{mn}$ (which coincides with $X_{1\nu}^{mn}$ when the fermion arrows reversed) is not shown.

$$\mathcal{A}(r_1, -r_2, p_2, -p_1) = \bar{u}(r_2) g \gamma_\alpha t^a u(r_1) \frac{-i}{q^2} \int_{k_1} i\Gamma_{\alpha\mu'\nu'}^{am'n'}(q, -k_1, -k_2) \mathcal{T}_{mn}^{\mu\nu}(k_1, k_2, p_2, -p_1),$$

$$\mathcal{T}_{mn}^{\mu\nu}(k_1, k_2, p_2, -p_1) = \bar{u}(p_1) \left[i\Delta_{mm'}^{\mu\mu'}(k_1) i\Delta_{nn}^{\nu\nu'}(k_2) \mathcal{C}_{\mu'\nu'}^{m'n'}(k_1, k_2, p_2, -p_1) \right] u(p_2). \tag{6.25}$$

From the definition above we clearly see that $\mathcal{T}$ is the subamplitude $AA \to q\bar{q}$ with the gluon off-shell and the fermions on-shell. The next step is to carry out the usual PT vertex decomposition on the three-gluon vertex $\Gamma_{\alpha\mu'\nu'}^{am'n'}$ appearing inside the integrand on the rhs of (6.25), and concentrate on the action of its Γ^{P} part on the amplitude $\mathcal{T}$. Therefore, we need to determine the STI satisfied by the amplitude $\mathcal{T}$ of Eq. (6.25).

In order to get this STI, one starts from the trivial identity in configuration space (valid due to ghost charge conservation)

$$\langle T[\bar{c}^m(x) A_\nu^n(y) q(z) \bar{q}(w)] \rangle = 0, \tag{6.26}$$

where T denotes the time-ordered product of fields. By rewriting the fields in terms of their BRST transformed counterparts, using the equations of motions and the equal time commutation relations [62], and, finally, Fourier transforming the result to momentum space, one arrives at the following identity

$$k_1^\mu C_{\mu\nu}^{mn} = k_{2\nu} G_1^{mn} - ig f^{nrs} Q_{1\nu}^{mrs} + g X_{1\nu}^{mn} + g \bar{X}_{1\nu}^{mn}. \tag{6.27}$$

The various Green's functions that appears in the rhs of the equation above are shown in Fig. 59. The terms $X_{1\nu}$ and $\bar{X}_{1\nu}$ correspond to contributions that vanish when the external quarks are assumed to be on-shell, since they are missing one full quark propagator; at lowest order they are simply the terms proportional to the inverse tree-level propagators $(\not{p}_1 - m)$ and $(\not{p}_2 - m)$ appearing in the PT calculations. Indeed, if we multiply both sides of Eq. (6.27) by the product $S^{-1}(p_2) S^{-1}(-p_1)$ of the two inverse propagators of the external quarks, and then sandwich the resulting amplitude between the on-shell spinors $\bar{u}(p_1)$ and $u(p_2)$, the vanishing of the
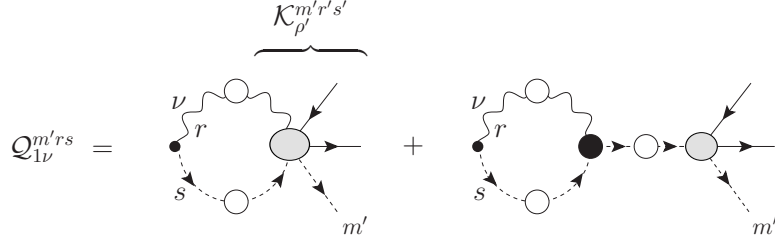
Fig. 60. Definition of the momentum space auxiliary function $\mathcal{Q}_{1\nu}^{m'rs}$. Gray blobs represent connected kernels, while black (respectively white) blobs represent 1PI (respectively connected) n-point Green's functions. Notice that the kernel $\mathcal{K}_{\rho'}^{m'r's'}$ is 1PI with respect to s-channel cuts.

aforementioned terms follows by virtue of the (all-order) Dirac equation. Thus we arrive at the on-shell STI

$$
\begin{aligned}
k_1^\mu \mathcal{T}_{\mu\nu}^{mn}(k_1, k_2, p_2, -p_1) &= \mathcal{S}_{1\nu}^{mn}(k_1, k_2, p_2, -p_1), \\
\mathcal{S}_{1\nu}^{mn}(k_1, k_2, p_2, -p_1) &= \bar{u}(p_2) \left[k_{2\nu} iD^{mm'}(k_1) iD^{nn'}(k_2) \mathcal{G}_1^{m'n'}(k_1, k_2, p_2, -p_1) \right. \\
&\quad \left. - ig f^{nrs} iD^{mm'}(k_1) \mathcal{Q}_{1\nu}^{m'rs}(k_1, k_2, p_2, -p_1) \right] u(p_2),
\end{aligned}
\tag{6.28}
$$

where the auxiliary function $\mathcal{Q}_{1\nu}^{m'rs}$ is shown in Fig. 60. A similar (Bose-symmetric) relation will hold when hitting the kernel with the k_2 momentum.

6.2.2 The fundamental all-order s-t cancellation

Having established the STIs of Eq. (6.28), we now turn to the main conceptual point related to the all orders PT construction. The basic observation is the following. In perturbation theory the quantities $\mathcal{T}_{\mu\nu}^{mn}$, $\mathcal{S}_{1\nu}^{mn}$, and $\mathcal{S}_{2\mu}^{mn}$ are given by Feynman diagrams, which can be separated into distinct classes, depending on their kinematic dependence (s/t separation) and their geometrical properties (1PI/1PR separation). We recall that s graphs are those which do not contain information about the kinematic details of the incoming test-quarks (self-energy graphs), whereas t graphs are those that depend also on the mass of the test quarks (vertex graphs). Thus, the Feynman graphs allow the following separation (see also Fig. 61, where we show the decomposition below at an arbitrary perturbative order n)

$$
\begin{aligned}
\mathcal{T}_{\mu\nu}^{mn} &= [\mathcal{T}_{\mu\nu}^{mn}]_{s,\mathrm{I}} + [\mathcal{T}_{\mu\nu}^{mn}]_{s,\mathrm{R}} + [\mathcal{T}_{\mu\nu}^{mn}]_{t,\mathrm{I}} + [\mathcal{T}_{\mu\nu}^{mn}]_{t,\mathrm{R}}, \\
\mathcal{S}_{1\nu}^{mn} &= [\mathcal{S}_{1\nu}^{mn}]_{s,\mathrm{I}} + [\mathcal{S}_{1\nu}^{mn}]_{s,\mathrm{R}} + [\mathcal{S}_{1\nu}^{mn}]_{t,\mathrm{I}} + [\mathcal{S}_{1\nu}^{mn}]_{t,\mathrm{R}},
\end{aligned}
\tag{6.29}
$$

On the other hand, we know by now that the action of the (longitudinal) momenta k_1^μ or k_2^ν on $\mathcal{T}_{\mu\nu}^{mn}$ does not respect, in general, the above separation; their action mixes propagator- with vertex-like terms, since the latter generate (through pinching) effectively propagator-like terms. Similarly, the separation between 1PI and 1PR terms is no longer unambiguous, since 1PR diagrams are converted (again through pinching) into effectively 1PI ones (the opposite cannot happen). An early example of this effect appeared in the construction of the PT three-gluon
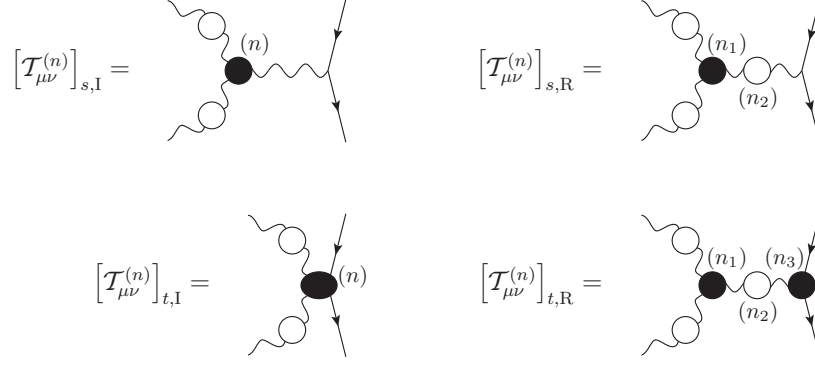
$$\left[\mathcal{T}_{\mu\nu}^{(n)}\right]_{s,\mathrm{I}} = \qquad\qquad \left[\mathcal{T}_{\mu\nu}^{(n)}\right]_{s,\mathrm{R}} =$$

$$\left[\mathcal{T}_{\mu\nu}^{(n)}\right]_{t,\mathrm{I}} = \qquad\qquad \left[\mathcal{T}_{\mu\nu}^{(n)}\right]_{t,\mathrm{R}} =$$

Fig. 61. Decomposition at an arbitrary perturbative level n of the fundamental amplitude $\mathcal{T}_{\mu\nu}^{mn}$ in terms of s and t channel, 1PI and 1PR components.

vertex in Section 2, and was encountered again in subsection 6.1.1.

Therefore, even though Eq (6.28) holds for the entire amplitude $\mathcal{T}_{\mu\nu}^{mn}$, it is not true for the individual subamplitudes defined in Eqs (6.29), *i.e.*, we have

$$k_1^\mu [\mathcal{T}_{\mu\nu}^{mn}]_{x,\mathrm{Y}} \neq [\mathcal{S}_{1\nu}^{mn}]_{x,\mathrm{Y}}, \qquad x = s, t; \ \mathrm{Y} = \mathrm{I}, \mathrm{R}, \tag{6.30}$$

where I (respectively R) indicates the one-particle *irreducible* (respectively *reducible*) parts of the amplitude involved. The reason for this inequality are precisely the propagator-like terms, such as those found in the one- and two-loop calculations (see Fig. 62). One should notice that the situation is exactly analogous to that encountered when studying the OT, which holds at the level of the full amplitude but not at the level of individual subamplitudes.

In particular, for individual subamplitudes we have that

$$k_1^\mu [\mathcal{T}_{\mu\nu}^{mn}]_{s,\mathrm{R}} = [\mathcal{S}_{1\nu}^{mn}]_{s,\mathrm{R}} + [\mathcal{R}_{1\nu}^{mn}]_{s,\mathrm{I}}^{\mathrm{int}},$$
$$k_1^\mu [\mathcal{T}_{\mu\nu}^{mn}]_{s,\mathrm{I}} = [\mathcal{S}_{1\nu}^{mn}]_{s,\mathrm{I}} - [\mathcal{R}_{1\nu}^{mn}]_{s,\mathrm{I}}^{\mathrm{int}} + [\mathcal{R}_{1\nu}^{mn}]_{s,\mathrm{I}}^{\mathrm{ext}},$$
$$k_1^\mu [\mathcal{T}_{\mu\nu}^{mn}]_{t,\mathrm{R}} = [\mathcal{S}_{1\nu}^{mn}]_{t,\mathrm{R}} + [\mathcal{R}_{1\nu}^{mn}]_{t,\mathrm{I}}^{\mathrm{int}},$$
$$k_1^\mu [\mathcal{T}_{\mu\nu}^{mn}]_{t,\mathrm{I}} = [\mathcal{S}_{1\nu}^{mn}]_{t,\mathrm{I}} - [\mathcal{R}_{1\nu}^{mn}]_{t,\mathrm{I}}^{\mathrm{int}} - [\mathcal{R}_{1\nu}^{mn}]_{s,\mathrm{I}}^{\mathrm{ext}}, \tag{6.31}$$

with similar equations holding when acting with the momentum k_2^ν. In the above equations the superscript "ext" and "int" stands for "external" and "internal" respectively, and refers to whether or not the pinching part of the diagram at hand has touched the external on-shell fermion legs. At order n, some example of the $\mathcal{R}^{(n)}$ terms introduced in the equations above are shown in Fig. 63. The structure of the $[\mathcal{R}_{1\nu}^{mn}]_{s,\mathrm{Y}}$ terms is very characteristic: kinematically they only depend on s; whereas this is obviously true for the first two equations of (6.31) (since these terms originate from the action of k_1^μ on an s-dependent piece $[\mathcal{T}_{\mu\nu}^{mn}]_{s,\mathrm{Y}}$), it is far less obvious for those appearing in the last two equations of (6.31), since they stem from the action of k_1^μ on a t-dependent term $[\mathcal{T}_{\mu\nu}^{mn}]_{t,\mathrm{Y}}$. In addition, all the $\mathcal{R}$ terms share a common feature, *i.e.*, they *cannot* be written in terms of conventional Feynman rules; instead they are built out of unphysical vertices, which do not correspond to any term in the original Lagrangian. It should be clear by now that the $\mathcal{R}$ terms are precisely the terms that cancel against each other when we carry out the PT procedure *diagrammatically*.
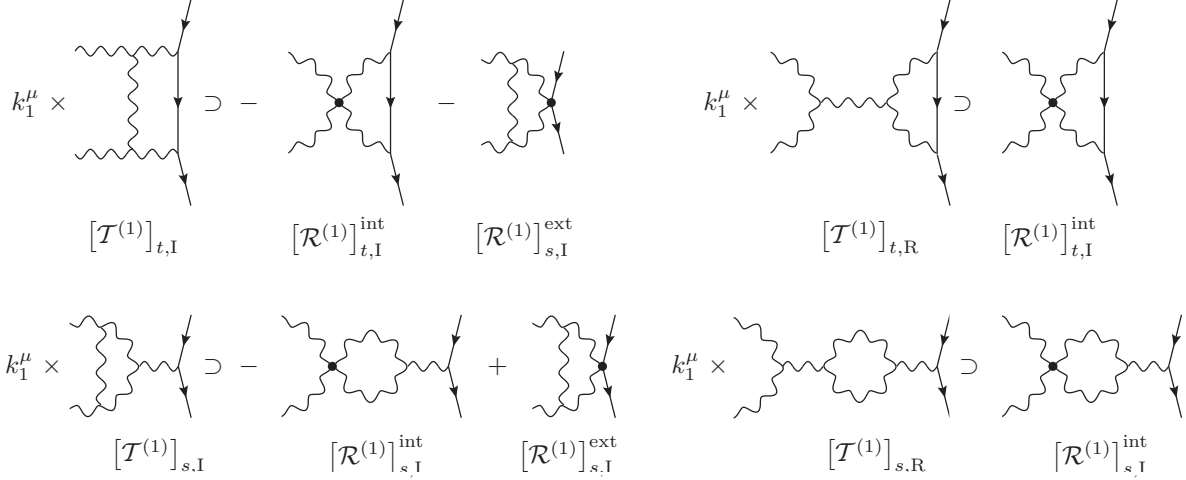
160

Fig. 62. Some two-loop examples of the $\mathcal{R}$ terms, together with the Feynman diagrams from which they originate.

Thus, after the PT cancellations have been enforced, we find that for the 1PI t-channel part of the amplitude we have the equality

$$[k_1^\mu \mathcal{T}_{\mu\nu}^{mn}]_{t,\mathrm{I}}^{\mathrm{PT}} = [\mathcal{S}_{1\nu}^{mn}]_{t,\mathrm{I}}, \qquad (6.32)$$

What is crucial in the above result is that it automatically takes care of both the s-t as well as the 1PR and 1PI cancellations of the $\mathcal{R}$ terms, which is characteristic of the PT, without having to actually trace them down. Thus, on hindsight, the PT algorithm as applied *e.g.*, in Section 2 and 4, and even in the two-loop generalization carried out in the initial part of this section, has amounted to enforcing diagram-by-diagram the vast, BRST-driven s-t channel cancellations, without making explicit use of the all-order STIs. Evidently, tracing down the action of the longitudinal momenta and the resulting exchanges between vertex and self-energy graphs, is equivalent to deriving (loop-by-loop) Eq. (6.32). Therefore, the non-trivial step for generalizing the PT to all orders is to recognize that the result obtained after the implementation of the PT algorithm on the lhs of Eq. (6.32) is already encoded on the rhs! Indeed, the rhs involves only conventional (ghost) Green's functions, expressed in terms of normal Feynman rules, with no reference to unphysical vertices.

This last point merits some additional comments. It should be clear that no pinching is possible when looking at the t-channel irreducible part of the rhs of Eq. (6.28). So, if we were to enforce the PT cancellations on both sides of the t irreducible part of these equations, on the rhs there would be nothing to pinch (all the vertices are internal), and therefore, there would be no unphysical vertices generated. Therefore, on the lhs, where pinching is possible, all contributions containing unphysical vertices must cancel. The only way to distort this equality is to violate the PT rules, allowing, for example, the generation of additional longitudinal momenta by carrying out sub-integrations, or by decomposing internal vertices. Violating these rules, however, will result in undesirable consequences: in the first case the appearance of terms of the form $q \cdot k$ in the denominators will interfere with the manifest analyticity of the PT Green's functions constructed, whereas, in the second, the special unitarity properties of the PT Green's functions will be inevitably compromised.
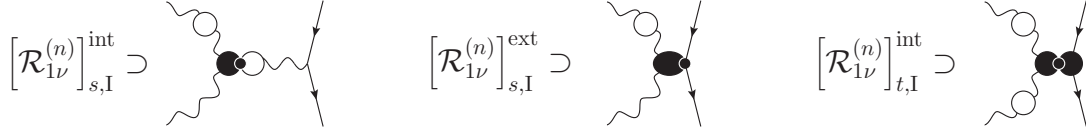
161

Fig. 63. Examples of the generic structures included in the $\mathcal{R}$ terms. A black dot indicates that a propagator has been removed through pinching.

6.2.3 The PT to all orders: the quark-gluon vertex and the gluon propagator

The considerations just presented can be used in order to accomplish in a rather compact form the all-order generalization of the PT construction.

To begin with, it is immediate to recognize that, in the R_ξ Feynman gauge (RFG for short), box diagrams of arbitrary order n, to be denoted by $B^{(n)}$, coincide with the PT boxes $\widehat{B}^{(n)}$, since all three-gluon vertices are "internal", *i.e.*, they do not provide longitudinal momenta. Thus, they coincide with the BFG boxes, $\tilde{B}^{(n)}$, *i.e.*,

$$\widehat{B}^{(n)} = B^{(n)} = \tilde{B}^{(n)} \tag{6.33}$$

for every n. The same is true for the PT quark self-energies; for exactly the same reason, they coincide with their RFG (and BFG) counterparts, *i.e.*,

$$\widehat{\Sigma}^{ij\,(n)} = \Sigma^{ij\,(n)} = \tilde{\Sigma}^{ij\,(n)}. \tag{6.34}$$

The next step will be the construction of the all-order PT quark-gluon 1PI vertex $\widehat{\Gamma}_\alpha^a$. Now, of all the diagrams that contribute to this vertex in the RFG (shown in Fig. 64), the only one receiving the action of the longitudinal pinching momenta is diagram (a); in fact, we know from the two-loop construction that (in the RFG) when the external gluon couples to a diagram through any type of interaction vertex other than a three-gluon vertex, then that diagram is inert, as far as pinching is concerned. Thus, we carry out the PT vertex decomposition of Eq. (2.38) in diagram (a), and concentrate on the Γ^{P} part only; specifically

$$(a)^{\mathrm{P}} = g f^{amn} \int_{k_1} (g_\alpha^\nu k_1^\mu - g_\alpha^\mu k_2^\nu) \left[\mathcal{T}_{\mu\nu}^{mn}(k_1, k_2, p_2, -p_1) \right]_{t,\mathrm{I}}. \tag{6.35}$$

Following the discussion presented in the previous subsection, the pinching action amounts to the replacements

$$k_1^\mu \left[\mathcal{T}_{\mu\nu}^{mn} \right]_{t,\mathrm{I}} \rightarrow \left[k_1^\mu \mathcal{T}_{\mu\nu}^{mn} \right]_{t,\mathrm{I}}^{\mathrm{PT}} = \left[\mathcal{S}_{1\nu}^{mn} \right]_{t,\mathrm{I}},$$

$$k_2^\nu \left[\mathcal{T}_{\mu\nu}^{mn} \right]_{t,\mathrm{I}} \rightarrow \left[k_2^\nu \mathcal{T}_{\mu\nu}^{mn} \right]_{t,\mathrm{I}}^{\mathrm{PT}} = \left[\mathcal{S}_{2\mu}^{mn} \right]_{t,\mathrm{I}}, \tag{6.36}$$

or, equivalently,

$$(a)^{\mathrm{P}} \rightarrow g f^{amn} \int_{k_1} \left\{ [\mathcal{S}_{1\alpha}^{mn}(k_1, k_2)]_{t,\mathrm{I}} - [\mathcal{S}_{2\alpha}^{mn}(k_1, k_2)]_{t,\mathrm{I}} \right\}. \tag{6.37}$$

In the formula above, and in what follows, we indicate only the momenta of the gluons k_i, omitting the momenta of the external fermions p_i.
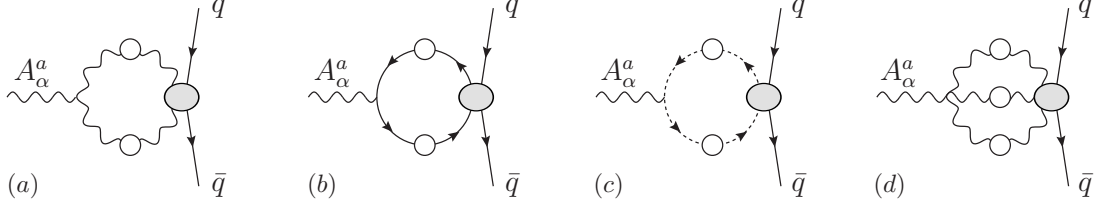
Fig. 64. The Feynman diagrams contributing to the quark-gluon vertex Γ_α^a in the R_ξ gauge. Kernels appearing in these diagrams are t-channel and 1PI. Not shown are the contribution (b') and (c') corresponding to diagrams (b) and (c) with the fermion and ghost arrows reversed.

At this point the construction of the effective PT quark-gluon vertex has been completed, and we have

$$\widehat{\Gamma}_\alpha^a(q, p_2, -p_1) = (a)^{\text{F}} + (b) + (b') + (c) + (c') + (d)$$
$$+ g f^{amn} \int_{k_1} \left\{ [\mathcal{S}_{1\alpha}^{mn}(k_1, k_2)]_{t,\text{I}} - [\mathcal{S}_{2\alpha}^{mn}(k_1, k_2)]_{t,\text{I}} \right\}. \tag{6.38}$$

We emphasize that in the construction presented thus far we have never resorted to the BFM formalism, but have only used the BRST identities of Eq. (6.28), together with (6.32).

The next crucial question will be then to establish the connection between the effective PT vertex and the quark-gluon vertex $\widetilde{\Gamma}_\alpha^a$ written in the BFG. To that end, we start be observing that all the inert terms contained in the original RFG Γ_α^a vertex carry over to the same sub-groups of BFG graphs. In order to facilitate this identification we recall (see also Appendix B) that to lowest order one has the identities $\Gamma^{\text{F}} = \Gamma_{\widehat{A}AA}$, while $\Gamma_{Aq\bar{q}} = \Gamma_{\widehat{A}q\bar{q}}$ and $\Gamma_{AAAA} = \Gamma_{\widehat{A}AAA}$, so that

$$(a)^{\text{F}} = (\widehat{a}), \qquad (b) = (\widehat{b}) \quad (b') = (\widehat{b'}), \qquad (d) = (\widehat{d}), \tag{6.39}$$

where a "hat" on the corresponding diagram means that the (external) gluon A_α^a has been effectively converted into a background gluon $\widehat{A}_\alpha^a$.

As should be familiar by now, the only exception to this rule are the ghost diagrams (d) and (d'), which need to be combined with the remaining terms from the PT construction in order to arrive at (see Fig. 65) both the *symmetric* ghost gluon vertex $\Gamma_{\widehat{A}c\bar{c}}$, characteristic of the BFG, as well as at the four-particle ghost vertex $\Gamma_{\widehat{A}Ac\bar{c}}$, totally absent in the conventional R_ξ diagrams.

Indeed, using Eq. (6.28), we find (omitting the spinors)

$$g f^{amn} \int_{k_1} [\mathcal{S}_{1\alpha}^{mn}(k_1, k_2)]_{t,\text{I}} = -g f^{amn} \int_{k_1} k_{2\alpha} D^{mm'}(k_1) D^{nn'}(k_2) \left[\mathcal{G}_1^{m'n'}(k_1, k_2) \right]_{t,\text{I}}$$
$$+ g^2 f^{amn} f^{nrs} \int_{k_1} D^{mm'}(k_1) \left[\mathcal{Q}_{1\alpha}^{m'rs}(k_1, k_2) \right]_{t,\text{I}}, \tag{6.40}$$

with a similar relation holding for the $\mathcal{S}_2$ term. Then, we find

$$(c) - g f^{amn} \int_{k_1} k_{2\alpha} D^{mm'}(k_1) D^{nn'}(k_2) \left[\mathcal{G}_1^{m'n'}(k_1, k_2) \right]_{t,\text{I}}$$
$$= g f^{amn} \int_{k_1} (k_1 - k_2)_\alpha D^{mm'}(k_1) D^{nn'}(k_2) \left[\mathcal{G}_1^{m'n'}(k_1, k_2) \right]_{t,\text{I}} = (\widehat{c}), \tag{6.41}$$
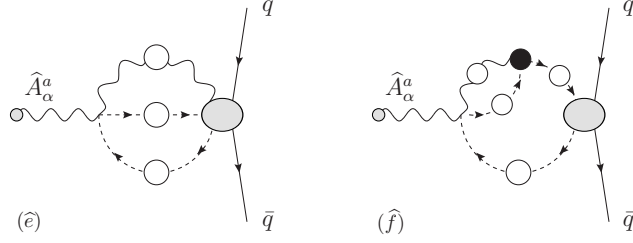
163

Fig. 65. Additional topologies present in the BFM quark-gluon vertex. As before, not shown are two similar contributions (e') and (f') with the ghost arrows reversed.

and, using the decomposition for the $\mathcal{Q}_{1\nu}^{m'rs}$ shown in Fig. 60,

$$
\begin{aligned}
g^2 f^{amn} f^{nrs} & \int_{k_1} D^{mm'}(k_1) \left[\mathcal{Q}_{1\alpha}^{m'rs}(k_1, k_2) \right]_{t,\mathrm{I}} \\
&= ig^2 f^{amn} f^{nrs} g_{\alpha\rho} \int_{k_1}\int_{k_3} D^{mm'}(k_1) D^{ss'}(k_3) \Delta_{rr'}^{\rho\rho'}(k_4) \left\{ \left[\mathcal{K}_{\rho'}^{m'r's'}(k_1, k_3, k_4) \right]_{t,\mathrm{I}} \right. \\
&\quad \left. + i\Gamma_{\rho'}^{gr's'}(-k_2, k_3, k_4) D^{gg'}(k_2) \left[\mathcal{G}_1^{m'g'}(k_1, k_2) \right]_{t,\mathrm{I}} \right\} \\
&= (\widehat{e}) + (\widehat{f}),
\end{aligned}
\tag{6.42}
$$

with $\mathcal{K}_{\sigma'}^{m'r's'}$ representing the 1PI five-particle kernel shown in Fig. 60, while $\Gamma_{\sigma'}^{gr's'}$ is the usual ghost-gluon vertex.

In exactly the same way, the remaining $\mathcal{S}_2$, when added to the R_ξ ghost diagram (c'), will give rise to graphs $(\widehat{c'})$, $(\widehat{e'})$, and $(\widehat{f'})$; so, we finally arrive at the relation

$$
\widehat{\Gamma}_\alpha^a(q, p_2, -p_1) = \widetilde{\Gamma}_\alpha^a(q, p_2, -p_1).
\tag{6.43}
$$

The final step is to construct the all-order PT gluon self-energy $\widehat{\Pi}_{\alpha\beta}^{ab}(q)$. Notice that at this point one would expect that it too coincides with the BFG gluon self-energy $\widetilde{\Pi}_{\alpha\beta}^{ab}(q)$, since both the boxes $\widehat{B}$ and the vertex $\widehat{\Gamma}_\alpha^a$ do coincide with the corresponding BFG boxes $\widetilde{B}$ and vertex $\widetilde{\Gamma}_\alpha^a$, and the S-matrix is unique. We will conclude this Section by furnishing an indirect proof of this statement by means of the "strong induction principle", which states that a given predicate $P(n)$ on $\mathbb{N}$ is true $\forall\, n \in \mathbb{N}$, if $P(k)$ is true whenever $P(j)$ is true $\forall\, j \in \mathbb{N}$ with $j < k$. In order to avoid notational clutter, we will use the schematic notation where all the group, Lorentz, and momentum indices will be suppressed.

At one- and two-loop (*i.e.*, $n = 1, 2$), we know that the result is true from our explicit calculations. Let us then assume that the PT construction has been successfully carried out up to the order $n - 1$ (strong induction hypothesis): we will show then that the PT gluon self-energy is equal to the BFG gluon self-energy at order n, *i.e.*, $\widehat{\Pi}^{(n)} \equiv \widetilde{\Pi}^{(n)}$; hence, by the strong induction principle, this last result will be valid at any given n, showing finally that the PT construction holds true to all orders.

From the strong inductive hypothesis, we know that

$$
\widehat{\Pi}^{(\ell)} \equiv \widetilde{\Pi}^{(\ell)}, \quad \widehat{\Gamma}^{(\ell)} \equiv \widetilde{\Gamma}^{(\ell)}, \quad \widehat{B}^{(\ell)} \equiv \widetilde{B}^{(\ell)} \equiv B^{(\ell)},
\tag{6.44}
$$

where $\ell = 1, \ldots, n-1$.

Now, the S-matrix element of order n, to be denoted as $S^{(n)}$, assumes the form

$$S^{(n)} = \{\Gamma\Delta\Gamma\}^{(n)} + B^{(n)}. \tag{6.45}$$

Moreover, since it is unique, regardless if it is written in the Feynman gauge, in the BFG, as well as before and after the PT rearrangement, we have that $S^{(n)} \equiv \widehat{S}^{(n)} \equiv \widetilde{S}^{(n)}$. Using then Eq. (6.33) (which holds to all orders, implying that Eq. (6.44) holds true also when $\ell = n$), we find that

$$\{\Gamma\Delta\Gamma\}^{(n)} \equiv \{\widehat{\Gamma}\widehat{\Delta}\widehat{\Gamma}\}^{(n)} \equiv \{\widetilde{\Gamma}\widetilde{\Delta}\widetilde{\Gamma}\}^{(n)}. \tag{6.46}$$

The above amplitudes can then be split into 1PR and 1PI parts; in particular, due to the strong inductive hypothesis of Eq. (6.44), the 1PR part after the PT rearrangement coincides with the 1PR part written in the BFG, since

$$\{\Gamma\Delta\Gamma\}_{\mathrm{R}}^{(n)} = \Gamma^{(n_1)}\Delta^{(n_2)}\Gamma^{(n_3)}, \qquad \begin{cases} n_1, n_2, n_3 < n, \\ n_1 + n_2 + n_3 = n. \end{cases} \tag{6.47}$$

Then Eq. (6.46) state the equivalence of the 1PI parts, *i.e.*,

$$\{\widehat{\Gamma}\widehat{\Delta}\widehat{\Gamma}\}_{\mathrm{I}}^{(n)} \equiv \{\widetilde{\Gamma}\widetilde{\Delta}\widetilde{\Gamma}\}_{\mathrm{I}}^{(n)}, \tag{6.48}$$

which implies

$$\left[\widehat{\Gamma}^{(n)} - \widetilde{\Gamma}^{(n)}\right]\Delta^{(0)}\Gamma^{(0)} + \Gamma^{(0)}\Delta^{(0)}\left[\widehat{\Gamma}^{(n)} - \widetilde{\Gamma}^{(n)}\right] + \Gamma^{(0)}\Delta^{(0)}\left[\widehat{\Pi}^{(n)} - \widetilde{\Pi}^{(n)}\right]\Delta^{(0)}\Gamma^{(0)} = 0. \tag{6.49}$$

At this point we do not have the equality we want yet, but only that

$$\begin{aligned}
\widehat{\Gamma}^{(n)} &= \widetilde{\Gamma}^{(n)} + f^{(n)}\Gamma^{(0)}, \\
\widehat{\Pi}^{(n)} &= \widetilde{\Pi}^{(n)} - 2iq^2 f^{(n)},
\end{aligned} \tag{6.50}$$

with $f^{(n)}$ an arbitrary function of q^2. However, by means of the *explicit* construction of the PT vertex just presented, we know that $\widehat{\Gamma}^{(n)} \equiv \widetilde{\Gamma}^{(n)}$, and therefore $f = 0$. Then one immediately concludes that

$$\widehat{\Pi}^{(n)} \equiv \widetilde{\Pi}^{(n)}. \tag{6.51}$$

Hence, by strong induction, the above relation is true for any given order n, *i.e.*, inserting back the Lorentz and gauge group structures, we arrive at the announced result

$$\widehat{\Pi}_{\alpha\beta}^{ab}(q) \equiv \widetilde{\Pi}_{\alpha\beta}^{ab}(q). \tag{6.52}$$

The same techniques described in this section have been used in [94] to generalize the PT algorithm to all orders in the electroweak sector of the SM.

7 PT in the Batalin-Vilkovisky framework

In the previous section we demonstrated how the PT algorithm can be generalized beyond the one-loop level. In passing from the two-loop to the all-order construction we abandoned the diagrammatic treatment, and resorted instead to a more formal procedure, where the longitudinal pinching momenta trigger the STIs satisfied by specific subsets of fully dressed vertices appearing in the ordinary perturbative expansion. Due to the non-linearity of the BRST transformation, we have also seen that the Green's functions generated by this process involve composite operators of the type $\langle 0|T[s\Phi(x)\cdots]|0\rangle$, with s the BRST operator and Φ a generic QCD field.

While it is rather satisfactory that the PT could be generalized to all orders, the way this was actually accomplished leaves some important issues still open, mainly for the following reasons.

* The PT quark-gluon vertex was constructed explicitly, but was only partially off-shell, since the external fermions were assumed (as always up to now) to be on-shell; however, for the upcoming SD analysis (next section) we should be able to construct *fully off-shell* vertices. To be sure, a fully off-shell quark-gluon vertex can be constructed through appropriate embedding (as was done for the completely off-shell three-gluon vertex in Section 2), but this would take us further away from the non-diagrammatic formulation that we are striving for.

* The only fully off-shell Green's function considered was the PT gluon propagator; however, it was not *explicitly* constructed, but rather indirectly shown to coincide with the corresponding BFG gluon propagator. It is clearly preferable to devise an *explicit* procedure for obtaining the PT gluon propagator to all orders.

* During the all-order construction presented, no pinching contributions have actually been ever identified; rather, all cancellations of such terms were concealed in the crucial steps corresponding to Eqs (6.36). However, the determination of closed expressions for the pinching contributions is instrumental for understanding the process-independence of the algorithm, as well as for determining crucial identities relating the R_ξ Green's functions with those of the BFG.

As it turns out [165], the most efficient framework for dealing with the type of quantities appearing in the PT procedure is the so-called Batalin-Vilkovisky (BV) formalism [46]. This formalism not only streamlines the derivation of the STIs satisfied by 1PI Green's functions and connected kernels, but has two additional important key features [165,167]: it allows for the construction of the auxiliary (ghost) Green's functions in terms of a well-defined set of Feynman rules, and furnishes a set of useful identities, the so-called Background-Quantum Identities (BQIs), which relate Green's functions involving background fields to Green's functions involving quantum fields. As we will see, these latter identities will allow for the effortless identification of the PT Green's functions with those of the BFG, and constitute one of the main advantages gained from employing the BV formalism [165].

In this section we present an introduction to the BV formalism, providing the minimum amount of information needed to establish notation, and arrive at the relevant generating functionals and master equations, together with the differentiation rules needed to generate from
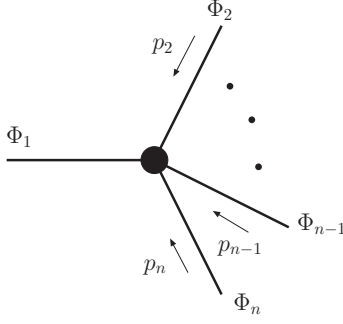
Fig. 66. Our conventions for the (1PI) Green's functions $\Gamma_{\Phi_1\cdots\Phi_n}(p_1,\ldots,p_n)$. All momenta $p_2,\ldots,p_n$ are assumed to be incoming, and are assigned to the corresponding fields starting from the rightmost one. The momentum of the leftmost field Φ_1 is determined through momentum conservation ($\sum_i p_i = 0$) and will be suppressed.

the latter useful identities. We will then concentrate on putting to work all the machinery introduced, by casting in the BV language the one- and two-loop results presented in earlier sections.

Thus, this introductory section sets up the stage for an alternative, and more efficient, way of generalizing the PT to all orders. In fact, as will be shown in the next section, casting the PT in the BV language permits to go on step further, allowing for the generalization of the PT algorithm to the Schwinger-Dyson equations of QCD.

7.1 Green's functions: conventions

The Green's functions of the theory can be constructed in terms of time-ordered products of free fields $\Phi_1^0 \cdots \Phi_n^0$ and vertices of the interaction Lagrangian $\mathcal{L}_{\text{int}}$ (constructed from the pieces of $\mathcal{L}$ which are not bilinear in the fields) through the standard Gell-Man-Low formula for the 1PI truncated Green's functions

$$
\begin{aligned}
\Gamma_{\Phi_1\cdots\Phi_n}(x_1,\ldots,x_n) &= \langle T[\Phi_1(x_1)\cdots\Phi_n(x_n)]\rangle^{\text{1PI}} \\
&= \langle T[\Phi_1^0(x_1)\cdots\Phi_n^0(x_n)]\exp(-i\int d^4x\,\mathcal{L}_{\text{int}})\rangle^{\text{1PI}}.
\end{aligned} \tag{7.1}
$$

The complete set of Green's functions can be handled most efficiently by introducing a generating functional (see also Section 3), which in Fourier space reads

$$
\Gamma[\Phi] = \sum_{n=0}^{\infty}\frac{(-i)^n}{n!}\int\prod_{i=0}^{n}d^4p_i\,\delta^4(\sum_{j=1}^{n}p_j)\Phi_1(p_1)\cdots\Phi_n(p_n)\Gamma_{\Phi_1\cdots\Phi_n}(p_1,\ldots,p_n), \tag{7.2}
$$

with p_i the (in-going) momentum of the Φ_i field. Since in perturbation theory $\Gamma_{\Phi_1\cdots\Phi_n}$ is a formal power series in $\hbar$, we will denote its m-loop contribution as $\Gamma_{\Phi_1\cdots\Phi_n}^{(m)}$. Then, the Green's functions of the theory may be obtained from the generating functional $\Gamma[\Phi]$ by means of functional

Φ	A_μ	ψ	$\bar{\psi}$	c	$\bar{c}$	A_μ^*	ψ^*	$\bar{\psi}^*$	c^*	$\bar{c}^*$	Ω_μ^a
$\mathrm{gh}(\Phi)$	0	0	0	1	-1	-1	-1	-1	-2	0	1
$\mathrm{st}(\Phi)$	B	F	F	F	F	F	B	B	B	B	F

Table 2
Ghost charges and statistics (B for Bose, F for Fermi) of the QCD fields, anti-fields and BFM sources.

differentiation:

$$\Gamma_{\Phi_1\cdots\Phi_n}(p_1,\ldots,p_n) = i^n \left. \frac{\delta^n\Gamma}{\delta\Phi_1(p_1)\delta\Phi_2(p_2)\cdots\delta\Phi_n(p_n)}\right|_{\Phi_i=0}, \tag{7.3}$$

where $\Phi(p)$ denotes the Fourier transform of $\Phi(x)$, and our convention on the external momenta is summarized in Fig. 66. From the definition given in Eq. (7.3) it follows that the Green's functions $i^{-n}\Gamma_{\Phi_1\cdots\Phi_n}$ are simply given by the corresponding Feynman diagrams in Minkowsky space. Finally, notice that upon inversion of two (adjacent) fields we have

$$\Gamma_{\Phi_1\cdots\Phi_i\Phi_{i+1}\cdots\Phi_n}(p_1,\ldots,p_i,p_{i+1},\ldots,p_n) = \pm\Gamma_{\Phi_1\cdots\Phi_{i+1}\Phi_i\cdots\Phi_n}(p_1,\ldots,p_{i+1},p_i,\ldots,p_n), \quad (7.4)$$

with the minus appearing only when both fields Φ_i and Φ_{i+1} obey Fermi statistics.

The Green's functions defined so far are sufficient for building all possible amplitudes involved in the S-matrix computation; however, due to the non-linearity of the BRST transformations, they do not cover the complete set of Green's functions appearing in the STIs of the theory (and therefore needed for its renormalization, as well as the PT construction).

7.2 The Batalin-Vilkovisky formalism for pedestrians

Let us now introduce for each field Φ appearing in the theory [4] a corresponding anti-field, to be denoted by Φ^*. The anti-field Φ^* has opposite statistics with respect to Φ; its ghost charge, $\mathrm{gh}(\Phi^*)$, is related to the ghost charge $\mathrm{gh}(\Phi)$ of the field Φ by $\mathrm{gh}(\Phi^*) = -1 - \mathrm{gh}(\Phi)$. For convenience, we summarize the ghost charges and statistics of the various QCD fields and anti-fields in Table 2. Next, we add to the original gauge invariant Lagrangian $\mathcal{L}_\mathrm{I}$ of Eq. (2.2) a term coupling the anti-fields with the BRST variation of the corresponding fields, to get

$$\mathcal{L}_\mathrm{BV} = \mathcal{L}_\mathrm{I} + \mathcal{L}_\mathrm{BRST}, \tag{7.5a}$$

$$\mathcal{L}_\mathrm{BRST} = \sum_\Phi \Phi^* s\Phi$$

$$= A_\mu^{*a}(\partial^\mu c^a + gf^{abc}A_\mu^b c^c) - \frac{1}{2}gf^{abc}c^{*a}c^b c^c + ig\bar{\psi}^* c^a t^a\psi - igc^a\bar{\psi}t^a\psi^*. \tag{7.5b}$$

Notice that we have suppressed all spinor indices (both flavor and color), since they play no role in the ensuing construction.

---

[4] In the rest of this report, quark fields will be denoted by the generic letter ψ

Then, the action $\Gamma^{(0)}[\Phi, \Phi^*]$ constructed from $\mathcal{L}_{\mathrm{BV}}$, will satisfy the master equation

$$\int d^4x \sum \frac{\delta\Gamma^{(0)}}{\delta\Phi^*}\frac{\delta\Gamma^{(0)}}{\delta\Phi} = 0. \tag{7.6}$$

To verify this, observe that, on one hand, the terms in $\delta\Gamma^{(0)}/\delta\Phi$ that are independent of the anti-fields Φ^* are zero, due the BRST (actually the gauge) invariance of the action

$$\int d^4x \sum s\Phi\frac{\delta\Gamma^{(0)}_{\mathrm{I}}}{\delta\Phi} = \int d^4x\,(s\Gamma^{(0)}_{\mathrm{I}}[\Phi]) = 0\,; \tag{7.7}$$

on the other hand, terms in $\delta\Gamma^{(0)}/\delta\Phi$ that are linear in the anti-fields vanish, due to the nihilpotency of the BRST operator

$$\int d^4x \sum s\Phi'\frac{\delta(s\Phi)}{\delta\Phi'} = \int d^4x \sum s^2\Phi' = 0. \tag{7.8}$$

Now, since the anti-fields are external sources, we must constrain them to suitable values before the action $\Gamma^{(0)}$ can be used for calculating the S-matrix elements of the theory [39]. To that end, we introduce an arbitrary fermionic functional, $\Psi[\Phi]$, with ghost charge -1, and set for all the anti-fields Φ^*

$$\Phi^* = \frac{\delta\Psi[\Phi]}{\delta\Phi}. \tag{7.9}$$

Then the action becomes

$$\begin{aligned}\Gamma^{(0)}[\Phi, \delta\Psi/\delta\Phi] &= \Gamma^{(0)}[\Phi] + (s\Phi)\frac{\delta\Psi[\Phi]}{\delta\Phi}\\ &= \Gamma^{(0)}[\Phi] + s\Psi[\Phi],\end{aligned} \tag{7.10}$$

and therefore, choosing the functional Ψ to satisfy the relation

$$s\Psi = \int d^4x\,(\mathcal{L}_{\mathrm{GF}} + \mathcal{L}_{\mathrm{FPG}})\,, \tag{7.11}$$

we see that the action $\Gamma^{(0)}$ (obtained from $\mathcal{L}_{\mathrm{BV}}$) is equivalent to the gauge-fixed action obtained from the original Lagrangian $\mathcal{L}$ of Eq. (2.1). The functional Ψ is often referred to as the "gauge fixing fermion".

It is well-known that the BRST symmetry is crucial for endowing a (gauge) theory with a unitary S-matrix and gauge-independent physical observables; therefore, it must be implemented to all orders. For doing so we establish the quantum corrected version of the master equation (7.6) in the form of the STI functional

$$\begin{aligned}\mathcal{S}(\Gamma)[\Phi] &= \int d^4x \sum \frac{\delta\Gamma}{\delta\Phi^*}\frac{\delta\Gamma}{\delta\Phi}\\ &= \int d^4x \left\{ \frac{\delta\Gamma}{\delta A_m^{*\mu}}\frac{\delta\Gamma}{\delta A_\mu^m} + \frac{\delta\Gamma}{\delta c^{*m}}\frac{\delta\Gamma}{\delta c^m} + \frac{\delta\Gamma}{\delta\psi^*}\frac{\delta\Gamma}{\delta\bar\psi} + \frac{\delta\Gamma}{\delta\psi}\frac{\delta\Gamma}{\delta\bar\psi^*} + B^m\frac{\delta\Gamma}{\delta\bar c^m} \right\}\\ &= 0,\end{aligned} \tag{7.12}$$

where $\Gamma[\Phi, \Phi^*]$ is now the effective action.

In order to simplify the structure of the STI generating functional of Eq. (7.12), let us notice that the anti-ghost $\bar{c}^a$ and the multiplier B^a have *linear* BRST transformations; therefore they do not present the usual complications (due to non-linearity) of the other QCD fields. Together with their corresponding anti-field, they enter bi-linearly in the action, and one can write the complete action (which we now explicitly indicate with a C subscript) as a sum of a minimal and non-minimal sector

$$\Gamma_{\mathrm{C}}^{(0)}[\Phi, \Phi^*] = \Gamma^{(0)}[A_\mu^a, A_\mu^{*a}, \psi, \psi^*, \bar{\psi}, \bar{\psi}^*, c^a, c^{*a}] + \bar{c}^{*a} B^a. \qquad (7.13)$$

The last term has no effect on the master equation (7.6), which is satisfied by $\Gamma^{(0)}$ alone; the fields $\{A_\mu^a, A_\mu^{*a}, \psi, \psi^*, \bar{\psi}, \bar{\psi}^*, c^a, c^{*a}\}$ are usually called *minimal variables* while $\bar{c}^a$ and B^a are referred to as non-minimal variables or "trivial pairs". Equivalently, one can introduce the minimal (or reduced) action by subtracting from the complete one the local term corresponding to the gauge-fixing Lagrangian, *i.e.*,

$$\Gamma = \Gamma_{\mathrm{C}} - \int d^4x \, \mathcal{L}_{\mathrm{GF}}. \qquad (7.14)$$

In either cases, the result is that the STI functional is now written as

$$\mathcal{S}(\Gamma)[\Phi] = \int d^4x \left\{ \frac{\delta\Gamma}{\delta A_m^{*\mu}} \frac{\delta\Gamma}{\delta A_\mu^m} + \frac{\delta\Gamma}{\delta c^{*m}} \frac{\delta\Gamma}{\delta c^m} + \frac{\delta\Gamma}{\delta\psi^*} \frac{\delta\Gamma}{\delta\bar{\psi}} + \frac{\delta\Gamma}{\delta\psi} \frac{\delta\Gamma}{\delta\bar{\psi}^*} \right\} = 0. \qquad (7.15)$$

In practice, the STIs of Eq. (7.15), generated from the reduced functional Γ, coincide with those obtained from Γ_{C} after the implementation of the Faddeev-Popov equation, described in the next subsection [168]. One should also keep in mind that the Green's functions involving unphysical fields that are generated by Γ coincide with those generated by Γ_{C} only up to constant terms proportional to the gauge fixing parameter, *e.g.*, $\Gamma_{A_\mu A_\nu}(q) = \Gamma_{A_\mu A_\nu}^{\mathrm{C}}(q) - i\xi^{-1}q_\mu q_\nu$. The differences between employing Γ or Γ_{C} is further explored in Appendix C; there, all relevant identities needed for the generalization of the PT procedure to the SDEs of QCD (next section) are derived and discussed.

Taking functional derivatives of $\mathcal{S}(\Gamma)[\Phi]$ and setting afterwards all fields and anti-fields to zero will generate the complete set of the all-order STIs of the theory; this is in exact analogy to what happens with the effective action, where taking functional derivatives of $\Gamma[\Phi]$ and setting afterwards all fields to zero generates the Green's functions of the theory, see Eq. (7.3). However, in order to reach meaningful expressions, one needs to keep in mind that:

* $\mathcal{S}(\Gamma)$ has ghost charge 1;

* functions with non-zero ghost charge vanish, since the ghost charge is a conserved quantity.

Thus, in order to extract non-trivial identities from Eq. (7.15) one needs to differentiate the latter with respect to a combination of fields, containing either one ghost field, or two ghost fields and one anti-field. The only exception to this rule is when differentiating with respect to a ghost anti-field, which needs to be compensated by three ghost fields. In particular, identities

involving one or more gauge fields are obtained by differentiating Eq. (7.15) with respect to the set of fields in which one gauge boson has been replaced by the corresponding ghost field. This is due to the fact that the linear part of the BRST transformation of the gauge field is proportional to the ghost field: $sA_\mu^a|_{\text{linear}} = \partial_\mu c^a$. For completeness we also notice that, for obtaining STIs involving Green's functions that contain ghost fields, one ghost field must be replaced by two ghost fields, due to the non linearity of the BRST ghost field transformation [$sc^a \propto f^{abc}c^b c^c$, see Eq. (2.9)]. The last technical point to be clarified is the dependence of the STIs on the (external) momenta. One should notice that the integral over d^4x present in Eq. (7.15), together with the conservation of momentum flow of the Green's functions, implies that no momentum integration is left over; as a result, the STIs will be expressed as a sum of products of (at most two) Green's functions.

An advantage of working with the BV formalism is the fact that the STI functional (7.15) is valid in any gauge, *i.e.*, it will not be affected when switching from one gauge to another. In particular, if we want to consider the BFM gauge, the only additional step we need to take is to implement the equations of motion for the background fields at the quantum level. This is achieved most efficiently by extending the BRST symmetry to the background gluon field, through the relations

$$s\widehat{A}_\mu^m = \Omega_\mu^m, \qquad s\Omega_\mu^m = 0, \tag{7.16}$$

where Ω_μ^m represents a (classical) vector field, with the same quantum numbers as the gluon, ghost charge $+1$, and Fermi statistics (see also Table 2). The dependence of the Green's functions on the background fields is then controlled by the modified STI functional

$$\mathcal{S}'(\Gamma')[\Phi] = \mathcal{S}(\Gamma')[\Phi] + \int d^4x \, \Omega_m^\mu \left(\frac{\delta\Gamma'}{\delta\widehat{A}_\mu^m} - \frac{\delta\Gamma'}{\delta A_\mu^m} \right) = 0, \tag{7.17}$$

where Γ' denotes the effective action that depends on the background sources Ω_μ^m (with $\Gamma \equiv \Gamma'|_{\Omega=0}$), and $\mathcal{S}(\Gamma')[\Phi]$ is the STI functional of Eq. (7.15). Differentiation of the STI functional (7.17) with respect to the background source and background or quantum fields will then provide the BQIs, which relate 1PI Green's functions involving background fields with the ones involving quantum fields. The BQIs are particularly useful in the PT context, since they allow for a direct comparison between PT and BFM Green's functions.

Finally, the background gauge invariance of the BFM effective action implies that Green's functions involving background fields satisfy linear WIs when contracted with the momentum corresponding to a background leg. They are generated by taking functional differentiations of the WI functional

$$\mathcal{W}_\vartheta[\Gamma'] = \int d^4x \sum_{\Phi, \Phi^*} \left(\delta_{\vartheta(x)}\Phi \right) \frac{\delta\Gamma'}{\delta\Phi} = 0, \tag{7.18}$$

where $\vartheta^a(x)$ are the local infinitesimal parameters corresponding to the $SU(3)$ generators t^a, which now play the role of the ghost field. The transformations $\delta_\vartheta\Phi$ are thus given by

$$
\begin{aligned}
\delta_\vartheta A_\mu^a &= g f^{abc} A_\mu^b \vartheta^c & \delta_\vartheta \widehat{A}_\mu^a &= \partial_\mu \vartheta^a + g f^{abc} \widehat{A}_\mu^b \vartheta^c, \\
\delta_\vartheta c^a &= -g f^{abc} c^b \vartheta^c & \delta_\vartheta \bar{c}^a &= -g f^{abc} \bar{c}^b \vartheta^c, \\
\delta_\vartheta \psi_{\text{f}}^i &= ig\vartheta^a (t^a)_{ij} \psi_{\text{f}}^j & \delta_\vartheta \bar{\psi}_{\text{f}}^i &= -ig\vartheta^a \bar{\psi}_{\text{f}}^j (t^a)_{ji},
\end{aligned}
\tag{7.19a}
$$

171

and the background transformations of the anti-fields $\delta_\vartheta \Phi^*$ coincide with the gauge transformations of the corresponding quantum gauge fields according to their specific representation. Notice that, in order to obtain the WIs satisfied by the Green's functions involving background gluons $\widehat{A}$, one has to differentiate the functional (7.18) with respect to the corresponding parameter ϑ.

The STIs and BQIs needed for the PT construction have been derived in [169], together with the method for constructing the auxiliary functions appearing in these identities; they are reported for convenience in Appendix C.2 and C.3.

7.3 *Faddeev-Popov equation(s)*

The Faddev-Popov equation is a highly non-trivial identity, which is extremely useful in the PT context, since it determines the result of the contraction of longitudinal momenta on auxiliary Green's functions. The FPE is also instrumental in proving the equivalence between the STIs and BQIs derived using Γ or Γ_C (see Appendix). Since the FPE depends crucially on the form of the ghost Lagrangian, which, in turn, depends on the gauge fixing function [see Eq. (2.7)], we will first present the corresponding derivation in the R_ξ gauges, and then generalize it to the BFM.

To derive the FPE in the R_ξ gauges, one observes that in the QCD action the only term proportional to the anti-ghost fields comes from the Faddeev-Popov Lagrangian density, which can be rewritten as

$$\mathcal{L}^{R_\xi}_{\mathrm{FPG}} = -\bar{c}^m \partial^\mu (s A^m_\mu) = -\bar{c}^m \partial^\mu \frac{\delta\Gamma}{\delta A^{*m}_\mu}. \tag{7.20}$$

Differentiation of the action with respect to $\bar{c}^a$ yields the FPE in the form of the identity

$$\frac{\delta\Gamma}{\delta\bar{c}^m} + \partial^\mu \frac{\delta\Gamma}{\delta A^{*m}_\mu} = 0, \tag{7.21}$$

so that, taking the Fourier transform, we arrive at

$$\frac{\delta\Gamma}{\delta\bar{c}^m} + iq^\mu \frac{\delta\Gamma}{\delta A^{*m}_\mu} = 0. \tag{7.22}$$

Thus, in the R_ξ case, the FPE amounts to the simple statement that the contraction of a leg corresponding to a gluon anti-field (A^{*m}_μ) by its own momentum (q^μ) converts it to an anti-ghost leg ($\bar{c}^m$). Functional differentiation of this identity with respect to QCD fields (but not background sources and fields, see below) furnishes useful identities, that will be used extensively in our construction.

For obtaining FPEs for Green's functions involving background gluons and sources, one has to modify Eq. (7.22), in order to account for the presence of extra terms in the BFM gauge fixing function (and therefore in the BFM Faddeev-Popov ghost Lagrangian). Eq. (7.21) gets then generalized to

$$\frac{\delta\Gamma'}{\delta\bar{c}^m} + \left(\widehat{\mathcal{D}}^\mu \frac{\delta\Gamma'}{\delta A^*_\mu}\right)^m - (\mathcal{D}^\mu \Omega_\mu)^m = 0. \tag{7.23}$$
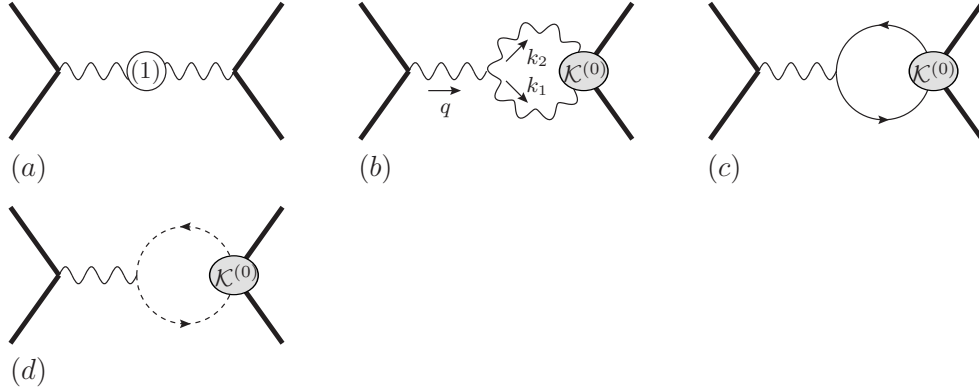
Fig. 67. The S-matrix PT setup for constructing the gluon propagator at one loop. The external particles are left unspecified since, due to the process-independence of the algorithm, they can equally well be quarks or gluons. When the external particles are, *e.g.*, gluons, the kernel $\mathcal{K}^{(0)}$ appearing in diagram (b) is the tree-level version of the one shown in Fig. 71. Mirror diagrams having the kernels on the opposite side are not shown.

Once again, the specific FPEs needed for the PT construction have been derived in [169], and are reported in Appendix C.1.

7.4 The (one-loop) PT algorithm in the BV language

After introducing all this formal machinery, it would be important to make contact with the PT algorithm. This is clearly best done at the one-loop level, since in this case all calculations are rather straightforward, and it is relatively easy to compare the standard diagrammatic results with those coming from the BV formalism. This comparison will (*i*) help us identify the pieces that will be generated when applying the PT algorithm, and (*ii*) establish the rules for distributing the pieces obtained in (*i*) among the different Green's functions appearing in the calculation.

The starting point is the usual embedding of the (one-loop) gluon propagator into an S-matrix element (Fig. 67). Choosing the external legs to be, *e.g.*, gluons, and carrying out the PT decomposition $\Gamma = \Gamma^{\mathrm{P}} + \Gamma^{\mathrm{F}}$ on the tree-level three-gluon vertex of diagram (b) [see Eqs (2.39)], we find

$$(b) = (b)^{\mathrm{F}} + (b)^{\mathrm{P}},$$
$$(b)^{\mathrm{P}} = -\frac{1}{2}gf^{am'n'}\int_{k_1}(g_{\alpha\nu'}k_{1\mu'} - g_{\alpha\mu'}k_{2\nu'})\Delta^{(0)\mu'\mu}_{m'm}(k_1)\Delta^{(0)\nu'\nu}_{n'n}(k_2)\mathcal{K}^{(0)}_{A^m_\mu A^n_\nu A^r_\rho A^s_\sigma}(k_2,p_2,-p_1).$$
$$= -gf^{amn}g^\nu_\alpha\int_{k_1}\frac{1}{k_1^2}\frac{1}{k_2^2}k_1^\mu\mathcal{K}^{(0)}_{A^m_\mu A^n_\nu A^r_\rho A^s_\sigma}(k_2,p_2,-p_1). \tag{7.24}$$

The $1/2$ symmetry factor carried by the kernel $\mathcal{K}$ is due to the explicit presence of the crossing term. Then, expanding at tree-level the STI (C.35), dropping the terms proportional to the

inverse gluon propagator $\Gamma^{(0)}_{AA}(p_i)$, since they vanish for "on-shell" gluons, and finally making use of Eq. (C.44), we get

$$(b)^{\mathrm{P}} = -\Gamma^{(1)}_{\Omega^a_\alpha A^{*\gamma}_d}(-q)\Gamma^{(0)}_{A^d_\gamma A^r_\rho A^s_\sigma}(p_2, -p_1) + (b')$$

$$(b') = -gf^{amn}g^\nu_\alpha \int_{k_1} \frac{1}{k_1^2}\frac{1}{k_2^2}\mathcal{K}^{(0)}_{c^m A^r_\rho A^s_\sigma A^{*\gamma}_d}(p_2, -p_1, k_2)\Gamma^{(0)}_{A^d_\gamma A^n_\nu}(k_2). \tag{7.25}$$

At this point the PT calculation is over, and one needs to reshuffle the pieces generated. Since (b') is a vertex-like contribution, the PT vertex $\widehat{\Gamma}_{AAA}$, which is obtained by considering the corresponding Green's function embedded in the S-matrix element, will be given by

$$(b)^{\mathrm{F}} + (b') + (c) + (d) = (b) + (c) + (d) + (b') - (b)^{\mathrm{P}}, \tag{7.26}$$

or

$$i\widehat{\Gamma}^{(1)}_{A^a_\alpha A^r_\rho A^s_\sigma}(p_2, -p_1) = i\Gamma^{(1)}_{A^a_\alpha A^r_\rho A^s_\sigma}(p_2, -p_1) + \Gamma^{(1)}_{\Omega^a_\alpha A^{*\gamma}_d}(-q)\Gamma^{(0)}_{A^d_\gamma A^r_\rho A^s_\sigma}(p_2, -p_1). \tag{7.27}$$

The PT self-energy will be given instead by the combination $(a) + 2(b)^{\mathrm{P}}$ [the factor of 2 coming from the mirror diagram of (b)], *i.e.*,

$$\widehat{\Pi}^{(1)}_{\alpha\beta}(q) = \Pi^{(1)}_{\alpha\beta}(q) + \Pi^{\mathrm{P}(1)}_{\alpha\beta}(q), \tag{7.28}$$

where we have defined, with the aid of Eq. (C.16),

$$\Pi^{\mathrm{P}(1)}_{\alpha\beta}(q) = 2i\Gamma^{(1)}_{\Omega_\alpha A^{*\gamma}}(q)\Gamma^{(0)}_{A_\gamma A_\beta}(q). \tag{7.29}$$

We can now proceed to the comparison of the PT Green's functions with those of the BFG, by resorting to the BQIs. Clearly, Eq. (7.27) represents the one-loop expansion of the BQI (C.48), and we immediately conclude that

$$\widehat{\Gamma}^{(1)}_{A^a_\alpha A^r_\rho A^s_\sigma}(p_2, -p_1) = \Gamma^{(1)}_{\widehat{A}^a_\alpha A^r_\rho A^s_\sigma}(p_2, -p_1). \tag{7.30}$$

For the self-energy we have instead [recall that in our conventions $-\Gamma_{AA}(q) = \Pi(q)$]

$$\delta^{ab}\widehat{\Pi}^{(1)}_{\alpha\beta}(q) = -\Gamma^{(1)}_{A^a_\alpha A^b_\beta}(q) + 2i\Gamma^{(1)}_{\Omega^a_\alpha A^{*\gamma}_d}(q)\Gamma^{(0)}_{A^d_\gamma A^b_\beta}(q), \tag{7.31}$$

which represents the one-loop version of the BQI of Eq. (C.39), *i.e.*, we have

$$\delta^{ab}\widehat{\Pi}^{(1)}_{\alpha\beta}(q) = -\Gamma^{(1)}_{\widehat{A}^a_\alpha \widehat{A}^b_\beta}(q). \tag{7.32}$$

7.5 *The two-loop case*

As can be inferred on the basis of the analysis carried out in the previous section, at the two-loop level all the diagrams appearing in the skeleton expansion of the propagator and vertex are

participating in the PT construction. Thus, it would be useless to carry out the same comparison between the diagrammatic and the BV formulation as we did at the one-loop level: while the level of difficulty would be the same as that of the all-order analysis, no deeper understanding would be gained in the process.

However, what we can still show is how the BV formalism enormously facilitates the comparison between the final PT result and the corresponding BFG Green's function, drastically reducing the additional effort required in order to compare the PT self-energy to the corresponding BFG one. This is particularly relevant in the SM case, where the use of the BQIs has been instrumental for generalizing the PT algorithm to two loops [170]. Let us start with the two-loop gluon self-energy, which is given by [see Eq. (6.20)]

$$\widehat{\Pi}^{(2)}_{\alpha\beta}(q) = \Pi^{(2)}_{\alpha\beta}(q) + \Pi^{\mathrm{P}\,(2)}_{\alpha\beta}(q) - R^{\mathrm{P}\,(2)}_{\alpha\beta}(q), \tag{7.33}$$

with

$$
\begin{aligned}
\Pi^{\mathrm{P}\,(2)}_{\alpha\beta}(q) - R^{\mathrm{P}\,(2)}_{\alpha\beta}(q) = q^2 P^{\gamma}_{\beta}(q) \bigg\{ & I_4 L_{\alpha\gamma}(\ell,k) + I_3 g_{\alpha\rho} \\
& - I_1 \left[k_\gamma g_{\alpha\sigma} + \Gamma^{(0)}_{\sigma\gamma\alpha}(-k,-\ell,k+\ell) \right] (\ell-q)^\sigma \bigg\} \\
& + i V^{\mathrm{P}\,(1)\,\gamma}_{\beta}(q) \Pi^{(1)}_{\gamma\alpha}(q) - q^2 I_2 P_{\alpha\beta}(q).
\end{aligned}
\tag{7.34}
$$

On the other hand, the two loop version of the BQI (C.39) satisfied by the gluon two-point function gives

$$
\begin{aligned}
\widehat{\Pi}^{(2)}_{\alpha\beta}(q) = & \Pi^{(2)}_{\alpha\beta}(q) + 2i\Gamma^{(2)}_{\Omega_\alpha A^{*\gamma}}(q)\Gamma^{(0)}_{A_\gamma A_\beta}(q) + 2i\Gamma^{(1)}_{\Omega_\alpha A^{*\gamma}}(q)\Gamma^{(1)}_{A_\gamma A_\beta}(q) \\
& + \Gamma^{(1)}_{\Omega_\alpha A^{*\gamma}}(q)\Gamma^{(0)}_{A_\gamma A_\epsilon}(q)\Gamma^{(1)}_{\Omega_\beta A^{*\epsilon}}(q),
\end{aligned}
\tag{7.35}
$$

where we have used the fact that $-\Gamma_{A_\alpha A_\beta} = \Pi_{\alpha\beta}$. From the one-loop results of the previous subsections it is immediate to establish the identity

$$2i\Gamma^{(1)}_{\Omega_\alpha A^{*\gamma}}(q)\Gamma^{(1)}_{A_\gamma A_\beta}(q) + \Gamma^{(1)}_{\Omega_\alpha A^{*\gamma}}(q)\Gamma^{(0)}_{A_\gamma A_\epsilon}(q) = i V^{\mathrm{P}\,(1)\,\gamma}_{\beta}(q)\Pi^{(1)}_{\gamma\alpha}(q) - q^2 I_2 P_{\alpha\beta}(q). \tag{7.36}$$

Finally, the perturbative expansion at the two-loop level of the auxiliary function $\Gamma_{\Omega A^*}$ is shown in Fig. 68; one has the results

$$
\begin{aligned}
(a) &= \frac{1}{2} I_1 \Gamma^{(0)}_{\sigma\gamma\alpha}(-k,-\ell,k+\ell)(\ell-q)^\sigma, & (b) &= \frac{1}{2} I_1 (\ell-q)_\alpha k_\gamma, \\
(c) &= -\frac{1}{2} I_4 L_{\alpha\gamma}(\ell,k), & (d) &= -\frac{1}{2} I_3 g_{\alpha\gamma},
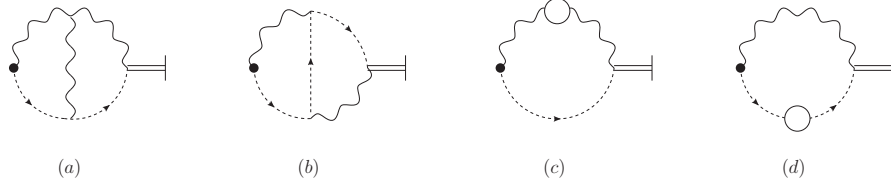\end{aligned}
\tag{7.37}
$$

or

175

Fig. 68. The two-loop diagrams contributing to the auxiliary function $\Gamma_{\Omega A^*}$.

$$2i\Gamma^{(2)}_{\Omega_\alpha A^{*\gamma}}(q)\Gamma^{(0)}_{A_\gamma A_\beta}(q) = q^2 P^\gamma_\beta(q)\left\{I_4 L_{\alpha\gamma}(\ell, k) + I_3 g_{\alpha\gamma}\right.$$
$$\left. - I_1\left[k_\gamma g_{\alpha\sigma} + \Gamma^{(0)}_{\sigma\gamma\alpha}(-k, -\ell, k+\ell)\right](\ell - q)^\sigma\right\}. \tag{7.38}$$

Putting everything together, we see that

$$\Pi^{\mathrm{P}\,(2)}_{\alpha\beta}(q) - R^{\mathrm{P}\,(2)}_{\alpha\beta}(q) = 2i\Gamma^{(2)}_{\Omega_\alpha A^{*\gamma}}(q)\Gamma^{(0)}_{A_\gamma A_\beta}(q) + 2i\Gamma^{(1)}_{\Omega_\alpha A^{*\gamma}}(q)\Gamma^{(1)}_{A_\gamma A_\beta}(q)$$
$$+ \Gamma^{(1)}_{\Omega_\alpha A^{*\gamma}}(q)\Gamma^{(0)}_{A_\gamma A_\epsilon}(q), \tag{7.39}$$

which thus implies

$$\widehat{\Pi}^{(2)}_{\alpha\beta}(q) = \widetilde{\Pi}^{(2)}_{\alpha\beta}(q), \tag{7.40}$$

where $\widetilde{\Pi}^{(2)}_{\alpha\beta}(q) = -\Gamma_{A_\alpha A_\beta}$ is the BFG two-loop gluon self-energy. The proof in the case of the PT two-loop quark-gluon vertex is even easier; after using the one-loop result, the two-loop PT vertex can be cast in the form

$$\widehat{\Gamma}^{(2)}_\alpha(p_1, p_2) = \Gamma^{(2)}_\alpha(p_1, p_2) + \frac{i}{2}V^{\mathrm{P}\,(1)\,\rho}_\alpha(q)\Gamma^{(1)}_\rho(p_1, p_2) - \frac{1}{2}\left\{I_4 L_{\alpha\rho}(\ell, k) + I_3 g_{\alpha\rho}\right.$$
$$\left. - I_1\left[k_\rho g_{\alpha\sigma} + \Gamma^{(0)}_{\sigma\rho\alpha}(-k, -\ell, k+\ell)\right](\ell - q)^\sigma\right\}\gamma^\rho. \tag{7.41}$$

The two-loop BQI (C.57) for the gluon-quark vertex reads

$$i\Gamma^{(2)}_{\widehat{A}^a_\alpha \psi\bar\psi}(p_2, -p_1) = i\Gamma^{(2)}_{\widehat{A}^a_\alpha \psi\bar\psi}(p_2, -p_1) + \Gamma^{(2)}_{\Omega_\alpha A^{*\gamma}}(q)\Gamma^{(0)}_{A^a_\gamma \psi\bar\psi}(p_2, -p_1)$$
$$+ \Gamma^{(1)}_{\Omega_\alpha A^{*\gamma}}(q)\Gamma^{(1)}_{A^a_\gamma \psi\bar\psi}(p_2, -p_1), \tag{7.42}$$

where we have neglected pieces that vanish on-shell. Then one has

176

$$\Gamma^{(1)}_{\Omega_\alpha A^{*\rho}}(q)\Gamma^{(1)}_{A^a_\rho \psi\bar\psi}(p_2, -p_1) = \frac{i}{2}V^{(1)\,\mathrm{P}\,\rho}_\alpha(q)\Gamma^{(1)}_{A^a_\rho \psi\bar\psi}(p_2, -p_1), \tag{7.43a}$$

$$\Gamma^{(2)}_{\Omega_\alpha A^{*\gamma}}(q)\Gamma^{(0)}_{A_\gamma \psi\bar\psi}(p_2, -p_1) = -\frac{1}{2}\left\{ I_4 L_{\alpha\rho}(\ell, k) + I_3 g_{\alpha\rho} \right.$$

$$\left. - I_1\left[k_\rho g_{\alpha\sigma} + \Gamma^{(0)}_{\sigma\rho\alpha}(-k, -\ell, k+\ell)\right](\ell - q)^\sigma \right\}\gamma^\rho, \tag{7.43b}$$

where in (7.43b) we have suppressed a factor gt^a. Thus we get the equality between the two-loop PT and BFG quark-gluon vertex [one needs to take into account that, due to the different conventions used, $\Gamma_\alpha(p_1, p_2) = i\Gamma_{A_\alpha \psi\bar\psi}(p_2, -p_1)$].

8 The PT Schwinger-Dyson Equations for QCD Green's functions

After recasting the PT algorithm in the BV language, and making contact with the original diagrammatic formulation, we are now ready to face the final challenge: apply the PT program to the (non-perturbative) Schwinger-Dyson equations (SDEs) of QCD. In fact, historically, this was the main motivation for introducing the method in the first place [5–8].

In this section, after briefly discussing the difficulties encountered when attempting to truncate the SDEs within the conventional formalism, we will scrutinize, in detail how the PT algorithm can be extended to the construction of new SDEs for the QCD Green's functions. Next we proceed to the actual construction of the new SDEs for the gluon two- and three-point functions. We will finally discuss in depth the theoretical and practical advantages of the new SDE series.

8.1 *SDEs for non-Abelian gauge theories: difficulties with the conventional formulation*

The SDEs provide a formal framework for tackling physics problems requiring a non perturbative treatment. In fact, even though these equations are derived from an expansion about the free-field vacuum, they finally make no reference to it, or to perturbation theory, and can be used to address problems related to chiral symmetry breaking, dynamical mass generation, formation of bound states, and other non-perturbative effects [26,27].

In practice, however, their usefulness hinges crucially on one's ability to devise a self-consistent truncation scheme that would select a tractable subset of these equations, without compromising the physics one hopes to describe. Inventing such a scheme for the SDE of gauge theories is a highly non-trivial proposition. The problem originates from the fact that the SDEs are built out of unphysical Green's functions; thus, the extraction of reliable physical information depends critically on the delicate all-order cancellations we have been describing in this review, which may be inadvertently distorted in the process of the truncation. For example, several of the issues related to the truncation of the SDEs of QED have been addressed in [171–180]; it goes without saying that the situation becomes even more complicated for strongly coupled non-Abelian gauge theories, such as QCD [181], mainly because of the following two reasons.

i. As we have seen, the complications caused by the dependence of the Green's functions on the gfp are more acute in non-Abelian gauge-theories. For example, recall that in QED the photon self-energy (vacuum polarization) is independent of the gfp, both perturbatively (to all orders) and non-perturbatively; when multiplied by e^2 it forms a physical observable, the QED effective charge. In contradistinction, the gluon self-energy is gfp-dependent already at one loop; depending on the gauge-fixing scheme employed, this dependence may be more or less virulent. This difference is clearly of little practical importance when computing S-matrix elements at a fixed order in perturbation theory, but has far-reaching consequences when attempting to truncate the corresponding SDEs, written in some gauge. Moreover, contrary to what happens in the perturbative calculation, even if one were to put together the non-perturbative expressions from these truncated SDEs to form a physical observable, the
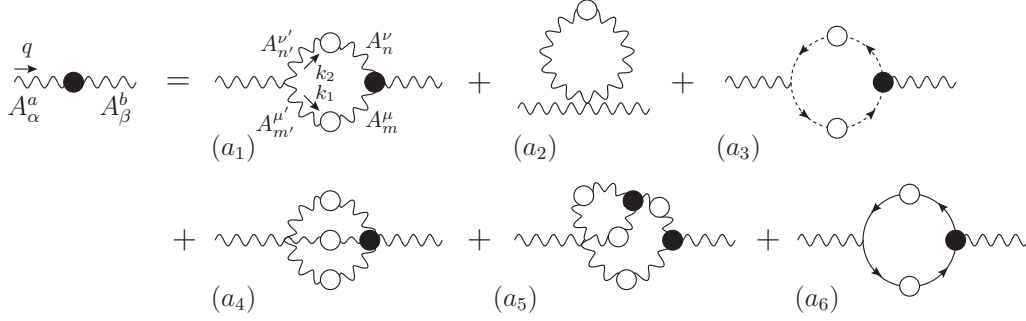
Fig. 69. The SDE satisfied by the gluon self-energy $-\Gamma_{AA}$. The symmetry factors of the diagrams are $s_{a_1} = s_{a_2} = s_{a_6} = 1/2$, $s_{a_3} = s_{a_4} = -1$, $s_{a_5} = 1/6$.

gauge-cancellations may not go through completely, because the process of the truncation might have distorted them. Thus, there is a high probability of ending up with a residual gauge-dependence infesting one's non-perturbative prediction for a physical observable.

ii. In Abelian gauge theories the Green's functions satisfy linear WIs, which in non-Abelian theories are replaced by the non-linear STIs, involving, in addition to the basic Green's functions of the theory, various composite ghost operators. In order to appreciate how the fact that the Green's functions satisfy STIs may complicate the truncation procedure of the SDEs, let us consider the simplest STI (and WI in this case) satisfied by the photon and gluon self-energies alike, namely

$$q^\alpha \Pi_{\alpha\beta}(q) = 0. \tag{8.1}$$

Eq. (8.1) is without a doubt the most fundamental statement at the level of Green's functions that one can obtain from the BRST symmetry: it affirms the transversality of the gauge-boson self-energy, be it a photon or a gluon, and is valid both perturbatively to all orders as well as non-perturbatively. The problem stems from the fact that in the SDE of $\Pi_{\alpha\beta}$ enter higher order Green's functions, namely the fully-dressed fundamental vertices of the theory. It is these latter Green's functions that in the Abelian context satisfy WIs, whereas in the non-Abelian context satisfy STIs. Thus, whereas in QED the validity of Eq. (8.1) can be easily seen at the level of the SDE, simply because $q^\alpha \Gamma_\alpha(p, p + q) = e\left[S^{-1}(p + q) - S^{-1}(p)\right]$, in QCD proving Eq. (8.1) explicitly, *i.e.*, by contracting with q^α the SDE of the gluon self-energy, requires a subtle conspiracy of all the (fully-dressed) vertices appearing in it. Truncating the SDE naively usually amounts to leaving out some of these vertices, and, as a result, Eq. (8.1) is compromised.

To be concrete, consider the SDE for the gluon propagator shown in Fig. 69; then, Eq. (8.1) translates at the level of the SDE to the statement

$$q^\alpha \sum_{i=1}^{6} (a_i)_{\alpha\beta} = 0. \tag{8.2}$$

The diagrammatic verification of (8.2), *i.e.*, through contraction of the individual graphs by q^α, is practically very difficult, essentially due to the complicated STIs satisfied by the vertices involved. The most typical example of such an STI is the one satisfied by the conventional three-gluon vertex of Eq. (2.94). In addition, some of the pertinent STIs are either too complicated,

such as that of the conventional four-gluon vertex, or they cannot be cast in a particularly convenient form. For instance, in the case of the conventional gluon-ghost vertex, $\Gamma_\mu(q,p)$, the STI that one may obtain formally for $q^\mu\Gamma_\mu(q,p)$ is the sum of two terms, one of which is $p^\mu\Gamma_\mu(q,p)$; this clearly limits its usefulness in applications.

The main practical consequence of these complicated STIs is that one cannot truncate (8.2) in any obvious way without violating the transversality of the resulting $\Pi_{\alpha\beta}(q)$. For example, keeping only graphs (a_1) and (a_2) is not correct even perturbatively, since the ghost loop is crucial for the transversality of $\Pi_{\alpha\beta}$ already at one-loop; adding (a_3) is still not sufficient for a SD analysis, because (beyond one-loop) $q^\alpha[(a_1)+(a_2)+(a_3)]_{\alpha\beta}\neq 0$.

Last but not least, these complications are often compounded by additional problems related to the loss of multiplicative renormalizability and the inability to form renormalization-group invariant quantities.

It should be clear by now that the difficulties pointed out are exactly of the type that can be circumvented using a PT approach (in fact, a gauge invariant truncation scheme for SDEs has been the original motivation for introducing it). In particular, the way *e.g.*, point (*i*) is resolved, for the prototype case of the gluon self-energy, is the following. The BFG is a privileged gauge, in the sense that it is selected *dynamically* when the gluon self-energy is embedded into a physical observable (such as an on-shell test amplitude). Specifically, the BFG captures the net propagator-like subamplitude emerging after QED-like conditions have been replicated inside the test-amplitude, by means of the PT procedure. Thus, once the PT rearrangements have taken place, the propagator is removed from the amplitude and is studied in isolation: one considers the SDE for the background gluon self-energy, $\widehat{\Pi}_{\alpha\beta}$, at $\xi_Q = 1$. Solving the SDE in the BFG eliminates any gauge-related exchanges between the solutions obtained for $\widehat{\Pi}_{\alpha\beta}$ and other Green's functions, when put together to form observables; thus, the solutions are free of gauge artifacts. Regarding point (*ii*), all full vertices appearing in the new SDE satisfy now Abelian WIs; as a result, gluonic and ghost contributions are *separately* transverse, within *each* order in the "dressed-loop" expansion (as was already noticed in our discussion of the BFM two-loop gluon self-energy, see subsection 3.3.2). Thus, as we will see explicitly in the next section, it is much easier to devise truncation schemes that manifestly preserve the validity of Eq. (8.1). Let us for now turn to the problem of how the PT algorithm can be generalized to a non-perturbative setting.

8.2 *The PT algorithm for Schwinger-Dyson equations*

The BV (re)formulation of the PT algorithm reveals its true power when dealing with the problem of constructing (off-shell) PT Green's functions without resorting to fixed order calculations, as it is the case when dealing with SDEs [182,183,169]. In particular, it is immediate to realize that the (one-loop) procedure described at the end of the previous section for the various QCD Green's functions carries over practically unaltered to the construction of the corresponding (non-perturbative) SDEs. This is basically due to the following three crucial observations [182,183,169]:

∗ the pinching momenta will be always determined from the tree-level decomposition given in

Eq. (2.38);

* their action is completely fixed by the structure of the STIs they trigger;

* the kernels encountered in these STIs are those appearing in the corresponding BQIs; thus, it is always possible to write the result of the action of the pinching momenta in terms of the auxiliary Green's functions of the BQIs.

The only operational difference is that, in the case of the SDEs for vertices, *all* external legs will be *off-shell*. This is of course unavoidable, because the (fully dressed) vertices are nested inside, for example, the SDE of the off-shell gluon self-energy, (see Fig. 69); thus, all legs are off-shell (the external leg because the physical four-momentum (q^2) is off-shell, and the legs inside the diagrams because they are irrigated by the virtual off-shell momenta). As a result, the equations of motion employed in the previous section in order to drop some of the resulting terms cannot be used in this case; therefore, the corresponding contributions, proportional to inverse self-energies, do not vanish, and form part of the resulting BQI.

Thus the PT rules for the construction of SDEs may be summarized as follows:

* For the SDEs of vertices, with *all three* external legs *off-shell*, the pinching momenta, coming from the only external three-gluon vertex undergoing the decomposition (2.38), generate four types of terms: one of them, corresponding to the term (b') in Eq. (7.25), is a genuine vertex-like contribution that must be included in the final PT answer for the vertex under construction, while the remaining three-terms will form part of the emerging BQI (and thus would be discarded from the PT vertex). These latter terms have a very characteristic structure, which facilitates their identification in the calculation. Specifically, one of them is always proportional to the auxiliary function $\Gamma_{\Omega A^*}$, while the other two are proportional to the inverse propagators of the fields entering into the two legs that did *not* undergo the decomposition of Eq. (2.38).

* In the case of the SDE for the gluon propagator, the pinching momenta will only generate pieces proportional to $\Gamma_{\Omega A^*}$; these terms should be discarded from the PT answer for the gluon two-point function (since they are exactly those that cancel against the contribution coming from the corresponding vertices), and will contribute instead to the corresponding BQI.

Thus, using these rules, and starting from the corresponding SDEs written in the Feynman gauge of the R_ξ, we will first derive the new SDEs for the $\widehat{\Gamma}_{AAA}$ vertex (the quark-gluon vertex $\widehat{\Gamma}_{A\psi\bar{\psi}}$) has been also explicitly constructed in [169]), and will then address the more complicated case of the SDE for the PT gluon propagator $\widehat{\Gamma}_{AA}$.

8.2.1 Three-gluon vertex

The SDE for the conventional three-gluon vertex is shown in Fig. 70. Before starting the calculation, let us emphasize that the purpose of this exercise is to generate dynamically the vertex
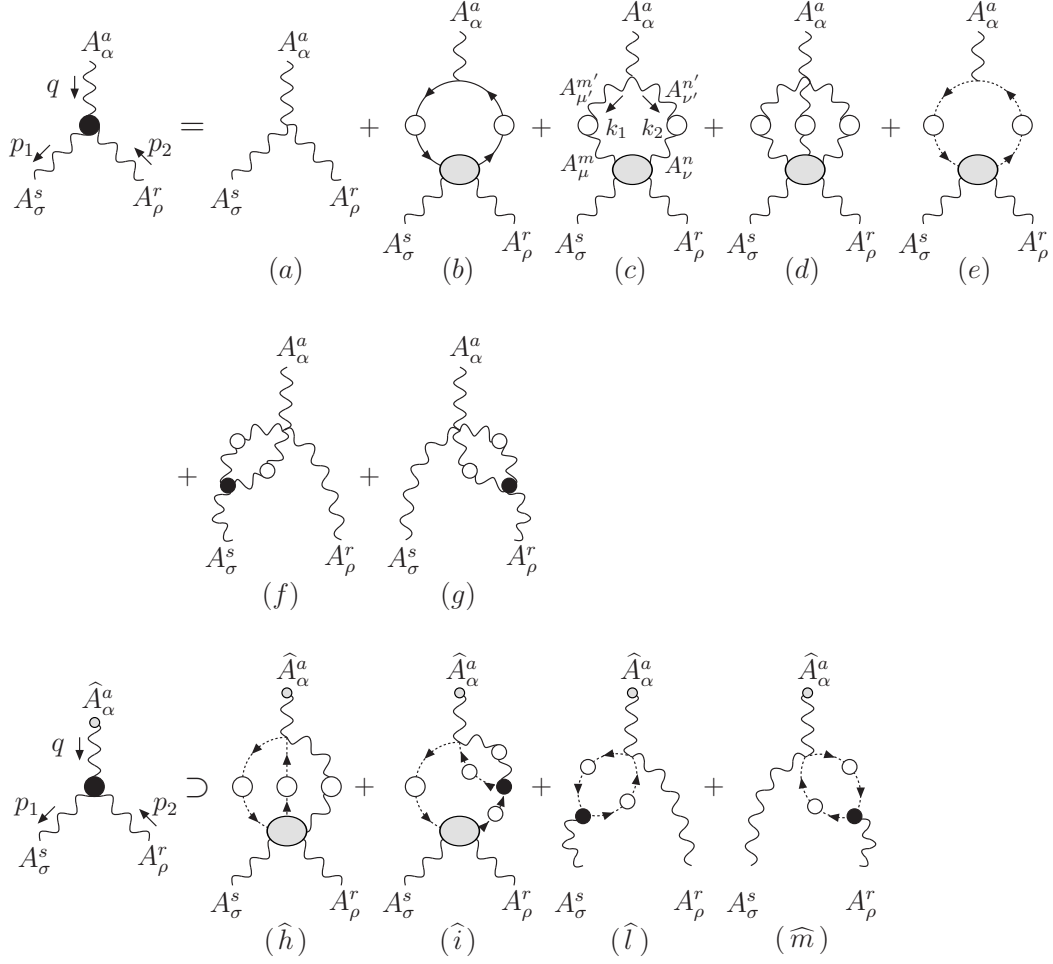
Fig. 70. The SDE of the three-gluon vertex. The symmetry factors of the R_ξ (first and second line of the figure) diagrams are $s(a,b) = 1$. $s(c) = 1/2$, $s(d) = 1/6$, $s(e) = -1$, $s(f,g) = 1/2$. In the third line we show the additional topologies present in the BFM version of the equation $[s(\widehat{h}, \widehat{i}, \widehat{l}, \widehat{m}) = -1]$, generated during the PT procedure.

$\Gamma_{\widehat{A}AA}$ and *not* the fully Bose-symmetric vertex [8,65] $\Gamma_{\widehat{A}\widehat{A}\widehat{A}}$ studied in Section 2. The reason for this is the fact that it is the former vertex that appears in the SDEs for the gluon propagator [see, e.g., diagram (d_1) in Fig. 77], making it the relevant vertex to be studied at this level.

We then begin by carrying out the decomposition of Eq. (2.38) to the tree-level vertex appearing in diagram (c), which will be the only one modified in our construction. Concentrating on the Γ^P part, we find

$$(c)^{\mathrm{P}} = g f^{amn'} g_{\alpha\nu'} \int_{k_1} \frac{1}{k_1^2} \Delta_{n'n}^{\nu'\nu}(k_2) k_1^\mu \mathcal{K}_{A_\mu^m A_\nu^n A_\rho^r A_\sigma^s}(k_2, p_2, -p_1), \tag{8.3}$$

where the kernel K_{AAAA} is shown in Fig. 71.

Using the STI (C.35) satisfied by this kernel, we obtain from Eq. (8.3) four terms, namely $(c)^{\mathrm{P}} = (s_1) + (s_2) + (s_3) + (s_4)$. Then, using Eqs (C.44) and (C.45), it is fairly straightforward to prove that

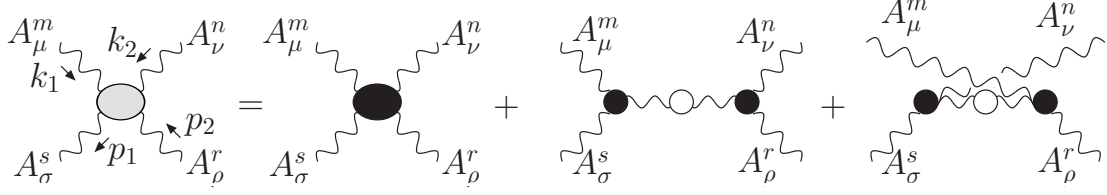Fig. 71. Skeleton expansion of the kernel appearing in the SDE for the three-gluon vertex [diagram (c) of Fig. 70]

$$(s_1) = -\Gamma_{\Omega_\alpha^a A_d^{*\gamma}}(-q)\Gamma_{A_\gamma^d A_\rho^r A_\sigma^s}(p_2, -p_1),$$
$$(s_2) = -\Gamma_{\Omega_\alpha^a A_\sigma^s A_d^{*\gamma}}(-p_1, p_2)\Gamma_{A_\gamma^d A_\rho^r}(p_2),$$
$$(s_3) = -\Gamma_{\Omega_\alpha^a A_\rho^r A_d^{*\gamma}}(p_2, -p_1)\Gamma_{A_\gamma^d A_\sigma^s}(p_1). \tag{8.4}$$

Evidently, the term (s_1) gives rise to the propagator-like contribution, [5] which, in the S-matrix PT, would be allotted to the new two-point function, $\widehat{\Gamma}_{AA}$. As for (s_2) and (s_3), they correspond to terms that would vanish on-shell, but now, due to the off-shell condition of the external legs, must be retained in the final answer.

Finally, let us consider the term (s_4), given by

$$(s_4) = gf^{am'n'}g_{\alpha\nu'}\int_{k_1} D^{m'm}(k_1)\Delta^{\nu'\nu}_{n'n}(k_2)\mathcal{K}_{c^m A_d^{*\gamma} A_\rho^r A_\sigma^s}(k_2, p_2, -p_1)\Gamma_{A_\gamma^d A_\nu^n}(k_2), \tag{8.5}$$

and show how it combines with the remaining R_ξ diagrams to generate the BFG vertex $\Gamma_{\widehat{A}AA}$. To this end, using Eq. (C.17) and the FPE satisfied by the kernel $\mathcal{K}_{cA^*AA}$, we can write $(s_4) = (s_{4a}) + (s_{4b})$, with

$$(s_{4a}) = -igf^{am'd}g_{\alpha\gamma}\int_{k_1} D^{m'm}(k_1)\mathcal{K}_{c^m A_d^{*\gamma} A_\rho^r A_\sigma^s}(k_2, p_2, -p_1),$$
$$(s_{4b}) = -gf^{am'n'}g_{\alpha\nu'}\int_{k_1} \delta^{dn'}\frac{k_2^{\nu'}}{k_2^2}D^{m'm}(k_1)\mathcal{K}_{c^m \bar{c}^d A_\rho^r A_\sigma^s}(k_2, p_2, -p_1). \tag{8.6}$$

The kernel $\mathcal{K}_{c\bar{c}AA}$ is defined by replacing in Eq. (C.36) every anti-field leg A^* by the corresponding anti-ghost field $\bar{c}$. First of all, notice that the apparently missing topologies $(\widehat{l})$ and $(\widehat{m})$ of Fig. 70 will be generated by the tree-level contribution appearing in the SDE of the auxiliary function Γ_{cAA^*}. To prove this, let us write

$$\mathcal{K}_{c^m A_d^{*\gamma} A_\rho^r A_\sigma^s}(k_2, p_2, -p_1) = \mathcal{K}'_{c^m A_d^{*\gamma} A_\rho^r A_\sigma^s}(k_2, p_2, -p_1) - igf^{dre'}g_\rho^\gamma\Gamma_{c^m A_\sigma^s \bar{c}^{e'}}(-p_1, \ell)D^{ee'}(\ell)$$
$$- igf^{dse}g_\sigma^\gamma D^{ee'}(\ell')\Gamma_{c^m A_\rho^r \bar{c}^{e'}}(p_2, -\ell'), \tag{8.7}$$

---

[5] Note that this term is identical to the one found in the construction of the SDE for the quark-gluon vertex [169]. This is the (all-order) manifestation of the PT process-independence (see 2.4.3): the propagator-like contributions do not depend on the details of the external (embedding) particles.
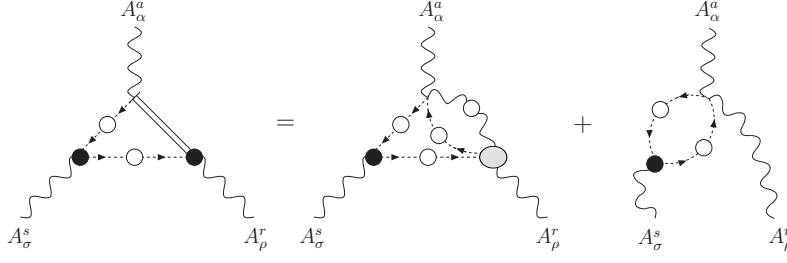
Fig. 72. The 1PR terms appearing in $\mathcal{K}_{c^m A_d^{*\gamma} A_\rho^r A_\sigma^s}$ contain a tree-level contribution generating the missing BFM topologies. Here we show the case for $(\widehat{l})$; a symmetric term generates $(\widehat{m})$. The first term on the rhs is part of the skeleton expansion of diagram $(\widehat{h})$ of Fig. 70. Notice that the lhs is simply a pictorial representation of the rhs: the anti-fields are static sources and do not propagate.

where the prime denotes that the Γ_{cAA^*} appearing in the corresponding 1PR terms starts at one-loop. We then find (see also Fig. 72)

$$
(s_{4a}) = (s'_{4a}) + (\widehat{l}) + (\widehat{m}),
$$
$$
(s'_{4a}) = -igf^{am'd}g_{\alpha\gamma}\int_{k_1} D^{m'm}(k_1)\mathcal{K}'_{c^m A_d^{*\gamma} A_\rho^r A_\sigma^s}(k_2, p_2, -p_1). \tag{8.8}
$$

Consider then the terms (s'_{4a}) and (s_{4b}). Their general structure suggests that (s'_{4a}) should give rise to the ghost quadrilinear vertex, while (s_{4b}), when added to diagram (e), should symmetrize the trilinear ghost gluon coupling. It turns out that this expectation is essentially correct, but its realization is not immediate, mainly due to the fact that the (s_{4b}) contains a tree-level instead of a full ghost propagator $[(k_2^2)^{-1}$ instead of $D(k_2)]$, while (s'_{4a}) can reproduce, at most, diagram $(\widehat{h})$ of Fig. 70, but not $(\widehat{i})$. The solution to this apparent mismatch is rather subtle: one must employ the SDE satisfied by the *ghost propagator*. This SDE is common to both the R_ξ-gauge and the BFM, given that there are no background ghosts.

To show how this works in detail, we add and subtract to the sum $(s'_{4a}) + (s_{4b})$ the missing term (see Fig. 73), obtaining

$$
(s'_{4a}) = -igf^{am'd}g_{\alpha\gamma}\int_{k_1} D^{m'm}(k_1)\left[\mathcal{K}'_{c^m A_d^{*\gamma} A_\rho^r A_\sigma^s}(k_2, p_2, -p_1)\right.
$$
$$
\left. - \Gamma'_{c^g A_d^{*\gamma}}(k_2)iD^{gg'}(k_2)\mathcal{K}_{c^m \bar{c}^{g'} A_\rho^r A_\sigma^s}(k_2, p_2, -p_1)\right]
$$
$$
= -igf^{am'd}g_{\alpha\gamma}\int_{k_1} D^{m'm}(k_1)\mathcal{K}^{\text{full}}_{c^m A_d^{*\gamma} \psi\bar{\psi}}(k_2, p_2, -p_1)
$$
$$
(s_{4b}) = -gf^{am'n'}g_\alpha^{\nu'}\int_{k_1}\left[\delta^{dn'}\frac{k_{2\nu'}}{k_2^2} - \Gamma'_{c^e A_{\nu'}^{*n'}}(k_2)D^{ed}(k_2)\right]\times
$$
$$
\times D^{m'm}(k_1)\mathcal{K}_{c^m \bar{c}^d A_\rho^r A_\sigma^s}(k_2, p_2, -p_1). \tag{8.9}
$$

Then, using Eq (C.40) (which can be safely done now, since tree-level contribution has been already taken into account)

$$
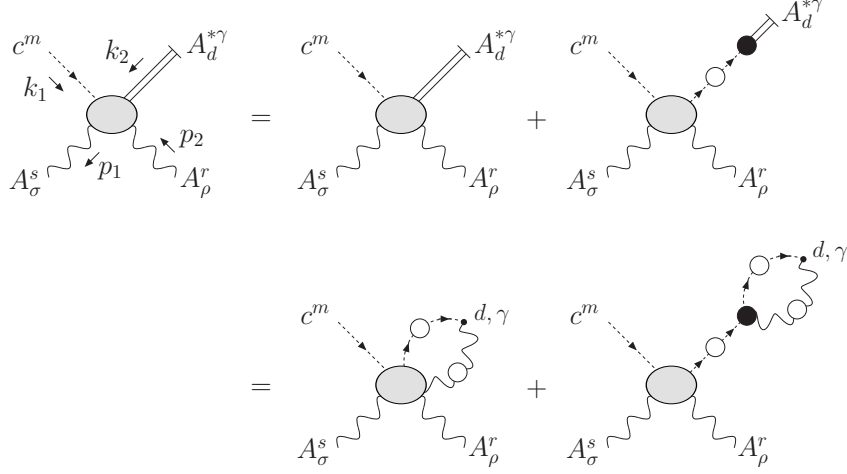(s'_{4a}) = (\widehat{h}) + (\widehat{i}). \tag{8.10}
$$

Fig. 73. Diagrammatic decomposition of the kernel $\mathcal{K}^{\text{full}}_{c^m A_d^{*\gamma} A_\rho^r A_\sigma^s}$ introduced in Eq. (8.9). The first term represents the kernel $\mathcal{K}'_{c^m A_d^{*\gamma} A_\rho^r A_\sigma^s}$; therefore the Γ_{cAA^*} appearing in the corresponding 1PR terms start at one-loop. The second term is the one added (and subtracted) to the original sum $(s'_{4a}) + (s_{4b})$. After replacing the gluon anti-field $A_d^{*\gamma}$ with the corresponding composite operator (second line), this kernel generates the BFM terms $(\hat{h}) + (\hat{i})$.

We finally turn to (s_{4b}) and consider the ghost SD equation of Fig. 74. One has

$$iD^{dn'}(k_2) = i\frac{\delta^{dn'}}{k_2^2} + i\frac{\delta^{dg}}{k_2^2}\left[-\Gamma'_{c^g \bar{c}^{g'}}(k_2)\right]iD^{g'n'}(k_2),\qquad(8.11)$$

where $\Gamma'_{c^g \bar{c}^{g'}}$ is given by $\Gamma_{c^g \bar{c}^{g'}}$ minus its tree-level part. Multiplying the above equation by k_2^2, using the FPE (C.1), and factoring out a $k_{2\nu'}$ we get the relation

$$k_{2\nu'}D^{dn'}(k_2) = \delta^{dn'}\frac{k_{2\nu'}}{k_2^2} - \Gamma'_{c^g A_{\nu'}^{*n'}}(k_2)D^{gd}(k_2).\qquad(8.12)$$

Therefore, we obtain

$$(s_{4b}) = -gf^{am'n'}\int_{k_1} k_{2\alpha}D^{m'm}(k_1)D^{n'n}(k_2)\mathcal{K}_{c^m \bar{c}^n A_\rho^r A_\sigma^s}(k_2, p_2, -p_1),\qquad(8.13)$$

so that

$$(s_{4b}) + (e) = (\hat{e}).\qquad(8.14)$$

Using the tree-level Feynman rules (see Appendix B), it is straightforward to establish that the graphs (b), (d), (f), and (g) can be converted to hatted ones automatically, and that $(c)^{\text{F}} = (\hat{c})$. Thus, collecting all the pieces we have, and using the standard PT decomposition (2.38) on the tree-level contribution (a), we get

$$\begin{aligned}
i\Gamma_{A_\alpha^a A_\rho^r A_\sigma^s}(p_2, -p_1) =& -\Gamma_{\Omega_\alpha^a A_d^{*\gamma}}(-q)\Gamma_{A_\gamma^d A_\rho^r A_\sigma^s}(p_2, -p_1) - \Gamma_{\Omega_\alpha^a A_\sigma^s A_d^{*\gamma}}(-p_1, p_2)\Gamma_{A_\gamma^d A_\rho^r}(p_2)\\
&-\Gamma_{\Omega_\alpha^a A_\rho^r A_d^{*\gamma}}(p_2, -p_1)\Gamma_{A_\gamma^d A_\sigma^s}(p_1) + [(\hat{a}) + (\hat{b}) + (\hat{c}) + (\hat{d}) + (\hat{e})\\
&+ (\hat{f}) + (\hat{g}) + (\hat{h}) + (\hat{i}) + (\hat{l}) + (\hat{m})]^{ars}_{\alpha\rho\sigma} - igf^{ars}\Gamma^{\text{P}}(p_2, -p_1).\quad(8.15)
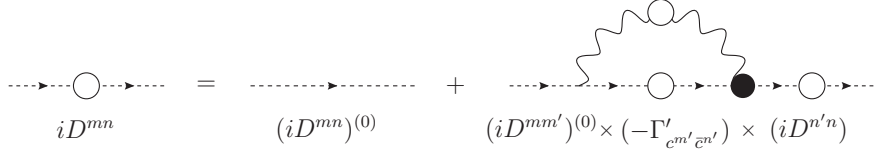\end{aligned}$$

Fig. 74. The SDE (8.11) satisfied by the ghost propagator.

As in the previous case, the sum of diagrams in the brackets is nothing but the kernel expansion of the SDE governing the vertex $\Gamma_{\widehat{A}AA}$, *i.e.*,

$$
\begin{aligned}
i\Gamma_{\widehat{A}^a_\alpha A^r_\rho A^s_\sigma}(p_2, -p_1) = {} & [(\widehat{a}) + (\widehat{b}) + (\widehat{c}) + (\widehat{d}) + (\widehat{e})) \\
& + (\widehat{f}) + (\widehat{g}) + (\widehat{h}) + (\widehat{i}) + (\widehat{l}) + (\widehat{m})]^{ars}_{\alpha\rho\sigma}.
\end{aligned}
\tag{8.16}
$$

This, in turn, implies that Eq. (8.15) represents the BQI of Eq. (C.48) up to the last (tree-level) term on the rhs. Of course, this tree-level discrepancy is to be expected, since the PT algorithm cannot possibly work at tree-level if the external legs are amputated, as is the case in the SDEs we are considering. To be sure, if we start from the tree-level $\Gamma^{(0)}_{AAA}$ only, *i.e.*, without hooking (two of) the external legs to (conserved) external currents, we can still carry out the decomposition of Eq. (2.38), but the Γ^P term will have nothing to act upon.

In summary, the application of the PT to the conventional SDE for the trilinear gluon vertex (*i*) has converted the initial kernel expansion [graphs (*a*) through (*g*) in Fig. 70] into the graphs corresponding to the kernel expansion of the vertex $\Gamma_{\widehat{A}AA}$; (*ii*) all other pinching terms extracted from the original diagram (*c*) are precisely the combinations of auxiliary Green's functions appearing in the BQI that relates the two vertices.

Notice at this point that the skeleton expansion of the multi-particle kernels appearing in the SDE for $\Gamma_{\widehat{A}AA}$ is still written in terms of the conventional fully dressed vertices and propagators (involving only quantum fields). Thus, Eq. (8.16) is not manifestly dynamical, *i.e.*, it does not involve the same unknown quantities on the right and left hand side. Specifically, in order to convert (8.16) into a genuine SDE, one has two possibilities, both involving the use of the above BQI: (*i*) substitute the lhs of Eq. (8.15) into the rhs of Eq. (8.16) and solve for the conventional Γ_{AAA} vertex, or (*ii*) invert Eq. (8.15) and use it to convert every Γ_{AAA} vertex appearing in the rhs of Eq. (8.16) into a $\Gamma_{\widehat{A}AA}$ vertex. It would seem that the latter option is operationally more cumbersome, especially taking into account that a similar procedure has to be followed for all the Green's functions that appear in the coupled system of SDEs that one considers.

8.2.2 *The gluon propagator*

In this section we turn to the SDE of the gluon self-energy. From a technical point of view, the construction is somewhat more involved compared to that of the the vertices, simply because the PT decomposition of Eq. (2.38) must be carried out on both sides of the self-energy diagram. Put in a different way, now we must convert not one, but two external gluons to background gluons. This is achieved through a procedure consisting of the following three basic steps [183,169]: (*i*) Start with the conventional SDE for Γ_{AA} and convert (through pinching) A to $\widehat{A}$; this generates
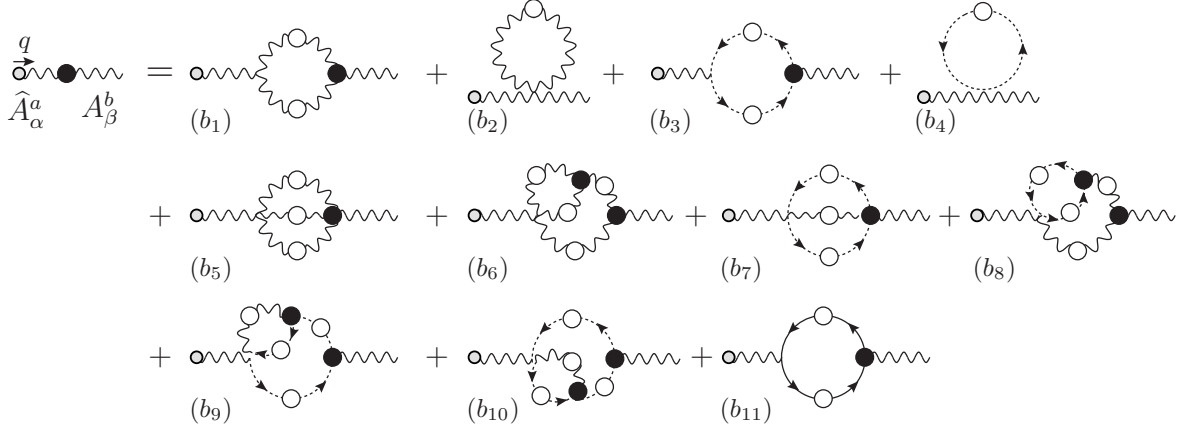
Fig. 75. The SDE satisfied by the gluon self-energy $-\Gamma_{\widehat{A}A}$. The symmetry factors of the diagrams are $s(b_1, b_2, b_6) = 1/2$, $s(b_5) = 1/6$, and all the remaining diagrams have $s = -1$.

the SDE for $\Gamma_{\widehat{A}A}$. (ii) Use the symmetry of $\Gamma_{\widehat{A}A}$ to interchange legs: $\Gamma_{\widehat{A}A} = \Gamma_{A\widehat{A}}$; this saves a lot of algebra in the next step. (iii) In the SDE for $\Gamma_{A\widehat{A}}$, convert (through pinching) A to $\widehat{A}$; this generates the SDE for $\Gamma_{\widehat{A}\widehat{A}}$. Let us now go over these steps in detail.

$*$ *First step*

The starting point is diagram (a_1) of Fig. 69. Following the PT procedure, we decompose the tree-level three-gluon vertex according to (2.38), and concentrate on the pinching part,

$$(a_1)^{\mathrm{P}} = ig f^{amn'} g_{\alpha\nu'} \int_{k_1} \frac{1}{k_1^2} \Delta^{\nu'\nu}_{n'n}(k_2) k_1^\mu \Gamma_{A_\mu^m A_\nu^n A_\beta^b}(k_2, -q). \tag{8.17}$$

The application of the STI of Eq. (C.10), together with Eq. (C.17) and the FPE (C.5), results in the following terms

$$
\begin{aligned}
(a_1)^{\mathrm{P}} &= ig f^{am'n'} g_{\alpha\nu'} \int_{k_1} D^{m'm}(k_1) \Delta^{\nu'\nu}_{n'n}(k_2) \Gamma_{c^m A_\nu^n A_d^{*\gamma}}(k_2, -q) \Gamma_{A_\gamma^d A_\beta^b}(q) \\
&\quad + g f^{am'd} g_{\alpha\gamma} \int_{k_1} D^{m'm}(k_1) \Gamma_{c^m A_\beta^b A_d^{*\gamma}}(-q, k_2) \\
&\quad - ig f^{am'n'} g_{\alpha\nu'} \int_{k_1} \delta^{dn'} \frac{k_2^{\nu'}}{k_2^2} D^{m'm}(k_1) \Gamma_{c^m A_\beta^b \bar{c}^d}(-q, k_2) \\
&= (s_1) + (s_2) + (s_3). \tag{8.18}
\end{aligned}
$$

Using the SDE of the auxiliary function $\Gamma_{\Omega A^*}$, shown in Eq. (C.44), one has immediately that

$$(s_1) = -i\Gamma_{\Omega_\alpha^a A_d^{*\gamma}}(q) \Gamma_{A_\gamma^d A_\beta^b}(q). \tag{8.19}$$

This corresponds to half of the pinching contribution coming from the vertex in the S-matrix PT.

As far as the (s_2) and (s_3) terms are concerned, let us start by adding and subtracting to them
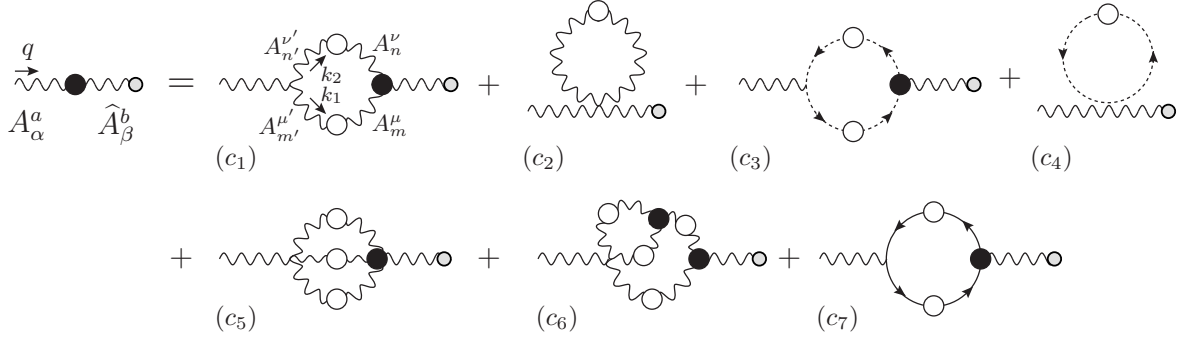
Fig. 76. The SDE satisfied by the gluon self-energy $-\Gamma_{A\widehat{A}}$. The symmetry factors of the diagrams are $s(c_1, c_2, c_6) = 1/2$, $s(c_3, c_4, c_7) = -1$, $s(c_5) = 1/6$.

the expression needed to convert the tree-level ghost propagator of (s_3) into a full one; making use of the ghost SDE (8.12), we obtain

$$
\begin{aligned}
(s_2) =&\, -g f^{am'd} g_{\alpha\gamma} \int_{k_1} i D^{m'm}(k_1) \Big[i\Gamma_{c^m A^b_\beta A^{*\gamma}_d}(-q, k_2) \\
&+ \Gamma'_{c^{g'} A^{*\gamma}_d}(k_2) D^{g'g}(k_2) \Gamma_{c^m A^b_\beta \bar{c}^g}(-q, k_2) \Big], \\
(s_3) =&\, -i g f^{am'n'} \int_{k_1} k_{2\alpha} D^{m'm}(k_1) D^{n'n}(k_2) \Gamma_{c^m A^b_\beta \bar{c}^n}(-q, k_2).
\end{aligned}
\tag{8.20}
$$

The second term symmetrizes the trilinear ghost-gluon coupling, and one has

$$
(s_3) + (a_3) = (b_3),
\tag{8.21}
$$

where (b_3) is shown in Fig. 75. The term (s_2) will finally generate all the remaining terms. To see how this happens, we denote by (s_{2a}) and (s_{2b}) the two terms appearing in the square brackets of (s_2), and concentrate on the first one. Making use of the SDE (C.43) satisfied by the auxiliary function Γ_{cAA^*}, and the decomposition (C.46) of the kernel appearing in the latter, we get

$$
\begin{aligned}
(s_{2a}) =&\, g^2 f^{am'd} f^{mdb} g_{\alpha\beta} \int_{k_1} D^{m'm}(k_1) \\
&+ g^2 f^{am'd} f^{dn's'} g_{\alpha\sigma'} \int_{k_1} \int_{k_3} D^{m'm}(k_1) \Delta^{\sigma'\sigma}_{s's}(k_3) D^{n'n}(k_4) \mathcal{K}_{c^m A^b_\beta A^s_\sigma \bar{c}^n}(-q, k_3, k_4) \\
=&\, (b_4) + (b_7) + (b_8) + (b_{10}).
\end{aligned}
\tag{8.22}
$$

For the second term, using the SDE satisfied by Γ_{cA^*}, shown in Eq. (C.42), we obtain

$$
\begin{aligned}
(s_{2b}) =&\, i g^2 f^{am'd} f^{dse} g^\sigma_\alpha \int_{k_1} \int_{k_3} D^{m'm}(k_1) \Delta^{\sigma\sigma'}_{ss'}(k_3) D^{ee'}(k_4) \Gamma_{c^{g'} A^{\sigma'}_{s'} \bar{c}^{e'}}(k_3, k_4) D^{g'g}(k_2) \times \\
&\times \Gamma_{c^m A^b_\beta \bar{c}^g}(-q, k_2) \\
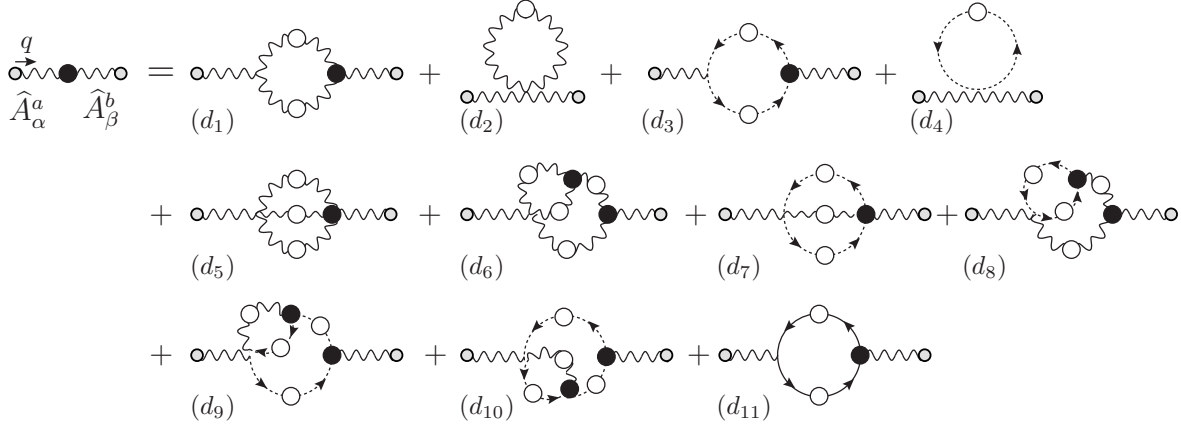=&\, (b_9).
\end{aligned}
\tag{8.23}
$$

Fig. 77. The SDE satisfied by the gluon self-energy $-\Gamma_{\widehat{A}\widehat{A}}$. The symmetry factors are the same as the one described in Fig. 75.

Finally, since the diagrams (a_2), (a_4) (a_5), and (a_6) carry over directly to the corresponding BFM ones (b_2), (b_5), (b_6), and (b_{11}), and given that $(a_1)^{\mathrm{F}} = (b_1)$, we have the final identity

$$(s_2) + (s_3) + \left[(a_1)^{\mathrm{F}} + \sum_{i=2}^{6}(a_i)\right] = \sum_{i=1}^{11}(b_i), \tag{8.24}$$

and therefore

$$-\Gamma_{A_\alpha^a A_\beta^b}(q) = -i\Gamma_{\Omega_\alpha^a A_d^{*\gamma}}(q)\Gamma_{A_\gamma^d A_\beta^b}(q) - \Gamma_{\widehat{A}_\alpha^a A_\beta^b}(q), \tag{8.25}$$

which is the BQI of Eq. (C.38).

* *Second step*

The second step in the propagator construction is to employ the obvious relation

$$\Gamma_{\widehat{A}_\alpha^a A_\beta^b}(q) = \Gamma_{A_\alpha^a \widehat{A}_\beta^b}(q), \tag{8.26}$$

that is to interchange the background and quantum legs (the SDE for the self-energy $-\Gamma_{A\widehat{A}}$ is shown in Fig. 76). This apparently trivial operation introduces a considerable simplification. First of all, it allows for the identification of the pinching momenta from the usual PT decomposition of the (tree-level) Γ appearing in diagram (c_1) of Fig. 76 [something not directly possible from diagram (b_1)]; thus, from the operational point of view, we remain on familiar ground. In addition, it avoids the need to employ the (formidably complicated) BQI for the four-gluon vertex; indeed, the equality between diagrams (c_5), (c_6), (c_7) of Fig. 76, and (d_5), (d_6), (d_{11}) of Fig. 77, respectively, is now immediate [as it was before, between the diagrams (a_4), (a_5), (a_6) and (b_5), (b_6), (b_{11}), respectively].

* *Third step*

We now turn to diagram (c_1) and concentrate on its pinching part, given by

$$(c_1)^{\mathrm{P}} = igf^{amn'}g_{\alpha\nu'}\int_{k_1}\frac{1}{k_1^2}\Delta_{n'n}^{\nu'\nu}(k_2)k_1^\mu\Gamma_{A_\mu^m A_\nu^n \widehat{A}_\beta^b}(k_2, -q). \tag{8.27}$$
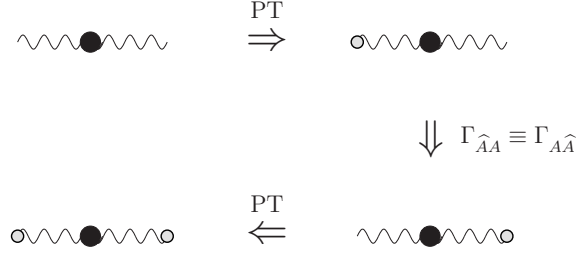
189

Fig. 78. Summary of the PT procedure employed for the construction of the new SDE describing the gluon propagator.

Notice the appearance of the full BFM vertex $\Gamma_{AA\widehat{A}}$ instead of the standard Γ_{AAA} (in the R_ξ). The STI satisfied by the former vertex has been derived in Eq. (C.30). Now, the first three terms, (s_1), (s_2) and (s_3), appearing in this STI, will give rise to PT contributions exactly equal to those encountered in first step described above, the only difference being that the A_β^b field appearing there is now a background field $\widehat{A}_\beta^b$. Thus, following exactly the reasoning described before, we find [see again Fig. 77 for the diagrams corresponding to each (d_i)]

$$(s_1) \rightarrow -i\Gamma_{\Omega_\alpha^a A_\epsilon^{*e}}(q)\Gamma_{A_\epsilon^e \widehat{A}_\beta^b}(q),$$

$$(s_2) + (s_3) + (c_3) = (d_3) + (d_4) + (d_7) + (d_8) + (d_9) + (d_{10}). \tag{8.28}$$

For the term (s_4) we have instead

$$(s_4) \rightarrow g^2 f^{am'e} f^{ebm} g_{\alpha\mu'} g_{\beta\mu} \int_{k_1} \Delta_{m'm}^{\mu'\mu}(k_1). \tag{8.29}$$

Clearly this has a seagull-like structure; in particular, it is immediate to prove that when added to (c_2) it will convert it into (d_2)

$$(s_4) + (c_2) = (d_2). \tag{8.30}$$

Thus, since as always $(c_1)^{\mathrm{F}} = (d_1)$ we get

$$(s_2) + (s_3) + (s_4) + \left[(c_1)^{\mathrm{F}} + \sum_{i=2}^{7}(c_i)\right] = \sum_{i=1}^{11}(d_i), \tag{8.31}$$

and therefore

$$-\Gamma_{A_\alpha^a \widehat{A}_\beta^b}(q) = -i\Gamma_{\Omega_\alpha^a A_\epsilon^{*e}}(q)\Gamma_{A_\epsilon^e \widehat{A}_\beta^b}(q) - \Gamma_{\widehat{A}_\alpha^a \widehat{A}_\beta^b}(q), \tag{8.32}$$

which is the BQI of Eq. (C.38). This concludes our proof.

In Fig. 78 we summarize the steps that allowed the successful construction of the SDE for the PT propagator.

8.3   *The new Schwinger-Dyson series*

We will now have a closer look at the structure and physical consequences of the new SDEs obtained in the previous subsections. We focus, for concreteness, on the SDE for the gluon

propagator; notice, however, that the following analysis applies with minimal modification to the three-point functions SDEs.

The PT rearrangement gives rise dynamically to the new SD series (shown in Fig. 79) which has the following characteristics:

∗ On the rhs, it is as if the external gluons had been converted dynamically into background gluons, since we have graphs that are made out of new vertices, which coincide precisely with the BFG ones. Notice, however, an important point: the graphs contain inside them the same gluon propagator as before, namely Δ.

∗ On the lhs, we have the sum of three terms: in addition to the term $\Delta^{-1}(q^2)P_{\alpha\beta}(q)$, present there from the beginning, we have two additional contributions, $2G(q^2)\Delta^{-1}(q^2)P_{\alpha\beta}(q)$ and $G^2(q^2)\Delta^{-1}(q^2)P_{\alpha\beta}(q)$, which appear during the PT rearrangement of the rhs (and are subsequently carried to the lhs). Thus, the term appearing on the lhs of the new SDE is $\Delta^{-1}(q^2)[1+G(q^2)]^2 P_{\alpha\beta}(q)$, with the function $G(q^2)$ defined through

$$\Gamma_{\Omega_\alpha A_\beta^*}(q) = ig_{\alpha\beta}G(q^2) + \dots, \tag{8.33}$$

where the omitted terms are proportional to $q_\alpha q_\beta$ (and therefore irrelevant due to transversality).

Summarizing, one may write schematically

$$\Delta^{-1}(q^2)[1 + G(q^2)]^2 P_{\alpha\beta}(q) = q^2 P_{\alpha\beta}(q) + i\sum_{1=1}^{11}(d_i)_{\alpha\beta}, \tag{8.34}$$

which is nothing but a rewriting of the BQI relating the background and the conventional gluon two-point function [see Eq. (C.39)]. Equivalently, one can cast Eq. (8.34) into a more conventional form by isolating on the lhs the inverse of the unknown quantity, thus writing

$$\Delta^{-1}(q^2)P_{\alpha\beta}(q) = \frac{q^2 P_{\alpha\beta}(q) + i\sum_{1=1}^{11}(d_i)_{\alpha\beta}}{[1 + G(q^2)]^2}. \tag{8.35}$$

8.3.1 The PT as a gauge-invariant truncation scheme: advantages over the conventional SDEs

The new SD series of Eqs (8.34) and (8.35) has a very special structure. In order to gain a deeper understanding of the situation at hand, let us first step back and consider the one-loop case again, in which the application of the intrinsic PT algorithm to the (one-loop) gluon self-energy, amounts to carry out the PT rearrangement of Eq. (2.71) of the two elementary three-gluon vertices appearing in diagram (a) of Fig. 9, thus getting the result

$$\widehat{\Pi}_{\alpha\beta}^{(1)}(q) = \frac{1}{2}g^2 C_A \left\{ \int_k \frac{\Gamma_{\alpha\mu\nu}^F \Gamma_\beta^{F\ \mu\nu}}{k^2(k+q)^2} - \int_k \frac{2(2k+q)_\alpha(2k+q)_\beta}{k^2(k+q)^2} \right\} - 2g^2 C_A \int_k \frac{q^2 P_{\alpha\beta}(q)}{k^2(k+q)^2}. \tag{8.36}$$
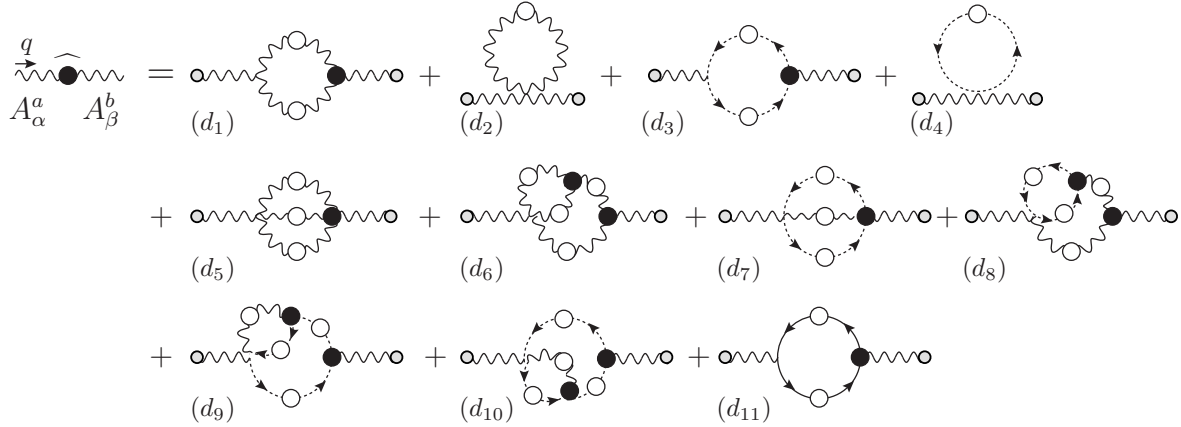
Fig. 79. The new SD series projected out dynamically by the PT algorithm.

It is elementary to verify that each of the two terms in braces on the rhs of the equation above are transverse; thus, the PT rearrangement has created three manifestly transverse structures. That in itself might not be so important, if it were not for the fact that, as we know, these structures admit a special diagrammatic representation and a unique field-theoretic interpretation. Specifically, the two terms in the square bracket correspond precisely to diagrams $(\widehat{a})$ and $(\widehat{b})$ of Fig. 80, defining the one-loop gluon self-energy in the BFG, while the third term on the rhs of Eq. (8.36) is the one-loop expression of the special auxiliary Green's function $\Gamma_{\Omega A^*}$, identified in the BV formulation of the PT (or, more precisely, the $g_{\alpha\beta}$ part of this latter function); it corresponds to diagram (c) in Fig. 80. Since the one-loop PT self-energy is obtained by simply dropping this last term from the rhs of Eq. (8.36), one has

$$\Pi_{\alpha\beta}^{(1)}(q) = \widehat{\Pi}_{\alpha\beta}^{(1)}(q) + (c)_{\alpha\beta}, \tag{8.37}$$

which, as we know from Section 7 [see Eq. (7.31)], is nothing but the one-loop version of the BQI of Eq. (C.39) [and, therefore, also of the SDE (8.34)]. Let us now focus on $\Pi_{\alpha\beta}^{(1)}(q)$, and imagine for a moment that no ghost loops may be considered when computing it, *i.e.*, the graphs $(\widehat{b})_{\alpha\beta}$ must be omitted; in a SDE context this "omission" would amount to a "truncation" of the series. One may still obtain a *transverse* approximation for $\Pi_{\alpha\beta}^{(1)}(q)$ with no ghost-loop, given by

$$\Pi_{\alpha\beta}^{(1)}(q) = (\widehat{a})_{\alpha\beta} + (c)_{\alpha\beta} = 4q^2 f(q^2) P_{\alpha\beta}(q), \tag{8.38}$$

where the function $f(q^2)$ has been defined in Eq. (3.37). Interestingly enough, the PT rearrangement offers already at one-loop the ability to truncate gauge-invariantly, *i.e.*, preserving the transversality of the truncated answer.

Turning now to the full SDE (8.35), one can prove that the special transversality property found above holds true non-perturbatively, with gluonic and ghost contributions separately transverse, and, in addition, no mixing between the one- and two-loop dressed diagrams. In the BFM context this property has been already seen explicitly for the divergent parts of the two-loop gluon self-energy diagrams (Section 3); here we will show that this is in fact a consequence of the all-orders WIs satisfied by the full vertices appearing in the diagrams defining the PT self-energy (Fig. 77). There are four fully dressed vertices appearing in $\widehat{\Pi}$, whose WIs we need: $\Gamma_{\widehat{A}AA}$, $\Gamma_{c\widehat{A}\bar{c}}$, $\Gamma_{\widehat{A}AAA}$ and, finally, $\Gamma_{c\widehat{A}\bar{c}A}$. One way to derive their WIs is to differentiate

192

Fig. 80. The conventional one-loop gluon self-energy before (first line) and after (second line) the PT rearrangement.

the WI functional of Eq. (7.18) with respect to the corresponding field combination where the background field has been replaced by the corresponding gauge parameter ϑ. On the other hand, a much more expeditious way is to derive the corresponding tree-level WIs, and then use linearity to generalize them to all orders, as we do in QED. Either way, one obtains the following results

$$
\begin{aligned}
q^{\alpha}\Gamma_{\widehat{A}^a_\alpha A^m_\mu A^n_\nu}(k_1, k_2) &= gf^{amn}\left[\Delta^{-1}_{\mu\nu}(k_1) - \Delta^{-1}_{\mu\nu}(k_2)\right], \\
q^{\alpha}\Gamma_{c^n \widehat{A}^a_\alpha \bar{c}^m}(q, -k_1) &= igf^{amn}\left[D^{-1}(k_2) - D^{-1}(k_1)\right], \\
q^{\alpha}\Gamma_{\widehat{A}^a_\alpha A^b_\beta A^m_\mu A^n_\nu}(k_1, k_2, k_3) &= gf^{adb}\Gamma_{A^d_\beta A^m_\mu A^n_\nu}(k_2, k_3) + gf^{adm}\Gamma_{A^d_\mu A^b_\beta A^n_\nu}(k_1, k_3) \\
&\quad + gf^{adn}\Gamma_{A^d_\nu A^b_\beta A^m_\mu}(k_1, k_2), \\
q^{\alpha}\Gamma_{c^n \widehat{A}^a_\alpha A^b_\beta \bar{c}^m}(q, k_3, -k_1) &= gf^{adb}\Gamma_{c^n A^d_\beta \bar{c}^m}(q + k_3, -k_1) + gf^{adm}\Gamma_{c^n A^b_\beta \bar{c}^d}(k_3, q - k_1) \\
&\quad + gf^{adn}\Gamma_{c^d A^b_\beta \bar{c}^m}(k_3, -k_1).
\end{aligned}
\tag{8.39}
$$

Armed with these WIs, we can now prove that the four groups identified (at two-loop level) in Eq. (3.41) are in fact independently transverse even non-perturbatively.

Let's start from the one-loop dressed gluonic contributions given by the combination of $(d_1) + (d_2)$ of Fig. 77. Using the first WI of Eq. (8.39) we get

$$
q^{\beta}(d_1)^{ab}_{\alpha\beta} = -g^2 C_A \delta^{ab} q_\alpha \int_k \Delta^\mu_\mu(k),
\tag{8.40}
$$

while, by simply computing the divergence of the tree-level vertex $\Gamma_{\widehat{A}\widehat{A}AA}$ given in Appendix B, we get

$$
q^{\beta}(d_2)^{ab}_{\alpha\beta} = g^2 C_A \delta^{ab} q_\alpha \int_k \Delta^\mu_\mu(k),
\tag{8.41}
$$

so that clearly

$$
q^{\beta}\left[(d_1) + (d_2)\right]^{ab}_{\alpha\beta} = 0.
\tag{8.42}
$$

Exactly the same procedure yields for the one-loop dressed ghost contributions

$$q^\beta (d_3)^{ab}_{\alpha\beta} = -2g^2 C_A \delta^{ab} q_\alpha \int_k D(k),$$

$$q^\beta (d_4)^{ab}_{\alpha\beta} = 2g^2 C_A \delta^{ab} q_\alpha \int_k D(k),$$

(8.43)

and therefore

$$q^\beta \left[(d_3) + (d_4) \right]^{ab}_{\alpha\beta} = 0.$$

(8.44)

For the two-loop dressed contributions the proof is only slightly more involved. We begin with the gluonic contributions. Using the third WI of Eq. (8.39) in diagram (d_5), after appropriate manipulation of the the terms produced, and taking into account the symmetry factor of $1/6$, we obtain

$$q^\beta (d_5)^{ab}_{\alpha\beta} = \frac{i}{2} g f^{bmn} \Gamma^{(0)}_{\widehat{A}^a_\alpha A^m_{\mu'} A^g_{\gamma'} A^e_{\epsilon'}} \int_k\!\!\int_\ell \Delta^{\epsilon'\epsilon}(k) \Delta^{\gamma'\gamma}(\ell + k) \Gamma_{A^g_\gamma A^e_\epsilon A^n_\mu}(k,\ell) \Delta^{\mu'\mu}(\ell + q).$$

(8.45)

Similarly, after making use the full Bose symmetry of the three-gluon vertex, graph (d_6) gives

$$q^\beta (d_6)^{ab}_{\alpha\beta} = \frac{i}{2} g f^{bmn} \Gamma^{(0)}_{\widehat{A}^a_\alpha A^m_{\mu'} A^g_{\gamma'} A^e_{\epsilon'}} \int_k\!\!\int_\ell \Delta^{\epsilon'\epsilon}(k) \Delta^{\gamma'\gamma}(\ell + k) \Gamma_{A^g_\gamma A^e_\epsilon A^{n'}_{\nu'}}(k,\ell) \times$$

$$\times \left[\Delta^{\nu'\nu}(\ell) g^{\mu'}_\nu - \Delta^{\mu'\mu}(\ell + q) g^{\nu'}_\mu \right].$$

(8.46)

The first term in the square brackets vanishes (the integral is independent of q, and therefore the free Lorentz index β cannot be saturated). Furthermore, the second term is exactly equal but opposite in sign to the one appearing in Eq. (8.45), so that we obtain

$$q^\beta \left[(d_5) + (d_6) \right]^{ab}_{\alpha\beta} = 0.$$

(8.47)

Finally, we turn to the two-loop dressed ghost contributions. Using the last WI of Eq. (8.39), we see that the divergence of diagram (d_7) gives us three terms, namely

$$q^\beta (d_7)^{ab}_{\alpha\beta} = -i\Gamma^{(0)}_{\widehat{A}^a_\alpha A^{r'}_{\rho'} \bar{c}^{n'}} \int_k\!\!\int_\ell D^{m'm}(\ell + k) D^{n'n}(\ell + q) \Delta^{\rho'\rho}_{r'r}(k) \times$$

$$\times \left[g f^{ber} \Gamma_{c^n A^e_\rho \bar{c}^e}(k - q, -\ell - k) + g f^{ben} \Gamma_{c^e A^r_\rho \bar{c}^m}(k, -\ell - k) \right.$$

$$\left. + g f^{ben} \Gamma_{c^n A^r_\rho \bar{c}^n}(k, -q - \ell - k) \right].$$

(8.48)

Each one of these three terms can be easily shown to cancel exactly against the individual divergences of the remaining three graphs. To see this in detail, let us consider for example diagram (d_{10}) and use the WI (8.39) to obtain

$$q^\beta (d_{10})^{ab}_{\alpha\beta} = -i g f^{bmn} \Gamma^{(0)}_{c^{m'} \widehat{A}^a_\alpha A^{r'}_{\rho'} \bar{c}^{n'}} \int_k\!\!\int_\ell D^{m'm}(\ell + k) D^{n'd}(\ell + q) D^{d'n}(\ell + k + q) \Delta^{\rho'\rho}_{r'r}(k) \times$$

$$\times \Gamma_{c^d A^r_\rho \bar{c}^{d'}}(k, -q - \ell - k) \left[D^{-1}(\ell + k + q) - D^{(-1)}(\ell + k) \right].$$

(8.49)

Then, we see that the second inverse propagator in the square brackets will give rise to a q-independent integral that will integrate to zero, while the first term will cancel exactly the third

term appearing in the square brackets of Eq. (8.48). It is not difficult to realize that the same pattern will be encountered when calculating the divergence of diagrams (d_8) and (d_9), so that one has the identity

$$q^\beta \left[(d_7) + (d_8) + (d_9) + (d_{10})\right]^{ab}_{\alpha\beta} = 0. \tag{8.50}$$

This concludes the proof of the special transversality property of $\widehat{\Pi}^{ab}_{\alpha\beta}(q)$, showing that gluon and ghost loops are separately transverse, and that dressing loops of different orders do not mix.

This last property has far-reaching practical consequences for the treatment of the SD series [183,169]. Specifically, it furnishes a systematic gauge-invariant truncation scheme that preserves the transversality of the answer. In fact, we can drastically reduce the number of coupled SDEs that must be included in order to maintain the gauge (or BRST) symmetry of the theory intact, as reflected, for example, in the validity of Eq.(8.1). For example, keeping only the diagrams in the first group, we obtain the truncated SDE

$$\Delta^{-1}(q^2)P_{\alpha\beta}(q) = \frac{q^2 P_{\alpha\beta}(q) + i[(d_1) + (d_2)]_{\alpha\beta}}{[1 + G(q^2)]^2}, \tag{8.51}$$

and from Eq. (8.42) we know that $[(d_1) + (d_2)]_{\alpha\beta}$ is transverse, *i.e.*,

$$[(d_1) + (d_2)]_{\alpha\beta} = (d-1)^{-1}[(d_1) + (d_2)]^\mu_\mu P_{\alpha\beta}(q). \tag{8.52}$$

Thus, the transverse projector $P_{\alpha\beta}(q)$ appears *exactly* on both sides of (8.51); one may subsequently isolate the scalar cofactors on both sides, obtaining a scalar equation of the form

$$\Delta^{-1}(q^2) = \frac{q^2 + i[(d_1) + (d_2)]^\mu_\mu}{[1 + G(q^2)]^2}. \tag{8.53}$$

A truncated equation similar to (8.51) may be written for any other of the four groups previously isolated, or for sums of these groups, without compromising the transversality of the answer. The price one has to pay for this advantageous situation is that one must consider, in addition, the equation determining the scalar function $G(q^2)$. This price is, however, rather modest, since one can approximate this function via a dressed-loop expansion [see, *e.g.*, Fig. C.1 together with Eq. (C.44)], without jeopardizing the transversality of $\Pi_{\alpha\beta}(q)$, given that $[1 + G(q^2)]^2$ affects only the size of the scalar prefactor.

Thus, in the case of pure Yang-Mills, within this new formulation, the minimum number of equations that one must consider is only two: The SDE for the gluon self-energy, given by the first gauge-invariant subset *only* (*i.e.*, $[(d_1) + (d_2)]_{\alpha\beta}$ in Fig. 79), and the SDE for the full three-gluon vertex, shown in Fig. 70 (which is instrumental in assuring the gauge invariance of the subset chosen). This is to be contrasted to what happens within the conventional formulation: there the SDEs for *all* vertices must be considered, or else Eq. (8.1) is violated (which is what usually happens).

8.3.2 *Some important theoretical and practical issues*

We now turn to some additional points that, due to their theoretical and practical relevance, deserve further elaboration.

It is important to emphasize that the analysis presented here does *not* furnish a simple diagrammatic truncation, analogous to that of the gluon self-energy, for the SDE of the three gluon vertex $\Gamma_{\widehat{A}AA}$, shown in Fig. 70. Thus, if one were to truncate the SDE for the three-gluon vertex by keeping any subset of the graphs appearing in Fig.70, one would violate the validity of the *all-order* WI of $\Gamma_{\widehat{A}AA}$ [Eq. (8.39) first line]; this, in turn, would lead immediately to the violation of Eq. (8.1), thus making the entire truncation scheme collapse.

The strategy one should adopt is instead the following (see also the discussion in the next section). Given that the proposed truncation scheme hinges crucially on the validity of the WI of $\Gamma_{\widehat{A}AA}$, one should start out with an approximation that manifestly preserves it. The way to enforce this, familiar to the SDE practitioners already from the QED era, is to resort to the "gauge-technique" [184], namely "solve" the WI. Specifically, one must express the three-gluon vertex as a functional of the corresponding self-energies, in such a way that (by construction) its WI is automatically satisfied. For example, an Ansatz with this property would be

$$
\Gamma_{\widehat{A}_\alpha A_\mu A_\nu}(k_1, k_2) = \Gamma^{(0)}_{\widehat{A}_\alpha A_\mu A_\nu}(k_1, k_2) - i \frac{(k_2 - k_1)_\alpha}{k_2^2 - k_1^2} \left[\Pi_{\mu\nu}(k_2) - \Pi_{\mu\nu}(k_1) \right]. \tag{8.54}
$$

Contracting the rhs with $q_\alpha = (k_1 + k_2)_\alpha$ yields automatically the first WI of Eq. (8.39). Thus, the minimum amount of ingredients for initiating a *self-consistent* non-perturbative treatment is the SD for the gluon self-energy, consisting of $[(d_1) + (d_2)]_{\alpha\beta}$, supplemented by an Ansatz for the three-gluon vertex like the one given in (8.54). Note that the "gauge-technique" leaves the transverse (*i.e.*, automatically conserved) part of the vertex undetermined. This is where the SDE for the vertex enters; it is used precisely to determine the transverse parts. Specifically, following standard techniques [45,65], one must expand the vertex into a suitable tensorial basis, consisting of fourteen independent tensors, and then isolate the transverse subset. This procedure will lead to a large number of coupled integral equations, one for each of the form-factors multiplying the corresponding tensorial structures, which may or may not be tractable. However, at this point, one may simplify the resulting equations (*e.g.*, linearize, etc) without jeopardizing the transversality of $\Pi_{\alpha\beta}$, which only depends on the "longitudinal" part of the vertex, *i.e.*, the one determined by (8.54). Thus, the transverse parts will be approximately determined, but gauge invariance, as captured by $q^\alpha \Pi_{\alpha\beta} = 0$, will remain exact.

Note by the way that the methodology described above constitutes, even to date, the standard procedure even in the context of QED, where the structure of the SDE is much simpler, given that the SDE for the photon contains one single graph [diagram (a_6) in Fig. 69], and the photon-electron vertex satisfies automatically a naive all-order WI. Thus, while the PT approach described here replicates QED-like properties at the level of the SDEs of QCD, admittedly a striking fact in itself, does not make QCD easier to solve than QED.

One should appreciate an additional point: any attempt to apply the approach described above in the context of the conventional SDE is bound to lead to the violation of the transversality of $\Pi_{\alpha\beta}$, because (*i*) the vertices satisfy complicated STI's instead of the WIs of Eq. (8.39), a fact that makes the application of the "gauge-technique" impractical, and (*ii*) even if one came up with the analogue of Eq. (8.54) for all vertices, one should still keep all self-energy diagrams in Fig. 69 to guarantee that $q^\alpha \Pi_{\alpha\beta} = 0$. From this point of view, the improvement of the PT approach over the standard formulation becomes evident.

Finally, one should be aware of the fact that there is no a-priori guarantee that the gauge-

invariant subset kept (*i.e.*, $[(d_1) + (d_2)]_{\alpha\beta}$) capture necessarily most of the dynamics, or, in other words, that they represent the numerically dominant contributions (however, for a variety of cases it seems to be true, see next section). But, the point is that one can *systematically* improve the picture by including more terms, without worrying that the initial approximation is plagued with artifacts, originating from the violation of the gauge invariance or of the BRST symmetry.

Now, in going from Eq. (8.34) to Eq. (8.35) one essentially chooses to retain the original propagator $\Delta(q)$ as the unknown quantity, to be dynamically determined from the SDE. There is, of course, an alternative strategy: one may define a new "variable" from the quantity appearing on the lhs (8.34), namely

$$\widehat{\Delta}(q) \equiv \left[1 + G(q^2)\right]^{-2} \Delta(q), \tag{8.55}$$

which leads to a new form for (8.34),

$$\widehat{\Delta}^{-1}(q^2)P_{\alpha\beta}(q) = q^2 P_{\alpha\beta}(q) + i \sum_{i=1}^{11} (d_i)_{\alpha\beta}. \tag{8.56}$$

Obviously, the special transversality properties established above hold as well for Eq. (8.56); for example, one may truncate it gauge-invariantly as

$$\widehat{\Delta}^{-1}(q^2)P_{\alpha\beta}(q) = q^2 P_{\alpha\beta}(q) + i[(d_1) + (d_2)]_{\alpha\beta}. \tag{8.57}$$

Should one opt for treating $\widehat{\Delta}(q)$ as the new unknown quantity, then an additional step must be carried out: one must use (8.55) to rewrite the entire rhs of (8.56) in terms of $\widehat{\Delta}$ instead of Δ, *i.e.*, carry out the replacement $\Delta \rightarrow [1 + G]^2 \, \widehat{\Delta}$ *inside* every diagram on the rhs of Eq. (8.56) that contains Δ's.

Thus, while Eq. (8.51) furnishes a gauge-invariant approximation for the conventional gluon self-energy $\Delta(q)$, Eq. (8.56) is the gauge-invariant approximation for the effective PT self-energy $\widehat{\Delta}$. The crucial point is that one may switch from one to the other by means of Eq. (8.55). For practical purposes this means, for example, that one may reach a gauge-invariant approximation not just for the PT quantity (BFG) but also for the *conventional* self-energy computed in the Feynman gauge (RFG). Eq. (8.55), which is the all-order generalization of the one-loop relation given in Eq. (8.37), plays an instrumental role in this entire construction, allowing one to convert the SDE series into a dynamical equation for either $\widehat{\Delta}(q)$ or $\Delta(q)$.

Let us end this section by observing that the new SDEs constructed in the previous subsections have been dynamically projected out in the BFG, which captures, as usual, the net gauge-independent and universal (*i.e.*, process-independent) contribution contained in any physical quantity. In practice, however, one would like to be able to truncate gauge-invariantly (*i.e.*, maintaining transversality) sets of SDEs written in different gauges. This becomes particularly relevant, for example, when one attempts to compare SDE predictions with lattice simulations, carried out usually in the Landau gauge, as we do in the next section.

This can be achieved by using the GPT algorithm described in subsection 3.6. As described there, the GPT modifies the starting point of the PT algorithm distributing differently the longitudinal momenta between $\Gamma^{\rm F}_{\alpha\mu\nu}$ and $\Gamma^{\rm P}_{\alpha\mu\nu}$. Specifically, the non-pinching part, *i.e.*, the analogue of $\Gamma^{\rm F}_{\alpha\mu\nu}$, must satisfy, instead of (2.40), a WI whose rhs is the difference of two inverse tree-level

propagators in the gauge one wishes to consider. In the context of SDEs, one starts out with the conventional SDE in the chosen gauge, carrying out the generalized PT vertex decomposition. Then, the action of the corresponding $\Gamma^{\mathrm{P}}_{\alpha\mu\nu}$ projects one to the corresponding BFM gauge. This new SD series contains full vertices that, even though they are in a different gauge, satisfy the same QED-like WIs given in Eq. (8.39). Therefore, the truncation properties of this SDE are the same as those just discussed for the case of the Feynman gauge. The analogy is completed by realizing that the BQIs in the corresponding gauge allow one to switch back and forth from the conventional to the BFM Green's function. Thus, one may obtain, for example, transverse approximations for the gluon propagator in the conventional Landau gauge by studying the SDE written in the BFM Landau gauge, computing the $[1 + G(q^2)]^2$ in the same gauge, *i.e.*, by employing Eq. (8.35) and using for the diagrams on its rhs the BFM Feynman rules in the Landau gauge.

9 Applications part II: Infrared properties of QCD Green's functions and dynamically generated gluon mass

The generation of mass gaps in QCD is one of the most fundamental problems in particle physics. In part the difficulty lies in the fact that the symmetries governing the QCD Lagrangian prohibit the appearance of mass terms at tree-level for all fundamental degrees of freedom and, provided that these symmetries are not violated through the procedure of regularization, this masslessness persists to all orders in perturbation theory. Thus, mass generation in QCD becomes an inherently non-perturbative problem, whose tackling requires the use of rather sophisticated calculational tools and approximation schemes [27].

Whereas the generation of quark masses is intimately connected with the breaking of chiral symmetry [185], Cornwall argued long ago [7] that an effective gluon mass can be generated *dynamically*, while preserving the local $SU(3)_c$ invariance of QCD, in close analogy to what happens in QED$_2$ (Schwinger model) [186], where the photon acquires a mass without violating the Abelian gauge symmetry (see discussion below). The gluon mass furnishes, at least in principle, a regulator for all infrared (IR) divergences of QCD. It must be emphasized that the gluon mass is not a directly measurable quantity, and that its value is determined by relating it to other dimensionful non-perturbative parameters, such as the string tension, glueball masses, gluon condensates, and the vacuum energy of QCD [187].

Since gluon mass generation is a purely non-perturbative effect, the most standard way for studying it in the continuum is through the SDEs governing the relevant Green's functions, and most importantly the gluon self-energy. One of the cornerstones in the original analysis of [7] was the insistence on preserving, at every level of approximation, crucial properties such as gauge-invariance, gauge-independence, and invariance under the renormalization group. With this motivation, a physical gluon propagator, $\widehat{\Delta}_{\mu\nu}$, was derived through the systematic rearrangement of Feynman graphs, which led to the birth of the PT. As the reader knows very well by now, the self-energy $\widehat{\Pi}_{\mu\nu}$ of this propagator is gauge-independent, and captures the leading logarithms of the theory, exactly as happens with the vacuum polarization in QED. The central result of [7] was that, when solving a simplified (one-loop inspired) SDE governing the PT propagator, one finds (under special assumptions for the form of the three-gluon vertex) solutions that are free of the Landau singularity, and reach a finite (non-vanishing) value in the deep IR. These solutions may be successfully fitted by a "massive" propagator of the form $\Delta^{-1}(q^2) = q^2 + m^2(q^2)$; the crucial characteristic, enforced by the SDE itself, is that $m^2(q^2)$ is not "hard", but depends non-trivially on the momentum transfer q^2. Specifically, $m^2(q^2)$ is a monotonically decreasing function, starting at a non-zero value in the IR ($m^2(0) > 0$) and dropping "sufficiently fast" in the deep UV.

Arguments based on the Operator Product Expansion (OPE) suggest that $m^2(q^2)$ should display power-law running, of the type $m^2(q^2) \sim \langle G^2 \rangle / q^2$, where $\langle G^2 \rangle$ is the gauge-invariant gluon condensate of dimension four: $\langle G^2 \rangle = \langle 0 | : G^a_{\mu\nu} G^{\mu\nu}_a : |0\rangle$. The unambiguous connection between the gluon mass and the gluon condensate established by Lavelle [188] merits further comments, because it constitutes another important success of the PT (for early calculations relating the gluon condensate and the effective gluon mass, see [189]). Specifically, the OPE was used to find the contribution of the $\langle G^2 \rangle$ condensate to the *conventional* gluon propagator, but the results turned out to be of limited usefulness: in addition to $\langle G^2 \rangle$, gauge-dependent conden-

sates involving the ghost fields c and $\bar{c}$ also appeared [188]. This calculation amply demonstrates that no physical results can be obtained from the OPE for a gauge-dependent quantity, such as the usual gluon propagator. Then, the same calculation was repeated for the PT propagator with very different results [190]: *only* the gauge-invariant condensate $\langle G^2 \rangle$ appeared, and in just such a way that it could be interpreted as contributing to a running mass. This result is equivalent to saying that, at large Euclidean momentum, $\widehat{\Delta}$ in $SU(N)$ behaves as

$$\widehat{\Delta}^{-1}(q) \to q^2 + \frac{17N}{18(N^2 - 1)} \frac{\langle G^2 \rangle}{q^2}. \tag{9.1}$$

Note that the multiplicative constant is positive, so this OPE correction has the right sign to represent a running mass, since the condensate $\langle G^2 \rangle$ is also positive (actually, powers of logarithms of q^2 can also occur, but we ignore them here). We emphasize also that this kind of power-law running has also been obtained from independent SDE studies [7,191,192].

An effective low-energy field theory for describing the gluon mass is the gauged non-linear sigma model known as "massive gauge-invariant Yang-Mills" [193], with Lagrangian density

$$\mathcal{L}_{\mathrm{MYM}} = \frac{1}{2} G^2_{\mu\nu} - m^2 \mathrm{Tr} \left[A_\mu - g^{-1} U(\theta) \partial_\mu U^{-1}(\theta) \right]^2, \tag{9.2}$$

where $A_\mu = \frac{1}{2i} \sum_a \lambda_a A^a_\mu$, the λ_a are the SU(3) generators (with $\mathrm{Tr} \lambda_a \lambda_b = 2\delta_{ab}$), and the $N \times N$ unitary matrix $U(\theta) = \exp \left[i \frac{1}{2} \lambda_a \theta^a \right]$ describes the scalar fields θ_a. Note that $\mathcal{L}_{\mathrm{MYM}}$ is locally gauge-invariant under the combined gauge transformation

$$A'_\mu = V A_\mu V^{-1} - g^{-1} \left[\partial_\mu V \right] V^{-1}, \qquad U' = U(\theta') = V U(\theta), \tag{9.3}$$

for any group matrix $V = \exp \left[i \frac{1}{2} \lambda_a \omega^a(x) \right]$, where $\omega^a(x)$ are the group parameters. One might think that, by employing (9.3), the fields θ_a can always be transformed to zero, but this is not so if the θ_a contain vortices. To use the $\mathcal{L}_{\mathrm{MYM}}$ in (9.2), one solves the equations of motion for U in terms of the gauge potentials and substitutes the result in the equations for the gauge potential. One then finds Goldstone-like massless modes, that, as we will see later in this section, are instrumental for enforcing gauge-invariance. This model admits vortex solutions [193], with a long-range pure gauge term in their potentials, which endows them with a topological quantum number corresponding to the center of the gauge group [Z_N for $SU(N)$], and is, in turn, responsible for quark confinement and gluon screening [193,194]. Specifically, center vortices of thickness $\sim m^{-1}$, where m is the induced mass of the gluon, form a condensate because their entropy (per unit size) is larger than their action. This condensation furnishes an area law to the fundamental representation Wilson loop, thus confining quarks. On the other hand, the adjoint potential shows a roughly linear regime followed by string breaking when the potential energy is about $2m$, corresponding to gluon screening [7,193]. Of course, $\mathcal{L}_{\mathrm{MYM}}$ is not renormalizable, and breaks down in the ultraviolet. This breakdown simply reflects the fact that the gluon mass m in (9.2) is assumed to be constant, while, as commented above, both the OPE and the SDEs furnish a momentum-dependent gluon mass, vanishing at large q^2.

The main theoretical tool for quantitative calculations in the infrared region of QCD, aside from the SDEs, is the lattice. In this framework, QCD is approximated by a lattice gauge theory with a non-zero lattice spacing and a finite space-time volume. In this way, one reduces
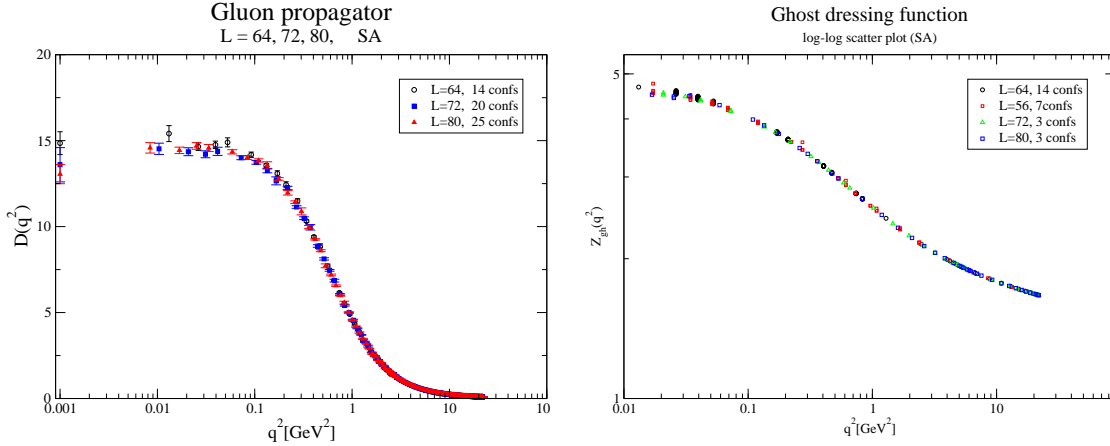
Fig. 81. (*Left panel*) The gluon propagator calculated for different lattice sizes at $\beta = 5.7$, from Ref. [195]. The data points drawn at $q^2 = 0.001$ represent the zero-momentum gluon propagator $\Delta(0)$. (*Right panel*) The ghost dressing function $Z_{\mathrm{gh}}(q^2) = q^2 D(q^2)$ for the same value of β. Notice that no power-law enhancement is observed for this quantity (see discussion in subsection 9.3).

the infinite functional integrals to a finite number of finite integrations, thus allowing the computation of correlation functions by numerical evaluations of these integrals via Monte-Carlo methods. The gluon and ghost propagators (in various gauges) have been studied extensively on the lattice [196–198]. To be sure, lattice simulations of gauge-dependent quantities are known to suffer from the problem of the Gribov copies, especially in the infrared regime, but it is generally believed that the effects are quantitative rather than qualitative. The effects of the Gribov ambiguity on the ghost propagator become more pronounced in the infrared, while their impact on the gluon propagator usually stay within the statistical error of the simulation [199–201]. It turns out that a large body of lattice data, produced over several years, confirm that the gluon propagator reaches indeed a finite (non-vanishing) value in the deep IR, as predicted by Cornwall. This rather characteristic behavior was already suggested by early studies, and has been firmly established recently using large-volume lattices, for pure Yang-Mills (no quarks included), for both $SU(2)$ [202] and $SU(3)$ [195] (see Fig. 81).

9.1 PT Schwinger-Dyson equations for the gluon and ghost propagators

As mentioned above, in the original analysis of gluon mass generation a simplified (and linearized) SDE was considered, that involved only the gluon self-energy, with no ghost loops included [7]. In this section we go one step further: we will exploit the powerful machinery offered by the SDE truncation scheme introduced in the previous section, in order to study gauge-invariantly the gluon-ghost system. In particular, we will show how to obtain self-consistently an infrared finite gluon propagator and a divergent (but non-enhanced) ghost propagator, in qualitative agreement with recent lattice data [195]. It is worth emphasizing that this behavior has also been confirmed within the Gribov-Zwanziger formalism [203].

In the previous sections we have employed the standard notation of the BV formalism, where all Green's functions are denoted by the letter Γ, and all incoming fields (together with their
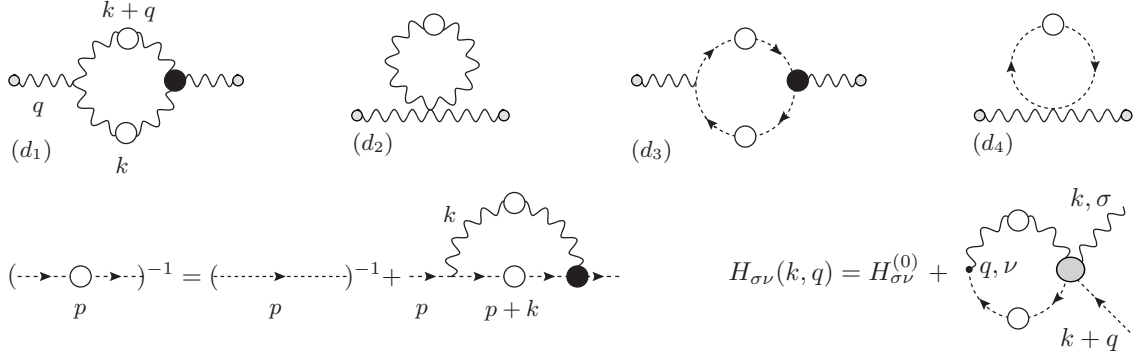
Fig. 82. The new SDE for the gluon-ghost system. Wavy lines with white blobs are full gluon propagators, dashed lines with white blobs are full-ghost propagators, black blobs are full vertices, and the gray blob denotes the scattering kernel. The circles attached to the external gluons denote that, from the point of view of Feynman rules, they are treated as background fields.

color and Lorentz indices) are explicitly displayed as subscripts. This notation is completely unambiguous, and is particularly suited for formal manipulations carried out so far, but is rather cumbersome for actual applications. Therefore, in this section we will switch to a simplified notation, that will result much more familiar to the SDE practitioners.

The SDEs for the gluon-ghost system are shown in Fig. 82. Evidently, we only consider the "one-loop dressed" contributions, leaving out (gauge-invariantly!) two-loop dressed diagrams. Indeed, as we know from the previous analysis this truncation preserves gauge-invariance, in the sense that it does *not* compromise the transversality of the gluon self-energy. In the case of pure (quark-less) QCD these SDEs read

$$\Delta^{-1}(q^2)P_{\mu\nu}(q) = \frac{q^2 P_{\mu\nu}(q) + i\sum_{i=1}^4 (d_i)_{\mu\nu}}{[1+G(q^2)]^2},$$

$$iD^{-1}(p^2) = p^2 + i\lambda \int_k \Gamma^\mu \Delta_{\mu\nu}(k)\mathbf{\Gamma}^\nu(p,k)D(p+k),$$

$$i\Lambda_{\mu\nu}(q) = \lambda \int_k H_{\mu\rho}^{(0)} D(k+q)\Delta^{\rho\sigma}(k) H_{\sigma\nu}(k,q), \tag{9.4}$$

where $\lambda = g^2 C_A$. Γ_μ is the standard (asymmetric) gluon-ghost vertex at tree-level, and $\mathbf{\Gamma}^\nu$ the fully-dressed one. $G(q^2)$ is the $g_{\mu\nu}$ component of the auxiliary two-point function $\Lambda_{\mu\nu}(q)$, and the function $H_{\sigma\nu}$ is defined diagrammatically in Fig. 82. $H_{\sigma\nu}$, and is related to the full gluon-ghost vertex by $q^\sigma H_{\sigma\nu}(p,r,q) = -i\mathbf{\Gamma}_\nu(p,r,q)$; at tree-level, $H_{\sigma\nu}^{(0)} = ig_{\sigma\nu}$.

Using the BFM rules of Appendix B to evaluate the diagrams (d_i), we find

$$(d_1) = \frac{\lambda}{2} \int_k \widetilde{\Gamma}_{\mu\alpha\beta} \Delta^{\alpha\rho}(k) \widetilde{\mathbf{\Gamma}}_{\nu\rho\sigma} \Delta^{\beta\sigma}(k+q),$$

$$(d_2) = -i\lambda g_{\mu\nu} \int_k \Delta^{\rho}_{\rho}(k) - i\lambda \left(\frac{1}{\xi} - 1\right) \int_k \Delta_{\mu\nu}(k),$$

$$(d_3) = -\lambda \int_k \widetilde{\Gamma}_{\mu} D(k) D(k+q) \widetilde{\mathbf{\Gamma}}_{\nu},$$

$$(d_4) = 2i\lambda g_{\mu\nu} \int_k D(k). \tag{9.5}$$

In the above formulas, $\widetilde{\Gamma}_{\mu\alpha\beta}(q, p_1, p_2) = \Gamma_{\mu\alpha\beta}(q, p_1, p_2) + \xi^{-1}\Gamma^{\mathrm{P}}_{\mu\alpha\beta}(q, p_1, p_2)$, where $\Gamma_{\mu\alpha\beta}$ is the standard QCD three-gluon vertex, and $\widetilde{\mathbf{\Gamma}}_{\mu\alpha\beta}$ its the fully-dressed version. Similarly, $\widetilde{\Gamma}_{\mu}$ denotes the *symmetric* gluon-ghost vertex at tree-level and $\widetilde{\mathbf{\Gamma}}_{\mu}$ its fully-dressed counterpart. Due to the Abelian all-order WIs that these two full vertices satisfy (for all ξ), namely

$$q^{\mu}\widetilde{\mathbf{\Gamma}}_{\mu\alpha\beta} = i\Delta^{-1}_{\alpha\beta}(k+q) - i\Delta^{-1}_{\alpha\beta}(k),$$

$$q^{\mu}\widetilde{\mathbf{\Gamma}}_{\mu} = iD^{-1}(k+q) - iD^{-1}(k), \tag{9.6}$$

one can easily demonstrate that $q^{\mu}[(d_1) + (d_2)]_{\mu\nu} = 0$ and $q^{\mu}[(d_3) + (d_4)]_{\mu\nu} = 0$ [90].

In order to make contact with the lattice results of [195,202] shown in Fig. 81, we will have to project the above system of coupled SDEs in the LG ($\xi = 0$). This is a subtle exercise, because one cannot set directly $\xi = 0$ in the integrals on the rhs of Eqs (9.5), due to the terms proportional to ξ^{-1}. Instead, one has to use the expressions for general ξ, carry out explicitly the set of cancellations produced when the terms proportional to ξ generated by the identity

$$k^{\mu}\Delta_{\mu\nu}(k) = -i\xi k_{\nu}/k^2, \tag{9.7}$$

are used to cancel ξ^{-1} terms, and set $\xi = 0$ only at the very end (this exercise is very similar to the BFM pinching we have carried at the one-loop level in subsection 3.5).

Let us focus on graph (d_1). First of all, it is relatively straightforward to establish that only the bare part of the full $\widetilde{\mathbf{\Gamma}}$ may furnish contributions proportional to ξ^{-1}. To see why this is so, consider the SDE of $\widetilde{\mathbf{\Gamma}}$ shown in Fig. 70. Evidently, the ξ^{-1} parts of the bare vertex are longitudinal; therefore, by virtue of Eq. (9.7), they cancel when contracted with an internal gluon propagator. Moreover, all kernels appearing in this SDE are regular in the LG, since all the fields entering are quantum ones (it is like computing the kernels in the normal LG, where no ξ^{-1} terms exist). Therefore, writing $\widetilde{\mathbf{\Gamma}}_{\nu\alpha\beta} = \widetilde{\Gamma}_{\nu\alpha\beta} + \widetilde{\mathbf{K}}_{\nu\alpha\beta}$, we have that $\widetilde{\mathbf{K}}_{\nu\alpha\beta}$ is regular in the limit $\xi \to 0$; we will denote by $\mathbf{K}_{\nu\alpha\beta}$ its value at $\xi = 0$. Thus, the only divergent contributions contained in (d_1) reside in the product $\widetilde{\Gamma}_{\mu\alpha\beta}\widetilde{\Gamma}_{\nu\rho\sigma}$. It is then a simple algebraic exercise to demonstrate that they cancel exactly against the part of the seagull diagram (d_2) proportional to ξ^{-1}. Thus, taking the LG limit we obtain

$$\sum_{i=1}^{2}(d_i)_{\mu\nu} = \lambda \left\{ \frac{1}{2} \int_k \Gamma_\mu^{\alpha\beta} \Delta_{\alpha\rho}^{\rm t}(k) \Delta_{\beta\sigma}^t(k+q) \mathbf{L}_\nu^{\rho\sigma} - \frac{9}{4} g_{\mu\nu} \int_k \Delta(k) \right.$$
$$\left. + \int_k \Delta_{\alpha\mu}^{\rm t}(k) \frac{(k+q)_\beta}{(k+q)^2} [\Gamma + \mathbf{L}]_\nu^{\alpha\beta} + \int_k \frac{k_\mu(k+q)_\nu}{k^2(k+q)^2} \right\}, \tag{9.8}$$

where $\Delta_{\mu\nu}^{\rm t}(q) = P_{\mu\nu}(q)\Delta(q^2)$, and $\mathbf{L}_{\mu\alpha\beta} \equiv \Gamma_{\mu\alpha\beta} + \mathbf{K}_{\mu\alpha\beta}$. Note that $\mathbf{L}_{\mu\alpha\beta}$ satisfies the WI

$$q^\mu \mathbf{L}_{\mu\alpha\beta} = {\rm P}_{\alpha\beta}(k+q)\Delta^{-1}(k+q) - {\rm P}_{\alpha\beta}(k)\Delta^{-1}(k), \tag{9.9}$$

as a direct consequence of (9.6). Therefore, one can verify that the lhs of (9.8) vanishes when contracted by q^μ, thus proving the announced transversality of this subset of graphs.

In order to proceed with our analysis, we need to furnish some information about the all-order vertices $\mathbf{L}_{\mu\alpha\beta}$, $\widetilde{\boldsymbol{\Gamma}}_\mu$, $\boldsymbol{\Gamma}_\mu$, and $H_{\mu\nu}$, entering in our system of SDEs. Of course, these vertices satisfy their own SDEs; so, in principle, one should couple all these equations together, to form an even more extended (and more intractable) system of coupled integral equations. As mention at the end of the previous section, given the practical difficulties of such a task, one resorts to the "gauge technique" [184,204,205], expressing the vertices as functionals of the various self-energies involved, in such a way as to satisfy by construction the correct WIs [6]. The Ansatz we will use for $\mathbf{L}_{\mu\alpha\beta}$ and $\widetilde{\boldsymbol{\Gamma}}_\mu$ is

$$\mathbf{L}_{\mu\alpha\beta} = \Gamma_{\mu\alpha\beta} + i\frac{q_\mu}{q^2} \left[\Pi_{\alpha\beta}(k+q) - \Pi_{\alpha\beta}(k) \right],$$
$$\widetilde{\boldsymbol{\Gamma}}_\mu = \widetilde{\Gamma}_\mu - i\frac{q_\mu}{q^2} \left[L(k+q) - L(k) \right]. \tag{9.10}$$

where L denotes the ghost self-energy, $D^{-1}(p^2) = p^2 - iL(p^2)$. As announced, the corresponding WIs, (9.6) and (9.6), are identically satisfied. On the other hand, for the conventional ghost-gluon vertex $\boldsymbol{\Gamma}_\mu$, appearing in the SDE of (9.4) we will use its tree-level expression, *i.e.*, $\Gamma_\nu \to \Gamma_\mu = -p_\mu$. Note that, unlike $\widetilde{\boldsymbol{\Gamma}}_\mu$, the conventional $\boldsymbol{\Gamma}_\mu$ satisfies a STI of rather limited usefulness; the ability to employ such a different treatment for $\widetilde{\boldsymbol{\Gamma}}_\mu$ and $\boldsymbol{\Gamma}_\mu$ without compromising gauge-invariance is indicative of the versatility of the new SD formalism used here. Finally, for $H_{\mu\nu}$ we use its tree-level value, $H_{\mu\nu}^{(0)} = ig_{\mu\nu}$.

The above Ansatz for the vertices needs further explaining, in view of the fact that it contains a longitudinally coupled pole $1/q^2$. We hasten to emphasize that the origin of this pole is not kinematic but rather dynamical, *i.e.*, it is a composite (bound-state) pole, whose presence is instrumental for the realization of the Schwinger mechanism in $d = 4$, leading to $\Delta^{-1}(0) \neq 0$. Given the importance of this mechanism to our approach, and the subtlety of the various concepts invoked, in the next subsection we present a brief overview of the Schwinger mechanism and its connection with the Goldstone phenomenon and the Higgs mechanism [206,207].

---

[6] As already mentioned, this method leaves the transverse (*i.e.*, identically conserved) part of the vertex undetermined. The transverse parts are known to be subleading in the IR, when a mass gap is formed, but must be supplied in the UV, because they are instrumental for enforcing the cancellation of the overlapping divergences and the correct renormalization group properties.
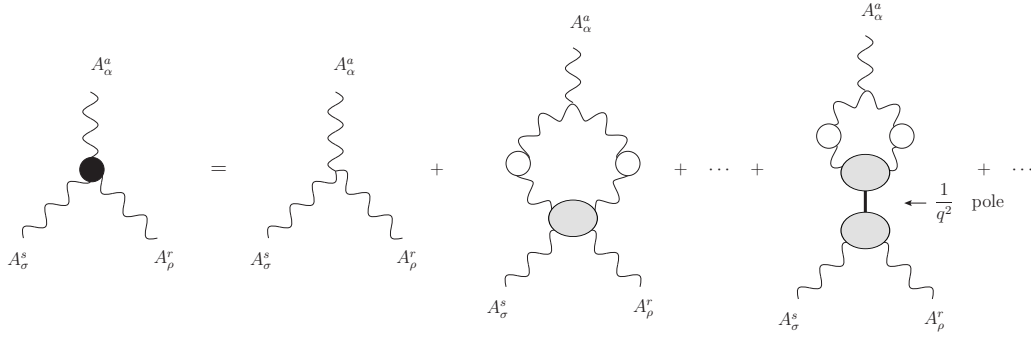
Fig. 83. The new SDE for the three-gluon vertex. Note that, as always, the kernels are one-particle irreducible; thus, the $1/q^2$ pole is not kinematic but dynamical, and is completely non-perturbative, *i.e.*, it vanishes to all orders in perturbation theory. Physically it corresponds to a longitudinally coupled massless composite excitation, acting as the (composite) Goldstone mode necessary for maintaining the local gauge invariance [208].

9.2   Schwinger mechanism, dynamical gauge-boson mass generation, and bound-state poles

According to Goldstone's theorem [209–211], the spontaneous breaking of a continuous global symmetry is accompanied by massless excitations, known as "Goldstone" particles [7]. Even though Goldstone's theorem is most frequently realized by a scalar field acquiring a vacuum expectation value, Nambu and Jona-Lasinio [212,213] introduced the notion of a dynamical Goldstone boson, demonstrating that the Goldstone mechanism can take place even when the Lagrangian does not include scalar fields. Thus, when chiral symmetry is broken, the associated Goldstone boson (the pion) is not an elementary excitation of a fundamental scalar field, but it is rather formed as a quark-antiquark bound state.

Goldstone's theorem, however, does not apply when the symmetry that is spontaneously broken is not global but local, accompanied by the associated massless gauge boson mediating the interaction (equivalently, one may say that the theorem does not apply in the presence of gauge-invariant long range forces). In such a case the Goldstone phenomenon is replaced by the Higgs phenomenon: no massless excitations appear in the spectrum, because the would-be Goldstone bosons combine with the transverse gauge boson to furnish the third helicity state of a massive spin one particle [214–218]. In addition, a massive scalar particle, the Higgs boson, also appears in the spectrum, and is instrumental for the renormalizability of the theory. Of course, both mechanisms may co-exist; if a local and a global symmetry are broken, one may have both phenomena. For example, the spontaneous breaking of a gauge symmetry through the Higgs mechanism gives mass to the gauge bosons; if, in addition, a global symmetry (e.g. chiral symmetry) is broken, then massless Goldstone bosons are present in the spectrum. As we will see in a moment, the opposite may also happen: the breaking of a global symmetry may furnish the Goldstone bosons that (in the absence of elementary scalar fields) will be absorbed by the gauge bosons, which will thus become massive.

Independently of the above consideration, and before the Higgs mechanism was even in-

---

[7]   In most cases these particles are scalars, and are hence referred to as bosons, even though spin $\frac{1}{2}$ Goldstone particles may exist, as for example when supersymmetry is spontaneously broken.

vented, Schwinger argued that the gauge invariance of a vector field does not necessarily imply zero mass for the associated particle, if the current vector coupling is sufficiently strong [186]. Schwinger's fundamental observation was that if (for some reason) the vacuum polarization tensor $\Pi_{\mu\nu}(q)$ acquires a pole at zero momentum transfer, then the vector meson becomes massive, even if the gauge symmetry forbids a mass at the level of the fundamental Lagrangian [219]. Indeed, casting the self-energy in the familiar form

$$\Delta^{\mu\nu}(q^2) = \left(g^{\mu\nu} - \frac{q^{\mu}q^{\nu}}{q^2}\right)\frac{-i}{q^2[1 + \mathbf{\Pi}(q^2)]}, \tag{9.11}$$

it is clear that if $\mathbf{\Pi}(q^2)$ has a pole at $q^2 = 0$ with positive residue μ^2, then the vector meson is massive, even though it is massless in the absence of interactions ($g = 0$, $\mathbf{\Pi} = 0$).

Indeed, there is *no* physical principle which would preclude $\mathbf{\Pi}(q^2)$ from acquiring a pole. Since bound states are expected to exist in most physical systems, and to produce poles in $\Pi_{\mu\nu}$ at time-like momenta, one may suppose that for sufficiently strong binding, the mass of such a bound state will be reduced to zero, thus generating a mass for the vector meson without interfering with gauge invariance. Schwinger demonstrated his general ideas in two-dimensional massless spinor QED ("Schwinger model"), which, by virtue of the special properties of the Dirac algebra at $d = 2$, is explicitly solvable: $\Pi_{\mu\nu}$ *does* indeed have a pole at $q^2 = 0$, and the photon acquires a mass, $\mu^2 = e^2/\pi$ (in $d = 2$, e has dimensions of mass) [8].

Perhaps the most appealing feature of the Schwinger mechanism is that the appearance of the required pole may happen for purely dynamical reasons, and, in particular, without the need to introduce fundamental scalar field in the Lagrangian. In fact, the Higgs mechanism can be viewed as just a *very special realization* of the Schwinger mechanism: the vacuum expectation value v of a canonical scalar field coupled to the vector meson gives rise to tadpole contributions to $\mathbf{\Pi}(q^2)$, which produce a pole. Thus, the Higgs mechanism corresponds to the special case where the residue of the pole is saturated by v^2, furnishing a gauge-boson mass $\mu^2 = 2g^2v^2$; the pole required is provided by the would-be Goldstone particles, which decouple from the spectrum.

In order to employ the Schwinger mechanism in realistic field theories, ultimately one must be able to demonstrate that a pole is generated somehow. Of course, the Higgs mechanism guarantees that, at the classical or semi-classical level. In the absence of fundamental scalar fields the realization of the mechanism is more subtle, but, at the same time, conceptually superior, because one does not have to assume the existence of fundamental scalars (not observed in Nature, to date). Therefore, in the seventies, an appealing alternative to the Higgs mechanism was extensively considered. The idea was to combine the *dynamical* Goldstone mechanism (*i.e.*, the Nambu–Jona-Lasino mechanism with composite Goldstone particles) with a gauge theory, in order to give *dynamical gauge-invariant masses* to the vector mesons. In this two-step scenario, mass generation is proceeded by the spontaneous breaking of a global (chiral) symmetry; the required pole in $\Pi_{\mu\nu}$ is provided by composite Goldstone bosons (fermion-antifermion bound states). Gauge invariance (long range forces), on the other hand, ensures that these massless ex-

---

[8] The generation of the pole in the Schwinger model is related to the anomaly of the axial-vector current, which is the reason why Godstone's theorem is evaded in this case. This is in fact consistent with Coleman's theorem [220], stating the absence of Goldstone bosons in $d = 2$.

citations will decouple from the complete physical scattering amplitude. The actual realization of the decoupling goes through a rather subtle mechanism, as has been demonstrated explicitly in the toy models considered [208,221].

Even though this activity was mainly directed towards an alternative descriptions (*i.e.*, without resorting to tree-level Higgs mechanism and elementary scalars) of the electroweak sector, Grand Unified Theories, and general model-building, these profound ideas invariably influenced our approach to the strong interactions. The general philosophy adopted when applying some of the dynamical concepts described above to pure Yang-Mills theories (without matter fields), such as quarkless QCD, is the following [222]. One assumes that, in a strongly-coupled gauge theory, longitudinally coupled, zero-mass bound-state excitations are dynamically produced. To be sure, the demonstration of the existence of a bound state, and in particular a zero-mass bound state, in realistic field theories is a difficult dynamical problem, usually studied by means of integral equations, known as Bethe-Salpeter equations (see, e.g., [223]). Thus, it is clear that a vital ingredient for this scenario is strong coupling, which can only come from the infrared instabilities of a non-Abelian gauge theories. The aforementioned excitations are *like* dynamical Nambu-Goldstone bosons, in the sense that they are massless, composite, and longitudinally coupled; but, at the same time, they differ from Nambu-Goldstone bosons as far as their origin is concerned: they do *not* originate from the spontaneous breaking of any global symmetry. The main role of these excitations is to trigger the Schwinger mechanism, i.e. to provide the required pole in the gluon self-energy [specifically, the gauge-independent $\widehat{\Pi}(q^2)$ obtained with the PT] thus furnishing (gauge-invariantly) a dynamical mass for the gluons. The additional important step is then to demonstrate that every such Goldstone-like scalar that is "eaten" by a gluon to give it mass is actually canceled out of the S-matrix by other massless poles, or by current conservation.

Exactly how should the idea of a composite excitation be incorporated at the level of Green's functions and the corresponding SDEs? A composite excitation is represented as a pole in an off-shell Green's function representing a field that does not exist in the classical action, but that occurs in the solution of the SDE for that Green's function, as a sort of bound state. To make contact with our starting point, i.e. the Ansatz of (9.10)-(9.10), we turn to the following simplified situation. Consider the WI of Eq. (3.59), and ask the following question: supposing that $\Delta^{(0)}_{\mu\nu}$ develops a mass, how must one modify $\tilde{\Gamma}_{\alpha\mu\nu}$ in order for the WI to continue been valid, which is tantamount to saying that the gauge-invariance remains intact? Thus, replace in $\Delta^0_{\mu\nu}$ of (2.31) the $d^{-1}(k) = k^2$ by $d_m^{-1}(k) = k^2 + m^2$, and substitute the resulting $\Delta^{(0)}_{m\,\mu\nu}$ in the rhs of Eq. (3.59). In order to maintain the validity of the WI one must simultaneously replace $\tilde{\Gamma}_{\alpha\mu\nu}$ on the lhs by $\tilde{\Gamma}^m_{\alpha\mu\nu}$ given by

$$\tilde{\Gamma}^m_{\alpha\mu\nu}(q, k_1, k_2) = \tilde{\Gamma}_{\alpha\mu\nu}(q, k_1, k_2) - \left[\frac{m^2}{2} \frac{q_\alpha k_{1\mu}(q - k_1)_\nu}{q^2 k_1^2} + \text{c.p.} \right], \qquad (9.12)$$

where "c.p." stands for cyclic permutations. The new vertex $\tilde{\Gamma}^m_{\alpha\mu\nu}(q, k_1, k_2)$ has, as we mentioned above, terms with longitudinally-coupled massless poles, whose residue is m^2. If the propagator is transverse and has mass, this is the only way that the original WI can be satisfied, just as the only way a massive gauge-boson propagator can be transverse is if it has similar poles in the transverse projector $P_{\mu\nu}$.

Substituting into the system of SDEs the expressions for the various vertices, as discussed above, and carrying out elementary but lengthy algebraic manipulations, we arrive at the final form of the SDEs, presented in [224].

The crucial point is the behavior of (9.4) as $q^2 \to 0$, where the "freezing" of the gluon propagator is observed. In this limit, Eq.(9.4) yields

$$\Delta^{-1}(0) \sim 15 \int_k \Delta(k) - 6 \int_k k^2 \Delta^2(k). \tag{9.13}$$

The rhs of Eq.(9.13) vanishes perturbatively, by virtue of the dimensional regularization result

$$\int_k \frac{\ln^n k^2}{k^2} = 0, \qquad n = 0, 1, 2, \ldots \tag{9.14}$$

which ensures the masslessness of the gluon to all orders. However, $\Delta^{-1}(0)$ does *not* have to vanish non-perturbatively, provided that the quadratically divergent integrals defining it can be properly regulated and made finite, *without* introducing counterterms of the form $m_0^2(\Lambda_{\mathrm{UV}}^2)A_\mu^2$, which are forbidden by the local gauge invariance of the fundamental QCD Lagrangian. It turns out that this is indeed possible: the divergent integrals can be regulated by subtracting appropriate combinations of "dimensional regularization zeros". Specifically, for large enough k^2 the $\Delta(k^2)$ goes over to its perturbative expression, to be denoted by $\Delta_{\mathrm{pert}}(k^2)$; it has the form

$$\Delta_{\mathrm{pert}}(k^2) = \sum_{n=0}^{N} a_n \frac{\ln^n k^2}{k^2}, \tag{9.15}$$

where the coefficient a_n are known from the perturbative expansion. Thus, we obtain for the regularized $\Delta_{\mathrm{reg}}^{-1}(0)$

$$\Delta_{\mathrm{reg}}^{-1}(0) \sim 15 \int_0^s dy\, y\, [\Delta(y) - \Delta_{\mathrm{pert}}(y)] - 6 \int_0^s dy\, y^2 \left[\Delta^2(y) - \Delta_{\mathrm{pert}}^2(y)\right]. \tag{9.16}$$

The obvious ambiguity of the regularization described above is the choice of the point s, past which the two curves, $\Delta(y)$ and $\Delta_{\mathrm{pert}}(y)$, are assumed to coincide. Due to this ambiguity one cannot pin down $\Delta_{\mathrm{reg}}(0)$ completely, which must be treated, at this level, as an arbitrary initial (boundary) condition. In [224] $\Delta_{\mathrm{reg}}(0)$ was fixed by resorting to the lattice data of [195]; specifically, when solving the system of SDEs numerically, $\Delta_{\mathrm{reg}}^{-1}(0)$ was chosen to have the same value as the lattice data at the origin $\Delta_{\mathrm{reg}}(0) = 7.3\,\mathrm{GeV}^{-2}$. Once this boundary condition is imposed, the system of SDE is solved for the entire range of (Euclidean) momenta, from the deep IR to the deep UV. The solutions obtained are shown in Fig. 84, where we show the numerical results for $\Delta(q^2)$ and the ghost dressing function renormalized at $\mu = M_b = 4.5\,\mathrm{GeV}$, and the comparison with the corresponding lattice data of Ref.[195].

It is interesting to mention that the non-perturbative transverse gluon propagator, being finite in the IR, is automatically less singular than a simple pole, thus satisfying the corresponding Kugo-Ojima confinement criterion [226,227]. Note that for $q^2 \le 10\,\mathrm{GeV}^2$ both gluon propagators (lattice and SDE) shown in Fig. 84 may be fitted very accurately using a unique functional
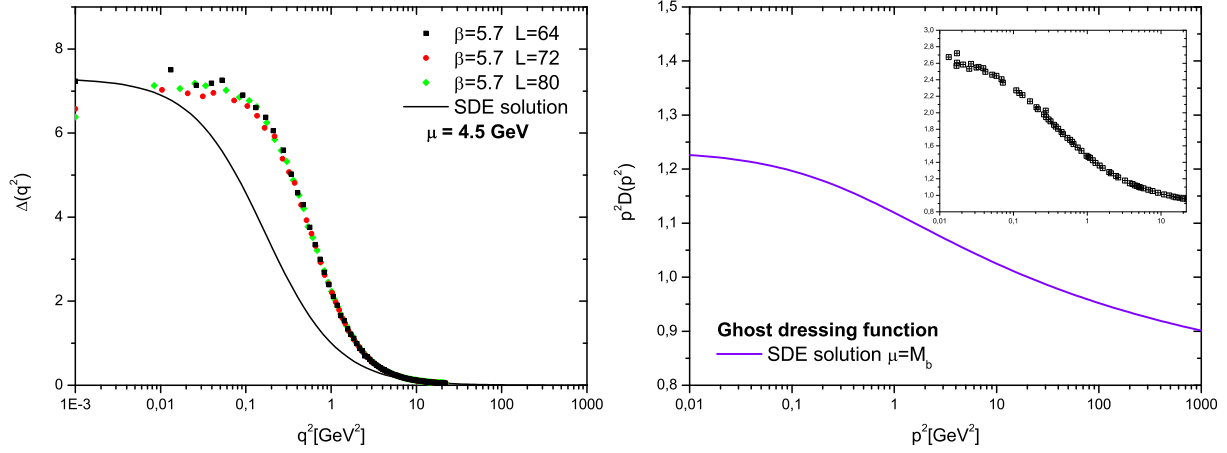
Fig. 84. (*Left panel*) The numerical solution for the gluon propagator from the SDE (black continuous line) compared to the lattice data of Ref. [195]. (*Right panel*) The ghost dressing function $p^2 D(p^2)$ obtained from the SDE. In the insert we show the lattice data for the same quantity; notice that there is no "infrared enhancement" [225]; instead, the dressing function saturates at a finite value

form, given by $\Delta^{-1}(q^2) = a + b\,(q^2)^{c-1}$. Specifically, measuring q^2 in GeV^2, the lattice data are fitted by $a = 0.14$, $b = 0.31$, and $c = 2.51$, while the SDE solution is described setting $a = 0.14$, $b = 0.86$, and $c = 2.02$.

Let us now take a closer look at the ghost propagator, $D(p^2)$. First of all, the $D(p^2)$ obtained from the ghost SDE diverges at the origin, in qualitative agreement with the lattice data. From the SDE point of view, this divergent behavior is due to the fact that the vertex Γ_μ employed does not contain $1/p^2$ poles, as suggested by previous lattice studies [228]; actually, Γ_μ was fixed at its tree-level value. Notice, however, that away from the LG one may obtain an IR finite (massive-like) $D(p^2)$, due to the contribution of the longitudinal form factor of the vertex Γ_μ (i.e. proportional to the gluon momentum k_μ); the latter gets annihilated in the LG when contracted with the gluon propagator, but contributes away from it [229].

Of particular theoretical interest is the IR behavior of the ghost dressing function $p^2 D(p^2)$, because it is intimately related to the Kugo-Ojima confinement criterion for the ghost propagator. This criterion would be satisfied if the non-perturbative ghost propagator (in the LG) were more singular in the IR than a simple pole; this type of behaviour is usually referred to as IR "enhancement". Thus, if we were to fit the dressing function $p^2 D(p^2)$ [obtained either from the lattice data or the corresponding SDE] with a function of the form form $p^2 D(p^2) = c_1 (p^2)^{-\gamma}$, a positive γ would indicate that the aforementioned criterion is satisfied.

It is relatively obvious from both the lattice data and our SDE solutions that no such "enhancement" is observed; $p^2 D(p^2)$ reaches a finite (positive) value as $p^2 \to 0$; a detailed fitting exercise confirms this point. Indeed, a IR-finite fit of the form $p^2 D(p^2) = \kappa_1 - \kappa_2 \ln(p^2 + \kappa_3)$, [with κ_3 acting as an effective gluon mass; p^2 in GeV^2, $k_1 = 1.12$, $k_2 = 0.04$, and $k_3 = 0.08$,

valid for the range $p^2 < 10$] is far superior to any power-law fit that has been tried [224]. The absence of power-law enhancement has also been verified in alternative SDE studies [225]. The fact that the Kugo-Ojima criterion is not satisfied is by no means an inconsistency, since a criterion is a sufficient but not a necessary condition. In that sense, the old confinement criterion associated with a gluon propagator going like $1/k^4$ in the IR is not valid either; this simply indicates that the real relation between the gluon propagator and confinement is more sophisticated than simply calculating a Fourier transform (see, for example, [230]).

Comparing the PT solution for the gluon propagator with the lattice data we notice that, whereas their asymptotic behavior coincides (perturbative limits), there is a discrepancy of about a factor of 1.5–2 in the intermediate region of momenta, especially around the fundamental QCD mass-scale [reflected also in the different values of the two sets of fitting parameters (a, b, c)]. In the case of the ghost dressing function, a relative difference of similar size is observed. These discrepancies may be accounted for by extending the gluon SDE to include the "two-loop dressed" graphs, omitted (gauge-invariantly) from the original analysis presented in [224], and/or by supplying to the vertex given in (9.10) the missing transverse parts.

9.4   The non-perturbative effective charge of QCD

As we have seen in detail in subsection 5.1.2, the PT permits the generalization of the prototype QED construction of an effective charge in the case of non-Abelian gauge theories, and in particular QCD. To remind the reader of the basic steps, we recall that, due to the Abelian WIs satisfied by the PT effective Green's functions, the PT self-energy $\widehat{\Delta}^{-1}(q^2)$ absorbs all the RG-logs, exactly as happens in QED with the photon self-energy; specifically, in the deep UV,

$$\widehat{\Delta}^{-1}(q^2) = q^2 \left[1 + bg^2 \ln \left(\frac{q^2}{\mu^2} \right) \right],$$

(9.17)

where $b = 11C_A/48\pi^2$ is the first coefficient of the QCD β-function. Equivalently, since Z_g and $\widehat{Z}_A$, the renormalization constants of the gauge-coupling and the effective self-energy, respectively, satisfy the QED relation $Z_g = \widehat{Z}_A^{-1/2}$, the product $\widehat{d}(q^2) = g^2 \widehat{\Delta}(q^2)$ forms a RG-invariant (μ-independent) quantity [7]; for large momenta q^2,

$$\widehat{d}(q^2) = \frac{\overline{g}^2(q^2)}{q^2},$$

(9.18)

where $\overline{g}^2(q^2)$ is the RG-invariant effective charge of QCD,

$$\overline{g}^2(q^2) = \frac{g^2}{1 + bg^2 \ln (q^2/\mu^2)} = \frac{1}{b \ln (q^2/\Lambda^2)}.$$

(9.19)

Let us now address the following question: assuming that one has non-perturbative information about the IR behavior of the *conventional* gluon propagator $\Delta(q^2)$, how should one extract an effective charge, which, perturbatively, will go over to Eq. (9.19)? To accomplish this, one must use an additional field-theoretic ingredient, namely the BQI of Eq. (C.39), relating the
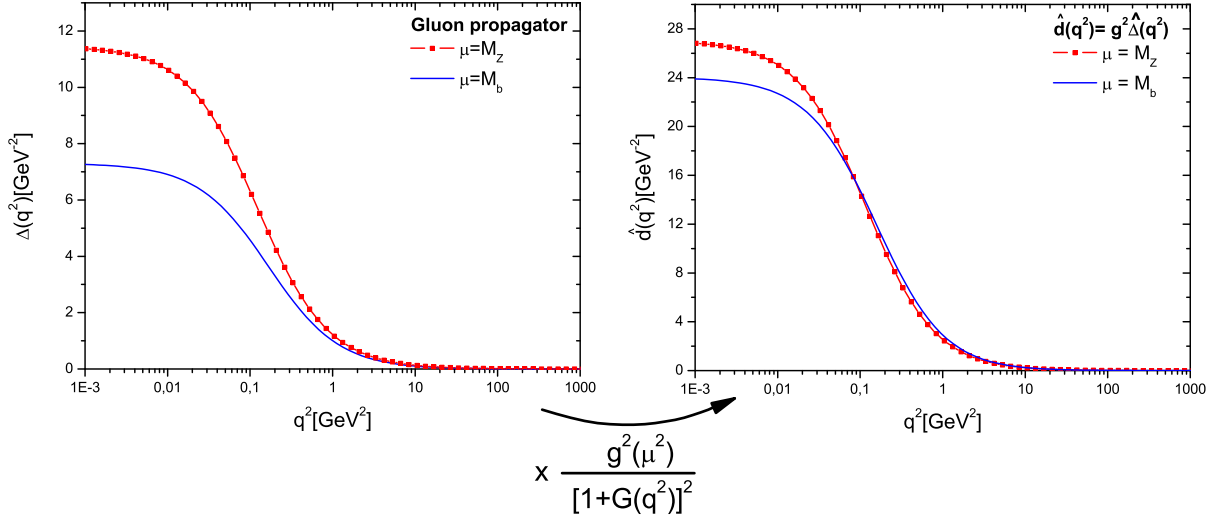
Fig. 85. (*Left panel*) The solution of SDE renormalized at $\mu = M_b = 4.5\,\text{GeV}$ (continuous blue curve) and $\mu = M_Z = 91\,\text{GeV}$ (red line plus square curve). (*Right panel*) The corresponding PT-BFM $\widehat{\Delta}(q^2)$ obtained as the convolution of $\Delta(q^2)$ and the function $g^2(\mu^2)/[1+G(q^2)]^2$.

conventional $\Delta(q^2)$ and the PT-BFM $\widehat{\Delta}(q^2)$ in any R_ξ-like gauge, *i.e.*,

$$\Delta(q^2) = \left[1 + G(q^2)\right]^2 \widehat{\Delta}(q^2). \tag{9.20}$$

Note that the $G(q^2)$ already appears in Eq. (9.4) and Fig. 82. The dynamical equation for $G(q^2)$ is obtained from the $g_{\mu\nu}$ part of $\Lambda_{\mu\nu}$ in (9.4); after using some of the aforementioned approximations for the vertices, we obtain

$$G(q^2) = -\frac{\lambda}{3} \int_k \left[2 + \frac{(k \cdot q)^2}{k^2 q^2}\right] \Delta(k) D(k+q). \tag{9.21}$$

First of all, it is easy to verify that, at lowest order, the $G(q^2)$ obtained from Eq. (9.21) restores the β function coefficient in front of ultraviolet logarithm. In that limit

$$1 + G(q^2) = 1 + \frac{9}{4}\frac{C_A g^2}{48\pi^2} \ln(\frac{q^2}{\mu^2}),$$

$$\Delta^{-1}(q^2) = q^2 \left[1 + \frac{13}{2}\frac{C_A g^2}{48\pi^2} \ln(\frac{q^2}{\mu^2})\right]. \tag{9.22}$$

Thus, using Eq. (9.20) we recover the $\widehat{\Delta}^{-1}(q^2)$ of Eq. (9.17), as we should. Then, non-perturbatively, one substitutes into Eq. (9.20) the $G(q^2)$ and $\Delta(q^2)$ obtained from solving the system in Eq. (8.35), to obtain $\widehat{\Delta}(q^2)$. This latter quantity is the non-perturbative generalization of
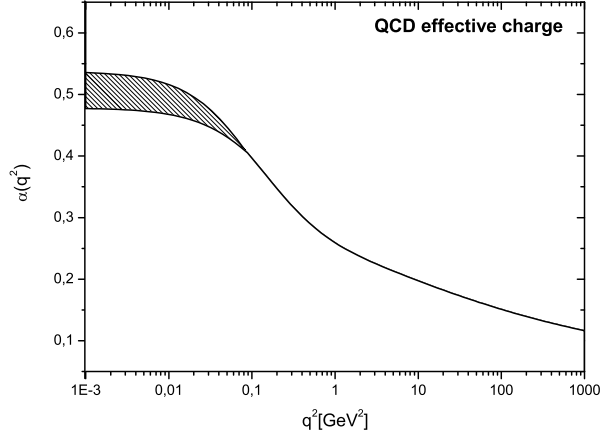
211

Fig. 86. The QCD effective charge, $\alpha(q^2) = \overline{g}^2(q^2)/4\pi$, extracted from Fig. 85 by factoring out $(q^2 + m^2(0))^{-1}$, with a gluon mass of $m(0)$=500 MeV.

Eq. (9.17); for the same reasons explained above, when multiplied by g^2 it should form an RG-invariant quantity, *e.g.*, the non-perturbative generalization of $\widehat{d}(q^2)$. In Fig. 85 we present the combined result of the above steps: $\widehat{d}(q^2)$ is obtained from two different sets of solutions of the system of Eqs (9.4) one renormalized at $\mu = M_b = 4.5\,\text{GeV}$ and one at $\mu = M_Z = 91\,\text{GeV}$. Ideally the two curves of $\widehat{d}(q^2)$ should be identical; even though this does not happen, due to the approximations employed when solving the SDE system, the two curves are fairly close, indicating that $\widehat{d}(q^2)$ is to a very good approximation an RG-invariant quantity, as it should.

We are now in the position to define the non-perturbative QCD effective charge from the RG-invariant quantity $\widehat{d}(q^2)$. Of course, as already mentioned in subsection 5.1.2, given that $\widehat{d}(q^2)$ reaches a finite value in the deep infrared, it would be unwise to define the effective charge by factoring out of $\widehat{d}(q^2)$ a factor of $1/q^2$, because this would give rise to the unphysical situation where the strong QCD coupling vanishes in the deep IR. This is wrong not only operationally, *i.e.*, forcing the coupling to vanish when it does not want to, but also conceptually, because it suggests that QCD in the presence of a gluon mass in non-interactive [9] . Of course, nothing could be further from the physical reality. First of all, a multitude of phenomenological studies find, with virtually no exception, that the QCD effective charge freezes at a non-zero value [231–236]. Second, a finite QCD effective charge constitutes a central assumption of the QCD/CFT correspondence [237,238]. Third, as we mentioned in detail at the beginning of this section [see discussion following (9.2)], the dynamical gluon mass is responsible for a very rich dynamical structure, being intimately connected, among other things, to both quark confinement and gluon

---

[9] To see how unphysical this procedure is, imagine applying it to the electroweak sector. Specifically, given that the propagators of the W and Z are finite in the IR, (due to the standard Higgs mechanism), pulling a factor $1/q^2$ out of them, instead of $(q_E^2 + M^2)$ [*viz.* (5.36), with $q^2 \to -q_E^2$], would give rise to an electroweak coupling that vanishes in the IR. Does that mean that the electroweak theory is non-interacting in the IR? Does Fermi's constant vanish all of a sudden? Or is β decay no longer observed?

screening. The correct procedure corresponds to factor out a "massive" propagator, *i.e.*, write

$$\widehat{d}(q^2) = \frac{\overline{g}^2(q^2)}{q^2 + m^2(q^2)}.$$ (9.23)

Of course, as we have emphasized, $m^2(q^2)$ itself is running, which must also be taken into account in a more sophisticated treatment. For the purposes of this report, however, we assume that $m^2(q^2)$ is constant, $m^2(q^2) = m^2(0)$, and use for $m(0)$ the value of $500\,\mathrm{MeV}$ favored by phenomenology [239]. The $\alpha(q^2)$ obtained is shown in Fig. 86; as announced, at low energies it freezes to a finite value, indicating the appearance of an infrared fixed point of QCD.

10 Concluding remarks

In this report we have given a detailed account of the pinch technique and some of its most characteristic applications. The present work may be separated in a natural way, into two large parts. The first part, comprising of sections 2 to 5, contains practically the entire one-loop PT, both in QCD and the electroweak sector, and the connection with the BFM formalism. The second part contains the developments following the non-diagrammatic formulation of the PT, the streamlining achieved by resorting to the Batalin-Vilkovisky formalism, and finally the non-perturbative QCD applications, with particular highlights the gauge-invariant truncation of the SDE series and the dynamical generation of an effective gluon mass.

We hope to have conveyed to the reader the underlying unity of the multitude of topics covered, and to have succeeded in demonstrating the versatility of the PT formalism and the wide range of its applicability. The reader should be able to appreciate, for example, how a simple one-loop calculation contains the seed of a non-trivial truncation of the SDEs, accomplished a quarter of a century later; or how a seemingly innocuous (or even redundant, according to some) rearrangement of graphs is able to give rise to a resummation formalism for resonant transition amplitudes that satisfies such a plethora of tightly interwoven physical constraints.

Throughout this report we have attempted to maintain a balance between the technical presentation (how to pinch) and the physical motivations and phenomenological applications (when to pinch and why). Even so, there is a considerable number of additional important applications that we could not possibly cover. Let us mention a few. There have been several application in the area of finite temperature field theory, starting with the early work by Cornwall and collaborators [162,191], the calculation of the plasmon decay constant by Nadkarni [240], the gauge-independent thermal β function computed by Sasaki [241,242], and the work on magnetic screening for the quark-gluon plasma by Alexanian and Nair [243]. In addition, the explicit one-loop PT calculations in the context of the Coulomb and temporal axial gauges have been presented by Passera and Sasaki in [244]. Moreover, Pilaftsis applied the PT to the resonant CP violation a decade ago [245,246], and recently to resonant leptogenesis [247,248]. The PT has also been used in order to obtain scale and gauge-independent mixing angles for scalar particles [249,250] and [251]. In addition, Caporaso and Pasquetti applied to the non-commutative QED [252], and non-commutative (softly broken) supersymmetric Chern-Simons theory [253].

To be sure, there are still many things one would like to know about the PT and its field-theoretic origin. Most importantly, as mentioned in the Introduction, a formal definition of the PT Green's functions in terms of fundamental fields, encoding "ab initio" their special properties, still eludes us. Ideally, one would like to find that particular combination of fields or operators, which, when appropriately combined, will furnish the PT answer without pinching, *i.e.*, regardless of whether or not one tracks down the various cancellations explicitly, and in any gauge-fixing scheme considered. Such a situation would be, of course, far superior than what happens now with the BFG, where there is no pinching only because of a kinematic accident, namely the lack of pinching momenta in that particular gauge.

One basic and rather obvious question, that, perhaps surprisingly, has not been addressed to date, is the following. It is well known that one can construct a gauge-invariant operator out of a gauge-variant one by means of a path-order exponential containing the gauge field A [254]. For example, in the case of the fermion propagator $S(x,y) = \langle 0|\psi(x)\bar{\psi}(y)|0\rangle$ the corresponding

gauge-invariant propagator S_{PO} reads ("PO" stands for "path-ordered")

$$S_{PO}(x,y) = \langle 0|\psi(x)P\exp\left(i\int_x^y dz\cdot A(z)\right)\bar\psi(y)|0\rangle. \qquad (10.1)$$

Is this gauge-invariant propagator related in any way to the PT fermion propagator, constructed in Section 2? Of course, completely related to this question is the construction presented in [255]; in fact, the distinction made there between the Wightman and the causal two-point function might be worth pursuing from the PT point of view.

Anyone remotely familiar with the PT gets the tantalizing feeling that, in addition to the BRST symmetry, some other powerful (yet undiscovered) mechanism must be at work, enforcing the PT properties. The remarkable supersymmetric relations discovered by Binger and Brodsky [65] (see Section 2) intensify this impression; their results indeed beg the question of whether one has actually stumbled into something bigger. Could it be, for example, that the PT rearrangements end up exposing some sort of hidden symmetry? Such a possibility is not unprecedented; an interesting 3-d example of a (topological) field-theory, which, when formulated in the background Landau gauge ($\xi_Q = 0$), displays an additional (non-BRST related) rigid supersymmetry, is given in [256].

Finally, it would be most interesting to explore possible connections with other field-theoretic methods [257–259], [260], [261,262], [10], [263], or string-inspired approaches [66,67,264], [265], [266], in order to either acquire a more formal understanding of the PT, or to encompass various related approaches into a unique coherent framework.

Acknowledgments

A $SU(N)$ group theoretical identities

In this Appendix we collect some useful group theoretical identities for the $SU(N)$ gauge group.

For any representation of $SU(N)$ the generators t^a ($a = 1, 2...N^2-1$) are hermitian, traceless matrices, generating the closed algebra

$$[t^a, t^b] = i f^{abc} t^c, \tag{A.1}$$

where f^{abc} are the (totally antisymmetric) structure constants, which satisfy the Jacobi identity

$$f^{abx} f^{cdx} + f^{acx} f^{dbx} + f^{adx} f^{bcx} = 0. \tag{A.2}$$

The fundamental representation t_f^a is N-dimensional, with the normalization

$$\text{Tr}(t_f^a t_f^b) = \frac{1}{2} \delta^{ab} \tag{A.3}$$

In the case of QCD, the fundamental $t_f^a = \lambda^a/2$, where λ^a are the Gell-Mann matrices.

The adjoint representation has dimension $N^2 - 1$, and its generators t_A^a have matrix elements given by the relation

$$(t_A^a)_{bc} = -i f^{abc}. \tag{A.4}$$

The Casimir eigenvalue C_r of a representation r is defined as

$$t_r^a t_r^a = C_r \, 1 \tag{A.5}$$

while the Dynkin index d_r is defined as

$$\text{Tr}(t_r^a t_r^b) = d_r \delta^{ab} \tag{A.6}$$

The Casimir eigenvalue and the Dynkin index of a representation of a group G are related by the general formula

$$C_r = \frac{\dim(G)}{\dim(r)} d_r \tag{A.7}$$

where $\dim(G)$ is the dimension of the group and $\dim(r)$ the dimension of the representation. Thus, for the adjoint representation $r = A$, $\dim(G) = \dim(A)$, and therefore $C_A = d_A$. Specializing to the $SU(N)$ case, one has $C_A = N$, and from Eq. (A.3) we have that $d_f = \frac{1}{2}$, and thus $C_f = (N^2 - 1)/2N$; for QCD, $C_f = 4/3$.

We conclude by quoting some identities involving the structure functions

$$f^{aex} f^{bex} = C_A \delta^{ab}, \tag{A.8a}$$

$$f^{axm} f^{bmn} f^{cnx} = \frac{1}{2} C_A f^{abc}, \tag{A.8b}$$

$$f^{alm} f^{bmn} f^{cne} f^{del} - f^{alm} f^{bmn} f^{dne} f^{cel} = -\frac{1}{2} C_A f^{abx} f^{cdx}. \tag{A.8c}$$

$m,\mu \sim\!\!\sim\!\!\sim\!\!\sim n,\nu$	$-i\frac{\delta^{mn}}{k^2}\left[g_{\mu\nu}-(1-\xi)\frac{k_\mu k_\nu}{k^2}\right]$	$i\Delta^{mn}_{\mu\nu}(k)$
$m \dashrightarrow n$	$i\frac{\delta^{mn}}{k^2}$	$iD^{mn}(k)$
$i,\mathrm{f} \longrightarrow j,\mathrm{f}'$	$i\frac{\delta^{ij}\delta^{\mathrm{ff}'}}{k^\mu\gamma_\mu-m_{\mathrm f}}$	$iS^{\mathrm{ff}'}_{ij}(k)$
m,μ $k_1\downarrow$ k_2 a,α q n,ν	$gf^{amn}\left[g_{\mu\nu}(k_1-k_2)_\alpha+g_{\alpha\nu}(k_2-q)_\mu \right.$ $\left.+g_{\alpha\mu}(q-k_1)_\nu\right]$	$i\Gamma_{A^a_\alpha A^m_\mu A^n_\nu}(k_1,k_2)$
a,α $q\downarrow$ k_2 $\bar c^m$ k_1 c^n	$gf^{amn}k_{1\alpha}$	$i\Gamma_{c^n A^a_\alpha \bar c^m}(q,-k_1)$
a,α $q\downarrow$ p_2 $\bar\psi^i$ p_1 ψ^j	$ig\gamma^\alpha(t^a)_{ij}$	$i\Gamma_{\psi^j A^a_\alpha \bar\psi^i}(q,-p_1)$
m,μ k_2 n,ν k_1 k_3 s,σ k_4 r,ρ	$-ig^2\left[f^{mse}f^{ern}(g_{\mu\rho}g_{\nu\sigma}-g_{\mu\nu}g_{\rho\sigma})\right.$ $+f^{mne}f^{esr}(g_{\mu\sigma}g_{\nu\rho}-g_{\mu\rho}g_{\nu\sigma})$ $\left.+f^{mre}f^{esn}(g_{\mu\sigma}g_{\nu\rho}-g_{\mu\nu}g_{\rho\sigma})\right]$	$\Gamma_{A^m_\mu A^n_\nu A^r_\rho A^s_\sigma}(k_2,k_3,k_4)$

Fig. B.1. Feynman rules for QCD in the R_ξ gauges. The first two columns show the lowest order Feynman diagrams and rule respectively, while the last one shows the corresponding all-order Green's function according to the conventions of Eq.(7.3).

B   Feynman rules

B.1 R_ξ and BFM gauges

The Feynman rules for QCD in R_ξ gauges are given in Fig. B.1. In the case of the BFM gauge, since the gauge fixing term is quadratic in the quantum fields, apart from vertices involving ghost fields only vertices containing exactly two quantum fields might differ from the conventional ones. Thus, the vertices $\Gamma_{\widehat A\psi\bar\psi}$ and $\Gamma_{\widehat AAAA}$ have to lowest order the same expression as the corresponding R_ξ ones $\Gamma_{A\psi\bar\psi}$ and Γ_{AAAA} (to higher order their relation is described by the corresponding BQIs).

m,μ ... a,α ... q ... n,ν ... k_1 ... k_2	$gf^{amn}\left[g_{\mu\nu}(k_1-k_2)_\alpha + g_{\alpha\nu}(k_2-q+\frac{1}{\xi}k_1)_\mu \right.$ $\left. +g_{\alpha\mu}(q-k_1-\frac{1}{\xi}k_2)_\nu\right]$	$i\Gamma_{\widehat{A}^a_\alpha A^m_\mu A^n_\nu}(k_1,k_2)$
a,α ... q ... k_2 ... $\bar{c}^m$ ... k_1 ... c^n	$gf^{amn}(k_1+k_2)_\alpha$	$i\Gamma_{c^n\widehat{A}^a_\alpha \bar{c}^m}(q,-k_1)$
m,μ ... k_2 ... n,ν ... k_1 ... p_2 ... s,σ ... p_1 ... r,ρ	$-ig^2\left[f^{mse}f^{ern}(g_{\mu\rho}g_{\nu\sigma}-g_{\mu\nu}g_{\rho\sigma}+\frac{1}{\xi}g_{\mu\sigma}g_{\nu\rho})\right.$ $+f^{mne}f^{esr}(g_{\mu\sigma}g_{\nu\rho}-g_{\mu\rho}g_{\nu\sigma}-\frac{1}{\xi}g_{\mu\nu}g_{\rho\sigma})$ $\left.+f^{mre}f^{esn}(g_{\mu\sigma}g_{\nu\rho}-g_{\mu\nu}g_{\rho\sigma})\right]$	$\Gamma_{\widehat{A}^m_\mu A^n_\nu \widehat{A}^r_\rho A^s_\sigma}(k_2,p_2,p_1)$
a,α ... k_3 ... r,ρ ... q ... k_2 ... $\bar{c}^m$ ... k_1 ... c^n	$-ig^2 g_{\alpha\rho}f^{mae}f^{ern}$	$\Gamma_{c^n\widehat{A}^a_\alpha A^r_\rho \bar{c}^m}(q,k_3,-k_1)$
a,α ... k_3 ... r,ρ ... q ... k_2 ... $\bar{c}^m$ ... k_1 ... c^n	$-ig^2 g_{\alpha\rho}(f^{mae}f^{ern}+f^{mre}f^{ean})$	$\Gamma_{c^n\widehat{A}^a_\alpha \widehat{A}^r_\rho \bar{c}^m}(q,k_3,-k_1)$

Fig. B.2. Feynman rules for QCD in the BFM gauge. We only include those rules which are different from the R_ξ ones to lowest order. A gray circle on a gluon line indicates a background field.

B.2 Anti-fields

The couplings of the anti-fields Φ^* with fields is entirely encoded in the BRST Lagrangian of Eq. (7.5b). When choosing the BFM gauge the additional coupling $gf^{amn}A^{*m}_\mu \widehat{A}^n_\nu c^a$ will arise in the BRST Lagrangian $\mathcal{L}_{\mathrm{BRST}}$ as a consequence of the BFM splitting $A \to \widehat{A} + A$. One then gets the Feynman rules given in Fig. B.3.

B.3 BFM sources

The coupling of the BFM source Ω^m_μ with the ghost and gluon fields can be derived from the Faddeev-Popov ghost Lagrangian, since making use of the BRST transformation of Eq. (7.16) we get

$$\mathcal{L}_{\mathrm{FPG}} = -\bar{c}^a s\mathcal{F}^a_{\mathrm{BFM}} \supset -\bar{c}^a gf^{amn}(s\widehat{A}^m_\mu)A^\mu_n = -gf^{amn}\bar{c}^a\Omega^m_\mu A^\mu_n. \tag{B.1}$$

c^n q A_μ^{*m}	$-q^\mu \delta^{mn}$	$-\Gamma_{c^n A_\mu^{*m}}(q)$
n, ν $k_2 \downarrow$ q c^a k_1 A_μ^{*m}	$igf^{amn}g_{\mu\nu}$	$i\Gamma_{c^a A_\nu^n A_\mu^{*m}}(k_2, q)$
n, ν $k_2 \downarrow$ q c^a k_1 A_μ^{*m}	$igf^{amn}g_{\mu\nu}$	$i\Gamma_{c^a \widehat{A}_\nu^n A_\mu^{*m}}(k_2, q)$
c^a $k_2 \downarrow$ q ψ^i p_2 $\bar\psi^{*j}$	$-g(t^a)_{ji}$	$i\Gamma_{\psi^i c^a \bar\psi^{*j}}(k_2, q)$
$\bar\psi^j$ $p_1 \uparrow$ k_2 ψ^{*i} q c^a	$g(t^a)_{ji}$	$i\Gamma_{\psi^{*i} \bar\psi^j c^a}(-p_1, k_2)$
c^n $k_2 \downarrow$ q c^a k_1 c^{*m}	$-igf^{amn}$	$i\Gamma_{c^a c^n c^{*m}}(k_2, q)$

Fig. B.3. Feynman rules for QCD anti-fields.

n, ν $k_2 \downarrow$ k_1 Ω_μ^m q $\bar c^a$	$-igf^{amn}g_{\mu\nu}$	$i\Gamma_{\Omega_\mu^m A_\nu^n \bar c^a}(k_2, -k_1)$

Fig. B.4. Feynman rule for the BFM gluon source Ω_μ^m.

The corresponding Feynman rule is given in Fig. B.4. In general Feynman rules involving the BFM source Ω can be derived by the one involving the (gluon) anti-field A^* through the replacements $A^* \to \Omega$ and $c \to \bar c$.

C Faddev-Popov equations, Slavnov-Taylor Identities and Background Quantum Identities for QCD

C.1 *Faddeev-Popov Equations*

As a first example of the use of the FPE introduced in Section 7.3, let us differentiate the functional equation (7.22) with respect to the ghost field c^b; after setting the fields/anti-fields to zero we get (relabeling the color and Lorentz indices)

$$\Gamma_{c^m \bar{c}^n}(q) + iq^\nu \Gamma_{c^m A_\nu^{*n}}(q) = 0, \tag{C.1}$$

which can be used to relate the auxiliary function $\Gamma_{c^m A_\nu^{*n}}(q)$ with the full ghost propagator $D^{ab}(q)$. Due to Lorentz invariance, we can in fact write $\Gamma_{c^m A_\nu^{*n}}(q) = q_\nu \Gamma_{c^m A^{*n}}(q)$, and therefore

$$\Gamma_{c^m \bar{c}^n}(q) = -iq^\nu \Gamma_{c^m A_\nu^{*n}}(q) = -iq^2 \Gamma_{c^m A^{*n}}(q). \tag{C.2}$$

On the other hand, due to our definition of the Green's functions [see Eq. (7.3)], one has that

$$iD^{mr}(q)\Gamma_{c^r \bar{c}^n}(q) = \delta^{mn}, \tag{C.3}$$

and therefore we get the announced relation:

$$\begin{aligned}
\Gamma_{c^m A_\nu^{*n}}(q) &= q_\nu \Gamma_{c^m A^{*n}}(q) \\
&= q_\nu [q^2 D^{mn}(q)]^{-1}.
\end{aligned} \tag{C.4}$$

As a second example, let us differentiate Eq. (7.22) twice, once with respect to A_ν^n and once with respect to c^r, and then set the fields/anti-fields to zero; in this way we get the identity

$$\Gamma_{c^r A_\nu^n \bar{c}^m}(k, q) + iq^\mu \Gamma_{c^r A_\nu^n A_\mu^{*m}}(k, q) = 0, \tag{C.5}$$

which is particularly useful for the PT construction. All these identities can be easily checked at tree-level; for example, using the Feynman rules of Appendix B, we have

$$iq^\mu \Gamma^{(0)}_{c^r A_\nu^n A_\mu^{*m}}(k, q) = igf^{mnr}q_\nu = -\Gamma^{(0)}_{c^r A_\nu^n \bar{c}^m}(k, q). \tag{C.6}$$

Differentiation of the functional (7.23) with respect to a BFM source Ω and a quantum gluon field A or a ghost field c and a background gluon $\widehat{A}$, provides instead the identities ($k_1 + k + q = 0$)

$$\Gamma_{\Omega_\rho^r A_\nu^n \bar{c}^m}(k, q) + iq^\mu \Gamma_{\Omega_\rho^r A_\nu^n A_\mu^{*m}}(k, q) = gf^{mnr}g_{\nu\rho}, \tag{C.7}$$

$$\Gamma_{c_\rho^r \widehat{A}_\nu^n \bar{c}^m}(k, q) + iq^\mu \Gamma_{c^r \widehat{A}_\nu^n A_\mu^{*m}}(k, q) = -igf^{mne}\Gamma_{c^r A_\nu^{*e}}(-k_1), \tag{C.8}$$

that can be easily checked at tree-level.

C.2 Slavnov-Taylor Identities

STIs are obtained by functional differentiation of the STI functional of Eq. (7.15) with respect to suitable combinations of fields chosen following the rules discussed in Section 7.

C.2.1 STIs for gluon proper vertices

Let us start by deriving the well-known STI for the trilinear gluon vertex which in the conventional formalism has been introduced in Eq. (2.94). By considering the functional differentiation

$$\frac{\delta^3 \mathcal{S}(\Gamma)}{\delta c^a(q)\delta A_\mu^m(k_1)\delta A_\nu^n(k_2)}\bigg|_{\Phi,\Phi^*=0} = 0 \qquad q + k_1 + k_2 = 0, \tag{C.9}$$

and using Eq. (C.4) one obtains

$$q^\alpha \Gamma_{A_\alpha^a A_\mu^m A_\nu^n}(k_1, k_2) = [q^2 D^{aa'}(q)] \left\{ \Gamma_{c^{a'} A_\nu^n A_d^{*\gamma}}(k_2, k_1)\Gamma_{A_\gamma^d A_\mu^m}(k_1) \right.$$
$$\left. + \Gamma_{c^{a'} A_\mu^m A_d^{*\gamma}}(k_1, k_2)\Gamma_{A_\gamma^d A_\nu^n}(k_2) \right\}. \tag{C.10}$$

At this point one would need to find out the relation between the (full) gluon propagator and the two point function $\Gamma_{A_\alpha^a A_\beta^b}$. First of all let us notice that since we are working in the Feynman gauge [see also Eq. (2.25)]

$$i\Delta_{\alpha\beta}^{ab\,(0)}(q) = -\frac{i}{k^2}\left\{ P_{\alpha\beta}(q) + \frac{k_\alpha k_\beta}{k^2} \right\}\delta^{ab} \qquad P_{\alpha\beta}(q) = g_{\alpha\beta} - \frac{q_\alpha q_\beta}{q^2}, \tag{C.11}$$

which translates to the all order formula

$$i\Delta_{\alpha\beta}^{ab}(q) = -i\delta^{ab}\left\{ P_{\alpha\beta}(q)\Delta(q^2) + \frac{q_\alpha q_\beta}{q^4} \right\}, \tag{C.12}$$

with

$$\Delta(q^2) = \frac{1}{q^2 + i\Pi(q^2)}, \qquad \Pi_{\alpha\beta}(q) = P_{\alpha\beta}(q)\Pi(q^2). \tag{C.13}$$

Notice that the way the gluon self-energy $\Pi_{\alpha\beta}(q)$ has been defined in the above equation, *i.e.*, with the imaginary i factor in front, implies that it is given simply by the corresponding Feynman diagrams in Minkowski space. Imposing then the condition

$$i\Delta_{\alpha\mu}^{am}(q)(\Delta^{-1})_{mb}^{\mu\beta}(q) = \delta^{ab}g_\beta^\alpha, \tag{C.14}$$

we get

$$(\Delta^{-1})_{mb}^{\mu\beta}(q) = i\delta^{mb}\left\{ P^{\mu\beta}(q)\Delta^{-1}(q^2) + q^\mu q^\beta \right\}. \tag{C.15}$$

On the other hand, recall that we are working with minimal variables, and thus with the reduced functional Γ; in the case of linear gauge fixings (as the R_ξ and the BFM are) the latter is equivalent to the complete one after subtracting the local term $\int d^4x\,\mathcal{L}_{\mathrm{GF}}$. This implies in turn that

Green's functions involving unphysical fields generated by the reduced functional coincide with the ones generated by the complete one only up to constant terms. In our case this affects only the two point function of the gluon field, for which one has the tree level expression

$$\Gamma^{(0)}_{A^a_\alpha A^b_\beta}(q) = iq^2 \delta^{ab} P_{\alpha\beta}(q), \tag{C.16}$$

which furnishes the sought-for all-order formula

$$\begin{aligned}\Gamma_{A^a_\alpha A^b_\beta}(q) &= (\Delta^{-1})^{ab}_{\alpha\beta}(q) - i\delta^{ab}q_\alpha q_\beta \\ &= i\delta^{ab} P_{\alpha\beta}(q)\Delta^{-1}(q^2).\end{aligned} \tag{C.17}$$

Using the above relation, we can now check the identity at tree-level; we get

$$\begin{aligned}q^\alpha \Gamma^{(0)}_{A^a_\alpha A^m_\mu A^n_\nu}(k_1, k_2) &= \left\{ \Gamma^{(0)}_{c^a A^n_\nu A^{*\gamma}_d}(k_2, k_1)\Gamma^{(0)}_{A^d_\gamma A^m_\mu}(k_1) + \Gamma^{(0)}_{c^a A^m_\mu A^{*\gamma}_d}(k_1, k_2)\Gamma^{(0)}_{A^d_\gamma A^n_\nu}(k_2) \right\} \\ &= igf^{amn} \left[(g_{\mu\nu}k_1^2 - k_{1\mu}k_{1\nu}) - (g_{\mu\nu}k_2^2 - k_{2\mu}k_{2\nu}) \right].\end{aligned} \tag{C.18}$$

Notice also that Eq. (C.17) allows us to compare the STI of Eq. (C.10) with the one written in the conventional formalism of Eq. (2.94). Factoring out the color structure, one arrive at the following identification

$$H_{\mu\gamma}(k_1, k_2) = \Gamma_{cA_\mu A^*_\gamma}(k_1, k_2), \tag{C.19}$$

which also shows that the FPE (C.5) corresponds to the well-known relation existing between the auxiliary function $H_{\alpha\beta}$ and the conventional gluon-ghost vertex Γ_β shown in Eq. (2.96).

We pause here to show what would have happened had we worked with the complete generating functional. In this case, due to the extra term appearing in the master equation (7.12) satisfied by the complete action, the differentiation carried out in Eq. (C.9) would generate two more terms with respect to the ones already appearing in Eq. (C.10), namely

$$\delta^{dn} k_{2\nu} \Gamma_{c^a A^m_\mu \bar{c}^d}(k_1, k_2) + \delta^{dm} k_{2\mu} \Gamma_{c^a A^n_\nu \bar{c}^d}(k_2, k_1). \tag{C.20}$$

To get to the terms above we have used the equation of motion of the Nakanishi-Lautrup multiplier B eliminating the latter in favor of the corresponding gauge-fixing function $\mathcal{F}$. Then, making use of the FPE (C.5), we get

$$-i\delta^{dn} k_{2\nu} k_{2\gamma} \Gamma_{c^a A^m_\mu A^{*\gamma}_d}(k_1, k_2) - i\delta^{dm} k_{1\mu} k_{1\gamma} \Gamma_{c^a A^n_\nu A^{*\gamma}_d}(k_2, k_1), \tag{C.21}$$

so that we finally would get the STI

$$\begin{aligned}q^\alpha \Gamma_{A^a_\alpha A^m_\mu A^n_\nu}(k_1, k_2) &= [q^2 D^{aa'}(q)] \left\{ \Gamma_{c^{a'} A^n_\nu A^{*\gamma}_d}(k_2, k_1) \left[\Gamma^{\mathrm{C}}_{A^d_\gamma A^m_\mu}(k_1) - i\delta^{dm} k_{1\mu} k_{1\gamma} \right] \right. \\ &\quad \left. + \Gamma_{c^{a'} A^m_\mu A^{*\gamma}_d}(k_1, k_2) \left[\Gamma^{\mathrm{C}}_{A^d_\gamma A^n_\nu}(k_2) - i\delta^{dn} k_{2\gamma} k_{2\nu} \right] \right\},\end{aligned} \tag{C.22}$$

where we have indicated explicitly that the two-point functions are to be evaluated from the completed functional (for the three point functions appearing in the STI above there is no difference). We then see that the difference amounts to a tree-level piece appearing in the two-point function, as has been anticipated in our general discussion of subsection 7.2 (recall that we are using the Feynman gauge $\xi = 1$). In particular notice that we correctly find the relation $\Gamma^{\mathrm{C}}_{A^a_\alpha A^b_\beta}(q) = (\Delta^{-1})^{ab}_{\alpha\beta}(q)$.

Another STI that will be needed in the PT construction is the one involving the quadrilinear gluon vertex; carrying out the functional differentiation

$$\left.\frac{\delta^4 \mathcal{S}(\Gamma)}{\delta c^m(k_1)\delta A^n_\nu(k_2)\delta A^r_\rho(p_2)\delta A^s_\sigma(-p_1)}\right|_{\Phi,\Phi^*=0} = 0 \qquad k_1 + k_2 + p_2 = p_1, \qquad \text{(C.23)}$$

and using Eq. (C.4), we arrive at the result

$$k_1^\mu \Gamma_{A^m_\mu A^n_\nu A^r_\rho A^s_\sigma}(k_2, p_2, -p_1) = [k_1^2 D^{mm'}(k_1)]\Big\{ \Gamma_{c^{m'} A^s_\sigma A^{*\gamma}_d}(-p_1, k_2 + p_2)\Gamma_{A^d_\gamma A^n_\nu A^r_\rho}(k_2, p_2)$$

$$+ \Gamma_{c^{m'} A^r_\rho A^{*\gamma}_d}(p_2, k_2 - p_1)\Gamma_{A^d_\gamma A^n_\nu A^s_\sigma}(k_2, -p_1) + \Gamma_{c^{m'} A^n_\nu A^{*\gamma}_d}(k_2, p_2 - p_1)\Gamma_{A^d_\gamma A^r_\rho A^s_\sigma}(p_2, -p_1)$$

$$+ \Gamma_{c^{m'} A^r_\rho A^s_\sigma A^{*\gamma}_d}(p_2, -p_1, k_2)\Gamma_{A^d_\gamma A^n_\nu}(k_2) + \Gamma_{c^{m'} A^n_\nu A^s_\sigma A^{*\gamma}_d}(k_2, -p_1, p_2)\Gamma_{A^d_\gamma A^r_\rho}(p_2)$$

$$+ \Gamma_{c^{m'} A^n_\nu A^r_\rho A^{*\gamma}_d}(k_2, p_2, -p_1)\Gamma_{A^d_\gamma A^s_\sigma}(p_1) \Big\}. \qquad \text{(C.24)}$$

C.2.2 *STIs for mixed quantum/background Green's functions*

Let us consider a Green's function involving background as well as quantum fields. Clearly, when contracting such a function with the momentum corresponding to a background leg it will satisfy a linear WI [such as the ones presented in Eq.s (8.39), (8.39), (8.39), and (8.39)], whereas when contracting it with the momentum corresponding to a quantum leg it will satisfy a non-linear STI. Let us then study the particularly interesting case of the STI satisfied by the vertex $\Gamma_{\widehat{A}AA}$ when contracted with the momentum of one of the quantum fields. Taking the functional differentiation

$$\left.\frac{\delta^3 \mathcal{S}'(\Gamma')}{\delta c^m(k_1)\delta \widehat{A}^a_\alpha(q)\delta A^n_\nu(k_2)}\right|_{\Phi,\Phi^*,\Omega=0} = 0 \qquad q + k_1 + k_2 = 0, \qquad \text{(C.25)}$$

we get

$$k_1^\mu \Gamma_{\widehat{A}^a_\alpha A^m_\mu A^n_\nu}(k_1, k_2) = [k_1^2 D^{mm'}(k_1)] \Big\{ \Gamma_{c^{m'} A^n_\nu A^{*\epsilon}_e}(k_2, q)\Gamma_{\widehat{A}^a_\alpha A^e_\epsilon}(q)$$

$$+ \Gamma_{c^{m'} \widehat{A}^a_\alpha A^{*\epsilon}_e}(q, k_2)\Gamma_{A^e_\epsilon A^n_\nu}(k_2) \Big\}. \qquad \text{(C.26)}$$

Notice that the same result can be achieved by contracting directly the BQI of Eq. (C.55) with the momentum of one of the quantum fields and then using the STI of Eq. (C.10) together with the BQIs of Eq.s(C.38) and (C.59) to bring the result in the above form.

It is particularly important to correctly identify, in the above identity, the missing tree-level contributions (due to the use of the reduced functional, see also the discussion in Section C.3.2). In order to do that, one can either work with the complete functional and use the FPE (C.8), or add them by hand using Eq. (C.55), obtaining in either cases the STI

$$
k_1^\mu \Gamma_{\widehat{A}_\alpha^a A_\mu^m A_\nu^n}(k_1,k_2) = [k_1^2 D^{mm'}(k_1)] \left\{ \Gamma_{c^{m'} A_\nu^n A_e^{*\epsilon}}(k_2,q) \Gamma_{\widehat{A}_\alpha^a A_e^\epsilon}(q) \right.
$$
$$
\left. + \Gamma_{c^{m'} \widehat{A}_\alpha^a A_e^{*\epsilon}}(q,k_2) \Gamma_{A_\epsilon^e A_\nu^n}(k_2) \right\} - ig f^{amn}(k_1^2 g_{\alpha\nu} - k_{1\alpha} k_{2\nu}). \tag{C.27}
$$

This STI can be further manipulate by using Eq. (C.17) and the FPE (C.8) for rewriting the term proportional to $\Gamma_{AA}(k_2)$ as

$$
\Gamma_{c^{m'} \widehat{A}_\alpha^a A_e^{*\epsilon}}(q,k_2) \Gamma_{A_\epsilon^e A_\nu^n}(k_2) = \Gamma_{c^{m'} \widehat{A}_\alpha^a A_e^{*\epsilon}}(q,k_2)(\Delta^{-1})_{\epsilon\nu}^{en}(k_2) + k_{2\nu} \Gamma_{c^{m'} \widehat{A}_\alpha^a \bar{c}^n}(q,k_2)
$$
$$
+ ig f^{aen} k_{2\nu} \Gamma_{c^{m'} A_\alpha^{*\epsilon}}(-k_1). \tag{C.28}
$$

On the other hand, employing Eq. (C.4) we find

$$
[k_1^2 D^{mm'}(k_1)](ig f^{nae} k_{2\nu}) \Gamma_{c^{m'} A_\alpha^{*\epsilon}}(-k_1) = -ig f^{amn} k_{1\alpha} k_{2\nu}; \tag{C.29}
$$

so, inserting Eq. (C.28) back into Eq. (C.27) we see that the term above partially cancels the tree level contribution, thus leaving us with the STI

$$
k_1^\mu \Gamma_{\widehat{A}_\alpha^a A_\mu^m A_\nu^s}(k_1,k_2) = [k_1^2 D^{mm'}(k_1)] \left\{ \Gamma_{c^{m'} A_\nu^n A_e^{*\epsilon}}(k_2,q) \Gamma_{\widehat{A}_\alpha^a A_e^\epsilon}(q) \right.
$$
$$
\left. + \Gamma_{c^{m'} \widehat{A}_\alpha^a A_e^{*\epsilon}}(q,k_2)(\Delta^{-1})_{\epsilon\nu}^{en}(k_2) + k_{2\nu} \Gamma_{c^{m'} \widehat{A}_\alpha^a \bar{c}^n}(q,k_2) \right\} - ig f^{amn} k_1^2 g_{\alpha\nu}. \tag{C.30}
$$

C.2.3   STIs for the gluon SD kernel

In the construction of the SDEs for the gluon self-energy and three-gluon vertex, one needs the knowledge of the STI satisfied by the kernel (see Fig. 71)

$$
\mathcal{K}_{A_\mu^m A_\nu^n A_\rho^r A_\sigma^s}(k_2,p_2,-p_1) = \Gamma_{A_\mu^m A_\nu^n A_\rho^r A_\sigma^s}(k_2,p_2,-p_1)
$$
$$
+ i\Gamma_{A_\sigma^s A_\mu^m A_e^e}(k_1,\ell) i\Delta_{ee'}^{\epsilon\epsilon'}(\ell) i\Gamma_{A_{\epsilon'}^{e'} A_\nu^n A_\rho^r}(k_2,p_2)
$$
$$
+ i\Gamma_{A_\sigma^s A_\nu^n A_e^e}(k_2,\ell') i\Delta_{ee'}^{\epsilon\epsilon'}(\ell') i\Gamma_{A_{\epsilon'}^{e'} A_\mu^m A_\rho^r}(k_1,p_2). \tag{C.31}
$$

Using the above relation, together with STI of Eq. (C.10), we find the following result

$$
k_1^\mu i\Gamma_{A_\sigma^s A_\mu^m A_\epsilon^e}(k_1,\ell) i\Delta_{ee'}^{\epsilon\epsilon'}(\ell) i\Gamma_{A_{\epsilon'}^{e'} A_\nu^n A_\rho^r}(k_2,p_2) = -[k_1^2 D^{mm'}(k_1)]\Gamma_{A_{\epsilon'}^{e'} A_\nu^n A_\rho^r}(k_2,p_2) \times
$$
$$
\times \left\{ \Gamma_{c^{m'} A_\sigma^s A_\epsilon^{*e'}}(-p_1,\ell) P^{\epsilon\epsilon'}(\ell) + i\Gamma_{c^{m'} A_\epsilon^e A_d^{*\gamma}}(\ell,-p_1) \Gamma_{A_\gamma^d A_\sigma^s}(p_1) \Delta_{ee'}^{\epsilon\epsilon'}(\ell) \right\}. \tag{C.32}
$$

In this case this is, however, not the end of the story, since the first term in the equation above still contains (virtual) longitudinal momenta, which will trigger the STI of Eq. (C.10) together with the FPE (C.5). After taking this into account, we obtain

$$
\begin{aligned}
k_1^\mu i\Gamma_{A_\sigma^s A_\mu^m A_\epsilon^e}(k_1,\ell) i\Delta_{ee'}^{\epsilon\epsilon'}(\ell) i\Gamma_{A_{\epsilon'}^{e'} A_\nu^n A_\rho^r}(k_2,p_2) &= -[k_1^2 D^{mm'}(k_1)] \times \\
\times \Big\{ &\Big[\Gamma_{c^{m'} A_\sigma^s A_{\epsilon'}^{*\epsilon'}}(-p_1,\ell) + i\Gamma_{c^{m'} A_\epsilon^e A_d^{*\gamma}}(\ell,-p_1)\Gamma_{A_\gamma^d A_\sigma^s}(p_1)\Delta_{ee'}^{\epsilon\epsilon'}(\ell)\Big]\Gamma_{A_{\epsilon'}^{e'} A_\nu^n A_\rho^r}(k_2,p_2) \\
&+i\Gamma_{c^{m'} A_\sigma^s \bar{c}^e}(-p_1,\ell)D^{ee'}(\ell)\Big[\Gamma_{c^{e'} A_\rho^r A_d^{*\gamma}}(p_2,k_2)\Gamma_{A_\gamma^d A_\nu^n}(k_2) \\
&+\Gamma_{c^{e'} A_\nu^n A_d^{*\gamma}}(k_2,p_2)\Gamma_{A_\gamma^d A_\rho^r}(p_2)\Big]\Big\}.
\end{aligned}
$$
(C.33)

Similarly we find

$$
\begin{aligned}
k_1^\mu i\Gamma_{A_\sigma^s A_\nu^n A_\epsilon^e}(k_2,\ell') i\Delta_{ee'}^{\epsilon\epsilon'}(\ell') i\Gamma_{A_{\epsilon'}^{e'} A_\mu^m A_\rho^r}(k_1,p_2) &= -[k_1^2 D^{mm'}(k_1)] \times \\
\times \Big\{ &\Gamma_{A_\sigma^s A_\nu^n A_\epsilon^e}(k_2,\ell')\Big[\Gamma_{c^{m'} A_\rho^r A_e^{*\epsilon}}(p_2,-\ell') + i\Delta_{ee'}^{\epsilon\epsilon'}(\ell')\Gamma_{c^{m'} A_{\epsilon'}^{e'} A_d^{*\gamma}}(-\ell',p_2)\Gamma_{A_\gamma^d A_\rho^r}(p_2)\Big] \\
&+iD^{ee'}(\ell')\Big[\Gamma_{c^e A_\nu^n A_d^{*\gamma}}(k_2,-p_1)\Gamma_{A_\gamma^d A_\sigma^s}(p_1) + \Gamma_{c^e A_\sigma^s A_d^{*\gamma}}(-p_1,k_2)\Gamma_{A_\gamma^d A_\nu^n}(k_2)\Big] \times \\
&\times\Gamma_{c^{m'} A_\rho^r \bar{c}^{e'}}(p_2,-\ell')\Big\}.
\end{aligned}
$$
(C.34)

As before, after combining these results with the four-gluon 1PI vertex STI of Eq. (C.24) we arrive at the needed STI for the four-gluon SD kernel, namely

$$
\begin{aligned}
k_1^\mu \mathcal{K}_{A_\mu^m A_\nu^n A_\rho^r A_\sigma^s}(k_2,p_2,-p_1) = [k_1^2 D^{mm'}(k_1)]\Big\{ &\Gamma_{c^{m'} A_\nu^n A_d^{*\gamma}}(k_2,-k_1-k_2)\Gamma_{A_\gamma^d A_\rho^r A_\sigma^s}(p_2,-p_1) \\
&+\mathcal{K}_{c^{m'} A_\nu^n A_\sigma^s A_d^{*\gamma}}(k_2,-p_1,p_2)\Gamma_{A_\gamma^d A_\rho^r}(p_2) \\
&+\mathcal{K}_{c^{m'} A_\nu^n A_\rho^r A_d^{*\gamma}}(k_2,p_2,-p_1)\Gamma_{A_\gamma^d A_\sigma^s}(p_1) \\
&+\mathcal{K}_{c^{m'} A_\rho^r A_\sigma^s A_d^{*\gamma}}(p_2,-p_1,k_2)\Gamma_{A_\gamma^d A_\nu^n}(k_2)\Big\},
\end{aligned}
$$
(C.35)

where the following auxiliary kernels have been defined

$$\mathcal{K}_{c m' A_\nu^n A_\sigma^s A_d^{*\gamma}}(k_2, -p_1, p_2) = \Gamma_{c m' A_\nu^n A_\sigma^s A_d^{*\gamma}}(k_2, -p_1, p_2)$$
$$+ i\Gamma_{A_\sigma^s A_\nu^n A_\epsilon^e}(k_2, \ell') i\Delta_{ee'}^{\epsilon\epsilon'}(\ell') i\Gamma_{c m' A_{\epsilon'}^{e'} A_d^{*\gamma}}(-\ell', p_2)$$
$$+ i\Gamma_{c m' A_\sigma^s \bar{c}^e}(-p_1, \ell) iD^{ee'}(\ell) i\Gamma_{c e' A_\nu^n A_d^{*\gamma}}(k_2, p_2),$$

$$\mathcal{K}_{c m' A_\nu^n A_\rho^r A_d^{*\gamma}}(k_2, p_2, -p_1) = \Gamma_{c m' A_\nu^n A_\rho^r A_d^{*\gamma}}(k_2, p_2, -p_1)$$
$$+ i\Gamma_{c m' A_\epsilon^e A_d^{*\gamma}}(\ell, -p_1) i\Delta_{ee'}^{\epsilon\epsilon'}(\ell) i\Gamma_{A_{\epsilon'}^{e'} A_\rho^r A_\nu^n}(k_2, p_2)$$
$$+ i\Gamma_{c e A_\nu^n A_d^{*\gamma}}(k_2, -p_1) iD^{ee'}(\ell') i\Gamma_{c m' A_\rho^r \bar{c}^{e'}}(p_2, -\ell'),$$

$$\mathcal{K}_{c m' A_\rho^r A_\sigma^s A_d^{*\gamma}}(p_2, -p_1, k_2) = \Gamma_{c m' A_\rho^r A_\sigma^s A_d^{*\gamma}}(p_2, -p_1, k_2)$$
$$+ i\Gamma_{c m' A_\sigma^s \bar{c}^{e'}}(-p_1, \ell) iD^{ee'}(\ell) i\Gamma_{c e' A_\rho^r A_d^{*\gamma}}(p_2, k_2)$$
$$+ i\Gamma_{c e A_\sigma^s A_d^{*\gamma}}(-p_1, k_2) iD^{ee'}(\ell') i\Gamma_{c m' A_\rho^r \bar{c}^{e'}}(p_2, -\ell'). \qquad (C.36)$$

C.3 Background-Quantum Identities

BQIs are obtained by functional differentiation of the STI functional of Eq. (7.17) with respect to combinations of background fields, quantum fields and background sources.

C.3.1 BQIs for two-point functions

The first BQI we can construct is the one relating the conventional with the BFM gluon self-energies. To this end, consider the following functional differentiation

$$\left. \frac{\delta^2 \mathcal{S}'(\Gamma')}{\delta\Omega_\alpha^a(p)\delta A_\beta^b(q)} \right|_{\Phi, \Phi^*, \Omega = 0} = 0 \qquad q + p = 0,$$
$$\left. \frac{\delta^2 \mathcal{S}'(\Gamma')}{\delta\Omega_\alpha^a(p)\delta \widehat{A}_\beta^b(q)} \right|_{\Phi, \Phi^*, \Omega = 0} = 0 \qquad q + p = 0, \qquad (C.37)$$

which will give the relations

$$i\Gamma_{\widehat{A}_\alpha^a A_\beta^b}(q) = \left[ig_\alpha^\gamma \delta^{ad} + \Gamma_{\Omega_\alpha^a A_d^{*\gamma}}(q) \right] \Gamma_{A_\gamma^d A_\beta^b}(q),$$
$$i\Gamma_{\widehat{A}_\alpha^a \widehat{A}_\beta^b}(q) = \left[ig_\alpha^\gamma \delta^{ad} + \Gamma_{\Omega_\alpha^a A_d^{*\gamma}}(q) \right] \Gamma_{A_\gamma^d \widehat{A}_\beta^b}(q). \qquad (C.38)$$

We can now combine Eq.s (C.38) and (C.38) such that the two-point function mixing background and quantum fields drops out, to get the BQI
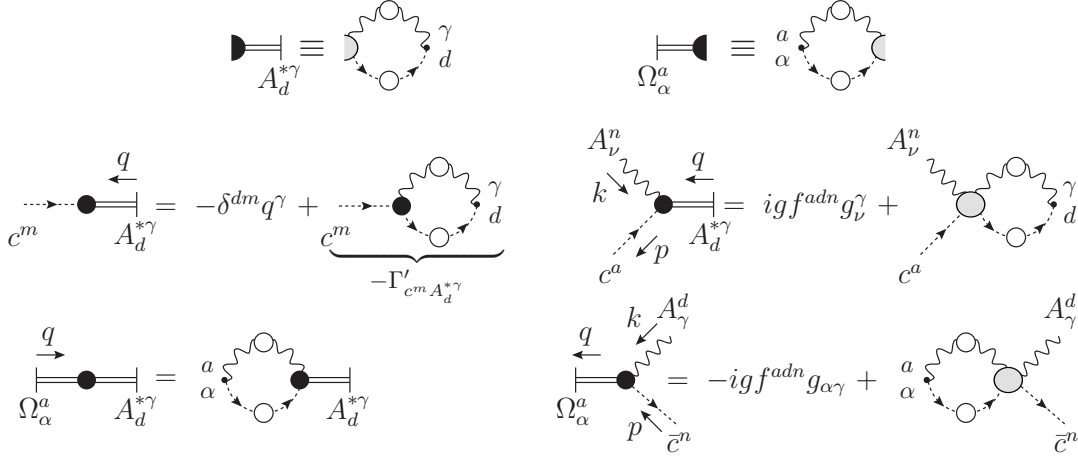
Fig. C.1. Expansions of the gluon anti-field and BFM source in terms of the corresponding composite operators. Notice that if the anti-field or the BFM sources are attached to a 1PI vertex, as shown in the first line, such an expansion will, in general, convert the 1PI vertex into a (connected) SD kernel. The equivalence shown is therefore not valid at tree-level (*e.g.*, in the case of three-point functions such an equivalence would imply that the kernels shown on the rhs of the corresponding expansions would be disconnected); when present, the tree-level needs to be added by hand, as explicitly shown in the two expansions of the second line and the last one of the third line. This type of expansion allows one to express the terms appearing in the BQIs in a form that reveals kernels appearing in the STIs [see, *e.g.*, Eq.s (C.49) and (C.50)]

$$
\begin{aligned}
i\Gamma_{\widehat{A}_\alpha^a \widehat{A}_\beta^b}(q) &= i\Gamma_{A_\alpha^a A_\beta^b}(q) + \Gamma_{\Omega_\alpha^a A_d^{*\gamma}}(q)\Gamma_{A_\gamma^d A_\beta^b}(q) + \Gamma_{\Omega_\beta^b A_d^{*\gamma}}(q)\Gamma_{A_\alpha^a A_\gamma^d}(q) \\
&\quad - i\Gamma_{\Omega_\alpha^a A_d^{*\gamma}}(q)\Gamma_{A_\gamma^d A_\epsilon^e}(q)\Gamma_{\Omega_\beta^b A_e^{*\epsilon}}(q) \\
&= i\Gamma_{A_\alpha^a A_\beta^b}(q) + 2\Gamma_{\Omega_\alpha^a A_d^{*\gamma}}(q)\Gamma_{A_\gamma^d A_\beta^b}(q) - i\Gamma_{\Omega_\alpha^a A_d^{*\gamma}}(q)\Gamma_{A_\gamma^d A_\epsilon^e}(q)\Gamma_{\Omega_\beta^b A_e^{*\epsilon}}, \quad (\text{C.39})
\end{aligned}
$$

where the last identity is due to the transversality of the Γ_{AA} two-point function.

In order for our PT procedure to be self-contained, it is important to express the 1PI auxiliary Green's function involved in the various STIs and the BQIs in terms of kernels that also appear in the relevant STIs. The key observation that makes this possible is that one may always replace an anti-field or BFM source with its corresponding BRST composite operator. Thus, for example, one has (see Fig. C.1)

$$
A_d^{*\gamma}(q) \rightarrow i\Gamma^{(0)}_{c^{e'} A_{\nu'}^{n'} A_d^{*\gamma}} \int_{k_1} i\Delta_{n'n}^{\nu'\nu}(k_2) iD^{e'e}(k_1), \tag{C.40}
$$

$$
\Omega_\alpha^a(q) \rightarrow i\Gamma^{(0)}_{\Omega_\alpha^a A_{\nu'}^{n'} \bar{c}^{e'}} \int_{k_1} i\Delta_{n'n}^{\nu'\nu}(k_2) iD^{e'e}(k_1), \tag{C.41}
$$

where k_1 and k_2 are related through $k_2 = q - k_1$. In this way we get the following SDEs (see again Fig. C.1)
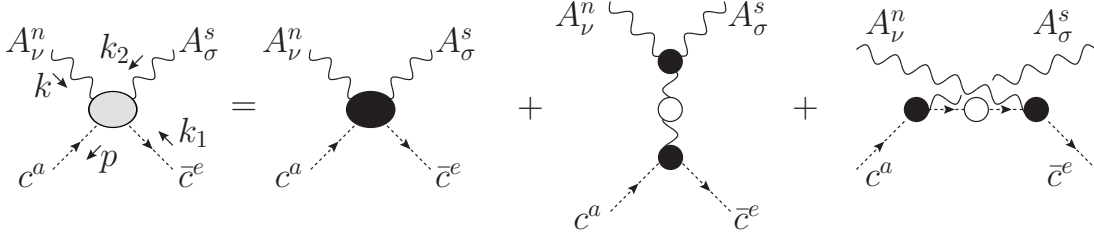
Fig. C.2. Skeleton expansion of the kernel appearing in the SDE for the auxiliary function Γ_{cAA^*}.

$$-\Gamma_{c^m A_d^{*\gamma}}(q) = -\delta^{dm} q_\gamma - \Gamma'_{c^m A_d^{*\gamma}}(q)$$

$$= -\delta^{dm} q_\gamma + g f^{dn'e'} g_{\nu'}^\gamma \int_{k_1} D^{e'e}(k_1)\Delta_{\nu'\nu}^{nn'}(k_2)\Gamma_{c^m A_\nu^n \bar{c}^e}(k_2, k_1), \qquad (C.42)$$

$$i\Gamma_{c^a A_\nu^n A_d^{*\gamma}}(k, q) = i g f^{adn} g_\nu^\gamma - i g f^{e'ds'} g_{\sigma'}^\gamma \int_{k_1} D^{ee'}(k_1)\Delta_{ss'}^{\sigma\sigma'}(k_2)\mathcal{K}_{c^a A_\nu^n A_\sigma^s \bar{c}^e}(k, k_2, k_1), \quad (C.43)$$

$$-\Gamma_{\Omega_\alpha^a A_d^{*\gamma}}(q) = g f^{ae'n'} g_{\alpha\nu'} \int_{k_1} D^{e'e}(k_1)\Delta_{n'n}^{\nu'\nu}(k_2)\Gamma_{c^e A_\nu^n A_d^{*\gamma}}(k_2, -q), \qquad (C.44)$$

$$i\Gamma_{\Omega_\alpha^a A_\gamma^d \bar{c}^n}(k, p) = -i g f^{adn} g_{\alpha\gamma} - i g f^{ae'n'} g_{\alpha\nu'} \int_{k_1} D^{e'e}(k_1)\Delta_{n'n}^{\nu'\nu}(k_2)\mathcal{K}_{c^e A_\nu^n A_\gamma^d \bar{c}^n}(k_2, k, p).$$
$$(C.45)$$

The kernel $\mathcal{K}_{cAA\bar{c}}$ appearing in the SDEs (C.43) and (C.45) is shown in Fig. C.2 and reads

$$\mathcal{K}_{c^a A_\nu^n A_\sigma^s \bar{c}^e}(k, k_2, k_1) = \Gamma_{c^a A_\nu^n A_\sigma^s \bar{c}^e}(k, k_2, k_1)$$
$$+ i\Gamma_{A_\nu^n A_\sigma^s A_\rho^r}(k_2, -k-k_2)i\Delta_{rr'}^{\rho\rho'}(k+k_2)i\Gamma_{c^m A_{\rho'}^{r'} \bar{c}^e}(k+k_2, k_1)$$
$$+ i\Gamma_{c^a A_\sigma^s \bar{c}^r}(k_2, -k_1-k_2)iD^{rr'}(k_1+k_2)i\Gamma_{c^{r'} A_\nu^n \bar{c}^e}(k, k_1). \qquad (C.46)$$

C.3.2 BQIs for three-point functions

The relation between the trilinear gluon vertex and the trilinear background gluon vertex, can be obtained by considering the following functional differentiation

$$\frac{\delta^3 \mathcal{S}'(\Gamma')}{\delta\Omega_\alpha^a(q)\delta A_\rho^r(p_2)\delta A_\sigma^s(-p_1)}\bigg|_{\Phi,\Phi^*,\Omega=0} = 0 \qquad q + p_2 = p_1. \qquad (C.47)$$

We then get

$$i\Gamma_{\widehat{A}_\alpha^a A_\rho^r A_\sigma^s}(p_2, -p_1) = [i g_\alpha^\gamma \delta^{ad} + \Gamma_{\Omega_\alpha^a A_d^{*\gamma}}(-q)]\Gamma_{A_\gamma^d A_\rho^r A_\sigma^s}(p_2, -p_1)$$
$$+ \Gamma_{\Omega_\alpha^a A_\sigma^s A_d^{*\gamma}}(-p_1, p_2)\Gamma_{A_\gamma^d A_\rho^r}(p_2) + \Gamma_{\Omega_\alpha^a A_\rho^r A_d^{*\gamma}}(p_2, -p_1)\Gamma_{A_\gamma^d A_\sigma^s}(p_1).$$
$$(C.48)$$

In order to explore further the all-order structure of these two auxiliary Green's functions, replace the BFM source with the corresponding composite operator using Eq. (C.41), thus obtaining

$$i\Gamma_{\Omega^a_\alpha A^s_\sigma A^{*\gamma}_d}(-p_1, p_2) = i\Gamma^{(0)}_{\Omega^a_\alpha A^{n'}_{\nu'} \bar{c}^{m'}} \int_{k_1} iD^{m'm}(k_1) i\Delta^{\nu'\nu}_{n'n}(k_2) \mathcal{K}_{c^m A^n_\nu A^s_\sigma A^{*\gamma}_d}(k_2, -p_1, p_2),$$

$$\text{(C.49)}$$

$$i\Gamma_{\Omega^a_\alpha A^r_\rho A^{*\gamma}_d}(p_2, -p_1) = i\Gamma^{(0)}_{\Omega^a_\alpha A^{n'}_{\nu'} \bar{c}^{m'}} \int_{k_1} iD^{m'm}(k_1) i\Delta^{\nu'\nu}_{n'n}(k_2) \mathcal{K}_{c^m A^n_\nu A^r_\rho A^{*\gamma}_d}(k_2, p_2, -p_1),$$

$$\text{(C.50)}$$

with the corresponding kernels defined in Eq.s (C.36) and (C.36). Notice the emergence of the pattern exploited in the application of the PT to the SDEs of QCD: namely that the auxiliary functions appearing in the BQI satisfied by a particular Green's function can be written in terms of kernels appearing in the STIs triggered when the PT procedure is applied to that same Green's function.

Now, the BQI of Eq. (C.48) gives at tree-level the result

$$\Gamma_{\widehat{A}^a_\alpha A^r_\rho A^s_\sigma}(p_2, -p_1) = \Gamma_{A^a_\alpha A^r_\rho A^s_\sigma}(p_2, -p_1). \qquad \text{(C.51)}$$

This is once again due to the use of the reduced functional: in fact in such case the two (tree-level) vertices need to coincide, since the difference between them is proportional to the inverse of the gauge fixing parameter (see Appendix B) and therefore entirely due to the gauge fixing Lagrangian. To restore the correct tree-level terms one would have to use the complete functional; in that case the differentiation of Eq. (C.47) shows the two additional terms

$$-\delta^{ds} p_{1\sigma} \Gamma_{\Omega^a_\alpha A^r_\rho \bar{c}^d}(p_2, -p_1) + \delta^{dr} p_{2\rho} \Gamma_{\Omega^a_\alpha A^s_\sigma \bar{c}^d}(-p_1, p_2), \qquad \text{(C.52)}$$

which, with the help of Eq. (C.7) become

$$-i\delta^{ds} p_{1\sigma} p_{1\gamma} \Gamma_{\Omega^a_\alpha A^r_\rho A^{*\gamma}_d}(p_2, -p_1) - i\delta^{dr} p_{2\rho} p_{2\gamma} \Gamma_{\Omega^a_\alpha A^s_\sigma A^{*\gamma}_d}(-p_1, p_2) + g f^{ars}(q_{\alpha\rho} p_{1\sigma} + g_{\alpha\sigma} p_{2\rho}).$$

$$\text{(C.53)}$$

Therefore we get the final identity

$$i\Gamma^{\text{C}}_{\widehat{A}^a_\alpha A^r_\rho A^s_\sigma}(p_2, -p_1) = [ig^\gamma_\alpha \delta^{ad} + \Gamma_{\Omega^a_\alpha A^{*\gamma}_d}(-q)]\Gamma_{A^d_\gamma A^r_\rho A^s_\sigma}(p_2, -p_1) + g f^{ars}(q_{\alpha\rho} p_{1\sigma} + g_{\alpha\sigma} p_{2\rho})$$

$$+ \Gamma_{\Omega^a_\alpha A^s_\sigma A^{*\gamma}_d}(-p_1, p_2) \left[\Gamma^{\text{C}}_{A^d_\gamma A^r_\rho}(p_2) - i\delta^{dr} p_{2\rho} p_{2\gamma} \right]$$

$$+ \Gamma_{\Omega^a_\alpha A^r_\rho A^{*\gamma}_d}(p_2, -p_1) \left[\Gamma^{\text{C}}_{A^d_\gamma A^s_\sigma}(p_1) - i\delta^{ds} p_{1\sigma} p_{1\gamma} \right], \qquad \text{(C.54)}$$

which gives the expected tree-level result. Once again we see that the difference between working with the reduced and complete functional lies in some constant (tree-level) terms that one recovers after applying the FPE for writing the STI/BQI at hand in the same form using Γ or Γ_{C}. Thus, opting for the fast way of deriving the STI/BQI with the reduced functional and adding the correct tree-level term, we write the BQI in its final form

$$i\Gamma_{\widehat{A}_\alpha^a A_\rho^r A_\sigma^s}(p_2, -p_1) = [ig_\alpha^\gamma \delta^{ad} + \Gamma_{\Omega_\alpha^a A_d^{*\gamma}}(-q)]\Gamma_{A_\gamma^d A_\rho^r A_\sigma^s}(p_2, -p_1)$$
$$+ \Gamma_{\Omega_\alpha^a A_\sigma^s A_d^{*\gamma}}(-p_1, p_2)\Gamma_{A_\gamma^d A_\rho^r}(p_2) + \Gamma_{\Omega_\alpha^a A_\rho^r A_d^{*\gamma}}(p_2, -p_1)\Gamma_{A_\gamma^d A_\sigma^s}(p_1)$$
$$+ gf^{ars}\left(p_{2\rho}g_{\alpha\sigma} + p_{1\sigma}g_{\alpha\rho}\right). \tag{C.55}$$

We conclude by giving the relation between the trilinear quantum gluon-quark vertex and the trilinear background gluon-quark vertex; this can be obtained by considering the following functional differentiation

$$\left.\frac{\delta^3 \mathcal{S}'(\Gamma')}{\delta\Omega_\alpha^a(q)\delta\psi(p_2)\delta\bar\psi(-p_1)}\right|_{\Phi,\Phi^*,\Omega=0} = 0 \qquad q + p_2 = p_1. \tag{C.56}$$

We then get

$$i\Gamma_{\widehat{A}_\alpha^a \psi\bar\psi}(p_2, -p_1) = [ig_\alpha^\gamma \delta^{ad} + \Gamma_{\Omega_\alpha^a A_d^{*\gamma}}(-q)]\Gamma_{A_\gamma^d \psi\bar\psi}(p_2, -p_1)$$
$$+ \Gamma_{\psi^*\bar\psi\Omega_\alpha^a}(-p_1, q)\Gamma_{\psi\bar\psi}(p_2) + \Gamma_{\psi\bar\psi}(p_1)\Gamma_{\psi\Omega_\alpha^a \bar\psi^*}(q, -p_1). \tag{C.57}$$

C.3.3   BQI for the ghost-gluon trilinear vertex

In this section we are going to derive the BQIs relating the R_ξ ghost sector with the BFM ones. We start from the trilinear ghost-gluon coupling, for which we choose the following functional differentiation

$$\left.\frac{\delta^3 \mathcal{S}'(\Gamma')}{\delta\Omega_\alpha^a(-q)\delta c^m(k_1)\delta\bar c^n(k_2)}\right|_{\Phi,\Phi^*,\Omega=0} = 0 \qquad k_1 + k_2 = q, \tag{C.58}$$

thus getting the result

$$i\Gamma_{c^m \widehat{A}_\alpha^a \bar c^n}(-q, k_2) = [i\delta^{da} g_\alpha^\gamma + \Gamma_{\Omega_\alpha^a A_d^{*\gamma}}(q)]\Gamma_{c^m A_\gamma^d \bar c^n}(-q, k_2)$$
$$- \Gamma_{c^m A_d^{*\gamma}}(-k_1)\Gamma_{\Omega_\alpha^a A_\gamma^d \bar c^n}(k_1, k_2) - \Gamma_{\Omega_\alpha^a c^m c^{*d}}(k_1, k_2)\Gamma_{c^d \bar c^n}(k_2). \tag{C.59}$$

References

[1] E. S. Abers, B. W. Lee, Gauge Theories, Phys. Rept. 9 (1973) 1–141.

[2] M. Froissart, Asymptotic behavior and subtractions in the Mandelstam representation, Phys. Rev. 123 (1961) 1053–1057.

[3] C. Becchi, A. Rouet, R. Stora, Renormalization of Gauge Theories, Annals Phys. 98 (1976) 287–321.

[4] I. V. Tyutin, Gauge invariance in field theory and statistical physics in operator formalism, LEBEDEV-75-39.

[5] J. M. Cornwall, Confinement and Infrared Properties of Yang-Mills Theory, Invited talk given at the US-Japan Seminar on Geometric Models of the Elementary Particles, Osaka, Japan, Jun 7-11, 1976.

[6] J. M. Cornwall, Nonperturbative mass gap in continuum QCD, UCLA/81/TEP/12, In *Marseille 1981, Proceedings, Theoretical Aspects Of Quantum Chromodynamics*, 96-116.

[7] J. M. Cornwall, Dynamical Mass Generation in Continuum QCD, Phys. Rev. D26 (1982) 1453.

[8] J. M. Cornwall, J. Papavassiliou, Gauge Invariant Three Gluon Vertex in QCD, Phys. Rev. D40 (1989) 3474.

[9] J. Papavassiliou, Gauge Invariant Proper Selfenergies and Vertices in Gauge Theories with Broken Symmetry, Phys. Rev. D41 (1990) 3179.

[10] Y. J. Feng, C. S. Lam, Diagrammatic analysis of QCD gauge transformations and gauge cancellations, Phys. Rev. D53 (1996) 2115–2127.

[11] J. M. Cornwall, G. Tiktopoulos, Infrared Behavior of Nonabelian Gauge Theories. 2, Phys. Rev. D15 (1977) 2937.

[12] N. J. Watson, The gauge-independent QCD effective charge, Nucl. Phys. B494 (1997) 388–432.

[13] S. J. Brodsky, G. P. Lepage, P. B. Mackenzie, On the Elimination of Scale Ambiguities in Perturbative Quantum Chromodynamics, Phys. Rev. D28 (1983) 228.

[14] A. H. Mueller, The QCD perturbation series, Talk given at Workshop on QCD: 20 Years Later, Aachen, Germany, 9-13 Jun 1992.

[15] S. J. Brodsky, Perspectives and challenges for QCD phenomenology, In the Proceedings of APS / DPF / DPB Summer Study on the Future of Particle Physics (Snowmass 2001), Snowmass, Colorado, 30 Jun - 21 Jul 2001, pp E211.

[16] M. Binger, S. J. Brodsky, Physical renormalization schemes and grand unification, Phys. Rev. D69 (2004) 095007.

[17] K. Fujikawa, B. W. Lee, A. I. Sanda, Generalized Renormalizable Gauge Formulation of Spontaneously Broken Gauge Theories, Phys. Rev. D6 (1972) 2923–2943.

[18] J. Papavassiliou, K. Philippides, Gauge invariant three boson vertices in the Standard Model and the static properties of the W, Phys. Rev. D48 (1993) 4255–4268.

[19] J. Papavassiliou, C. Parrinello, Gauge invariant top quark form-factors from e+ e- experiments, Phys. Rev. D50 (1994) 3059–3075.

[20] J. Bernabeu, L. G. Cabral-Rosetti, J. Papavassiliou, J. Vidal, On the charge radius of the neutrino, Phys. Rev. D62 (2000) 113012.

[21] J. Bernabeu, J. Papavassiliou, J. Vidal, On the observability of the neutrino charge radius, Phys. Rev. Lett. 89 (2002) 101802.

[22] M. J. G. Veltman, Unitarity and causality in a renormalizable field theory with unstable particles, Physica 29 (1963) 186–207.

[23] J. Papavassiliou, A. Pilaftsis, Gauge invariance and unstable particles, Phys. Rev. Lett. 75 (1995) 3060–3063.

[24] F. J. Dyson, The S matrix in quantum electrodynamics, Phys. Rev. 75 (1949) 1736–1755.

[25] J. S. Schwinger, On the Green's functions of quantized fields. 1, Proc. Nat. Acad. Sci. 37 (1951) 452–455.

[26] J. M. Cornwall, R. Jackiw, E. Tomboulis, Effective Action for Composite Operators, Phys. Rev. D10 (1974) 2428–2445.

[27] W. J. Marciano, H. Pagels, Quantum Chromodynamics: A Review, Phys. Rept. 36 (1978) 137.

[28] B. S. DeWitt, Quantum theory of gravity. II. The manifestly covariant theory, Phys. Rev. 162 (1967) 1195–1239.

[29] J. Honerkamp, The Question of invariant renormalizability of the massless Yang-Mills theory in a manifest covariant approach, Nucl. Phys. B48 (1972) 269–287.

[30] R. E. Kallosh, The Renormalization in Nonabelian Gauge Theories, Nucl. Phys. B78 (1974) 293.

[31] H. Kluberg-Stern, J. B. Zuber, Renormalization of Nonabelian Gauge Theories in a Background Field Gauge. 1. Green Functions, Phys. Rev. D12 (1975) 482–488.

[32] I. Y. Arefeva, L. D. Faddeev, A. A. Slavnov, Generating Functional for the S-Matrix in Gauge Theories, Theor. Math. Phys. 21 (1975) 1165.

[33] G. 't Hooft, The Background Field Method in Gauge Field Theories, In *Karpacz 1975, Proceedings, Acta Universitatis Wratislaviensis No.368, Vol.1*, Wroclaw 1976, 345-369.

[34] L. F. Abbott, The Background Field Method Beyond One Loop, Nucl. Phys. B185 (1981) 189.

[35] S. Weinberg, Effective Gauge Theories, Phys. Lett. B91 (1980) 51.

[36] G. M. Shore, Symmetry restoration and the background field method in gauge theories, Ann. Phys. 137 (1981) 262.

[37] L. F. Abbott, M. T. Grisaru, R. K. Schaefer, The Background Field Method and the S Matrix, Nucl. Phys. B229 (1983) 372.

[38] C. F. Hart, Theory and renormalization of the gauge invariant effective action, Phys. Rev. D28 (1983) 1993–2006.

[39] S. Weinberg, The quantum theory of fields. Vol 2: Modern applications, Cambridge, UK: Univ. Pr. (1996) 489 p, 1996.

[40] A. Denner, G. Weiglein, S. Dittmaier, Gauge invariance of green functions: Background field method versus pinch technique, Phys. Lett. B333 (1994) 420–426.

[41] S. Hashimoto, J. Kodaira, Y. Yasui, K. Sasaki, The Background field method: Alternative way of deriving the pinch technique's results, Phys. Rev. D50 (1994) 7066–7076.

[42] A. Pilaftsis, Generalized pinch technique and the background field method in general gauges, Nucl. Phys. B487 (1997) 467–491.

[43] J. Papavassiliou, The pinch technique at two loops, Phys. Rev. Lett. 84 (2000) 2782–2785.

[44] D. Binosi, J. Papavassiliou, The pinch technique to all orders, Phys. Rev. D66 (2002) 111901(R).

[45] J. S. Ball, T.-W. Chiu, Analytic properties of the vertex function in gauge theories. 2, Phys. Rev. D22 (1980) 2550.

[46] I. A. Batalin, G. A. Vilkovisky, Quantization of Gauge Theories with Linearly Dependent Generators, Phys. Rev. D28 (1983) 2567–2582.

[47] M. E. Peskin, D. V. Schroeder, An Introduction to quantum field theory, Reading, USA: Addison-Wesley, 842 p, 1995.

[48] C. Becchi, A. Rouet, R. Stora, Renormalization of the Abelian Higgs-Kibble Model, Commun. Math. Phys. 42 (1975) 127–162.

[49] N. Nakanishi, Covariant quantization of the electromagnetic field in the landau gauge, Prog. Theor. Phys. 35 (6) (1966) 1111–1116.

[50] B. Lautrup, Canonical quantum electrodynamics in covariant gauges, Mat. Fys. Medd. Dan. Vid. Selsk. 35 (11) (1966) 1.

[51] R. Delbourgo, A. Salam, J. A. Strathdee, Scalar multiplets and asymptotic freedom, Nuovo Cim. A23 (1974) 237–256.

[52] W. Kummer, Ghost Free Nonabelian Gauge Theory, Acta Phys. Austriaca 41 (1975) 315–334.

[53] W. Konetschny, W. Kummer, Ghost free nonabelian gauge theory: Renormalization and gauge-invariance, Nucl. Phys. B100 (1975) 106.

[54] J. Frenkel, A class of ghost free nonabelian gauge theories, Phys. Rev. D13 (1976) 2325–2334.

[55] Y. L. Dokshitzer, D. Diakonov, S. I. Troian, Hard Processes in Quantum Chromodynamics, Phys. Rept. 58 (1980) 269–395.

[56] G. Leibbrandt, Introduction to Noncovariant Gauges, Rev. Mod. Phys. 59 (1987) 1067.

[57] D. M. Capper, G. Leibbrandt, On Ward Identities in a general axial gauge. 1. Yang-Mills Theory, Phys. Rev. D25 (1982) 1002.

[58] A. Andrasi, J. C. Taylor, Ghosts and renormalization in the planar gauge, Nucl. Phys. B192 (1981) 283.

[59] L. F. Abbott, Introduction to the Background Field Method, Acta Phys. Polon. B13 (1982) 33.

[60] J. Papavassiliou, On the connection between the pinch technique and the background field method, Phys. Rev. D51 (1995) 856–861.

[61] D. Binosi, J. Papavassiliou, Gauge-independent off-shell fermion self-energies at two loops: The cases of QED and QCD, Phys. Rev. D65 (2002) 085003.

[62] P. Pascual, R. Tarrach, QCD: Renormalization for the practitioner, Lect. Notes Phys. 194 (1984) 1–277.

[63] N. J. Watson, Universality of the pinch technique gauge boson selfenergies, Phys. Lett. B349 (1995) 155–164.

[64] U. Bar-Gadda, Infrared behavior of the effective coupling in quantum chromodynamics: a nonperturbative approach, Nucl. Phys. B163 (1980) 312–332.

[65] M. Binger, S. J. Brodsky, The form factors of the gauge-invariant three-gluon vertex, Phys. Rev. D74 (2006) 054016.

[66] Z. Bern, L. J. Dixon, D. C. Dunbar, D. A. Kosower, One loop n point gauge theory amplitudes, unitarity and collinear limits, Nucl. Phys. B425 (1994) 217–260.

[67] Z. Bern, L. J. Dixon, D. C. Dunbar, D. A. Kosower, Fusing gauge theory tree amplitudes into loop amplitudes, Nucl. Phys. B435 (1995) 59–101.

[68] A. I. Davydychev, P. Osland, O. V. Tarasov, Three-gluon vertex in arbitrary gauge and dimension, Phys. Rev. D54 (1996) 4087–4113.

[69] J. Papavassiliou, The gauge invariant four gluon vertex and its Ward Identity, Phys. Rev. D47 (1993) 4728–4738.

[70] J. D. Bjorken, S. D. Drell, Relativistic Quantum Field Theory, Mc Graw-Hill, Inc. (1965), 1965.

[71] R. J. Eden, P. V. Landshoff, P. J. Olive, J. C. Polkinghorne, The analytic S matrix, Cambridge, UK: Univ. Pr. (1966), 1966.

[72] J. Papavassiliou, A. Pilaftsis, Gauge-invariant resummation formalism for two point correlation functions, Phys. Rev. D54 (1996) 5315–5335.

[73] J. Papavassiliou, E. de Rafael, N. J. Watson, Electroweak effective charges and their relation to physical cross sections, Nucl. Phys. B503 (1997) 79–116.

[74] J. Papavassiliou, A. Pilaftsis, A Gauge independent approach to resonant transition amplitudes, Phys. Rev. D53 (1996) 2128–2149.

[75] J. Papavassiliou, A. Pilaftsis, Effective charge of the Higgs boson, Phys. Rev. Lett. 80 (1998) 2785–2788.

[76] J. Papavassiliou, The pinch technique approach to the physics of unstable particles, In 6th Hellenic School and Workshop on Elementary Particle Physics: Corfu, Greece, 6-26 Sep 1998.

[77] B. S. DeWitt, Quantum theory of gravity. III. Applications of the covariant theory, Phys. Rev. 162 (1967) 1239–1256.

[78] J. Honerkamp, Chiral multiloops, Nucl. Phys. B36 (1972) 130–140.

[79] S. Sarkar, Mixing of Operators in Wilson Expansions, Nucl. Phys. B82 (1974) 447.

[80] S. Sarkar, H. Strubbe, Anomalous Dimensions in Background Field Gauges, Nucl. Phys. B90 (1975) 45.

[81] H. Kluberg-Stern, J. B. Zuber, Renormalization of Nonabelian Gauge Theories in a Background Field Gauge. 2. Gauge Invariant Operators, Phys. Rev. D12 (1975) 3159–3180.

[82] G. 't Hooft, An algorithm for the poles at dimension four in the dimensional regularization procedure, Nucl. Phys. B62 (1973) 444–460.

[83] M. T. Grisaru, P. van Nieuwenhuizen, C. C. Wu, Background Field Method Versus Normal Field Theory in Explicit Examples: One Loop Divergences in S Matrix and Green's Functions for Yang-Mills and Gravitational Fields, Phys. Rev. D12 (1975) 3203.

[84] B. S. DeWitt, A gauge invariant effective action, NSF-ITP-80-31.

[85] D. G. Boulware, Gauge Dependence of the Effective Action, Phys. Rev. D23 (1981) 389.

[86] D. M. Capper, A. MacLean, The background field method at two loops: a general gauge Yang-Mills calculation, Nucl. Phys. B203 (1982) 413.

[87] H. D. Politzer, Reliable perturbative results for strong interactions?, Phys. Rev. Lett. 30 (1973) 1346–1349.

[88] D. J. Gross, F. Wilczek, Ultraviolet behavior of non-Abelian gauge theories, Phys. Rev. Lett. 30 (1973) 1343–1346.

[89] D. R. T. Jones, Two Loop Diagrams in Yang-Mills Theory, Nucl. Phys. B75 (1974) 531.

[90] A. C. Aguilar, J. Papavassiliou, Gluon mass generation in the PT-BFM scheme, JHEP 12 (2006) 012.

[91] B. Haeri Jr, The ultraviolet improved gauge technique and the effective quark propagator in QCD, Phys. Rev. D38 (1988) 3799.

[92] G. Degrassi, A. Sirlin, Gauge invariant selfenergies and vertex parts of the Standard Model in the pinch technique framework, Phys. Rev. D46 (1992) 3104–3116.

[93] J. Papavassiliou, Gauge independent transverse and longitudinal self energies and vertices via the pinch technique, Phys. Rev. D50 (1994) 5958–5970.

[94] D. Binosi, Electroweak pinch technique to all orders, J. Phys. G30 (2004) 1021–1064.

[95] A. Denner, G. Weiglein, S. Dittmaier, Application of the background field method to the electroweak standard model, Nucl. Phys. B440 (1995) 95–128.

[96] G. Passarino, M. J. G. Veltman, One Loop Corrections for e+ e- Annihilation Into mu+ mu- in the Weinberg Model, Nucl. Phys. B160 (1979) 151.

[97] A. Denner, Techniques for calculation of electroweak radiative corrections at the one loop level and results for W physics at LEP-200, Fortschr. Phys. 41 (1993) 307–420.

[98] S. Weinberg, Physical Processes in a Convergent Theory of the Weak and Electromagnetic Interactions, Phys. Rev. Lett. 27 (1971) 1688–1691.

[99] S. Y. Lee, Finite higher-order weak and electromagnetic corrections to the strangeness-conserving hadronic beta decay in weinberg's theory of weak interactions, Phys. Rev. D6 (1972) 1803–1807.

[100] T. Appelquist, H. R. Quinn, Divergence cancellations in a simplified weak interaction model, Phys. Lett. B39 (1972) 229–232.

[101] J. Papavassiliou, A. Sirlin, Renormalizable W selfenergy in the unitary gauge via the pinch technique, Phys. Rev. D50 (1994) 5951–5957.

[102] W. Alles, C. Boyer, A. J. Buras, W Boson Production in e+ e- Collisions in the Weinberg-Salam Model, Nucl. Phys. B119 (1977) 125.

[103] J. Papavassiliou, CP violation in the Weinberg multi-Higgs model, Presented at the Conference on Standard Model IV, Lake Tahoe, Dec 13-18, 1995. In *Tahoe City 1994, Proceedings, Beyond the standard model 4* 509-513.

[104] M. Gell-Mann, F. E. Low, Quantum electrodynamics at small distances, Phys. Rev. 95 (1954) 1300–1312.

[105] G. 't Hooft, in The Whys of Subnuclear Physics, Ed. A. Zichichi, Plenum Press, New York (1979).

[106] F. David, The Operator Product Expansion and Renormalons: A Comment, Nucl. Phys. B263 (1986) 637–648.

[107] M. Beneke, V. M. Braun, Heavy quark effective theory beyond perturbation theory: Renormalons, the pole mass and the residual mass term, Nucl. Phys. B426 (1994) 301–343.

[108] A. Pilaftsis, Enhancement of CP violating phenomena at tree level due to heavy quark propagator singularities, Z. Phys. C47 (1990) 95–104.

[109] A. Sirlin, Theoretical considerations concerning the Z0 mass, Phys. Rev. Lett. 67 (1991) 2127–2130.

[110] A. Sirlin, Observations concerning mass renormalization in the electroweak theory, Phys. Lett. B267 (1991) 240–242.

[111] U. Baur, D. Zeppenfeld, Finite width effects and gauge invariance in radiative W productions and decay, Phys. Rev. Lett. 75 (1995) 1002–1005.

[112] J. R. Ellis, S. Kelley, D. V. Nanopoulos, Probing the desert using gauge coupling unification, Phys. Lett. B260 (1991) 131–137.

[113] U. Amaldi, W. de Boer, H. Furstenau, Comparison of grand unified theories with electroweak and strong coupling constants measured at LEP, Phys. Lett. B260 (1991) 447–455.

[114] P. Langacker, N. Polonsky, The Bottom mass prediction in supersymmetric grand unification: Uncertainties and constraints, Phys. Rev. D49 (1994) 1454–1467.

[115] E. de Rafael, Lectures on Quantum Electrodynamics. 1UAB-FT-D-1, May 1976. 185pp. GIFT lectures given at Barcelona, Autonoma U., May 1976.

[116] B. N. Taylor, E. R. Cohen, Recommended values of the fundamental physical constants: A status report, J. Res. Natl. Inst. Stand. Technol. (95) (1990) 497.

[117] N. J. Watson, Effective charges in non-Abelian gauge theories, In Proceedings of the French-American Seminar on Theoretical Aspects of Quantum Chromodynamics, Marseille, France, 1981, ed. J. W. Dash (Centre de Physique Théorique report no. CPT-81/P-1345, 1982).

[118] D. Binosi, J. Papavassiliou, The QCD effective charge to all orders, Nucl. Phys. Proc. Suppl. 121 (2003) 281–284.

[119] L. Baulieu, R. Coquereaux, Photon - Z mixing in the Weinberg-Salam model: effective charges and the a=-3 gauge, Ann. Phys. 140 (1982) 163.

[120] D. C. Kennedy, B. W. Lynn, Electroweak Radiative Corrections with an Effective Lagrangian: Four Fermion Processes, Nucl. Phys. B322 (1989) 1.

[121] K. Philippides, A. Sirlin, Application of the Pinch Technique to Neutral Current Amplitudes and the Concept of the Z Mass, Phys. Lett. B367 (1996) 377–385.

[122] M. S. Bilenky, J. L. Kneur, F. M. Renard, D. Schildknecht, Trilinear couplings among the electroweak vector bosons and their determination at LEP-200, Nucl. Phys. B409 (1993) 22–68.

[123] K. Hagiwara, S. Matsumoto, D. Haidt, C. S. Kim, A Novel approach to confront electroweak data and theory, Z. Phys. C64 (1994) 559–620.

[124] J. S. Schwinger, On Quantum electrodynamics and the magnetic moment of the electron, Phys. Rev. 73 (1948) 416–417.

[125] W. A. Bardeen, R. Gastmans, B. Lautrup, Static quantities in Weinberg's model of weak and electromagnetic interactions, Nucl. Phys. B46 (1972) 319–331.

[126] E. N. Argyres, G. Katsilieris, A. B. Lahanas, C. G. Papadopoulos, V. C. Spanos, One loop corrections to three vector boson vertices in the Standard Model, Nucl. Phys. B391 (1993) 23–41.

[127] J. Bernabeu, J. Papavassiliou, J. Vidal, The neutrino charge radius is a physical observable, Nucl. Phys. B680 (2004) 450–478.

[128] S. Sarantakos, A. Sirlin, W. J. Marciano, Radiative Corrections to Neutrino-Lepton Scattering in the SU(2)-L x U(1) Theory, Nucl. Phys. B217 (1983) 84.

[129] J. Papavassiliou, J. Bernabeu, M. Passera, Neutrino nuclear coherent scattering and the effective neutrino charge radius, PoS HEP2005 (2006) 192.

[130] J. Bernabeu, Low-Energy Elastic Neutrino-Nucleon and Nuclear Scattering and Its Relevance for Supernovae, CERN-TH-2073.

[131] L. M. Sehgal, Differences in the coherent interactions of electron-neutrino, muon-neutrino and tau-neutrino, Phys. Lett. B162 (1985) 370.

[132] F. J. Botella, C. S. Lim, W. J. Marciano, Radiative corrections to neutrino indices of refraction, Phys. Rev. D35 (1987) 896.

[133] G. Degrassi, B. A. Kniehl, A. Sirlin, Gauge invariant formulation of the S, T, and U parameters, Phys. Rev. D48 (1993) 3963–3966.

[134] C. D. Carone, Electroweak constraints on extended models with extra dimensions, Phys. Rev. D61 (2000) 015008.

[135] T. Appelquist, H.-C. Cheng, B. A. Dobrescu, Bounds on universal extra dimensions, Phys. Rev. D64 (2001) 035002.

[136] J. F. Oliver, J. Papavassiliou, A. Santamaria, Universal extra dimensions and Z –¿ b anti-b, Phys. Rev. D67 (2003) 056002.

[137] S. Dawson, C. B. Jackson, One-loop Corrections to the S Parameter in the Four-site Model, Phys. Rev. D79 (2009) 013006.

[138] G. Burdman, L. Da Rold, Renormalization of the S Parameter in Holographic Models of Electroweak Symmetry Breaking, JHEP 11 (2008) 025.

[139] S. Dawson, C. B. Jackson, Chiral-logarithmic corrections to the S and T parameters in Higgsless models, Phys. Rev. D76 (2007) 015014.

[140] G. Cacciapaglia, C. Csaki, G. Marandella, A. Strumia, The minimal set of electroweak precision parameters, Phys. Rev. D74 (2006) 033011.

[141] N. D. Christensen, R. Shrock, Technifermion representations and precision electroweak constraints, Phys. Lett. B632 (2006) 92–98.

[142] J. Montano, G. Tavares-Velasco, J. J. Toscano, F. Ramirez-Zavaleta, Su(L) (2) x U(Y) (1) -invariant description of the bilepton contribution to the WWV vertex in the minimal 331 model, Phys. Rev. D72 (2005) 055023.

[143] M. J. G. Veltman, Limit on Mass Differences in the Weinberg Model, Nucl. Phys. B123 (1977) 89.

[144] M. S. Chanowitz, M. A. Furman, I. Hinchliffe, Weak Interactions of Ultraheavy Fermions, Phys. Lett. B78 (1978) 285.

[145] M. S. Chanowitz, M. A. Furman, I. Hinchliffe, Weak Interactions of Ultraheavy Fermions. 2, Nucl. Phys. B153 (1979) 402.

[146] M. B. Einhorn, D. R. T. Jones, M. J. G. Veltman, Heavy Particles and the rho Parameter in the Standard Model, Nucl. Phys. B191 (1981) 146.

[147] J. J. van der Bij, F. Hoogeveen, Two Loop Correction to Weak Interaction Parameters Due to a Heavy Fermion Doublet, Nucl. Phys. B283 (1987) 477.

[148] G. Degrassi, S. Fanchiotti, P. Gambino, Current algebra approach to heavy top effects in delta (rho), Int. J. Mod. Phys. A10 (1995) 1377–1392.

[149] G. Degrassi, S. Fanchiotti, F. Feruglio, B. P. Gambino, A. Vicini, Two loop electroweak top corrections: Are they under control?, Phys. Lett. B350 (1995) 75–84.

[150] J. Papavassiliou, K. Philippides, K. Sasaki, Two loop electroweak corrections to the rho parameter beyond the leading approximation, Phys. Rev. D53 (1996) 3942–3961.

[151] J. M. Cornwall, D. N. Levin, G. Tiktopoulos, Derivation of Gauge Invariance from High-Energy Unitarity Bounds on the s Matrix, Phys. Rev. D10 (1974) 1145; Erratum–ibid. D11, (1975) 972.

[152] C. E. Vayonakis, Born Helicity Amplitudes and Cross-Sections in Nonabelian Gauge Theories, Nuovo Cim. Lett. 17 (1976) 383.

[153] M. S. Chanowitz, M. K. Gaillard, The TeV Physics of Strongly Interacting W's and Z's, Nucl. Phys. B261 (1985) 379.

[154] S. Willenbrock, G. Valencia, On the definition of the Z boson mass, Phys. Lett. B259 (1991) 373–376.

[155] R. G. Stuart, General renormalization of the gauge invariant perturbation expansion near the Z0 resonance, Phys. Lett. B272 (1991) 353–358.

[156] R. G. Stuart, Gauge invariance, analyticity and physical observables at the Z0 resonance, Phys. Lett. B262 (1991) 113–119.

[157] R. G. Stuart, The Structure of the Z0 resonance and the physical properties of the Z0 boson, Phys. Rev. Lett. 70 (1993) 3193–3196.

[158] H. G. J. Veltman, Mass and width of unstable gauge bosons, Z. Phys. C62 (1994) 35–52.

[159] G. J. Gounaris, R. Kogerler, H. Neufeld, Relationship Between Longitudinally Polarized Vector Bosons and their Unphysical Scalar Partners, Phys. Rev. D34 (1986) 3257.

[160] J. Papavassiliou, Asymptotic properties of Born-improved amplitudes with gauge bosons in the final state, Phys. Rev. D60 (1999) 056001.

[161] J. Papavassiliou, The pinch technique at two-loops: The case of massless Yang-Mills theories, Phys. Rev. D62 (2000) 045006.

[162] J. M. Cornwall, W.-S. Hou, J. E. King, Gauge invariant calculations in finite temperature QCD: Landau ghost and magnetic mass, Phys. Lett. B153 (1985) 173.

[163] J. M. Cornwall, How d = 3 QCD resembles d = 4 QCD, Physica A158 (1989) 97–110.

[164] J. M. Cornwall, On one-loop gap equations for the magnetic mass in d = 3 gauge theory, Phys. Rev. D57 (1998) 3694–3700.

[165] D. Binosi, J. Papavassiliou, Pinch technique and the Batalin-Vilkovisky formalism, Phys. Rev. D66 (2002) 025024.

[166] D. Binosi, J. Papavassiliou, Pinch technique self-energies and vertices to all orders in perturbation theory, J. Phys. G30 (2004) 203.

[167] P. A. Grassi, T. Hurth, M. Steinhauser, Practical algebraic renormalization, Annals Phys. 288 (2001) 197–248.

[168] C. Itzykson, J. B. Zuber, Quantum Field Theory, International Series in Pure and Applied Physics, New York, USA: Mcgraw-Hill (1980) 705 p., 1980.

[169] D. Binosi, J. Papavassiliou, New Schwinger-Dyson equations for non-Abelian gauge theories, JHEP 11 (2008) 063.

[170] D. Binosi, J. Papavassiliou, The two-loop pinch technique in the electroweak sector, Phys. Rev. D66 (2002) 076010.

[171] D. C. Curtis, M. R. Pennington, Truncating the Schwinger-Dyson equations: How multiplicative renormalizability and the Ward identity restrict the three point vertex in QED, Phys. Rev. D42 (1990) 4165–4169.

[172] D. C. Curtis, M. R. Pennington, D. A. Walsh, On the gauge dependence of dynamical fermion masses, Phys. Lett. B249 (1990) 528–530.

[173] D. C. Curtis, M. R. Pennington, Nonperturbative study of the fermion propagator in quenched QED in covariant gauges using a renormalizable truncation of the Schwinger- Dyson equation, Phys. Rev. D48 (1993) 4933–4939.

[174] A. Bashir, M. R. Pennington, Gauge independent chiral symmetry breaking in quenched QED, Phys. Rev. D50 (1994) 7679–7689.

[175] A. Bashir, M. R. Pennington, Constraint on the QED Vertex from the Mass Anomalous Dimension $\gamma_m = 1$, Phys. Rev. D53 (1996) 4694–4697.

[176] A. Bashir, A. Kizilersu, M. R. Pennington, The non-perturbative three-point vertex in massless quenched QED and perturbation theory constraints, Phys. Rev. D57 (1998) 1242–1249.

[177] A. Bashir, A. Huet, A. Raya, Gauge dependence of mass and condensate in chirally asymmetric phase of quenched QED3, Phys. Rev. D66 (2002) 025029.

[178] A. Bashir, A. Raya, Dynamical fermion masses and constraints of gauge invariance in quenched QED3, Nucl. Phys. B709 (2005) 307–328.

[179] K.-i. Kondo, Y. Kikukawa, H. Mino, The phase structure of quantum electrodynamics in the framework of the Schwinger Dyson equation, Phys. Lett. B220 (1989) 270–275.

[180] V. Sauli, Minkowski solution of Dyson-Schwinger equations in momentum subtraction scheme, JHEP 02 (2003) 001.

[181] S. Mandelstam, Approximation Scheme for QCD, Phys. Rev. D20 (1979) 3223.

[182] D. Binosi, J. Papavassiliou, Pinch Technique for Schwinger-Dyson Equations, JHEP 03 (2007) 041.

[183] D. Binosi, J. Papavassiliou, Gauge-invariant truncation scheme for the Schwinger-Dyson equations of QCD, Phys. Rev. D77 (2008) 061702(R).

[184] A. Salam, Renormalizable electrodynamics of vector mesons, Phys. Rev. 130 (1963) 1287–1290.

[185] K. D. Lane, Asymptotic Freedom and Goldstone Realization of Chiral Symmetry, Phys. Rev. D10 (1974) 2605.

[186] J. S. Schwinger, Gauge Invariance and Mass, Phys. Rev. 125 (1962) 397–398.

[187] M. A. Shifman, A. I. Vainshtein, V. I. Zakharov, QCD and Resonance Physics: Applications, Nucl. Phys. B147 (1979) 448–518.

[188] M. J. Lavelle, M. Schaden, Propagators and condensates in QCD, Phys. Lett. B208 (1988) 297.

[189] F. R. Graziani, The gluon condensate and the effective gluon mass, Z. Phys. C33 (1987) 397.

[190] M. Lavelle, Gauge invariant effective gluon mass from the operator product expansion, Phys. Rev. D44 (1991) 26–28.

[191] J. M. Cornwall, W.-S. Hou, Extension of the gauge technique to broken symmetries and finite temperature, Phys. Rev. D34 (1986) 585.

[192] A. C. Aguilar, J. Papavassiliou, Power-law running of the effective gluon mass, Eur. Phys. J. A35 (2008) 189–205.

[193] J. M. Cornwall, Quark Confinement and Vortices in Massive Gauge Invariant QCD, Nucl. Phys. B157 (1979) 392.

[194] C. W. Bernard, Adjoint Wilson lines and the effective gluon mass, Nucl. Phys. B219 (1983) 341.

[195] I. L. Bogolubsky, E. M. Ilgenfritz, M. Muller-Preussker, A. Sternbeck, The Landau gauge gluon and ghost propagators in 4D SU(3) gluodynamics in large lattice volumes.

[196] C. Alexandrou, P. de Forcrand, E. Follana, The gluon propagator without lattice Gribov copies, Phys. Rev. D63 (2001) 094504.

[197] C. Alexandrou, P. de Forcrand, E. Follana, The gluon propagator without lattice Gribov copies on a finer lattice, Phys. Rev. D65 (2002) 114508.

[198] C. Alexandrou, P. De Forcrand, E. Follana, The Laplacian gauge gluon propagator in SU(N(c)), Phys. Rev. D65 (2002) 117502.

[199] A. G. Williams, Nonperturbative QCD, gauge-fixing, Gribov copies, and the lattice, Prog. Theor. Phys. Suppl. 151 (2003) 154.

[200] A. Sternbeck, E. M. Ilgenfritz, M. Muller-Preussker, A. Schiller, The influence of Gribov copies on the gluon and ghost propagator, AIP Conf. Proc. 756 (2005) 284–286.

[201] P. J. Silva, O. Oliveira, Gribov copies, lattice QCD and the gluon propagator, Nucl. Phys. (B690) (2004) 177.

[202] A. Cucchieri, T. Mendes, What's up with IR gluon and ghost propagators in Landau gauge? A puzzling answer from huge lattices.

[203] D. Dudal, J. A. Gracey, S. P. Sorella, N. Vandersickel, H. Verschelde, A refinement of the Gribov-Zwanziger approach in the Landau gauge: infrared propagators in harmony with the lattice results, Phys. Rev. D78 (2008) 065047.

[204] A. Salam, R. Delbourgo, Renormalizable electrodynamics of scalar and vector mesons. II, Phys. Rev. 135 (1964) B1398–B1427.

[205] R. Delbourgo, P. C. West, A Gauge Covariant Approximation to Quantum Electrodynamics, J. Phys. A10 (1977) 1049.

[206] E. Farhi, R. Jackiw, Dynamical gauge symmetry breaking. A collection of reprints, Singapore, Singapore: World Scientific (1982) 403p.

[207] R. Jackiw, Dynamical Symmetry BreakingIn *Erice 1973, Proceedings, Laws Of Hadronic Matter*, New York 1975, 225-251 and M I T Cambridge - COO-3069-190 (73,REC.AUG 74) 23p.

[208] R. Jackiw, K. Johnson, Dynamical Model of Spontaneously Broken Gauge Symmetries, Phys. Rev. D8 (1973) 2386–2398.

[209] Y. Nambu, Quasi-particles and gauge invariance in the theory of superconductivity, Phys. Rev. 117 (1960) 648–663.

[210] J. Goldstone, Field Theories with Superconductor Solutions, Nuovo Cim. 19 (1961) 154–164.

[211] J. Goldstone, A. Salam, S. Weinberg, Broken Symmetries, Phys. Rev. 127 (1962) 965–970.

[212] Y. Nambu, G. Jona-Lasinio, Dynamical model of elementary particles based on an analogy with superconductivity. I, Phys. Rev. 122 (1961) 345–358.

[213] Y. Nambu, G. Jona-Lasinio, Dynamical model of elementary particles based on an analogy with superconductivity. II, Phys. Rev. 124 (1961) 246–254.

[214] P. W. Higgs, Broken Symmetries and the Masses of Gauge Bosons, Phys. Rev. Lett. 13 (1964) 508–509.

[215] P. W. Higgs, Broken symmetries, massless particles and gauge fields, Phys. Lett. 12 (1964) 132–133.

[216] F. Englert, R. Brout, Broken Symmatry and the Mass of Vector Mesons, Phys. Rev. Lett. 13 (1964) 321–322.

[217] G. S. Guralnik, C. R. Hagen, T. W. B. Kibble, Global Conservation Laws and Massless Particles, Phys. Rev. Lett. 13 (1964) 585–587.

[218] P. W. Higgs, Spontaneous Symmetry Breakdown Without Massless Bosons, Phys. Rev. 145 (1966) 1156–1163.

[219] J. S. Schwinger, Gauge Invariance and Mass. 2, Phys. Rev. 128 (1962) 2425–2429.

[220] S. R. Coleman, There are no Goldstone bosons in two-dimensions, Commun. Math. Phys. 31 (1973) 259–264.

[221] J. M. Cornwall, R. E. Norton, Spontaneous Symmetry Breaking Without Scalar Mesons, Phys. Rev. D8 (1973) 3338–3346.

[222] E. Eichten, F. Feinberg, Dynamical Symmetry Breaking of Nonabelian Gauge Symmetries, Phys. Rev. D10 (1974) 3254–3279.

[223] E. C. Poggio, E. Tomboulis, S. H. H. Tye, Dynamical Symmetry Breaking in Nonabelian Field Theories, Phys. Rev. D11 (1975) 2839.

[224] A. C. Aguilar, D. Binosi, J. Papavassiliou, Gluon and ghost propagators in the Landau gauge: Deriving lattice results from Schwinger-Dyson equations, Phys. Rev. D78 (2008) 025010.

[225] P. Boucaud, J. P. Leroy, A. Le Yaouanc, J. Micheli, O. Pene, J. Rodriguez-Quintero, On the IR behaviour of the Landau-gauge ghost propagator, JHEP 06 (2008) 099.

[226] T. Kugo, I. Ojima, Local Covariant Operator Formalism of Nonabelian Gauge Theories and Quark Confinement Problem, Prog. Theor. Phys. Suppl. 66 (1979) 1.

[227] C. S. Fischer, Infrared properties of QCD from Dyson-Schwinger equations, J. Phys. G32 (2006) R253–R291.

[228] A. Cucchieri, T. Mendes, A. Mihara, Numerical study of the ghost-gluon vertex in Landau gauge, JHEP 12 (2004) 012.

[229] A. C. Aguilar, J. Papavassiliou, Infrared finite ghost propagator in the Feynman gauge, Phys. Rev. D77 (2008) 125022.

[230] J. Greensite, The confinement problem in lattice gauge theory, Prog. Theor. Phys. Suppl. 51 (2003) 1, and references therein.

[231] Y. L. Dokshitzer, G. Marchesini, B. R. Webber, Dispersive Approach to Power-Behaved Contributions in QCD Hard Processes, Nucl. Phys. B469 (1996) 93–142.

[232] S. J. Brodsky, S. Menke, C. Merino, J. Rathsman, On the behavior of the effective QCD coupling alpha(tau)(s) at low scales, Phys. Rev. D67 (2003) 055008.

[233] A. C. Aguilar, A. A. Natale, P. S. Rodrigues da Silva, Relating a gluon mass scale to an infrared fixed point in pure gauge QCD, Phys. Rev. Lett. 90 (2003) 152001.

[234] A. C. Aguilar, A. Mihara, A. A. Natale, Phenomenological tests for the freezing of the QCD running coupling constant, Int. J. Mod. Phys. A19 (2004) 249–269.

[235] G. M. Prosperi, M. Raciti, C. Simolo, On the running coupling constant in QCD, Prog. Part. Nucl. Phys. 58 (2007) 387–438.

[236] J. L. Albacete, N. Armesto, J. G. Milhano, C. A. Salgado, Non-linear QCD meets data: A global analysis of lepton- proton scattering with running coupling BK evolution.

[237] G. F. de Teramond, S. J. Brodsky, The hadronic spectrum of a holographic dual of QCD, Phys. Rev. Lett. 94 (2005) 201601.

[238] S. J. Brodsky, R. Shrock, Maximum Wavelength of Confined Quarks and Gluons and Properties of Quantum Chromodynamics, Phys. Lett. B666 (2008) 95–99.

[239] A. C. Aguilar, A. Mihara, A. A. Natale, Freezing of the QCD coupling constant and solutions of Schwinger-Dyson equations, Phys. Rev. D65 (2002) 054011.

[240] S. Nadkarni, Linear response and plasmon decay in hot gluonic matter, Phys. Rev. Lett. 61 (1988) 396.

[241] K. Sasaki, Gauge-independent resummed gluon self-energy in hot QCD, Nucl. Phys. B490 (1997) 472–504.

[242] K. Sasaki, Gauge-independent Thermal β Function In Yang-Mills Theory, Phys. Lett. B369 (1996) 117–122.

[243] G. Alexanian, V. P. Nair, A Selfconsistent inclusion of magnetic screening for the quark - gluon plasma, Phys. Lett. B352 (1995) 435–439.

[244] M. Passera, K. Sasaki, The gluon self-energy in the Coulomb and temporal axial gauges via the pinch technique, Phys. Rev. D54 (1996) 5763–5776.

[245] A. Pilaftsis, Higgs-Z Mixing and Resonant CP Violation at mu+ mu- Colliders, Phys. Rev. Lett. 77 (1996) 4996–4999.

[246] A. Pilaftsis, Resonant CP violation induced by particle mixing in transition amplitudes, Nucl. Phys. B504 (1997) 61–107.

[247] A. Pilaftsis, T. E. J. Underwood, Resonant leptogenesis, Nucl. Phys. B692 (2004) 303–345.

[248] A. Pilaftsis, Electroweak Resonant Leptogenesis in the Singlet Majoron Model, Phys. Rev. D78 (2008) 013008.

[249] Y. Yamada, Gauge dependence of the on-shell renormalized mixing matrices, Phys. Rev. D64 (2001) 036008.

[250] J. R. Espinosa, Y. Yamada, Scale- and gauge-independent mixing angles for scalar particles, Phys. Rev. D67 (2003) 036003.

[251] A. Pilaftsis, Gauge and scheme dependence of mixing matrix renormalization, Phys. Rev. D65 (2002) 115013.

[252] N. Caporaso, S. Pasquetti, Gauge-invariant resummation formalism and unitarity in non-commutative QED, JHEP 04 (2006) 016.

[253] N. Caporaso, S. Pasquetti, Non-commutative (softly broken) supersymmetric Yang-Mills-Chern-Simons.

[254] K. G. Wilson, J. B. Kogut, The Renormalization group and the epsilon expansion, Phys. Rept. 12 (1974) 75–200.

[255] S. Catani, E. D'Emilio, Gauge Invariant Chromoelectromagnetic Field And Hot Gluon Plasma Oscillations, Fortsch. Phys. 41 (1993) 261–287.

[256] D. Birmingham, M. Rakowski, G. Thompson, Renormalization of topological field theory, Nucl. Phys. B329 (1990) 83.

[257] M. D'Attanasio, T. R. Morris, Gauge Invariance, the Quantum Action Principle, and the Renormalization Group, Phys. Lett. B378 (1996) 213–221.

[258] S. Arnone, T. R. Morris, O. J. Rosten, A Generalised Manifestly Gauge Invariant Exact Renormalisation Group for SU(N) Yang-Mills, Eur. Phys. J. C50 (2007) 467–504.

[259] T. R. Morris, O. J. Rosten, A manifestly gauge invariant, continuum calculation of the SU(N) Yang-Mills two-loop beta function, Phys. Rev. D73 (2006) 065003.

[260] C. Schubert, An introduction to the worldline technique for quantum field theory calculations, Acta Phys. Polon. B27 (1996) 3965–4001.

[261] N. K. Nielsen, Gauge Invariance and Broken Conformal Symmetry, Nucl. Phys. B97 (1975) 527.

[262] N. K. Nielsen, On the Gauge Dependence of Spontaneous Symmetry Breaking in Gauge Theories, Nucl. Phys. B101 (1975) 173.

[263] Y. A. Simonov, Perturbative theory in the nonperturbative QCD vacuum, Phys. Atom. Nucl. 58 (1995) 107–123.

[264] Z. Bern, D. C. Dunbar, A Mapping between Feynman and string motivated one loop rules in gauge theories, Nucl. Phys. B379 (1992) 562–601.

[265] Y. J. Feng, C. S. Lam, String organization of field theories: Duality and gauge invariance, Phys. Rev. D50 (1994) 7430–7439.

[266] P. Di Vecchia, L. Magnea, A. Lerda, R. Russo, R. Marotta, String techniques for the calculation of renormalization constants in field theory, Nucl. Phys. B469 (1996) 235–286.

[267] D. Binosi, L. Theussl, JaxoDraw: A graphical user interface for drawing Feynman diagrams, Comput. Phys. Commun. 161 (2004) 76–86.

[268] D. Binosi, J. Collins, C. Kaufhold and L. Theussl, JaxoDraw: A graphical user interface for drawing Feynman diagrams. Version 2.0 release notes, Comput. Phys. Commun. 180 (2009) 1709–1715.